frontiers | Research Topics

Neuroprotection and neurorestoration: Natural medicinal products in preventing and ameliorating cognitive impairment

Edited by
Jianxun Liu, Guibo Sun, Dennis Chang and Qian Hua

Coordinated by
Yehao Zhang

Published in
Frontiers in Neuroscience
Frontiers in Pharmacology

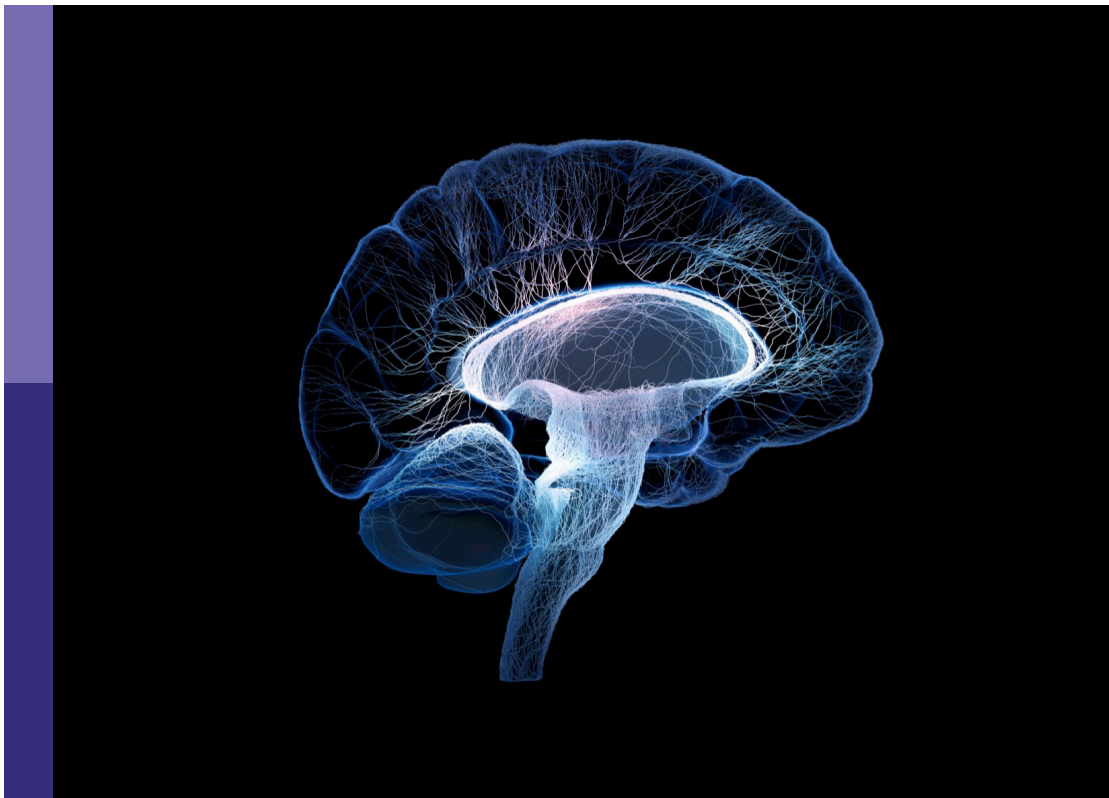

ISSN 1664-8714
ISBN 978-2-8325-4387-0
DOI 10.3389/978-2-8325-4387-0

About Frontiers

Frontiers is more than just an open access publisher of scholarly articles: it is a pioneering approach to the world of academia, radically improving the way scholarly research is managed. The grand vision of Frontiers is a world where all people have an equal opportunity to seek, share and generate knowledge. Frontiers provides immediate and permanent online open access to all its publications, but this alone is not enough to realize our grand goals.

Frontiers journal series

The Frontiers journal series is a multi-tier and interdisciplinary set of open-access, online journals, promising a paradigm shift from the current review, selection and dissemination processes in academic publishing. All Frontiers journals are driven by researchers for researchers; therefore, they constitute a service to the scholarly community. At the same time, the *Frontiers journal series* operates on a revolutionary invention, the tiered publishing system, initially addressing specific communities of scholars, and gradually climbing up to broader public understanding, thus serving the interests of the lay society, too.

Dedication to quality

Each Frontiers article is a landmark of the highest quality, thanks to genuinely collaborative interactions between authors and review editors, who include some of the world's best academicians. Research must be certified by peers before entering a stream of knowledge that may eventually reach the public - and shape society; therefore, Frontiers only applies the most rigorous and unbiased reviews. Frontiers revolutionizes research publishing by freely delivering the most outstanding research, evaluated with no bias from both the academic and social point of view. By applying the most advanced information technologies, Frontiers is catapulting scholarly publishing into a new generation.

What are Frontiers Research Topics?

Frontiers Research Topics are very popular trademarks of the *Frontiers journals series*: they are collections of at least ten articles, all centered on a particular subject. With their unique mix of varied contributions from Original Research to Review Articles, Frontiers Research Topics unify the most influential researchers, the latest key findings and historical advances in a hot research area.

Find out more on how to host your own Frontiers Research Topic or contribute to one as an author by contacting the Frontiers editorial office: frontiersin.org/about/contact

Neuroprotection and neurorestoration: Natural medicinal products in preventing and ameliorating cognitive impairment

Topic editors

Jianxun Liu — Xiyuan Hospital, China Academy of Chinese Medical Sciences, China

Guibo Sun — Chinese Academy of Medical Sciences and Peking Union Medical College, China

Dennis Chang — Western Sydney University, Australia

Qian Hua — Beijing University of Chinese Medicine, China

Topic Coordinator

Yehao Zhang — Institute of Basic Medical Sciences, Xiyuan Hospital, China Academy of Chinese Medical Sciences, China

Citation

Liu, J., Sun, G., Chang, D., Hua, Q., Zhang, Y., eds. (2024). *Neuroprotection and neurorestoration: Natural medicinal products in preventing and ameliorating cognitive impairment*. Lausanne: Frontiers Media SA.

doi: 10.3389/978-2-8325-4387-0

Table of contents

frontiers | Frontiers in Neuroscience

TYPE Review
PUBLISHED 24 November 2022
DOI 10.3389/fnins.2022.1044572

OPEN ACCESS

EDITED BY
Jianxun Liu,
China Academy of Chinese Medical Sciences, China

REVIEWED BY
Zequn Yin,
Hefei University of Technology, China
Shuang Zhang,
Hefei University of Technology, China

*CORRESPONDENCE
Jian-gang Liu
liujiangang2002@sina.com
Hao Li
xyhplihao1965@126.com

SPECIALTY SECTION
This article was submitted to Neuropharmacology, a section of the journal Frontiers in Neuroscience

RECEIVED 14 September 2022
ACCEPTED 04 November 2022
PUBLISHED 24 November 2022

CITATION
Chang S-r, Liu J-g, Li H, Liu M-x, Shi D-d and Zhou L-j (2022) Pharmaceutical and pharmacological studies of Shen Ma Yi Zhi granule for prevention of vascular dementia: A review.
Front. Neurosci. 16:1044572.
doi: 10.3389/fnins.2022.1044572

Pharmaceutical and pharmacological studies of Shen Ma Yi Zhi granule for prevention of vascular dementia: A review

Su-rui Chang[1,2], Jian-gang Liu[1,3]*, Hao Li[1,4,5]*, Mei-xia Liu[1,4], Dan-dan Shi[1,4] and Li-juan Zhou[1,4]

[1]Xiyuan Hospital, China Academy of Chinese Medical Sciences, Beijing, China, [2]Graduate School, China Academy of Chinese Medical Sciences, Beijing, China, [3]National Clinical Research Center for Chinese Medicine Cardiology, Beijing, China, [4]Institute of Geriatrics of China Academy of Chinese Medical Sciences, Beijing, China, [5]Wangjing Hospital, China Academy of Chinese Medical Sciences, Beijing, China

Background: With dementia significantly increasing hospitalization and disability rates, worldwide aging of the population presents major challenges to public health. The majority of cases of cognitive dysfunction among the elderly, however, are characterized by an identifiable, preventable and treatable vascular component. As such, increased study of preventative methods in the context of dementia is warranted. Traditional Chinese medicine compounds have been reported to be neuroprotective and improve cognitive function via a variety of mechanisms. Shen Ma Yi Zhi granule (SMYZG) is one such collection of compounds that has been proven clinically effective. Pharmacological mechanisms of action, pharmacokinetics and clinical applications of SMYZG have been previously studied using a variety of vascular dementia animal models. SMYZG activates and regulates four main signaling pathways relevant to vascular dementia including the AMPK/PPARα/PGC-1α/UCP2, Nrf2/HO-1, HIF-1/VEGF/Notch, and VEGF/Flk-1/p8 MAPK pathways. Furthermore, SMYZG influences anti-inflammatory and anti-oxidant stress responses, reverses demyelination of brain white matter and vascular endothelium, regulates pericyte function and normalizes mitochondrial metabolism. Neuroprotective effects of SMYZG, as well as those promoting regeneration of vascular endothelium, have also been reported in studies of rat models of vascular dementia. Future research concerning SMYG is warranted for development of vascular dementia preventative management strategies.

KEYWORDS

Shen Ma Yi Zhi, VaD, traditional compounds, animal models, signal pathway

Introduction

Cognitive impairment significantly impairs thought, communication, comprehension, and memory formation processes. Vascular risk factors are among the leading etiologies of cognitive impairment among the elderly. Therapies capable of effectively delaying, preventing or treating cognitive decline, however, remain to be developed for clinical use. Recently, a number of studies have reported success in treating Alzheimer's disease and vascular dementia with traditional Chinese medicine compounds as demonstrated using behavioral tests, histopathological examinations and indexes relevant to neurotransmitter catabolism. Importantly, these studies underscored the excellent potential that traditional Chinese medicine compounds have in future clinical use (Lecordier et al., 2021).

Shen Ma Yi Zhi granule (SMYZG), a Chinese herbal prescription, was demonstrated effective in treating vascular disease (Chang Surui, 2020). This compound consists of ginseng (*Panax Ginseng C.A. Mey*), Gastrodia elata (*Gastrodia elata Bl*), Euonymus alatus [*Euonymus alatus (Thunb.) Sieb*], and Ligustici (*Ligusticum chuanxiong Hort*). Pharmaceutical, pharmacodynamic and toxicological have been finished to determine the pharmaceutical extractions routing. *In vivo* studies have similarly been conducted (Li, 2017; Kun et al., 2020; Sun et al., 2021a,b; Lijuan et al., 2022). Importantly, aqueous extracts of SMYZG were reported to not only be neuroprotective but also beneficially affect learning and memory, hippocampal structure, central cholinergic system function as well as suppress the inflammatory and oxidative stress responses based on 2-VO and MID models; the primary active functional components were reported to be ginsenosides, gastrodin, ferulic acid, and quercetin (Nan-Nan et al., 2019). Toxicological studies revealed no negative effects on organs or critical biological parameters. Furthermore, SMYZG was awarded a National Invention Patent (Meixia, 2020) and recorded in the national registry of Chinese medicine preparations (No. Z20200005000).

Chemistry of Shen Ma Yi Zhi granule

Preparation processes

Shen Ma Yi Zhi granule is composed of ginseng (*Panax Ginseng C.A. Mey*), Gastrodia elata (*Gastrodiaelata Bl*), Euonymus alatus [*Euonymus alatus (Thunb.) Sieb*], and Ligustici (*Ligusticum chuanxiong Hort*) in a respective 3:3:3:2 ratio. All components meet the standards set forth by the Chinese Pharmacopoeia Commission (2015). Constituent weighting is achieved using the analytic hierarchy process (AHP) method. Orthogonal and single factor analyses were applied for optimization of extraction and purification technology used to prepare SMYZG by measuring yield rates of extraction and transition probability of gastrodin, *p*-hydroxybenzylalcohol, and ferulic acid. Briefly, Gastrodia elata, Euonymus alatus, and Ligustici slices are mixed, with water added to the mixture three times for 1 h each time. Ten times the amount of water per compound is added the first time while eight times the amount of water is added the second and third times. Ginseng slices are soaked in water for compound extraction twice and at 2 h per time; 12 times the amount of water is added to the ginseng the first time and 10 times the second. Mixing the extracts together in the Drug Manufacturing Room of Xiyuan Hospital, Chinese Academy of Chinese Medical Sciences, produces a crude drug extract of 2.44 g (**Figure 1**).

Chemical components of Shen Ma Yi Zhi granule

Ginseng (*Panax Ginseng C.A. Mey*), a root of Panax (Araliaceae), contains panaxosides A, B, C, D, E, and F, volatile oil, Ginseng ene, vitamin B1, vitamin B2, nicotinic acid, niacinamide, pantothenic acid, choline, maltase, invertase, esterase, and a variety of amino acids (Jian and Shao-wa, 2021). Gastrodia elata (*Gastrodiaelata Bl*), i.e., dried Gastrodia elata plant content, contains compounds such as Gastrodia elata glucoside and Gastrodia elata ether glucoside (Wei et al., 2021). Euonymus alatus [*Euonymus alatus (Thunb.) Sieb*], the twig outgrowths of celastraceae plants, contains compounds such as stigmast-4-en-3-one, quercetin, β-sitosterol, dehydrodicatechin, aromadendrin, d-catechin, 4 β-sitosterone, alatamine, and wilfordine (Lei et al., 2015; Rui-xi et al., 2015; Yanxiu et al., 2021). Ligustici (*Ligusticum chuanxiong Hort*), i.e., dried Ligusticum plant content, contains compounds such as tetramethylpyrazine, perlolyrine, ligustilide, wallichilide, senkyunolide, vanillic acid, caffeic acid, protocatechuic acid, and ferulic acid (Jiangang et al., 2019; Li Qian, 2020; Zhonghui et al., 2020).

Importantly, there are four major clinically effective components of SMYZG, including *b*-D-glucopyranoside (3b, 12b)-3,12-dihydroxydammar-24-en-20-yl, 4 -(hydroxymethyl)phenyl-β-D-glucopyranoside, 4H-1-benzopyran-4-one, 2-(3,4-dihydroxyphenyl)-3,5,7-trihydroxy-flavone, 2–propenoic acid and 3-(4-hydroxy-3-methoxyphenyl). Molecular structures are detailed in **Figure 2**.

High-performance liquid chromatography parameters of SMYZG, shown in **Figure 3**, are as follows: chromatographic column, Tnature C18 column (4.6 mm × 250 mm, 5 min); drug elution times: 0–5 min, 0–14%; 6–10 min, 14–19%; 11–15 min, 19–20%; 16–20 min, 20–24%; 21–25 min, 20–24%. Mobile phase: methanol (A) approximately 0.1%; acetum (B) approximately 0.1%. Flow rate: 0.25 ml/min. UV detection wavelength: 321 nm. Injection volume: 5 μl (**Figure 3**).

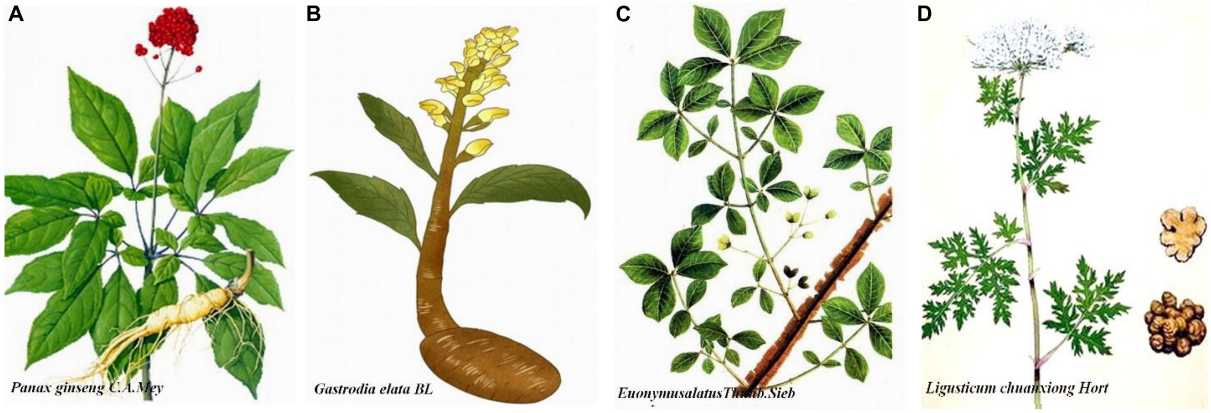

FIGURE 1
Detailing of herbal Shen Ma Yi Zhi granule (SMYZG) components. **(A)** *Panax Ginseng C.A. Mey*; **(B)** *Gastrodia elata Bl*; **(C)** *Euonymus alatus (Thunb.) Sieb*; **(D)** *Ligusticum chuanxiong Hort*. Sources for the images within this figure: 699pic.com and Chinese Pharmacopoeia.

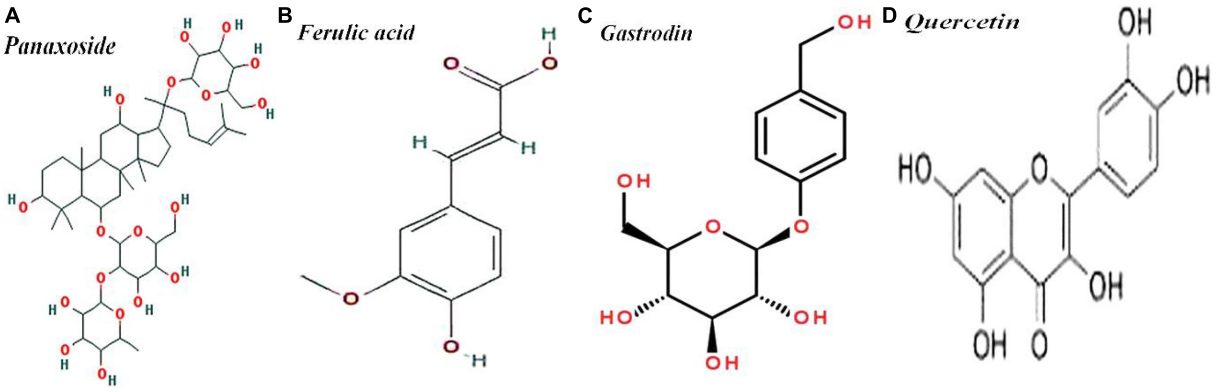

FIGURE 2
Molecular structures of **(A)** panaxoside/C36H62O8, **(B)** ferulic acid/C10H10O4, **(C)** gastrodin/C13H18O7, and **(D)** Quercetin/C15H10O7.

Clinical studies concerning Shen Ma Yi Zhi granule

Vascular dementia (VaD), the second commonest form of dementia after Alzheimer's disease (Huang et al., 2016), is primarily characterized by poor athletic performance, executive functioning, information processing, concentration, and memory (O'Brien et al., 2003; Hachinski et al., 2006; Moorhouse and Rockwood, 2008). Diagnosis is not always straightforward as a number of non-specific signs and wide variety of risk factors are often present among older patients. In contrast to Alzheimer's, VaD generally manifests more acutely with executive functioning gradually declining and memory impairment fluctuating (Hachinski et al., 2006; Moorhouse and Rockwood, 2008). Functional regions (vascular control areas) involved in cortical dementia are shown in **Figure 4**.

Wu et al. (2017) recruited 60 mild and moderate VaD patients previously diagnosed according to Chinese guidelines for diagnosis and treatment of vascular cognitive impairment (Cognitive Impairment Committee NBCM, 2019), then observed the hemorheological indexes and tested their cognitive functioning. Mini-Mental State Exam (MMSE) scores of patients treated with SMYZG were found to have markedly improved; as such, SMYZG treatment was concluded to effectively improve cognition among this patient population. And it increased erythrocyte deformability, inhibited platelet function, reduced blood viscosity and improved the blood rheology.

One randomized controlled trial (Zhang et al., 2020) evaluating the clinical effectiveness of treating VaD patients with SMYZG in combination with Ginkgo biloba tablets revealed that this regimen increases MMSE scores, decreases Alzheimer's Disease Assessment Scale-Cognitive Subscale (ADAS-Cog) scores, improves patient memory, attenuates mood fluctuations

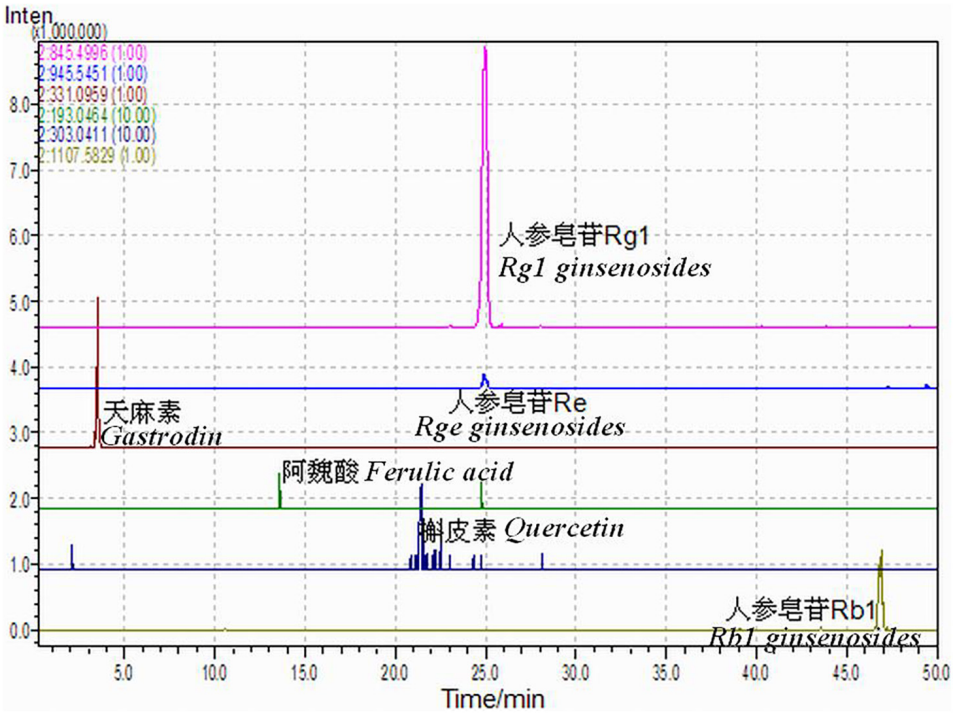

FIGURE 3
Shen Ma Yi Zhi granule (SMYZG) sample chromatogram absorption peaks and HPLC retention times.

and improves ADL capacities. Furthermore, these compounds were noted to increase blood levels of both nitric oxide (NO) and vascular endothelial growth factor (VEGF) and thus improve endothelial function. In experimental group, the level of neuronspecific enolase (NSE) decreased and the level of brain-derived neurotrophic factor (BNDF) increased indicated that SMYZ had a certain clinical effect in nourishing nerves and repairing damaged nerves.

Model animal experiments

Selection of suitable animal models is key in successful experimental design and is also critical to result accuracy and objectivity. At least 10 methods of creating VaD animal models have been reported and include procedures such as vessel occlusion (VO), lacunar infarct embolization (MID) and photochemical induction (Lin et al., 2014). Studying multiple VaD animal models is therefore helpful in evaluating pharmacological mechanisms more precisely.

2-VO rat model data

The 2-VO rat model leads to chronic cerebral hypoperfusion and subsequent development of secondary cerebrovascular pathophysiological alterations, critical risk factors for VaD pathogenesis (Zhang et al., 2018). Advantages of this model include lower levels of injury inflicted on animals and rapid operating time. This model simulates hypoperfused (Tomimoto et al., 2003; Farkas et al., 2007) and hypoxic (Hu et al., 2017) states of the human brain, especially in structures related to recognition such as the hippocampus and cerebral cortex. These brain regions are more easily affected by oxidative stress, with resultant structural neuronal and cholinergic system damage significantly impairing learning, memory, and behavior (Luo et al., 2019; Zhu et al., 2019; Fan et al., 2020). Relevant mechanisms of these pathological processes are closely related with those of chronic cerebral ischemia (CCI) (Cheng et al., 2019).

Frequency of Morris water maze platform searching, frequency of original platform crossing and percentage of time spent swimming in the quadrant of the original platform location among rats in SMYZG treatment groups increased significantly. These data underscore that SMYZG improves learning and memory function among 2-VO rats. Importantly, SMYZG repairs 2-VO rat cortical damage by improving the loose arrangement of pyramidal cells, reducing axonotmesis and neuronal shrinkage, protecting the morphology and structure of neuronal mitochondria, as well as increasing the number of neuronal mitochondrial and surrounding microvasculature density.

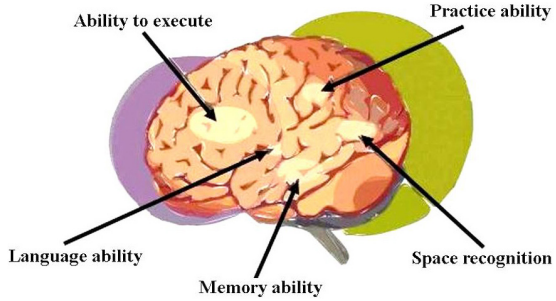

FIGURE 4
Functional regions (vascular control areas) involved in cortical dementia.

MID rat model data

Multiple cerebral infarction, also known as white matter disease, is most commonly caused by systemic disease or brain lesions (Kalaria, 2016). Cerebral small vessel disease (CSVD) is related to the occurrence and development of MID and is one of the most common causes of VaD. MID patients with cognitive impairment frequently exhibit significant small vessel ischemic changes along with areas of cerebral infarction (Jiang et al., 2021). Many studies have utilized sludged blood or kelp microgelation (KMG) to construct MID rat models (Qun and Yongjun, 2015). Successful model construction is demonstrated by confirmation of multiple deep lacunar infarctions. Model rats exhibit obvious post-operative cognitive disorders (Qun and Yongjun, 2015).

Zhou et al. (Hao, 2020) utilized KMG for MID rat model construction. Among SMYZG treatment group rats, escape latency and swim distance in the platform quadrant were significantly shortened; the frequency of original platform crossing and percentage of swimming time, as well as percentage of swimming distance in the original platform quadrant were all significantly increased. Wen et al. reported that SMYZG ameliorates neuronal pathogenesis, shortens distances between pyramidal cells, increases Nissl body quantities, attenuates mitochondrial dysfunction and improves endoplasmic reticular function in the MID rat model (Li, 2017).

APOE$^{-/-}$ mice data

The Apolipoprotein E knock-out (ApoE$^{-/-}$) mouse model is widely used to study atherosclerosis. ApoE$^{-/-}$ mice possess risk factors such as cerebral arteriosclerosis and lipometabolic disturbances. Blood-brain barrier disruptions and synaptic injury are among the pathological characteristics seen in this mouse model, as in VaD. Masliah et al. (1997) reported that 3-month-old ApoE$^{-/-}$ mice exhibit poorer learning and memory functionality as compared to control mice. Other studies similarly reported ApoE$^{-/-}$ mice to manifest neuropathologic changes resulting in worsened memory formation, among others. Along with worsened defense against oxidative damage in the ApoE$^{-/-}$ mouse brain, antioxidant enzyme levels decrease (Shea et al., 2002) and the hippocampus is significantly affected (Charles et al., 2000).

Screening of proteins expressed in vascular endothelium involved in brain lacunar infarcts (Wang et al., 2018) revealed pathologic changes in cerebral vascular endothelial cell permeability and vasodilation among ApoE$^{-/-}$ mice. Proteomics and network pharmacology suggests that SMYZG improves cognition via regulation of eNOS and CAV1 expression (Qiong et al., 2019).

Mechanistic studies concerning prevention of vascular dementia by Shen Ma Yi Zhi granule

Vascular dementia is commonly caused by hypoxic-ischemic brain damage via a number of mechanisms. Multiple infarcts can occur in the setting of numerous cardiovascular and cerebrovascular diseases as well as thrombotic conditions.

Effect on cholinergic levels

Central cholinergic system dysfunction induces hippocampal neuronal loss, decreased choline acetyltransferase and acetyl cholinesterase activity, and decreased muscarinic and nicotinic receptor density. Resultant neuronal damage manifests with memory and learning disorders (Jiamou et al., 2020; Ying et al., 2022).

The phenolic compounds erulic acid and alkaloid ligustrazine found in Ligustici are not metabolized and freely permeate the blood-brain barrier to reach the hippocampus (Mancuso and Santangelo, 2014; Koh, 2015; Qian and Zengchun, 2019). Like acetyl cholinesterase inhibitors, these compounds increase the amount of acetylcholine and exert neuroprotective effects (Yunfeng and Huixia, 2011). Gastrodin extract treatment was reported to shorten mouse escape time and platform search distance, as well as increase the amount of cerebral acetylcholine and alleviate dysmnesia induced by scopolamine (Chunni et al., 2014). Ginseng (Ying et al., 2014; Md et al., 2018), and in particular ginsenosides, play important roles in protecting against oxidative stress and regulating cholinergic signaling. Most notably, ginsenoside Rb1 was reported to increase hippocampal antioxidant levels (Rui-xi et al., 2015; Zhu et al., 2019). Quercetin extracted from Euonymus alatus was similarly reported to increase acetylcholinesterase levels (Rui-xi et al., 2015; Sharma et al., 2021; Poonam et al., 2022).

Effect on levels of inflammatory mediators

Neuroinflammation promotes VaD pathogenesis and imbalances in proinflammatory and antinflammatory factor secretion is relevant to involved pathomechanisms. A number of inflammatory markers have attracted attention as potential novel biomarkers due to changes in their levels early in VaD pathology. The inflammatory cascade is activated (Roux et al., 2001; Wyss-Coray and Mucke, 2002) by TNF-α, a monokine mainly produced by monocytes and macrophages. Belkhelfa et al. (2018) reported levels of TNF-α and IL-1β in the VaD hippocampus to be significantly higher as compared to those of control individuals. Their interaction with TLR-4, a receptor distributed mainly on the microglial cell surface, results in proinflammatory factor activation and neurodegeneration. Importantly, SMYZG decreases levels of IL-1β and TNF-α in VaD model rats.

Ferulic acid, a component of Ligustici, likely functions via ERK signaling (Guifang et al., 2021; Yuanyuan et al., 2021) to repress microglial activation and neuroinflammation. Ginsenosides (Bo et al., 2019) decrease levels of TLR3 and TRIF mRNA, resulting in activation of the TLR3/TRIF pathway and attenuation of inflammation in VaD rats. Gastrodia elata (Huan et al., 2017) ameliorates oxidative stress and inflammation and promotes humoral immunity, while quercetin (Poonam et al., 2022) decreases IL-6, IL-10, TNF-α, and acetylcholinesterase levels in VaD rats, attenuating endothelial dysfunction associated with hypertension.

Studies based on 2-VO rats suggest (Sun et al., 2020; Lijuan et al., 2022) that the level of 1L-1β and TNF-α increased in the model group, while decreased in SMYZ groups and had dose-effect relationship. Indicated that SMYZ can improve the learning and memory ability of rats with vascular cognitive disorder by inhibiting inflammatory response and improving oxidative stress state.

Effect on antioxidative stress system

The oxidative stress response increases the level of reactive oxygen species depletes antioxidative compound stores and negatively impacts neuronal survival (Agdeppa et al., 2003), thus damaging synaptic activity in the area of involvement. Alterations in subsequent neurotransmission result in cognitive impairment (Tönnies and Trushina, 2017).

Ginsenosides are known to exhibit antioxidative properties (Dongmin et al., 2020); the ginsenoside Rg1 was reported to reduce oxidative injury and attenuate cognitive impairment (Chen et al., 2018). In addition, this compound was reported to exert positive effects in the setting of cerebral ischemia-reperfusion injury (Chu et al., 2019). Ferulic acid is neuroprotective primarily via mechanisms that decrease intracellular oxidative stress (Jianliang et al., 2015; Ling et al., 2019). Both LT and aqueous extract of Ligustici decrease malondialdehyde (MDA) levels in hypoxic neurons and increase superoxide dismutase activity. Gastrodia extract passes through the blood-brain barrier and exerts effects directly on brain tissue to normalize hemangiectasis and increase blood flow to the ischemic area (Chunyan et al., 2009), thereby lessening neuronal injury. This extract also reduces cellular calcium overload and decreases toxic effects of excitatory amino acids to produce an anti-apoptotic effect (Yunlin, 2006; Qihai et al., 2011; Aili, 2018). Debin and Shaofen (2006) reported that flavonoids prevent MDA generation via decreasing levels of H_2O_2; quercetin (Wei Si-Can and Tian-lai, 2020) was found to decrease MDA levels and increase superoxide dismutase activity.

Studies based on 2-VO rats suggested (Yu Cao, 2019; Sun et al., 2020) that the level of SOD, GSH, and GSH-Px decreased significantly, the level of MDA increased in the model group. While the level of SOD, GSH, and GSH-Px increased, the level of MDA decreased in SMYZ groups. Indicated that SMYZ can depress activation and proliferation of glial cells in hippocampal CA1 region, and improve mitochondrial ultrastructure.

Effect on cerebral white matter myelination

Cerebral white matter lesions are the most common pathological marker of VaD (Prins and Scheltens, 2015; Alber et al., 2019), manifesting in myelin discontinuity (Hill and Grutzendler, 2019). Levels of myelin basic protein, a membrane protein found on the serosal myelin surface, is significantly related to the severity of myelinoclasis. It also serves as an important indicator of demyelinating disease severity and remyelination (Choi et al., 2016; Nasrabady et al., 2018). White matter lesions occur due to a number of etiologies such as hypoxia, oxidative stress and the resultant inflammatory response, blood-brain barrier permeability and neurovascular unit disorder (Li Zehui, 2020).

The ginsenoside Rb1 was previously reported to improve symptoms of neurologic impairment by increasing lacunar infarct density in areas of infarction via the promotion of angiogenesis-related factor expression, such as VEGF and Ang-2 (Xiao et al., 2019). This compound was also reported to promote cortical neuronal stem cell proliferation and differentiation toward neuroglia–like cells (Wang et al., 2009). *In vitro* studies of LT (Qin et al., 2018) revealed that phthalide compounds such as ligustilide and senkyunolide A facilitate the penetration by certain medications of the blood-brain barrier. Ligustilide protects damaged nerves by attenuating cerebral ischemia-reperfusion injury via antioxidant and anti-apoptotic activity (Peng et al., 2007; Li et al., 2017). Studies on models of corneal endothelial injury (Guofeng et al., 2012)

revealed that LT protects the endothelia via amelioration of cell damage by inhibiting expression of COX-2 and NF-κB proteins, as well as decreasing MAPK phosphorylation. Phenolic compounds found in Gastrodia were reported to exert neuroprotective effects by decreasing hippocampal NO content and NOS activity, reducing nNOS and iNOS expression and promoting eNOS expression (Xiaohua et al., 2011; **Table 1**).

Signaling pathways relevant to vascular dementia treatment by Shen Ma Yi Zhi granule

Mechanistic studies of VaD have investigated apolipoprotein, tau and lipid metabolism, as well as immune and oxidative stress responses. Although amyloid-ß is currently considered to be the initiator of pathological changes in the setting of Alzheimer's disease, genetic susceptibility factors mediating reactions to amyloid-ß such as metabolic processes, immunity and lysosomal function are of vital importance in the pathogenesis of VaD and Alzheimer's.

Effect on mitochondrial metabolism

Chronic cerebral hypoperfusion refers to cerebral low-flow ischemia and hypoxic conditions due to angiostenosis. Chronic cerebral hypoperfusion is itself a risk factor for cognitive impairment and patients suffering cognitive decline commonly suffer significant cerebral hypoperfusion (Cao et al., 2016; Kalaria, 2016; Kazumata et al., 2019), and vice versa (Jessica et al., 2017).

Gastrodin was reported to increase neuronal oxygen metabolism, neuronal levels of ATP, promote neuronal glucose uptake and utilization, enhance memory and decrease lactate generation in the setting of ischemia (Meikang et al., 2010). The ginsenoside Re was reported to regenerate damaged neurons and improve cognition in rats via normalization of mitochondrial physiology (Wang et al., 2009).

Shen Ma Yi Zhi granule improves neuronal mitochondrial metabolism in 2-VO rats via the AMPK/PPARα/PGC-1α/UCP2 pathway (Sun et al., 2021b). Levels of AMPK, PPARα, PGC-1α, and ATP5A protein and mRNA were reported to be increased in the setting of SMYZG treatment, while levels of UCP2 gene expression were reported to be decreased (**Figure 5**).

Effect on anti-oxidative stress and ant-inflammatory signaling

Oxidative stress and inflammation directly damage cells (Beydoun et al., 2022). Bioactive products in the setting of oxidative stress initiate the inflammatory response (Wang et al., 2007) and are known to significantly aggravate cerebral injury. Astrocytes supply neuronal energy (Elkabes et al., 1996; Nakajima et al., 2001; Changhai and Rui, 2007; Gardiner et al., 2009), improve neuronal function, and promote memory generation and consolidation via secretion of BNDF (Allen et al., 2013). The hippocampal inflammatory response is the main pathologic characteristic of VaD (Stefaniak and O'Brien, 2016; Price et al., 2018). Nrf2 and HO-1, key signal molecules of the Nrf2/HO-1 pathway, exert anti-oxidative and ant-inflammatory effects (Wang et al., 2015).

The ginsenoside Rb1 improves learning and memory via attenuation of the hippocampal inflammatory response in a rat model of cerebral ischemia-reperfusion (Wang et al., 2009). Senkyunolide I reduces cerebral inflammation caused by oxidative stress and glucose deprivation as well as reoxygenation. Flavonoids and total steroids found in Euonymus alatus were found to possess signaling capabilities relevant to maintenance of oxygen free radical levels (Debin and Shaofen, 2006). Studies on VaD rats revealed that quercetin (Wei Si-Can and Tian-lai, 2020) administration resulted in increased neuronal lactate dehydrogenase activity and ATP levels as well as inhibition of cerebral NOS activity. Neuronal NO and lactate dehydrogenase levels as well as serum ET-1 levels were reported to be decreased, while serum levels of calcitonin gene-related peptide increased, thus promoting physiological neuronal metabolism and functioning. SMYZG (Kun et al., 2020; Wei Si-Can and Tian-lai, 2020) improves cognitive function and exerts neuroprotective effects by promoting the proliferation of reactive astrocyte-type cells via upregulation of the Nrf2/HO1 pathway.

Effect on the neurovascular unit

The neurovascular unit consists of the blood-brain barrier, neurons and glial cells including astrocytes, oligodendrocytes microglia. The neurovascular unit is a fairly novel concept that has attracted interest for consideration in research of stroke treatment (Muoio et al., 2014). The neurovascular unit together with pericytes as well as the corneal epithelial cells are critically important in the pathogenesis of ischemic cerebrovascular and hemorrhagic cerebral vascular diseases (Ozgur et al., 2017).

Effect on pericyte signal

Pericytes play critical roles in areas of lacunar infarction (Mark, 2009). Pericytes function to regulate blood-brain barrier permeability, clearing cellular components (Ferland-McCollough et al., 2017), maintaining homeostasis of cerebral vascular and protecting the central nervous system.

Surgeries (Sun et al., 2021a) can cause vascular injury and angiogenic instability via downregulation of Ang1 and PDGFR-β protein expression in corneal epithelial cells of brains among MID rats. SMYZG was reported to promote Ang1 and Ang1 mRNA expression in pericytes, increase neuronal PDGFR-β and PDGFR-β mRNA levels, and increase NG2 and NG2 mRNA levels. These results underscore that SMYZG protects pericytes and improves neurovascular homeostasis.

TABLE 1 Pharmacologic effects of active ingredients composing Shen Ma Yi Zhi granule (SMYZG).

Article	Plant name	Active ingredient	Chemical structure type	Pharmacological action index	Signaling pathways	Effects
Koh (2015) and Qian and Zengchun (2019)	Ligustici	Ferulic acid	Phenolic compounds C10H10O4	MDA,SOD, GSH, IL-6, IL-10, TNF-α, AchE	(1) Nrf2/HO-1 pathway	(1) Anti-oxidative stress
Mancuso and Santangelo (2014)		Ligustrazine (LT)		AchE	(1) Nrf2/HO-1 pathway	(1) Anti-oxidative stress
Xiao et al. (2019)	Ginseng	Ginsenoside Rg1		TLR3 protein, TLR3 mRNA, TRIF protein, and TRIF mRNA	(1) Nrf2/HO-1 pathway (2) VEGF/Flk-1/P38MAPK signaling	(1) Anti-oxidative stress (2) Repair neure injury
		Ginsenoside Rb1		B-Secretases, Presenilin-1 (PS-1)	(1) AMPK/PPARα/PGC-1α/UCP2 pathway (2) Nrf2/HO-1 pathway (3) HIF-1/VEGF/Notch signaling (4) Pericyte signal	(1) Repair neure injury and mitochondrial injury inhippocampus (2) Suppress inflammatory response (3) Increase microvessel density
Chunyan et al. (2009), Xiaohua et al. (2011), and Wei et al. (2019)	Gastrodia elata	Gastrodin	Phenolic compounds	NO, iNOS, AchE, and VEGF	(1) Nrf2/HO-1 pathway (2) Pericyte signal (3) AMPK/PPARα/PGC-1α/UCP2 pathway (4) VEGF/Flk-1/P38MAPK signaling	(1) Anti-oxidative stress, suppress inflammatory response and anti-apoptosis (2) Maintain and recover physiological function of cerebrovascular (3) Increase oxygen utilization rate of brain and improve energy metabolism (4) Anti-oxidative stress, anti-apoptosis, suppress calcium overload and decrease excitatory toxicity
Wei Si-Can and Tian-lai (2020)	Euonymus alatus	Quercetin		MDA, SOD, IL-6, IL-10, TNF-α, and AchE	(1) Nrf2/HO-1 pathway	(1) Improve energy metabolism and improve blood rheology (2) Anti-oxidative stress
Debin and Shaofen (2006)		Flavonoids		MDA and SOD	(1) Nrf2/HO-1 pathway	(1) Scavenging free radical (2) Anti-oxidative stress

Effect on angiogenesis signaling

Vascular endothelial growth factor, astrocytes, Ang-1, Notch, and pericytes were found to synergistically interact to stimulate regeneration and maturation of blood vessels (Li, 2017; Kun et al., 2020). The hypoxia inducible factor-1 (HIF-1)-VEGF and Notch pathways are two main signaling pathways in angiogenesis. HIF-1 is one transcription factor relevant to intracellular oxygen homeostasis that is evoked by hypoxia. VEGF, another neuroprotective factor increased in neuronal tissue in the setting of cerebrovascular trauma, decreases blood-brain barrier permeability and promotes angiogenesis (Lian Jin et al., 2011). The Notch gene plays a key role in HIF-1/VEGF/Notch signaling and thus promotes blood vessel regeneration (Luttun et al., 2002; Yin, 2016).

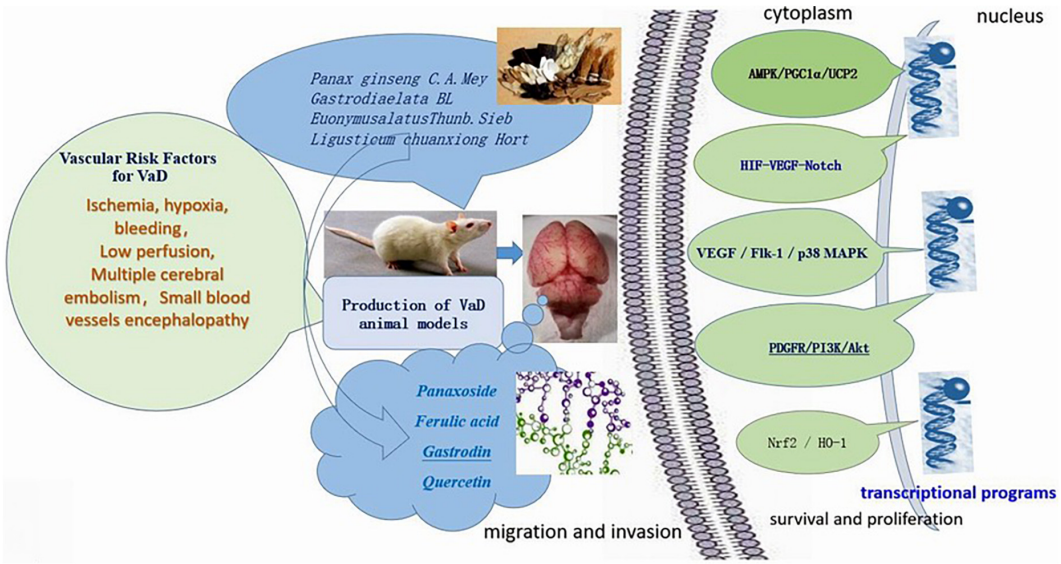

FIGURE 5
Signaling pathways of Shen Ma Yi Zhi granule (SMYZG) in the context of vascular dementia (VaD) treatment. Sources for the images within this figure: 699pic.com and Chinese Pharmacopoeia.

TABLE 2 Likely signaling pathways of Shen Ma Yi Zhi granule (SMYZG).

Articles	Signal pathways	Animal models	Target proteins	Regulate trends	Mechanism
Sun et al. (2021b)	AMPK/PGC-1α/UCP2/ATP5A	2-VO	AMPK, PPARα, PGC-1α, and ATP5A	Up	Mitochondrial related proteins, mitochondrial energy metabolism
			UCP2	Down	
Sun et al. (2021a)	Pericytes, Ang1, PDGFR-β protein	MID	Ang1 and PDGFR-β	Up	Pericytes, pathogenesis of neovascularization
Kun et al. (2020)	HIF/VEGF Notch	MID	HIF1α, VEGF, VEGF mRNA, and notch	Up	Pathogenesis of neovascularia
Xuemei et al. (2019) and Yu et al. (2019)	Nrf2/HO-1	MID	Nrf2mRNA, HO-1mRNA	Up	Antioxidant stress response
Li (2017)	VEGF/Flk-1/P38MAPK	2-VO	P38MARK,NMDAR1, PSD-95, VEGF, FLK-1 mRNA, and proteins	Up	Synaptic plasticity improving via vascular endothelium

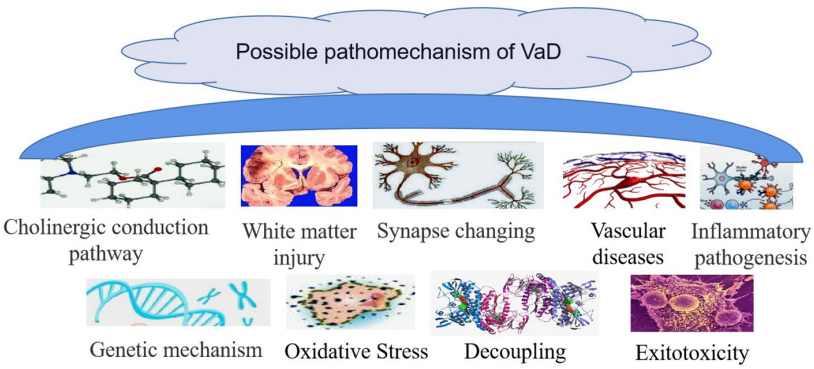

FIGURE 6
Possible pathomechanism of vascular dementia (VaD). Sources for the images within this figure: 699pic.com and Chinese Pharmacopoeia.

Effect on endothelial cells and synaptic plasticity in the context of lacunar infarction

Endothelial cells of the blood-brain barrier are important early in the pathogenesis of VaD. Injury of proteins involved in neural synaptic plasticity is also important in cognitive impairment. Endothelial cells regulate neuronal activation via secretion of compounds such as VEGF, BDNF, and NO. Similarly, endothelial cells regulate synaptic plasticity via VEGF/Flk-1/p8 MAPK signaling.

Studies (Lian Jin et al., 2011; Li, 2017; Xuemei et al., 2019) of VaD rat models reported that SMYZG promotes expression of P38MAPK, NMDAR1, PSD-95, VEGF, and FLK-1 mRNA and protein in rat neuronal tissue, promotes expression of choline acetyltransferase, inhibits MMP9 expression. SMYZG was reported to improve cognition via inhibition of neuroglial cell activation and proliferation in the CA1 region. SMYZG also improves endothelial cellular function, activates VEGF/Flk-1/P38MAPK signaling and improves synaptic plasticity (**Table 2**).

Conclusion and perspectives

Vascular dementia (Gorelick et al., 2011) is a common, highly heterogeneous condition that manifests due to stroke, neurovascular trauma or cerebrovascular disease. The four major subtypes of VaD that can be further subclassified include MID, post-stroke dementia, subcortical ischemic vascular dementia and mixed dementia (Skrobot et al., 2016a,b, 2018; Hao et al., 2021). VaD is the second commonest dementia after Alzheimer's, and although Alzheimer's is characterized by episodic disturbances in memory, both conditions are clinically similar and challenging to distinguish (Laukka et al., 2004). Interestingly, VaD and Alzheimer's were reported to commonly coexist in patients suffering cognitive impairment (Schneider et al., 2005; Sonnen et al., 2007; Launer et al., 2008; Wu, 2019). And end-stage VaD patients share the similar pathological basis with AD patients (Wu, 2019). As interest in VaD research increases, particular focus on treatment improvement, pathological mechanism elucidation and conduction of prospective drug development studies is warranted (Cognitive Impairment Committee NBCM, 2019; Hao et al., 2021).

Chronic cerebral hypoperfusion is the main etiological mechanism of VaD (Cao et al., 2016; Jessica et al., 2017; Kazumata et al., 2019), with half of VaD patients suffering subcortical white matter infarction (Kalaria, 2016). However, white matter lesions are considered to also be an etiology for chronic cerebral hypoperfusion and a pathologic characteristic common in both Alzheimer's and VaD (**Figure 6**).

The concept of the neurovascular unit underscores the relationship between VaD and other cerebrovascular diseases. Investigation of interactions among neurons, glial cells and the cerebral vasculature should be encouraged from a holistic perspective. A variety of active compounds compose SMYZG such as ferulic acid, LT, ginsenoside Rg1, ginsenoside Rb1, gastrodin, and quercetin, as well as a number of flavonoids. Treatment targets have been reported to include dementia-associated proteins (e.g., beta-secretase, PS-1), apoptosis-associated factors (e.g., TLR3, TRIF), vascular endothelium--associated factors (i.e., VEGF), components of cholinergic signaling (e.g., acetylcholinesterase, choline), inflammatory factors (e.g., IL-6, IL-10, NF-α) and factors important in oxidative stress (e.g., MDA, SOD, GSH, NO, iNOS). To further clarify effects of SMYZG in the clinical setting, multi-center randomized controlled trials with large sample sizes are required. Clinical monitoring of SMYZG blood levels as well as investigation of pharmacokinetic properties, are also warranted.

This article reviewed previously published data from studies using different animal models relevant to the pharmacological mechanism, pharmacokinetics and clinical applications of SMYZG, as well as the pathophysiological characteristics of VaD. Important processes ameliorated by SMYZG treatment include neuronal oxidative stress, cerebral white matter demyelination, pericyte function, neuronal mitochondrial metabolism, cerebral endothelial function and neuroinflammation. Relevant signaling pathways include the AMPK/PPARα/PGC-1α/UCP2, Nrf2/HO-1, HIF-1/VEGF/Notch, and VEGF/Flk-1/p8 MAPK pathways.

In this manuscript, we collected around 10 years reports for SMYZ of VaD prevention and treatment. For future applications, more approaches need to be designed in further studies along with the development of proteomics, metabonomics, transcriptomics, network pharmacology, and interdisciplinary research. To identify active ingredients based on the sense of system biology. To evaluate pharmaceutical and pharmacological effects of active ingredients based on metabonomics. To research complex components of herbal medicines by establishing combination-activity relationship (CAR) according to the relevance of herbal combination and bioactivity based on systems modeling (Liu et al., 2016; Liu, 2017). Various metabolites will be produced during the whole process after oral administration of SMYZ to form pharmaco-metabonomics (Xiao, 2014; National Medical Products Administration, 2020). We shall test active components in plasma, prototype components, gut bacteria and metabolites with approaches like nuclear magnetic resonance (NMR), gas chromatography-mass spectrometry (GC-MC) and ultra performance liquid chromatography-tandem mass spectrometry (UPLC-MS/MS). This methods are conducted by modern equipments that are characterized by high resolution, high-throughput and high sensitivity. Using of all above mentioned technologies is consistent with concept of holism of Traditional Chinese Medicine (TCM).

Chinese medicines are complicated chemical systems based on systematic chemical separation, biological expression, separation and preparation of herb components. For further study, our research group will put more efforts on figuring out

the compatibility regularity and integrating multi-components. The basic pharmacology, mechanism of action and the relationship between active components and clinical efficacy of the drug must be determined including toxicologic effects. Upgrade the preparation technique and make new traditional Chinese medicines with controllable quality, low toxic and clearly mechanisms.

Author contributions

J-GL and HL conceived the topic and helped to draft the manuscript. J-GL and S-RC wrote the manuscript together. M-XL, D-DS, and L-JZ participated in the research. All authors contributed to the article and approved the submitted version.

Funding

We gratefully acknowledge the financial support from National Natural Science Foundation of China (Grant no. 81403266). Our research gain support as key project of basic research of "Major new drug development" projects of Ministry of Science and Technology, PRC (Grant no. 2019ZX09301-114), "Innovation Research Projects" of G20 engineering of Beijing Municipal Science and Technology Commission (Grant no. Z171100001717016).

Acknowledgments

We gratefully thank for pharmaceutical technology support from Rui Zheng of Xiyuan Hospital of China Academy of Chinese Medical Sciences. We thank for pharmaceutical analysis support from Yun Wei of State Key Laboratory of chemical resource engineering of Beijing University of Chemical Technology. We also thank for Sir Yuyang Liu to assist in reviewing and giving suggestions for revising this manuscript.

Conflict of interest

The authors declare that the research was conducted in the absence of any commercial or financial relationships that could be construed as a potential conflict of interest.

Publisher's note

References

Agdeppa, E. D., Kepe, V., Liu, J., Small, G. W., Huang, S. C., Petric, A., et al. (2003). 2-Dialkylamino-6-acylmalononitrile substituted naphthalenes (DDNP analogs): Novel diagnostic and therapeutic tools in Alzheimer's disease. *Mol. Imaging Biol.* 5, 404–417. doi: 10.1016/j.mibio.2003.09.010

Aili, W. (2018). Analysis of clinical and pharmacological effects of ligustrazine on cerebral infarction. *Electron. J. Clin. Med. Lit.* 5, 163–166.

Alber, J., Alladi, S., Bae, H., Barton, D. A., Beckett, L. A., Bell, J. M., et al. (2019). White matter hyperintensities in vascular contributions to cognitive impairment and dementia (VCID): Knowledge gaps and opportunities. *Alzheimers Dement.* 5, 107–117. doi: 10.1016/j.trci.2019.02.001

Allen, S. J., Watson, J. J., Shoemark, D. K., Barua, N. U., and Patel, N. K. (2013). GDNF, NGF and BDNF as therapeutic options for neurodegeneration. *Pharmacol. Therap.* 138, 155–175. doi: 10.1016/j.pharmthera.2013.01.004

Belkhelfa, M., Beder, N., Mouhoub, D., Amri, M., Hayet, R., Tighilt, N., et al. (2018). The involvement of neuroinflammation and necroptosis in the hippocampus during vascular dementia. *J. Neuroimmunol.* 320, 48–57. doi: 10.1016/j.jneuroim.2018.04.004

Beydoun, M. A., Beydoun, H. A., Fanelli-Kuczmarski, M. T., Weiss, J., Hossain, S., Canas, J. A., et al. (2022). Association of serum antioxidant vitamins and carotenoids with incident Alzheimer disease and all-cause dementia among US adults. *Neurology* 98, e2150–e2162. doi: 10.1212/WNL.0000000000200289

Bo, L., Xiaolei, H., and Chunyuan, Z. (2019). Research progress on anti-inflammatory effect and molecular mechanism of ginsenosides. *Chin. J. Pharm.* 54, 253–258.

Cao, Y., Liang, L., Xu, J., Wu, J., Yan, Y., Lin, P., et al. (2016). The effect of *Scutellaria baicalensis* stem-leaf flavonoids on spatial learning and memory in chronic cerebral ischemia-induced vascular dementia of rats. *Acta Biochim. Biophys. Sin. (Shanghai)* 48, 437–446. doi: 10.1093/abbs/gmw024

Chang Surui, L. J. L. M. (2020). Experimental study on acute toxicity of ShenmaYizhi decoction. *Chin. J. integr. Med. Cardio Cereb. Vasc. Dis.* 18, 424–426.

Changhai, Y., and Rui, Z. (2007). Stars of expectation: Astrocytes. *Science* 59, 13–16.

Charles, R., Pascale, K., Diana, A., Lussier-Cacan, S., Theroux, L., Christen, Y., et al. (2000). Impact of apoE deficiency on oxidative insults and antioxidant levels in the brain. *Mol. Brain Res.* 86, 76–83. doi: 10.1016/S0169-328X(00)00268-0

Chen, L., Yao, H., Chen, X., Wang, Z., Xiang, Y., Xia, J., et al. (2018). Ginsenoside Rg1 decreases oxidative stress and down-regulates Akt/mTOR signalling to attenuate cognitive impairment in mice and senescence of neural stem cells induced by D-galactose. *Neurochem. Res.* 43, 430–440. doi: 10.1007/s11064-017-2438-y

Cheng, C. S., Jiangang, L., Meixia, L., Hao, L., and Zenggang, L. (2019). Exploration of pathological mechanism of vascular dementia induced by chronic cerebral hypoperfusion and production of several common animal models. *Acta Neuropharmacol.* 9, 13–17.

Chinese Pharmacopoeia Commission (2015). *Pharmacopoeia of the people' s republic of China*. Beijing: China Medical Science and Technology Press, 28–29.

Choi, B. R., Kim, D. H., and Back, D. B. (2016). Characterization of white matter injury in a rat model of chronic cerebral hypoperfusion. *Stroke* 47, 542–547. doi: 10.1161/STROKEAHA.115.011679

Chu, S. F., Zhang, Z., Zhou, X., He, W. B., Chen, C., Luo, P., et al. (2019). Ginsenoside Rg1 protects against ischemic/reperfusion-induced neuronal injury through miR-144/Nrf2/ARE pathway. *Acta Pharmacol. Sin.* 40, 13–25. doi: 10.1038/s41401-018-0154-z

Chunni, H., Fangyan, H., Ye, T., and Xiaohua, D. (2014). Effects of *Gastrodia elata* extract on cholinergic system in rats with memory acquisition disorder. *China Pharm.* 23.

Chunyan, Z., Yuping, L., Maoxu, L., and Ruilian, W. (2009). Effect of gastrodin on vascular dementia. *J. Emerg. Tradit. Chin. Med.* 18, 1220–1221.

Cognitive Impairment Committee NBCM (2019). 2019 Guidelines for the Diagnosis and Treatment of Vascular cognitive Impairment in China. *Chin. Med. J. Pek.* 99, 2737–2744.

Debin, H., and Shaofen, Y. (2006). The effect of three extracts of podophylla SPP. On oxygen free radical. *J. Hubei Univ. Natl.* 2006, 4–6.

Dongmin, C., Qinxiao, G., Yali, L., and Shumei, W. (2020). Serum metabolomics study of ginsenosides in the treatment of ischemic stroke based on 1 H-NMR. *China J. Chin. Mater. Med.* 45, 1142–1148.

Elkabes, S., DiCicco-Bloom, E. M., and Black, I. B. (1996). Brain microglia/macrophages express neurotrophins that selectively regulate microglial proliferation and function. *J. Neurosci.* 16, 2508–2521. doi: 10.1523/JNEUROSCI.16-08-02508.1996

Fan, W., Huang, Y., Zheng, H., Li, S., Li, Z., Yuan, L., et al. (2020). Ginsenosides for the treatment of metabolic syndrome and cardiovascular diseases: Pharmacology and mechanisms. *Biomed. Pharmacother.* 132:110915. doi: 10.1016/j.biopha.2020.110915

Farkas, E., Luiten, P. G. M., and Bari, F. (2007). Permanent, bilateral common carotid artery occlusion in the rat: A model for chronic cerebral hypoperfusion-related neurodegenerative diseases. *Brain Res. Rev.* 54, 162–180. doi: 10.1016/j.brainresrev.2007.01.003

Ferland-McCollough, D., Slater, S., Richard, J., Reni, C., and Mangialardi, G. (2017). Pericytes, an overlooked player in vascular pathobiology. *Pharmacol. Therap.* 171, 30–42. doi: 10.1016/j.pharmthera.2016.11.008

Gardiner, J., Barton, D., Overall, R., and Marc, J. (2009). Neurotrophic support and oxidative stress: Converging effects in the normal and diseased nervous system. *Neuroscientist* 15, 47–61. doi: 10.1177/1073858408325269

Gorelick, P. B., Scuteri, A., Black, S. E., Decarli, C., Greenberg, S. M., Iadecola, C., et al. (2011). Vascular contributions to cognitive impairment and dementia: A statement for healthcare professionals from the American heart association/American stroke association. *Stroke* 42, 2672–2713. doi: 10.1161/STR.0b013e3182299496

Guifang, L., Congshu, H., and Guihua, Z. (2021). Ferulic acid inhibits radiation-induced microglial inflammation through NLRP3 inflammasome. *Pharmacol. Clin. Chin. Mater. Med.* 37, 76–80.

Guofeng, W., Feng, L., Xia, Z., and Yang, C. (2012). Effects of ligustrazine on endothelial cell inflammation induced by oxidized low density lipoprotein. *Chin. J. Hypertens.* 20, 347–351.

Hachinski, V., Iadecola, C., Petersen, R. C., Breteler, M. M., Nyenhuis, D. L., Black, S. E., et al. (2006). National institute of neurological disorders and stroke-canadian stroke network vascular cognitive impairment harmonization standards. *Stroke* 37, 2220–2241. doi: 10.1161/01.STR.0000237236.88823.47

Hao, S., Dong, S., and Junjian, Z. (2021). Interpretation of 'the diagnosis and treatment guideline of VaD of China' (2019). *Chin. J. Clin.* 49, 655–657.

Hao, Z. L. L. N. (2020). Influence of Shen Ma Yizhi decoction on learning memory, inflammatory factors and antioxidant effects in vascular cognitive impaired rats induced by multiple cerebral infarction. *Tradit. Chin. Drug Res. Clin. Pharmacol.* 31, 294–299.

Hill, R. A., and Grutzendler, J. (2019). Uncovering the biology of myelin with optical imaging of the live brain. *Glia* 67, 2008–2019. doi: 10.1002/glia.23635

Hu, C., Lau, A. J., Wang, R., and Chang, T. K. H. (2017). Comparative analysis of ginsenosides in human glucocorticoid receptor binding, transactivation, and transrepression. *Eur. J. Pharmacol.* 815, 501–511. doi: 10.1016/j.ejphar.2017.10.019

Huan, W., Dayan, Z., Wei, W., Gao, J., Rao, C., Peng, C., et al. (2017). Effects of gastrodin on the expression of NF-kB inflammatory cascade in glucose and oxygen deprivation redonor cortical neurons. *Chin. J. Exp. Tradit. Med. Formulae* 23, 104–111.

Huang, Y., Chen, J., Yuan, J., and Shanquan, Z. (2016). Cognitive variations among vascular dementia subtypes caused by small-, large-, or mixed-vessel disease. *Arch. Med. Sci.* 12, 747–753. doi: 10.5114/aoms.2016.60962

Jessica, D., Akihiro, K., Yoshiki, H., Ihara, M., Kalaria, R. N., and Horsburgh, K. (2017). Chronic cerebral hypoperfusion: A key mechanism leading to vascular cognitive impairment and dementia. Closing the translational gap between rodent models and human vascular cognitive impairment and dementia. *Clin. Sci. (Lond)* 131, 2451–2468. doi: 10.1042/CS20160727

Jiamou, R., Yumei, G., Changxue, W., Yi, L., and Fan, W. (2020). Expression of cholinesterase and cholinacetylase in rats with vascular cognitive dysfunction. *Chin. J. Gerontol.* 40, 2396–2401.

Jian, G., and Shao-wa, L. (2021). Research progress in chemical constituents and pharmacological action of Renshen (Ginseng). *Guid. J. Tradit. Chin. Med. Pharm.* 27, 127–130.

Jiang, Y., Müller, K., Khan, M. A., Assmann, J. C., Lampe, J., Kilau, K., et al. (2021). Cerebral angiogenesis ameliorates pathological disorders in Nemo-deficient mice with small-vessel disease. *J. Cereb. Blood Flow. Metab.* 41, 219–235. doi: 10.1177/0271678X20910522

Jiangang, L., Dawu, Z., Yuyang, L., Jiatao, F., Jie, L., Dazhuo, S., et al. (2019). Separation of extracts from chuanxiong rhizoma and the pharmacological effects on myocardium of ischemia/reperfusion injury in rats. *Chin. J. Mordern Appl. Pharm.* 36, 2369–2375.

Jianliang, W., Minmin, S., Shuixin, Y., Xiang, W., and Zengchun, M. (2015). Inhibition of microglial inflammatory response by ferulic acid. *Chin. Pharmacol. Bull.* 31, 97–102.

Kalaria, R. N. (2016). Neuropathological diagnosis of vascular cognitive impairment and vascular dementia with implications for Alzheimer's disease. *Acta Neuropathol.* 131, 659–685. doi: 10.1007/s00401-016-1571-z

Kazumata, K., Tokairin, K., Sugiyama, T., Ito, M., Uchino, H., Osanai, T., et al. (2019). Association of cognitive function with cerebral blood flow in children with moyamoya disease. *J. Neurosurg. Pediatr.* 25, 1–7. doi: 10.3171/2019.7.PEDS19312

Koh, P. (2015). Ferulic acid attenuates the down-regulation of MEK/ERK/p90RSK signaling pathway in focal cerebral ischemic injury. *Neurosci. Lett.* 588, 18–23. doi: 10.1016/j.neulet.2014.12.047

Kun, L., Hui, P., Yu, C., Lina, M., and Hao, L. (2020). Effects of Shenma Yizhi prescription on Nrf2/HO-1 pathway and microglia in rats with vascular dementia. *Chin. J. Inf. TCM* 27, 38–42.

Laukka, E. J., Jones, S., Small, B. J., Fratiglioni, L., and Bäckman, L. (2004). Similar patterns of cognitive deficits in the preclinical phases of vascular dementia and Alzheimer's disease. *J. Int. Neuropsychol. Soc.* 10, 382–391. doi: 10.1017/S1355617704103068

Launer, L. J., Petrovitch, H., Ross, G. W., Markesbery, W., and White, L. R. (2008). AD brain pathology: Vascular origins? Results from the HAAS autopsy study. *Neurobiol. Aging* 29, 1587–1590. doi: 10.1016/j.neurobiolaging.2007.03.008

Lecordier, S., Manrique-Castano, D., El Moghrabi, Y., and ElAli, A. (2021). Neurovascular alterations in vascular dementia: Emphasis on risk factors. *Front. Aging Neurosci.* 13:727590. doi: 10.3389/fnagi.2021.727590

Lei, Z., Yan, Z., Xian-sheng, Y., Zhang, J., Zhang, W. K., and Li, P. (2015). Chemical constituents from twigs of Euonymus alatus. *China J. Chin. Mater. Med.* 40, 2612–2616.

Li Qian, W. X. (2020). New progress in research on chemical constituents and pharmacological action of *Ligusticum* chuanxiong Hort. *Chem. Eng.* 34, 62–64.

Li Zehui, C. Y. L. J. (2020). Effects of Shenma Yizhi prescription on cognitive function and white matter damage of vascular dementia rats with multiple cerebral infarction. *World Chin. Med.* 15, 1120–1123.

Li, J., Yu, J., Ma, H., Yang, N., Li, L., Zheng, D. D., et al. (2017). Intranasal pretreatment with Z-ligustilide, the main volatile component of rhizoma chuanxiong, confers prophylaxis against cerebral ischemia via Nrf2 and HSP70 signaling pathways. *J. Agric. Food Chem.* 65, 1533–1542. doi: 10.1021/acs.jafc.6b04979

Li, K. (2017). Effects of Shenma Yizhi prescription on hippocampal morphology and oxidative stress in vascular dementia model rats. *Beijing Tradit. Chin. Med.* 36, 397–400.

Lian Jin, H., Pennant, W. A., Hyung Lee, M., Su, S., Ah Kim, H., Lu Liu, M., et al. (2011). Neural stem cells modified by a hypoxia-inducible VEGF gene expression system improve cell viability under hypoxic conditions and spinal cord injury. *Spine* 36, 857–864. doi: 10.1097/BRS.0b013e3181e7f34b

Lijuan, Z., Meixia, L., Jiangang, L., Chengcheng, S., and Nannan, L. (2022). Research ideas and methods of traditional Chinese medicine compound in the treatment of vascular dementia development and research on the prevention and treatment of vascular dementia with Shenma Yizhi decoction. *Modern Tradit. Chin. Med. Mater. Med. World Sci. Technol.* 24, 217–233.

Lin, W., Xiaomei, M., and Haitao, Z. (2014). Advances in animal models of vascular dementia. *J. Guangxi Univ. Chin. Med.* 17, 93–96.

Ling, L., Zheng, X., and Youcai, W. (2019). Protective effect of ferulic acid on oxidative stress injury of H9c2 cardiomyocytes induced by advanced glycation end products. *Chin. J. Clin. Pharmacol.* 35, 1446–1448.

Liu, C. X., Chen, S. L., and Xiao, X. H. (2016). Quality marker of traditional Chinese medicine (Q-Marker): A new concept for quality control of traditional Chinese medicine products. *Chin. Tradit. Herb. Drugs* 47, 1443–1457.

Liu, X. (2017). Construction of TCM quality traceability system based on TCM quality markers. *Chin. Tradit. Herb. Drugs* 48, 3669–3676.

Luo, C., Xu, X., Wei, X., Feng, W., Huang, H., Liu, H., et al. (2019). Natural medicines for the treatment of fatigue: Bioactive components, pharmacology, and mechanisms. *Pharmacol. Res.* 148:104409. doi: 10.1016/j.phrs.2019.104409

Luttun, A., Carmeliet, G., and Carmeliet, P. (2002). Vascular progenitors: From biology to treatment. *Trends Cardiovasc. Med.* 12, 88–96. doi: 10.1016/S1050-1738(01)00152-9

Mancuso, C., and Santangelo, R. (2014). Ferulic acid: Pharmacological and toxicological aspects. *Food Chem. Toxicol.* 65, 185–195. doi: 10.1016/j.fct.2013.12.024

Mark, F. (2009). Pericyte signaling in the neurovascular unit. *Stroke* 40(Suppl. 3), S13–S15. doi: 10.1161/STROKEAHA.108.533117

Masliah, E., Samuel, W., Veinbergs, I., Mallory, M., Mante, M., and Saitoh, T. (1997). Neurodegeneration and cognitive impairment in apoE-deficient mice is ameliorated by infusion of recombinant apoE. *Brain Res.* 751, 307–314. doi: 10.1016/S0006-8993(96)01420-5

Md, J., Ezazul, H. M., Joonsoo, K., Cho, D. Y., Kim, I. S., and Choi, D. K. (2018). Active ginseng components in cognitive impairment: Therapeutic potential and prospects for delivery and clinical study. *Oncotarget* 9, 33601–33620. doi: 10.18632/oncotarget.26035

Meikang, W., Chunmei, M., and Xiangdang, W. (2010). Effect of gastrodin injection on cognitive dysfunction in vascular dementia. *Chin. J. Med.* 45, 58–59.

Meixia, L. (2020). *New TCM compounds of preventing VaD- researching and development of shenmayizhi*. Beijing: CNKI.

Moorhouse, P., and Rockwood, K. (2008). Vascular cognitive impairment: Current concepts and clinical developments. *Lancet Neurol.* 7, 246–255. doi: 10.1016/S1474-4422(08)70040-1

Muoio, V., Persson, P. B., and Sendeski, M. M. (2014). The neurovascular unit-concept review. *Acta Physiol. (Oxf)* 4, 790–798. doi: 10.1111/apha.12250

Nakajima, K., Honda, S., Tohyama, Y., Imai, Y., Kohsaka, S., and Kurihara, T. (2001). Neurotrophin secretion from cultured microglia. *J. Neurosci. Res.* 65, 322–331. doi: 10.1002/jnr.1157

Nan-Nan, L., Jian-Gang, L., and Rui, Z. (2019). Comparativestudy on pharmacological effects of Shenma Yizhi formula processed with three kinds of preparation techniques. *Beijing J. Tradit. Chin. Med.* 38, 427–432.

Nasrabady, S. E., Rizvi, B., Goldman, J. E., and Brickman, A. M. (2018). White matter changes in Alzheimer's disease: A focus on myelin and oligodendrocytes. *Acta Neuropathol. Commun.* 6:22. doi: 10.1186/s40478-018-0515-3

National Medical Products Administration (2020). *Circular of the center for drug control of the state food and drug administration on issuing the technical guidelines for the study of biological effects of traditional Chinese medicine (Trial) (No. 50 of 2020)*. Beijing: National Medical Products Administration.

O'Brien, J. T., Erkinjuntti, T., Reisberg, B., Roman, G., Sawada, T., Pantoni, L., et al. (2003). Vascular cognitive impairment. *Lancet Neurol.* 2, 89–98. doi: 10.1016/S1474-4422(03)00305-3

Ozgur, O., Ihsan, S., and Yasemin, G. (2017). The role of pericytes in neurovascular unit: Emphasis on stroke. *Curr. Drug Targets* 18, 1386–1391. doi: 10.2174/1389450117666160613104523

Peng, H., Du, J., Zhang, G., Kuang, X., Liu, Y. X., Qian, Z. M., et al. (2007). Neuroprotective effect of Z-ligustilide against permanent focal ischemic damage in rats. *Biol. Pharm. Bull.* 30, 309–312. doi: 10.1248/bpb.30.309

Poonam, S., Nikita, G., Shalini, J., Sharma, B. M., Singh, B., Kharkwal, H., et al. (2022). Salubrious effects of ulinastatin and quercetin alone or in combination in endothelial dysfunction and vascular dementia. *Pharmacol. Rep.* 74, 481–492. doi: 10.1007/s43440-022-00364-1

Price, B. R., Norris, C. M., Sompol, P., and Wilcock, D. M. (2018). An emerging role of astrocytes in vascular contributions to cognitive impairment and dementia. *J. Neurochem.* 144, 644–650. doi: 10.1111/jnc.14273

Prins, N. D., and Scheltens, P. (2015). White matter hyperintensities, cognitive impairment and dementia: An update. *Nat. Rev. Neurol.* 11, 157–165. doi: 10.1038/nrneurol.2015.10

Qian, H., and Zengchun, M. (2019). Research progress of ferulic acid in the treatment of Alzheimer's disease. *MIL Med.* 43, 230–235.

Qihai, G., Jingshan, S., Danli, Y., Bin, H., and Xiaolong, X. (2011). Pharmacological action and mechanism of gastrodin in central nervous system. *Chin. J. N. Drugs Clin. Med.* 30, 176–179.

Qin, Z., Yu, T., Peng-Yi, H., Liu, D., Zhang, D., Yue, P., et al. (2018). The influence and mechanism of ligustilide, senkyunolide I, and senkyunolide A on echinacoside transport through MDCK-MDR1 cells as blood-brain barrier in vitro model. *Phytother. Res.* 32, 426–435. doi: 10.1002/ptr.5985

Qiong, W., Yu, C., Meixia, L., Liu, F., Brantner, A. H., Yang, Y., et al. (2019). Traditional Chinese medicine Shenmayizhi decoction ameliorates memory and cognitive impairment induced by scopolamine via preventing hippocampal cholinergic dysfunction in rats. *Neuropsychiatr. Dis. Treat.* 15, 3167–3176. doi: 10.2147/NDT.S214976

Qun, W., and Yongjun, W. (2015). An animal model of vascular dementia in rodents. *Chin. J. Stroke* 10, 279–283.

Roux, P. P., Bhakar, A. L., Kennedy, T. E., and Barker, P. A. (2001). The p75 neurotrophin receptor activates Akt (protein kinase B) through a phosphatidylinositol 3-kinase-dependent pathway. *J. Biol. Chem.* 276, 23097–23104. doi: 10.1074/jbc.M011520200

Rui-xi, S., Jing, P., Jian, G., Maoting, W., Heqing, H., and Ling, L. (2015). Mordern research on pharmacological action of *Euonymus alatus* (Thunb.) Sieb. *Glob. Tradit. Chin. Med.* 8, 245–249.

Schneider, J. A., Bienias, J. L., Wilson, R. S., Berry-Kravis, E., Evans, D. A., and Bennett, D. A. (2005). The apolipoprotein E epsilon4 allele increases the odds of chronic cerebral infarction [corrected] detected at autopsy in older persons. *Stroke* 36, 954–959. doi: 10.1161/01.STR.0000160747.27470.2a

Sharma, P., Aggarwal, K., Awasthi, R., Kulkarni, G. T., and Sharma, B. (2021). Behavioral and biochemical investigations to explore the efficacy of quercetin and folacin in experimental diabetes induced vascular endothelium dysfunction and associated dementia in rats. *J. Basic Clin. Physiol. Pharmacol.* doi: 10.1515/jbcpp-2020-0159

Shea, T. B., Rogers, E., Ashline, D., Ortiz, D., and Sheu, M. S. (2002). Apolipoprotein E deficiency promotes increased oxidative stress and compensatory increases in antioxidants in brain tissue. *Free Radic. Biol. Med.* 33, 1115–1120. doi: 10.1016/S0891-5849(02)01001-8

Skrobot, O. A., Attems, J., Esiri, M., Hortobágyi, T., Ironside, J. W., Kalaria, R. N., et al. (2016a). Vascular cognitive impairment neuropathology guidelines (VCING): The contribution of cerebrovascular pathology to cognitive impairment. *Brain* 139, 2957–2969. doi: 10.1093/brain/aww214

Skrobot, O. A., O'Brien, J., Black, S., Chen, C., DeCarli, C., Erkinjuntti, T., et al. (2016b). The vascular impairment of cognition classification consensus study. *Alzheimers Dement.* 13, 624–633.

Skrobot, O. A., Black, S. E., Chen, C., DeCarli, C., Erkinjuntti, T., Ford, G. A., et al. (2018). Progress toward standardized diagnosis of vascular cognitive impairment: Guidelines from the vascular impairment of cognition classification consensus study. *Alzheimers Dement.* 14, 280–292. doi: 10.1016/j.jalz.2017.09.007

Sonnen, J. A., Larson, E. B., Crane, P. K., Haneuse, S., Li, G., Schellenberg, G. D., et al. (2007). Pathological correlates of dementia in a longitudinal, population-based sample of aging. *Ann. Neurol.* 62, 406–413. doi: 10.1002/ana.21208

Stefaniak, J., and O'Brien, J. (2016). Imaging of neuroinflammation in dementia: A review. *J. Neurol. Neurosurg. Psychiatry* 87, 21–28.

Sun, C. C., Liu, J., Liu, M., Luo, Z. G., and Li, H. (2020). Intervention of Shenma Yizhi prescription on learning and memory in rats with vascular cognitive impairment induced by chronic cerebral ischemia. *Chin. J. Exp. Tradit. Med. Formulae* 26, 153–159.

Sun, C., Liu, J., Li, N., Liu, M., Luo, Z., and Li, H. (2021a). Traditional Chinese medicine Shenmayizhi decoction ameliorates memory and cognitive impairment induced by multiple cerebral infarctions. *Evid Based Compl. Alternat. Med.* 2021:6648455. doi: 10.1155/2021/6648455

Sun, C., Liu, M., Liu, J., Zhang, T., Zhang, L., Li, H., et al. (2021b). ShenmaYizhi decoction improves the mitochondrial structure in the brain and ameliorates cognitive impairment in VCI rats via the AMPK/UCP2 signaling pathway. *Neuropsychiatr. Dis. Treat.* 17, 1937–1951. doi: 10.2147/NDT.S302355

Tomimoto, H., Ihara, M., Wakita, H., Ohtani, R., Lin, J. X., Akiguchi, I., et al. (2003). Chronic cerebral hypoperfusion induces white matter lesions and loss of oligodendroglia with DNA fragmentation in the rat. *Acta Neuropathol.* 106, 527–534. doi: 10.1007/s00401-003-0749-3

Tönnies, E., and Trushina, E. (2017). Oxidative stress, synaptic dysfunction, and Alzheimer's disease. *J. Alzheimers Dis.* 57, 1105–1121. doi: 10.3233/JAD-161088

Wang, F., Cao, Y., Ma, L., Pei, H., Rausch, W. D., and Li, H. (2018). Dysfunction of cerebrovascular endothelial cells: Prelude to vascular dementia. *Front. Aging Neurosci.* 10:376. doi: 10.3389/fnagi.2018.00376

Wang, Q., Tang, X. N., and Yenari, M. A. (2007). The inflammatory response in stroke. *J. Neuroimmunol.* 184, 53–68. doi: 10.1016/j.jneuroim.2006.11.014

Wang, X. R., Shi, G. X., Yang, J. W., Yan, C. Q., Lin, L. T., Du, S. Q., et al. (2015). Acupuncture ameliorates cognitive impairment and hippocampus neuronal loss in experimental vascular dementia through Nrf2-mediated antioxidant response. *Free Radic. Biol. Med.* 89, 1077–1084. doi: 10.1016/j.freeradbiomed.2015.10.426

Wang, Y., Chen, J., Chu, S., Wang, Y. S., Wang, X. Y., Chen, N. H., et al. (2009). Improvement of memory in mice and increase of hippocampal excitability in rats by ginsenoside Rg1' s metabolites ginsenoside Rh1 and protopanaxatriol. *J. Pharmacol. Sci.* 109, 504–510. doi: 10.1254/jphs.08060FP

Wei Si-Can, L. I. N., and Tian-lai, H. L. S. Z. (2020). Quercetin activates mitochondrial autophagy via PINK1/parkin pathway to alleviate cerebral ischemia-reperfusion injury in rats. *Chin. J. Pathophysiol.* 36, 2251–2257.

Wei, L., Linhua, D., Dongli, Q., and Yingqiang, Z. (2021). Overview of the pharmacological effects of Gastrodia and its active ingredients. *Pharmacol. Clin. Chin. Mater. Med.* 37, 240–244.

Wei, Z., Yingqiang, Z., Jianguo, Z., Tian, L., and Juan, W. (2019). The influence of Tianm Gouteng decoction on the VEGF, TNF-α and EPCs mobilization in spontaneously hypertensive rats. *Chin. J. Integr. Med. Cardio Cerebrovasc. Dis.* 17, 2425–2429.

Wu, J. (2019). Comparison of pathological mechanisms and clinical studies between Alzheimer's disease and vascular dementia. *Zhejiang Med. J.* 41, 1227–1231.

Wu, Q., Fang, L., and Jiangang, L. (2017). Effect of Shenma Yizhi decoction cognitive function hemorheological statein mildand moderate vascular dementia. *Chin. J. Integr. Med. Cardio Cerebrovasc. Dis.* 15, 2381–2385.

Wyss-Coray, T., and Mucke, L. (2002). Inflammation in neurodegenerative disease–a double-edged sword. *Neuron* 35, 419–432. doi: 10.1016/S0896-6273(02)00794-8

Xiao, X. H. (2014). Research and application of biological evaluation in quality standardization of traditional Chinese medicine. *World Sci. Technol. Modern. Tradit. Chin. Med.* 16, 514–518.

Xiao, Z., Jinzhi, Z., Zhenzhen, L., and Yan, L. (2019). Effect and mechanism of ginsenoside Rb1 on angiogenesis in rats with cerebral infarction. *Med. Pharm. J. Chin. Peoples Liberat. Army* 31, 10–15.

Xiaohua, D., Rong, D., Xiufang, L., Weigang, D., and Shengyou, W. (2011). Effects of gastrodiol on nitric oxide and nitric oxide synthase in hippocampus of cerebral ischemia model rats. *Chin. J. Geriatr. Cardio Cerebrovasc. Dis.* 13, 653–655.

Xuemei, D., Yu, C., and Yang, Y. (2019). Effects of Shenma Yizhi decoction on the cognitive function and hippocampal oxidative stress in rats with alcohol associated dementia. *Chin. J. Integr. Med Cardio Cerebrovasc. Dis.* 24, 3922–3928.

Yanxiu, G., Xi, S., Yi, M., Lin, L., Zhilai, Z., Ling, J., et al. (2021). Advances in the chemical constituents and pharmacological activities of the *Euonymus alatus*. *Chin. J. Mordern Appl. Pharm.* 38, 2305–2316.

Yin, C. (2016). Role of vascular endothelial growth factor in angiogenesis after ischemic brain injury West China. *J. Pharm.* 31, 103–107.

Ying, X., Eamonn, E., Jurgen, F., Pinsker, D., Thomas, P., Latter, M., et al. (2022). Reduced cortical cholinergic innervation measured using [18F]-FEOBV PET imaging correlates with cognitive decline in mild cognitive impairment. *Neuroimage* 34:102992. doi: 10.1016/j.nicl.2022.102992

Ying, Z., Li, L., Guang-Yu, L., Liu, J. X., and Li, T. (2014). [Pharmacokinetics and brain distribution of ginsenosides after administration of sailuotong]. *Zhongguo Zhong Yao Za* 39, 316–321.

Yu Cao, X. D. Z. L. (2019). The influence of ShenmaYizhi decoction hippocampal cognitive function in rats with bilateral carotid artery ligation. *Chin. J. Integr. Med. Cardio Cerebrovasc. Dis.* 17, 1151–1155.

Yu, C., Xuemei, D., Zehui, L., Kun, L., Meixia, L., Hui, P., et al. (2019). The influence of Shenma Yizhi decoction on hippocampal cognitive function in rats with bilateral carotid artery ligation. *Chin. J. Integr. Tradit. West. Med. Cardio Cerebrovasc. Dis.* 17, 1151–1155.

Yuanyuan, W., Hao, Z., and Yuhuan, S. (2021). Mechanism of ferulic acid alleviating hepatic fibrosis in rats by inhibiting MAPK and NF-κB/IκBα signaling pathways. *Cent. South Pharm.* 19, 2489–2495.

Yunfeng, J., and Huixia, L. (2011). Effects of ligusticum chuanxiong alkaloid on SOD activity, NO, NOS and MDA contents in rat brain tissue. *Chin. Tradit. Med. modern Distance Educ.* 9, 212–213.

Yunlin, Z. (2006). Treatment of senile vascular dementia with integrated traditional Chinese and Western medicine. *Chin. J. Clin.* 2006, 2–4.

Zhang, H., Cao, Y., Pei, H., Wang, H., Ma, L., Wang, Z., et al. (2020). Shenmayizhi formula combined with ginkgo extract tablets for the treatment of vascular dementia: A randomized, double-blind, controlled trial. *Evid. Based Compl. Alternat. Med.* 2020:8312347. doi: 10.1155/2020/8312347

Zhang, Y., Liu, J., and Yang, B. (2018). *Ginkgo biloba* extract inhibits astrocytic lipocalin-2 expression and alleviates neuroinflammatory injury via the JAK2/STAT3 pathway after ischemic brain stroke. *Front. Pharmacol.* 9:518. doi: 10.3389/fphar.2018.00518

Zhonghui, P., Min, D., Cheng, P., and Liang, X. (2020). Research progress on substance basis and pharmacological action of alkaloids in *Ligusticum* chuanxiong. *China Pharm.* 31, 1020–1024.

Zhu, H., Liu, C., Hou, J., Long, H., Wang, B., Guo, D., et al. (2019). *Gastrodia elata* blume polysaccharides: A review of their acquisition, analysis, modification, and pharmacological activities. *Molecules* 24:2436. doi: 10.3390/molecules24132436

frontiers | Frontiers in Neuroscience

TYPE Systematic Review
PUBLISHED 14 December 2022
DOI 10.3389/fnins.2022.1053283

OPEN ACCESS

EDITED BY
Jianxun Liu,
Xiyuan Hospital, China Academy of Chinese Medical Sciences, China

REVIEWED BY
Mukaila Raji,
University of Texas Medical Branch at Galveston, United States
Chao-Qun Yan,
Dongzhimen Hospital, Beijing University of Chinese Medicine, China

*CORRESPONDENCE
Hui Pei
phxydoctor@126.com
Hao Li
xyhplihao1965@126.com

SPECIALTY SECTION
This article was submitted to Neuropharmacology, a section of the journal Frontiers in Neuroscience

RECEIVED 25 September 2022
ACCEPTED 28 November 2022
PUBLISHED 14 December 2022

CITATION
Wen J, Cao Y, Chang S, Huang Q, Zhang Z, Wei W, Yao J, Pei H and Li H (2022) A network meta-analysis on the improvement of cognition in patients with vascular dementia by different acupuncture therapies.
Front. Neurosci. 16:1053283.
doi: 10.3389/fnins.2022.1053283

A network meta-analysis on the improvement of cognition in patients with vascular dementia by different acupuncture therapies

Jiayu Wen[1,2], Yu Cao[2], Surui Chang[2], Qiaoyi Huang[1,2], Zhen Zhang[2], Wei Wei[3], Jiuxiu Yao[2,4], Hui Pei[2]* and Hao Li[3]*

[1]Graduate College, Beijing University of Chinese Medicine, Beijing, China, [2]Department of Geriatrics, Xiyuan Hospital, China Academy of Chinese Medical Sciences, Beijing, China, [3]Wangjing Hospital, China Academy of Chinese Medical Sciences, Beijing, China, [4]First Clinical College, Shandong University of Traditional Chinese Medicine, Jinan, China

Introduction: The second most prevalent cause of dementia is vascular dementia (VaD). Furthermore, acupuncture is a relatively safe and effective traditional therapy for individuals with VaD. We performed a network meta-analysis to assess the effectiveness and safety of various acupuncture therapies for VaD based on existing research.

Methods: We searched six electronic databases to screen for randomized controlled trials (RCTs) comparing different acupuncture treatments in VaD patients. The Cochrne tool (Review Manager 5.3) was used to evaluate the risk of bias of the included RCTs. Based on the Grading of Recommendations Assessment, Development and Evaluation framework, we assessed the confidence in the evidence using the Confidence In the results from Network Meta-Analysis approach. We used the frequency approach to perform the network meta-analysis. Data were analyzed using R 4.1.1.

Results: In total, we included 46 eligible studies. The results of the network analysis showed that the combined interventions of moxibustion (MB) with body acupuncture (BA) (MB + BA) and electroacupuncture (EA) with scalp acupuncture (SA) with BA (EA + SA + BA) were more effective in improving cognitive functions and activities of daily living compared with SA or BA alone. However, in the subgroup analysis, EA + SA + BA showed better efficacy in short- and mid-term acupuncture compared with other acupuncture therapies.

Conclusion: Combined acupuncture therapy may be a safe and effective intervention for individuals with VaD, and MB + BA and EA + SA + BA appear to be the most effective interventions. However, because the analysis of this study was based on low-to-moderate evidence, there remains no strong supporting evidence. Thus, high-quality, large-scale, and long-term studies should be conducted in the future to assess the effectiveness and safety of acupuncture in VaD.

Systematic review registration: https://www.crd.york.ac.uk/prospero/, identifier: CRD42022354573.

KEYWORDS

vascular dementia, electroacupuncture, scalp acupuncture, body acupuncture, moxibustion, cognitive function, ability of daily life, frequentist network meta-analysis

Introduction

Vascular dementia (VaD) is the second most prevalent cause of dementia (Yang et al., 2022), accounting for roughly 15% to 20% of dementia cases in North America and Europe, and about 30% of dementia cases in Asia (Wolters and Ikram, 2019). The risk of VaD doubles every 5.3 years, with the incidence rate increasing with age. Age-related dementia has become one of the major health problems worldwide (Iadecola et al., 2019). According to the World Health Organization, 35.6 million individuals worldwide suffer from dementia, and this figure is anticipated to quadruple by 2050 (World Health, 2012), which would place a huge burden on families, primary caregivers, and the economic cost to society. In the United States, such costs have exceeded those of cancer and heart disease (Hurd et al., 2013). Although the average cognitive impairment rates of VaD and Alzheimer's disease are similar, the mortality rate is higher in VaD than that in Alzheimer's disease (Kua et al., 2014). Therefore, there is an urgent need to identify suitable treatments for VaD.

VaD is characterized by progressive deterioration of memory and other cognitive functions due to cerebrovascular disease. The major cause of VaD is chronic cerebral hypoperfusion (Wang et al., 2020) and tissue hypoxia (Iadecola et al., 2019) after cerebral ischemia, which enhances the permeability of the blood-brain barrier permeability and plasma protein extravasation into the brain, resulting in a severe inflammatory response and oxidative stress, further leading to white matter damage (Rouhl et al., 2012). Although several advancements have been made in understanding the relationship between cerebrovascular disease and dementia, the underlying pathogenesis of VaD remains poorly understood. Currently, beneficial therapies include cholinesterase inhibitors and memantine, which are licensed drugs for Alzheimer's disease (O'Brien and Thomas, 2015). Several large studies have shown that cholinesterase inhibitors and memantine are effective in the treatment of VaD; however, the magnitude of their effectiveness is limited. Therefore, the regulators and guideline panels of these trials have recommended that memantine and cholinesterase inhibitors are inappropriate for the treatment of patients with VaD (Joshua et al., 2018). The same phenomenon is observed with N-methyl-D-aspartate antagonists (Orgogozo et al., 2002; Wilcock et al., 2002). For these reasons, alternative approaches, including acupuncture, have been adopted for VaD.

Abbreviations: RCTs, Randomized controlled trials; MB, moxibustion; BA, body acupuncture; EA, electroacupuncture; SA, scalp acupuncture; VaD, Vascular dementia; NMA, Network meta-analysis; MMSE, Mini-Mental State Examination; ADLs, Activities of daily living; CINeMA, Confidence In the results from Network Meta-Analysis; CI, Confidence interval.

Acupuncture, which is a traditional Chinese medical therapy, is one of the most commonly employed non-pharmacological therapies, and has been used in many countries for the treatment of neurological disorders (Wu et al., 2010; Wan et al., 2016). Accumulated evidence has also shown that acupuncture can improve the symptoms of VaD through its antioxidant, anti-inflammatory, and anti-apoptotic effects (Ye et al., 2017; Yang et al., 2018; Zhu et al., 2018). The network meta-analysis (NMA) method is effective for comparing and ranking various therapies; therefore, this study aimed to assess the efficacy and safety of different acupuncture techniques for the treatment of patients with VaD, and to determine the most suitable method for the acupuncture treatment of VaD.

Methods

This review was conducted according to the Preferred Reporting Items for Systematic Reviews and Meta-Analyses for Network Meta-Analyses (Moher et al., 2009; Page et al., 2021). In addition, our study protocol has been registered with the International Prospective Register of Systematic Reviews (PROSPERO) (registration number: CRD42022354573).

Search strategy for identification of studies

We conducted a systematic search of six databases, including PubMed, Cochrane Library, Embase, Web of Science, MEDLINE, and China National Knowledge Infrastructure, from their establishment on July 31, 2022. The following keywords were used during the search: (acupuncture therapy, acupuncture, acupuncture treatment, electro-acupuncture, needling, scalp acupuncture, electrostimulation, body acupuncture, electroacupuncture, moxibustion) and (dementia, vascular dementia, infarct dementia, post-stroke dementia, and vascular cognitive impairment). We adjusted and specified the retrieval strategies according to the different databases. The specifics of the search strategies are listed in the Supplementary Appendix 1.

Study selection

Two reviewers (JYW and SRC) independently evaluated the included studies. Any discrepancies were reviewed by a third reviewer (ZZ) and resolved by discussion among all the reviewers. Included studies fulfilled the following criteria: (i) randomized controlled trials (RCTs); (ii) included patients who matched the established diagnostic criteria for VaD, including the Diagnostic and Statistical Manual of Mental Disorders, the National Institute of Neurological Disorders and

Stroke, and the Association Internationale pour la Recherche et l'Enseignement en Neurosciences criteria, Hachinski Ischemic Score $\geq$ 7, and the outcomes of computed tomography or magnetic resonance imaging; (iii) types of acupuncture included were electroacupuncture (EA), scalp acupuncture (SA) (including traditional SA and modern SA) (Jian-Li et al., 2019), body acupuncture (BA), and moxibustion (MB); and (iv) the control group received sham acupuncture, blank control, wait-list control and anti-dementia medications (for whom the observation group used acupuncture combined with anti-dementia medications). Studies that met the following criteria were excluded: (i) comprised of patients with Alzheimer's disease or dementia caused by other factors; (ii) included patients with Hachinski Ischemic Score $<$ 7; (iii) included patients with a score $>$ 8 on the Cornell Scale for Depression in Dementia and who were diagnosed according to the Diagnostic and Statistical Manual of Mental Disorders criteria as having evident mental depression, or patients with other mental diseases or disorders; and (iv) included patients with severe neurological deficits or serious medical conditions, such as dysopia, aphasia and dysacusis, and malignancy.

Data abstraction

Two reviewers (JYW and QYH) independently extracted data from the included RCTs. The extracted data included study characteristics such as first author, title of study, participants (sex, age, month of diagnoses, sample sizes), study design (randomization, blinding), interventions, controlled interventions, outcome measures, results and adverse events, we recorded these characteristics in advance. The four categories of acupuncture treatments were EA, SA, BA, and MB. The control groups included patients receiving anti-dementia medications, for whom the observation group used acupuncture combined with anti-dementia medications; sham acupuncture; blank control; wait-list control. Any discrepancies were evaluated by a third reviewer (JXY) and resolved by discussion among all the reviewers.

Outcomes

The Mini-Mental State Examination (MMSE) and Hasegawa Dementia Scale (HDS) were defined as the primary efficiency outcome measures. When more than one measure of cognitive function was used in a study, we preferentially used the MMSE in all cases for inclusion in our meta-analysis. However, due to the high similarity in scoring criteria, total score and content between MMSE and HDS (Kim et al., 2005; Senda et al., 2020), we included a very small number of HDS scores to analyze together. The Barthel Index of ADLs and activities of daily living (ADLs) were identified as the secondary efficacy outcome indicators.

Quality assessment

Two independent reviewers (SRC and WW) evaluated the identified trials. The revised Cochrane risk-of-bias tool for randomized trials (Review Manager 5.3) was used to assess the bias risk of the included RCTs. Any disagreements were reviewed by a third reviewer (QYH) and resolved by discussion among all the reviewers.

Data synthesis and analysis

A pairwise meta-analysis was performed in this study using the random-effects model in Stata 14 (StataCorp LLC, College Station, Texas 77845, USA). Then, the "netmeta" version 0.9–2 of the R-4.1.1 software was used to conduct a frequentist NMA (Rücker, 2012; Krahn et al., 2013) in this study. To display and describe the geometric features of different acupuncture treatments, we used the "networkPlot" function of Stata 14 (College Station, Texas 77,845 USA) to draw and generate network graphs. Different nodes represented different treatments, and edges represented head-to-head comparisons between different treatments. We used the "decomp.design" function to evaluate the consistency of entire network, homogeneity within designs, and homogeneity/consistency between designs. We used a node-splitting method (Rücker and Schwarzer, 2015) to evaluate the inconsistency between direct and indirect comparisons. The different interventions were ranked in accordance with the P-score, which were based only on the standard errors of the network and point estimations. These scores, which gauge the degree of certainty between comparisons of different interventions, are averaged across all competing treatments (Brehm et al., 2009).

We calculated pooled estimates and 95% confidence intervals (95% CIs) by performing a random-effects NMA. Generally speaking, when studies use the same evaluation method to assess our results of interest, the mean difference in the change scores between the final and baseline scores on the scale was regarded as a treatment effect to evaluate the outcomes. Since lower scores represented more severe cognitive impairment, the final minus the baseline scores served as the change scores definition. One treatment was considered more effective than the other if the corresponding estimate of the mean difference in the change score was positive and the 95% CI did not include zero.

Moreover, to investigate the probable sources of heterogeneity more thoroughly in this study, we performed

subgroup analyses according to different acupuncture treatment durations. Based on the duration of treatment, all results from the included studies were divided into three groups i.e., short-term ($1 \leq \times \leq 30$ days), mid-term ($30 < \times \leq 60$ days), and long-term ($\times > 60$ days).

Assessing confidence of the evidence

Confidence in the results from Network Meta-Analysis (CINeMA) was used to assess the confidence of the evidence in all the trials, and ratings were assigned using the CINeMA application (Nikolakopoulou et al., 2020).

CINeMA evaluates six domains as follows: within-study bias, reporting bias, indirectness, imprecision, heterogeneity, and incoherence. With the exception of reporting bias, which is classified as suspect or undetected, they are graded as no concerns, some concerns, or major concerns. The conclusions are then presented for each treatment comparison across these six dimensions as high, moderate, low, or very low confidence (Papakonstantinou et al., 2020).

All or most comparisons from industry-funded trials were considered to be at a risk of reporting bias. For comparisons with poor network connections, indirection is downgraded. For imprecision, the threshold was set to a mean difference of 0 for continuous comparisons.

Results

Study identification

For the present study, a total of 1,814 studies were identified. After reviewing the titles and abstracts, 102 studies were chosen for further review. Of these, 50 were excluded: 14 did not report the related data, 13 did not include the relevant target populations, 11 were not RCTs, and 12 did not investigate the target interventions. After qualitative synthesis, 8 studies were excluded. In total, 46 RCTs met the inclusion criteria and were included in this meta-analysis study (Huang et al., 1992, 2007, 2012; Liu et al., 1997, 1998, 2016; Lai et al., 1998; Li et al., 1999, 2014; Lun et al., 2003; Lai and Huang, 2005; Wu, 2006; Xu, 2006; Zhang et al., 2006, 2008; Ling et al., 2007; Chu et al., 2008; Han, 2009; Peng, 2009; Wang, 2009, 2014; Zhao et al., 2009; Teng, 2011; Yin et al., 2011; Teng and Lai, 2012; Zhou and Zhou, 2012; Dai et al., 2013a,b; Gao et al., 2013; Sheng et al., 2013; He and Guo, 2014; Shi et al., 2014; Jin, 2015; Li, 2015; Luo et al., 2015; Xie and Junming, 2016; Chen, 2017; Sheng and Cai, 2017; Wang and Wang, 2018; Wang et al., 2018; Feng, 2020; Guo, 2020; Ouyang, 2020; Yao, 2020; Zhu, 2020; Han et al., 2021). The detailed selection process is illustrated in Figure 1.

Characteristics of the included studies

The aggregated characteristics of the included RCTs are shown in Table 1.

The included studies were released between 1992 and 2022. Forty-six of the RCTs originated in China. Thirty-seven studies were published in Chinese, whereas nine studies were published in English. Thirty RCTs were two-arm trials, 13 were three-arm trials, and three were multi-arm trials. Courses of acupuncture and other therapies ranged from 4 to 12 weeks in the included studies.

Quality of evidence

Figure 2 presents the evaluation results of the risk of bias (Supplementary Appendix 2). All 46 included studies were RCTs. Methods for generating random sequences were clearly stated in 30 studies, of which 3 studies (Liu et al., 1997; Sheng and Cai, 2017; Wang et al., 2018) were classified as high risk of bias due to the use of hospital or clinical record numbers as sequence numbers. The remaining 16 studies demonstrated an unclear risk of bias, as the random sequence generation method was not specified. Fifteen studies demonstrated a low risk of bias and the remaining 31 studies showed an unclear risk of bias in allocation concealment.

Due to the specificity of the interventions evaluated in this review, blinding between patients and clinicians was difficult to implement. Thirteen studies showed a low risk of bias and 33 studies showed an unclear risk of bias in the blinding of the participants and personnel. Fourteen studies showed a low risk of bias and 32 studies showed an unclear risk of bias in the blinding of outcome assessment.

Thirteen studies showed a low risk of bias in incomplete outcome data, whilst 33 studies showed an unclear risk of bias for incomplete outcome data. Regarding selective outcome reporting, one study (Guang-Xia et al., 2014) demonstrated a high risk of bias because it did not report pre-determined outcomes, 35 studies showed a low risk of bias, and the remaining 10 studies showed an unclear risk of bias. Twenty-eight studies showed an unclear risk of bias due to other bias.

Outcome analysis of cognitive function

Pairwise meta-analysis

We performed a pairwise meta-analysis of cognitive function and the results are shown in Supplementary Appendix 3. The results of the pairwise meta-analysis showed that although each acupuncture therapy had certain advantages compared with the control group (among which the advantages of MB + BA and EA + SA

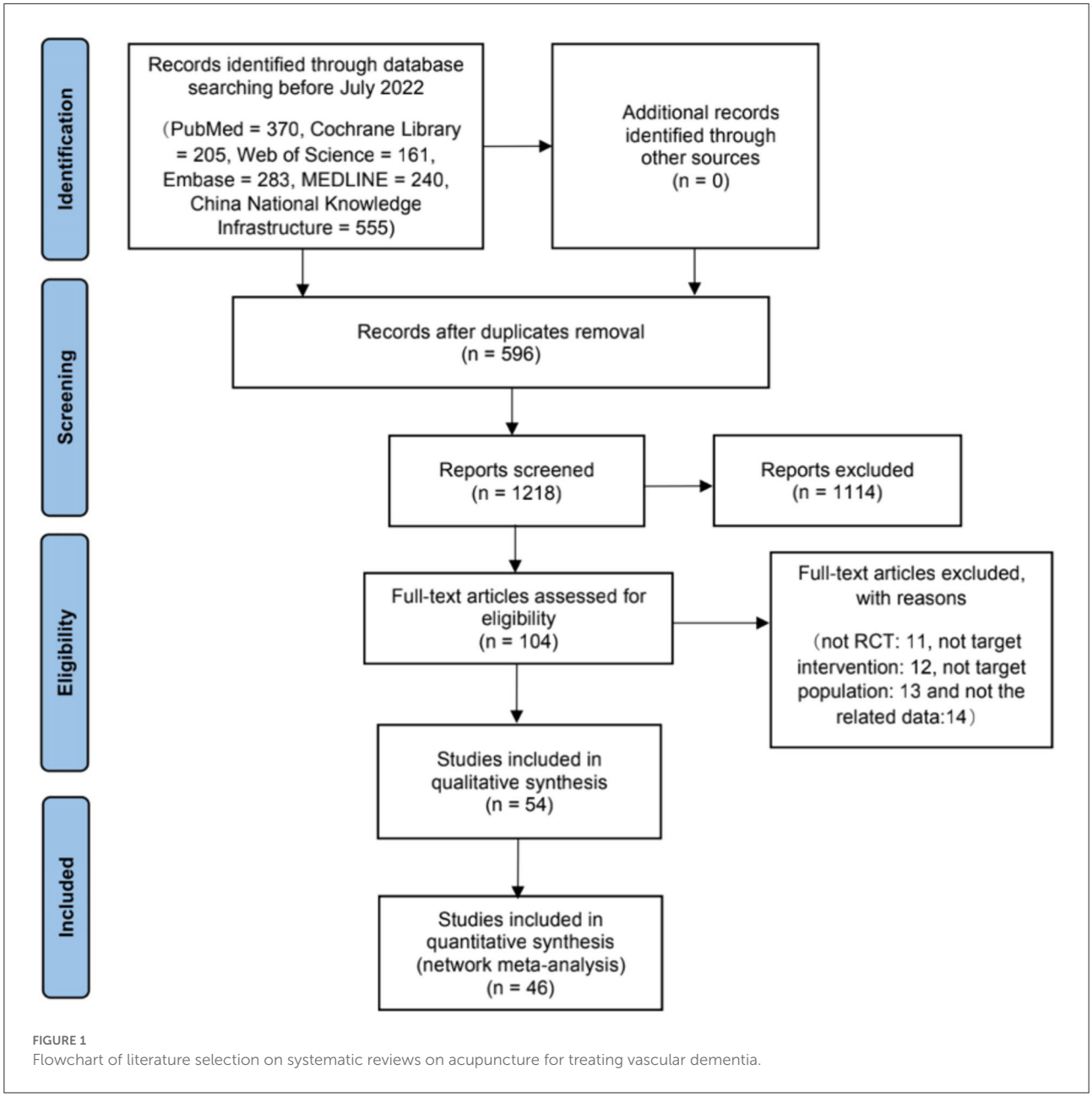

FIGURE 1
Flowchart of literature selection on systematic reviews on acupuncture for treating vascular dementia.

were larger), there was no significant difference in any of the comparisons.

Network meta-analysis

The network plot is shown in Figure 3. Eight interventions were involved i.e., EA + SA + BA, SA + BA, EA + SA, SA, BA, MB + BA, MB, and control.

Forty-six studies, which contributed 3,731 patients in the main NMA, reported changes in cognitive function scores using the MMSE and HDS. The results of the NMA of different interventions are shown in Table 2. Compared to the control group, MB + BA (1.31, 95% CI: 0.18–2.44), EA + SA + BA (1.17, 95% CI: 0.53–1.81), SA + BA (0.92, 95% CI: 0.52–1.33), SA (0.88, 95% CI: 0.45–1.31), EA + SA (0.84, 95% CI: 0.50–1.19), and BA (0.53, 95% CI: 0.06–1.00) showed better improvement in cognitive function.

Compared to simple SA and BA, the combined interventions EA + SA + BA (0.29, 95% CI: −0.46–1.04 and 0.64, 95% CI: −0.06–1.34, respectively) and SA + BA (0.05, 95% CI: −0.51–0.61 and 0.40, 95% CI: −0.04–0.84, respectively) showed better improvement in cognitive function. Compared to simple MB, the combined intervention MB + BA (0.50, 95% CI: −0.57–1.57) showed better improvement in cognitive function. SA

TABLE 1 The aggregated characteristics of the included RCTs.

Source	Study design	Age	Sample (men)	Duration	Intervention scheme	Duration of intervention	Outcome measure	
Wang et al. (2018)	Randomized controlled trial	SA: 70.0 ± 8.0 Control: 64.0 ± 7.0	SA: 60 (31) Control: 60 (32)	SA: 8.3 ± 3.3 Control: 8.2 ± 2.7 years	SA: 30 min, manipulate the needle for 60 s	2 times per day, 5 times per week for 7 weeks	MMSE	N/A
Han et al. (2021)	Randomized controlled trial	SA + BA: 64.0 ± 9.0 Control: 66.0 ± 8.0	SA: 59 (30) Control: 59 (29)	SA: 6.3 ± 2.6 Control: 6.7 ± 2.4 months	SA: 30 min, manipulate the needle until patients have the needling sensation	1 time per day, 5 times per week for 8 weeks	MMSE	Barthel
Guang-Xia et al. (2014)	Randomized controlled trial	SA + BA: 67.2 ± 9.3 Control: 67.5 ± 10.1	SA + BA: 22 (12) Control: 22 (11)	N/A	SA + BA: 30 min, manipulate the needle until patients have the needling sensation	1 time every two days for 6 weeks	MMSE	ADL
Liu et al. (2016)	Randomized controlled trial	SA + BA: 55.0 ± 7.0 Control: 56.0 ± 9.0	SA + BA:84 (54) Control: 84 (52)	SA + BA: 2.9 ± 0.7 Control: 3.2 ± 0.9 years	SA + BA: manipulate the needle for 1 min	1 time per day for 8 weeks	MMSE	N/A
Li et al. (1999)	Randomized controlled trial	58.0–82.0	32 (9)	3–60 years	SA + BA: 30 min	1 time per day for 2 months	HDS	N/A
Huang et al. (1992)	Randomized controlled trial	53.0–75.0	36 (27)	3–60 years	SA+BA	1 month	HDS	N/A
Jin (2015)	Randomized controlled trial	BA: 73.2 ± 5.3 Control: 71.9 ± 4.8	BA: 23 (15) Control: 23 (14)	BA: 2.4 ± 1.3 Control: 2.0 ± 1.7 years	BA: manipulate the needle for 1 min	1 time per day, 6 times per week for 2 months	MMSE	ADL
Li (2015)	Randomized controlled trial	SA + BA: (man) 50.3 ± 3.1, (woman) 51.5 ± 2.5 Control: (man) 53.3 ± 2.5, (woman) 50.6 ±3. 6	SA + BA: 43 (25) Control: 43 (26)	SA + BA: (man) 2.0 ± 1.5, (woman) 2.3 ± 0.9 Control: (man) 2.1 ± 0.5, (woman) 2.0 ± 1.6 years	SA + BA: 40 min, manipulate the needle 1 time	1 time per day, 5 times per week for 12 weeks	MMSE	ADL
Lun et al. (2003)	Randomized controlled trial	SA: 52.0–68.0 Control: 52.0–65.0	SA: 57 (35) Control: 32 (20)	N/A	SA: 30 min, manipulate the needle 2 times	1 time per day, 6 times per week for 4 months	HDS	N/A
Wang et al. (2018)	Randomized controlled trial	MB + BA: 54.0 ± 7 0.0 MB: 52.0 ± 7.0 BA: 52.0 ± 8.0	MB + BA: 38 (28) MB: 38 (29) BA: 38 (27)	MB + BA: 16.1 ± 4.7 MB: 15.9 ± 5.7 BA: 15.8 ± 3.9 months	MB + BA, MB: 30 min BA: 30 min, manipulate the needle until patients have the needling sensation	MB: 1 time per day, 2 times per week for 4 weeks BA: 1 time per day, 5 times per week for 4 weeks	MMSE	ADL
Lai et al. (1998)	Randomized controlled trial	EA + SA + BA: 68.6 ± 6.9 SA + BA: 66.1 ± 6.8	EA + SA + BA: 23 (14) SA + BA: 23 (17)	N/A	EA + SA + BA: 30 min, the frequency of EA is 120–250 times per minute; SA+BA: 30 min, manipulate the needle 1 time every 10 min	1 time per day, 5 times per week for 7 weeks	HDS	N/A

(Continued)

10.3389/fnins.2022.1053283

TABLE 1 (Continued)

Source	Study design	Age	Sample (men)	Duration	Intervention scheme	Duration of intervention	Outcome measure	
Zhang et al. (2008)	Randomized controlled trial	EA + SA: 64.7 ± 8.7 Control: 65.0 ± 8.2	EA + SA: 82 (50) Control: 81 (53)	N/A	EA + SA: 30 min, 3–15 Hz, 2–4 mA	1 time per day, 5 times per week for 6 weeks	MMSE	ADL-R
Zhao et al. (2009)	Randomized controlled trial	N/A	N/A	N/A	EA + SA: 30 min, the frequency of EA is 300–500 times per minute	1 time per day, 5 times per week for 6 weeks	MMSE	N/A
Liu et al. (1998)	Randomized controlled trial	EA + SA 1: 67.5 ± 7.2 Control 1: 65.5 ± 6.8 EA + SA 2: 68.2 ± 7.8 control 2: 65.2 ± 7.6	EA + SA 1: 30 (15) Control 1: 60 (34) EA + SA 2: 60 (38) Control 2: 30 (21)	EA + SA 1: 11.5 ± 8.7 Control 1: 11.1 ± 8.1 EA + SA 2: 11.8 ± 4.9 Control 2: 13.0 ± 5.4 months	EA + SA: 30 min, the frequency of EA is 200 times per minute	1 time per day, 5 times per week for 8 weeks	MMSE	ADL
Li et al. (2014)	Randomized controlled trial	SA: 63.0 ± 9.0 BA: 64.0 ± 8.0	SA: 31 (16) BA: 28 (14)	SA: 10.6 ± 3.3 BA: 10.7 ± 3.3 years	SA: 45 min, manipulate the needle until patients have the needling sensation	1 time per day for 6 weeks	MMSE	ADL
Lai and Huang (2005)	Randomized controlled trial	73.1 ± 5.8	50 (23)	2.35 ± 0.92 years	SA + BA, BA: 20 min, manipulate the needle 1 time every 5 min	1 time per day, 5 times per week for 4 weeks	HDS	ADL
Huang et al. (2007)	Randomized controlled trial	SA + BA 1: 71.3 ± 4.1 SA + BA 2: 71.6 ± 5.0 SA + BA 3: 69.3 ± 4.7 BA: 71.2 ± 4.8	SA + BA 1: 10 (6) SA + BA 2: 10 (5) SA + BA 3: 10 (5) BA: 10 (4)	SA + BA 1: 2.1 ± 0.7 SA + BA 2: 2.6 ± 0.5 SA + BA 3: 2.2 ± 0.6 BA: 2.2 ± 0.6 years	SA + BA, BA: 20 min, manipulate the needle 1 time every 5 min	1 time per day, 5 times per week for 4 weeks	MMSE	ADL
Liu et al. (1997)	Randomized controlled trial	BA: 64.8 ± 7.3 SA + BA: 64.7 ± 7.4	BA: 50 (40) SA + BA: 51 (33)	BA: 0.5–60 SA + BA: 0.5–36 months	BA, SA + BA: 20 min, manipulate the needle until patients have the needling sensation	1 time per day for 1 month	HDS	N/A
Teng (2011)	Randomized controlled trial	Control: 69.0 ± 6.0 EA + SA: 66.0 ± 6.0 BA: 68.0 ± 6.0	Control: 28 (18) EA + SA: 27 (16) BA: 25 (14)	Control: 2.0 ± 1.1 EA + SA: 2.1 ± 0.7 BA: 2.0 ± 1.1 years	EA + SA, BA: 30 min	1 time per day, 6 times per week for 1 month	MMSE	Barthel
Xu (2006)	Randomized controlled trial	EA + SA: 63.7 ± 7.7 Control: 63.3 ± 8.1	EA + SA: 30 (21) Control: 20 (12)	N/A	EA + SA: 30 min, dense-sparse waves	1 time per day for 3 months	MMSE	ADL

(Continued)

10.3389/fnins.2022.1053283

TABLE 1 (Continued)

Source	Study design	Age	Sample (men)	Duration	Intervention scheme	Duration of intervention	Outcome measure	
Yao (2020)	Randomized controlled trial	EA + SA: 64.5 ± 4.9 Control: 63.3 ± 5.5	EA + SA: 30 (15) Control: 30 (16)	EA + SA: 26.1 ± 6.5 Control: 25.9 ± 6.0 months	EA + SA: 30 min, continuous wave, 4 Hz	1 time per day for 4 weeks	MMSE	ADL
Wang (2014)	Randomized controlled trial	EA + SA + BA: 66.0 ± 7.9 SA + BA: 63.6 ± 8.0	EA + SA + BA: 30 (16) SA + BA: 30 (17)	EA + SA + BA: 61.6 ± 37.4 SA + BA: 59.6 ± 32.9 months	EA: 20 min, dense-sparse waves SA + BA: 40 min, manipulate the needle 1 time every 20 min	1 time per day, 5 times per week for 8 weeks	MMSE	ADL
Ling et al. (2007)	Randomized controlled trial	N/A	N/A	N/A	EA + SA: 30 min, continuous wave, the frequency of EA is 300–500 times per minute	1 time per day, 5 times per week for 6 weeks	MMSE	N/A
Yin et al. (2011)	Randomized controlled trial	EA + SA: 62.7 ± 5.1 Control: 62.8 ± 5.4	EA + SA: 30 (18) Control: 30 (17)	EA + SA: 1.7±0.3 Control: 1.6 ± 0.3 years	EA + SA: 30 min, continuous wave, 25–42 Hz	1 time per day, 5 times per week for 12 weeks	MMSE	N/A
Zhang et al. (2006)	Randomized controlled trial	EA + SA: 67.6 ± 7.0 Control: 63.0 ± 6.7	EA + SA: 27 (19) Control: 28 (17)	N/A	EA + SA: 30 min, continuous wave, the frequency of EA is 300–500 times per minute	1 time per day, 5 times per week for 6 weeks	MMSE	ADL
Han (2009)	Randomized controlled trial	EA + SA + BA: 62.5 ± 15.8 Control: 64.2 ± 16.3	EA + SA + BA: 92 (49) Control: 90 (47)	N/A	EA + SA + BA: 30 min, dense-sparse waves	1 time per day, 5 times per week for 8 weeks	LOCTA	N/A
Zhu (2020)	Randomized controlled trial	EA + SA + BA: 65.8 ± 6.7 SA + BA: 65.6 ± 7.2	EA + SA + BA: 32 (15) SA + BA: 31 (16)	EA + SA + BA: 12.6 ± 3.4 SA + BA: 12.2 ± 3.2 months	EA + SA + BA: 30 min, continuous wave, 2 Hz SA + BA: 30 min, manipulate the needle for 1 minute	2 time per day, 6 times per week for 4 weeks	MMSE	ADL
Peng (2009)	Randomized controlled trial	EA + SA: 63.7 ± 9.3 Control: 66.0 ±9 0.1	EA + SA: 24 (15) Control :26 (17)	N/A	EA + SA: 30 min, continuous wave, the frequency of EA is 300–500 times per minute	1 time per day, 5 times per week for 6 weeks	MMSE	ADL
Guo (2020)	Randomized controlled trial	EA + SA + BA: 67.4 ± 3.4 SA + BA: 66.7 ± 3.4	EA + SA + BA: 30 (13) SA + BA: 30 (16)	N/A	EA + SA + BA: 30 min, dense-sparse waves, manipulate the needle for 1 min	1 time per day, 6 times per week for 5 weeks	MMSE	N/A
Chu et al. (2008)	Randomized controlled trial	SA: 68.2 ± 9.2 Control: 67.7 ± 8.5	SA: 33 (20) Control: 32 (18)	SA: 5.2 ± 2.9 Control: 4.9 ± 2.8 months	SA: 10 h, manipulate the needle until patients have the needling sensation	1 time per day, 5 times per week for 8 weeks	MMSE	ADL

(Continued)

10.3389/fnins.2022.1053283

TABLE 1 (Continued)

Source	Study design	Age	Sample (men)	Duration	Intervention scheme	Duration of intervention	Outcome measure	
Chen (2017)	Randomized controlled trial	EA + SA: 58.1 ± 6.9 Control: 57.4 ± 6.7	EA + SA: 37 (20) Control: 37 (21)	EA + SA: 13.5 ± 4.7 Control: 13.5 ± 4.7 months	EA + SA: 30 min SA: 6 h	1 time per day, 6 times per week for 6 weeks	MMSE	N/A
Wu (2006)	Randomized controlled trial	64.7 ± 7.6	60 (38)	N/A	EA + SA: 20 min, the frequency of EA is 200 times per minute	1 time per day for 45 days	MMSE	N/A
Zhou and Zhou (2012)	Randomized controlled trial	SA + BA: 64.8 ± 6.2 BA: 66.3 ± 7.3	SA + BA: 30 (18) BA: 30 (20)	N/A	SA + BA, BA: 30 min, manipulate the needle 1 time every 10 min	1 time per day, 6 times per week for 6 weeks	MMSE	ADL
Sheng et al. (2013)	Randomized controlled trial	SA: 71.8 ± 2.7 Control: 67.3 ± 2.0	SA: 30 (22) Control: 30 (19)	SA: 10.4 ± 2.3 Control: 10.6 ± 2.3 months	SA: 30 min, manipulate the needle until patients have the needling sensation	1 time per day, 6 times per week for 12 weeks	MMSE	ADL
Dai et al. (2013b)	Randomized controlled trial	N/A	N/A	N/A	SA: 50 min, manipulate the needle 2 times, 2 min every time	1 time per day for 4 weeks	MMSE	ADL
Dai et al. (2013a)	Randomized controlled trial	SA 1: 66.0 ± 6.0 SA 2: 68 ± 6.0 Control: 69.0 ± 6.0	SA 1: 30 (17) SA 2: 30 (15) Control: 30 (10)	SA 1: 2.1 ± 0.7 SA 2: 2.0 ± 1.0 Control: 2.0 ± 1.0 years	SA 1, SA 2: 50 min, manipulate the needle 2 times, 2 min every time	1 time per day for 4 weeks	MMSE	ADL
He and Guo (2014)	Randomized controlled trial	EA + SA: 65.1 ± 8.5 BA: 66.4 ± 7.2	SA: 34 (18) BA: 33 (17)	SA: 9.8 ± 2.9 BA: 9.9 ± 2.9 years	SA, BA: 50 min, manipulate the needle until patients have the needling sensation	1 time per day for 8 weeks	MMSE	ADL
Gao et al. (2013)	Randomized controlled trial	SA: 71.6 ± 5.0 Control: 72.3 ± 4.0	EA + SA: 30 (13) Control: 30 (14)	EA + SA: 5.6 ± 2.1 Control: 5.0 ± 1.9 months	EA + SA: 30 min, continuous wave, the frequency of EA is 300–500 times per minute	1 time per day, 6 times per week for 8 weeks	MMSE	N/A
Teng and Lai (2012)	Randomized controlled trial	SA: 66.0 ± 6.0 BA: 68.0 ± 6.0	SA: 27 (16) BA: 25 (14)	SA: 2.1 ± 0.7 BA: 2.0 ± 1.1 years	SA: 30 min	1 time per day, 6 times per week for 1 month	MMSE	Barthel
Wang (2009)	Randomized controlled trial	EA + SA: 66.8 ± 8.6 EA + BA: 66.2 ± 8.1	EA + SA: 92 (51) EA + BA: 92 (59)	EA + SA: 3.6 ± 2.9 EA + BA: 3.6 ± 2.9 years	EA + SA, EA + BA: 30 min, dense-sparse waves, 80–100 Hz	1 time per day, 5 times per week for 3 months	MMSE	ADL

(Continued)

10.3389/fnins.2022.1053283

TABLE 1 (Continued)

Source	Study design	Age	Sample (men)	Duration	Intervention scheme	Duration of intervention	Outcome measure	
Huang et al. (2012)	Randomized controlled trial	EA + SA: 67.0 ± 9.0 EA + BA: 66.0 ± 8.0	EA + SA: 92 (51) EA + BA: 92 (59)	N/A	EA + SA, EA + BA: 30 min, dense-sparse waves, 1.3–1.7 Hz	1 time per day, 5 times per week for 3 months	MMSE	ADL
Xie and Junming (2016)	Randomized controlled trial	SA: 63.5 ± 7.8 Control: 62.8 ± 7.1	SA: 30 (17) Control: 30 (16)	SA: 2.7 ± 0. 5 Control: 2.9 ± 0. 3 years	SA: 45 min, manipulate the needle 2 times every 10 min, 10–15 s per time	1 time per day for 3 months	MMSE	ADL
Ouyang (2020)	Randomized controlled trial	SA + BA: 63.8 ± 9.4 Control: 62.6 ± 9.6	SA + BA: 30 (12) Control: 30 (11)	SA + BA: 1.3 ± 0.7 Control: 1.4 ± 0.7 years	SA + BA: 30 min, manipulate the needle until patients have the needling sensation	1 time per day, 6 times per week for 4 weeks	MMSE	ADL
Feng (2020)	Randomized controlled trial	EA + SA: 65. 8± 5.3 Control: 64.3 ± 6.0	EA + SA: 30 (17) Control: 30 (16)	EA + SA: 14.3 ± 2.5 Control: 14.7 ± 1.7 months	EA + SA: 30 min, dense-sparse waves, 1 Hz	1 time per day, 5 times per week for 8 weeks	MMSE	ADL
Luo et al. (2015)	Randomized controlled trial	MB: 72.1 ± 3.4 BA: 71.8 ± 3. 9	MB: 30 (13) BA: 30 (15)	MB: 1.4 ± 0.3 BA: 1.4 ± 0.2 years	MB: 30 min BA: 30 min, manipulate the needle for 30 s	1 time every two days for 8 weeks	MMSE	N/A
Sheng and Cai (2017)	Randomized controlled trial	MB: 55.5 ± 4.9 Control: 54.9 ± 5.2	MB: 30 (16) Control: 30 (18)	N/A	MB: 30 min	1 time per day, 6 times per week for 4 weeks	MMSE	ADL

10.3389/fnins.2022.1053283

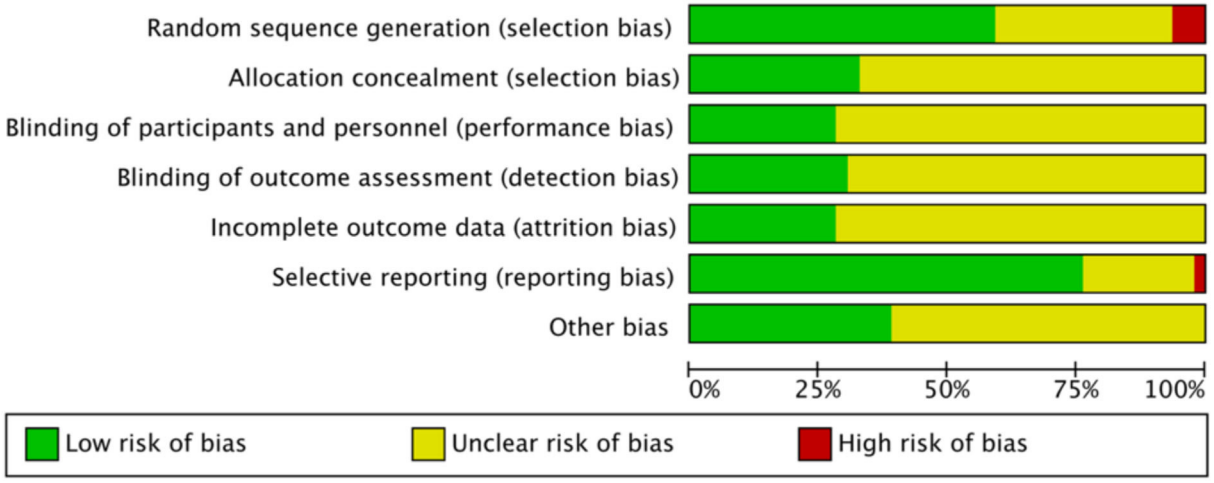

FIGURE 2
Risk of bias summery for 46 included studies.

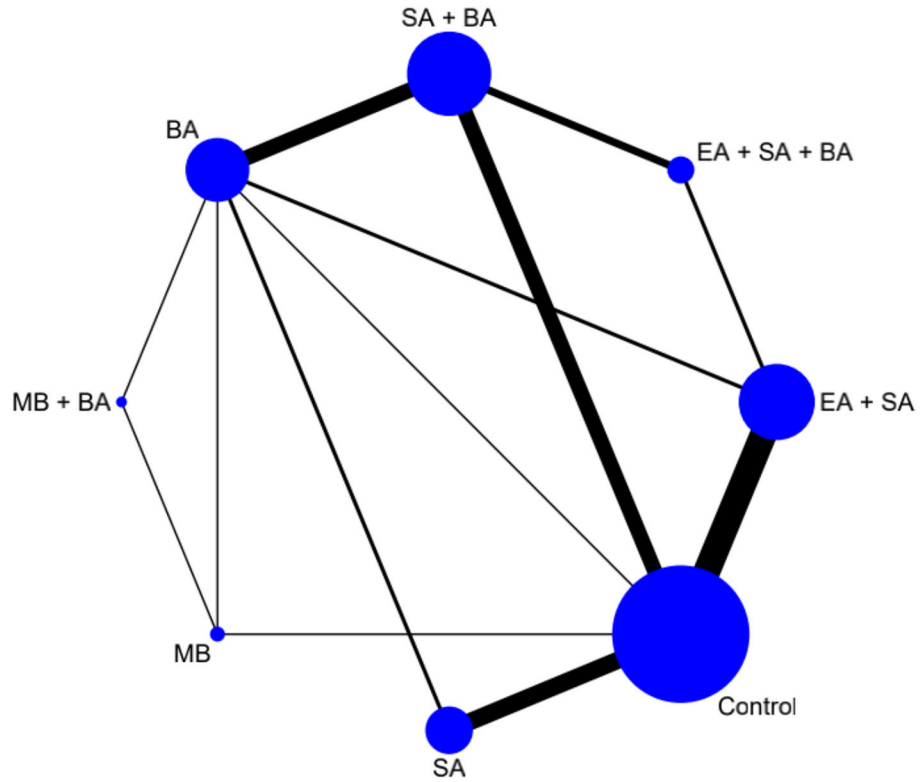

FIGURE 3
Network plot of cognitive function.

may be more effective in relieving dementia symptoms than BA (0.35, 95% CI: −0.22–0.92). However, there were no appreciable differences between these acupuncture therapies in terms of improving cognitive function. However, acupuncture combined with EA or MB was better than SA or BA alone. Moreover, MB + BA showed the greatest possibility of becoming the most effective intervention for improving cognitive function (P-score = 0.80, Figure 4).

TABLE 2 Results of network meta-analysis for all possible treatment effects (cognitive function).

MB + BA	.	.	.	.	0.61 (−0.77–1.98)	0.68 (−0.70–2.05)	.
0.14 (−1.11–1.40)	**EA + SA + BA**	0.73 (0.03–1.44)	.	−0.56 (−1.50–0.38)	.	.	.
0.39 (−0.75–1.52)	0.24 (−0.35–0.83)	**SA + BA**	.	.	.	0.23 (−0.31–0.76)	1.31 (0.82–1.81)
0.43 (−0.75–1.62)	0.29 (−0.46–1.04)	0.05 (−0.51–0.61)	**SA**	.	.	0.49 (−0.50–1.48)	0.85 (0.38–1.31)
0.47 (−0.70–1.63)	0.32 (−0.32–0.97)	0.08 (−0.40–0.56)	0.03 (−0.51–0.57)	**EA + SA**	.	0.60 (−0.39–1.59)	0.66 (0.29–1.04)
0.50 (−0.57–1.57)	0.36 (−0.73–1.44)	0.12 (−0.84–1.07)	0.07 (−0.93–1.07)	0.03 (−0.93–1.00)	**MB**	0.18 (−1.21–1.57)	1.02 (−0.38–2.43)
0.78 (−0.29–1.85)	0.64 (−0.06–1.34)	0.40 (−0.04–0.84)	0.35 (−0.22–0.92)	0.32 (−0.21–0.84)	0.28 (−0.62–1.18)	**BA**	0.00 (−1.42–1.42)
1.31 (0.18–2.44)	1.17 (0.53–1.81)	0.92 (0.52–1.33)	0.88 (0.45–1.31)	0.84 (0.50–1.19)	0.81 (−0.12–1.74)	0.53 (0.06–1.00)	**Control**

MB + BA, moxibustion with body acupuncture; EA + SA + BA, electroacupuncture with scalp acupuncture with body acupuncture; SA + BA, scalp acupuncture with body acupuncture; EA + SA, electroacupuncture with scalp acupuncture; MB, moxibustion; BA, body acupuncture. The estimates of mean difference of treatments in the columns vs. rows are presented in the lower diagonal elements, whereas those of the row treatments vs. column treatments are presented in the upper diagonal elements. The . symbol indicates results not reported in the studies.

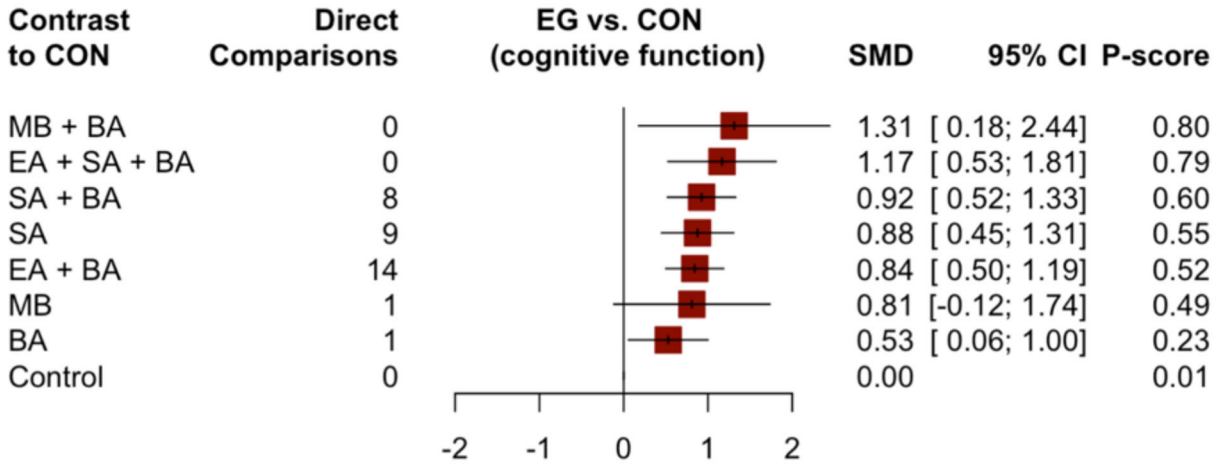

FIGURE 4
Forest plot compared with the control group (cognitive function).

Inconsistency between direct and indirect comparisons of cognitive function scores

Inconsistency between direct and indirect comparisons was assessed using a node-splitting model, showing no inconsistencies among the studies ($P > 0.05$). Details of the results are presented in Table 3.

Subgroup analysis

An improvement in cognition scores in the short-term ($1 \leq \times \leq 30$ days) was reported in 16 trials; 22 trials reported an improvement in cognition scores in the mid-term ($30 < \times \leq 60$ days), and eight trials reported an improvement in cognition scores in the long-term ($\times > 60$ days). Data from different treatments were evaluated separately in accordance with different treatment durations in each subgroup. There were eight different interventions in the short-term. Paired meta-analysis showed that EA + SA + BA vs. BA (1.13, 95% CI: 0.43–1.84), SA + BA vs. EA + SA + BA (−0.93, 95% CI: −1.52– −0.35), control vs. EA + SA + BA (−1.53, 95% CI: −2.78– −0.27), and control vs. EA + SA (−0.88, 95% CI: −1.48– −0.28) were all statistically significantly different (Supplementary Appendix 7). In the NMA, the EA + SA + BA treatment showed the best improvement in cognitive function (0.96), followed by MB + BA (0.84), EA + SA (0.61), MB (0.54), SA + BA (0.46), SA (0.37), and BA (0.22). The details are illustrated in Figure 5. There were significant differences in the curative effects between EA + SA + BA and SA + BA (0.93, 95% CI: 0.37–1.49), SA (1.02, 95% CI: 0.24–1.80), and BA (1.17, 95% CI: 0.52–1.82, Supplementary Appendix 7).

For the mid-term, there were no statistically significant differences between the groups in the paired meta-analysis (Supplementary Appendix 7). In the NMA, the highest probability of enhancing cognitive function was observed for EA + SA + BA, with a probability of 0.88, followed by SA and SA + BA with probabilities of 0.71 and 0.70, respectively (Figure 6, Supplementary Appendix 7). For the long-term, eight studies with five treatments (SA + BA, SA, EA + SA, control, and EA + SA + BA) were included. However, we failed to

perform the corresponding network analysis because of the long-term network was disconnected.

Nine studies (Lai et al., 1998; Ling et al., 2007; Huang et al., 2012; Luo et al., 2015; Liu et al., 2016; Xie and Junming, 2016; Sheng and Cai, 2017; Feng, 2020; Ouyang, 2020) reported change scores using syndrome differentiation score of vascular dementia; however, failed to perform the corresponding network analysis due to the limited number of studies included.

Outcome analysis of living ability

Pairwise meta-analysis

We performed a pairwise meta-analysis of living ability and the results are shown in Supplementary Appendix 3. The results of the pairwise meta-analysis showed that although each acupuncture therapy had slight advantages compared with the control group, there was no significant difference in any of the comparisons.

Network meta-analysis

The network plot is shown in Figure 7. Eight interventions were involved: EA + SA + BA, SA + BA, EA + SA, SA, BA, MB + BA, MB, and control.

Thirty studies with 2,486 patients in the main NMA reported changes in ADL scores using the ADLs and Barthel index. The results of the NMA of different treatments are shown in Table 4. Compared to the control group, MB + BA (1.97, 95% CI: 0.95–2.99), EA + SA + BA (1.04, 95% CI: 0.37–1.71), EA + SA (0.87, 95% CI: 0.51–1.24), and SA + BA (0.72, 95% CI: 0.24–1.19) showed better improvement in ADLs. However, other acupuncture treatments showed no significant difference compared to the control group. MA + BA may be more suitable for improving the activity of daily living compared to MB (1.38, 95% CI: 0.44–2.32) and BA (1.53, 95% CI: 0.59–2.47). Furthermore, combined acupuncture MB + BA (P-score = 0.99) and EA + SA + BA (P-score = 0.76, Figure 8) are likely to be the best intervention to improve the ADLs of patients with VaD.

Inconsistency between direct and indirect comparisons of life function scores

Inconsistency between direct and indirect comparisons was assessed using a node-splitting model, showing no inconsistencies among the studies ($P > 0.05$). Details of the results are presented in Table 5.

Adverse events

Forty participants from eight studies (Zhang et al., 2008; Huang et al., 2012; Shi et al., 2014; Wang, 2014; Wang et al., 2018; Feng, 2020; Ouyang, 2020; Yao, 2020) reported the presence of adverse events. The main adverse effects reported in the acupuncture group were "discomfort at the acupuncture site" (16 patients), "skin bruising at acupoints" (15 patients), "fainting during acupuncture treatment" (seven patients), and "bleeding at acupuncture points" (two patients). These symptoms are mild and persist for a short period of time.

Confidence in evidence

The confidence ratings for these comparisons with CINeMA (Supplementary material) were mostly low to moderate confidence. This was mainly because of within-study bias, lack of precision, and/ or heterogeneity. Poor reporting of the randomization and blinding procedures explained the concerns of within-study bias. The relatively small number of studies with direct evidence included in all the comparisons explains the imprecision. The observed heterogeneity is likely because of the small number of trials in some comparisons, whereas some of the RCTs focused on different subgroups of VaD.

Discussion

To the best of our knowledge, this study is the first NMA to explore the efficacy of different acupuncture treatments for VaD. The MMSE scale (Cui et al., 2019) is currently the most widely used neuropsychological scale for clinical cognitive function screening, which can comprehensively reflect the cognitive state and cognitive characteristics of patients. Cognitive impairment is a core symptom of VaD; therefore, we chose to assess changes in cognitive impairment as the primary efficiency outcome of this review. In addition, the decline in the ability to perform ADLs is also one of the main symptoms of VaD; thus, we choose the ADLs as secondary efficacy outcome indicators. We used direct and indirect evidence to evaluate the relative effects of different acupuncture therapies on cognitive function and the ability to perform ADLs in patients with VaD. Based on the currently available data, our NMA suggests that combined acupuncture interventions (EA + SA + BA and MB + BA) show better efficacy in improving cognitive function and the ability to perform ADLs compared with MB, SA, and BA alone. SA was more effective than BA in improving cognitive function. Using a subgroup analysis of cognitive function, we found that EA + SA + BA achieved the best effect among the therapies analyzed for both the short- and mid-terms. However, for the short-term, EA + SA was more effective than SA + BA, whereas the opposite was true for the mid-term. This may be why there is a certain degree of heterogeneity in our review. Furthermore, the efficacy of EA in improving the ADLs was better than that of non-EA treatments.

TABLE 3 Node-splitting analysis of inconsistency (cognitive function).

Comparison	Direct RoM 95% CI	Indirect RoM 95% CI	Network RoM 95% CI	*P*-value
BA vs. EA + SA	−0.60 (−1.59–0.39)	−0.20 (−0.82–0.41)	−0.39 (−1.56–0.77)	0.554
BA vs. SA	−0.49 (−1.48–0.50)	−0.28 (−0.98–0.42)	−0.21 (−1.43–1.00)	0.983
BA vs. SA + BA	−0.23 (−0.76–0.31)	−0.74 (−1.51–0.03)	0.52 (−0.42–1.46)	0.171
EA + SA vs. EA + SA + BA	0.56 (−0.38–1.50)	−1.09 (−1.97–0.21)	1.65 (0.36–2.94)	1.000
EA + SA + BA vs. SA + BA	0.73 (0.03–1.44)	−0.92 (−2.00–0.16)	1.65 (0.36–2.94)	0.268
BA vs. MB	−0.18 (−1.57–1.21)	−0.35 (−1.54–0.83)	0.17 (−1.65–2.00)	0.853
EA + SA vs. Control	0.66 (0.29–1.04)	1.83 (0.95–2.70)	−1.16 (−2.11–0.21)	0.000
SA vs. Control	0.85 (0.38–1.31)	1.06 (−0.06–2.18)	−0.21 (−1.43–1.00)	0.732

RoM, ratio of mean.

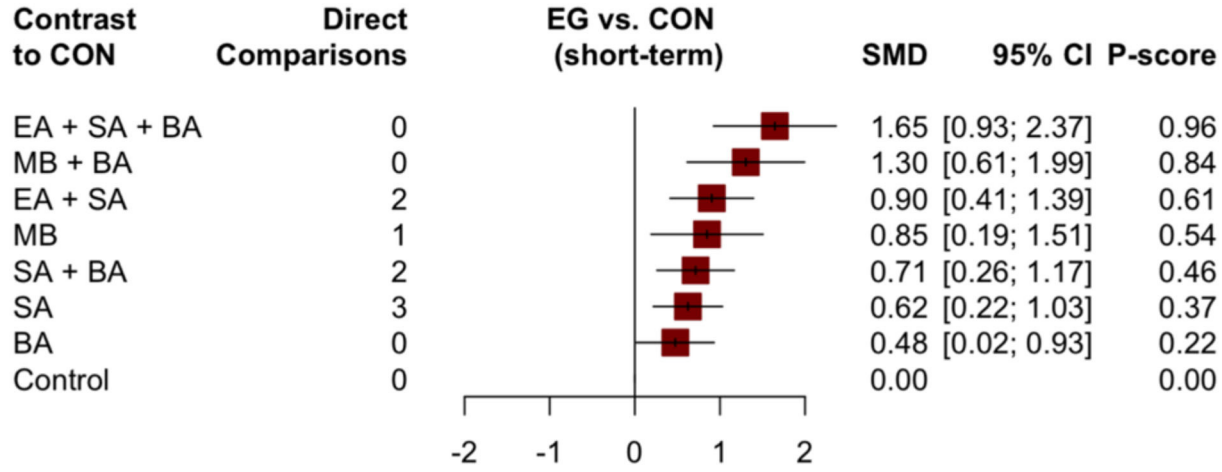

FIGURE 5
Forest plot compared with the control group of cognitive function (short-term).

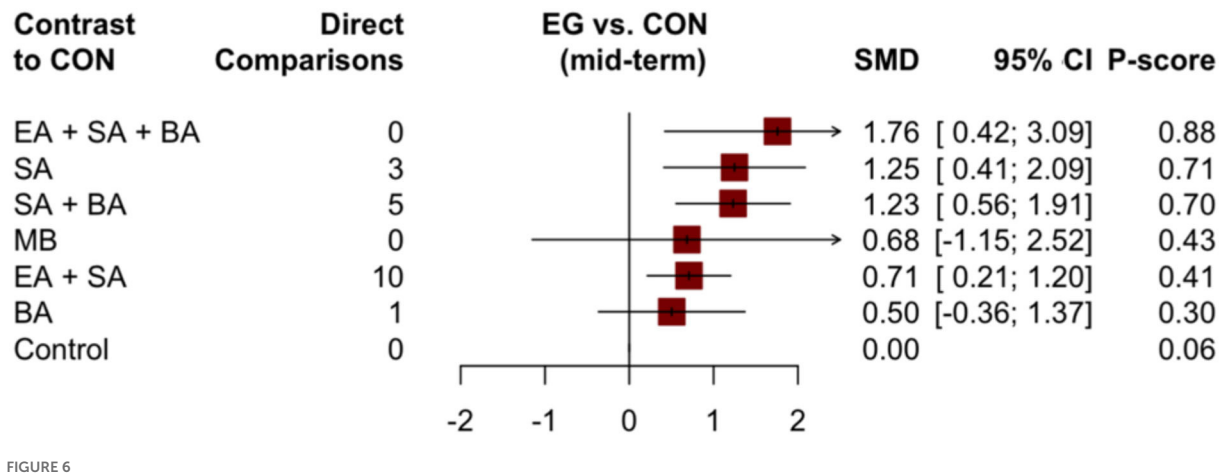

FIGURE 6
Forest plot compared with the control group of cognitive function (mid-term).

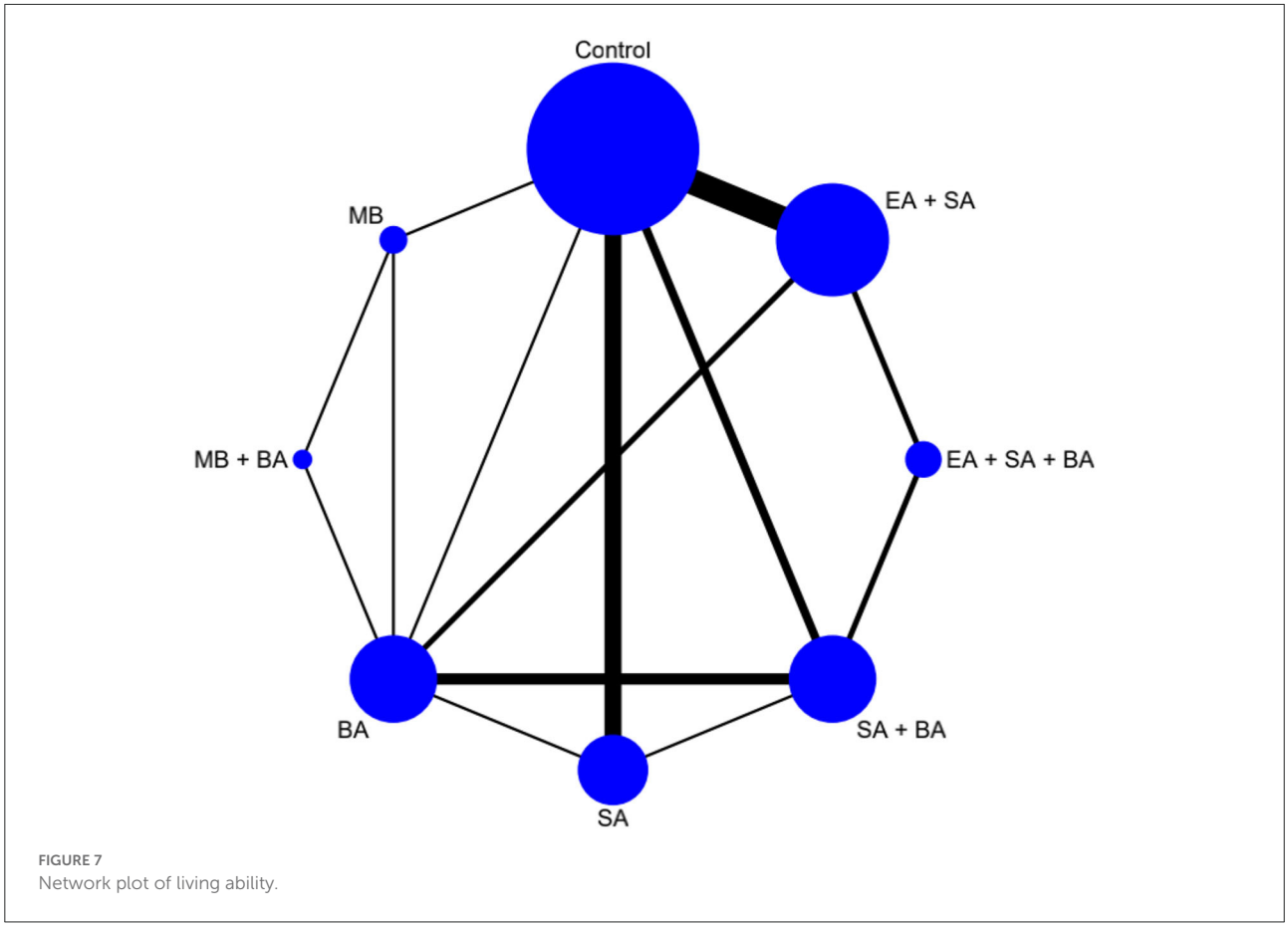

FIGURE 7
Network plot of living ability.

TABLE 4 Results of network meta-analysis for all possible treatment effects (living ability).

MB + BA	.	.	.	1.42 (0.21–2.62)	1.50 (−0.29–2.70)	.	.
0.93 (−0.24– 2.10)	**EA + SA + BA**	0.13 (−0.93–0.68)	0.66 (−0.20–1.52)	.	.	.	.
1.10 (0.05–2.14)	0.17 (−0.47–0.80)	**EA + SA**	.	.	0.21 (−0.64–1.07)	.	0.85 (0.44–1.25)
1.25 (0.21–2.29)	0.32 (−0.33–0.97)	0.16 (−0.38–0.69)	**SA + BA**	.	0.21 (−0.46–0.88	−0.17 (−1.38–1.04)	1.16 (0.47–1.85)
1.38 (0.44–2.32)	0.45 (−0.56–1.46)	0.28 (−0.58–1.14)	0.13 (−0.75–1.00)	**MB**	0.12 (−1.06–1.30)	.	0.67 (−0.55–1.88)
1.53 (0.59–2.47)	0.61 (−0.13–1.34)	0.44 (−0.09–0.97)	0.28 (−0.23–0.79)	0.16 (−0.63–0.94)	**BA**	−0.20 (−1.43–1.02)	−0.12 (−1.36–1.11)
1.56 (0.49–2.64)	0.63 (−0.14–1.40)	0.47 (−0.09–1.02)	0.31 (−0.27–0.89)	0.18 (−0.71–1.08)	0.03 (−0.57–0.62)	**SA**	0.29 (−0.20–0.78)
1.97 (0.95–2.99)	1.04 (0.37–1.71)	0.87 (0.51–1.24)	0.72 (0.24–1.19)	0.59 (−0.23–1.41)	0.43 (−0.07–0.94)	0.41 (−0.03–0.85)	**Control**

MB + BA, moxibustion with body acupuncture; EA + SA + BA, electroacupuncture with scalp acupuncture with body acupuncture; SA + BA, scalp acupuncture with body acupuncture; EA + SA, electroacupuncture with scalp acupuncture; MB, moxibustion; BA, body acupuncture. The estimates of mean difference of treatments in the columns vs. rows are presented in the lower diagonal elements, whereas those of the row treatments vs. column treatments are presented in the upper diagonal elements. The . symbol indicates results not reported in the studies.

Based on the analysis of adverse reactions from all included studies, all included acupuncture treatments were relatively safe for patients with VaD. Although some cases of adverse reactions have been reported, these adverse reactions are mild, and there is no direct association between adverse reactions and interventions. Therefore, these cases were justified.

Numerous studies have reported that VaD may be caused by hypoperfusion (Ruitenberg et al., 2005) and hypoxia (Fernando et al., 2006) after cerebral ischemia, resulting in alterations in blood–brain barrier permeability (Candelario-Jalil et al., 2011; Wardlaw et al., 2013), oxidative stress, and inflammation (Gallacher et al., 2010; Rouhl et al., 2012), which in turn can lead to white matter damage (Iadecola et al., 2019). The exact mechanism by which EA + SA + BA and MB + BA show better therapeutic efficiency in patients with VaD is still not fully understood. However, studies have shown that EA can enhance the secretion of brain-derived neurotrophic factors to exert neuroprotective effects after cerebral ischemia (Tao et al., 2016).

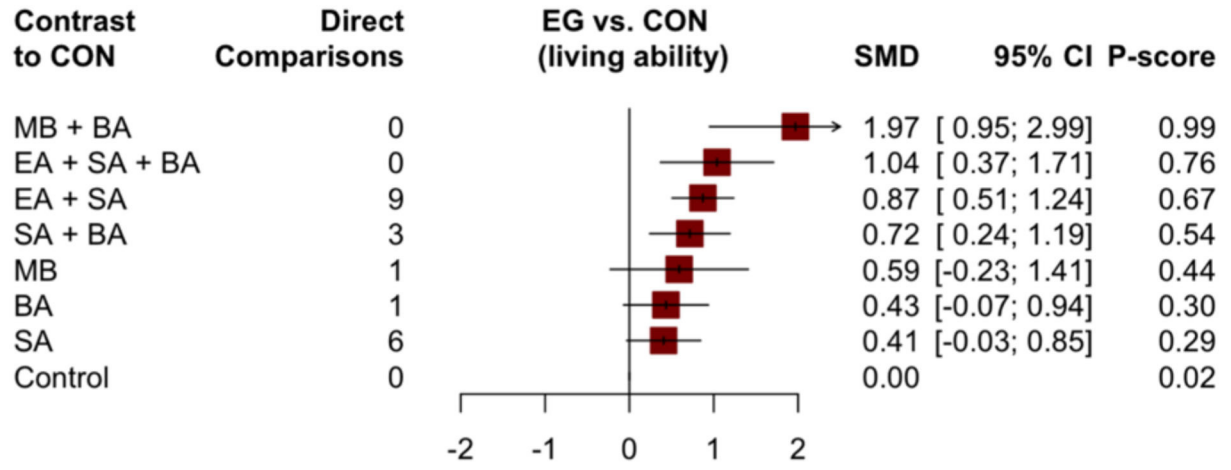

FIGURE 8
Forest plot compared with the control group (living ability).

TABLE 5 Node-splitting analysis of inconsistency (living ability).

Comparison	Direct RoM 95% CI	Indirect RoM 95% CI	Network RoM 95% CI	*P*-value
BA vs. EA + SA	−0.21 (−1.07–0.64)	−0.58 (−1.26–0.10)	−0.37 (−0.72–1.46)	0.960
BA vs. SA	−0.20 (−1.43–1.02)	−0.10 (−0.58–0.78)	−0.30 (−1.70–1.10)	0.621
EA + SA vs. EA + SA + BA	0.13 (−0.68–0.93)	−0.67 (−1.72–0.38)	0.80 (−0.52–2.12)	1.000
EA + SA + BA vs. SA + BA	0.66 (−0.20–1.52)	−0.14 (−1.14 to −0.86)	0.80 (−0.52–2.12)	0.236
EA + SA vs. control	0.85 (0.44–1.25)	0.98 (0.12–1.84)	−0.13 (−1.08–0.81)	0.000
SA vs. control	0.29 (−0.20–0.78)	0.86 (−0.11–1.84)	−0.57 (−1.67–0.52)	0.569

RoM, ratio of mean.

EA can reduce oxidative stress and anti-apoptotic cell death by increasing superoxide dismutase activity in the brain (Wang et al., 2011). MB can inhibit apoptosis and oxidative stress and improve vascular endothelial growth factor inflammation (Lai et al., 2022). MB may improve cognitive function in VaD patients by inhibiting hippocampal neuronal apoptosis (Yang et al., 2021). SA can improve blood supply to the brain and enhance neuronal metabolism (Chen et al., 2020). EA + SA can improve the learning and memory ability of VaD rats by down-regulating inflammatory factors, reducing neuronal apoptosis, and improving synaptic plasticity (Ma et al., 2022). SA + BA can improve cognitive function by inhibiting brain oxidative stress and inflammation, alleviating neuronal death in VaD rats (Du et al., 2018). Therefore, we speculate that the reason why EA + SA + BA and MB + BA are superior to other acupuncture treatments may be that the combination therapy brings together the advantages of individual acupuncture treatments. However, to determine whether these findings are attributed to simple additive effects or due to the interaction of multiple signaling pathways *in vivo* requires further research.

Limitations

This study had the following limitations: (i) the included RCTs were mainly conducted in China, (ii) Reliability of results may be affected by incomplete reporting of test details, (iii) testing indexes other than the scale could not be included because of the limited number of studies, and (iv) due to the limited number of studies retrieved, we could not extend our review more beneficially, such as whether the analysis results varied by patient sex (male vs. female), or whether effect size corresponds to the atherosclerotic cardiovascular disease (ASCVD) burden.

The lack of long-term follow-up studies makes it hard to conclude substantial implications of the study. The disease cycle in patients with VaD usually has longer chronic progression. More evidence is required to confirm whether acupuncture has long-term efficacy in addition to short-term improvement in cognitive function.

Conclusion

Combined acupuncture therapy may be an effective and safe intervention for patients with VaD, and MB + BA and EA + SA + BA emerged as the most effective interventions in this study. EA + SA + BA shows the best efficacy when the course of acupuncture is short or moderate. However, because the analysis in this study was based on low-to-moderate evidence, there is no strong supporting evidence in this regard. High-quality, large-scale, long-term studies should be performed in the future to investigate the efficacy and safety of acupuncture in VaD.

Data availability statement

The datasets presented in this study can be found in online repositories. The names of the repository/repositories and accession number(s) can be found in the article/Supplementary material.

Author contributions

JW: research design and writing. YC, HP, and HL: guidance of the relevant methodology. JW, SC, and ZZ: study selection. JW, QH, and JY: data abstraction. WW, SC, and QH: quality assessment. JW and SC: data statistics and analysis. All authors examined the results of this study and approved the final submission.

Funding

This study was supported by the Scientific and Technological Innovation Project of China Academy of Chinese Medical Sciences (CI2021A01401 and CI2021A01403).

Acknowledgments

The authors thank the Editage (http://www.editage.cn) for the English language editing of this article.

Conflict of interest

The authors declare that the research was conducted in the absence of any commercial or financial relationships that could be construed as a potential conflict of interest.

The handling editor declared a shared affiliation with the authors JW, YC, QH, ZZ, and HP at the time of review.

Publisher's note

All claims expressed in this article are solely those of the authors and do not necessarily represent those of their affiliated organizations, or those of the publisher, the editors and the reviewers. Any product that may be evaluated in this article, or claim that may be made by its manufacturer, is not guaranteed or endorsed by the publisher.

Supplementary material

The Supplementary Material for this article can be found online at: https://www.frontiersin.org/articles/10.3389/fnins.2022.1053283/full#supplementary-material

References

Brehm, B. J., Lattin, B. L., Summer, S. S., Boback, J. A., Gilchrist, G. M., Jandacek, R. J., et al. (2009). One-year comparison of a high-monounsaturated fat diet with a high-carbohydrate diet in type 2 diabetes. *Diabetes Care* 32, 215–220. doi: 10.2337/dc08-0687

Candelario-Jalil, E., Thompson, J., Taheri, S., Grossetete, M., Adair, J. C., Edmonds, E., et al. (2011). Matrix metalloproteinases are associated with increased blood-brain barrier opening in vascular cognitive impairment. *Stroke* 42, 1345–1350. doi: 10.1161/STROKEAHA.110.600825

Chen, J. (2017). Effects of scalp acupuncture on cognitive function and limb motor function in patients with vascular dementia. *J. Pract. Tradit. Chin. Med.* 33, 711. doi: 10.3696/j.issn.1004-2814.2017.06.086

Chen, J., Li, H., Zeng, C., Li, J., and Zhao, B. (2020). Evaluation of the recovery outcome of poststroke cognitive impairment after cluster needling of scalp acupuncture therapy based on functional near-infrared spectroscopy. *Brain Behav.* 10, e01731. doi: 10.1002/brb3.1731

Chu, J.-M., Bao, Y.-H., and Zou, C. (2008). Effect of long-time retention of scalp needle on the abilities of cognition, daily living activity and P300 in vascular dementia patients. *Acupunct. Res.* 33, 334–338. doi: 10.3969/j.issn.1000-0607.2008.05.010

Cui, S., Chen, N., Yang, M., Guo, J., Zhou, M., Zhu, C., et al. (2019). Cerebrolysin for vascular dementia. *Cochrane Database Syst. Rev.* 2019, CD008900. doi: 10.1002/14651858.CD008900.pub3

Dai, X. H., Guo, Y., Zhang, H., and Zou, W. (2013a). Clinical observation of 35 cases of mild vascular dementia treated mainly by scalp acupuncture with rapid needling manipulations. *J. Clin. Acupunct. Moxibustion* 29, 10–11. doi: 10.3969/j.issn.1005-0779.2013.08.005

Dai, X. H., Guo, Y. H., Zhang, H. W., and Wei, Z. (2013b). Therapeutic observation on the treatment of vascular dementia majorly with scalp acupuncture with rapid needling manipulations. *Shanghai J. Acupunct. Moxibustion* 32, 709–710. doi: 10.3969/j.issn.1005-0957.2013.09.709

Du, S.-Q., Wang, X.-R., Zhu, W., Ye, Y., Yang, J.-W., Ma, S.-M., et al. (2018). Acupuncture inhibits TXNIP-associated oxidative stress and inflammation to attenuate cognitive impairment in vascular dementia rats. *CNS Neurosci. Ther.* 24, 39–46. doi: 10.1111/cns.12773

Feng, L. (2020). *Clinical observation on the treatment of mild vascular dementia after stroke with zhiqi acupuncture* (Master thesis). Guangzhou University of Chinese Medicine, Guangzhou, China. doi: 10.27465/d.cnki.gzzyc.2020.000004

Fernando, M. S., Simpson, J. E., Matthews, F., Brayne, C., Lewis, C. E., Barber, R., et al. (2006). White matter lesions in an unselected cohort of the elderly: molecular pathology suggests origin from chronic hypoperfusion injury. *Stroke* 37, 1391–1398. doi: 10.1161/01.STR.0000221308.94473.14

Gallacher, J., Bayer, A., Lowe, G., Fish, M., Pickering, J., Pedro, S., et al. (2010). Is sticky blood bad for the brain?: hemostatic and inflammatory systems and dementia in the caerphilly prospective study. *Arterioscler. Thromb. Vasc. Biol.* 30, 599–604. doi: 10.1161/ATVBAHA.109.197368

Gao, Q., Su, C., and Huang, Y. (2013). Effect of scalp acupuncture therapy on post-stroke mild vascular dementia. *J. Pract. Trad. Chin. Med.* 29, 891. doi: 10.3969/j.issn.1004-2814.2013.11.001

Guang-Xia, S., Cun-Zhi, L., Wei, G., Zhan-Kui, W., Lei, W., Chuan, X., et al. (2014). Effects of acupuncture on Chinese medicine syndromes of vascular dementia. *Chin. J. Integr. Med.* 20, 661–666. doi: 10.1007/s11655-013-1323-4

Guo, P. (2020). *The clinical study on treatment of cognitive function of subcortical adterioscleroyic encephalopathy by scalp electroacupuncture* (Master thesis). Heilongjiang University of Chinese Medicine, Harbin, China. doi: 10.27127/d.cnki.ghlzu.2020.000263

Han, B. (2009). Electric acupuncture treating 92 vascular dementia patients. *Shanxi J. Trad. Chin. Med.* 30, 1523–1524. doi: 10.3969/j.issn.1000-7369.2009.11.066

Han, H., Li, X., Jiang, H.-N., Xu, K., and Wang, Y. (2021). Effect of early acupuncture on cognitive function in patients with vascular dementia after cerebral infarction. *Zhongguo Zhen Jiu* 41, 979–983. doi: 10.13703/j.0255-2930.20210117-k0008

He, J., and Guo, S. (2014). Effects of scalp acupuncture combined with auricular point sticking on clinical symptoms and cognitive behavior ability in eldly patients with vascular dementia. *Chin. J. Gerontol.* 34, 5576–5577. doi: 10.3969/j.issn.1005-9202.2014.19.123

Huang, L. N., An, J. M., Su, T. S., Pu, W., Dong, L., Zhang, R. P., et al. (2012). Therapeutic efficacy observation on scalp acupuncture for vascular dementia. *J. Acupunct. Tuina Sci.* 10, 38–43. doi: 10.1007/s11726-012-0567-z

Huang, W. C., Xu, J., and Wang, X. (1992). Study on the acupuncture in treating multiple infarctional dementia. *Zhongguo Zhen Jiu* 12, 113–115.

Huang, Y., Lai, X., and Tang, A. (2007). Comparative study of the specificities of needling acupoints DU20, DU26 and HT7 in intervening vascular dementia in different areas in the brain on the basis of scale assessment and cerebral functional imaging. *Chin. J. Integr. Med.* 13, 103–108. doi: 10.1007/s11655-007-0103-z

Hurd, M. D., Martorell, P., Delavande, A., Mullen, K. J., and Langa, K. M. (2013). Monetary costs of dementia in the United States. *N. Engl. J. Med.* 368, 1326–1334. doi: 10.1056/NEJMsa1204629

Iadecola, C., Duering, M., Hachinski, V., Joutel, A., Pendlebury, S. T., Schneider, J. A., et al. (2019). Vascular cognitive impairment and dementia: JACC scientific expert panel. *J. Am. Coll. Cardiol.* 73, 3326–3344. doi: 10.1016/j.jacc.2019.04.034

Jian-Li, W. U., Xin, H. N., Wang, D. L., Zhu, Z. W., and Sun, Z. R. (2019). Origin and development situation of scalp acupuncture therapy. *J. Guangzhou Univ. Trad. Chin. Med.* 36, 1783–1787. doi: 10.13359/j.cnki.gzxbtcm.2019.11.022

Jin, Z. (2015). Efficacy of acupuncture combined with nimodipine in the treatment of vascular dementia. *China Foreign Med. Treat.* 35, 3–4. doi: 10.1662/j.cnki.1674-0742.2015.14.074

Joshua, P., John, O., Louise, R., and Damien, L. (2018). Dementia: assessment, management and support: summary of updated NICE guidance. *BMJ Clin. Res.* 361, k2438. doi: 10.1136/bmj.k2438

Kim, K. W., Lee, D. Y., Jhoo, J. H., Youn, J. C., Suh, Y. J., Jun, Y. H., et al. (2005). Diagnostic accuracy of mini-mental status examination and revised hasegawa dementia scale for Alzheimer's disease. *Dement. Geriatr. Cogn. Disord.* 19, 324–330. doi: 10.1159/000084558

Krahn, U., Binder, H., and König, J. (2013). A graphical tool for locating inconsistency in network meta-analyses. *BMC Med. Res. Methodol.* 13, 35. doi: 10.1186/1471-2288-13-35

Kua, E. H., Ho, E., Tan, H. H., Tsoi, C., Thng, C., and Mahendran, R. (2014). The natural history of dementia. *Psychogeriatrics* 14, 196–201. doi: 10.1111/psyg.12053

Lai, X., and Huang, Y. (2005). A comparative study on the acupoints of specialty of Baihui, Shuigou and Shenmen in treating vascular dementia. *Chin. J. Integr. Med.* 11, 161–166. doi: 10.1007/BF02836497

Lai, X., Mo, F., and Jiang, G. (1998). Observation of clinical effect of acupuncture on vascular dementia and its influence on superoxide dismutase, lipid peroxide and nitric oxide. *Chin. J. Int. Trad. Western Med.* 18, 648–651.

Lai, Z., Zhang, Q., Liang, L., Wei, Y., Duan, G., Mai, W., et al. (2022). Efficacy and mechanism of moxibustion treatment on mild cognitive impairment patients: an fMRI study using ALFF. *Front. Mol. Neurosci.* 15, 852882. doi: 10.3389/fnmol.2022.852882

Li, B. (2015). Governor vessel acupuncture method in the treatment of vascular dementia for 43 cases. *Chin. Med. Mod. Dist. Educ. China* 13, 70–72. doi: 10.3969./j.issn.1672-2779.2015.15.036

Li, S.-K., Ding, D.-M., Zhang, Z.-L., Ma, L., Huang, H.-Y., and Wu, X.-H. (2014). Effects of scalp acupuncture combined with auricular point sticking on cognitive behavior ability in patients with vascular dementia. *Zhongguo Zhen Jiu* 34, 417–420. doi: 10.13703/j.0255-2930.2014.05.012

Li, Y., Zhuang, L., Zheng, L., and Yang, W. (1999). Study on treatment of vascular dementia with acupuncture and moxibustion principally. *World J. Acupunct. Moxibustion*. 9, 6–11.

Ling, Z., Hong, Z., and Zhong, Z. (2007). The clinical research on scalp electric acupuncture improving the cognition function of 90 vascular dementia patients. *J. Sichuan Trad. Chin. Med.* 25, 105–108. doi: 10.3969/j.issn.1000-3649.2007.09.066

Liu, H., Hou, D., Diao, Z., and Yun, W. (1997). Observation on the clinical curative effects of turbit-clearing and intelligence-improving acupuncture therapy on vascular dementia and the study on its mechanisms. *Chin. Acuponct. Moxibustion* 9, 521–525.

Liu, J., Peng, X., and Lin, D. (1998). Clinical study on treatment of vascular dementia by electroacupuncture of scalp- acupoints. *Chin. Acupunct. Moxibustion* 4, 197–200.

Liu, Q., Wang, X.-J., Zhang, Z.-C., Xue, R., Li, P., and Li, B. (2016). Neuroprotection against vascular dementia after acupuncture combined with donepezil hydrochloride: P300 event related potential. *Neural Rege. Res.* 11, 460–464. doi: 10.4103/1673-5374.179059

Lun, X., Rong, L., and Yang, W. (2003). Observation on efficacy of CT positioning scalp circum-needling combined with Chinese herbal medicine in treating poly-infarctional vascular dementia. *Chin. J. Int. Trad. Western Med.* 23, 423–425. doi: 10.3221/j.issn:1003-5370.2003.06.008

Luo, B. H., Jian-Chun, Y. U., Yue-Qiang, H. U., Xue, L. F., Liang, Y. J., and Qin, B. N. (2015). Clinical observation about treatment of 30 cases of mild and moderate vascular dementia with "Yi Qi, Tiao Xue, Fu Ben, Pei Yuan" Moxibustion of Zhuang medicated thread. *Lishizhen Med. Materia Medica Res.* 26, 649–651. doi: 10.3969/j.issn.1008-0805.2015.03.053

Ma, C., Zhou, Y., Yi, W., Zhou, X., Guo, W., Xu, X., et al. (2022). Electroacupuncture of the Baihui and Shenting acupoints for vascular dementia in rats through the miR-81/IL-16/PSD-95 pathway. *Ann. Transl. Med.* 10, 540. doi: 10.21037/atm-22-2068

Moher, D., Liberati, A., Tetzlaff, J., and Altman, D. G. (2009). Preferred reporting items for systematic reviews and meta-analyses: the PRISMA statement. *BMJ* 339, b2535. doi: 10.1136/bmj.b2535

Nikolakopoulou, A., Higgins, J. P. T., Papakonstantinou, T., Chaimani, A., Del Giovane, C., Egger, M., et al. (2020). CINeMA: an approach for assessing confidence in the results of a network meta-analysis. *PLoS Med.* 17, e1003082. doi: 10.1371/journal.pmed.1003082

O'Brien, J. T., and Thomas, A. (2015). Vascular dementia. *Lancet* 386, 1698–1706. doi: 10.1016/S0140-6736(15)00463-8

Orgogozo, J.-M., Rigaud, A.-S., Stöffler, A., Möbius, H.-J., and Forette, F. (2002). Efficacy and safety of memantine in patients with mild to moderate vascular dementia: a randomized, placebo-controlled trial (MMM 300). *Stroke* 33, 1834–1839. doi: 10.1161/01.STR.0000020094.08790.49

Ouyang, C. (2020). *Clinical study on acupuncture treatment of mild to moderate vascular dementia* (Master thesis). Guangzhou University of Chinese Medicine, Guangzhou, China. doi: 10.27044/d.cnki.ggzzu.2020.000791

Page, M. J., McKenzie, J. E., Bossuyt, P. M., Boutron, I., Hoffmann, T. C., Mulrow, C. D., et al. (2021). The PRISMA 2020 statement: an updated guideline for reporting systematic reviews. *BMJ* 372, n71. doi: 10.1136/bmj.n71

Papakonstantinou, T., Nikolakopoulou, A., Higgins, J. P. T., Egger, M., and Salanti, G. (2020). CINeMA: software for semiautomated assessment of the confidence in the results of network meta-analysis. *Campbell Syst. Rev.* doi: 10.1002/cl2.1080

Peng, X. (2009). Research on scalp electric acupuncture in improving the cognition function of vascular dementia patients. *J. Sich. Trad. Chin. Med.* 27, 113–115.

Rouhl, R., Damoiseaux, J., Lodder, J., Theunissen, R., Knottnerus, I., Staals, J., et al. (2012). Vascular inflammation in cerebral small vessel disease. *Neurobiol. Aging* 33, 1800–1806. doi: 10.1016/j.neurobiolaging.2011.04.008

Rücker, G. (2012). Network meta-analysis, electrical networks and graph theory. *Res. Synth. Method.* 3, 312–324. doi: 10.1002/jrsm.1058

Rücker, G., and Schwarzer, G. (2015). Ranking treatments in frequentist network meta-analysis works without resampling methods. *BMC Med. Res. Methodol.* 15, 58. doi: 10.1186/s12874-015-0060-8

Ruitenberg, A., den Heijer, T., Bakker, S. L. M., van Swieten, J. C., Koudstaal, P. J., Hofman, A., et al. (2005). Cerebral hypoperfusion and clinical onset of dementia: the rotterdam study. *Ann. Neurol.* 57, 789–794. doi: 10.1002/ana.20493

Senda, M., Terada, S., Takenoshita, S., Hayashi, S., Yabe, M., Imai, N., et al. (2020). Diagnostic utility of the addenbrooke's cognitive examination - III (ACE-III), mini-ACE, mini-mental state examination, montreal cognitive assessment, and hasegawa dementia scale-revised for detecting mild cognitive impairment and dementia. *Psychogeriatrics* 20, 156–162. doi: 10.1111/psyg.12480

Sheng, D., and Cai, S. (2017). Observation of the efficacy of wenyang bushen moxibustion treatment vascular dementia. *J. Pract. Trad. Chin. Med*. 33, 58–59. doi: 10.3969/j.issn.1004-2814.2017.01.049

Sheng, G., Zhao, Q., Guo, J., and Huang, L. (2013). Clinical observation on the treatment of post-stroke dementia with scalp acupuncture combined with Tianzhi gradules. *Acta Chin. Med. Pharmacol.* 41, 83–84. doi: 10.19664/j.cnki.1002-2392.2013.02.033

Shi, G., Liu, C., Guan, W., Wang, Z., Wang, L., Xiao, C., et al. (2014). Effects of acupuncture on Chinese medicine syndromes of vascular dementia. *Chin. J. Integr. Med.* 20, 661–666.

Tao, J., Zheng, Y., Liu, W., Yang, S., Huang, J., Xue, X., et al. (2016). Electro-acupuncture at LI11 and ST36 acupoints exerts neuroprotective effects via reactive astrocyte proliferation after ischemia and reperfusion injury in rats. *Brain Res. Bull.* 120, 14–24. doi: 10.1016/j.brainresbull.2015.10.011

Teng, X. (2011). Clinical study on vascular dementia treated by electroacupuncture at neck points plus scalp acupuncture. *Shanghai J. Acupunct. Moxibustion* 30, 84–86. doi: 10.3969/j/issn.1005-0957.2011.02.084

Teng, X. Y., and Lai, Z. J. (2012). Clinical efficacy observation of scalp-acupuncture-based therapy for vascular dementia. *J. Acupunct. Tuina Sci.* 10, 34–37. doi: 10.1007/s11726-012-0566-0

Wan, F., Niu, X., Song, Y.-L., and Si, Y.-C. (2016). The role of Chinese herbs and acupuncture on the inflammation reaction after cerebral ischemia. *Curr. Pharm. Des.* 22, 709–719. doi: 10.2174/1381612822666151204001348

Wang, F., and Wang, M. (2018). Acupuncture at five mind points combined with modified kidney decoction for vascular dementia of kidney essence deficiency. *Zhongguo Zhen Jiu* 38, 127–134. doi: 10.13703/j.0255-2930.2018.02.004

Wang, H., Pan, Y., Xue, B., Wang, X., Zhao, F., Jia, J., et al. (2011). The antioxidative effect of electro-acupuncture in a mouse model of Parkinson's disease. *PLoS ONE* 6, e19790. doi: 10.1371/journal.pone.0019790

Wang, J. (2014). *The clinical study of electro-acupuncture cephalic and nuchal points of du meridian with acupuncture back shu points in treatment of vascular dementia* (Master thesis). Heilongjiang University of Chinese Medicine, Harbin, China.

Wang, L., Yang, J.-W., Lin, L.-T., Huang, J., Wang, X.-R., Su, X.-T., et al. (2020). Acupuncture attenuates inflammation in microglia of vascular dementia rats by inhibiting miR-93-mediated TLR4/MyD88/NF-B signaling pathway. *Oxid. Med. Cell. Longev.* 2020, 8253904. doi: 10.1155/2020/8253904

Wang, P. (2009). *Clinical Study on Vascular Dementia with Liver-Kidney Deficiency and Phlegm Stasis Syndromes Treated by Scalp Acupuncture.* Master, Shaanxi University of Chinese Medicine.

Wang, S., Ye, G., Xu, C., Jia, A., Ru, Y., Guan, S., et al. (2018). Flipping moxibustion of medicine at acupoints in governor vessel combined with acupuncture for vascular dementia. *Zhongguo Zhen Jiu* 38, 919–924.

Wardlaw, J. M., Smith, C., and Dichgans, M. (2013). Mechanisms of sporadic cerebral small vessel disease: insights from neuroimaging. *Lancet Neurol.* 12, 483–497. doi: 10.1016/S1474-4422(13)70060-7

Wilcock, G., Möbius, H. J., and Stöffler, A. (2002). A double-blind, placebo-controlled multicentre study of memantine in mild to moderate vascular dementia (MMM500). *Int. Clin. Psychopharmacol.* 17, 297–305. doi: 10.1097/00004850-200211000-00005

Wolters, F. J., and Ikram, M. A. (2019). Epidemiology of vascular dementia. *Arterioscler. Thromb. Vasc. Biol.* 39, 1542–1549. doi: 10.1161/ATVBAHA.119.311908

World Health, O. (2012). *Dementia: A Public Health Priority*. Geneva: World Health Organization.

Wu, H. (2006). Effects of scalp acupuncture plus electrical stimulation on cognitive and limb motor functions in patients with vascular dementia. *J. Clin. Exp. Med.* 5, 1160. doi: 10.3969/j.issn.1671-4695.2006.08.069

Wu, P., Mills, E., Moher, D., and Seely, D. (2010). Acupuncture in poststroke rehabilitation: a systematic review and meta-analysis of randomized trials. *Stroke* 41, e171–e179. doi: 10.1161/STROKEAHA.109.573576

Xie, X., and Junming, A. N. (2016). Clinical randomized controlled study of applying scalp acupuncture in treating vascular dementia. *J. Sichuan Trad. Chin. Med.* 34, 182.

Xu, L. (2006). *Clinical study on the treatment of vascular dementia with EX-HN1* (Master thesis). Guangzhou University of Chinese Medicine, Guangzhou, China.

Yang, J.-W., Wang, X.-R., Zhang, M., Xiao, L.-Y., Zhu, W., Ji, C.-S., et al. (2018). Acupuncture as a multifunctional neuroprotective therapy ameliorates cognitive impairment in a rat model of vascular dementia: a quantitative iTRAQ proteomics study. *CNS Neurosci. Ther.* 24, 1264–1274. doi: 10.1111/cns.13063

Yang, K., Song, X.-G., Ruan, J.-R., Cai, S.-C., Zhu, C.-F., Qin, X.-F., et al. (2021). Effect of moxibustion on cognitive function and proteins related with apoptosis of hippocampal neurons in rats with vascular dementia. *Zhongguo Zhen Jiu* 41, 1371–1378. doi: 10.13703/j.0255-2930.20210124-k0006

Yang, Y., Zhao, X., Zhu, Z., and Zhang, L. (2022). Vascular dementia: a microglia's perspective. *Ageing Res. Rev.* 81, 101734. doi: 10.1016/j.arr.2022.101734

Yao, J. (2020). *Clinical effect of electroacupuncture at sishencong point combined with donepezil on subcortical arteriosclerotic encephalopathy* (Master thesis). Heilongjiang University of Chinese Medicine, Harbin, China. doi: 10.27127/d.cnki.ghlzu.2020.000201

Ye, Y., Li, H., Yang, J.-W., Wang, X.-R., Shi, G.-X., Yan, C.-Q., et al. (2017). Acupuncture attenuated vascular dementia-induced hippocampal long-term potentiation impairments via activation of D1/D5 receptors. *Stroke* 48, 1044–1051. doi: 10.1161/STROKEAHA.116.014696

Yin, J. Q., Li-Hong, L. I., and Feng, A. C. (2011). Clinical observation to improve symptoms in patients with vascular dementia treated with electric needle on scalp acupuncture. *Chin. Arch. Tradit. Chin. Med.* 29, 415–416. doi: 10.3109/9781841848433

Zhang, H., Zhao, L., He, C.-Q., Hu, K.-M., and Liu, J. (2008). Clinically multi-central randomized controlled study on scalp electroacupuncture for treatment of vascular dementia. *Zhongguo Zhen Jiu* 28, 783–787.

Zhang, H., Zhao, L., Zhu, M. J., and Fang, Y. J. (2006). Clinical research on cognition level and living quality of vascular dementia by scalp electric acupuncture. *J. Chengdu Univ. Tradit. Chin. Med.* 29, 6–15.

Zhao, L., Zhang, H., Zheng, Z., and Huang, J. (2009). Electroacupuncture on the head points for improving gnosia in patients with vascular dementia. *J. Tradit. Chin. Med.* 29, 29–34. doi: 10.1016/S0254-6272(09)60027-3

Zhou, W., and Zhou, Z. Y. (2012). Vascular dementia treated by scalp acupuncture plus body acupuncture therapy. *J. Clin. Acupunct. Moxibustion* 28, 11–14. doi: 10.3969/j.issn.1005-0779.2012.06.004

Zhu, H. (2020). *Clinical observation of cross-electric acupuncture in the treatment of vascular dementia* (Master thesis). Heilongjiang University of Chinese Medicine, Harbin, China. doi: 10.27127/d.cnki.ghlzu.2020.000252

Zhu, W., Wang, X.-R., Du, S.-Q., Yan, C.-Q., Yang, N.-N., Lin, L.-L., et al. (2018). Anti-oxidative and anti-apoptotic effects of acupuncture: role of thioredoxin-1 in the hippocampus of vascular dementia rats. *Neuroscience* 379, 281–291. doi: 10.1016/j.neuroscience.2018.03.029

frontiers | Frontiers in Neuroscience

TYPE Original Research
PUBLISHED 15 December 2022
DOI 10.3389/fnins.2022.1071068

OPEN ACCESS

EDITED BY
Guibo Sun,
Chinese Academy of Medical Sciences and Peking Union Medical College, China

REVIEWED BY
Ana Paula Pesarico,
Federal University of Pampa, Brazil
Ning Jiang,
Chinese Academy of Medical Sciences and Peking Union Medical College, China

*CORRESPONDENCE
Yan Huang
huangyan023@163.com
Wen-Xia Zhou
zhouwx@bmi.ac.cn

SPECIALTY SECTION
This article was submitted to Neuropharmacology, a section of the journal Frontiers in Neuroscience

RECEIVED 15 October 2022
ACCEPTED 28 November 2022
PUBLISHED 15 December 2022

CITATION
Wang C, Zhu M-H, Sun N, Shen W, Jiang N, Zhao Q-S, Zhang Y-X, Huang Y and Zhou W-X (2022) Isorhynchophylline ameliorates stress-induced emotional disorder and cognitive impairment with modulation of NMDA receptors. *Front. Neurosci.* 16:1071068. doi: 10.3389/fnins.2022.1071068

Isorhynchophylline ameliorates stress-induced emotional disorder and cognitive impairment with modulation of NMDA receptors

Chen Wang[1], Ming-Hao Zhu[1], Na Sun[1], Wei Shen[1], Ning Jiang[1], Qin-Shi Zhao[2], Yong-Xiang Zhang[1], Yan Huang[1]* and Wen-Xia Zhou[1]*

[1]State Key Laboratory of Toxicology and Medical Countermeasures, Beijing Institute of Pharmacology and Toxicology, Beijing, China, [2]State Key Laboratory of Phytochemistry and Plant Resources in West China, Kunming Institute of Botany, Chinese Academy of Sciences (CAS), Kunming, China

Introduction: Isorhynchophylline is one of the main active ingredients from *Uncaria rhynchophylla*, the effects and mechanisms of isorhynchophylline on stress-induced emotional disorders and cognitive impairment remain unclear.

Methods: Long-term potentiation (LTP) *in vivo* was used for synaptic plasticity evaluation; chronic unpredictable mild stress (CUMS) model was used to evaluate the effect of isorhynchophylline on stress induced emotional disorders and cognitive impairment; sucrose preference test (SPT), open field test (OFT), and elevated plus maze (EPM) were used to evaluate emotional disorders; morris water maze (MWM) test was used to evaluate cognitive impairment; Western blotting (WB) was used to the expression of proteins; high performance liquid chromatography (HPLC) was used to quantify neurotransmitters; Nissl staining was used to identify pathological changes induced by stress.

Results: In this study, we found that isorhynchophylline improved corticosterone-induced *in vivo* LTP impairment significantly, indicating positive effects on stress. Therefore, 28-day CUMS model was adopted to evaluate the anti-stress effects of isorhynchophylline. The results showed that isorhynchophylline improved CUMS-induced weight loss, anxiety- and depression-like behaviors, and spatial memory impairment. Isorhynchophylline reduced CUMS-induced corticosterone elevation. N-methyl-D-aspartic acid (NMDA) receptors play an important role in the process of emotion and memory. Glutamate and the expression of GluN2B increased in the CUMS mice, while D-serine and the expression of serine racemase (SR) decreased significantly, and isorhynchophylline restored these changes to normal level.

Conclusion: These results indicated that isorhynchophylline ameliorated stress-induced emotional disorders and cognitive impairment, modulating NMDA receptors might be one of the underlying mechanisms.

KEYWORDS

isorhynchophylline (PubChem CID: 3037048), corticosterone, long-term potentiation, chronic unpredictable mild stress, D-serine, NMDA receptors

1 Introduction

Stress is broadly defined as an anticipated disruption of homeostasis or a threat to wellbeing (Kim and Diamond, 2002; McEwen, 2007; Ulrich-Lai and Herman, 2009). A number of stress-associated diseases have been identified in humans, such as hypertension, diabetes, gastric-intestinal ulceration (Kim et al., 2006). High-intensity stress could not only cause anxiety and depression symptoms (Willner, 2017; Lupien et al., 2018), but also increase the risk of various neurological disorders (McEwen, 2000; Radahmadi et al., 2014). Alleviating the symptoms like anxiety and depression is the primary treatment in clinic, the commonly used drugs are serotonin reuptake inhibitors, such as sertraline and fluoxetine (Giacomini et al., 2016; Noorafshan et al., 2019; Rauch et al., 2019). Recently, the N-methyl-D-aspartate (NMDA) receptors antagonist ketamine or its S (+)-isomer has been used for the treatment of stress-induced depressive disorders and post-traumatic stress disorder (PTSD) in both humans and animals (Feder et al., 2014; Brachman et al., 2016; McGowan et al., 2018; Wang et al., 2022). However, the current drugs could only alleviate stress-induced emotional disorders like anxiety and depression with little improvement on stress-induced cognitive impairment, and these drugs might even cause cognitive impairment in long-term use (Luo et al., 2021).

Isorhynchophylline is one of the main active ingredients from *Uncaria rhynchophylla*. *Uncaria rhynchophylla*, a traditional Chinese medicine, which is mainly used to treat cardiovascular and central nervous systems diseases, such as lightheadedness, convulsions, numbness, and hypertension (Shi et al., 2003). Modern pharmacological researches reveal that isorhynchophylline has multiple neural protective effects. Isorhynchophylline could improve cognitive impairment in Alzheimer's disease (Xian et al., 2014a), D-galactose (Xian et al., 2014b), aluminum chloride (Li et al., 2018) and ischemia (Kang et al., 2004) animal models. Isorhynchophylline could also ameliorate neural plasticity deficits caused by many factors, such as ischemia, D-galactose and aluminum chloride (Kang et al., 2004; Xian et al., 2014b; Li et al., 2018). Reducing beta-amyloid peptide (Aβ)-induced neurotoxicity, neuronal apoptosis and tau protein hyperphosphorylation (Xian et al., 2012, Xian et al., 2013, 2014a) contributed to isorhynchophylline's neural protective effects. NMDA and 5-HT_2 receptors (Kang et al., 2002, 2004) were the potential targets for isorhynchophylline. Recently, it has reported that isorhynchophylline had antidepressant-like effects (Xian et al., 2017, 2019). These results indicate that isorhynchophylline has potential effects on stress-induced emotional disorders and cognitive impairment. Thus, this study is to investigate whether isorhynchophylline has protective effect against stress-induced emotional disorders and cognitive impairment.

Corticosterone is both the biomarker and effector molecule of stress in rodents. Excess corticosterone could cause cognitive (Dominguez et al., 2019) and neural plasticity impairments (Wang et al., 2021; Huang et al., 2022). Therefore, corticosterone induced long-term potentiation (LTP) impairment was used for preliminary evaluation of isorhynchophylline. Then the 28-day chronic unpredictable mild stress (CUMS) model was adopted to confirm whether isorhynchophylline could alleviate emotional disorders and cognitive impairment, and finally observing the effect of isorhynchophylline on CUMS-induced dysfunction of NMDA receptor.

2 Materials and methods

2.1 Animals and drug treatment

Two-month-old male C57BL/6J mice, which is commonly used for CUMS model (Lu et al., 2019), were purchased from Beijing Vital River Laboratory Animal Technology Co., Ltd. Mice were kept in plastic cages and allowed free access to food and water under standard housing conditions (room temperature 23 ± 1°C and humidity of 55 ± 5%) with a 12-h light/12-h dark cycle. Experiments started after 7 days acclimating to the laboratory environment. The Institute of Animal Care and Use Committee of the National Beijing Center for Drug Safety Evaluation and Research approved all the experiments (No.: IACUC-DWZX-2021-590).

For *in vivo* electrophysiology, 50 mg/kg corticosterone (CORT, TCIchemicals, Shanghai, China) was used to mimic stress 60 min before high frequency stimulation (HFS). Both intracerebroventricular and intragastric administration were used in this study. Intracerebroventricular administration only used for preliminary evaluation; intragastric administration, which is like clinical routine, was used for further evaluation. For intracerebroventricular administration, 2 μg per animal

(isorhynchophylline) was used; For intragastric administration, 20/40/80 mg/kg isorhynchophylline was used.

For intracerebroventricular injection, the coordinates are: −0.22 mm from Bregma, 1 mm lateral to the sagittal suture and 2.5 mm deep from the skull surface, according to *Mouse Brain in Stereotaxic Coordinates* (Franklin and Paxinos, 2008). A syringe pump, at a rate of 1 μl/min, was used to deliver the drug into the right lateral ventricle. The needle was left in place for 1 min after discontinuation of plunger movement to prevent backflow.

For CUMS, mice were separated into three groups, which were Control group (Control), chronic unpredictable mild stress group (CUMS) and chronic unpredictable mild stress + isorhynchophylline group (Iso). Isorhynchophylline was intragastric administered 20 mg/kg/day from the −7 to 28 d. Mice in Control and CUMS groups were given equal volumes of 0.5% sodium carboxymethyl cellulose (Sigma-Aldrich Corporation).

2.2 *In vivo* LTP recording

In vivo LTP recording was conducted as previously described (Huang et al., 2013). Mice were anesthetized with pentobarbital sodium,then fitted with ear cuffs and placed in a stereotaxic frame. A stimulating electrode (stainless steel bipolar) was placed in the perforant path (PP), the evoked potentials were recorded with a stainless-steel electrode in the cell body layer of dentate gyrus (DG). The WinLTP program[1] was used to initiate the electrical stimulus and record the data. After obtaining a stable stimulus–response curve baseline at fixed current intensity, the current intensity was regulated to evoke a 1/3–1/2 maximum population spike (PS) amplitude. After recording the 30 min baseline, LTP was induced by high-frequency stimulus (HFS) (250 Hz, three trains 10 s apart, eight 0.1 ms pulses in each train), and PSs were recorded for another 60 min. The mean PS amplitudes during 0–30 min was normalized to 100% as baseline; the relative PS amplitudes (31–90 min) were normalized relative to the baseline period before HFS.

2.3 Chronic unpredictable mild stress procedure

According to the previous description (Willner, 2017; Liu M. Y. et al., 2018), the CUMS procedure was conducted for 28 days. CUMS-treated mice were subjected to 14 stressors with a random schedule. These stressors include food deprivation (24 h), water deprivation (24 h), cage tilt (24 h, 45°), dark during the day (12 h), lights on at night (12 h), damp bedding (24 h), no bedding (24 h), noise stimulation (1 h, 100 dB), electric shock (1 h, 0.8 mA, 5 s/min), tail pinch (1 min), tail suspension (30 min), cage shake (1 h, 220 r/min), restrained in tube (2 h) and cold water swimming (6 min, 10 °C), the detailed schedule is shown in **Table 1**.

2.4 Behavior tests

2.4.1 Sucrose preference test (SPT)

The SPT was according to previous description (Liu M. Y. et al., 2018). Four days before CUMS, all animals were habituated to drink sucrose solution (1%, w/v) by replacing normal water for 2 days (48 h). The position of the bottles was changed several times during the period. During test, all mice were deprived of food and water for 24 h, starting at 10 a.m. 24 h later. Each animal was provided with 1% sucrose solution and normal water individually for 1 h, and the weights of sucrose solution and water consumed were recorded accordingly.

2.4.2 Open field test

The OFT was performed as described previously (Huang et al., 2017). The arena was partitioned into peripheral area and central area. After 30 min acclimation in the test room, mice were allowed to explore the open field for 5 min and then they were returned to home age. Central area duration and visits were recorded as indicators of anxiety and exploratory behaviors.

2.4.3 Elevated plus maze (EPM)

The elevated plus-maze apparatus was elevated 100 cm above the floor. The maze consisted of two open arms (50 cm × 10 cm) and two closed arms (50 cm × 10 cm × 10 cm) joined by a central square (10 cm × 10 cm). mice were put in the central square and allowed to explore for 5 min, then they were returned to home age.

TABLE 1 The protocol of 28 days chronic unpredictable mild stress.

Day week	Day 1	Day 2	Day 3	Day 4	Day 5	Day 6	Day 7
Week 1	LN	FD	CT	DB	DD	NB	WD
	RS	CW	TP	ES	TS	CS	NS
Week 2	NB	WD	DB	RS	DD	FD	DB
	CW	DD	TS	TP	CW	CT	CS
Week 3	NB	WD	RS	CT	DD	FD	LN
	TS	NB	NS	ES	TP	CT	TS
Week 4	DD	WD	CT	DB	FD	LN	WD
	CW	ES	CS	RS	TP	TS	NS

FD, food deprivation (24 h); WD, water deprivation (24 h); CT, cage tilt (24 h, 45°); DD, dark during the day (12 h); LN, lights on at night (12 h); DB, damp bedding (24 h); NB, no bedding (24 h); NS, noise stimulation (1 h, 100 dB); ES, electric shock (1 h, 0.8 mA, 5 s/min), TP, tail pinch (1 min), TS, tail suspension (30 min); CS, cage shake (1 h, 220r/min); RS, restrained in tube (2 h); CW, cold water swimming (6 min, 10°C).

1 http://www.winltp.com

2.4.4 Morris water maze (MWM) test

The MWM test was performed as described previously (Vorhees and Williams, 2006). The learning phase contained four trials per day for five consecutive days and the probe trial was carried out on the sixth day. During the learning phase, mice were allowed to find the platform for 60 s, if the mouse failed to find the platform on time, it was guided to the platform and remained on the platform for 15 s. During the probe trial phase, mice were given a 60 s exploring period in the pool without platform, the latency and time in the target quadrant were regarded as indicators of memory.

The order of these tests is: Sucrose Preference Test, Open Field Test, Elevated plus Maze, Morris Water Maze Test.

2.5 Corticosterone evaluation

Plasma corticosterone was measured by an enzyme-linked immunosorbent assay kit (Cloud-Clone Corp, USA) according to the Instruction manual.

2.6 Western blotting (WB)

Western blotting was performed as described previously with minor modifications (Taylor and Posch, 2014). Ten mg hippocampal samples were homogenized in 0.1 ml lysis buffer and then centrifuged at 15,000 g for 15 min at 4°C. The concentrations of protein were determined by Bradford protein assay kit (PR102, Galen Biopharm International Co., Ltd.). Equal amounts of protein were boiled in loading buffer (100 mM Tris–HCl of pH 6.8, 4% sodium dodecyl sulfate, 200 mM DTT, 0.2% bromophenol blue, and 20% glycerol) for 5 min before loading on a SDS polyacrylamide gel. Electrophoresis was performed at 60 V for 30 min and then 100 V for 90 min, followed by wet transfer onto a nitrocellulose membrane at 100 V for 60 min. The membrane was blocked for 60 min in blocking solution (5% non-fat dry milk, 0.05% Tween-20, phosphate buffered saline) and then incubated at 4°C overnight with rabbit anti-SR antibody (1:1000, Sigma-Aldrich) and rabbit anti-NR2A/B antibody (1:1,000, Sigma-Aldrich). After 30 min washes with 0.05% Tween-20, PBS, the primary antibodies were detected with the horseradish peroxidase-conjugated secondary antibodies and chemiluminescent HRP substrate (Thermo Fisher Scientific Inc., Waltham, MA, USA). Band density values were normalized to β-actin.

2.7 High performance liquid chromatography (HPLC)

HPLC was performed as described previously with minor modifications (Grant et al., 2006). Hippocampal samples were homogenized in methanol and centrifuged for 15 min at 15,000 g at 4°C. The calculated amount of OPA was dissolved in 5 mL of methanol in a volumetric flask and diluted to the mark with a borate buffer solution (PH = 9.3). The sample was derivatizated for 35 min before loading sample. The mobile phase contains a buffered solution containing 0.1 M NaH_2PO_4, 20 m 0.1 mM Na_2EDTA and its pH was adjusted to 5.8 with phosphoric acid. The flow rate was 0.75 ml/min, the detector potential was + 0.75 V with respect to the calomel reference electrode and the sensitivity was set at 50 nA full-scale detection. Chromatographic column is an Agilent reversed-phase chromatographic column (C-18, 4.6 mm × 250 mm, 5 μm).

2.8 Nissl staining

The mice brains were removed after anesthesia and fixed in 4% paraformaldehyde. The sections (4 μm) were stained using 0.5% cresyl violet acetate (Beyotime, China). The integrated optical density (IOD) of Nissl bodies was quantified by using Image J software (Version 1.48, National Institutes of Health).

2.9 Statistical analysis

The data are presented as the mean ± SEM. GraphPad Prism 6.0 (Inc., La Jolla, CA, USA) was used to plot and analyze the data. Student's *t*-test was used to analyze two groups and one-way analysis of variance (ANOVA) followed by Dunnett's multiple comparisons test was used when comparing more than two groups. A two-way repeated measures ANOVA was adopted to analyze the changes of body weight during CUMS and MWM escape latency during learning phase. $P < 0.05$ was considered as statistically significant.

3 Results

3.1 Effects of isorhynchophylline on hippocampal LTP in corticosterone-treated mice

The average values of the relative PS amplitudes in CORT-treated mice were significantly lower than that in the control mice, while isorhynchophylline (2 μg, i.c.v.) significantly reverse the decreased PS amplitudes (one-way ANOVA followed by Dunnett's tests; $F_{2,12} = 52.66$, $P < 0.001$; Cort *vs.* control: $P < 0.001$; 2 μg Iso *vs.* Cort: $P < 0.001$; $n = 5$; **Figures 1A, B**).

Subsequently, we observed the effect of single administration of isorhynchophylline (20/40/80 mg/kg, i.g.) on corticosterone-induced LTP impairment. Results showed the average values of the relative PS amplitudes in

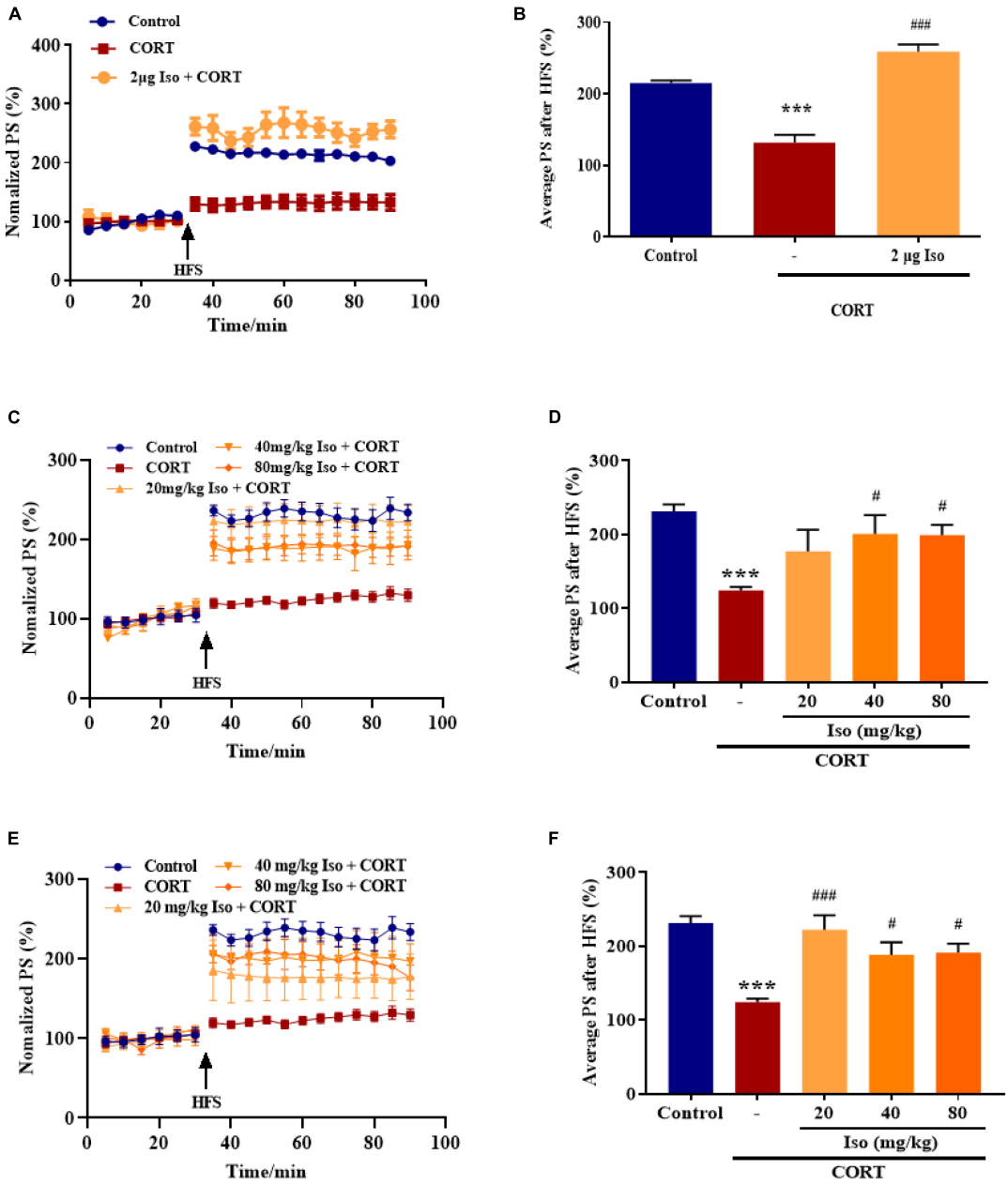

FIGURE 1
Effects of isorhynchophylline on hippocampal LTP in corticosterone (CORT)-treated mice. **(A)** The time course of average relative PS amplitudes. **(B)** The average relative PS amplitudes post-HFS (31–90 min). Isorhynchophylline (2 μg, i.c.v) significantly improved CORT-induced LTP impairment. CORT/vehicle was injected 60 min before HFS and isorhynchophylline was administrated 30 min before CORT/vehicle. **(C)** The time course of average relative PS amplitudes. **(D)** The average relative PS amplitudes post-HFS (31–90 min). Isorhynchophylline (40/80 mg/kg, i.g.) significantly improved CORT-induced LTP impairment. **(E)** The time course of average relative PS amplitudes. **(F)** The average relative PS amplitudes post-HFS (31–90 min). Isorhynchophylline (20/40/80 mg/kg for seven days, i.g.) significantly improved CORT-induced LTP impairment. The data are presented as mean ± SEM. $^{***}P < 0.001$ compared to the Control group; $^{\#}P < 0.05$, $^{\#\#\#}P < 0.001$ compared to the corticosterone group.

CORT-treated mice were significantly lower than that in the control mice, while 40 and 80 kg/mg isorhynchophylline significantly reverse the decreased PS amplitudes and 20 mg/kg isorhynchophylline showed no effect (one-way ANOVA followed by Dunnett's tests; $F_{4,20} = 6.204$, $P = 0.002$; Cort *vs.* control: $P < 0.001$; 20 mg/kg Iso *vs.* Cort: $P = 0.105$; 40 mg/kg Iso *vs.* Cort: $P = 0.013$; 80 mg/kg Iso *vs.* Cort: $P = 0.014$; n = 5; Figures 1C, D).

Then, we observed the effect of administration of isorhynchophylline (20/40/80 mg/kg, i.g.) for 7 consecutive days

on corticosterone-induced LTP impairment. Results showed that 20, 40 and 80 kg/mg isorhynchophylline significantly reverse the decreased PS amplitudes by corticosterone (one-way ANOVA followed by Dunnett's tests; $F_{4,20} = 9.177$, $P < 0.001$; Cort *vs.* control: $P < 0.001$; 20 mg/kg Iso *vs.* Cort: $P < 0.001$; 40 mg/kg Iso *vs.* Cort: $P = 0.026$; 80 mg/kg Iso *vs.* Cort: $P = 0.021$; $n = 5$; Figures 1E, F).

These results showed that both central and peripheral administration of isorhynchophylline significantly improved corticosterone-induced LTP impairment, indicating potential effects on stress.

3.2 Effects of isorhynchophylline on emotional disorder in CUMS mice

The body weight in the control group kept increasing stably; the body weight in the CUMS group was significantly lower than that of the control group on the 7th, 14th, 21st, and 28th day, and isorhynchophylline improved the body weights on the 28th day (two-way repeated measures ANOVA followed by Dunnett's tests; Time: $P < 0.001$; Treatment: $P < 0.001$; Day 1: CUMS *vs.* control: $P = 0.578$; Iso *vs.* CUMS: $P = 0.856$; Day 7: CUMS *vs.* control: $P = 0.039$; Iso *vs.* CUMS: $P = 0.837$; Day 14: CUMS *vs.* control: $P < 0.001$; Iso *vs.* CUMS: $P = 0.708$; Day 21: CUMS *vs.* control: $P < 0.001$; Iso *vs.* CUMS: $P = 0.979$; Day 28: CUMS *vs.* control: $P < 0.001$; Iso *vs.* CUMS: $P = 0.015$; $n = 10$; Figure 2A).

For SPT test, the results showed the sucrose preference index of mice in the CUMS group was significantly lower than that in the control group, and isorhynchophylline improved the sucrose preference indexes (one-way ANOVA followed by Dunnett's tests; $F_{2,27} = 8.566$, $P = 0.001$; CUMS *vs.* control: $P = 0.003$; Iso *vs.* CUMS: $P = 0.002$; $n = 10$; Figure 2B).

For OFT test, the results showed that the total distance increased in CUMS group significantly, while the central retention time is higher than that of the CUMS group, and isorhynchophylline improved theses changes in OFT (one-way ANOVA followed by Dunnett's tests; For total distance: $F_{2,27} = 8.784$, $P = 0.001$; CUMS *vs.* control: $P < 0.001$; Iso *vs.* CUMS: $P = 0.022$; For central retention time: $F_{2,27} = 7.509$, $P = 0.003$; CUMS *vs.* control: $P = 0.002$; Iso *vs.* CUMS: $P = 0.013$; $n = 10$; Figures 2C, D).

For EPM test, the results showed that the open arm time and open arm entries were significantly decreased in CUMS group, and isorhynchophylline improved theses changes in EPM (one-way ANOVA followed by Dunnett's tests; For open arm time: $F_{2,27} = 6.655$, $P = 0.005$; CUMS *vs.* control: $P = 0.003$; Iso *vs.* CUMS: $P = 0.029$; For open arm entries: $F_{2,27} = 6.401$, $P = 0.005$; CUMS *vs.* control: $P = 0.004$; Iso *vs.* CUMS: $P = 0.021$; $n = 10$; Figures 2E, F).

These results suggested that isorhynchophylline effectively alleviated anxiety- and depression- like behaviors of mice caused by CUMS.

3.3 Effects of isorhynchophylline on the spatial memory in CUMS mice

During the learning phase, the escape latency of mice in each group showed a downward trend and there was no statistical difference among groups (Figure 3A). During the probe phase, the escape latency in the CUMS group was significantly longer than that in the control group, and isorhynchophylline improved the latency significantly (one-way ANOVA followed by Dunnett's tests; $F_{2,27} = 5.770$, $P = 0.008$; CUMS *vs.* control: $P = 0.011$; Iso *vs.* CUMS: $P = 0.014$; $n = 10$; Figure 3B).The time in the target quadrant of the CUMS group was significantly shorter than that of the control group, and isorhynchophylline improved the time in the target quadrant significantly (one-way ANOVA followed by Dunnett's tests; $F_{2,27} = 7.769$, $P = 0.002$; CUMS *vs.* control: $P = 0.045$; Iso *vs.* CUMS: $P = 0.001$; $n = 10$; Figure 3C). There was no difference in the swimming speed of the mice in each group during the probe phase (Figure 3D).

The above results suggested that isorhynchophylline effectively improved the spatial memory deficit in mice caused by CUMS.

3.4 The mechanisms of isorhynchophylline on CUMS mice

The plasma corticosterone in the CUMS group was significantly increased compared with control, and corticosterone in the isorhynchophylline group was significantly lower than that in the CUMS group (one-way ANOVA followed by Dunnett's tests; $F_{2,12} = 13.16$, $P < 0.001$; CUMS *vs.* control: $P = 0.009$; Iso *vs.* CUMS: $P < 0.001$; $n = 5$; Figure 4A). The hippocampus glutamate in the CUMS group increased compared with control, and the glutamate in the isorhynchophylline group was significantly lower than that in the CUMS group (one-way ANOVA followed by Dunnett's tests; $F_{2,12} = 12.37$, $P = 0.001$; CUMS *vs.* control: $P = 0.011$; Iso *vs.* CUMS: $P < 0.001$; $n = 5$; Figure 4B). The hippocampus D-serine, the NMDA receptors co-agonist, was significantly reduced in the CUMS group, and the content of D-serine in the isorhynchophylline group was higher than that of the CUMS group (one-way ANOVA followed by Dunnett's tests; $F_{2,12} = 3.215$, $P = 0.076$; CUMS *vs.* control: $P = 0.048$; Iso *vs.* CUMS: $P = 0.299$; $n = 5$; Figure 4C).

The expression of SR, a key synthetase of hippocampal D-serine, was significantly decreased in the CUMS group, while the expression of SR in the isorhynchophylline group was significantly higher than that in the CUMS group (one-way ANOVA followed by Dunnett's tests; $F_{2,12} = 9.771$, $P = 0.003$; CUMS *vs.* control: $P = 0.003$; Iso *vs.* CUMS: $P = 0.007$; $n = 5$; Figure 4D). The expression of hippocampal GluN2A in the CUMS group showed an increasing trend, and the expression of

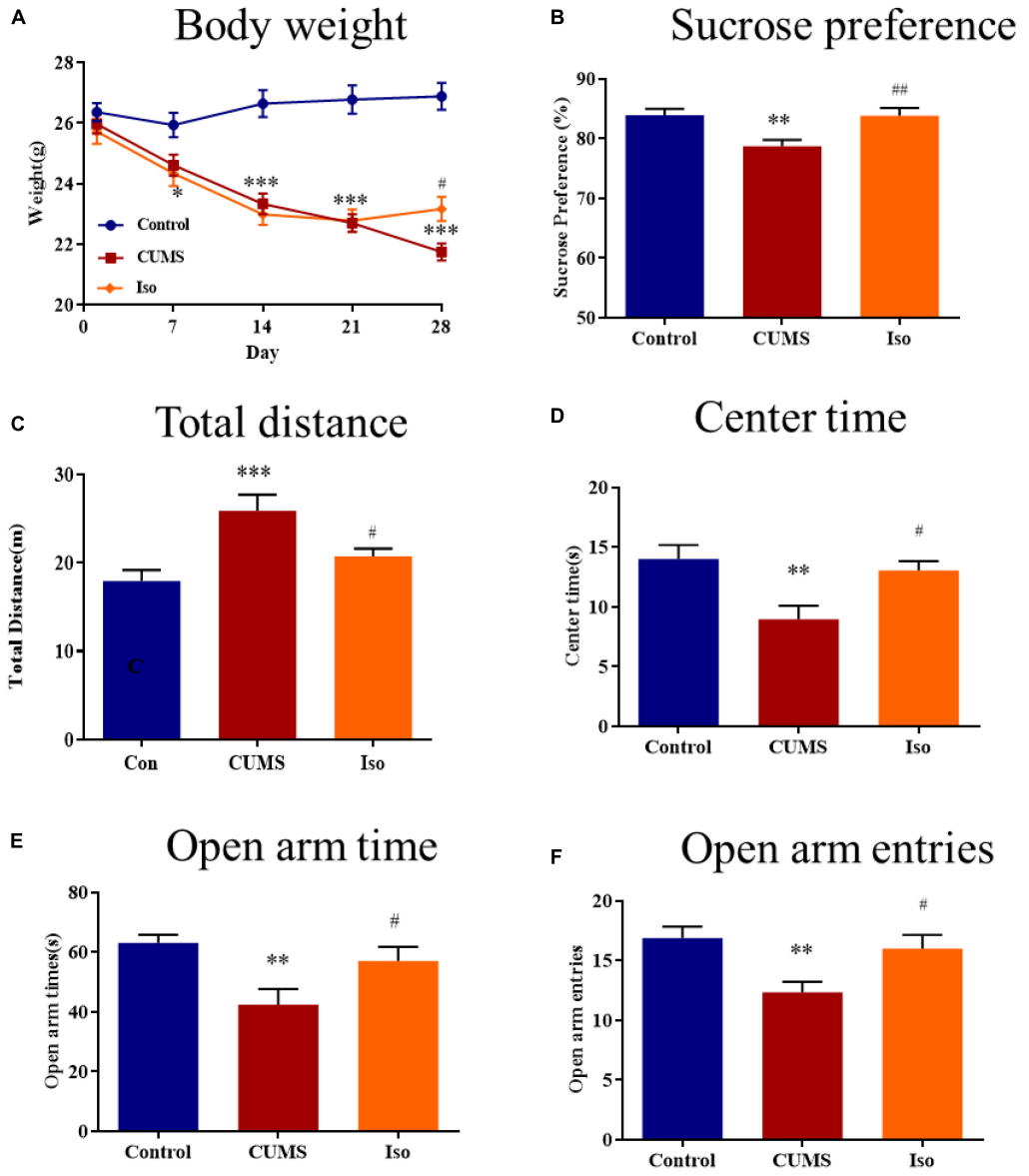

FIGURE 2
Effects of isorhynchophylline on body weight, sucrose preference, open field test and elevated plus maze in CUMS mice. **(A)** Isorhynchophylline significantly alleviated CUMS-induced body weight loss. **(B)** Isorhynchophylline significantly increased sucrose preference index in CUMS mice. **(C)** Isorhynchophylline significantly decreased total distance in CUMS mice. **(D)** Isorhynchophylline significantly increased central retention time in CUMS mice. **(E)** Isorhynchophylline significantly increased open arm times in CUMS mice. **(F)** Isorhynchophylline significantly open arm entries in CUMS mice. The data are presented as mean ± SEM. $^{**}P < 0.01$, $^{***}P < 0.001$ compared to the Con group; $^{\#}P < 0.05$, $^{\#\#}P < 0.01$ compared to the CUMS group.

GluN2A in the hippocampus in the isorhynchophylline group was significantly lower than that of the CUMS group (one-way ANOVA followed by Dunnett's tests; $F_{2,12} = 3.664$, $P = 0.057$; CUMS *vs.* control: $P = 0.171$; Iso *vs.* CUMS: $P = 0.038$; $n = 5$; Figure 4E). The expression of GluN2B in the CUMS group was significantly higher than that in the control group, and the GluN2B expression in the isorhynchophylline group was significantly lower than that in the CUMS group (one-way ANOVA followed by Dunnett's tests; $F_{2,12} = 6.32$, $P = 0.013$; CUMS *vs.* control: $P = 0.016$; Iso *vs.* CUMS: $P = 0.020$; $n = 5$; Figure 4F).

Nissl staining results showed that the IOD of Nissl bodies was significantly lower in the CUMS group than that in the control group, and IOD of Nissl bodies in isorhynchophylline group was significantly higher than that in CUMS group (one-way ANOVA followed by Dunnett's tests; $F_{2,12} = 5.230$, $P = 0.023$; CUMS *vs.* control: $P = 0.028$; Iso *vs.* CUMS: $P = 0.031$; $n = 5$; Figure 5).

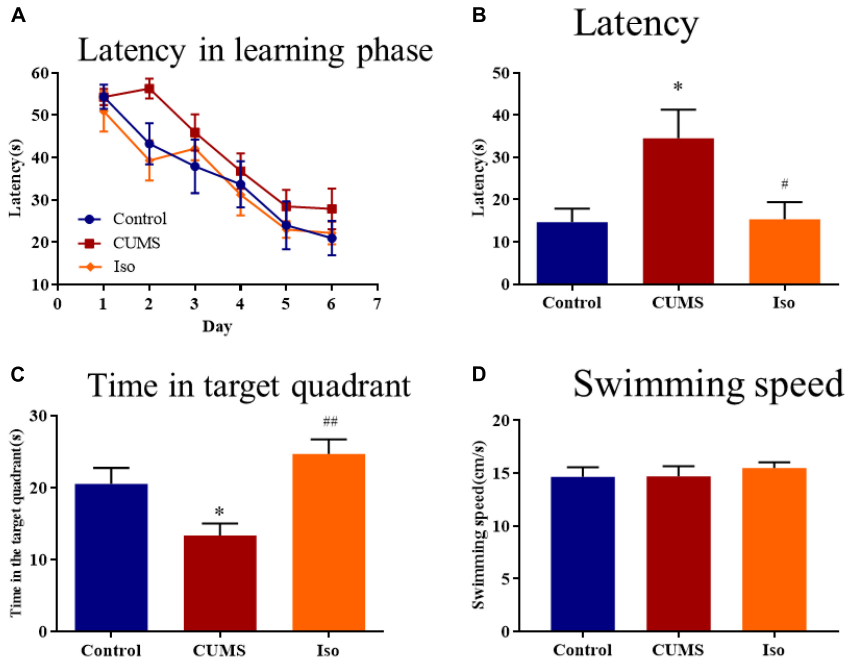

FIGURE 3
Effects of isorhynchophylline on the spatial memory in MWM test in CUMS mice. **(A)** The escape latency of mice in learning phase. **(B)** The escape latency in probe trial was significantly decreased by isorhynchophylline in CUMS mice. **(C)** The time spent in the target quadrant was significantly increased by isorhynchophylline in CUMS mice. **(D)** There was no difference in swimming speed in each group. The data are presented as mean ± SEM. $^{*}P < 0.05$ compared to the con group; $^{\#}P < 0.05$, $^{\#\#}P < 0.01$ compared to the CUMS group.

4 Discussion

When endogenous or exogenous environmental stimuli is perceived as aversive, or threatening, the systemic neuroendocrine response is activated, this process is called stress response (Lucassen et al., 2014). Stress can activate the HPA axis, and glucocorticoids are one of the main biomarkers for stress (Akirav, 2004; Mora et al., 2012). There are 2 types of receptors for glucocorticoids, the mineralocorticoid receptor (MR) and the glucocorticoid receptor (GR) (Reul and de Kloet, 1985). Both MR and GR expressed in hippocampus (Reul and De Kloet, 1986), and related to stress-induced cognition impairment and emotional disorders. Stress or glucocorticoids have been shown to modulate cognitive function and synaptic plasticity (McEwen and Sapolsky, 1995; Diamond et al., 1996; Kim et al., 1996; Sandi et al., 1997; Cao et al., 2016). Long-term stress has also been shown to induced morphological changes in the hippocampus (Lee et al., 2009; Schoenfeld and Gould, 2012). In addition, hippocampus also important to anxiety (Barkus et al., 2010) and depression (Sahay and Hen, 2007). Therefor this study focused on hippocampus.

The level of corticosterone was assessed as a biomarker of stress in rodents, it was reported that chronic stress could induce plasma corticosterone increasing sustainedly (Bernatova et al., 2018). Sustained corticosterone rise is a key factor for stress-induced memory deficits (Dominguez et al., 2019). It was also reported that corticosterone itself could cause hippocampal synaptic plasticity and cognitive impairment (Pavlides et al., 1993; Howland and Wang, 2008). Therefore, corticosterone was adopted to mimic stress. Results showed that single administration of corticosterone *via* subcutaneous injection impaired hippocampal LTP in mice *in vivo* significantly, both intracerebroventricular and intragastric administrated of isorhynchophylline reversed corticosterone-induced LTP impairment, suggesting that isorhynchophylline may have protective effect against stress-induced synaptic and cognitive impairment. Previous study reported that intragastric administration of isorhynchophylline 20 mg/kg for 7 days had anti-depression effects (Xian et al., 2017), and 20 mg/kg isorhynchophylline was sufficient to reverse corticosterone-induced LTP impairment in this study. So 20 mg/kg isorhynchophylline was adopted for further observing its effect on emotional disorders and cognitive impairment caused by chronic stress.

Chronic unpredictable mild stress is widely used to investigate stress induced disorders, such as depression and cognitive impairment (Shang et al., 2017; Willner, 2017; Antoniuk et al., 2019). Therefore, CUMS was adopted in this study. Results showed that CUMS caused weight loss, in accord with previous study (Willner et al., 1996), and isorhynchophylline significantly alleviated CUMS-induced weight loss. The plasma corticosterone was assessed as a

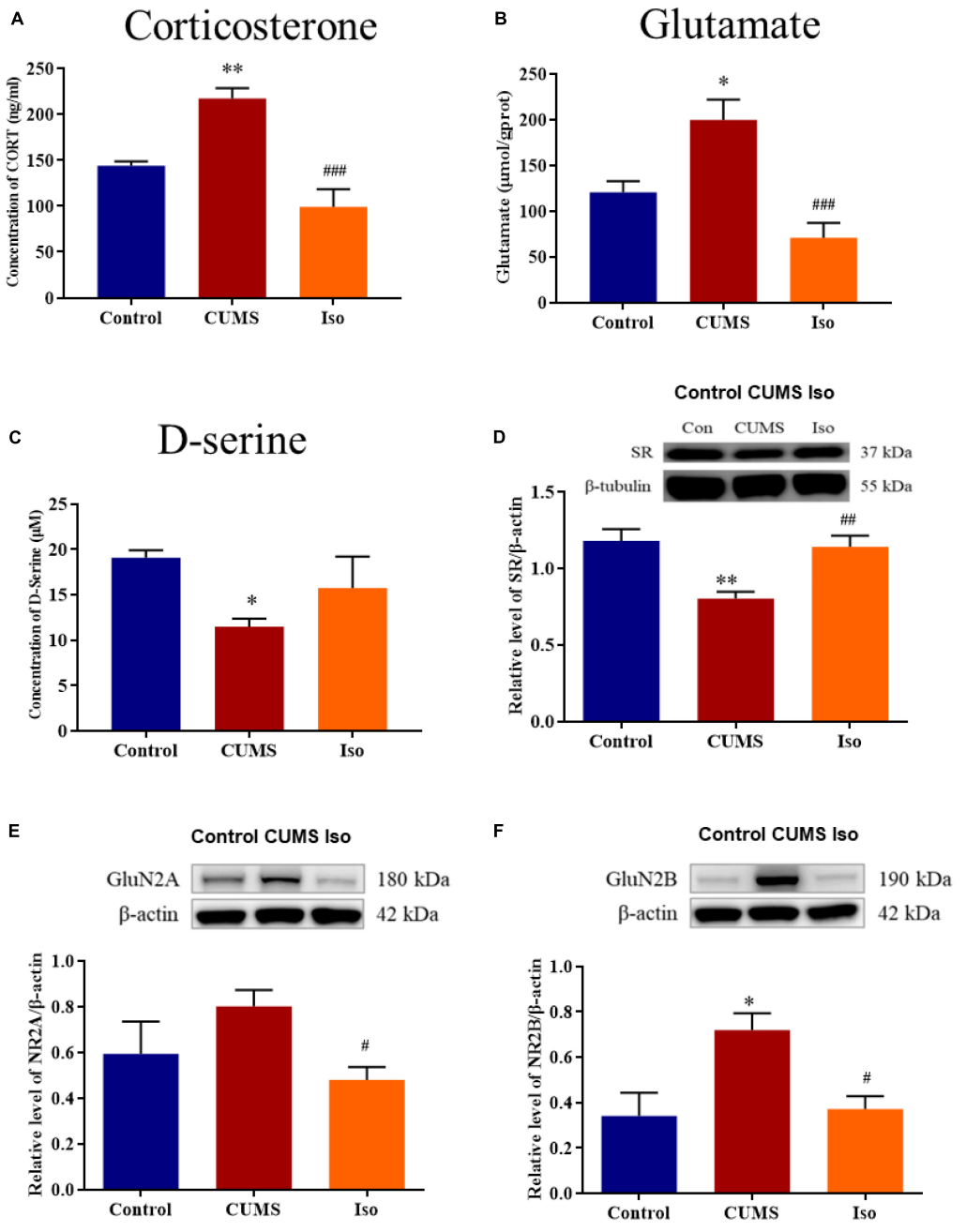

FIGURE 4
Effects of isorhynchophylline on plasma corticosterone, glutamate, SR, D-serine, GluN2A and GluN2B in CUMS mice. **(A)** Isorhynchophylline significantly decreased the serum corticosterone level in CUMS mice. **(B)** Isorhynchophylline significantly decreased the hippocampal glutamate level in CUMS mice. **(C)** Isorhynchophylline increased the level of D-serine in CUMS mice. **(D)** Isorhynchophylline significantly increased the expression of SR in CUMS mice. **(E)** Isorhynchophylline significantly decreased the expression of GluN2A in CUMS mice. **(F)** Isorhynchophylline significantly decreased the expression of GluN2B in CUMS mice. The data are presented as mean ± SEM. $^{*}P < 0.05$, $^{**}P < 0.01$ compared to the Con group; $^{\#}P < 0.05$, $^{\#\#}P < 0.01$, $^{\#\#}P < 0.001$ compared to the CUMS group.

biomarker of stress, previous research showed that attenuating corticosterone on the day of memory assessment prevented chronic stress-induced spatial memory impairments (Wright et al., 2006), our results also showed that isorhynchophylline decreased elevated corticosterone in CUMS mice, indicating that isorhynchophylline may reduce stress response. SPT was used to evaluate depression-like behavior, results showed that CUMS caused depression-like behavior, in accord with previous reports (Qiao et al., 2016; Liu W. et al., 2018), and isorhynchophylline alleviated CUMS-induced depression-like

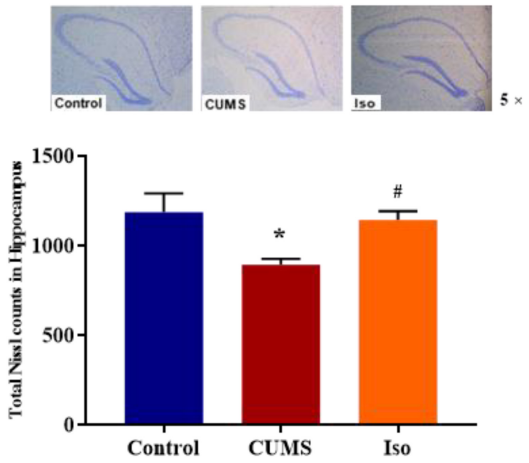

FIGURE 5
Effects of isorhynchophylline on Nissl staining in hippocampus. The data are presented as mean ± SEM. $^{*}P < 0.05$ compared to the Con group; $^{\#}P < 0.05$ compared to the CUMS group.

behavior in line with reported results (Xian et al., 2017). For anxiety-like behavior, OPT and EPM were adopted. The results showed that isorhynchophylline significantly enhanced the exploratory behavior of CUMS mice, suggesting that the anxiety symptoms were efficiently relieved by isorhynchophylline. MWM test is the most commonly used experiment to evaluate spatial learning and memory (Vorhees and Williams, 2006). CUMS-induced cognitive impairment has been widely reported (Gu et al., 2014; Shen et al., 2018, 2019), our results also showed that CUMS caused spatial memory deficit in mice and isorhynchophylline reversed this impairment. These results indicates that isorhynchophylline improved both emotional disorder and cognitive impairment.

Synaptic structure is the biological basis of learning and memory (Luscher and Malenka, 2012), normal synaptic transmission requires presynaptic glutamate and D-serine to bind to NMDA receptors to maintain synaptic plasticity and cognitive function (Hardingham and Bading, 2010). It's reported that chronic stress induced glutamate elevation (Garcia-Garcia et al., 2009; Hill et al., 2012; Willner, 2017) and NMDA receptors expression increasing (Liu et al., 2019; Lorigooini et al., 2020) in hippocampal tissue, indicating hyperfunction of NMDA receptors. On the other hand, chronic stress induced D-serine deficit (Wang et al., 2017), indicating hypofunction of NMDA receptors. Our previous studies provide possible explanation for this paradox. Previous data showed that acute stress or corticosterone administration may cause hypofunction of NMDA receptors by inhibiting D-serine release, despite of increasing glutamate (Wang et al., 2021). Long-term hypofunction of NMDA receptor, on the condition of chronic stress, might cause compensatory NMDA receptor expression, as showed in published data (Liu et al., 2019; Lorigooini et al., 2020) and this study. Isorhynchophylline improved LTP impairment by corticosterone *via* ICV administration, indicating isorhynchophylline improved corticosterone induced NMDA receptors hypofunction. Additionally, isorhynchophylline restored CUMS induced glutamate and D-serine disturbance, and modulated the expression of serine racemase (SR) and NMDA receptors. Altogether, these results indicate that modulating the function of NMDA receptor may be involved in the effect of

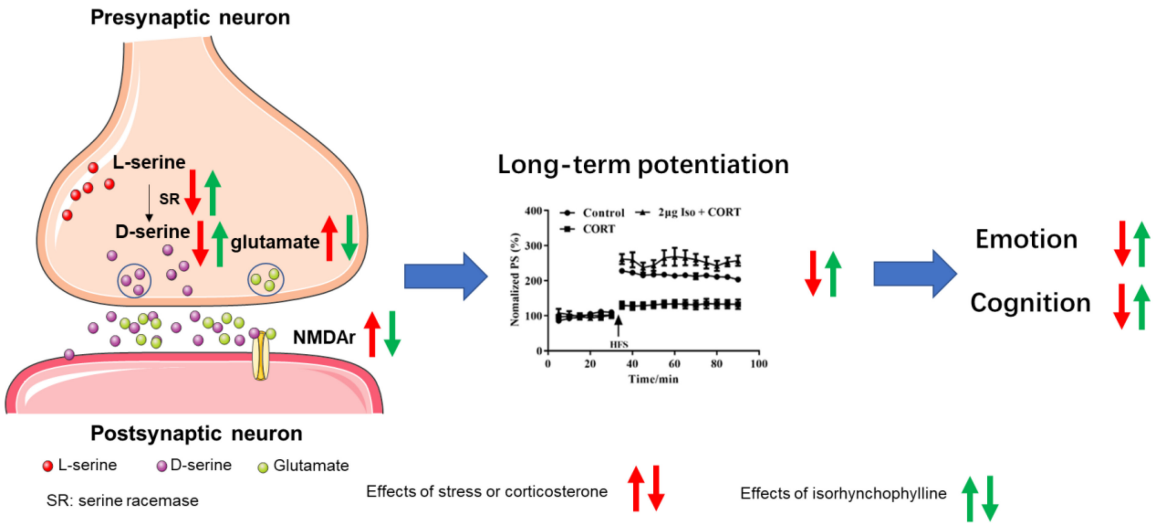

FIGURE 6
Sketch map for the mechanisms of isorhynchophylline on CUMS induced emotional disorders and cognitive impairment.

isorhynchophylline on alleviating cognitive deficits induced by CUMS (**Figure 6**).

5 Conclusion

In conclusion, isorhynchophylline has protective effect against stress-induced emotional disorders and cognitive impairment simultaneously, restoring the function of NMDA receptors to normal might be one of its mechanisms. Nevertheless, the underlying mechanisms are more complex than it was described above and further investigations are needed.

Data availability statement

The original contributions presented in this study are included in the article/supplementary material, further inquiries can be directed to the corresponding authors.

Ethics statement

This animal study was reviewed and approved by the Institute of Animal Care and Use Committee (IACUC) of the National Beijing Center for Drug Safety Evaluation and Research (NBCDSER).

Author contributions

YH, W-XZ, and Y-XZ conceived the study and participated in design. CW conducted most of the experiments. WS, M-HZ, and NJ conducted parts of the experiments. CW and YH wrote and revised the manuscript. W-XZ and Y-XZ revised the manuscript. NS participated in the analysis of the results of the electrophysiological experiment. Q-SZ provided isorhynchophylline used in this study. All authors contributed to the article and approved the submitted version.

Conflict of interest

The authors declare that the research was conducted in the absence of any commercial or financial relationships that could be construed as a potential conflict of interest.

Publisher's note

All claims expressed in this article are solely those of the authors and do not necessarily represent those of their affiliated organizations, or those of the publisher, the editors and the reviewers. Any product that may be evaluated in this article, or claim that may be made by its manufacturer, is not guaranteed or endorsed by the publisher.

References

Akirav, I. (2004). A facilitative role for corticosterone in the acquisition of a spatial task under moderate stress. *Learn. Mem.* 11, 188–195. doi: 10.1101/lm.61704

Antoniuk, S., Bijata, M., Ponimaskin, E., and Wlodarczyk, J. (2019). Chronic unpredictable mild stress for modeling depression in rodents: Meta-analysis of model reliability. *Neurosci. Biobehav. Rev.* 99, 101–116.

Barkus, C., Mchugh, S. B., Sprengel, R., Seeburg, P. H., Rawlins, J. N., and Bannerman, D. M. (2010). Hippocampal NMDA receptors and anxiety: At the interface between cognition and emotion. *Eur. J. Pharmacol.* 626, 49–56. doi: 10.1016/j.ejphar.2009.10.014

Bernatova, I., Puzserova, A., Balis, P., Sestakova, N., Horvathova, M., Kralovicova, Z., et al. (2018). Chronic stress produces persistent increases in plasma corticosterone, reductions in brain and cardiac nitric oxide production, and delayed alterations in endothelial function in young prehypertensive rats. *Front. Physiol.* 9:1179. doi: 10.3389/fphys.2018.01179

Brachman, R. A., Mcgowan, J. C., Perusini, J. N., Lim, S. C., Pham, T. H., Faye, C., et al. (2016). Ketamine as a prophylactic against stress-induced depressive-like behavior. *Biol. Psychiatry* 79, 776–786.

Cao, G., Gong, S., Zhang, F., and Fu, W. (2016). Xiao Yao San against corticosterone-induced stress injury via upregulating glucocorticoid receptor reaction element transcriptional activity. *Evid. Based Complement. Alternat. Med.* 2016:5850739. doi: 10.1155/2016/5850739

Diamond, D. M., Fleshner, M., Ingersoll, N., and Rose, G. M. (1996). Psychological stress impairs spatial working memory: Relevance to electrophysiological studies of hippocampal function. *Behav. Neurosci.* 110, 661–672. doi: 10.1037//0735-7044.110.4.661

Dominguez, G., Henkous, N., Prevot, T., David, V., Guillou, J. L., Belzung, C., et al. (2019). Sustained corticosterone rise in the prefrontal cortex is a key factor for chronic stress-induced working memory deficits in mice. *Neurobiol. Stress* 10:100161. doi: 10.1016/j.ynstr.2019.100161

Feder, A., Parides, M. K., Murrough, J. W., Perez, A. M., Morgan, J. E., Saxena, S., et al. (2014). Efficacy of intravenous ketamine for treatment of chronic posttraumatic stress disorder: A randomized clinical trial. *JAMA Psychiatry* 71, 681–688.

Franklin, K., and Paxinos, G. (2008). *The mouse brain in stereotaxic coordinates, compact*. Cambridge, MA: Academic Press.

Garcia-Garcia, A. L., Elizalde, N., Matrov, D., Harro, J., Wojcik, S. M., Venzala, E., et al. (2009). Increased vulnerability to depressive-like behavior of mice with decreased expression of VGLUT1. *Biol. Psychiatry* 66, 275–282. doi: 10.1016/j.biopsych.2009.02.027

Giacomini, A., Abreu, M. S., Giacomini, L. V., Siebel, A. M., Zimerman, F. F., Rambo, C. L., et al. (2016). Fluoxetine and diazepam acutely modulate stress induced-behavior. *Behav. Brain Res.* 296, 301–310. doi: 10.1016/j.bbr.2015.09.027

Grant, S. L., Shulman, Y., Tibbo, P., Hampson, D. R., and Baker, G. B. (2006). Determination of d-serine and related neuroactive amino acids in human plasma by high-performance liquid chromatography with fluorimetric detection. *J. Chromatogr. B Analyt. Technol. Biomed. Life Sci.* 844, 278–282. doi: 10.1016/j.jchromb.2006.07.022

Gu, H. F., Nie, Y. X., Tong, Q. Z., Tang, Y. L., Zeng, Y., Jing, K. Q., et al. (2014). Epigallocatechin-3-gallate attenuates impairment of learning and memory in chronic unpredictable mild stress-treated rats by restoring hippocampal autophagic flux. *PLoS One* 9:e112683. doi: 10.1371/journal.pone.0112683

Hardingham, G. E., and Bading, H. (2010). Synaptic versus extrasynaptic NMDA receptor signalling: Implications for neurodegenerative disorders. *Nat. Rev. Neurosci.* 11, 682–696. doi: 10.1038/nrn2911

Hill, M. N., Hellemans, K. G., Verma, P., Gorzalka, B. B., and Weinberg, J. (2012). Neurobiology of chronic mild stress: Parallels to major depression. *Neurosci. Biobehav. Rev.* 36, 2085–2117.

Howland, J. G., and Wang, Y. T. (2008). Synaptic plasticity in learning and memory: Stress effects in the hippocampus. *Prog. Brain Res.* 169, 145–158.

Huang, H. J., Zhu, X. C., Han, Q. Q., Wang, Y. L., Yue, N., Wang, J., et al. (2017). Ghrelin alleviates anxiety- and depression-like behaviors induced by chronic unpredictable mild stress in rodents. *Behav. Brain Res.* 326, 33–43. doi: 10.1016/j.bbr.2017.02.040

Huang, Y., Li, D., Wang, C., Sun, N., and Zhou, W. X. (2022). Stachyose alleviates corticosterone-induced long-term potentiation impairment via the gut-brain axis. *Front. Pharmacol.* 13:799244. doi: 10.3389/fphar.2022.799244

Huang, Y., Yang, S., Hu, Z. Y., Liu, G., Zhou, W. X. and Zhang, Y. X. (2012). A new approach to location of the dentate gyrus and perforant path in rats/mice by landmarks on the skull. *Acta Neurobiol. Exp.* 72, 468–472.

Kang, T. H., Murakami, Y., Matsumoto, K., Takayama, H., Kitajima, M., Aimi, N., et al. (2002). Rhynchophylline and isorhynchophylline inhibit NMDA receptors expressed in *Xenopus* oocytes. *Eur. J. Pharmacol.* 455, 27–34. doi: 10.1016/s0014-2999(02)02581-5

Kang, T. H., Murakami, Y., Takayama, H., Kitajima, M., Aimi, N., Watanabe, H., et al. (2004). Protective effect of rhynchophylline and isorhynchophylline on in vitro ischemia-induced neuronal damage in the hippocampus: Putative neurotransmitter receptors involved in their action. *Life Sci.* 76, 331–343. doi: 10.1016/j.lfs.2004.08.012

Kim, J. J., and Diamond, D. M. (2002). The stressed hippocampus, synaptic plasticity and lost memories. *Nat. Rev. Neurosci.* 3, 453–462.

Kim, J. J., Foy, M. R., and Thompson, R. F. (1996). Behavioral stress modifies hippocampal plasticity through N-methyl-D-aspartate receptor activation. *Proc. Natl. Acad. Sci. U.S.A.* 93, 4750–4753. doi: 10.1073/pnas.93.10.4750

Kim, J. J., Song, E. Y., and Kosten, T. A. (2006). Stress effects in the hippocampus: Synaptic plasticity and memory. *Stress* 9, 1–11.

Lee, T., Jarome, T., Li, S. J., Kim, J. J., and Helmstetter, F. J. (2009). Chronic stress selectively reduces hippocampal volume in rats: A longitudinal magnetic resonance imaging study. *Neuroreport* 20, 1554–1558. doi: 10.1097/WNR.0b013e328332bb09

Li, H. Q., Ip, S. P., Zheng, G. Q., Xian, Y. F., and Lin, Z. X. (2018). Isorhynchophylline alleviates learning and memory impairments induced by aluminum chloride in mice. *Chin. Med.* 13:29. doi: 10.1186/s13020-018-0187-8

Liu, M. Y., Yin, C. Y., Zhu, L. J., Zhu, X. H., Xu, C., Luo, C. X., et al. (2018). Sucrose preference test for measurement of stress-induced anhedonia in mice. *Nat. Protoc.* 13, 1686–1698.

Liu, W., Xue, X., Xia, J., Liu, J., and Qi, Z. (2018). Swimming exercise reverses CUMS-induced changes in depression-like behaviors and hippocampal plasticity-related proteins. *J. Affect. Disord.* 227, 126–135. doi: 10.1016/j.jad.2017.10.019

Liu, Y., Cao, L., Zhang, X., Liang, Y., Xu, Y., and Zhu, C. (2019). Memantine differentially regulates tau phosphorylation induced by chronic restraint stress of varying duration in mice. *Neural Plast.* 2019:4168472. doi: 10.1155/2019/4168472

Lorigooini, Z., Nouri, A., Mottaghinia, F., Balali-Dehkordi, S., Bijad, E., Dehkordi, S. H., et al. (2020). Ferulic acid through mitigation of NMDA receptor pathway exerts anxiolytic-like effect in mouse model of maternal separation stress. *J. Basic Clin. Physiol. Pharmacol.* doi: 10.1515/jbcpp-2019-0263

Lu, Q., Mouri, A., Yang, Y., Kunisawa, K., Teshigawara, T., Hirakawa, M., et al. (2019). Chronic unpredictable mild stress-induced behavioral changes are coupled with dopaminergic hyperfunction and serotonergic hypofunction in mouse models of depression. *Behav. Brain Res.* 372:112053.

Lucassen, P. J., Pruessner, J., Sousa, N., Almeida, O. F., Van Dam, A. M., Rajkowska, G., et al. (2014). Neuropathology of stress. *Acta Neuropathol.* 127, 109–135.

Luo, Y., Yu, Y., Zhang, M., He, H., and Fan, N. (2021). Chronic administration of ketamine induces cognitive deterioration by restraining synaptic signaling. *Mol. Psychiatry.* 26, 4702–4718. doi: 10.1038/s41380-020-0793-6

Lupien, S. J., Juster, R. P., Raymond, C., and Marin, M. F. (2018). The effects of chronic stress on the human brain: From neurotoxicity, to vulnerability, to opportunity. *Front. Neuroendocrinol.* 49:91–105. doi: 10.1016/j.yfrne.2018.02.001

Luscher, C., and Malenka, R. C. (2012). NMDA receptor-dependent long-term potentiation and long-term depression (LTP/LTD). *Cold Spring Harb. Perspect. Biol.* 4:a005710.

McEwen, B. S. (2000). Effects of adverse experiences for brain structure and function. *Biol. Psychiatry* 48, 721–731.

McEwen, B. S. (2007). Physiology and neurobiology of stress and adaptation: Central role of the brain. *Physiol. Rev.* 87, 873–904.

McEwen, B. S., and Sapolsky, R. M. (1995). Stress and cognitive function. *Curr. Opin. Neurobiol.* 5, 205–216.

McGowan, J. C., Hill, C., Mastrodonato, A., Lagamma, C. T., Kitayev, A., Brachman, R. A., et al. (2018). Prophylactic ketamine alters nucleotide and neurotransmitter metabolism in brain and plasma following stress. *Neuropsychopharmacology* 43, 1813–1821. doi: 10.1038/s41386-018-0043-7

Mora, F., Segovia, G., Del Arco, A., De Blas, M., and Garrido, P. (2012). Stress, neurotransmitters, corticosterone and body–brain integration. *Brain Res.* 1476, 71–85. doi: 10.1016/j.brainres.2011.12.049

Noorafshan, A., Yousefi, M., Hosseini, L., and Karbalay-Doust, S. (2019). Can sertraline and nortriptyline protect the neurons in submucosal and myenteric plexuses of rat's colon against stress? *Dig. Dis. Sci.* 64, 2548–2554. doi: 10.1007/s10620-019-05600-y

Pavlides, C., Watanabe, Y., and Mcewen, B. S. (1993). Effects of glucocorticoids on hippocampal long-term potentiation. *Hippocampus* 3, 183–192.

Qiao, H., Li, M. X., Xu, C., Chen, H. B., An, S. C., and Ma, X. M. (2016). Dendritic spines in depression: What we learned from animal models. *Neural Plast.* 2016:8056370.

Radahmadi, M., Hosseini, N., and Nasimi, A. (2014). Effect of chronic stress on short and long-term plasticity in dentate gyrus; study of recovery and adaptation. *Neuroscience* 280, 121–129. doi: 10.1016/j.neuroscience.2014.09.005

Rauch, S. A. M., Kim, H. M., Powell, C., Tuerk, P. W., Simon, N. M., Acierno, R., et al. (2019). Efficacy of prolonged exposure therapy, sertraline hydrochloride, and their combination among combat veterans with posttraumatic stress disorder: A randomized clinical trial. *JAMA Psychiatry* 76, 117–126.

Reul, J. M. H. M., and De Kloet, E. R. (1986). Anatomical resolution of two types of corticosterone receptor sites in rat brain with in vitro autoradiography and computerized image analysis. *J. Steroid Biochem.* 24, 269–272. doi: 10.1016/0022-4731(86)90063-4

Reul, J. M., and de Kloet, E. R. (1985). Two receptor systems for corticosterone in rat brain: Microdistribution and differential occupation. *Endocrinology* 117, 2505–2511. doi: 10.1210/endo-117-6-2505

Sahay, A., and Hen, R. (2007). Adult hippocampal neurogenesis in depression. *Nat. Neurosci.* 10, 1110–1115.

Sandi, C., Loscertales, M., and Guaza, C. (1997). Experience-dependent facilitating effect of corticosterone on spatial memory formation in the water maze. *Eur. J. Neurosci.* 9, 637–642. doi: 10.1111/j.1460-9568.1997.tb01412.x

Schoenfeld, T. J., and Gould, E. (2012). Stress, stress hormones, and adult neurogenesis. *Exp. Neurol.* 233, 12–21.

Shang, X., Shang, Y., Fu, J., and Zhang, T. (2017). Nicotine significantly improves chronic stress-induced impairments of cognition and synaptic plasticity in mice. *Mol. Neurobiol.* 54, 4644–4658.

Shen, J., Li, Y., Qu, C., Xu, L., Sun, H., and Zhang, J. (2019). The enriched environment ameliorates chronic unpredictable mild stress-induced depressive-like behaviors and cognitive impairment by activating the Sirt1/miR-134 signaling pathway in hippocampus. *J. Affect. Disord.* 248, 81–90.

Shen, J., Xu, L., Qu, C., Sun, H., and Zhang, J. (2018). Resveratrol prevents cognitive deficits induced by chronic unpredictable mild stress: Sirt1/miR-134 signalling pathway regulates CREB/BDNF expression in hippocampus in vivo and in vitro. *Behav. Brain Res.* 349, 1–7. doi: 10.1016/j.bbr.2018.04.050

Shi, J. S., Yu, J. X., Chen, X. P., and Xu, R. X. (2003). Pharmacological actions of *Uncaria* alkaloids, rhynchophylline and isorhynchophylline. *Acta Pharmacol. Sin.* 24, 97–101.

Taylor, S. C., and Posch, A. (2014). The design of a quantitative western blot experiment. *Biomed. Res. Int.* 2014:361590.

Ulrich-Lai, Y. M., and Herman, J. P. (2009). Neural regulation of endocrine and autonomic stress responses. *Nat. Rev. Neurosci.* 10, 397–409.

Vorhees, C. V., and Williams, M. T. (2006). Morris water maze: Procedures for assessing spatial and related forms of learning and memory. *Nat. Protoc.* 1, 848–858.

Wang, C., Yu, Q., Li, D., Sun, N., Huang, Y., Zhang, Y. X., et al. (2021). Reduced D-serine release may contribute to impairment of long-term potentiation by corticosterone in the perforant path-dentate gyrus. *Neurochem. Res.* 46, 2359–2375. doi: 10.1007/s11064-021-03380-4

Wang, J., Zhang, K., Chen, X., Liu, X., Teng, H., Zhao, M., et al. (2017). Epigenetic activation of Asct2 in the hippocampus contributes to depression-like behavior by regulating D-serine in mice. *Front. Mol. Neurosci.* 10:139. doi: 10.3389/fnmol.2017.00139

Wang, Q., Xiao, M., Sun, H., and Zhang, P. (2022). A study on the preventive effect of esketamine on postpartum depression (PPD) after cesarean section. *Comput. Math. Methods Med.* 2022:1524198. doi: 10.1155/2022/1524198

Willner, P. (2017). The chronic mild stress (CMS) model of depression: History, evaluation and usage. *Neurobiol. Stress* 6, 78–93. doi: 10.1016/j.ynstr.2016.08.002

Willner, P., Moreau, J. L., Nielsen, C. K., Papp, M., and Sluzewska, A. (1996). Decreased hedonic responsiveness following chronic mild stress is not secondary to loss of body weight. *Physiol. Behav.* 60, 129–134.

Wright, R. L., Lightner, E. N., Harman, J. S., Meijer, O. C., and Conrad, C. D. (2006). Attenuating corticosterone levels on the day of memory assessment prevents chronic stress-induced impairments in spatial memory. *Eur. J. Neurosci.* 24, 595–605.

Xian, Y. F., Fan, D., Ip, S. P., Mao, Q. Q., and Lin, Z. X. (2017). Antidepressant-like effect of isorhynchophylline in mice. *Neurochem. Res.* 42, 678–685.

Xian, Y. F., Ip, S. P., Li, H. Q., Qu, C., Su, Z. R., Chen, J. N., et al. (2019). Isorhynchophylline exerts antidepressant-like effects in mice via modulating neuroinflammation and neurotrophins: Involvement of the PI3K/Akt/GSK-3beta signaling pathway. *FASEB J.* 33, 10393–10408. doi: 10.1096/fj.201802743RR

Xian, Y. F., Lin, Z. X., Mao, Q. Q., Chen, J. N., Su, Z. R., Lai, X. P., et al. (2013). Isorhynchophylline protects PC12 Cells against beta-amyloid-induced apoptosis via PI3K/AKT signaling pathway. *Evid. Based Complement. Alternat. Med.* 2013:163057. doi: 10.1155/2013/163057

Xian, Y. F., Lin, Z. X., Mao, Q. Q., Ip, S. P., Su, Z. R., and Lai, X. P. (2012). Protective effect of isorhynchophylline against beta-amyloid-induced neurotoxicity in Pc12 cells. *Cell. Mol. Neurobiol.* 32, 353–360.

Xian, Y. F., Mao, Q. Q., Wu, J. C., Su, Z. R., Chen, J. N., Lai, X. P., et al. (2014a). Isorhynchophylline treatment improves the amyloid-beta-induced cognitive impairment in rats via inhibition of neuronal apoptosis and tau protein hyperphosphorylation. *J. Alzheimers Dis.* 39, 331–346. doi: 10.3233/JAD-131457

Xian, Y. F., Su, Z. R., Chen, J. N., Lai, X. P., Mao, Q. Q., Cheng, C. H., et al. (2014b). Isorhynchophylline improves learning and memory impairments induced by D-galactose in mice. *Neurochem. Int.* 76, 42–49. doi: 10.1016/j.neuint.2014.06.011

frontiers | Frontiers in Neuroscience

TYPE Original Research
PUBLISHED 20 January 2023
DOI 10.3389/fnins.2023.1093180

OPEN ACCESS

EDITED BY
Dennis Chang,
Western Sydney University, Australia

REVIEWED BY
Chaohua Li,
Peking University, China
He Zhang,
Guang'anmen Hospital, China Academy of Chinese Medical Sciences, China

*CORRESPONDENCE
Yu Cao
✉ yu.cao-xiyuan@outlook.com
Hao Li
✉ xyhplihao1965@126.com

†These authors have contributed equally to this work and share first authorship

SPECIALTY SECTION
This article was submitted to Neuropharmacology, a section of the journal Frontiers in Neuroscience

RECEIVED 08 November 2022
ACCEPTED 06 January 2023
PUBLISHED 20 January 2023

CITATION
Yao J, Wei W, Wen J, Cao Y and Li H (2023) The efficacy and mechanism of berberine in improving aging-related cognitive dysfunction: A study based on network pharmacology.
Front. Neurosci. 17:1093180.
doi: 10.3389/fnins.2023.1093180

The efficacy and mechanism of berberine in improving aging-related cognitive dysfunction: A study based on network pharmacology

Jiuxiu Yao[1†], Wei Wei[2,3†], Jiayu Wen[4], Yu Cao[3*] and Hao Li[2,3*]

[1]College of First Clinical Medicine, Shandong University of Traditional Chinese Medicine, Jinan, China, [2]Wangjing Hospital, China Academy of Chinese Medical Sciences, Beijing, China, [3]Department of Geriatrics, Xiyuan Hospital, China Academy of Chinese Medical Sciences, Beijing, China, [4]Graduate College, Beijing University of Chinese Medicine, Beijing, China

Objective: To analyze the effects and mechanisms of berberine in the treatment of aging-related cognitive dysfunction based on network pharmacology methods, molecular docking techniques, and animal experiments.

Methods: A mouse model of cognitive dysfunction was constructed by subcutaneous injection of D-galactose (D-gal) for 10 weeks, and the neuroprotective effects of berberine on aging-related cognitive dysfunction mice were evaluated by the Morris water maze (MWM) and immunofluorescence staining. The targets of berberine were obtained by SwissTargetPrediction, GeneCards, and PharmMapper. Putative targets of cognitive dysfunction were obtained by GeneCards, TTD, and DrugBank database. The STRING database and Cytoscape software were applied for protein-protein interaction (PPI) analysis and further screening of core targets. The DAVID database was used for Kyoto Encyclopedia of Genes and Genomes (KEGG) and gene ontology (GO) enrichment analysis to clarify the biological processes and pathways involved in the intersection targets, and AutoDockTools was adopted for molecular docking verification of core targets. Finally, the core genes were validated using real-time quantitative PCR.

Results: The MWM results showed that treatment with berberine significantly improved spatial learning and memory in mice with cognitive decline induced by D-gal. Immunofluorescence staining indicated that berberine modified the levels of aging-related markers in the brain. A total of 386 berberine putative targets associated with cognitive dysfunction were identified based on the public database. The core targets of berberine for improving cognitive function, include *Mapk1*, *Src*, *Ctnnb1*, *Akt1*, *Pik3ca*, *Tp53*, *Jun*, and *Hsp90aa1*. GO enrichment and KEGG pathway enrichment analyses indicated that the mechanism of berberine in the treatment of aging-related cognitive dysfunction is attributed to pathways such as PI3K-AKT and MAPK pathways. *In vivo* experiments further confirmed that *Akt1*, *Ctnnb1*, *Tp53*, and *Jun* were involved in the neuroprotective actions of berberine.

Conclusion: This study reveals the multi-target and multi-pathway effects of berberine on regulating aging-related cognitive dysfunction, which provides preclinical evidence and may promote new drug development in mitigating cognitive dysfunction.

KEYWORDS

berberine, cognitive dysfunction, D-galactose, RT-qPCR, network pharmacology

1. Introduction

Cognitive dysfunction, also known as cognitive impairment (CI), is characterized by memory loss, learning disabilities, and a decreased ability to concentrate on a particular task. The spectrum of CI can range from mild cognitive deficits that are not clinically detectable to dementia (Luchsinger, 2012). Dementia is usually diagnosed when acquired cognitive impairment becomes severe enough to impair social and/or occupational functioning (Hugo and Ganguli, 2014). The CI leads to a reduced quality of life in older adults and increases the risk of dementia and mortality (Park et al., 2013; Hu et al., 2020). The population aged 80 years and older is the fastest-growing segment of the global population, and prevention of age-related cognitive dysfunction is one of the greatest challenges facing healthcare today.

Mild cognitive impairment (MCI) is considered to be a state between normal cognitive aging and early dementia (Petersen, 2004). Notably, approximately 16% of subjects diagnosed with MCI returned to normal or near-normal cognition after approximately 1 year (Koepsell and Monsell, 2012). In a meta-analysis evaluating the rate of progression from MCI to dementia in 41 cohort studies stratified by population studies and clinical trials, more than half of the participants did not progress to dementia within 10 years, and the annual conversion rate for dementia and Alzheimer's disease (AD) was approximately 7% (McGirr et al., 2022). In addition to the modification of some modifiable risk factors, treatment with traditional Chinese medicine (TCM) may play a role in the recovery of cognitive function.

Berberine (BBR) is an isoquinoline alkaloid, mainly found in the rhizome of *Coptis* sp., and the cortex of *Berberis* sp., and *Phellodendron* sp. Numerous studies have demonstrated multiple pharmacological effects of BBR, including anti-inflammatory (Jeong et al., 2009), anti-proliferative (Choi et al., 2008), hypoglycemic (Zhang et al., 2010; Pirillo and Catapano, 2015), hypocholesterolemic (Pirillo and Catapano, 2015), and anti-hypertensive effects (Bova et al., 1992). Previous studies have shown that BBR has antioxidant properties as well as protective effects against neurodegenerative diseases (Cheng et al., 2022), improving the cognitive decline associated with diabetes in db/db mice (Li et al., 2018). Recent studies have highlighted the anti-aging effects of BBR (Xu et al., 2017; Dang et al., 2020), which is considered to be one of the greatest risk factors for neurodegenerative diseases. Taken together, it will be of interest to explore the protective effects of BBR in neurodegenerative diseases.

D-galactose (D-gal) is an aldohexose naturally existing in the body, including in the brain (Nagy and Pohl, 2015). D-gal predisposes to aging and long-term systemic administration has been used to artificially produce brain aging phenotypes in animal models, which causes the onset of behavioral and cognitive deficits (Shwe et al., 2018). Several studies have illustrated that D-gal-induced brain aging not only contributes to memory deficits, neuronal degeneration, and apoptosis, but also increased oxidative stress, and mitochondrial dysfunction, which has many similarities to human brain aging (Banji et al., 2014). All these deficits eventually lead to cognitive decline. The amelioration of cognitive dysfunction by BBR has been observed in animal models of AD (Durairajan et al., 2012; Panahi et al., 2013). BBR has previously been observed to reduce the levels of endogenous oxidants and DNA damage response (Zhao et al., 2013), with potential effects of anti-aging (Dang et al., 2020; Li et al., 2022). However, the effects of BBR on cognitive impairment during aging have not been sufficiently investigated. In the current study, we investigated whether BBR reverses D-gal-induced aging and improves cognitive function in mice. The flow chart of this study is shown in **Figure 1**.

2. Materials and methods

2.1. Animals and general procedures

Eight-week-old male ICR mice ($n = 32$) were housed in eight cages. All animals were allowed free access to food and water and maintained at constant temperature ($22 \pm 3°C$) and humidity ($50 \pm 10\%$) during a 12-h light/dark cycle. The project was authorized by the Ethics Committee of Xiyuan Hospital, China Academy of Chinese Medical Sciences (No. 2021XLC035-3).

After 1 week of adaptive rearing, D-gal-induced cognitive dysfunction was performed by subcutaneous injection of D-gal for 10 weeks according to a previously described procedure (Sun et al., 2018; Daroi et al., 2022). Similarly, BBR was administered orally as previously described (Ma et al., 2021; Wang et al., 2022) to observe the protective benefits against aging-related cognitive impairment. Mice were randomly divided into the following four groups ($n = 8$ per group). (1) Control: subcutaneous injections of saline and oral distilled water, (2) Model: subcutaneous injections of D-gal (150 mg/kg/d) and oral distilled water, (3) BBR-L: subcutaneous injections of D-gal (150 mg/kg/d) and BBR orally (50 mg/kg), (4) BBR-H: subcutaneous injections of D-gal (150 mg/kg/d) and BBR orally (100 mg/kg).

2.2. Drug

Berberine (BBR), purity ≧98% (LDSW220209-1), provided by Shaanxi Lande Biotechnology Co., Ltd. D- (+) galactose (ST1218-50 g) purchased from Shanghai Beyotime Biotechnology Co., Ltd. Pentobarbital sodium salt (P3761) was purchased from Sigma, USA.

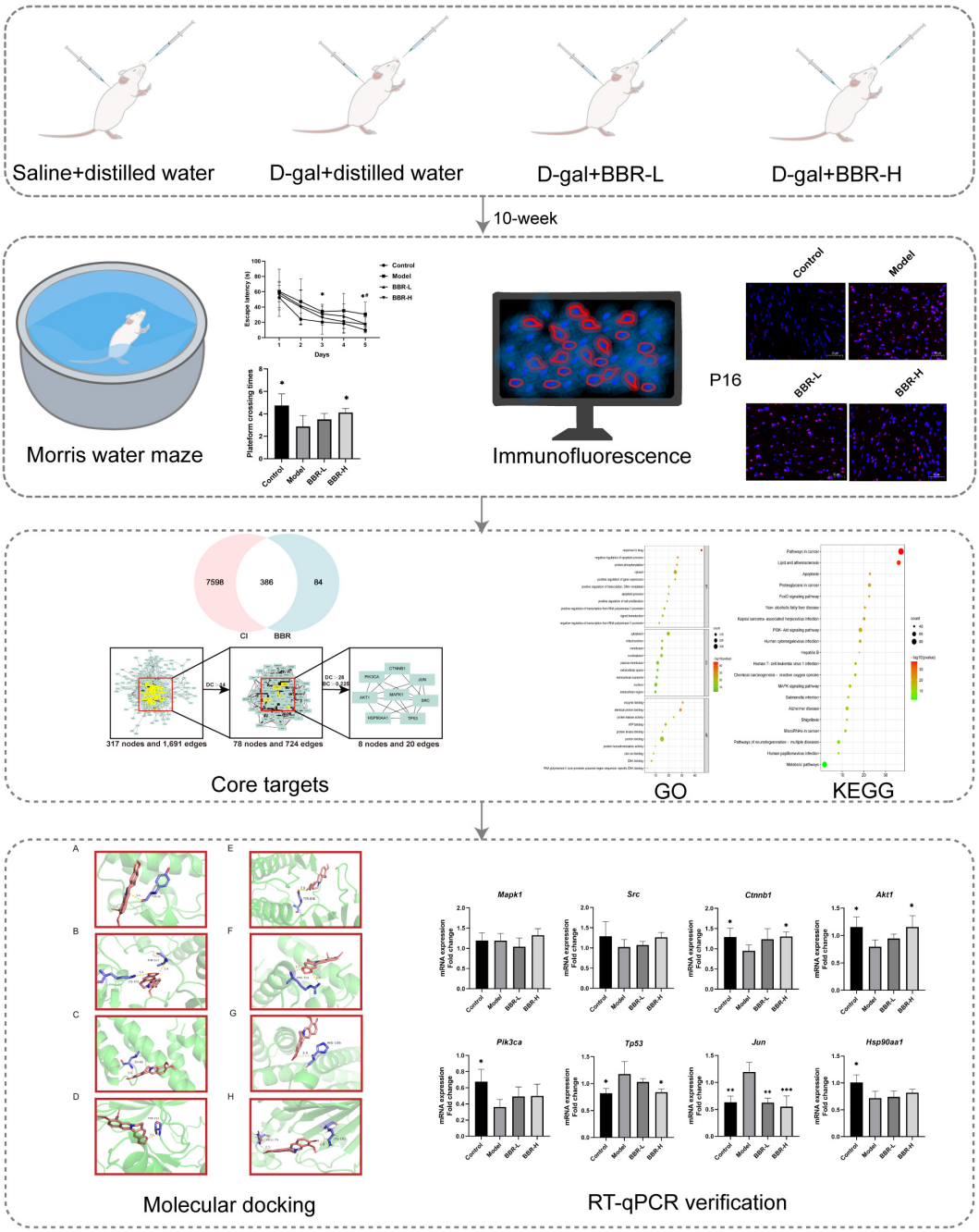

FIGURE 1
The flowchart of this study. Morris water maze: *$p < 0.05$ Control vs. Model; #$p < 0.05$ BBR-L/H vs. Model; RT-qPCR verification: *$p < 0.05$, **$p < 0.01$, and ***$p < 0.001$ vs. Model.

2.3. Morris water maze test

The Morris water maze (MWM) experiment was conducted for 6 days during the 10th week of dosing. The water maze apparatus consisted of a circular pool (120 cm in diameter and 50 cm in height), an automatic camera, and a computerized analysis system. The pool was divided equally into four quadrants, and a 12-cm diameter platform was placed in the first quadrant and filled with an appropriate amount of water so that the top of the platform was 1 cm below the water's surface. An appropriate amount of ink was poured into the water and mixed, and the water temperature was maintained at (23 ± 1)°C during the experiment. The MWM experiment consisted of two parts: navigation experiments and spatial probe experiments. On the day before the start of the experiment, each mouse was placed in the pool (without a platform) and swam freely for 90 s to adapt to the environment. The experiment started with 5 days of positioning navigation: each mouse was trained four times per day at 20-min intervals, with clockwise changes of entry points during the four training sessions. The mice were placed in the water facing the wall of the pool and the time between entering the water and finding the escape platform was recorded using a video tracking system, i.e., escape latency. If the platform could not be

found for 90 s, the mice were manually guided to the platform for 10 s. On day 6, the spatial exploration experiment was started: the escape platform for the positioning navigation experiment was removed, and the mice were placed in the water facing the wall of the pool (the entry point was the midpoint of the third quadrant), and the number of times they crossed the original platform area within 90 s was recorded, i.e., the number of times they crossed the platform.

2.4. Tissue preparation

Brain tissue was taken after MWM. Mice were deeply anesthetized with an intraperitoneal injection of sodium pentobarbital, and the brain was quickly removed from the skull. Three animals in each group were randomly selected. Each brain was divided into left and right halves through a mid-sagittal incision, and the left one was fixed with 4% paraformaldehyde for performing immunofluorescence staining. The remaining cortex was snap-freezing in liquid nitrogen and then transferred to −80°C for further analyses.

2.5. Immunofluorescence staining

Paraffin sections were dewaxed in xylene and rehydrated in ethanol and distilled water. After antigen retrieval with EDTA, sections were blocked in 3% BSA for 30 min at room temperature. The blocked solution was gently shaken off and the primary antibody, namely, Anti -CDKN2A/p16INK4a Rabbit pAb) (GB111143, Servicebio, Wuhan, China) was added to the sections and incubated overnight at 4°C. The next day, a secondary antibody (Cy3 conjugated Goat Anti-Rabbit IgG, GB21303, Servicebio, Wuhan, China) was added and incubated at room temperature for 1 h. After DAPI (G1012, Servicebio, Wuhan, China) stained the nuclei, the sections were dried slightly and then sealed with anti-fluorescence quenched sealing tablets. Images of the cortex were captured at ×20 magnification with a fluorescence microscope (Nikon DS-U3, Nikon).

2.6. Key targets screening for BBR to improve cognitive dysfunction

2.6.1. Identification of candidate targets for cognitive dysfunction

Three public disease-gene-related databases were used to retrieve important targets for Cognitive Dysfunction, including GeneCards[1] (Safran et al., 2021), DrugBank[2] (Wishart et al., 2018), and TTD (Zhou et al., 2022).[3] The search term "cognitive dysfunction" or "cognitive impairment" is used to screen potential disease targets for cognitive dysfunction, and the disease targets obtained from the three databases were combined and de-duplicated. UniProt[4] was used to standardize the gene names.

2.6.2. Identification of candidate targets for BBR

To identify the corresponding targets of BBR, target prediction of BBR was performed through three public databases, including GeneCards (see text footnote 1) (Safran et al., 2021), SwissTargetPrediction[5] (Daina et al., 2019), and PharmMapper[6] (Wang et al., 2017), while all targets were restricted to Homo sapiens. The genes obtained from these three databases were aggregated and duplicates were removed. The UniProt (see text footnote 4) (UniProt Consortium, 2020) database was used to standardize the gene names.

2.6.3. Construction of protein-protein interaction networks

Candidate target genes of BBR were intersected with CI-associated target genes to obtain intersecting genes and draw Venn diagrams, and these genes corresponding to both drugs and diseases were considered potential therapeutic targets. Online STRING 11.5[7] (Szklarczyk et al., 2021) was used to construct protein-protein interaction (PPI) networks. All networks were built with Cytoscape v3.8.2, software for analyzing and visualizing biological networks. The core networks were analyzed based on degree, betweenness centrality, close-ness centrality, and average shortest path length. In the network, the nodes represent the targets, while the edges represent the connections between them.

2.6.4. Enrichment analysis of GO and KEGG pathways

DAVID Bioinformatics Resource 2021[8] (Sherman et al., 2022) was used to analyze gene ontology (GO) enrichment and Kyoto Encyclopedia of Genes and Genomes (KEGG) pathway enrichment for key targets involved in biological process, cellular component, molecular function, and signaling pathway. The bioinformatics online analysis platform[9] was used to visualize the enrichment analysis results.

2.7. Molecular docking

The molecular structures of BBR were captured in the Traditional Chinese Medicine System Pharmacology database and Analysis Platform (TCMSP)[10] (Ru et al., 2014) and the molecular structures (crystal structures) of the target proteins were obtained from the PDB database (Protein Data Bank).[11] The molecular structures of BBR were captured in TCMSP (see text footnote 10) and the molecular structures (crystal structures) of the target proteins were obtained from the PDB database (Protein Data Bank, see text footnote 11). Pre-docking molecular processing was performed using AutoDockTools 1.5.7 software, and the pdbqt files were acquired. Molecular docking was performed using AutoDock Vina 1.1.2[12] software, and the affinity score was calculated, with a smaller value indicating a stronger

1 https://www.genecards.org/
2 https://go.drugbank.com/
3 https://db.idrblab.net/ttd/
4 https://www.uniprot.org/
5 http://swisstargetprediction.ch/
6 http://www.lilab-ecust.cn/pharmmapper/
7 https://string-db.org/
8 https://david.ncifcrf.gov/
9 https://www.bioinformatics.com.cn/
10 https://tcmsp-e.com/tcmsp.php
11 https://www.rcsb.org/
12 http://vina.scripps.edu/

bonding force. PyMOL2.4.0 software[13] was used to visualize the molecular docking results and calculate the Root Mean Square Deviation (RMSD) to verify the reliability, and the docking results were considered reliable with RMSD < 2A.

2.8. RT-qPCR

Total RNA was extracted from the mice's cerebral cortex using an RNA extraction kit (Servicebio, Wuhan, China, G3640-50T). Reverse-transcription of RNA to cDNA was performed using ReverTra Ace qPCR RT Master Mix (TOYOBO, FSQ-201) according to the manufacturer's instructions. Real-time qPCR was conducted on an ABI 7500 system using Applied Biosystems SYBR-Green PCR Master mix (Thermo Fisher Scientific, Inc., USA). The total reaction volume was 10 μL and primer sequences are shown in **Table 1**. The following amplification steps were used: initial denaturation at 95°C for 10 min, followed by 40 denaturation cycles at 95°C for 15 s, and elongation at 60°C for 60 s. *Gapdh* was used as a housekeeping gene. Relative mRNA expression was calculated using the $2^{-\Delta\Delta Ct}$ method. Three replicates were performed for each group.

3. Statistics

Data were presented as mean ± SEM. MWM task data were analyzed using repeated-measures analysis of variance (ANOVA). The results of Mauchly's test of sphericity were first used to determine whether there was a correlation between the repeated measures data and if there was a correlation ($p \leq 0.05$), a multivariate ANOVA was performed, or the Greenhouse–Geisser correction was applied. Pairwise comparisons between different subgroups at the same time point were performed using multivariate ANOVA. For data that did not involve repeated measures, two independent samples *t*-test or Mann–Whitney *U*-test was used for analysis. $p < 0.05$ was considered statistically significant. All statistical analyses were performed with SPSS software version 26.0. GraphPad Prism 8 was used for generating data plots.

4. Results

4.1. Effects of BBR on cognitive dysfunction

The MWM test is the most widely used laboratory behavioral test to assess cognitive deficits in rodents and the experimental protocol of MWM is as described previously (Vorhees and Williams, 2006). In the navigation test, as shown in **Figure 2A**, the escape latency of all mice gradually decreased with the increasing number of training sessions, indicating that their ability to locate the platform was enhanced. Compared with the control group, the escape latency of mice in the model group increased, with significant differences on days 3 and 5 ($p < 0.05$). The escape latency of mice in the BBR-L and BBR-H groups was diminished compared to the model group and exhibited a significant difference on day 5 ($p < 0.05$). In the exploratory experiment on day 6 (**Figure 2B**), the times of crossing the original platform were significantly reduced in the model group compared to the control group ($p < 0.05$). Both the BBR-L and BBR-H groups experienced an elevation in the number of mice crossing the original platform compared to the model group, with the BBR-H group showing a significant difference ($p < 0.05$). Collectively, these data suggest that we successfully induced aging-related cognitive dysfunction in mice, and more critically, we found that berberine ameliorated this cognitive impairment, although more studies are necessary to clarify the mechanisms involved.

4.2. BBR reduces the expression of P16 in brain tissue of cognitive dysfunctions mice

Aging is a common risk factor attributed to various neurodegenerative diseases, and aging of the brain eventually leads to CI. P16, a tumor suppressor gene can be considered the best biomarker of cellular senescence (Kim and Sharpless, 2006). Immunofluorescence staining of brain tissue for P16 at the end of administration to determine that D-gal caused aging-related cognitive dysfunction in mice. As shown in **Figure 2C**, P16 expression was significantly increased in the D-gal group compared with the control group, indicating that D-gal induced brain aging in mice. However, the administration of BBR altered the expression of senescence marker. Compared with the D-gal group, P16 expression was reduced in both the low- and high-dose groups of BBR. In conclusion, the above results suggest that BBR has anti-aging potential in the brain.

4.3. Results of network pharmacology study

4.3.1. Target network analysis

To further elucidate the mechanisms and targets of BBR for improving cognitive function, we conducted a network pharmacology study. We applied three public disease gene-related databases, including GeneCards, DrugBank, and TTD, to retrieve major targets for CI/cognitive dysfunction. Ultimately, a total of 7,984 recognized CI-associated genes were explored (**Supplementary Table 1**). To identify the corresponding targets for BBR, we aggregated all predicted targets from GeneCards, SwissTargetPrediction, and PharmMapper. Finally, 470 targets for BBR were obtained (**Supplementary Table 2**).

4.3.2. PPI network construction and core gene screening for BBR and CI

By intersecting candidate target genes of BBR with CI-related target genes, we identified genes intersecting with drugs and diseases as potential targets. The Venn diagram (**Figure 3A**) showed that there were 386 potential targets associated with both BBR and CI. Intersecting genes of BBR and CI were imported into the STRING database to construct the PPI network. We set the highest confidence level of 0.900 for the minimum required interaction score and hid the unlinked nodes in the network (**Figure 3B**). All network visualizations were implemented by Cytoscape. As shown in **Figure 3C**, the PPI network contains 317 nodes and 1,961 edges. Based on Degree and betweenness centrality, we selected the top 8 genes as hub genes (**Figures 3C–E**). These hub genes may represent the key molecular targets in the anti-CI action of BBR. Accordingly,

13 https://pymol.org/2/

TABLE 1 Primers used for quantitative real-time PCR.

Gene	Forward primer (5′-3′)	Reverse primer (5′-3′)
Mapk1	AACCTCCTGCTGAACACCACTT	CCACAGACCAAATATCAATGGACTT
Src	AGATCACTAGACGGGAATCAGAGC	GCACCTTTTGTGGTCTCACTCTC
Ctnnb1	GTTCTACGCCATCACGACACTG	AGGTCCTCATTATGTTTACTAAGGC
Akt1	TTTGGGAAGGTGATTCTGGTG	CAGGACACGGTTCTCAGTAAGC
Pik3ca	ATGGAGGAGAACCCTTATGTGAC	AGATTGAAAGGCAAAGGCGC
Tp53	CCCTCTGAGCCAGGAGACATT	CCCAGGTGGAAGCCATAGTTG
Jun	CCTTCTACGACGATGCCCTC	GGGTCGGTGTAGTGGTGATGT
Hsp90aa1	TTTACTCTGCCTATTTGGTTGCTG	CACAAAGAGAGTAATGGGATAGCC
Gapdh	CCTCGTCCCGTAGACAAAATG	TGAGGTCAATGAAGGGGTCGT

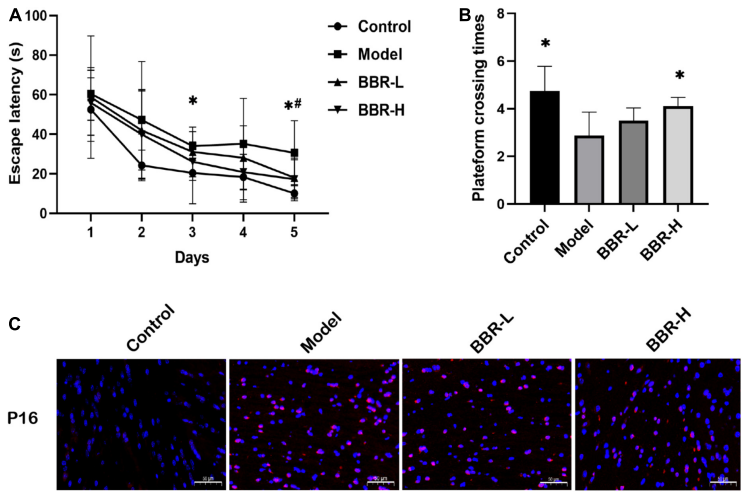

FIGURE 2
The results of Morris water maze (MWM) and immunofluorescence. **(A)** The escape latency. **(B)** The times across the platform (All data are mean ± SEM with $n = 8$, $^*p < 0.05$ Control vs. Model; $\#p < 0.05$ BBR-L/H vs. Model). **(C)** Immunofluorescence staining of P16 (×20, red = p16, blue = DAPI, scale bar 50 μm).

eight core target genes were obtained (Figure 3E), including *Mapk1*, *Src*, *Ctnnb1*, *Akt1*, *Pik3ca*, *Tp53*, *Jun*, and *Hsp90aa1*.

4.3.3. Enrichment analysis of BBR-CI target networks

Gene ontology (GO) analysis is commonly used to comprehensively characterize the contribution of genes in an organism, including biological processes, cellular components, and molecular functions. BBR therapeutic targets associated with CI were included in the analysis, and the results are shown in Figure 4A. KEGG is a database resource for understanding the high-level function and utility of biological systems from genomic and molecular level information. According to the KEGG pathway enrichment analysis (Figure 4B), the PI3K-Akt signaling pathway and MAPK signaling pathway were significantly enriched.

4.4. BBR-core targets molecular docking

Molecular docking of BBR and its corresponding core targets are achieved by AutoDock Vina software. It is generally believed that the smaller the affinity, the more stable the conformation of ligand-receptor binding and the higher the possibility of interaction. The molecular docking results demonstrated that BBR had a small affinity for all eight core targets (Table 2), indicating a favorable binding activity. The docking results are presented in Figure 5.

4.5. RT-qPCR validation of core genes

Further RT-qPCR was performed on brain tissues from mice in the four groups. The results (Figure 6) demonstrated that the expression of *Ctnnb1*, *Akt1*, *Pik3ca*, and *Hsp90aa1* was significantly lower in the model group compared with the control group ($p < 0.05$), the expression of *Src* showed a decreasing but not significant trend and the expression of *Tp53* and *Jun* was significantly higher ($p < 0.05$, $p < 0.01$, respectively). Compared with the model group, the expression of *Src*, *Ctnnb1*, *Akt1*, *Pik3ca*, and *Hsp90aa1* exhibited an increasing tendency in both the BBR-L and BBR-H groups, in which the expression of *Ctnnb1* and *Akt1* was significantly higher in the BBR-H group ($p < 0.05$). *Tp53* and *Jun* expression showed a decreasing trend and were significantly lower in the BBR-H group ($p < 0.05$, $p < 0.001$, respectively). Unfortunately,

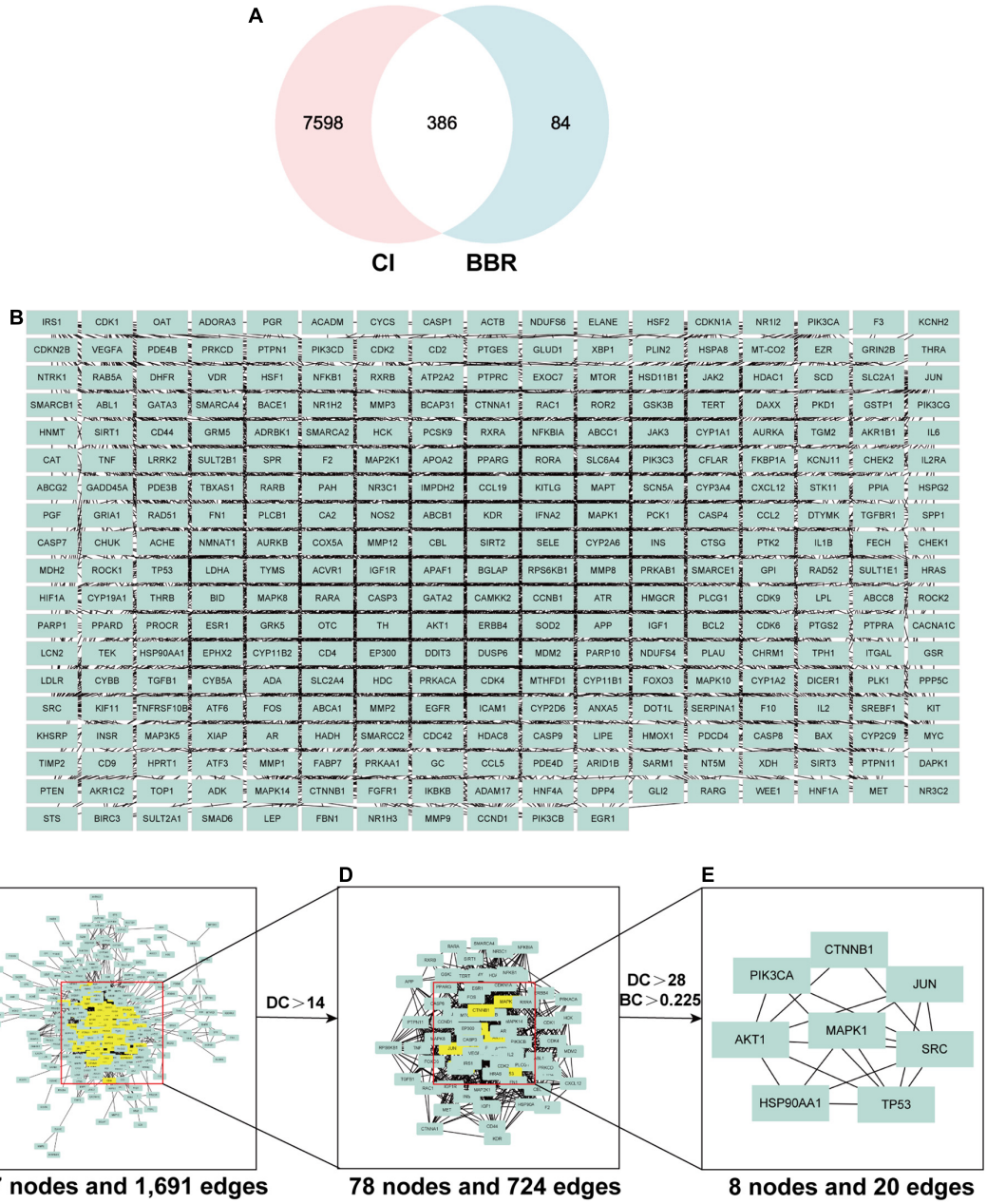

FIGURE 3
The screening process of core genes between cognitive impairment (CI) and berberine (BBR). **(A)** Venn diagram of CI and BBR overlapping genes. **(B)** Intersecting genes after screening. **(C)** Protein-protein interaction (PPI) network of intersecting genes. **(D)** PPI network of significant targets extracted from Panel **(C)**. **(E)** PPI network of candidate BBR targets for CI extracted from Panel **(D)**.

statistically significant results for *Mapk1* were not observed in our study.

5. Discussion

This study investigated the role and mechanism of BBR on aging-related spatial learning memory deficits due to D-gal with the assistance of network pharmacology and molecular docking techniques. Aging is considered to be the most important risk factor for neurodegenerative diseases, including AD. D-gal-induced aging mouse models have been widely used in aging studies, and long-term administration of D-gal induces aging, manifests neurological deficits, and shows significant spatial learning and memory deficits in the MWM test (Wei et al., 2008).

Based on a network pharmacological analysis, we constructed an animal model of aging-related cognitive impairment by subcutaneous injection of D-gal to evaluate the effects of BBR. Chronic administration of low doses of D-gal has been shown to induce changes that mimic the natural aging process in animals, including cognitive impairment (Wei et al., 2005). In our study, MWM behavioral tests were applied to detect changes in cognitive status after 10 weeks of subcutaneous injection of D-gal. We found that BBR treatment improved D-gal-induced learning and memory deficits. Previous studies have shown that BBR displays significant memory improvement activity in multiple animal models of memory

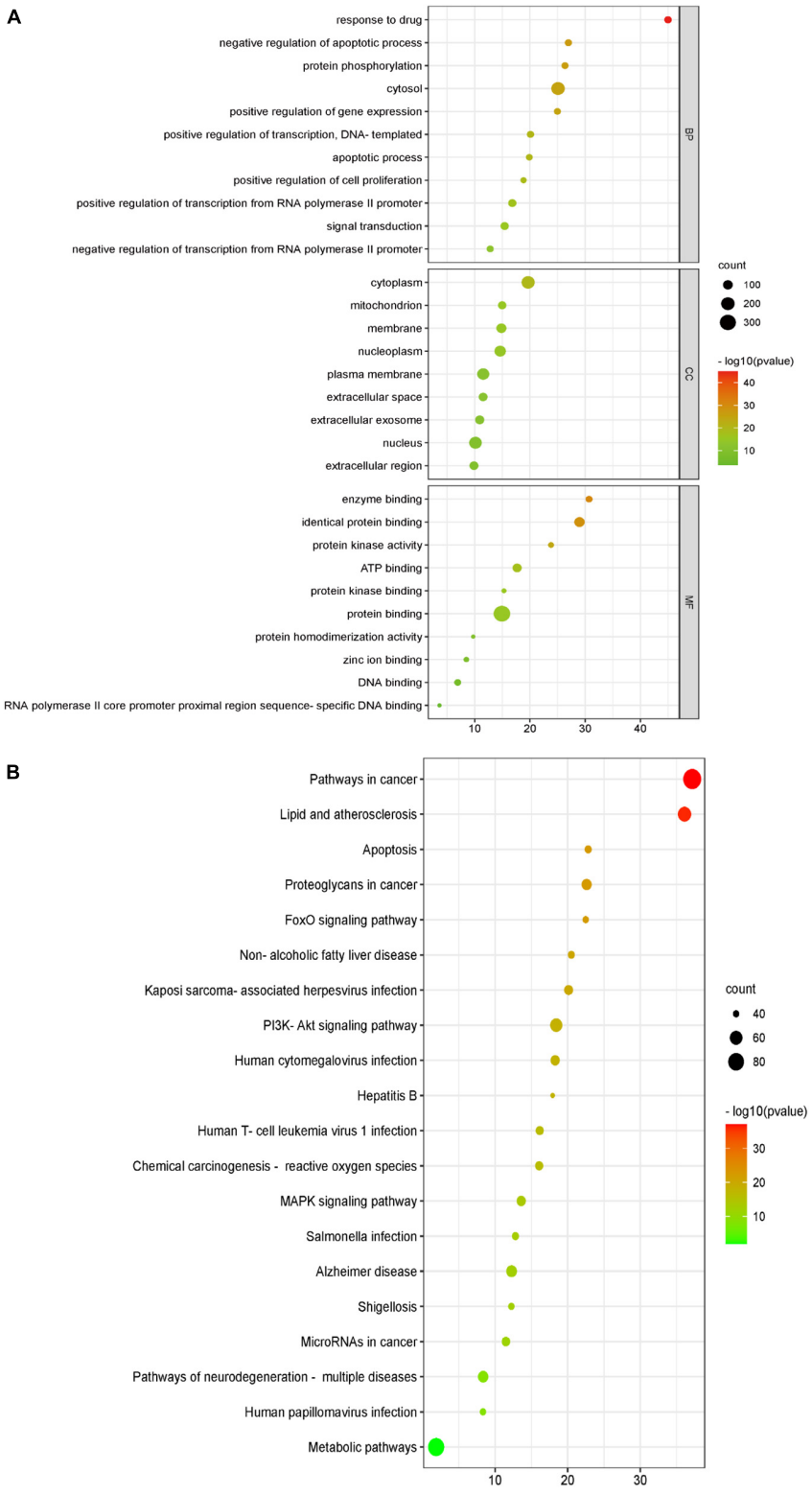

FIGURE 4
Gene ontology (GO) function and Kyoto Encyclopedia of Genes and Genomes (KEGG) pathway enrichment analyses of berberine (BBR) in the treatment of cognitive impairment (CI). **(A)** The GO function analysis, includes biological process (BP), cellular component (CC), and molecular function (MF). **(B)** Top 20 pathways in the BBR anti-CI bubble diagram of KEGG pathway enrichment.

deficits through various mechanisms, such as anti-inflammatory, anti-oxidative stress, cholinesterase inhibition, and anti-amyloid effects (Yuan et al., 2019). In addition, we explored the expression levels of aging markers and found that D-gal resulted in increased expression of the aging marker P16, and BBR administration ameliorated these changes. These results are consistent with previous studies (Dang et al., 2020). Administration of BBR for 6 months significantly improved cognitive deficits and insulin

TABLE 2 Molecular docking results of 8 core targets and berberine (BBR).

Target name	Affinity (kcal/mol)
Mapk1	−7.6
Src	−9.6
Ctnnb1	−6.9
Akt1	−10.2
Pik3ca	−8.1
Tp53	−7.7
Jun	−6.9
Hsp90aa1	−7.0

resistance in naturally aged rats (Yu et al., 2018). BBR emphasizes the induction of neuroprotective effects against Adriamycin-induced cognitive decline by modulating brain growth factors and exerting anti-inflammatory, anti-apoptotic, and antioxidant effects (Shaker et al., 2021). These results further support the ameliorative role of BBR in aging-related cognitive dysfunction.

Cognitive dysfunction is a common disorder in older individuals, and the incidence of MCI increases significantly with age (Petersen et al., 2018). MCI is a cognitive state between normal aging and dementia, and studies have shown that individuals with MCI are approximately three times more likely to progress to dementia over the next 2–5 years than age-matched controls (Petersen et al., 2018). It is well known that no drug is available to modify the disease process in AD, the most common type of dementia. Of particular note, it has been reported that 12.2% of MCI patients recover normal cognitive function within 3 years (McGirr et al., 2022). There are reasonable grounds to believe that reversing MCI to reduce the burden of dementia is a viable area of interest. There is compelling evidence to suggest that BBR was effective in improving cognitive function in Diabetes-related cognitive impairment and AD (Akbar et al., 2021; Hao et al., 2022). A spectrum of studies has demonstrated the ameliorative role of BBR in AD pathologies and cognitive dysfunction (He et al., 2017; Cai et al., 2018; Lin L. et al., 2020; Wu et al., 2021; Ye et al., 2021). BBR may improve cognitive impairment through a variety of mechanisms, including anti-inflammatory, anti-oxidative stress, improvement of insulin resistance, and inhibition

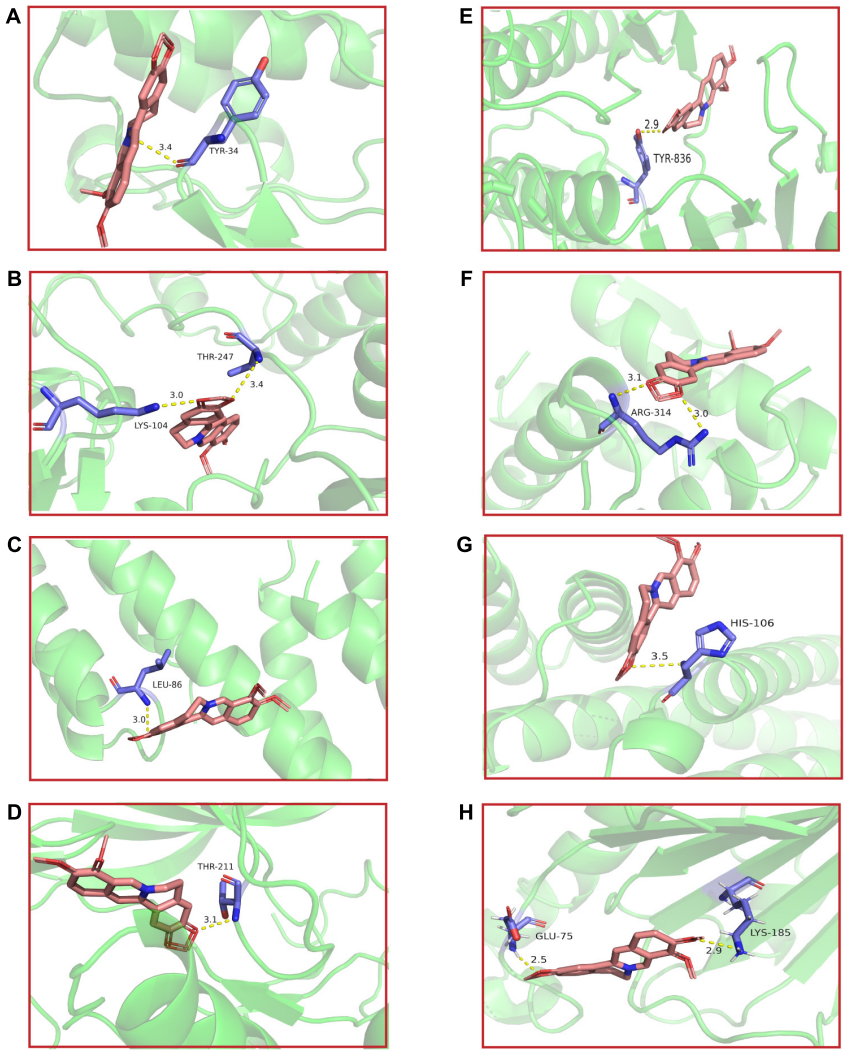

FIGURE 5
The molecular docking results of berberine (BBR) and key targets. BBR and **(A)** *Mapk1*; **(B)** *Src*; **(C)** *Ctnnb1*; **(D)** *Akt1*; **(E)** *Pik3ca*; **(F)** *Tp53*; **(G)** *Jun*; **(H)** *Hsp90aa1*.

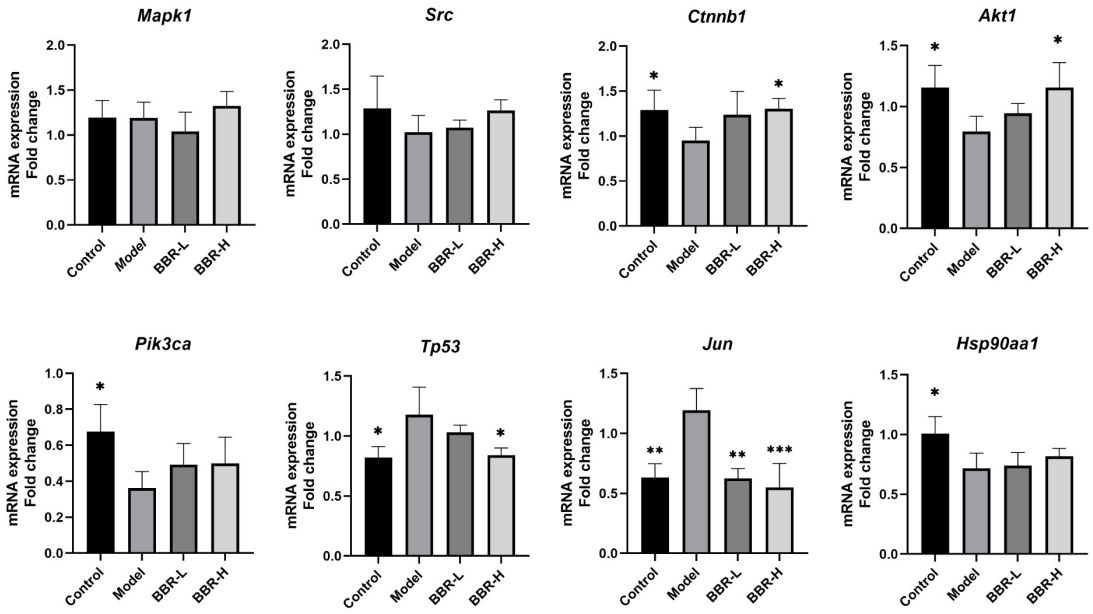

FIGURE 6
The results of RT-qPCR (All data are mean ± SEM with $n = 3$, $^{*}p < 0.05$, $^{**}p < 0.01$, $^{***}p < 0.001$ vs. Model).

of endoplasmic reticulum stress (Patil et al., 2015; Yu et al., 2018; Wang et al., 2019; Yuan et al., 2019; Shaker et al., 2021; Wu et al., 2021). Our study is the pioneer in exploring the mechanism by which BBR improves cognitive dysfunction with the assistance of network pharmacology and molecular docking techniques. To identify the therapeutic targets of BBR against CI, we identified 7,984 CI-validated targets and 470 BBR therapeutic targets using network pharmacology. We identified 386 potential targets associated with BBR and CI. In addition, BBR therapeutic targets associated with CI were used for GO and KEGG analyses. The results of GO analysis and KEGG analysis showed that BBR may exert its effects through MAPK and PI3K/Akt signaling pathways. Previous studies have shown that BBR can increase the levels of proteins located on neurosynapse through the MAPK signaling pathway (Zhou et al., 2016)and exert neuroprotective effects against tau protein hyperphosphorylation through PI3K/Akt pathway (Lin J. Y. et al., 2020).

The top 8 targets screened by network pharmacology were *Mapk1*, *Src*, *Ctnnb1*, *Akt1*, *Pik3ca*, *Tp53*, *Jun*, and *Hsp90aa1*. Molecular docking showed that the core targets dovetailed well with BBR, and RT-qPCR validated that the anti-aging-related cognitive dysfunction of BBR may be achieved by modulating *Akt1*, *Ctnnb1*, *Tp53*, and *Jun*. PI3K/Akt signaling pathway plays an essential role in regulating cell growth, proliferation, and survival. Akt activated by PI3K promotes cell growth and survival through the phosphorylation of multiple cytoplasmic proteins during senescence (Lin J. Y. et al., 2020). A previous study showed that berberine-induced PI3K/Akt activation exerts a protective effect by causing dephosphorylation of tau proteins and ameliorating neuronal axonal damage (Wang et al., 2018). In addition, BBR blocks Aβ production by activating the PI3K/Akt signaling pathway *in vitro* (Durairajan et al., 2012). Although our study only detected statistical differences in *Akt1*, *Pik3ca* showed the same trend of alteration, and it has also been shown that BBR can reduce tau hyperphosphorylation in 3 × Tg AD mice *via* the Akt/glycogen synthase kinase-3β (GSK3β) pathway (Chen et al., 2020). The *Ctnnb1* gene encodes β-catenin, a pivotal component of the Wnt signaling pathway that plays a significant role in the regulation of cell proliferation, differentiation, and apoptosis (Liu et al., 2022). Wnt signaling declines with age in the rat brain (Jessberger et al., 2009) and has been identified in the cerebral cortex of AD patients (Folke et al., 2019). Targeting recovery of the Wnt/β-catenin signaling pathway is a promising therapeutic strategy for AD (Jia et al., 2019). The *Tp53* gene produces the P53 protein, which functions as a transcription factor involved in cell cycle control, DNA repair, and regulation of cellular senescence and body aging (Rufini et al., 2013). A study reveals that BBR can depress the expression of P53 in primary neurons to keep cells in G0/G1 phase (Chai et al., 2013). *c-Jun* is an inducible transcription factor known to play a key role in neuronal cell death and survival (Raivich et al., 2004). Activated *c-Jun* expression is increased in the AD brain (Anderson et al., 1994; Raivich et al., 2004) and is present in the neurogenic fiber tangles of the AD brain (Pearson et al., 2006). Our results are in good agreement with previous studies and we support that BBR functions from multiple targets to improve cognitive function. In future studies, it is imperative to validate and explore our results more thoroughly and extensively.

6. Conclusion

Taken together, the results of this study suggest that BBR is able to attenuate spatial learning and memory impairment by inhibiting the expression of aging markers in the brain of the D-gal-induced senescence mice. Further network pharmacology and RT-qPCR validation suggest that this anti-aging effect may be achieved through the regulation of genes such as *Akt1*, *Ctnnb1*, *Tp53*, and *Jun*. These findings provide new evidence for the anti-aging protective effects of BBR and offer potential therapeutic directions for cognitive dysfunction. However, the specific targets of BBR in its anti-aging effects are not known, which is the main limitation of this study. Therefore, further studies are needed to identify whether BBR plays

a role in improving cognitive function through improving the aging of specific cell types in the CNS and to elucidate the mechanism.

Data availability statement

The original contributions presented in this study are included in this article/**Supplementary material**, further inquiries can be directed to the corresponding authors.

Ethics statement

The animal study was reviewed and approved by Ethics Committee of Xiyuan Hospital, China Academy of Chinese Medical Sciences (No. 2021XLC035-3).

Author contributions

JY and WW performed the experiments and data analysis and wrote the manuscript. JW assisted with the experiments. YC and HL assisted in conceptualizing and revising the manuscript. All authors reviewed and approved the manuscript.

Funding

This study was funded by the Fundamental Research Funds for the Central Public Welfare Research Institutes (ZZ15-YQ-013 and ZZ15-XY-PT-02) and the Science and Technology Innovation Project of Chinese Academy of Traditional Chinese Medicine (CI2021A01401 and CI2021A04618).

Conflict of interest

The authors declare that the research was conducted in the absence of any commercial or financial relationships that could be construed as a potential conflict of interest.

The handling editor declared a shared affiliation with the authors WW and YC at the time of review.

Publisher's note

All claims expressed in this article are solely those of the authors and do not necessarily represent those of their affiliated organizations, or those of the publisher, the editors and the reviewers. Any product that may be evaluated in this article, or claim that may be made by its manufacturer, is not guaranteed or endorsed by the publisher.

Supplementary material

The Supplementary Material for this article can be found online at: https://www.frontiersin.org/articles/10.3389/fnins.2023.1093180/full#supplementary-material

References

Akbar, M., Shabbir, A., Rehman, K., Akash, M. S. H., and Shah, M. A. (2021). Neuroprotective potential of berberine in modulating Alzheimer's disease via multiple signaling pathways. *J. Food Biochem.* 45:e13936. doi: 10.1111/jfbc.13936

Anderson, A. J., Cummings, B. J., and Cotman, C. W. (1994). Increased immunoreactivity for Jun-and Fos-related proteins in Alzheimer's disease: association with pathology. *Exp. Neurol.* 125, 286–295. doi: 10.1006/exnr.1994.1031

Banji, O. J., Banji, D., and Ch, K. (2014). Curcumin and hesperidin improve cognition by suppressing mitochondrial dysfunction and apoptosis induced by D-galactose in rat brain. *Food Chem. Toxicol.* 74, 51–59. doi: 10.1016/j.fct.2014.08.020

Bova, S., Padrini, R., Goldman, W., Berman, D., and Cargnelli, G. (1992). On the mechanism of vasodilating action of berberine: possible role of inositol lipid signaling system. *J. Pharmacol. Exp. Ther.* 261, 318–323.

Cai, Z., Wang, C., He, W., and Chen, Y. (2018). Berberine alleviates amyloid-beta pathology in the brain of APP/PS1 transgenic mice via inhibiting β/γ-secretases activity and enhancing α-secretases. *Curr. Alzheimer Res.* 15, 1045–1052. doi: 10.2174/1567205015666180702105740

Chai, Y. S., Hu, J., Lei, F., Wang, Y. G., Yuan, Z. Y., Lu, X., et al. (2013). Effect of berberine on cell cycle arrest and cell survival during cerebral ischemia and reperfusion and correlations with p53/cyclin D1 and PI3K/Akt. *Eur. J. Pharmacol.* 708, 44–55. doi: 10.1016/j.ejphar.2013.02.041

Chen, Y., Chen, Y., Liang, Y., Chen, H., Ji, X., and Huang, M. (2020). Berberine mitigates cognitive decline in an Alzheimer's disease Mouse Model by targeting both tau hyperphosphorylation and autophagic clearance. *Biomed. Pharmacother.* 121:109670. doi: 10.1016/j.biopha.2019.109670

Cheng, Z., Kang, C., Che, S., Su, J., Sun, Q., Ge, T., et al. (2022). Berberine: a promising treatment for neurodegenerative diseases. *Front. Pharmacol.* 13:845591. doi: 10.3389/fphar.2022.845591

Choi, M. S., Yuk, D. Y., Oh, J. H., Jung, H. Y., Han, S. B., Moon, D. C., et al. (2008). Berberine inhibits human neuroblastoma cell growth through induction of p53-dependent apoptosis. *Anticancer Res.* 28, 3777–3784.

Daina, A., Michielin, O., and Zoete, V. (2019). SwissTargetPrediction: updated data and new features for efficient prediction of protein targets of small molecules. *Nucleic Acids Res.* 47, W357–W364. doi: 10.1093/nar/gkz382

Dang, Y., An, Y., He, J., Huang, B., Zhu, J., Gao, M., et al. (2020). Berberine ameliorates cellular senescence and extends the lifespan of mice via regulating p16 and cyclin protein expression. *Aging Cell* 19:e13060. doi: 10.1111/acel.13060

Daroi, P. A., Dhage, S. N., and Juvekar, A. R. (2022). p-Coumaric acid protects against D-galactose induced neurotoxicity by attenuating neuroinflammation and apoptosis in mice brain. *Metab. Brain Dis.* 37, 2569–2579. doi: 10.1007/s11011-022-01007-3

Durairajan, S. S. K., Liu, L.-F., Lu, J.-H., Chen, L.-L., Yuan, Q., Chung, S. K., et al. (2012). Berberine ameliorates β-amyloid pathology, gliosis, and cognitive impairment in an Alzheimer's disease transgenic mouse model. *Neurobiol. Aging* 33, 2903–2919. doi: 10.1016/j.neurobiolaging.2012.02.016

Folke, J., Pakkenberg, B., and Brudek, T. (2019). Impaired Wnt signaling in the prefrontal cortex of Alzheimer's disease. *Mol. Neurobiol.* 56, 873–891. doi: 10.1007/s12035-018-1103-z

Hao, Y., Li, J., Yue, S., Wang, S., Hu, S., and Li, B. (2022). Neuroprotective effect and possible mechanisms of berberine in diabetes-related cognitive impairment: a systematic review and meta-analysis of animal studies. *Front. Pharmacol.* 13:917375. doi: 10.3389/fphar.2022.917375

He, W., Wang, C., Chen, Y., He, Y., and Cai, Z. (2017). Berberine attenuates cognitive impairment and ameliorates tau hyperphosphorylation by limiting the self-perpetuating pathogenic cycle between NF-κB signaling, oxidative stress and neuroinflammation. *Pharmacol. Rep.* 69, 1341–1348. doi: 10.1016/j.pharep.2017.06.006

Hu, C., Wang, L., Guo, Y., Cao, Z., Lu, Y., and Qin, H. (2020). Study of the risk and preventive factors for progress of mild cognitive impairment to dementia. *Am. J. Alzheimers Dis. Other Dement.* 35:1533317520925324. doi: 10.1177/1533317520925324

Hugo, J., and Ganguli, M. (2014). Dementia and cognitive impairment: epidemiology, diagnosis, and treatment. *Clin. Geriatr. Med.* 30, 421–442. doi: 10.1016/j.cger.2014.04.001

Jeong, H. W., Hsu, K. C., Lee, J.-W., Ham, M., Huh, J. Y., Shin, H. J., et al. (2009). Berberine suppresses proinflammatory responses through AMPK activation in macrophages. *Am. J. Physiol. Endocrinol. Metab.* 296, E955–E964.

Jessberger, S., Clark, R. E., Broadbent, N. J., Clemenson, G. D., Consiglio, A., Lie, D. C., et al. (2009). Dentate gyrus-specific knockdown of adult neurogenesis impairs spatial and object recognition memory in adult rats. *Learn. Mem.* 16, 147–154. doi: 10.1101/lm.1172609

Jia, L., Piña-Crespo, J., and Li, Y. (2019). Restoring Wnt/β-catenin signaling is a promising therapeutic strategy for Alzheimer's disease. *Mol. Brain* 12:104. doi: 10.1186/s13041-019-0525-5

Kim, W. Y., and Sharpless, N. E. (2006). The regulation of INK4/ARF in cancer and aging. *Cell* 127, 265–275. doi: 10.1016/j.cell.2006.10.003

Koepsell, T. D., and Monsell, S. E. (2012). Reversion from mild cognitive impairment to normal or near-normal cognition: risk factors and prognosis. *Neurology* 79, 1591–1598. doi: 10.1212/WNL.0b013e31826e26b7

Li, C., Jiang, S., Wang, H., Wang, Y., Han, Y., and Jiang, J. (2022). Berberine exerts protective effects on cardiac senescence by regulating the Klotho/SIRT1 signaling pathway. *Biomed. Pharmacother.* 151:113097. doi: 10.1016/j.biopha.2022.113097

Li, H. Y., Wang, X. C., Xu, Y. M., Luo, N. C., Luo, S., Hao, X. Y., et al. (2018). Berberine improves diabetic encephalopathy through the SIRT1/ER stress pathway in db/db mice. *Rejuvenation Res.* 21, 200–209. doi: 10.1089/rej.2017.1972

Lin, J. Y., Kuo, W. W., Baskaran, R., Kuo, C. H., Chen, Y. A., Chen, W. S., et al. (2020). Swimming exercise stimulates IGF1/ PI3K/Akt and AMPK/SIRT1/PGC1α survival signaling to suppress apoptosis and inflammation in aging hippocampus. *Aging* 12, 6852–6864. doi: 10.18632/aging.103046

Lin, L., Li, C., Zhang, D., Yuan, M., Chen, C.-H., and Li, M. (2020). Synergic effects of berberine and curcumin on improving cognitive function in an Alzheimer's disease mouse model. *Neurochem. Res.* 45, 1130–1141. doi: 10.1007/s11064-020-02992-6

Liu, J., Xiao, Q., Xiao, J., Niu, C., Li, Y., Zhang, X., et al. (2022). Wnt/β-catenin signalling: function, biological mechanisms, and therapeutic opportunities. *Signal. Transduct. Target. Ther.* 7:3. doi: 10.1038/s41392-021-00762-6

Luchsinger, J. A. (2012). Type 2 diabetes and cognitive impairment: linking mechanisms. *J. Alzheimers Dis.* 30, S185–S198. doi: 10.3233/JAD-2012-111433

Ma, C. Y., Shi, X. Y., Wu, Y. R., Zhang, Y., Yao, Y. H., Qu, H. L., et al. (2021). Berberine attenuates atherosclerotic lesions and hepatic steatosis in ApoE(−/−) mice by down-regulating PCSK9 via ERK1/2 pathway. *Ann. Transl. Med.* 9:1517. doi: 10.21037/atm-20-8106

McGirr, A., Nathan, S., Ghahremani, M., Gill, S., Smith, E. E., and Ismail, Z. (2022). Progression to dementia or reversion to normal cognition in mild cognitive impairment as a function of late-onset neuropsychiatric symptoms. *Neurology* 98, e2132–e2139. doi: 10.1212/wnl.0000000000200256

Nagy, G., and Pohl, N. L. (2015). Complete hexose isomer identification with mass spectrometry. *J. Am. Soc. Mass Spectrom.* 26, 677–685. doi: 10.1007/s13361-014-1072-z

Panahi, N., Mahmoudian, M., Mortazavi, P., and Hashjin, G. S. (2013). Experimental research effects of berberine on β-secretase activity in a rabbit model of Alzheimer's disease. *Arch. Med. Sci.* 9, 146–150. doi: 10.5114/aoms.2013.33354

Park, M. H., Kwon, D. Y., Jung, J. M., Han, C., Jo, I., and Jo, S. A. (2013). Mini-Mental Status Examination as predictors of mortality in the elderly. *Acta Psychiatr. Scand.* 127, 298–304. doi: 10.1111/j.1600-0447.2012.01918.x

Patil, S., Tawari, S., Mundhada, D., and Nadeem, S. (2015). Protective effect of berberine, an isoquinoline alkaloid ameliorates ethanol-induced oxidative stress and memory dysfunction in rats. *Pharmacol. Biochem. Behav.* 136, 13–20. doi: 10.1016/j.pbb.2015.07.001

Pearson, A. G., Byrne, U. T. E., MacGibbon, G. A., Faull, R. L. M., and Dragunow, M. (2006). Activated c-Jun is present in neurofibrillary tangles in Alzheimer's disease brains. *Neurosci. Lett.* 398, 246–250. doi: 10.1016/j.neulet.2006.01.031

Petersen, R. C. (2004). Mild cognitive impairment as a diagnostic entity. *J. Intern. Med.* 256, 183–194.

Petersen, R. C., Lopez, O., Armstrong, M. J., Getchius, T. S. D., Ganguli, M., Gloss, D., et al. (2018). Practice guideline update summary: mild cognitive impairment: report of the guideline development, dissemination, and implementation subcommittee of the American academy of neurology. *Neurology* 90, 126–135. doi: 10.1212/wnl.0000000000004826

Pirillo, A., and Catapano, A. L. (2015). Berberine, a plant alkaloid with lipid- and glucose-lowering properties: from *in vitro* evidence to clinical studies. *Atherosclerosis* 243, 449–461. doi: 10.1016/j.atherosclerosis.2015.09.032

Raivich, G., Bohatschek, M., Da Costa, C., Iwata, O., Galiano, M., Hristova, M., et al. (2004). The AP-1 transcription factor c-Jun is required for efficient axonal regeneration. *Neuron* 43, 57–67. doi: 10.1016/j.neuron.2004.06.005

Ru, J., Li, P., Wang, J., Zhou, W., Li, B., Huang, C., et al. (2014). TCMSP: a database of systems pharmacology for drug discovery from herbal medicines. *J. Cheminform.* 6:13. doi: 10.1186/1758-2946-6-13

Rufini, A., Tucci, P., Celardo, I., and Melino, G. (2013). Senescence and aging: the critical roles of p53. *Oncogene* 32, 5129–5143. doi: 10.1038/onc.2012.640

Safran, M., Rosen, N., Twik, M., BarShir, R., Stein, T. I., Dahary, D., et al. (2021). "The genecards suite," in *Practical Guide to Life Science Databases*, eds I. Abugessaisa and T. Kasukawa (Singapore: Springer Nature Singapore), 27–56.

Shaker, F. H., El-Derany, M. O., Wahdan, S. A., El-Demerdash, E., and El-Mesallamy, H. O. (2021). Berberine ameliorates doxorubicin-induced cognitive impairment (chemobrain) in rats. *Life Sci.* 269:119078. doi: 10.1016/j.lfs.2021.119078

Sherman, B. T., Hao, M., Qiu, J., Jiao, X., Baseler, M. W., Lane, H. C., et al. (2022). DAVID: a web server for functional enrichment analysis and functional annotation of gene lists (2021 update). *Nucleic Acids Res.* 50, W216–W221. doi: 10.1093/nar/gkac194

Shwe, T., Pratchayasakul, W., Chattipakorn, N., and Chattipakorn, S. C. (2018). Role of D-galactose-induced brain aging and its potential used for therapeutic interventions. *Exp. Gerontol.* 101, 13–36. doi: 10.1016/j.exger.2017.10.029

Sun, K., Yang, P., Zhao, R., Bai, Y., and Guo, Z. (2018). Matrine attenuates D-galactose-induced aging-related behavior in mice *via* inhibition of cellular senescence and oxidative stress. *Oxid. Med. Cell. Longev.* 2018:7108604. doi: 10.1155/2018/7108604

Szklarczyk, D., Gable, A. L., Nastou, K. C., Lyon, D., Kirsch, R., Pyysalo, S., et al. (2021). The STRING database in 2021: customizable protein-protein networks, and functional characterization of user-uploaded gene/measurement sets. *Nucleic Acids Res.* 49, D605–D612. doi: 10.1093/nar/gkaa1074

UniProt Consortium (2020). UniProt: the universal protein knowledgebase in 2021. *Nucleic Acids Res.* 49, D480–D489. doi: 10.1093/nar/gkaa1100

Vorhees, C. V., and Williams, M. T. (2006). Morris water maze: procedures for assessing spatial and related forms of learning and memory. *Nat. Protoc.* 1, 848–858. doi: 10.1038/nprot.2006.116

Wang, K., Chen, Q., Wu, N., Li, Y., Zhang, R., Wang, J., et al. (2019). Berberine ameliorates spatial learning memory impairment and modulates cholinergic anti-inflammatory pathway in diabetic rats. *Front. Pharmacol.* 10:1003. doi: 10.3389/fphar.2019.01003

Wang, Q., Sun, Y. N., Zou, C. M., Zhang, T. L., Li, Z., Liu, M., et al. (2022). Regulation of the kynurenine/serotonin pathway by berberine and the underlying effect in the hippocampus of the chronic unpredictable mild stress mice. *Behav. Brain Res.* 422:113764. doi: 10.1016/j.bbr.2022.113764

Wang, S., He, B., Hang, W., Wu, N., Xia, L., Wang, X., et al. (2018). Berberine alleviates tau hyperphosphorylation and axonopathy-associated with diabetic encephalopathy via restoring PI3K/Akt/GSK3β pathway. *J. Alzheimers Dis.* 65, 1385–1400. doi: 10.3233/jad-180497

Wang, X., Shen, Y., Wang, S., Li, S., Zhang, W., Liu, X., et al. (2017). PharmMapper 2017 update: a web server for potential drug target identification with a comprehensive target pharmacophore database. *Nucleic Acids Res.* 45, W356–W360. doi: 10.1093/nar/gkx374

Wei, H., Cai, Y., Chu, J., Li, C., and Li, L. (2008). Temporal gene expression profile in hippocampus of mice treated with d-galactose. *Cell. Mol. Neurobiol.* 28, 781–794. doi: 10.1007/s10571-007-9177-6

Wei, H., Li, L., Song, Q., Ai, H., Chu, J., and Li, W. (2005). Behavioural study of the d-galactose induced aging model in C57BL/6J mice. *Behav. Brain Res.* 157, 245–251. doi: 10.1016/j.bbr.2004.07.003

Wishart, D. S., Feunang, Y. D., Guo, A. C., Lo, E. J., Marcu, A., Grant, J. R., et al. (2018). DrugBank 5.0: a major update to the DrugBank database for 2018. *Nucleic Acids Res.* 46, D1074–D1082. doi: 10.1093/nar/gkx1037

Wu, Y., Chen, Q., Wen, B., Wu, N., He, B., and Chen, J. (2021). Berberine reduces Aβ(42) deposition and Tau hyperphosphorylation via ameliorating endoplasmic reticulum stress. *Front. Pharmacol.* 12:640758. doi: 10.3389/fphar.2021.640758

Xu, Z., Feng, W., Shen, Q., Yu, N., Yu, K., Wang, S., et al. (2017). Rhizoma coptidis and berberine as a natural drug to combat aging and aging-related diseases via anti-oxidation and AMPK activation. *Aging Dis.* 8, 760–777. doi: 10.14336/ad.2016.0620

Ye, C., Liang, Y., Chen, Y., Xiong, Y., She, Y., Zhong, X., et al. (2021). Berberine improves cognitive impairment by simultaneously impacting cerebral blood flow and β-amyloid accumulation in an APP/tau/PS1 mouse model of Alzheimer's disease. *Cells* 10:1161. doi: 10.3390/cells10051161

Yu, Y., Zhao, Y., Teng, F., Li, J., Guan, Y., Xu, J., et al. (2018). Berberine improves cognitive deficiency and muscular dysfunction via activation of the AMPK/SIRT1/PGC-1a pathway in skeletal muscle from naturally aging rats. *J. Nutr. Health Aging* 22, 710–717. doi: 10.1007/s12603-018-1015-7

Yuan, N.-N., Cai, C.-Z., Wu, M.-Y., Su, H.-X., Li, M., and Lu, J.-H. (2019). Neuroprotective effects of berberine in animal models of Alzheimer's disease: a systematic review of pre-clinical studies. *BMC Complement. Altern. Med.* 19:109. doi: 10.1186/s12906-019-2510-z

Zhang, H., Wei, J., Xue, R., Wu, J. D., Zhao, W., Wang, Z. Z., et al. (2010). Berberine lowers blood glucose in type 2 diabetes mellitus patients through increasing insulin receptor expression. *Metabolism* 59, 285–292. doi: 10.1016/j.metabol.2009.07.029

Zhao, H., Halicka, H. D., Li, J., and Darzynkiewicz, Z. (2013). Berberine suppresses gero-conversion from cell cycle arrest to senescence. *Aging* 5:623. doi: 10.18632/aging.100593

Zhou, J., Du, X., Long, M., Zhang, Z., Zhou, S., Zhou, J., et al. (2016). Neuroprotective effect of berberine is mediated by MAPK signaling pathway in experimental diabetic neuropathy in rats. *Eur. J. Pharmacol.* 774, 87–94. doi: 10.1016/j.ejphar.2016.02.007

Zhou, Y., Zhang, Y., Lian, X., Li, F., Wang, C., Zhu, F., et al. (2022). Therapeutic target database update 2022: Facilitating drug discovery with enriched comparative data of targeted agents. *Nucleic Acids Res.* 50, D1398–D1407. doi: 10.1093/nar/gkab953

frontiers | Frontiers in Pharmacology

TYPE Original Research
PUBLISHED 02 February 2023
DOI 10.3389/fphar.2023.1096309

OPEN ACCESS

EDITED BY
Jianxun Liu,
Xiyuan Hospital, China Academy of Chinese Medical Sciences, China

REVIEWED BY
Govindaiah Vinukonda,
New York Medical College, United States
Ivana Grković,
University of Belgrade, Serbia

*CORRESPONDENCE
Songbiao Cui,
sbcui@ybu.edu.cn
Dongyuan Xu,
dyxu@ybu.edu.cn

SPECIALTY SECTION
This article was submitted to Neuropharmacology, a section of the journal Frontiers in Pharmacology

RECEIVED 12 November 2022
ACCEPTED 20 January 2023
PUBLISHED 02 February 2023

CITATION
Xuan C, Cui H, Jin Z, Yue Y, Cao S, Cui S and Xu D (2023), Glutamine ameliorates hyperoxia-induced hippocampal damage by attenuating inflammation and apoptosis *via* the MKP-1/MAPK signaling pathway in neonatal rats.
Front. Pharmacol. 14:1096309.
doi: 10.3389/fphar.2023.1096309

Glutamine ameliorates hyperoxia-induced hippocampal damage by attenuating inflammation and apoptosis *via* the MKP-1/MAPK signaling pathway in neonatal rats

Chouhui Xuan[1], Haixia Cui[2], Zhengyong Jin[1], Yuyang Yue[3], Shuxia Cao[4], Songbiao Cui[5]* and Dongyuan Xu[6]*

[1]Department of Pediatrics, Yanbian University Hospital, Yanji, Jilin, China, [2]Department of Clinical Laboratory, Yanbian University Hospital, Yanji, Jilin, China, [3]Department of Dermatology, Yanbian University Hospital, Yanji, Jilin, China, [4]Department of Center of Morphological Experiment, Yanbian University, Yanji, Jilin, China, [5]Department of Neurology, Yanbian University Hospital, Yanji, Jilin, China, [6]Key Laboratory of Cellular Function and Pharmacology of Jilin Province, Yanbian University, Yanji, China

Glutamine (Gln) is an immunomodulatory protein that mediates oxidative stress, inflammation, and apoptosis, but has not been reported in the treatment of hyperoxia (Hyp)-induced brain injury. The aim of this study was to determine whether Gln could improve hyp-induced brain injury in neonatal rats to and later learning and memory dysfunction, and to explore its possible mechanisms. We prepared a model of neonatal rat brain injury caused by normobaric hyperoxia while administered with Gln for 7 days for evaluation. Learning memory function was assessed with the Morris water maze test. Histological analysis, protein expression analysis, oxidative stress and inflammation level analysis were performed using hippocampal tissue. Gln treatment significantly reduced brain tissue water content, oxidative stress levels, microglia activation and inflammatory factor expression, and attenuated tissue damage and apoptosis in the hippocampal region. Gln ameliorates hyp-induced learning, memory impairment in neonatal rats in water maze test. It also increased MKP-1 protein expression and decreased p-p38, p-ERK and p-JNK. Therefore, it is hypothesized that Gln may exert neuroprotective effects by increasing MKP-1 expression to negatively regulate MAPK signaling, with potential cognitive improvement in hyp-induced brain injury.

KEYWORDS

glutamine, hyperoxia, hippocampus, learning and memory impairment, inflammation, MKP-1, MAPK

Introduction

Gln, an L-alpha-amino acid, is the most abundant non-essential amino acid in the body. It is an important nutrient for the conversion of some amino acids and biomolecules and is frequently used as a source of energy for some rapidly dividing cells (Hu et al., 2020). Gln is used clinically as an immunotropic modulator (Kim, 2011) in the treatment of various diseases such as hyp-induced acute lung injury (Perng et al., 2010), traumatic brain injury, bronchial asthma, and ulcerative colitis. Gln stores are depleted and rapidly released in the presence of stressors, causing a decrease in intracellular Gln levels. Supplementation of Gln

via an external source increases expression of glutathione, which in turn reacts directly with reactive oxygen species (ROS) to prevent oxidative damage (Oliveira et al., 2010), effectively reduces ROS and inflammatory factor levels (Gong et al., 2017), and promotes neurotrophic factor expression and neurogenesis, thereby improving cell survival.

Oxygen therapy is one of the most common and important treatments used in the resuscitation of preterm infants. However, at the critical stage of life, increased oxygen levels may affect the process of brain development. ROS are formed in excess during oxygen therapy, causing oxidative stress and leading to cellular inflammation and apoptosis (Sifringer et al., 2013); neuronal development is also adversely affected (Al et al., 2020). Preterm infants are particularly susceptible to ROS-induced damage as their antioxidative systems are not completely developed at birth, and during childhood, these infants are at a tenfold risk of developing cognitive and learning disabilities as well as behavioral abnormalities (Hintz et al., 2018). Studies have shown that early postnatal intervention *via* administration of Gln may increase the volume of cerebral structures, improve brain development in preterm infants, and reduce occurrence of adverse outcomes such as neurocognitive dysfunction and attention deficit hyperactivity disorder (ADHD) in later life (de Kieviet et al., 2014). Therefore, it is necessary to develop a safe and effective neuroprotective drug for preterm infants with hyp-induced brain injuries.

MAPK pathway is increasingly recognized as playing a key role in regulating ROS production (Lv et al., 2020). Phosphatase-1, or MKP-1 (dual specificity phosphatase 1, also known as DUSP1), inactivates this pathway and is essential for the control of inflammation. MKP-1 not only suppresses inflammation by dephosphorylating the MAPK family of proteins at key modulation sites, but is also involved in negative feedback regulation and homeostatic function in cellular transduction. Regulation of the activity of related factors in the MKP-1/MAPK signaling pathway may be critical for preventing and counteracting neuroinflammation and apoptosis. Studies have shown that the anti-inflammatory and anti-apoptotic effects of Gln in acute lung injury are mediated by the MAPK signaling pathway (Huang et al., 2021). Additionally, Gln regulates the MAPK pathway *via* upregulation of MKP-1, which balances the inflammatory response (Kim et al., 2022).

To test the hypothesis that Gln may regulate the MKP-1/MAPK pathway and cause a decrease in oxidative stress, inflammation, and apoptosis, thereby preventing brain damage, learning difficulties and memory dysfunction caused by hyp-induced injury, in this study we investigated the protective role of Gln in hyp-induced brain injury in neonatal rats and its association with the MKP-1/MAPK signaling pathway using a neonatal rat brain subjected to normobaric hyperoxia as a model.

Material and methods

Main reagents

MKP-1 (#sc-373841), p-p38 (#sc-166182), p38 (#sc-81621), p-JNK (#sc-6254), JNK (#sc-7345), p-ERK (#sc-7383), ERK (#sc-135900), BDNF (#sc-65514), Synapsin Ia (#sc-376623), MBP (#sc-376995), Bax (#sc-20067), Bcl-2 (#sc-7382) antibodies were purchased from Santa cruz biotechnology (United States). Goat anti-rabbit IgG/horseradish enzyme labeling (#16K22C) was purchased from Boster Biological Technology (Wuhan, China), and goat anti-mouse IgG/horseradish enzyme labeling (#ZB-2305) was purchased from Zhongshanjinqiao biotechnology (Beijing, China). β-actin antibody (bsm-33036m) (1:1000) was purchased from Beijing Boaosen Biotechnology Co., Ltd. (Beijing, China). L-glutamine (G8540) was purchased from Sigma-Aldrich (United States). Rat IL-1β (SBJ-H0417), IL-6 (SBJ-H0465), TNF-α (SBJ-H0038) ELISA kit reagent kits were purchased from Nanjing Sempega Biotechnology Co. (Nanjing, China). ROS (MM-43700M2), GSH-PX (MM-20251R2), SOD (MM-20387R2), MDA (MM-0385R1) ELISA kits were purchased from Jiangsu Meimian Industrial Co., Ltd. (Yancheng, China). TUNEL kit was purchased from Promega (United States). H-E staining kit was purchased from Beijing Solarbio Science and Technology Co., Ltd. (Beijing, China). Iba-1 antibody was purchased from Santa cruz biotechnology (United States). DAB kit was purchased from Beijing Boaosen Biotechnology Co., Ltd. (Beijing, China).

Animals and experimental procedures

SD neonatal rats, weighing 6.7–8.2 g, were used in this study, provided by the Animal Section of Yanbian University. All animals were kept together with their dams in per cage on a 12 h light/dark cycle in a temperature-controlled room (22°C ± 1°C) with free access to water and food.

60 newborn rats were randomly divided into four groups ($n = 15$) 1 day after birth: control group (Con: 21% O_2), normal drug group (Con + Gln: 21% O_2), Hyp group (Hyp: 85% O_2) and drug group (Hyp + Gln: 85% O_2). The Hyp and Hyp + Gln groups were placed in glass chambers and oxygen concentrations were measured twice daily with a digital oximeter, and nitrogen dioxide and water were absorbed with soda lime. The dams were rotated between the hyperoxia- and normoxia-exposed pups every day to avoid undersupply of the young. Gln was dissolved in 0.9% Nacl to be used. Gln (1 μg/g B.W) was administered intraperitoneally to newborn rats in the Con + Gln and Hyp + Gln groups at the same time each day, and the same volume of 0.9% NaCl was administered intraperitoneally to newborn rats in the Con and Hyp groups at the same time for 7 days.

At P7, each group of randomly selected newborn rats ($n = 3$) was anesthetized, fixed on the operating table, and the thoracic cavity was exposed. After injection of chilled PBS solution from the apex of heart, the tissue was fixed by injection of 4% paraformaldehyde. The brain tissue was then quickly removed, immersed in 4% paraformaldehyde solution for 24 h and fixed, and subjected to histopathological analysis (HE staining, immunohistochemistry, TUNEL staining) after tissue pruning, dehydration, transparency, paraffin embedding and conventional sectioning. In each group, newborn rats ($n = 3$) were randomly selected and executed after anesthesia, and a pair of hippocampal tissues were rapidly isolated on ice, treated with liquid nitrogen and placed in an ultra-low temperature refrigerator at −80°C for backup (ELISA, Western Blot). And each group of newborn rats ($n = 3$) was then randomly selected and executed after anesthesia, and brain tissue was removed to determine the water content of brain tissue. At P30, each group of neonatal rats ($n = 6$) began the Morris water maze experiment (Figure 1).

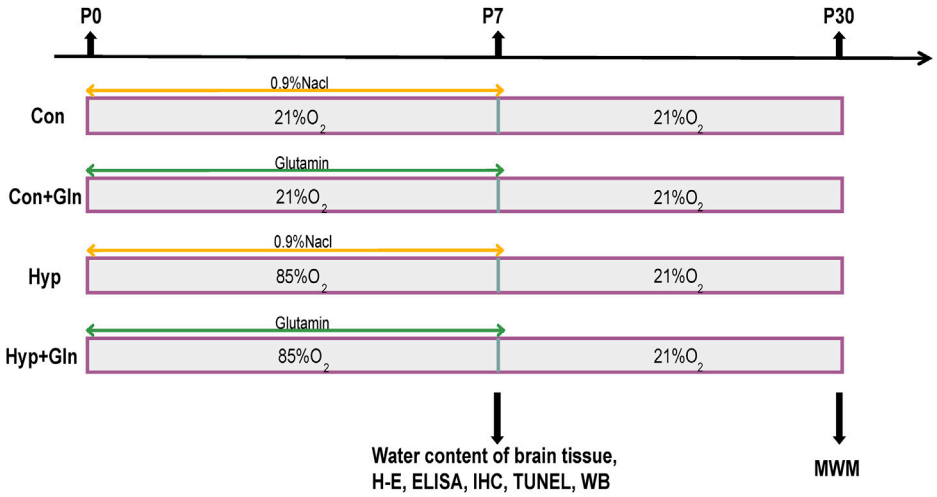

FIGURE 1
The experimental procedure. Newborn rats were randomly divided into four groups: Con, Con + Gln, Hyp and Hyp + Gln. The Hyp and Hyp + Gln groups were placed in 85% O_2 for 7 days, Con and Con + Gln groups were placed indoor (21% O_2). Gln [1 μg/g (B)W] was administered intraperitoneally to newborn rats in the Con + Gln and Hyp + Gln groups at the same time each day, and the same volume of 0.9% NaCl was administered intraperitoneally to newborn rats in the Con and Hyp groups at the same time for 7 days. At P7, each group of randomly selected newborn rats for histopathological analysis (n = 3), determine the water content of brain tissue (n = 3) and protein analysis (n = 3). At P30, each group of neonatal rats (n = 6) began the Morris water maze experiment. Con, control; Hyp, hyperoxia; Gln, glutamine; P0, postnatal day 0; P7, postnatal day 7; P30, postnatal day 30; IHC, immunohistochemistry; WB, western blot; MWM, morris water maze experiment.

Brain water content measurement

Newborn rats were selected at random from each group (n = 3), and following ether anesthesia, the brain tissues were immediately removed and weighed. The wet weight (W) of the brain tissues was marked and baked in a 60°C oven. The dry brain tissue weight (D) is measured when there is no weight change for two consecutive days. The brain tissue water content (%) was determined using the formula [(W-D)/W] 100%.

Assay for oxidative stress parameters

Hippocampal tissues were removed and washed with pre-cooled saline, dried on filter paper. The hippocampal samples with saline solution were homogenized at a ratio of 1:9 (g/mL) in a homogenizer, and the supernatant was collected by centrifugation at 3,000 rpm for 10 min. *Hippocampus* oxidation index was determined using malondialdehyde (MDA), ROS, superoxide dismutase (SOD) and glutathione (GSH) Elisa kits. The MDA level was measured by the absorbance of the sample at 532 nm, expressed as nmol/mg protein. The SOD level was measured by the absorbance of the sample at 550 nm, expressed as unit/mg protein. The ROS level was measured by the absorbance of the sample at 525 nm, expressed as RFU/mg protein. The GSH level expressed as ng/mg protein. All results were normalized by the total protein concentration in each sample.

ELISA assay

The hippocampal samples with saline solution were homogenized at a ratio of 1:9 (g/mL) in a homogenizer, and the supernatant was collected by centrifugation at 3,000 rpm for 10 min. The expression levels of TNF-α, IL-1β and IL-6 in hippocampus tissue were determined using quantitative ELISA kits according to the manufacturer's instructions.

Morris water maze (MWM) test

To observe the ability to reflect spatial learning and memory, the MWM test was conducted at P30-P34. The Morris water maze apparatus consisted mainly of a 160 cm-wide, 60 cm-high circular pool with a black interior and a water level 30 cm deep, which was kept at 20°C ± 1°C. A cylindrical platform with a diameter of 12 cm wide was set 1 cm below the water surface of the third quadrant. In the first phase, spatial learning ability was tested (localization-navigation test): each rat was tested four times a day (with a 2-min break in between) for 4 days. In each test, newborn rats (n = 6) were placed in the water facing the wall of the tube from quadrants 1 to 4 sequentially, swam for a maximum of 2 min to find the platform, and remained on the platform for 20 s. If the platform was not found within 2 min, they were guided to the platform for 20 s and the escape latency was recorded as 2 min. In the second phase, spatial memory was examined (spatial exploration test): the platform was removed and the rats were all placed in the water along the pool wall from the same quadrant and the swimming time and distance in the target quadrant and the number of times they crossed the platform in 2 min were recorded. The experimental process was recorded and analyzed by the data acquisition system.

Histopathological assessment of brain injury

The brain tissues were fixed in 4% PFA solution for 24 h, and then dehydrated with graded alcohol. Brain tissue was embedded in paraffin and sliced at a thickness of 5–7 μm. H&E staining kit was used according to the instructions. Finally, the sections were sealed with neutral gum.

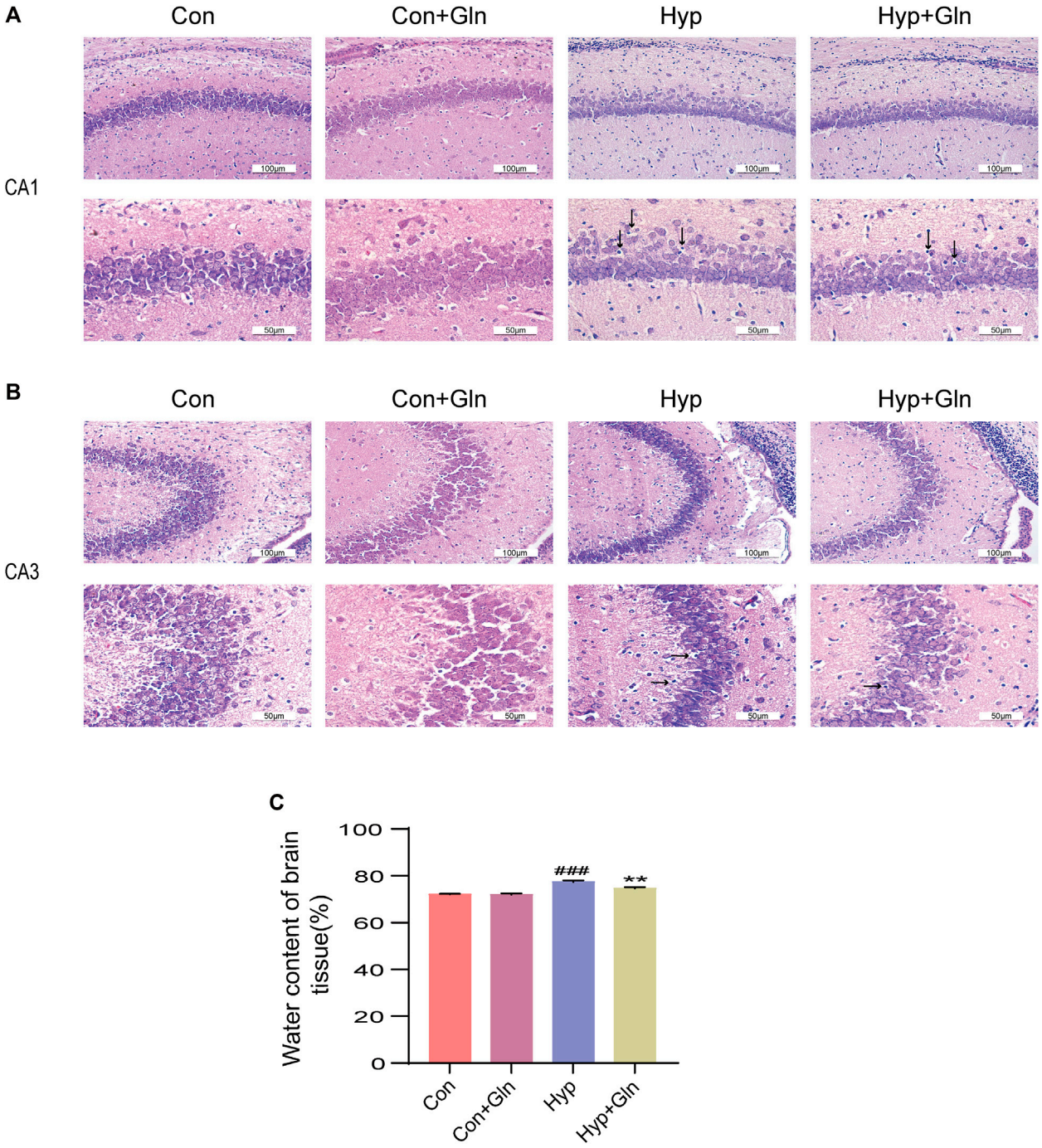

FIGURE 2
Gln ameliorates hyperoxia-induced cerebral edema and brain tissue damage. **(A)** Morphological changes of CA1 area of hippocampus in each group. Scale bar = 100 μm, 50 μm **(B)** Morphological changes of CA3 area of hippocampus in each group. Scale bar = 100 μm, 50 μm **(C)** Changes of brain water content in each group. Con (72.11 ± 0.12), Con + Gln (71.94 ± 0.32), Hyp (77.41 ± 0.37), Hyp + Gln (74.66 ± 0.29). $^{###}p < 0.001$ vs. the Con, $^{**}p < 0.01$ vs. the Hyp ($n = 3$). $p < 0.05$ was considered statistically significant. Areas of severe histopathological changes were marked by black arrows.

TUNEL staining

Brain tissue sections were dewaxed and treated with proteinase K working solution to permeabilize the cell and nuclear membranes and 3% H_2O_2 methanolic closure solution. The sections were incubated with TUNEL reaction mixture for 1 h at 37°C protected from light, and then reacted with anti-fluorescein antibody for 30 min protected from light. The sections were then incubated for 5 min using a 4, 6-diamidino-2-phenylindole (DAPI) (Santa Cruz, United States) solution. The apoptotic cells were quantitatively assessed, with three animals examined per group and three slices per hippocampal sample. TUNEL-positive hippocampal neurons of the CA1 zone were identified and counted under ×200 magnification, and the average number of positive apoptotic hippocampal neurons in the CA1 of three brains in a group was calculated.

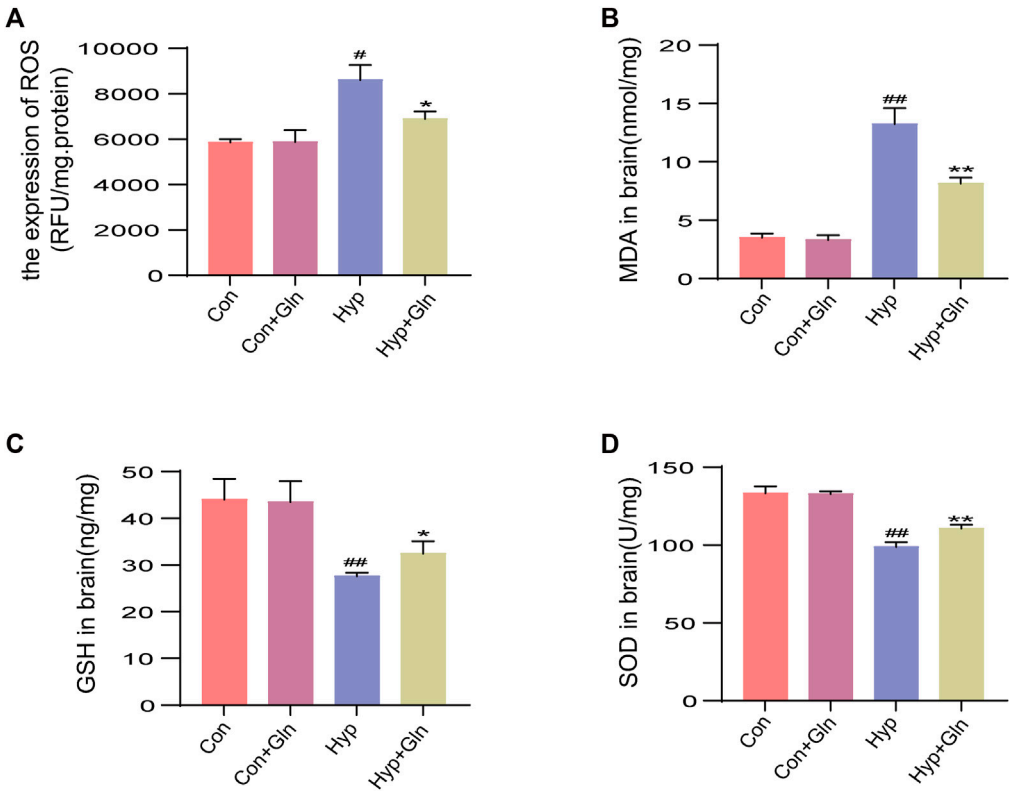

FIGURE 3
Gln improves oxidative stress after hyperoxia injury. **(A)** Total ROS content in hippocampus. Con (5851.05 ± 90.01), Con + Gln (5880.49 ± 303.02), Hyp (8160.46 ± 380.24), Hyp + Gln (6899.07 ± 184.10). **(B)** MDA content in hippocampus. Con (3.50 ± 0.21), Con + Gln (3.30 ± 0.23), Hyp (13.23 ± 0.78), Hyp + Gln (8.13 ± 0.29). **(C)** GSH content in hippocampus. Con (44.03 ± 2.54), Con + Gln (43.47 ± 2.58), Hyp (27.60 ± 0.44), Hyp + Gln (32.43 ± 1.53). **(D)** SOD content in hippocampus. Con (133.37 ± 2.49), Con + Gln (132.87 ± 1.00), Hyp (98.77 ± 1.78), Hyp + Gln (110.70 ± 1.36) ($n = 3$). $^{\#}p < 0.05$, $^{\#\#}p < 0.01$ vs. the Con, $^{*}p < 0.05$, $^{**}p < 0.01$ vs. the Hyp. $p < 0.05$ was considered statistically significant.

Immunohistochemical staining

The slides underwent dewaxing, dehydration, rehydration, antigen repair in boiling sodium citrate buffer, cold confirmed to room temperature and then rinsed in PBS. After 15 min of endogenous peroxide blocker blockade, the slides incubated with primary antibody Iba-1 (1:500) overnight at 4°C. After rewarming at room temperature for 1 h, PBS rinsing, they were then incubated with secondary antibodies (anti-goat anti-rabbit; Servicebio, Wuhan, China) at room temperature for 30 min. PBS rinsing them again and DAB color development for 5 min. The CA1 and CA3 regions of the hippocampus were analyzed. The images (200x, 400x) were captured by the microscope system (Leica, Germany). The experiment was repeated three times. The average number of activated microglia in the CA1 and CA3 area of three hippocampal in a group was calculated under ×400 magnification.

Western blotting

To investigate the expression of proteins by western blot analyses, hippocampal tissue samples were lysed in a protein cell lysis buffer (RIPA buffer (Solarbio, #R0010, Beijing, China): PMSF (Solarbio, #P0100, Beijing, China): phosphatase inhibitor (BestBio, #BB 1907, Shanghai, China) = 100:1:1). The protein concentration of the samples was determined using a bicinchoninic acid (BCA) protein assay kit (Thermo Scientific, #1859078, Shanghai, China). The samples were boiled for 10 min, and proteins were separated by electrophoresis using a 10% or 12% sodium dodecyl sulfate (SDS)-polyacrylamide gel. Then, proteins transferred to PVDF membranes (SigmaAldrich, #PR05505, United States). The membrane was blocked with 5% skim milk (diluted with TBST), incubated with primary antibody overnight at 4°C. The membrane was washed three times with 0.1% TBST, and incubated with secondary antibody for 1.5 h and then washed again with TBST. Then, the membranes were detected with an enhanced chemiluminescence kit (Boster, 16K22C02, China). The samples were wrapped in plastic wrap and transferred into the dark room. The processes of developing and fixing were done after the exposure of X-ray film. The results were scanned by a gel imaging system and analyzed by using ImageJ software. The grayscale value of each band was normalized to the grayscale value of the β-actin band, and the relative expression of the proteins was determined. The primary antibody included MKP-1 (1:1000), p-p38 (1:1000), p38 (1:1000), p-JNK (1:1000), JNK (1:1000), p-ERK (1:1000), ERK (1:1000), BDNF (1:1000), Synapsin Ia (1:1000), MBP (1:1000), Bax (1:1000), Bcl-2 (1:1000). The secondary antibodies include Goat anti-rabbit IgG/horseradish enzyme labeling (1:5000) and goat anti-mouse IgG/horseradish enzyme labeling (1:5000).

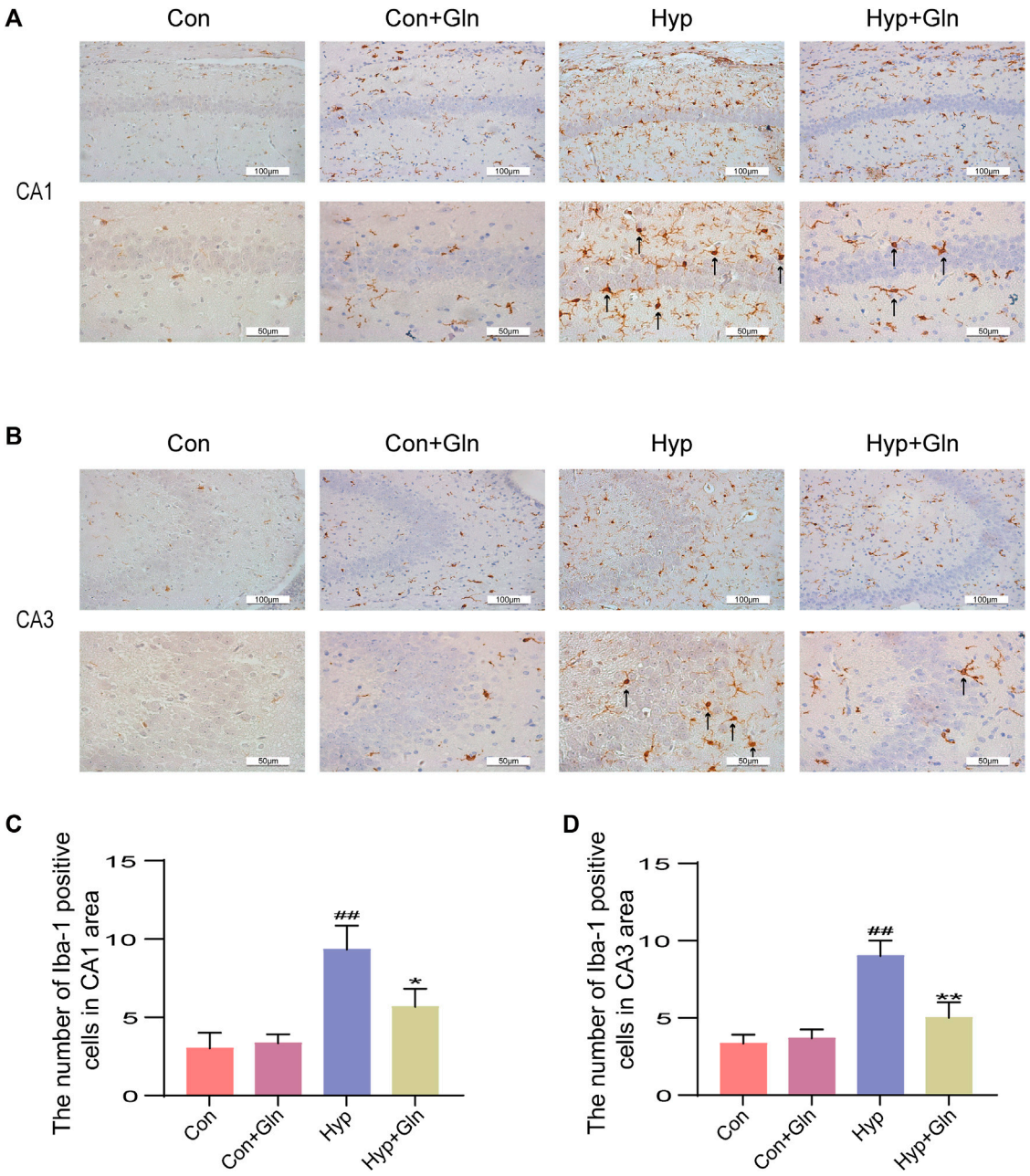

FIGURE 4
Gln inhibits microglia activation caused by hyperoxia. **(A)** Activation of microglia in the hippocampus (CA1) of each group. **(B)** Activation of microglia in the hippocampus (CA3) of each group. **(C)** Quantification of activated microglia (CA1). Con (3.00 ± 0.58), Con + Gln (3.33 ± 0.33), Hyp (9.33 ± 0.88), Hyp + Gln (5.67 ± 0.67) **(D)** Quantification of activated microglia (CA3). Con (3.33 ± 0.33), Con + Gln (3.67 ± 0.33), Hyp (9.00 ± 0.58), Hyp + Gln (5.00 ± 0.58) ($n = 3$). $^{\#\#}p < 0.01$ vs. the Con. $^{*}p < 0.05$, $^{**}p < 0.01$ vs. the Hyp. $p < 0.05$ was considered statistically significant. Activated microglia were marked by black arrows.

Statistical analysis

SPSS26.0 software was used for statistical analysis, and GraphPad Prism 8.0.1 software was used to crate figures. Values are presented as mean ± standard deviation, and statistical significance was determined by one-way ANOVA followed by Tukey and Bonferroni tests. Univariate repeated measures ANOVA was used to analyze escape latency (MWM) for independent group comparisons. $p < 0.05$ was considered statistically significant.

Result

Gln ameliorates hyp-induced elevated brain water content and hippocampal histopathological changes

In this study, brain edema was observed in each group by measuring brain tissue water content. As shown in Figure 2C, the brain tissue water content in the Hyp group was significantly higher

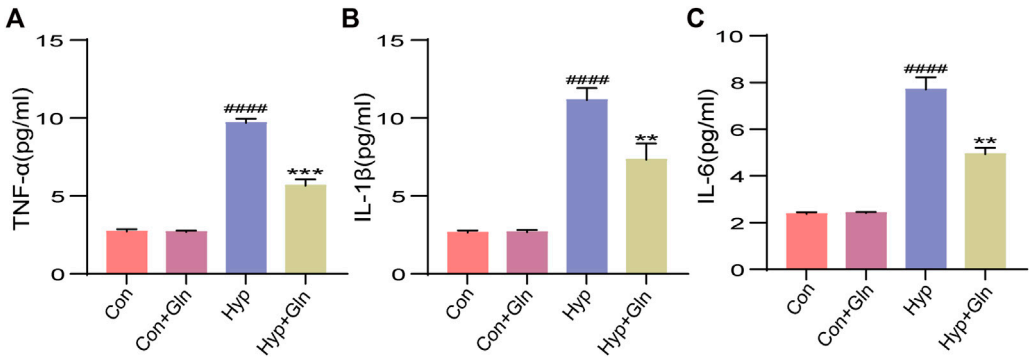

FIGURE 5
Gln inhibits inflammation caused by hyperoxia. **(A)** TNF-α content in hippocampus. Con (2.73 ± 0.84), Con + Gln (2.69 ± 0.41), Hyp (9.70 ± 0.15), Hyp + Gln (5.67 ± 0.22). **(B)** IL-1β content in hippocampus. Con (2.65 ± 0.08), Con + Gln (2.68 ± 0.08), Hyp (11.16 ± 0.44), Hyp + Gln (7.33 ± 0.60). **(C)** IL-6 content in hippocampus. Con (2.38 ± 0.05), Con + Gln (2.42 ± 0.02), Hyp (7.71 ± 0.30), Hyp + Gln (4.94 ± 0.16) ($n = 3$). $^{####}p < 0.0001$ vs. the Con, $^{**}p < 0.01$, $^{***}p < 0.001$ vs. the Hyp. $p < 0.05$ was considered statistically significant.

($p < 0.001$) than that in the Con group and that in the Hyp + Gln group was significantly lower ($p < 0.01$) than that in the Hyp group. Con (72.11 ± 0.12), Con + Gln (71.94 ± 0.32), Hyp (77.41 ± 0.37), Hyp + Gln (74.66 ± 0.29) ($n = 3$).

In addition, H&E staining was used to evaluate the success of the model preparation and to determine whether Gln ameliorates hyp-induced brain tissue damage. As shown in Figures 2A, B, the cells in the hippocampal CA1 and CA3 areas of neonatal rats in the Con and Con + Gln groups had regular morphology, neat arrangement, large and round nuclei, uniform nuclei color, and clear nucleoli. Compared with the Con group, the morphology of hippocampal CA1 and CA3 pyramidal cells in the Hyp group was less regular, with solid nuclei, cytoplasmic cavities, and a more diffuse arrangement of pyramidal neurons. However, the Hyp + Gln group showed improved cell morphology and arrangement and fewer cells with nuclear fixation. These results suggest that Gln ameliorated hyp-induced brain tissue damage and edema.

Gln improves oxidative stress after hyp-induced injury

The supernatant of the hippocampal tissue homogenate from each group of neonatal rats was tested using relevant kits to observe changes in oxidative stress levels. The results showed that total ROS levels ($p < 0.05$) (Figure 3A) and MDA levels ($p < 0.01$) (Figure 3B) were significantly higher and GSH ($p < 0.01$) (Figure 3C) and SOD (superoxide dismutase) levels ($p < 0.01$) (Figure 3D) were considerably lower in the Hyp group than in the Con group. However, the Hyp + Gln group showed significantly lower ROS ($p < 0.05$) and MDA ($p < 0.01$) content and considerably higher GSH ($p < 0.05$) and SOD ($p < 0.01$) content than the Hyp group. These results suggest that Gln reduces the level of oxidative stress induced by hyp. ROS: Con (5851.05 ± 90.01), Con + Gln (5880.49 ± 303.02), Hyp (8160.46 ± 380.24), Hyp + Gln (6899.07 ± 184.10); MDA: Con (3.50 ± 0.21), Con + Gln (3.30 ± 0.23), Hyp (13.23 ± 0.78), Hyp + Gln (8.13 ± 0.29); GSH: Con (44.03 ± 2.54), Con + Gln (43.47 ± 2.58), Hyp (27.60 ± 0.44), Hyp + Gln (32.43 ± 1.53); SOD: Con (133.37 ± 2.49), Con + Gln (132.87 ± 1.00), Hyp (98.77 ± 1.78), Hyp + Gln (110.70 ± 1.36) ($n = 3$).

Gln inhibits microglia activation and inflammation caused by hyp

Microglia were marked out with Iba-1, and microglia activation in CA1 (Figures 4A, C) and CA3 (Figures 4B, D) regions of hippocampus was observed and analysed in each group. In the Con and Con + Gln groups, scattered un-activated microglia, with thin, elongated cells and few branches were observed in a resting state in the hippocampal region. In the Hyp group, microglia had enlarged cytosomes, short and thick branches and protrusions, and the number of activated cells was significantly increased (CA1: $p < 0.01$, CA3: $p < 0.01$), suggesting microglial activation. However, Gln administration significantly reduced microglial activation after hyp (CA1: $p < 0.05$, CA3: $p < 0.01$). CA1: Con (3.00 ± 0.58), Con + Gln (3.33 ± 0.33), Hyp (9.33 ± 0.88), Hyp + Gln (5.67 ± 0.67). CA3: Con (3.33 ± 0.33), Con + Gln (3.67 ± 0.33), Hyp (9.00 ± 0.58), Hyp + Gln (5.00 ± 0.58) ($n = 3$).

To verify whether Gln could inhibit the inflammatory response caused by hyp, we examined the expression of TNF-α (Figure 5A), IL-1β (Figure 5B), and IL-6 (Figure 5C) in hippocampal tissues. Exposure to hyp significantly increased the expression levels of TNF-α ($p < 0.0001$), IL-1β ($p < 0.0001$), and IL-6 ($p < 0.0001$), showing that hyp induces an inflammatory response. However, these changes were significantly reversed after Gln application (TNF-α: $p < 0.001$, IL-1β: $p < 0.01$, IL-6: $p < 0.01$). TNF-α: Con (2.73 ± 0.84), Con + Gln (2.69 ± 0.41), Hyp (9.70 ± 0.15), Hyp + Gln (5.67 ± 0.22). IL-1β: Con (2.65 ± 0.08), Con + Gln (2.68 ± 0.08), Hyp (11.16 ± 0.44), Hyp + Gln (7.33 ± 0.60). IL-6: Con (2.38 ± 0.05), Con + Gln (2.42 ± 0.02), Hyp (7.71 ± 0.30), Hyp + Gln (4.94 ± 0.16) ($n = 3$).

Gln inhibits neuronal apoptosis in rats with hyperoxia-induced brain injury

TUNEL staining was performed to evaluate the inhibitory effect of Gln on apoptosis (Figure 6A). The results showed that the number of TUNEL-positive cells increased significantly after exposure to hyp ($p < 0.01$), while Gln administration exerted an inhibitory effect on hyp-

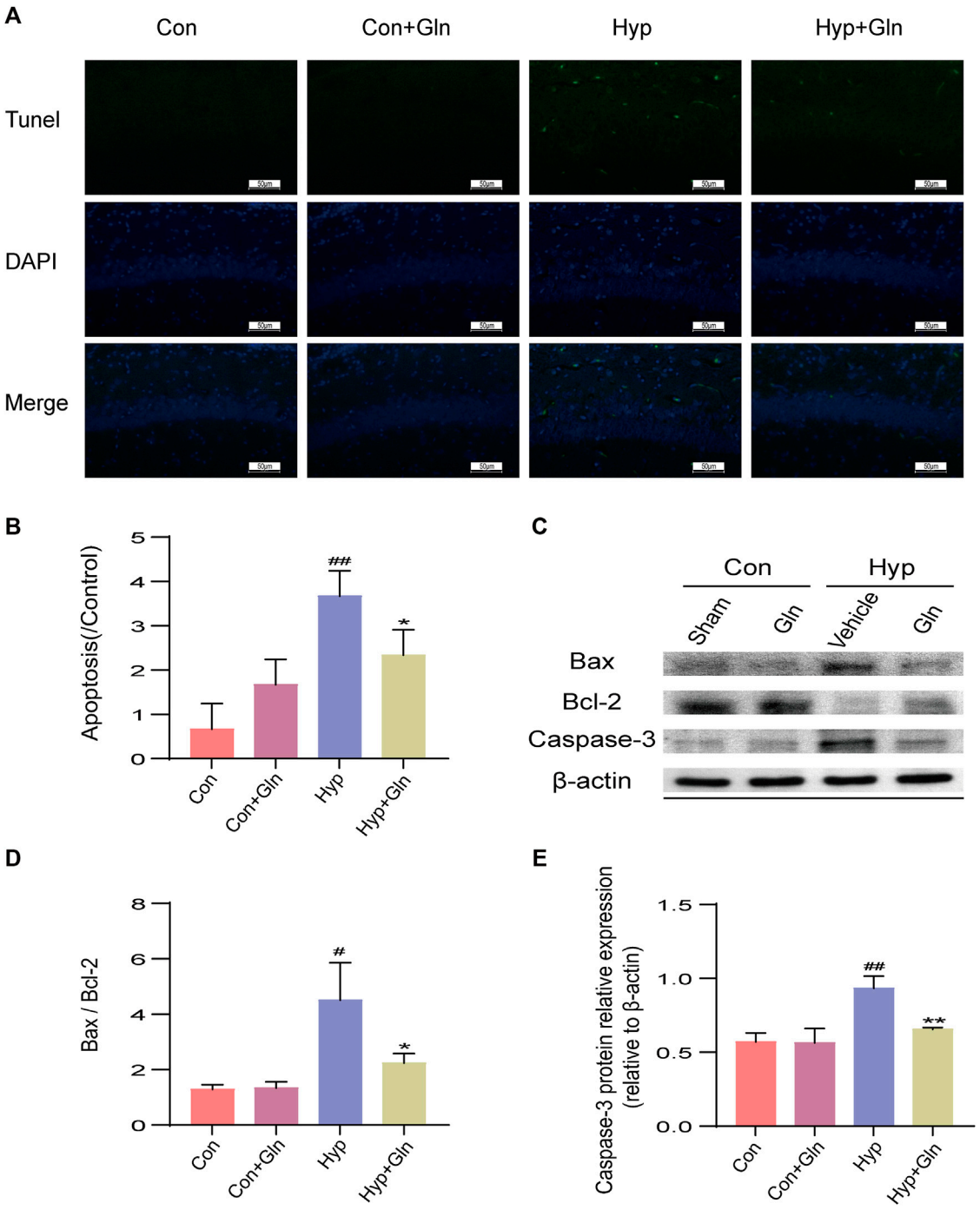

FIGURE 6
Gln inhibits neuronal apoptosis in rats with hyperoxia-induced brain injury. **(A)** TUNEL staining of hippocampal tissue. Scale bar = 50 μm **(B)** Hippocampal Apoptosis Index (AI). Con (0.67 ± 0.33), Con + Gln (1.67 ± 0.33), Hyp (3.67 ± 0.33), Hyp + Gln (2.33 ± 0.33) **(C)** Representative images of Western blotting analysis of Bax, Bcl-2 and Caspase-3 of each group. **(D)** Ratio of Bcl-2 to Bax. Con (1.29 ± 0.10), Con + Gln (1.34 ± 0.13), Hyp (4.50 ± 0.79), Hyp + Gln (2.24 ± 0.20). **(E)** Caspase-3 content in hippocampus. Con (0.57 ± 0.04), Con + Gln (0.56 ± 0.06), Hyp (0.93 ± 0.05), Hyp + Gln (0.66 ± 0.01) (n = 3). $^{\#}p < 0.05$, $^{\#\#}p < 0.01$ vs. the Con, $^{*}p < 0.05$, $^{**}p < 0.01$ vs. the Hyp. $p < 0.05$ was considered statistically significant.

induced apoptosis ($p < 0.05$) (Figure 6B). Con (0.67 ± 0.33), Con + Gln (1.67 ± 0.33), Hyp (3.67 ± 0.33), Hyp + Gln (2.33 ± 0.33) (n = 3).

To further clarify the apoptosis of hippocampal tissues in each group, caspase-3, Bax and Bcl-2 was determined by western blotting (Figure 6C). The results showed that the Bax/Bcl-2 ratio ($p < 0.05$) and caspase-3 content ($p < 0.01$) were significantly increased in the Hyp group; in contrast, it considerably improved in the Hyp + Gln group (Bax/Bcl-2: $p < 0.05$; Caspase-3: $p < 0.01$) (Figures 6D, E). Bax/Bcl-2: Con (1.29 ± 0.10), Con + Gln (1.34 ± 0.13), Hyp (4.50 ± 0.79), Hyp + Gln (2.24 ± 0.20); Caspase-3: Con (0.57 ± 0.04), Con + Gln (0.56 ± 0.06), Hyp (0.93 ± 0.05), Hyp + Gln (0.66 ± 0.01) (n = 3).

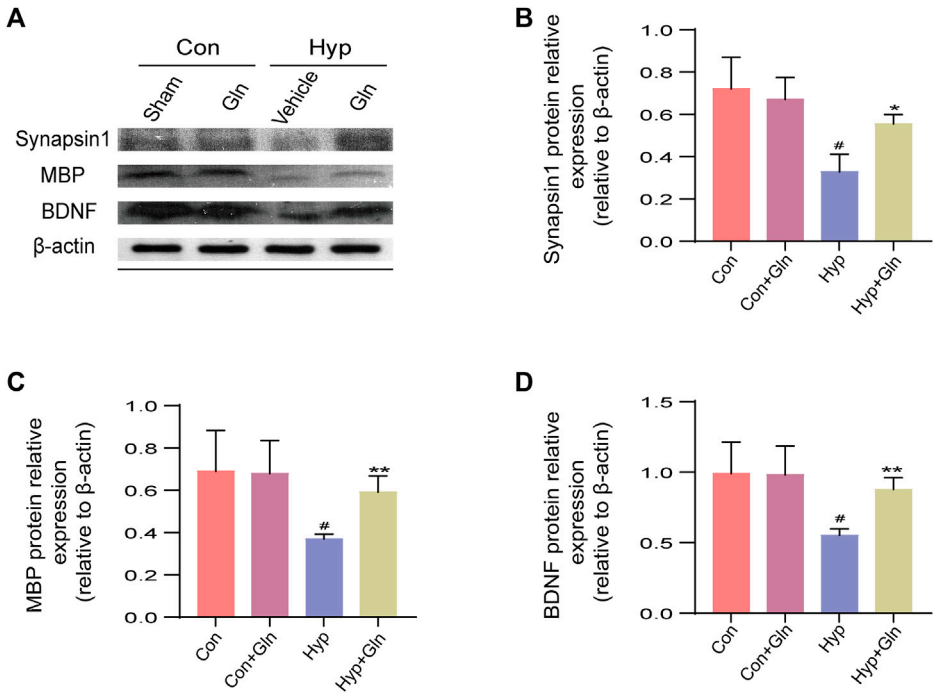

FIGURE 7
Gln increases BDNF, synapsin-1 and MBP expression in hippocampal tissue of rats with hyperoxia-induced brain injury. **(A)** Representative images of Western blotting analysis of synapsin-1, MBP and BDNF of each group. **(B)** Synapsin-1 content in hippocampus. Con (0.72 ± 0.09), Con + Gln (0.67 ± 0.06), Hyp (0.33 ± 0.05), Hyp + Gln (0.55 ± 0.03). **(C)** MBP content in hippocampus. Con (0.69 ± 0.11), Con + Gln (0.68 ± 0.09), Hyp (0.37 ± 0.01), Hyp + Gln (0.59 ± 0.04). **(D)** BDNF content in hippocampus. Con (0.99 ± 0.13), Con + Gln (0.98 ± 0.12), Hyp (00.55 ± 0.03), Hyp + Gln (0.88 ± 0.05). (n = 3). $^{\#}p < 0.05$ vs. the Con, $^{*}p < 0.05$, $^{**}p < 0.01$ vs. the Hyp. $p < 0.05$ was considered statistically significant.

Gln increases BDNF, Synapsin-1 and MBP expression in hippocampal tissue of rats with hyp-induced brain injury

To evaluate whether the neuroprotective effect of Gln is related to synaptic plasticity, impaired myelin formation, and the absence of neurotrophic factors, the expression of brain-derived neurotrophic factor (BDNF), synapsin I, and myelin basic protein (MBP) was examined after homogenizing hippocampal tissue obtained from each group of rats (Figure 7A). The results showed that the expression of synapsin I ($p < 0.05$), MBP ($p < 0.05$) and BDNF ($p < 0.05$) proteins decreased significantin the Hyp group. In the Hyp + Gln group, the expression of these proteins was significantly higher than that in the Hyp group (synapsin I: $p < 0.05$; MBP: $p < 0.01$; BDNF: $p < 0.01$). This indicated that Gln increased synapsin I (Figure 7B), MBP (Figure 7C) and BDNF (Figure 7D) expression in the hippocampal tissue of rats with hyp-induced brain injury to improve neural outcomes. Synapsin-1: Con (0.72 ± 0.09), Con + Gln (0.67 ± 0.06), Hyp (0.33 ± 0.05), Hyp + Gln (0.55 ± 0.03); MBP: Con (0.69 ± 0.11), Con + Gln (0.68 ± 0.09), Hyp (0.37 ± 0.01), Hyp + Gln (0.59 ± 0.04); BDNF: Con (0.99 ± 0.13), Con + Gln (0.98 ± 0.12), Hyp (00.55 ± 0.03), Hyp + Gln (0.88 ± 0.05) (n = 3).

Gln amelioration of hyp-induced brain injury may be related to the MKP-1/MAPK signaling pathway

The MAPK signaling pathway is closely associated with oxidative stress, inflammation, and apoptosis. To assess the role of Gln in a model of hyp-induced brain injury and its association with the MKP-1/MAPK signaling pathway, we examined the expression of MKP-1/MAPK signaling pathway-related proteins (Figure 8A). The results showed that compared with the Con group, MKP-1 expression ($p < 0.05$) (Figure 8B) was slightly increased, and p-p38/p38 ($p < 0.05$) (Figure 8C), p-ERK/ERK ($p < 0.01$) (Figure 8D), and p-JNK/JNK ($p < 0.01$) (Figure 8E) expression was significantly decreased in the Hyp group. Compared with the Hyp group, the Hyp + Gln group showed increased MKP-1 protein expression ($p < 0.01$) and significantly decreased p-p38/p38 ($p < 0.05$), p-ERK/ERK ($p < 0.05$), and p-JNK/JNK ($p < 0.01$) expression. MKP-1: Con (0.28 ± 0.01), Con + Gln (0.28 ± 0.01), Hyp (0.32 ± 0.01), Hyp + Gln (0.84 ± 0.11); p-p38/p38: Con (0.71 ± 0.00), Con + Gln (0.73 ± 0.05), Hyp (1.29 ± 0.17), Hyp + Gln (0.77 ± 0.02); p-ERK/ERK: Con (0.53 ± 0.04), Con + Gln (0.53 ± 0.03), Hyp (0.83 ± 0.04), Hyp + Gln (0.66 ± 0.04); p-JNK/JNK: Con (0.93 ± 0.03), Con + Gln (0.91 ± 0.04), Hyp (1.23 ± 0.01), Hyp + Gln (1.03 ± 0.02) (n = 3).

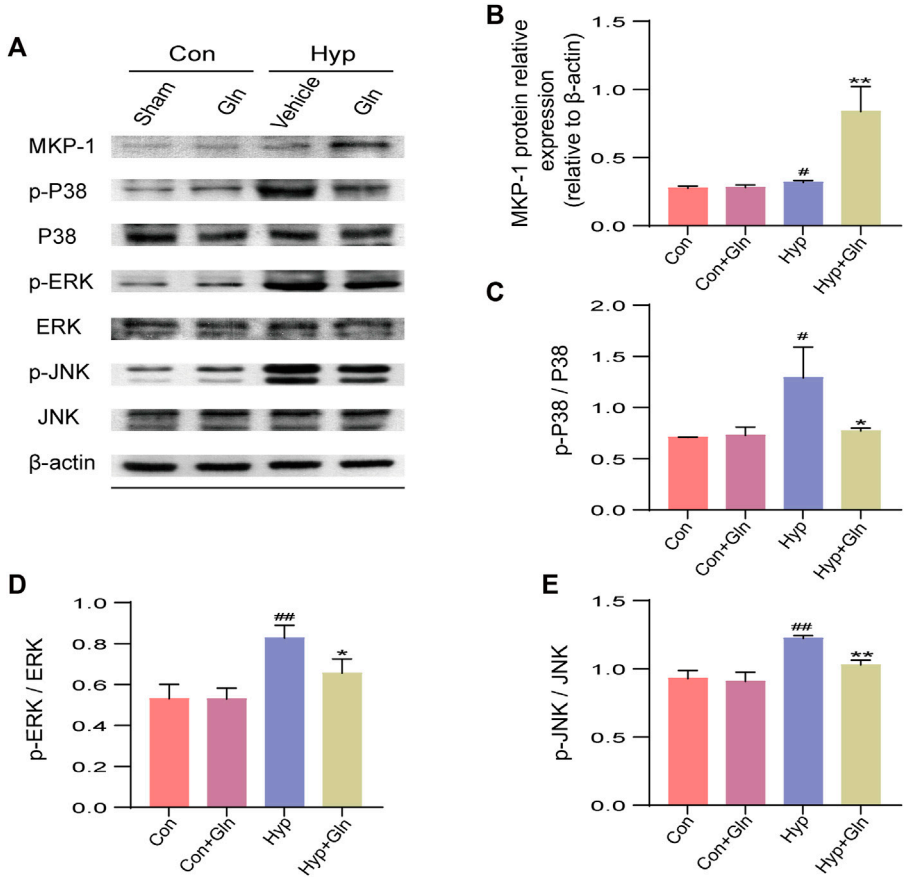

FIGURE 8
Gln amelioration of hyperoxia-induced brain injury may be related to MKP-1/MAPK signaling pathway. **(A)** Representative images of Western blotting analysis of MKP-1, p-p38, p38, p-ERK, ERK, p-JNK, and JNK of each group. **(B)** Quantification of MKP-1. Con (0.28 ± 0.01), Con + Gln (0.28 ± 0.01), Hyp (0.32 ± 0.01), Hyp + Gln (0.84 ± 0.11). **(C)** Ratio of p-p38 to p38. Con (0.71 ± 0.00), Con + Gln (0.73 ± 0.05), Hyp (1.29 ± 0.17), Hyp + Gln (0.77 ± 0.02). **(D)** Ratio of p-ERK to ERK. Con (0.53 ± 0.04), Con + Gln (0.53 ± 0.03), Hyp (0.83 ± 0.04), Hyp + Gln (0.66 ± 0.04). **(E)** Ratio of p-JNK to JNK. Con (0.93 ± 0.03), Con + Gln (0.91 ± 0.04), Hyp (1.23 ± 0.01), Hyp + Gln (1.03 ± 0.02). ($n = 3$). $^{\#}p < 0.05$, $^{\#\#}p < 0.01$ vs. the Con, $^{*}p < 0.05$, $^{**}p < 0.01$ vs. the Hyp. $p < 0.05$ was considered statistically significant.

Gln ameliorates neurobehavioral deficits in rats with hyp-induced brain injury

The Morris water maze assesses spatial learning and long-term memory. To further assess the neuroprotective effect of Gln, the neurobehavioral function of each group of adolescent rats was examined using the MWM experiment (P30-34). The escape latency (Figure 9A) showed a decreasing trend with increasing time in all groups. Gln administration failed to shorten escape latency after hyp-induced injury on the first day of testing. However, the mean escape latency was significantly shorter ($p < 0.05$; $p < 0.01$) in the Hyp + Gln group from Days three to four. These results suggest that rats in all groups had the ability to learn and remember. These abilities were impaired to varying degrees by hyp-induced brain injury; however, Gln improved the spatial learning abilities of rats with hyp-induced brain injury. In the observation of the swimming path on Day 5, it was found that the Hyp group rats crossed the platform position (Figure 9B) less ($p < 0.001$) often than the Con group did, and the percentage of distance traveled in the target quadrant (Figure 9C) was less ($p < 0.01$) than that of the Con group. In the Hyp + Gln group, the number of platform crossings increased ($p < 0.01$) compared to that in the Hyp group, and the percentage of distance traveled in the target quadrant increased ($p < 0.01$) compared to that in the Hyp group. These results suggest that hyp-induced brain damage during the neonatal period affects memory capacity in adolescent rats. However, administration of Gln significantly improved the duration spent in the plateau quadrant, suggesting that Gln effectively alleviated memory impairment induced by hyp. No significant difference was observed in the mean swimming speed between groups (Figure 9D). Latency to escape: Con (101.96 ± 7.86, 21.63 ± 4.05, 18.07 ± 3.71, 12.94 ± 3.68), Con + Gln (101.76 ± 10.43, 23.10 ± 4.09, 18.85 ± 4.16, 12.66 ± 3.85), Hyp (110.78 ± 4.19, 70.39 ± 13.85, 58.48 ± 8.53, 47.28 ± 4.24), Hyp + Gln (102.54 ± 8.82, 58.89 ± 8.76, 35.25 ± 5.99, 26.22 ± 4.50); Times crossing platform: Con (6.50 ± 0.62), Con + Gln (6.17 ± 0.70), Hyp (1.50 ± 0.56), Hyp + Gln (4.00 ± 0.37); Distance spend in the target quarter: Con (58.97 ± 5.46), Con + Gln (47.82 ± 4.06), Hyp (34.12 ± 4.42), Hyp + Gln (52.19 ± 2.92); Swim speed: Con (23.04 ± 1.22), Con + Gln (23.39 ± 1.58), Hyp (21.95 ± 2.37), Hyp + Gln (22.96 ± 0.86) (n = 6).

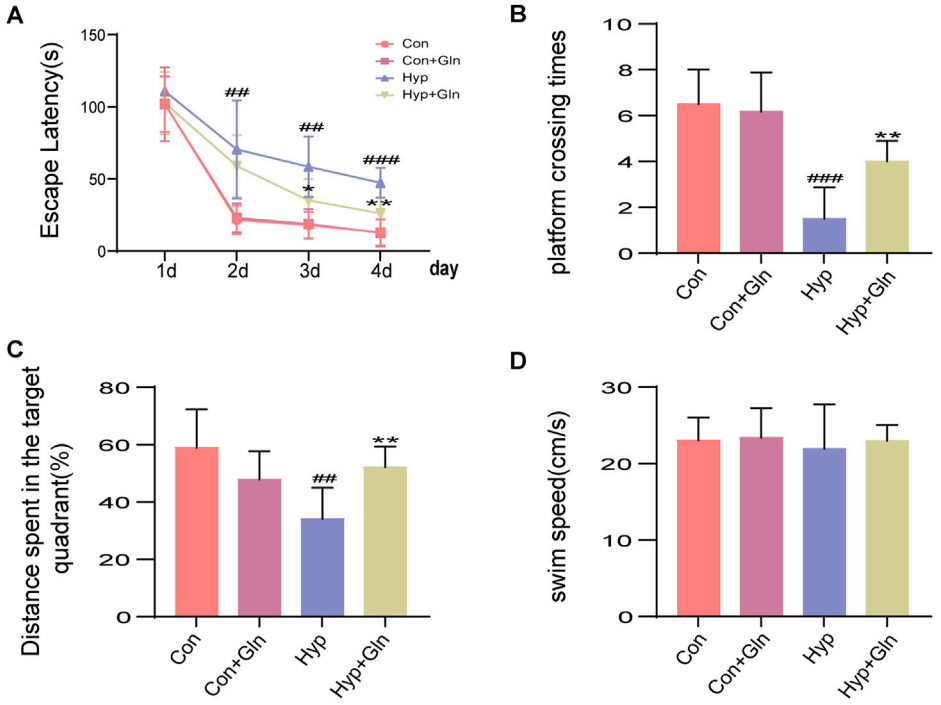

FIGURE 9
Gln ameliorates distant neurobehavioral deficits in rats with hyperoxia-induced brain injury. **(A)** Latency to escape in MWM. Con (101.96 ± 7.86, 21.63 ± 4.05, 18.07 ± 3.71, 12.94 ± 3.68), Con + Gln (101.76 ± 10.43, 23.10 ± 4.09, 18.85 ± 4.16, 12.66 ± 3.85), Hyp (110.78 ± 4.19, 70.39 ± 13.85, 58.48 ± 8.53, 47.28 ± 4.24), Hyp + Gln (102.54 ± 8.82, 58.89 ± 8.76, 35.25 ± 5.99, 26.22 ± 4.50). **(B)** Times crossing platform in MWM. Con (6.50 ± 0.62), Con + Gln (6.17 ± 0.70), Hyp (1.50 ± 0.56), Hyp + Gln (4.00 ± 0.37). **(C)** Distance spend in the target quarter in MWM. Con (58.97 ± 5.46), Con + Gln (47.82 ± 4.06), Hyp (34.12 ± 4.42), Hyp + Gln (52.19 ± 2.92). **(D)** Swim speed in MWM. Con (23.04 ± 1.22), Con + Gln (23.39 ± 1.58), Hyp (21.95 ± 2.37), Hyp + Gln (22.96 ± 0.86) ($n = 6$). $^{\#\#}p < 0.01$, $^{\#\#\#}p < 0.001$ vs. the Con, $^{*}p < 0.05$, $^{**}p < 0.01$ vs. the Hyp. $p < 0.05$ was considered statistically significant.

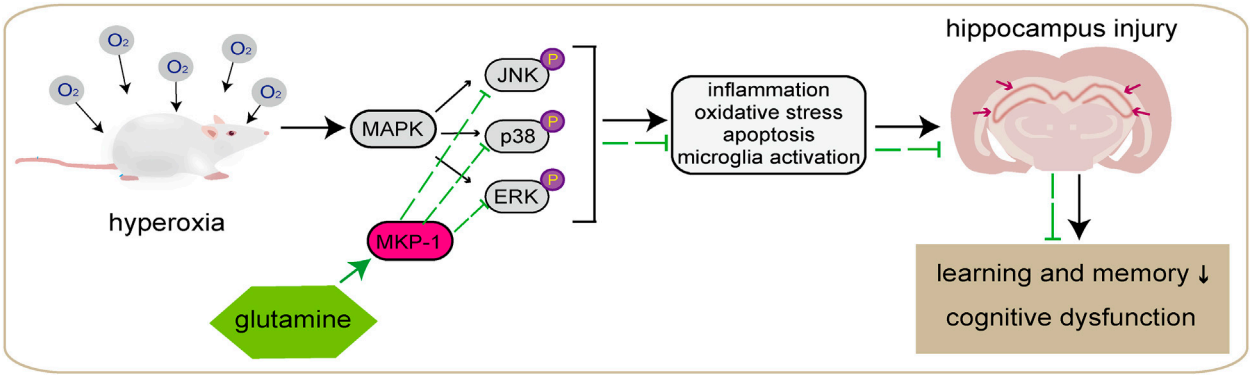

FIGURE 10
Graphical abstract. Hyperoxia can lead to behavioral abnormalities and neurocognitive and learning deficits in newborn rats, which is thought to be related to damage to hippocampal neurons caused by oxidative stress, inflammation, apoptosis, and microglial overactivation. Gln may induce MKP-1 and thereby inhibit activation of the MAPK signaling pathway, leading to a reduction in oxidative stress, inflammation, and apoptosis in cells and attenuating hyperoxia-induced damage to cerebral tissue, and improve learning and memory dysfunction.

Discussion

Long-term hyperoxia treatment can lead to behavioral abnormalities and neurocognitive and learning deficits in preterm infants, which is thought to be related to damage to hippocampal neurons caused by oxidative stress, inflammation, apoptosis, and reduced expression of neurotrophic factors (Sifringer et al., 2015). Spatial cognition and memory are inseparable from hippocampal function, and alterations in hippocampal structure and function are associated with reduced spatial, social, and mathematical abilities

(Banker et al., 2021). We found that hyperoxia caused brain tissue edema and hippocampal damage in neonatal rats, with significant deficits in spatial memory and learning ability observed during adolescence. Gln is an *in vivo* antioxidant precursor substance with multiple regulatory mechanisms and known antioxidant potential (Cetinbas et al., 2010), and its neuroprotective potential has been demonstrated in animal models of neonatal brain injury, including hypoxia-induced neuroinflammation. Gln ameliorates spatial learning and memory dysfunction in neonatal brain injury caused by hyperoxia. The neuroprotective effects of Gln appear to be associated with its anti-inflammatory and anti-apoptotic effects after attenuation of oxidative stress, which is beneficial for long-term brain development (de Kieviet et al., 2012). Thus, Gln is a promising drug for the treatment of hyp-induced brain injury.

Oxidative stress is a key factor in the complex cascade of brain injury mechanisms. In preterm infants, whose antioxidant systems are not yet well-developed, the excessive ROS generated in a hyperoxic environment trigger an inflammatory response that induces prostaglandin production and leads to the formation of intercellular interstitial edema (Lapi et al., 2020). Microglia, a major component of the immune defense system of the central nervous system, are overactivated by multiple diseases and external stimuli (including traumatic brain trauma and neurological infections) (Loane and Byrnes, 2010), and in response secrete ROS to induce oxidative stress and inflammatory responses, which can lead to further neurological diseases. It was found that increased levels of pro-inflammatory cytokines in the hippocampus, such as IL-6, IL-1β, and TNF-α, activate microglia and lead to neurotransmitter alterations, causing dysfunction in spatial learning and cognitive faculties (Hernández-Rabaza et al., 2016). Gln, a precursor of the endogenous antioxidant glutathione, has antioxidant potential and the ability to balance oxidative stress (Cetinbas et al., 2010). It may exert neuroprotective effects through inhibition of excessive inflammatory responses. In this study, administration of Gln was seen to significantly reduce hyp-induced edema in brain tissue, ameliorate hippocampal damage, decrease microglial activation, significantly decrease MDA and ROS levels, and significantly increase SOD and GSH levels. The results suggest that in the developing brain, Gln may have antioxidant activity against hyp-induced oxidative stress, inhibit microglial overactivation, and inhibit the synthesis and release of pro-inflammatory cytokines, thus exerting a protective effect by reducing neuronal inflammation and damage.

Many proteins also play important roles in the development and treatment of brain injury. BDNF is an important protein that can influence neuroplasticity, affecting cognition, brain structure and function (Roy et al., 2020). Synapsin I, the most abundant protein in synaptic vesicles, is involved in synaptic development and transmission, regulation of neurotransmitter release (Lu et al., 2018), neurodevelopment, and neuronal growth. It plays a key role in information processing and transmission and is thought to have a positive impact on learning and memory consolidation (Zhu et al., 2018). MBP is the main protein in the myelin sheath of the central nervous system, where it maintains sheath stability, structure, and function (Krugmann et al., 2020). MBP is involved in the myelination process as a major component of the myelin membrane in the CNS, and changes in MBP levels may reflect the degree of white matter damage in astrocytes, which has been identified as a sensitive and specific marker of brain damage in recent years (Zhou et al., 2015). Oxidative stress, inflammatory responses, and apoptosis triggered by hyperoxia in the developing brain are believed to have a major effect on the survival of immature oligodendrocytes (which are highly sensitive to oxygen concentration), leading to impaired myelin formation (Brehmer et al., 2012). We found that hyperoxia leads to decreased levels of BDNF, synapsin I, and MBP in the hippocampus, in agreement with previous findings (Kim et al., 2016). However, Gln may also play a therapeutic role by increasing neurotrophic factor levels and regulating signals related to synaptic plasticity.

MAPK mediates cellular responses to external stimuli and regulates a variety of cellular activities such as cell proliferation, differentiation, apoptosis, and neuronal plasticity (Keshet and Seger, 2010). Evidence suggests that the MAPK signaling pathway can regulate oxidative stress (Chen et al., 2020) and microglial activation (Na et al., 2014) to suppress inflammatory factor production. It is also involved in apoptosis (Hsieh et al., 2021). Negative regulation of MAPK activity is achieved through MKP. MKP-1 expression is upregulated both when oxidative damage occurs (Patterson et al., 2009) and on administration of neuroprotective drugs (Jeanneteau et al., 2010). MKP-1 is known to reduce levels of pro-inflammatory cytokines (Zhang et al., 2012) and apoptosis by accelerating MAPK inactivation, thus improving neuronal function by decreasing phosphorylation of JNK, ERK, and p38 (Horita et al., 2010). Gu et al. showed that Gln inhibited ROS production, increased antioxidant enzyme activity, and ameliorated intestinal inflammation and oxidative damage by reducing the activation of the MAPK pathway. In keeping with previous findings, we found that the administration of Gln increased MKP-1 expression, inhibited phosphorylation of JNK, ERK, and p38, and reduced oxidative stress, inflammation, and apoptosis. Therefore, we speculate that Gln may induce MKP-1 and thereby inhibit activation of the MAPK signaling pathway, leading to a reduction in oxidative stress, inflammation, and apoptosis in cells and attenuating hyp-induced damage to cerebral tissue.

Conclusion

This study shows that in newborn rats with hyp-induced brain injury, Gln has potent anti-inflammatory and antioxidant activities, reduces hippocampal damage and neurological dysfunction, ameliorates hyp-induced brain injury, and decreases apoptosis, thus alleviating learning difficulties and memory dysfunction in newborn rats with hyp-induced brain injury. Our results suggest that the molecular mechanism underlying these effects may be related to the MKP-1/MAPK signaling pathway (Figure 10). This study provides a theoretical basis for the possible pathological mechanisms underlying hyp-induced newborn neurological injury and its prevention. In summary, Gln has a neuroprotective effect in neonatal brain injury caused by hyperoxia and has potential as a drug candidate.

Data availability statement

The original contributions presented in the study are included in the article/supplementary material, further inquiries can be directed to the corresponding authors.

Ethics statement

The animal study was reviewed and approved by Institutional Animal Use and Care Committee of Yanbian University of Science and Technology.

Author contributions

All authors helped to perform the research; ZJ, SoC, and DX conceived and designed the experiments, and revised the manuscript; CX collected the data, wrote the manuscript, and analyzed the data; YY and SC provided the study materials.

Funding

The work was supported by National Nature Science Foundation of China (grant number: 81860279), National Nature Science Foundation of China (grant number: 31760330), and National Science Foundation of Jilin Province for Sciences and Technology (20220101355JC).

Conflict of interest

The authors declare that the research was conducted in the absence of any commercial or financial relationships that could be construed as a potential conflict of interest.

Publisher's note

References

Al, N., Çakir, A., Koç, C., Cansev, M., and Alkan, T. (2020). Antioxidative effects of uridine in a neonatal rat model of hyperoxic brain injury. *Turk J. Med. Sci.* 50 (8), 2059–2066. doi:10.3906/sag-2002-14

Banker, S. M., Pagliaccio, D., Ramphal, B., Thomas, L., Dranovsky, A., and Margolis, A. E. (2021). Altered structure and functional connectivity of the hippocampus are associated with social and mathematical difficulties in nonverbal learning disability. *Hippocampus* 31 (1), 79–88. doi:10.1002/hipo.23264

Brehmer, F., Bendix, I., Prager, S., van de Looij, Y., Reinboth, B. S., Zimmermanns, J., et al. (2012). Interaction of inflammation and hyperoxia in a rat model of neonatal white matter damage. *PLoS One* 7 (11), e49023. doi:10.1371/journal.pone.0049023

Cetinbas, F., Yelken, B., and Gulbas, Z. (2010). Role of glutamine administration on cellular immunity after total parenteral nutrition enriched with glutamine in patients with systemic inflammatory response syndrome. *J. Crit. Care* 25 (4), 661. e1-6. doi:10.1016/j.jcrc.2010.03.011

Chen, Q., Zhou, Y., Zhou, L., Fu, Z., Yang, C., Zhao, L., et al. (2020). TRPC6-dependent Ca(2+) signaling mediates airway inflammation in response to oxidative stress via ERK pathway. *Cell. Death Dis.* 11 (3), 170. doi:10.1038/s41419-020-2360-0

de Kieviet, J. F., Oosterlaan, J., Vermeulen, R. J., Pouwels, P. J., Lafeber, H. N., and van Elburg, R. M. (2012). Effects of glutamine on brain development in very preterm children at school age. *Pediatrics* 130 (5), e1121–e1127. doi:10.1542/peds.2012-0928

de Kieviet, J. F., Vuijk, P. J., van den Berg, A., Lafeber, H. N., Oosterlaan, J., and van Elburg, R. M. (2014). Glutamine effects on brain growth in very preterm children in the first year of life. *Clin. Nutr.* 33 (1), 69–74. doi:10.1016/j.clnu.2013.03.019

Gong, Z. Y., Yuan, Z. Q., Dong, Z. W., and Peng, Y. Z. (2017). Glutamine with probiotics attenuates intestinal inflammation and oxidative stress in a rat burn injury model through altered iNOS gene aberrant methylation. *Am. J. Transl. Res.* 9 (5), 2535–2547.

Hernández-Rabaza, V., Cabrera-Pastor, A., Taoro-González, L., Malaguarnera, M., Agustí, A., Llansola, M., et al. (2016). Hyperammonemia induces glial activation, neuroinflammation and alters neurotransmitter receptors in hippocampus, impairing spatial learning: Reversal by sulforaphane. *J. Neuroinflammation* 13, 41. doi:10.1186/s12974-016-0505-y

Hintz, S. R., Vohr, B. R., Bann, C. M., Taylor, H. G., Das, A., Gustafson, K. E., et al. (2018). Preterm neuroimaging and school-age cognitive outcomes. *Pediatrics* 142 (1), e20174058. doi:10.1542/peds.2017-4058

Horita, H., Wada, K., Rivas, M. V., Hara, E., and Jarvis, E. D. (2010). The dusp1 immediate early gene is regulated by natural stimuli predominantly in sensory input neurons. *J. Comp. Neurol.* 518 (14), 2873–2901. doi:10.1002/cne.22370

Hsieh, M. C., Lo, Y. S., Chuang, Y. C., Lin, C. C., Ho, H. Y., Hsieh, M. J., et al. (2021). Dehydrocrenatidine extracted from Picrasma quassioides induces the apoptosis of nasopharyngeal carcinoma cells through the JNK and ERK signaling pathways. *Oncol. Rep.* 46 (2), 166. doi:10.3892/or.2021.8117

Hu, H., Dai, S., Li, J., Wen, A., and Bai, X. (2020). Glutamine improves heat stress-induced oxidative damage in the broiler thigh muscle by activating the nuclear factor erythroid 2-related 2/Kelch-like ECH-associated protein 1 signaling pathway. *Poult. Sci.* 99 (3), 1454–1461. doi:10.1016/j.psj.2019.11.001

Huang, J., Liu, J., Chang, G., Wang, Y., Ma, N., Roy, A. C., et al. (2021). Glutamine supplementation attenuates the inflammation caused by LPS-induced acute lung injury in mice by regulating the TLR4/MAPK signaling pathway. *Inflammation* 44 (6), 2180–2192. doi:10.1007/s10753-021-01491-2

Jeanneteau, F., Deinhardt, K., Miyoshi, G., Bennett, A. M., and Chao, M. V. (2010). The MAP kinase phosphatase MKP-1 regulates BDNF-induced axon branching. *Nat. Neurosci.* 13 (11), 1373–1379. doi:10.1038/nn.2655

Keshet, Y., and Seger, R. (2010). The MAP kinase signaling cascades: A system of hundreds of components regulates a diverse array of physiological functions. *Methods Mol. Biol.* 661, 3–38. doi:10.1007/978-1-60761-795-2_1

Kim, H. (2011). Glutamine as an immunonutrient. *Yonsei Med. J.* 52 (6), 892–897. doi:10.3349/ymj.2011.52.6.892

Kim, J. M., Im, Y. N., Chung, Y. J., Youm, J. H., Im, S. Y., Han, M. K., et al. (2022). Glutamine deficiency shifts the asthmatic state toward neutrophilic airway inflammation. *Allergy* 77 (4), 1180–1191. doi:10.1111/all.15121

Kim, Y. E., Park, W. S., Sung, D. K., Ahn, S. Y., Sung, S. I., Yoo, H. S., et al. (2016). Intratracheal transplantation of mesenchymal stem cells simultaneously attenuates both lung and brain injuries in hyperoxic newborn rats. *Pediatr. Res.* 80 (3), 415–424. doi:10.1038/pr.2016.88

Krugmann, B., Radulescu, A., Appavou, M. S., Koutsioubas, A., Stingaciu, L. R., Dulle, M., et al. (2020). Membrane stiffness and myelin basic protein binding strength as molecular origin of multiple sclerosis. *Sci. Rep.* 10 (1), 16691. doi:10.1038/s41598-020-73671-3

Lapi, D., Stornaiuolo, M., Sabatino, L., Sommella, E., Tenore, G., Daglia, M., et al. (2020). The pomace extract taurisolo protects rat brain from ischemia-reperfusion injury. *Front. Cell. Neurosci.* 14, 3. doi:10.3389/fncel.2020.00003

Loane, D. J., and Byrnes, K. R. (2010). Role of microglia in neurotrauma. *Neurotherapeutics* 7 (4), 366–377. doi:10.1016/j.nurt.2010.07.002

Lu, J., Jiao, Z., Yu, Y., Zhang, C., He, X., Li, Q., et al. (2018). Programming for increased expression of hippocampal GAD67 mediated the hypersensitivity of the hypothalamic-pituitary-adrenal axis in male offspring rats with prenatal ethanol exposure. *Cell. Death Dis.* 9 (6), 659. doi:10.1038/s41419-018-0663-1

Lv, F., Li, N., Kong, M., Wu, J., Fan, Z., Miao, D., et al. (2020). CDKN2a/p16 antagonizes hepatic stellate cell activation and liver fibrosis by modulating ROS levels. *Front. Cell. Dev. Biol.* 8, 176. doi:10.3389/fcell.2020.00176

Na, K. S., Jung, H. Y., and Kim, Y. K. (2014). The role of pro-inflammatory cytokines in the neuroinflammation and neurogenesis of schizophrenia. *Prog. Neuropsychopharmacol. Biol. Psychiatry* 48, 277–286. doi:10.1016/j.pnpbp.2012.10.022

Oliveira, G. P., Dias, C. M., Pelosi, P., and Rocco, P. R. (2010). Understanding the mechanisms of glutamine action in critically ill patients. *Acad Bras Cienc* 82 (2), 417–430. doi:10.1590/s0001-37652010000200018

Patterson, K. I., Brummer, T., O'Brien, P. M., and Daly, R. J. (2009). Dual-specificity phosphatases: Critical regulators with diverse cellular targets. *Biochem. J.* 418 (3), 475–489. doi:10.1042/bj20082234

Perng, W. C., Huang, K. L., Li, M. H., Hsu, C. W., Tsai, S. H., Chu, S. J., et al. (2010). Glutamine attenuates hyperoxia-induced acute lung injury in mice. *Clin. Exp. Pharmacol. Physiol.* 37 (1), 56–61. doi:10.1111/j.1440-1681.2009.05239.x

Roy, N., Barry, R. J., Fernandez, F. E., Lim, C. K., Al-Dabbas, M. A., Karamacoska, D., et al. (2020). Electrophysiological correlates of the brain-derived neurotrophic factor (BDNF) Val66Met polymorphism. *Sci. Rep.* 10 (1), 17915. doi:10.1038/s41598-020-74780-9

Sifringer, M., Bendix, I., von Haefen, C., Endesfelder, S., Kalb, A., Bührer, C., et al. (2013). Oxygen toxicity is reduced by acetylcholinesterase inhibition in the developing rat brain. *Dev. Neurosci.* 35 (2-3), 255–264. doi:10.1159/000346723

Sifringer, M., von Haefen, C., Krain, M., Paeschke, N., Bendix, I., Bührer, C., et al. (2015). Neuroprotective effect of dexmedetomidine on hyperoxia-induced toxicity in the neonatal rat brain. *Oxid. Med. Cell. Longev.* 2015, 530371. doi:10.1155/2015/530371

Zhang, T., Lu, X., Arnold, P., Liu, Y., Baliga, R., Huang, H., et al. (2012). Mitogen-activated protein kinase phosphatase-1 inhibits myocardial TNF-α expression and improves cardiac function during endotoxemia. *Cardiovasc Res.* 93 (3), 471–479. doi:10.1093/cvr/cvr346

Zhou, W., Li, W., Qu, L. H., Tang, J., Chen, S., and Rong, X. (2015). Relationship of plasma S100B and MBP with brain damage in preterm infants. *Int. J. Clin. Exp. Med.* 8 (9), 16445–16453.

Zhu, L., Tang, T., Fan, R., Luo, J. K., Cui, H. J., Zhang, C. H., et al. (2018). Xuefu Zhuyu decoction improves neurological dysfunction by increasing synapsin expression after traumatic brain injury. *Neural Regen. Res.* 13 (8), 1417–1424. doi:10.4103/1673-5374.235297

frontiers | Frontiers in Pharmacology

TYPE Original Research
PUBLISHED 15 February 2023
DOI 10.3389/fphar.2023.1135934

OPEN ACCESS

EDITED BY
Morena Zusso,
University of Padua, Italy

REVIEWED BY
Eugenio Ragazzi,
University of Padua, Italy
Ricardo Benjamin Maccioni,
International Center for Biomedicine,
Chile

*CORRESPONDENCE
Xian Zhou,
p.zhou@westernsydney.edu.au

SPECIALTY SECTION
This article was submitted to Neuropharmacology, a section of the journal Frontiers in Pharmacology

RECEIVED 02 January 2023
ACCEPTED 31 January 2023
PUBLISHED 15 February 2023

CITATION
Liu Y, Chang D, Liu T and Zhou X (2023), Natural product-based bioactive agents in combination attenuate neuroinflammation in a tri-culture model. *Front. Pharmacol.* 14:1135934. doi: 10.3389/fphar.2023.1135934

Natural product-based bioactive agents in combination attenuate neuroinflammation in a tri-culture model

Yang Liu[1], Dennis Chang[1], Tianqing Liu[1,2] and Xian Zhou[1]*

[1]NICM Health Research Institute, Western Sydney University, Westmead, NSW, Australia, [2]School of Science, Western Sydney University, Penrith, NSW, Australia

Introduction: Neuroinflammation is an important pathological event contributing to the onset and progression of neurodegenerative diseases. The hyperactivation of microglia triggers the release of excessive proinflammatory mediators that lead to the leaky blood-brain barrier and impaired neuronal survival. Andrographolide (AN), baicalein (BA) and 6-shogaol (6-SG) possess anti-neuroinflammatory properties through diverse mechanisms of action. The present study aims to investigate the effects of the pair-combinations of these bioactive compounds in attenuating neuroinflammation.

Methods: A tri-culture model with microglial N11 cells, microvascular endothelial MVEC(B3) cells, and neuroblastoma N2A cells was established in a transwell system. AN, BA and 6-SG used alone (25 μM) or in pair-wised combinations (12.5 + 12.5 μM) were subjected to the tri-culture system. Upon the stimulation of lipopolysaccharides (LPS) at 1 μg/mL, tumor necrosis factor-alpha (TNF-α) and interleukin 6 (IL-6) levels were determined by ELISA assays. Immunofluorescence staining was applied to investigate the nuclear translocation of nuclear factor kappa B p65 (NF-κB p65) on N11 cells, expressions of protein zonula occludens-1 (ZO-1) on MVEC cells and phosphorylated tau (p-tau) on N2A cells, respectively. The endothelial barrier permeability of MVEC cells was assessed by the Evans blue dye, and the resistance from the endothelial barrier was measured by transepithelial/endothelial electrical resistance (TEER) value. Neuronal survival of N2A cells was determined by Alamar blue and MTT assays.

Results: Combinations of AN-SG and BA-SG synergistically lowered the TNF and IL-6 levels in LPS-induced N11 cells. Remarkably, the combined anti-neuroinflammatory effects of AN-SG and BA-SG remained significantly greater compared to their individual components at the same concentration level. The molecular mechanism of the attenuated neuroinflammation was likely to be mediated by downregulation of NF-κB p65 translocation ($p < 0.0001$ vs. LPS stimulation) in N11 cells. In the MVEC cells, both AN-SG and BA-SG restored TEER values, ZO-1 expression and reduced permeability. Furthermore, AN-SG and BA-SG significantly improved neuronal survival and reduced expressions of p-tau on N2A cells.

Discussion: The AN-SG and BA-SG combinations showed greater anti-neuroinflammatory potential than those used alone in mono- and tri-cultured N11 cells, thereby further protecting endothelial tight junction and neuronal survival. Taken together, AN-SG and BA-SG may provide improved anti-neuroinflammatory and neuroprotective activities.

KEYWORDS

neuroinflammantion, herbal compound formulation, tri-culture, BBB, neuroprotection

1 Introduction

Neurodegenerative diseases are a group of conditions, including motor neuron disease, Alzheimer's disease, Parkinson's disease and Huntington's disease, characterized by the progressive loss of structure or function of neurons (Fumia et al., 2022). According to World Health Organization, there are more than 55 million people suffering from dementia worldwide (World Health Organization, 2022). Due to the rapid growth of the aging population, neurodegenerative diseases are predicted to be the top disease burden in 2050 (Nichols et al., 2022). The conventional treatments for neurodegenerative diseases are largely symptomatic and present very limited effectiveness in curing or preventing the disease. Thus, it is imperative to explore effective therapeutic options (Yang et al., 2021a).

Neuroinflammation is inflammation occurring in the central nervous system (CNS). It is a pathological event that is related to the onset of neuronal damage and contribute to the progression of neurodegeneration and cognitive impairment (Guzman-Martinez et al., 2019). Neuroinflammation is primarily initiated by the activation of glial cells (mainly microglia) and consequential expression of proinflammatory mediators (Adriani et al., 2017; Bhowmick et al., 2019). Upon the activation, microglia secrete proinflammatory mediators/cytokines such as nitric oxide (NO), tumor necrosis factor (TNF)-α and interleukin (IL)-6 (Ha et al., 2012), of which the overproduction in a chronic condition can contribute to the impairment of the blood-brain barrier (BBB) and result in higher permeability of toxins (Takata et al., 2021). The breakdown of the BBB allows further immune cell recruitment, which then attack the myelin around nerves and result in nerve damage leading to escalated neuroinflammation (Kempuraj et al., 2016). In addition, emerging evidence has shown that the crosstalks among various groups of glial cells, and between microglia and neuron within the neurovascular unit (NVU) are important in the pathogenesis of neuroimmunomodulation in CNS (De la Fuente, 2008; Fernández et al., 2008; Maccioni et al., 2009; Maccioni et al., 2018). Although the understanding of how microglia-neuron cellular interaction occurs in CNS neuroinflammation remains limited, a recent study has shown that microglia-mediated neuroinflammation is linked with neuronal injury and phosphorylation of tau and tauopathies (Guzman-Martinez et al., 2019). The physiological function of the tau protein can be altered by the chronic stimulation of glial cells, which leads to the activation of enzymes that phosphorylate tau, then reduced neuronal capacity (Wyss-Coray and Mucke, 2002). All these interactions and positive feedback loop between the tau pathology and the activation of glial cells cause continuous neuroinflammatory cycles eventually leading to neurodegeneration (Morales et al., 2014).

Robust *in vitro* and *in vivo* models that can measure the multifaceted interactions are key to the understanding of complex pathophysiology of neuroinflammation and to the development of therapeutic interventions. Research has been devoted to establishing co- and tri-culture models as a practical *in vitro* tool for screening brain-targeted drug candidates before animal testing. For example, Park et al. (2018) established a three dimensional human tri-culture system (neuron, astrocyte, and microglia) modeling neuroinflammation, which demonstrated that the induced microglial recruitment released pro-inflammatory cytokines and chemokines, and resulted in the death of neurons and astrocytes . Our previous study established a tri-culture model (microglial, endothelial and neuronal cells) to simulate the NVU environment under neuroinflammation. It was observed that the activated microglia directly provoked the damage of the endothelial tight junction and triggered neuronal loss (Zheng et al., 2021).

The current treatment of neurodegenerative diseases largely focuses on symptomatic relief. Cholinesterase enzyme inhibitors such as galantamine, donepezil, rivastigmine, and N-methyl d-aspartate antagonists (i.e., memantine) have shown to improve memory, thinking, judgment and other thought processes. However, none of these treatments could prevent or stop the progression of the diseases (Van Bulck et al., 2019). Moreover, the etiologic and underlying pathophysiology of neurodegenerative diseases are variable and includes different factors (Leroi et al., 2006), and thus the multi-component and multi-target approach (as opposed to mono-component and mono-target therapy) may offer a better solution to combat the diseases (Liu et al., 2017). Herbal medicines have been extensively explored in recent years regarding their biological activities and potential therapeutic benefits for neurodegenerative disorders (Mohd Sairazi and Sirajudeen, 2020) (Mecocci et al., 2014; Makkar et al., 2020). Emerging evidence has shown that some herbal medicines and their bioactive components used in combination can illustrate synergistic and multi-target effects (Liebner et al., 2018; Choi et al., 2011; Lin, 2011; Calfio et al., 2020). Yang et al. (2021b) demonstrated that a herbal combination of *Aconitum carmichaelii* Debx. (*Fuzi*) and *Zingiber officinale* Rosc. (*Ganjiang*) exhibited a multi-target behavior against neuroinflammation as evidenced by reduced productions of IL-6, TNF-α, reactive oxygen species, NO, and prostaglandins E2 in microglia BV2 cells which were likely to be attributed to the interactions of their bioactive components.

Andrographolide (AN), a major bioactive component of *Andrographis paniculata*, exhibits a wide range of biological activities, including anti-inflammatory, antioxidant, anti-neuroinflammatory, and neuroprotective effects (Zhang et al., 2021). The mechanisms underlying its anti-neuroinflammatory effect were found to be associated with the inhibition of nuclear factor kappa B p65 (NF-κB) signaling and the activation of NLR family pyrin domain containing 3 (Li et al., 2018). Baicalein (BA), a flavone subclass of flavonoids, is a major bioactive constituent in the roots of *Scutellaria baicalensis* (Yang et al., 2019). This compound has been shown to possess various biological characteristics, including anti-bacterial, anti-hypertensive, and anti-neuroinflammatory effects (Zhang et al., 2017). BA was shown to reduce the levels of a broad range of pro-inflammatory cytokines, such as IL-1, TNF-α, and IL-6, *via* the NF-κB signaling inhibition (Zhang et al., 2017). 6-shogaol (6-SG), a pungent component derived from ginger *Zingiber officinale* Rosc., is another promising bioactive agent that exhibits neuroprotective and anti-inflammatory properties (Park et al., 2013). 6-SG was shown to significantly suppress TNF-α and NO levels through downregulation of cyclooxygenase (COX-2), p38 mitogen-activated protein kinase (MAPK), and NF-κB signaling pathways in the lipopolysaccharides (LPS)-induced microglia BV2 cells and a neuroinflammatory mouse model

(Ha et al., 2012). It appears that AN, BA and 6-SG all possess anti-neuroinflammatory properties, with the NF-κB signaling as the common pathway. However, it is plausible that their combined use can generate a multi-target behavior against neuroinflammation in NVU attributed to their versatile pharmacological actions.

This study aims to explore the anti-neuroinflammatory effects of AN-SG and BA-SG combinations on protecting neurons and endothelial tight junctions in an LPS-induced neuroinflammation tri-culture model.

2 Materials and methods

2.1 Cell culture

2.1.1 Cell lines

The mouse brain microvascular endothelial cell line MVEC(B3) was obtained from Dr Jia Li, Macquarie University. Mouse microglia N-11 (N11) and mouse neuroblastoma Neuro 2A cell lines (N2A) were kindly donated from Professor Gerald Muench, School of Medicine, Western Sydney University. They were cultured in complete Dulbecco's modified Eagle medium (DMEM, Lonza, Australia) supplemented with 10% foetal bovine serum (FBS, Thermo Fisher Scientific, Australia) and 1% penicillin.

2.1.2 Cell culture for the single cell line

N11 cells, MVEC cells and N2A cells were incubated at 37°C, 5% CO_2 in 95% air in a vented flask T75 cm^2 (Sigma-Aldrich, Australia), respectively. Cultured cells up to passage 35 with approximately 90% confluency were digested with 0.25% trypsin (Thermo Fisher Scientific, Australia) to perform experiments.

2.1.3 Mono-culture and tri-culture system

For mono-culture, N11 cells (1.0×10^6 cells/mL) were seeded in 96-well plates with DMEM containing 10% FBS. A tri-cultured neuroinflammation model was established using transwell polycarbonate membrane cell culture inserts in a 24-well plate (Corning®Costar®Transwell® Cell culture inserts, Sigma, Australia) with slight modification (Zheng, et al., 2021). The transwell with insert membrane was placed upside down and coated with 1% polylysine (Sigma, United States) for 1 h. Then 200 µL of N11 cells (2.0×10^6 cells/mL) were seeded on the top of the transwell with DMEM containing 10% FBS and kept upside down in the incubator to ensure N11 cells adhered to the top of the transwell by the surface tension. In parallel, 500 µL of N2A cells (1.0×10^6 cells/mL) were seeded in a fresh 24-well plate with DMEM containing 10% FBS. After 4 h, the transwell with N11 cells was inverted and placed within a 24-well plate immersed with 375 µL DMEM containing 10% FBS in each well, and the MVEC cells (1.0×10^6 cells/mL) were seeded with 250 µL DMEM containing 10% FBS in the same insert of N11 cells.

2.2 Drug preparation and lipopolysaccharides-induced neuroinflammation

The natural compounds, AN, BA and 6-SG (purity >98%), were purchased from Chengdu Biopurify (China). The identity and purity were confirmed by high-performance liquid chromatography (Supplementary material 1). Each compound was dissolved in dimethyl sulfoxide (DMSO) at a concentration of 100 mM. They were serially diluted with DMEM serum-free media before adding to the cells. After the three cell lines were cultured together in the transwell system for 24 h, the system was treated with individual AN, 6-SG, and BA at 25 µM, combined AN-SG [AN (12.5 µM) +6-SG (12.5 µM), the total concentration of 7.83 µg/mL], and BA-SG [BA (12.5 µM) + 6-SG (12.5 µM), total concentration of 6.83 µg/mL] or media with vehicle control (0.1% DMSO) for 1 h before the activation of LPS, 1 µg/mL. The cells and cell supernatant were then subjected to bioassays after 24 h.

2.3 Measurement of nitrite (NO_2^-) production using the griess reaction

After 24 h of LPS stimulation, the supernatants in the upper and lower compartment (90 µL) in the tri-culture system were collected for the measurement of nitrite (NO_2^-) level by mixing with an equal amount of the Griess reaction (1% sulfanilamide in 5% phosphoric acid and N-(1-naphthyl)-ethylene diamine dihydrochloride) (Tsikas, 2007; Yoon, et al., 2010). The measurement of nitrate/nitrite concentration or total nitrate and nitrite concentration (NOx) is routinely used as an index of NO production (Moncada et al., 1991; Sun et al., 2003). Griess assay has been popularly used to measure the nitric oxide (NO) level (Bohl and West, 2000; Saha et al., 2004; Schmölz et al., 2017). Nitrite production was determined by measuring the optical density at 540 nm using a microplate reader (BMG Labtech Fluostar Optima, Mount Eliza, Victoria, Australia). The concentration of nitrite was determined using a standard curve generated with sodium nitrite ($NaNO_2$). The rest of the cell supernatant was subjected to TNF-α and IL-6 ELISA assay.

2.4 TNF-α and IL-6 ELISA assay

The levels of IL-6 and TNF-α in the supernatant from the mono-cultured N11 cells, the upper and lower compartment of the tri-culture system were measured using commercial ELISA kits (murine IL-6 ELISA kit, cat. No. 431304, Biolegend; murine TNF-α ELISA kit, cat. No. 900- K45, Biogems) according to manufacturers' instructions. The absorbance was measured at 410 nm with a microplate reader (BMG Labtech Fluostar Optima, Mount Eliza, Victoria, Australia). The concentrations of IL-6 and TNF-α were calculated using standard curves.

2.5 Transendothelial electrical resistance values

The transendothelial electrical resistance (TEER) values in the tri-culture 24-well systems were measured by an epithelial volt/ohm resistance meter (ERS-2, cat. no. MERS00001; Merck) according to the manufacturer's instruction. The background TEER value was measured in the blank well with medium only. The final results were calculated by TEER in each group subtracted from the background TEER values. The values are shown as $\Omega \times cm^2$.

2.6 Evans blue permeability test

After the various treatments for 24 h in the tri-culture system, the medium in the lower compartment was replaced with 0.5 mL

phosphate-buffered saline (PBS), and the upper compartment was filled with 0.2 mL of 0.25% Evans blue (Sigma, Australia). After 0.5 h's incubation, the solution in the lower compartment was tested for absorbance at 450 nm using a microplate reader (BMG Labtech Fluostar Optima, Mount Eliza, Victoria, Australia).

2.7 Alamar blue and MTT assays

Cell viability of N2A cells in the tri-culture system was evaluated 24 h after the LPS stimulation. After removing the supernatants, the N2A cells were incubated with 100 µL of Alamar Blue (0.01 mg/mL resazurin) (Schober, et al., 2021). The plate was then incubated for another 2 h in a humidified incubator at 37°C. The optical density of each well was measured from excitation of 545 nm and emission of 595 nm using a microplate reader (BMG Labtech Fluostar Optima, Mount Eliza, Victoria, Australia).

The N2A cells were also co-incubated with MTT solution (0.5 mg/mL in PBS) 24 h after the LPS stimulation for 2 h at 37°C with 5% CO_2. DMSO was then added to dissolve the insoluble formazan crystal. The absorbance was measured at 510 nm using a microplate reader. The density of formazan formed in control (medium with the vehicle) cells was taken as 100% of cell viability. The cell viability of the measured sample was determined using the equation: Cell viability % = absorbance of treated cells/absorbance of cells and medium only (blank control) * 100%

2.8 Immunofluorescent staining

The N2A cells were seeded on a 1 cm cover slide in the 24-well. The tri-culture system was established and treated overnight using the same protocol as described above. Each cell line was washed with cold PBS and fixed with 4% paraformaldehyde for 20 min at room temperature. Triton-X 100 (0.1%) was added to cells for 20 min and followed by blocking with 3% Bovine Serum Albumin (BSA, Scientifix, Australia) for 1 h. Primary antibodies were then added to the system, including zonula occludens-1 (ZO-1; 1:100, cat no. 13663S), phosphorylated tau (p-tau; 1: 200, cat no. 49561) or NF-κB p65 (p65; 1:100, cat no.8242), all purchased from Cell Signaling Technologies, United States. The cells were then washed with PBS three times and each cell line was then stained with mixed secondary antibodies, including donkey anti-mouse IgG Alexa Fluor 488 (green; 1: 1,000, cat no. A32766), donkey anti-goat IgG Alexa Fluor 680 (yellow; 1: 250, cat no. A32680) and donkey anti-rabbit IgG Alexa Fluor 594 (red; 1: 1,000, cat no. A32754), all purchased from Thermo Fisher Scientific, Australia. The insert membrane was cut for the collection of either the N11 or the MVEC cells. Cotton was used to swap the other side of the membrane of the cell line and then put on the new slide. Finally, the anti-fade mounting medium with DAPI (Sigma, Australia) was added to the cells and subjected to immunofluorescent imaging using an Inverted Leica TCS SP5 laser scanning confocal microscope (School of Medicine, Western Sydney University, Australia).

2.9 Statistical analysis

Statistical analysis was conducted using GraphPad Prism 9.0 software (GraphPad Software Inc., United States). The data was shown as mean ± standard error of the mean (SEM) from at least three individual experiments. The relative half maximal inhibitory concentration (IC_{50}) values were determined from the constructed dose-response curves. The responses generated by nitrite, TNF and IL-6 assays were normalised to 0%–100%, where the averaged responses of blank control and LPS were normalised to 0% and 100% respectively. The IC_{50} value was then determined by the concentration that corresponds to 50% of the effect level. The statistical comparison between groups was conducted by one-way analysis of variance (ANOVA) with Tukey test, and $p < 0.05$ was considered statistically significant. The interaction of the substances in the ELISA experiment was ascertained using the combination index (CI) model. The data obtained from the dose-response curves in reducing IL-6 and TNF-α was entered into the Compusyn software 2.0 (ComboSyn, Inc., United States), which produced the isobologram figure, CI values, and CI-fraction affected (Fa, here refereed to IL-6/TNF-α inhibition) curve (El Hassouni et al., 2019).

3 Results

3.1 Enhanced anti-neuroinflammatory activities of AN-SG and BA-SG

3.1.1 Restored cell viability by AN-SG and BA-SG

Firstly, the cell viability of N11 cells in the mono-culture and tri-culture system treated by the individual and combined bioactive was examined. As shown in Figures 1A, B, AN and 6-SG (0.78–100 µM) did not exhibit any obvious cytotoxicity, which were all above 88.27% compared with the vehicle control (blank). Particularly, 6-SG showed the highest cell viability throughout the tested concentrations, which ranged from 92.72% ± 2.17% to 104.13% ± 4.85%. The treatments of BA and AN appeared to slightly affect the cell viability, which ranged from 89.07% ± 5.93% to 97.92% ± 0.85%, and 88.27% ± 8.34% to 96.25% ± 0.34%, respectively. BA at 3.125 and 6.25 µM showed significantly impaired cell viability compared to the blank control ($p < 0.05$). Interestingly, combinations of AN-SG and BA-SG did not show any obvious cytotoxicity. AN-SG seemed to lower reduction in cell viability compared to that of AN alone, and a similar trend was shown in BA-SG compared to that of BA alone.

In particular, the cell viability of mono-cultured N11 cells treated by AN, BA, 6-SG, AN-SG, and BA-SG at 25 µM were tested (Figures 1C, D). It was obvious that LPS stimulation significantly affected the cell viability of N11 cells compared to the vehicle control (79.00% ± 2.64% vs. blank 100%, $p < 0.05$). All the treatments did not exhibit any cytotoxicity at 25 µM compared with the blank, with cell viability all above 95.28% ± 8.59%. Particularly, AN-SG 25 µM (12.5 + 12.5 µM, 7.83 µg/mL), BA-SG 25 µM (12.5 + 12.5 µM, 6.83 µg/mL) maintained the cell viability at 97.89% ± 11.48% and 102.76% ± 7.14%.

3.1.2 Synergistic inhibition of IL-6 and TNF-α productions by AN-SG and BA-SG on mono-cultured N11 cells

Next, the IL-6 and TNF-α inhibitory effects of AN-SG were tested in LPS-induced mono-cultured N11 cells compared with AN and 6-SG used alone (Figures 2A, D). LPS-stimulated cells demonstrated significantly increased amounts of IL-6 (12.29 ± 1.13 ng/mL vs. 2.06 ± 0.08 ng/mL, $p < 0.0001$) and TNF-α (78.52 ± 0.35 ng/mL vs. 14.25 ± 0.14 ng/mL, $p < 0.0001$) compared to that of the blank control. All the individual and

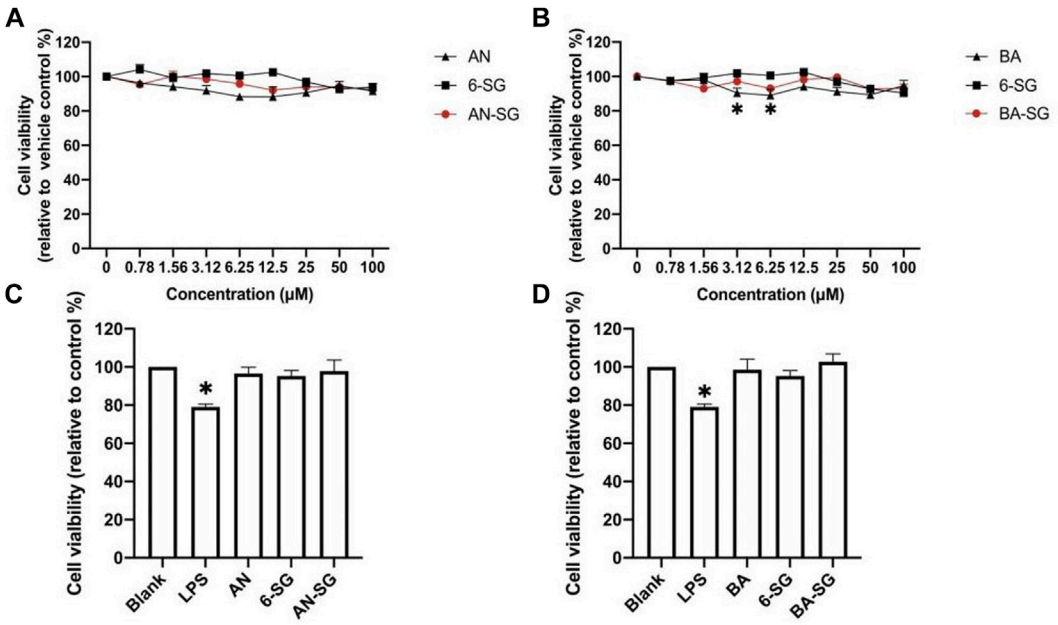

FIGURE 1
Cell viability of N11 cells in the mono-culture treated by AN, BA, 6-SG and their combinations, AN-SG and BA-SG. **(A)** The dose-response curve of the cell viability treated by AN, 6-SG and AN-SG at 0.78–100 μM in N11 cells. **(B)** The dose-response curve of the cell viability treated by BA, 6-SG and BA-SG at 0.78–100 μM in N11 cells. **(C)** Cell viability of N11 treated by AN, 6-SG and AN-SG at 25 μM. **(D)** Cell viability of N11 treated by BA, 6-SG and BA-SG at 25 μM *$p < 0.05$ vs. Blank (cells with vehicle control) analysed by one-way ANOVA with Tukey test. Data are shown as mean ± SEM ($n = 3$).

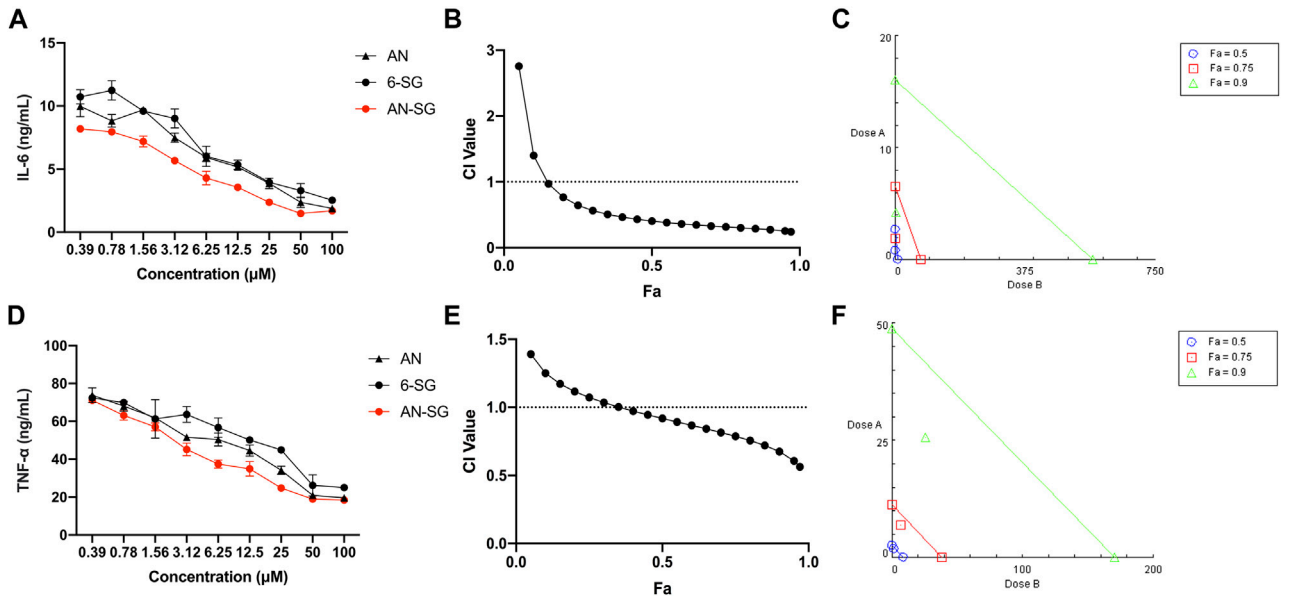

FIGURE 2
The AN-SG combination exhibited synergistic effects on inhibition of LPS-induced IL-6 and TNF-α productions in mono-cultured N11 cells. AN, 6-SG and AN-SG dose-dependently inhibited LPS-induced IL-6 **(A)** and TNF-α **(D)** in N11 cells ($n = 3$). The synergistic IL-6 **(B)** and TNF-α **(E)** inhibitory effects of AN-SG were determined by the CI-Fa curves. CI values represent the interaction in AN-SG, with CI < 1, CI = 1 and CI > 1 referring to synergy, addition and antagonism, respectively. Fa on the *X*-axis is defined as the fraction effect level, and herein it refers to the IL-6 and TNF-α inhibitory effect, respectively. Isobologram analysis of AN-SG in IL-6 **(C)** and TNF-α **(F)** inhibition when the default set of Fa values at 0.50, 0.75 and 0.90. Data are shown as mean ± SEM.

combined treatments showed dose-dependent reductions of IL-6 and TNF-α compared to that of LPS (all $p < 0.0001$) on mono-cultured N11 cells. AN-SG and BA-SG (0.39–100 μM) appeared to be more potent than their individuals used alone at all tested concentrations. The IC_{50} value of AN-SG in inhibiting IL-6 was determined to be 1.18 ± 0.38 μM, which was significantly lower than that of AN (3.54 ± 1.19 μM, $p < 0.01$) or 6-SG

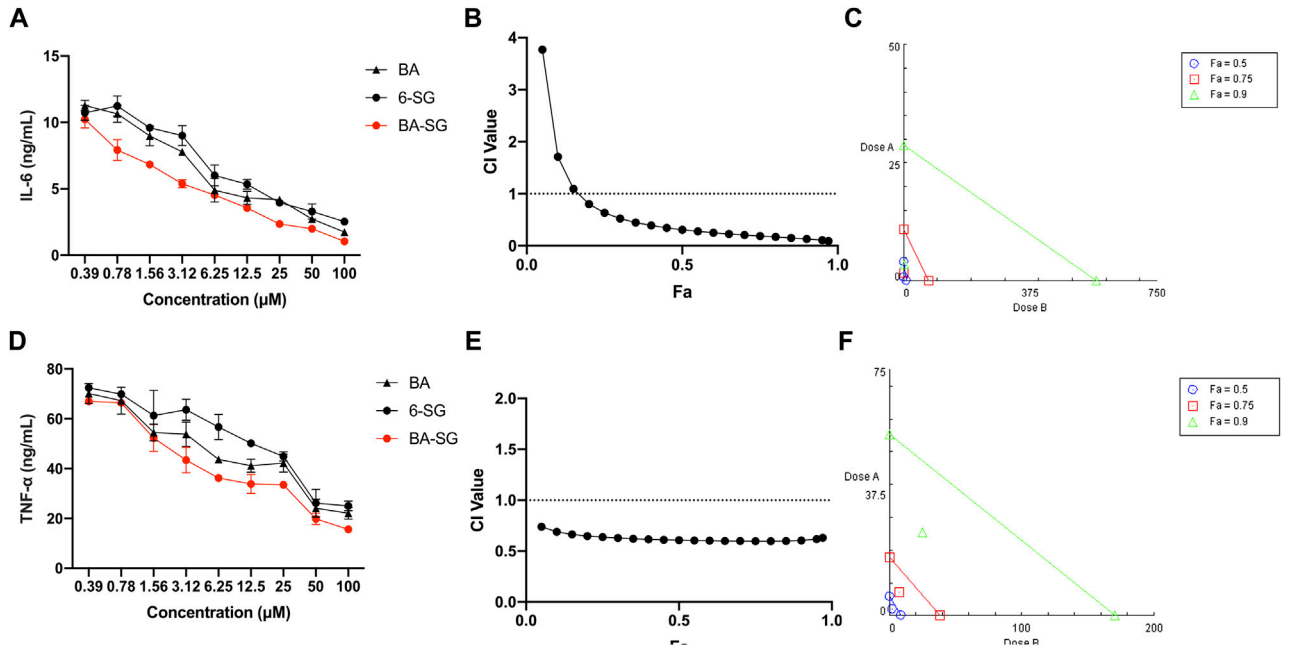

FIGURE 3
The BA-SG combination exhibited synergistic inhibitory effects on LPS-induced IL-6 and TNF-α productions in mono-cultured N11 cells. BA, 6-SG, and BA-SG dose-dependently inhibited LPS-induced IL-6 **(A)** and TNF-α **(D)** in N11 cells (n = 3). The synergistic IL-6 **(B)** and TNF-α **(E)** inhibitory effects of BA-SG were determined by the CI-Fa curves. CI values represent the interaction in BA-SG, with CI < 1, CI = 1 and CI > 1 referring to synergy, addition and antagonism, respectively. Fa on the X-axis is defined as the fraction effect level, and herein it refers to the IL-6 and TNF-α inhibitory effect, respectively. Isobologram analysis of BA-SG in IL-6 **(C)** and TNF-α **(F)** inhibition when the default set of Fa values at 0.50, 0.75, and 0.90. Data are shown as mean ± SEM.

(5.46 ± 1.41 μM, $p < 0.01$). Similarly, the IC_{50} value of AN-SG in inhibiting TNF-α was also the lowest (3.47 ± 0.64 μM) compared to that of AN (7.24 ± 1.90 μM, $p < 0.05$) or 6-SG (13.93 ± 6.37 μM, $p < 0.001$).

At 25 μM, the IL-6 production of AN-SG (2.51 ± 0.81 ng/mL) was significantly lower than that of the LPS stimulation (12.29 ± 1.13 ng/mL, $p < 0.0001$). In addition, IL-6 production by AN-SG was significantly lower than that of AN (4.14 ± 0.71 ng/mL, $p < 0.01$) or 6-SG (4.28 ± 0.77 ng/mL, $p < 0.01$). The TNF-α release of AN-SG (24.76 ± 1.41 ng/mL, $p < 0.0001$ vs. LPS) was also significantly lower than that of AN (34.22 ± 3.14 ng/mL, $p < 0.05$) or 6-SG (44.89 ± 2.63 ng/mL, $p < 0.001$) at 25 μM. Thus, this concentration was selected for AN, 6-SG and AN-SG to be tested in the tri-culture system.

The CI model was performed to evaluate whether the enhanced activity of the AN-SG combination was due to a synergistic interaction. In Figure 2B, the CI values ranged from 0.24 to 0.97 when the Fa was above 0.15 (15%–97% IL-6 inhibitory effect), suggesting a strong synergy of AN-SG combination in inhibiting IL-6. The isobologram (Figure 2C) also suggested a synergistic interaction between AN and 6-SG in reducing LPS-stimulated IL-6 with Fa values at 0.50, 0.75 and 0.9 (representing 50%, 75% and 90% of the IL-6 inhibition). Similarly, in Figure 2E, AN-SG synergistically inhibited TNF-α with CI values ranging from 0.56 to 0.97 when the Fa was above 0.4 (40%–97% TNF-α inhibitory effect). The results of the isobologram (Figure 2F) also supported this finding with Fa values at 0.50, 0.75 and 0.9.

The IL-6 and TNF-α inhibitory effects of BA-SG were examined in LPS-induced mono-cultured N11 cells against their individual components. Compared with LPS-stimulation, all the BA, 6-SG and BA-SG produced dose-dependent IL-6 and TNF-α inhibitory effects (Figures 3A, D). The IC_{50} value of BA-SG in inhibiting IL-6 was determined to be 1.44 ± 0.37 μM, which was significantly lower than that of BA (3.65 ± 0.90 μM, $p < 0.05$) or 6-SG (5.46 ± 1.41 μM, $p < 0.01$). Similarly, the IC_{50} value of BA-SG for the TNF-α inhibition was also the lowest (3.26 ± 1.09 μM) compared to that of BA (6.52 ± 2.93 μM, $p < 0.05$) or 6-SG (13.93 ± 6.37 μM, $p < 0.01$).

At 25 μM, BA-SG exhibited significant IL-6 inhibitory effects (2.47 ± 0.78 ng/mL, $p < 0.0001$) compared LPS stimulation only. In particular, the IL-6 production of BA-SG was significantly lower than that of BA (4.14 ± 0.63 ng/mL, $p < 0.05$) or 6-SG (4.28 ± 0.77 ng/mL, $p < 0.05$) alone. The TNF-α reduction by BA-SG was also significantly greater than that of BA (42.08 ± 3.62 ng/mL, $p < 0.05$) or 6-SG (44.89 ± 2.63 ng/mL, $p < 0.05$) alone at 25 μM. Thus, this concentration was selected for BA, 6-SG and BA-SG to be tested in the tri-culture system. CI and isobologram models (Figures 3B–F) demonstrated a synergistic effect of BA-SG in inhibiting IL-6 and TNF-α at the concentration range of 0.78–100 μM and 0.39–100 μM (CI < 1) were observed. The isobologram also supported the observed synergy of the BA-SG combination in reducing LPS-stimulated IL-6 (Figure 3C) and TNF-α (Figure 3F) when Fa values were at 0.50, 0.75, and 0.9.

3.1.3 Enhanced inhibitory effects of AN-SG and BA-SG on nitrite, IL-6 and TNF-α productions in tri-culture system

In the tri-culture model, nitrite, IL-6 and TNF-α inhibitory effects of AN-SG against LPS stimulation were compared to that of AN or 6-SG alone at 25 μM. As shown in Figure 4A, LPS generated an excessive amount of nitrite in the upper compartment at 29.71 ± 0.97 ng/mL ($p < 0.0001$ vs. blank control: 0.24 ± 0.13 ng/mL). The combination of AN-SG [AN (12.5 μM) + 6-SG (12.5 μM), total concentration of 7.83 μg/mL] significantly lowered the level of nitrite to 15.16 ±

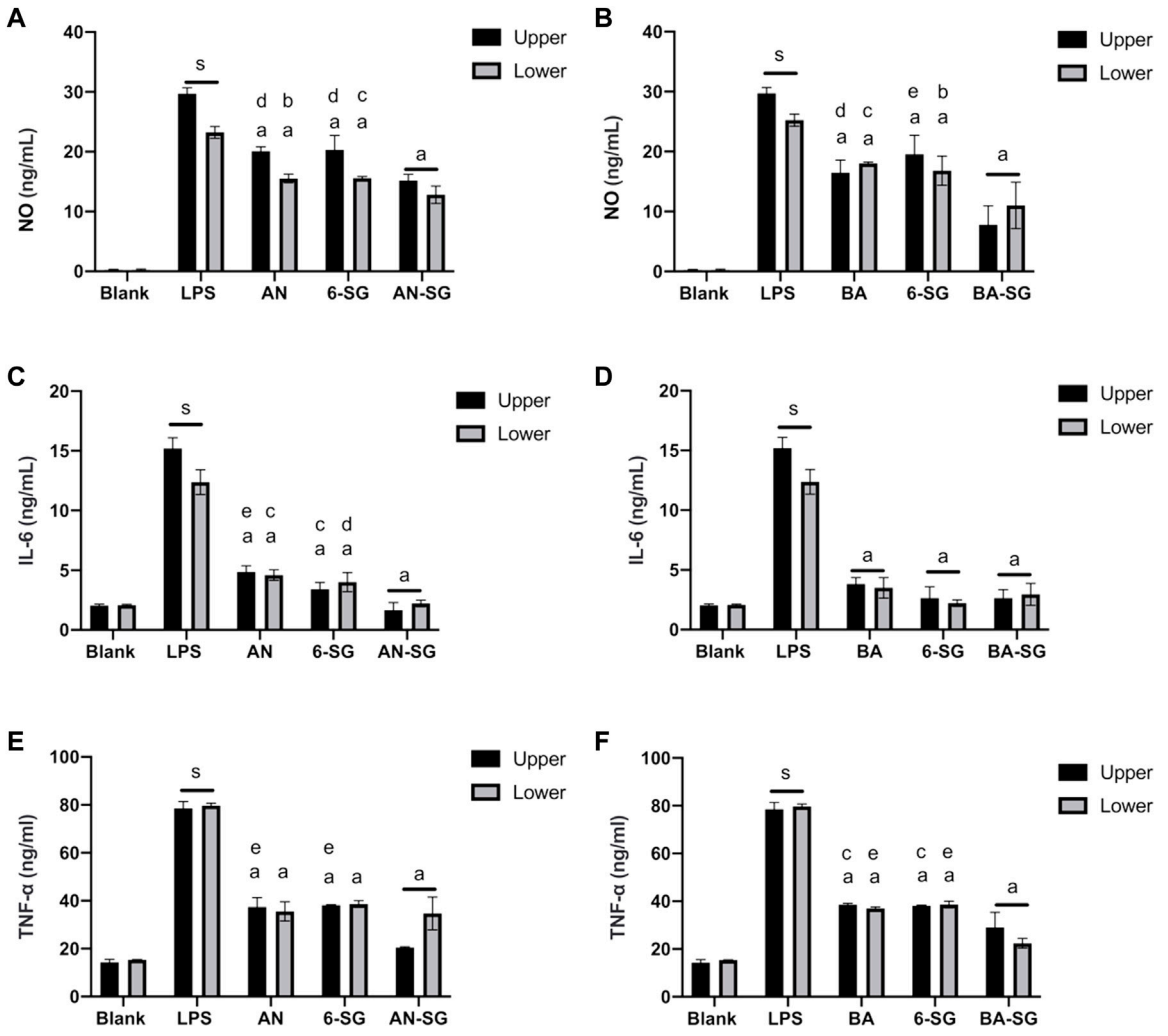

FIGURE 4
AN-SG and BA-SG generally exhibited greater effects in reducing nitrite, IL-6 and TNF-α productions than that of the individual component in the tri-culture system. AN-SG inhibited nitrite **(A)**, IL-6 **(C)**, and TNF-α **(E)** productions and BA-SG inhibited nitrite **(B)**, IL-6 **(D)** and TNF-α **(F)** productions in LPS-activated tri-culture model in both upper and lower compartments. Data are shown as mean ± SEM (n = 3). Figures generated by Graphpad prism 9.0. The statistical comparison between groups was conducted by one-way ANOVA analysis and Tukey test for group comparison. s: $p < 0.0001$ vs. Blank, a: $p < 0.0001$ vs. LPS, b: $p < 0.05$ vs. combinations, c: $p < 0.01$ vs. combinations, d: $p < 0.001$ vs. combinations, e: $p < 0.0001$ vs. combinations.

1.06 ng/mL ($p < 0.0001$ vs. LPS stimulation) and the reduction was significantly greater than that of AN (20.09 ± 0.71 ng/mL) or 6-SG (20.30 ± 2.42 ng/mL) alone at the same concentration level ($p < 0.001$ vs. AN, $p < 0.001$ vs. 6-SG). Similarly, BA-SG [BA (12.5 μM) + 6-SG (12.5 μM), total concentration of 6.83 μg/mL] significantly reduced nitrite to 7.78 ± 3.16 ng/mL, which was significantly greater than BA (16.49 ± 2.09 ng/mL) or 6-SG (19.56 ± 3.14 ng/mL) ($p < 0.0001$ vs. LPS stimulation, $p < 0.001$ vs. BA, $p < 0.0001$ vs. 6-SG) (Figure 4B).

The stimulation of LPS also generated an excessive amount of nitrite in the lower compartment to 23.23 ± 1.40 ng/mL ($p < 0.0001$ vs. blank control: 0.24 ± 0.17 ng/mL, Figure 4A). The combination of AN-SG significantly lowered the level of nitrite to 15.16 ± 1.06 ng/mL ($p < 0.0001$ vs. LPS stimulation), and the single compounds, AN and 6-SG also reduced nitrite productions to 15.52 ± 0.71 ng/mL and 15.57 ± 0.29 ng/mL, respectively. However, the combined activities of AN-SG were not significantly higher than that of the single components. Similarly, BA-SG significantly reduced nitrite to 11.00 ± 3.86 ng/mL, which was significantly greater than BA (19.34 ± 1.09 ng/mL) or 6-SG (16.81 ± 2.44 ng/mL) ($p < 0.0001$ vs. LPS stimulation, $p < 0.01$ vs. BA, $p < 0.05$ vs. 6-SG, Figure 4B).

As shown in Figures 4C–F, LPS-stimulated cells produced significantly higher IL-6 (12.53 ± 3.70 ng/mL vs. 2.04 ± 0.11 ng/mL, $p < 0.0001$) and TNF-α (79.67 ± 0.10 ng/mL vs. 15.35 ± 0.01 ng/mL, $p < 0.0001$) in the upper compartment compared to that of the blank control. AN-SG significantly lower the IL-6 production (Figure 4C, 1.66 ± 0.62 ng/mL, $p < 0.0001$ vs. LPS) and TNF-α productions (Figure 4E, 20.40 ± 0.03 ng/mL, $p < 0.0001$ vs. LPS) in the upper compartments. Furthermore, the IL-6 reduction by AN-SG was greater than that of AN (4.86 ± 0.51 ng/mL, $p < 0.0001$) or 6-SG (3.40 ± 0.57, $p < 0.01$) alone (Figure 4C). Similarly, in the Figure 4E, the TNF-α reduction by AN-SG was greater than that of AN (37.36 ± 3.89 ng/mL, $p < 0.0001$) or 6-SG (38.13 ± 0.20 ng/mL, $p < 0.0001$), alone.

Similarly, in the tri-culture model, the nitrite, IL-6 and TNF-α inhibitory effects of BA-SG against LPS stimulation were compared to that of BA or 6-SG at 25 μM. The combination of

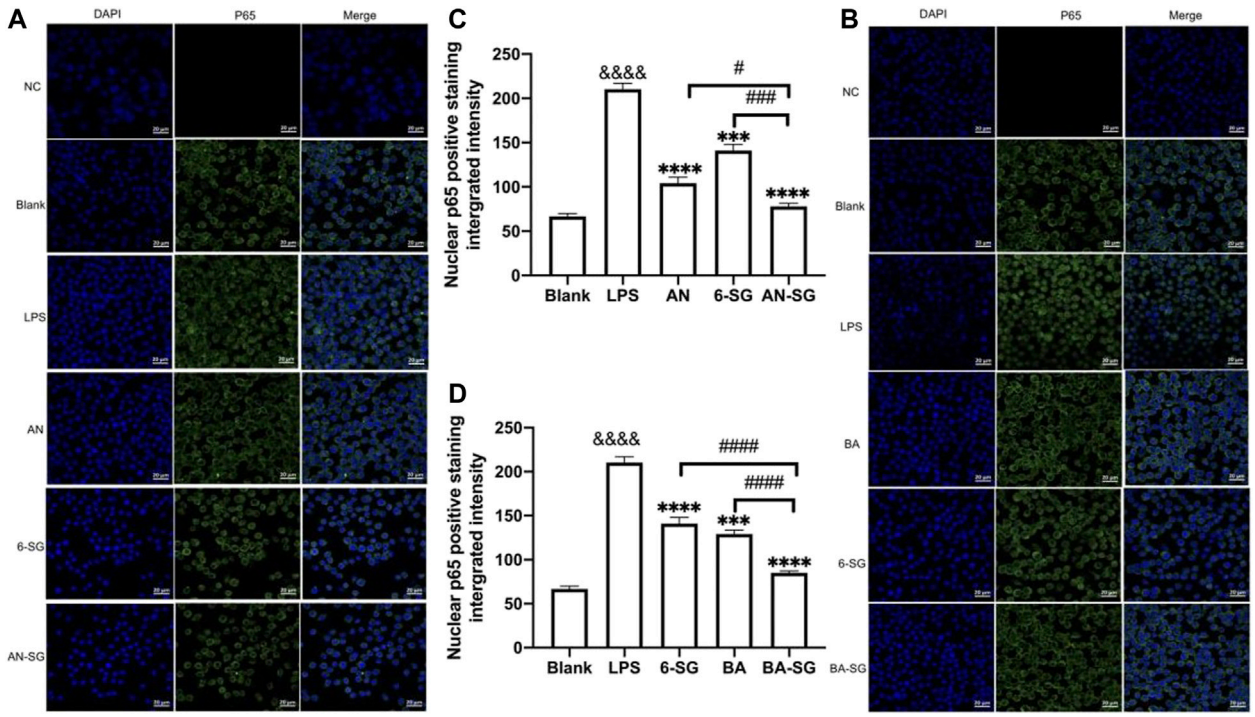

FIGURE 5
AN-SG and BA-SG exhibited greater effects in inhibiting LPS-induced NF-κB nuclear translocation than the individual component in the N11 cells of the tri-culture model. **(A)** AN-SG and **(B)** BA-SG for the immunofluorescence staining of NF-κB p65. Images were taken using a confocal microscope with × 63 magnification. Blue: DAPI in the nucleus, green: NF-κB p65 in the N11 cells. Scale bar = 20 μm. **(C, D)** Statistical analysis of the NF-κB p65 translocation activities by AN-SG and BA-SG using ImageJ. Data are shown as mean ± SEM ($n > 3$). &&&& $p < 0.0001$ vs. Blank, ***$p < 0.001$, ****$p < 0.0001$ vs. LPS, #$p < 0.05$, ###$p < 0.001$, ####$p < 0.0001$ vs. combination, by one-way ANOVA analysis and Tukey test for group comparison in GraphPad Prism 9.

BA-SG significantly lowered the IL-6 production (Figure 4D, 2.64 ± 0.70 ng/mL, $p < 0.0001$ vs. LPS) and TNF-α productions (Figure 4F, 29.00 ± 6.36 ng/mL, $p < 0.0001$ vs. LPS) in the upper compartments. However, there was no significant difference in the IL-6 reduction compared between BA-SG to BA (3.83 ± 0.52 ng/mL, $p > 0.05$) or 6-SG (2.63 ± 0.94 ng/mL, $p > 0.05$) in the Figure 4D. The TNF-α reduction by BA-SG was greater compared to BA (38.57 ± 0.56 ng/mL, $p < 0.01$) or 6-SG (38.13 ± 0.26 ng/mL, $p < 0.01$) either (Figure 4F). A similar trend of the IL-6 and TNF-α reduction was also found in the lower compartments, in which all the individual and combined activities showed significant and comparable effects.

3.1.4 Enhanced effects of AN-SG and BA-SG in inhibiting NF-κB p65 translocation of N11 cells in the tri-culture model

The results of our previous study suggested that in the tri-culture model, the LPS-induced neuroinflammation was mediated by the NF-κB p65 translocation in the microglia cells (Zheng et al., 2021). In this study, the effects of AN-SG and BA-SG in inhibiting neuroinflammation on N11 cells in the tri-culture model was examined on the NF-κB p65 translocation by immunofluorescence staining.

As shown in Figure 5, the blank control showed that the NF-κB p65 (green fluorescence) was mostly expressed outside the nucleus (DAPI, blue fluorescence). In response to the LPS stimulation, increased expressions of NF-κB p65 were observed in the nucleus, as evidenced by the overlapping green in the blue fluorescence, suggesting that LPS triggered the increased translocation of NF-κB p65 to the cell nucleus after the 0.5 h's incubation. All the individual and combined treatments appeared to inhibit the translocation to various degrees (Figures 5A,B). The statistical analysis (Figure 5C) demonstrated that AN-SG downregulated the integrated intensity of nuclear positive NF-κB p65 (77.96 ± 19.95, vs. LPS = 210.23 ± 28.00, $p < 0.0001$). The nuclear positive NF-κB p65 of AN-SG was significantly lower than that of AN (104.07 ± 24.78, $p < 0.05$) or 6-SG (140.93 ± 27.60, $p < 0.001$). BA-SG also significantly suppressed NF-κB p65 translocation (85.16 ± 8.91 vs. LPS = 210.23 ± 28.00, $p < 0.0001$), which the nuclear positive integrated intensity was significantly lower than that of BA (129.16 ± 19.34, $p < 0.0001$) or 6-SG (140.93 ± 27.60, $p < 0.0001$) alone (Figure 5D).

3.2 Enhanced effect of AN-SG and BA-SG in protecting endothelial tight junction of MVEC cells in the tri-culture system

In the MVEC cells of the tri-culture system, LPS exposure induced impaired endothelial tight junction as evidenced by a significant reduction of the TEER value in the LPS stimulated group (162 ± 12 Ω) compared with the blank control (207 ± 18 Ω, $p < 0.01$). As shown in Figure 6A, AN restored the TEER value to 181 ± 12 Ω ($p < 0.05$ vs. LPS), and 6-SG also increased the TEER value to 176 ± 6 Ω ($p < 0.01$ vs. LPS). However, AN-SG demonstrated the highest effect in restoring TEER value (205 ± 12 Ω, $p < 0.01$ vs. LPS), which was greater than that of AN and 6-SG alone (both $p < 0.01$).

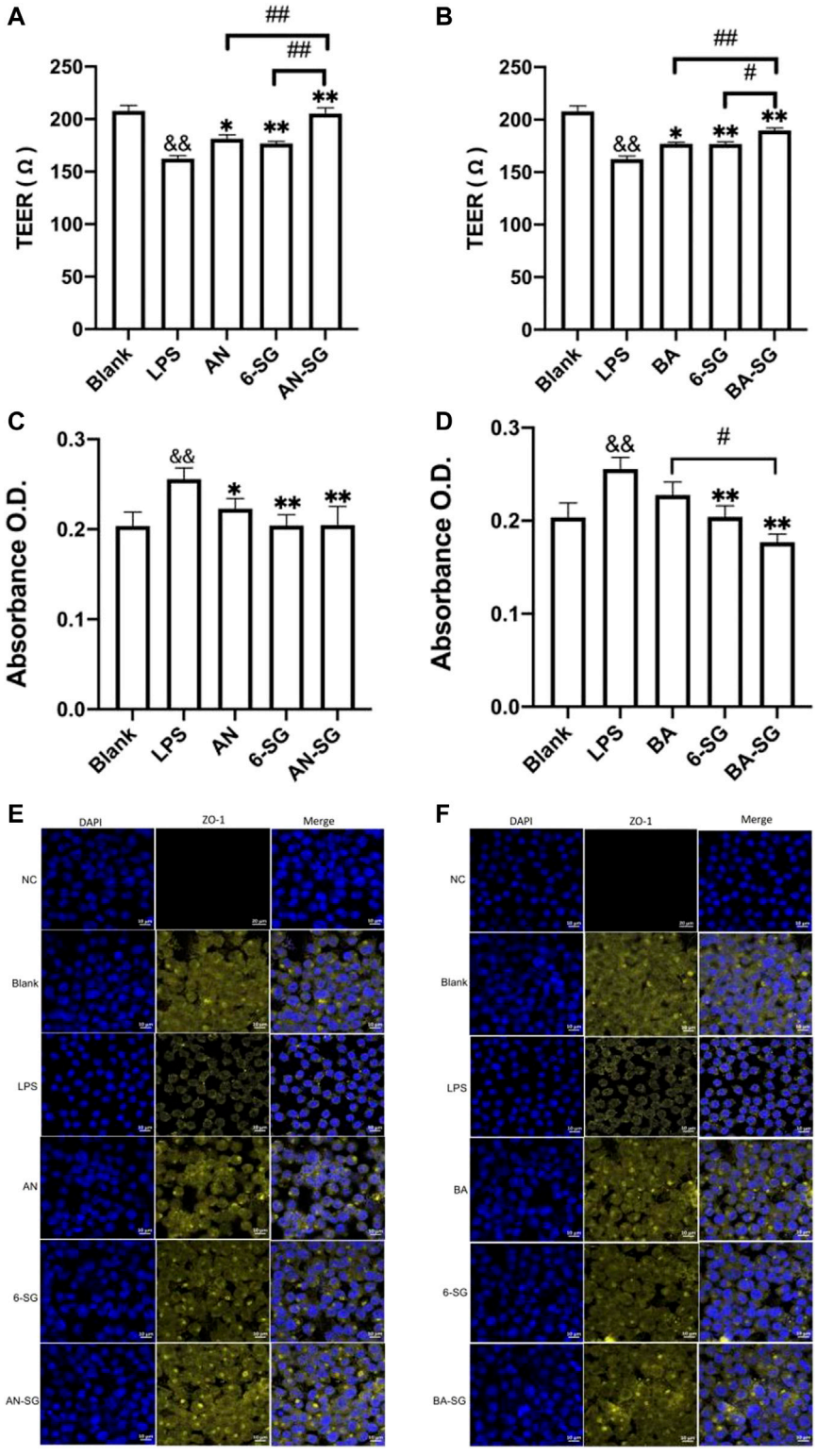

FIGURE 6
AN-SG and BA-SG demonstrated a more prominent effect in protecting the endothelial tight junction of MVEC cells in the tri-culture system against LPS-stimulated neuroinflammation. The measurements of TEER **(A)**, Evans blue absorbance **(C)** and tight junction protein ZO-1 **(E)** for AN-SG, and TEER **(B)**, Evans blue absorbance **(D)** and tight junction protein ZO-1 **(F)** for BA-SG in the LPS-activated tri-culture model. Immunofluorescence staining of ZO-1 in the MVEC cells of the tri-culture model. Images were taken using a confocal microscope with ×63 magnification. Blue: DAPI in the nucleus; yellow: ZO-1 in the microvascular endothelial cells. Scale bar = 10 μm && $p < 0.01$ vs. Blank, *$p < 0.05$, **$p < 0.01$ vs. LPS, #$p < 0.05$, ##$p < 0.01$ vs. combination, by one-way ANOVA analysis and Tukey test for group comparison in GraphPad Prism 9. O.D.: optical density.

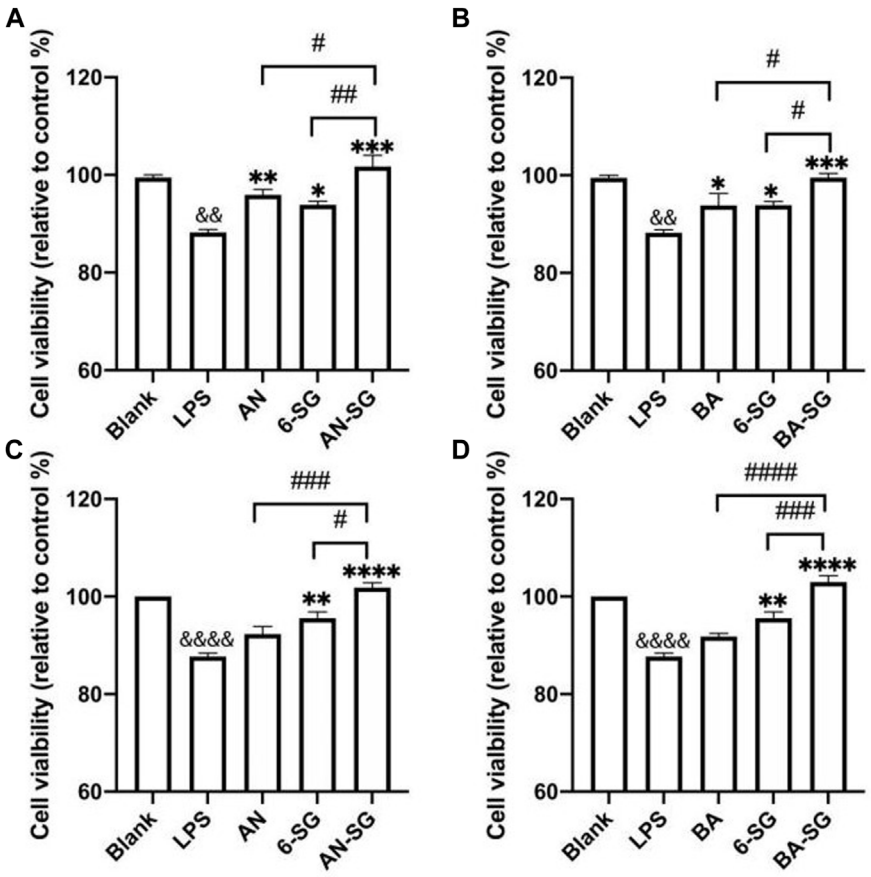

FIGURE 7
AN-SG and BA-SG exhibited greater restored cell viability in N2A cells of the tri-culture system against the LPS stimulation compared with their corresponding individual component. The Alamar blue assay was evaluated for **(A)** AN-SG and **(B)** BA-SG, and the MTT assay on **(C)** AN-SG and **(D)** BA-SG. Data are shown as mean ± SEM ($n > 3$). && $p < 0.01$, &&&& $p < 0.0001$ vs. Blank, *$p < 0.05$, **$p < 0.01$, ***$p < 0.001$, ****$p < 0.0001$ vs. LPS, #$p < 0.05$, ##$p < 0.01$, ###$p < 0.001$, ####$p < 0.0001$ vs. combination, by one-way ANOVA analysis and Tukey test for group comparison in GraphPad Prism 9.

The increased Evans blue absorbance also suggested the damaged endothelial tight junction upon the LPS simulation in the LPS group (0.28 ± 0.08) compared with the Blank group (Blank: 0.20 ± 0.06, $p < 0.01$, Figure 6C). Both AN and 6-SG alone significantly lowered the Evans blue absorbance to 0.22 ± 0.03 and 0.20 ± 0.04, respectively, $p < 0.01$ vs. LPS. AN-SG also lowered Evans blue absorbance (AN-SG: 0.21 ± 0.07, compared with LPS ($p < 0.01$). However, the combined treatment was not significantly stronger than the individual treatment.

In Figure 6B, both BA and 6-SG significantly increased the TEER value to 177 ± 5 Ω and 176 ± 6 Ω, respectively ($p < 0.05$ and $p < 0.01$ vs. LPS). BA-SG significantly restored TEER values (BA-SG: 190 ± 6 Ω, $p < 0.01$ vs. LPS) and showed greater ability than that of the BA ($p < 0.01$) and 6-SG ($p < 0.05$) alone. Similarly, BA-SG further lowered Evans blue absorbance (0.17 ± 0.02) than BA (0.22 ± 0.04) or 6-SG (0.20 ± 0.03) used alone ($p < 0.05$, Figure 6D).

The impaired tight junction in MVEC cells was further demonstrated by the immunofluorescence staining of ZO-1 upon the stimulation of LPS (Figures 6E, F). The tight junction protein ZO-1 in the blank tri-culture system was shown as a complete honeycomb structure, but the integrity was damaged after the LPS exposure for 24 h at 1 μg/mL. The single compounds AN, BA and 6-SG, and the AN-SG and BA-SG combinations increased the yellow honeycomb structure compared with the LPS and single component treatment. However, a prominent improved tight junction was seen after the treatment of AN-SG and BA-SG combinations. Compared with the AN and 6-SG used alone, AN-SG showed increased yellow honeycomb for the ZO-1 protein expression. Similarly, the BA-SG combination showed increased yellow honeycomb for the ZO-1 protein expression compared with the single compounds BA and 6-SG.

3.3 Enhanced effects of AN-SG and BA-SG in protecting neuronal survival and attenuating tau phosphorylation in the tri-culture model

3.3.1 Enhanced effects of AN-SG and BA-SG in restoring neuronal survival of N2A cells

The effects of AN, BA, 6-SG, AN-SG or BA-SG at 25 μM on cell viability of N2A cells in the tri-culture system was tested using Alamar blue and MTT assays. In Figure 7A, the Alamar blue assay demonstrated that the cell viability of N2A cells in the LPS group was significantly reduced compared with the blank group (88.23% ± 1.05% vs. Blank = 100%, $p < 0.0001$) after 24 h' exposure. All treatments of AN (95.90% ± 2.20%, $p < 0.01$), 6-SG (93.89% ± 1.46%, $p < 0.05$) and AN-SG (101.71% ± 3.96%, $p < 0.001$) significantly restored the cell viability compared with that of LPS. In particular, AN-SG demonstrated the highest cell viability compared to AN ($p < 0.05$) or 6-SG ($p < 0.01$) alone. Similarly, in Figure 7B, all the single compounds BA (92.23% ± 4.22% vs. LPS, $p < 0.05$), 6-SG (94.12% ± 1.46%

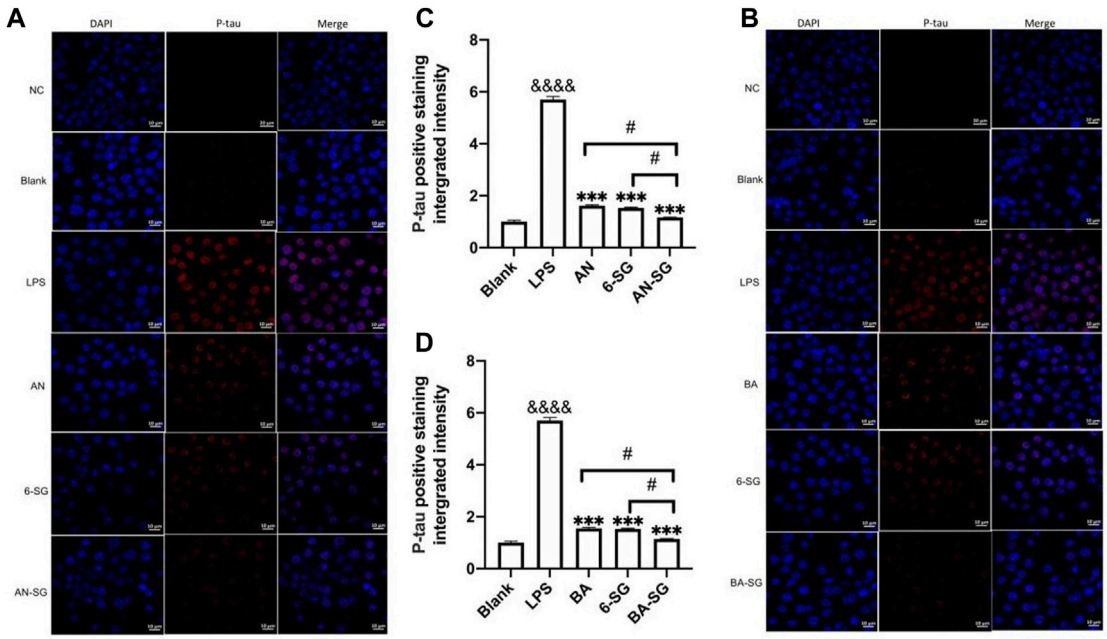

FIGURE 8
AN-SG and BA-SG exhibited greater p-tau reduction in N2A cells of the tri-culture system against the LPS stimulation compared with their corresponding individual component. Immunofluorescence staining of p-tau for **(A)** AN-SG and **(B)** BA-SG groups after the exposure of LPS for 0.5 h. Images were taken by a confocal microscope with × 63 magnification. Blue: DAPI in the nucleus. Red: p-tau in tri-cultured N2A cell lines. Scale bar = 10 μm. Use ImageJ to quantity the tau protein phosphorylation activity. **(C, D)** Statistical analysis of the p-tau expression by AN-SG and BA-SG using ImageJ. Data are shown as mean ± SEM ($n > 3$). &&&& $p < 0.0001$ vs. Blank, *** $p < 0.001$ vs. LPS, # $p < 0.05$ vs. combination, by one-way ANOVA analysis and Tukey test for group comparison in GraphPad Prism 9.

vs. LPS, $p < 0.05$) and combination BA-SG (100.21% ± 1.39% vs. LPS, $p < 0.001$) significantly restored the cell viability. BA-SG displayed the highest cell viability compared to BA or 6-SG (both $p < 0.05$).

MTT assay was conducted to confirm the data obtained from the Alamar blue assay, which showed a similar trend. In Figure 7C, LPS significantly decreased the cell viability compared with the blank group (87.74% ± 1.19% vs. Blank = 100%, $p < 0.0001$). AN (92.31% ± 2.68%, $p > 0.05$), 6-SG (95.55% ± 2.31%, $p < 0.01$) and AN-SG (101.83% ± 1.72%, $p < 0.0001$) significantly restored the cell viability compared with that of LPS. AN-SG demonstrated a higher cell viability level compared with AN ($p < 0.01$) or 6-SG ($p < 0.05$) alone. Similarly, in Figure 7D, BA-SG (102.97% ± 2.26% vs. LPS, $p < 0.0001$) also showed significantly enhanced cell viability, which was greater than that of BA ($p < 0.0001$) or 6-SG ($p < 0.001$) alone.

3.3.2 Enhanced effects of AN-SG and BA-SG in reducing tau phosphorylation in N2A cells of tri-culture system

Immunofluorescent staining of p-tau protein in N2A cells was conducted to examine the capacity of AN-SG and BA-SG to attenuate p-tau expression in the LPS-induced neuroinflammation tri-culture system. As shown in Figure 8, the phosphorylation of tau protein (red fluorescence) increased significantly in the N2A cells after the LPS exposure for 0.5 h compared to that of the blank control group (Blank: 1.00 ± 0.08, LPS: 5.70 ± 0.20, $p < 0.0001$). AN, 6-SG and AN-SG appeared to decrease the tau phosphorylation compared with the LPS (Figure 8A). The statistical analysis (Figure 8C) demonstrated that all the treatments have significantly reduced the p-tau accumulation compared with LPS ($p < 0.05$). Particularly, the p-tau accumulation in AN-SG (1.16 ± 0.01) was significantly lower than that of AN (1.62 ± 0.05) or 6-SG (1.53 ± 0.04) individually ($p < 0.05$, respectively).

Similarly, it was obvious that BA, 6-SG and BA-SG decreased tau phosphorylation compared with the LPS treatment (BA: 1.55 ± 0.06, 6-SG: 1.53 ± 0.04, BA-SG: 1.14 ± 0.02, $p < 0.001$, respectively, Figures 8B, D). However, BA-SG demonstrated a more effective p-tau reduction compared with the BA or 6-SG alone ($p < 0.05$, respectively).

4 Discussions

This study investigated the anti-neuroinflammatory activities of two combinations, AN-SG and BA-SG, in comparison to that of their individual components in the LPS-stimulated neuroinflammation tri-culture model. Our results demonstrated that these combinations exhibited pronounced effects in suppressing neuroinflammation mediated by N11 microglia cells and, in turn, protecting endothelial tight junction and restoring neuronal cell viability. Noticeably, the combined effects were generally greater than the single component used alone.

Neuroinflammation is a complex inflammatory process in the CNS that plays a vital defensive role against numerous pathogens, toxins, or factors that produce neurodegeneration. Recent research suggested that dysfunctional cell-cell signaling in the NVU is a defining feature of CNS illnesses (Zlokovic, 2005; Benarroch, 2007; Zarekiani et al., 2022). The CNS's structural and functional integrity is dependent on the function of NVU, which regulates transport across

the BBB (Erickson et al., 2020; Pluimer et al., 2020; Salmina et al., 2021). Increasing evidence showed that disruption of functional interactions among the cells in NVU is the early hallmark of Alzheimer's disease (Montagne et al., 2017; Liebner et al., 2018; Yu et al., 2020).

Our results suggested that the combinations of AN-SG and BA-SG significantly inhibited NO, IL-6, and TNF-α in mono-cultured N11 and the tri-culture cells. Microglia N11 cells are the resident innate immune cells in the NVU and produce several proinflammatory factors (IL-1, TNF-α, NO, PGE2, superoxide) within the brain (Block and Hong, 2005). Among these, high NO levels can increase neuroinflammation leading to tissue damage and neuronal death (Liy et al., 2021). IL-6 is a pleiotropic cytokine that participates in a variety of pathways, including immunological responses, inflammation, hematopoiesis, bone metabolism, and embryonic development (Tanaka et al., 2014). TNF-α is an inflammatory cytokine that promotes apoptosis and activates NF-κB, resulting in the generation of proinflammatory cytokines and glial activation, which leads to neuroinflammation and neuronal death (Jung et al., 2019). NF-κB is the key transcription factor that plays a central role in the neuroinflammatory pathways. It is a crucial regulator of cellular gene transcription that can regulate a variety of cytokines and receptors, such as NO, IL-6 and TNF-α (Zhang and Sun, 2015).

In this study, the single herbal compounds and their combinations effectively inhibited the NF-κB p65 translocation, which partly explains the mechanisms underlying their anti-neuroinflammatory activities. In particular, our results showed that the AN-SG and BA-SG combinations produced greater effects on many neuroinflammatory mediators, including nitrite, IL-6 and TNF-α compared with the single components. To the best of our knowledge, this is the first study that demonstrated the combined effects of AN and 6-SG for anti-neuroinflammatory activity. Our results of the BA-SG combination are somewhat in line with the findings from Suzuki et al., where a combination of aqueous extract of *Scutellaria* root (BA is a main bioactive ingredient) and 6-SG was shown to produce an advanced effect on cyclic adenosine monophosphate phosphodiesterase inhibitory activity (Suzuki et al., 1991), which may contribute to the attenuated neuroinflammation (Chuang et al., 2017).

In the NVU, astrocytes, microglia and pericytes are directly localized around the endothelial cells to aid the connection between blood supply and metabolic needs and also release several substances that improve and preserve the BBB integrity (Ronaldson and Davis, 2012). Excessive activation of microglia can have a negative impact on the BBB function. In particular, the excessive release of NO and IL-6 from the activated microglia has been demonstrated to impair the BBB's permeability, enabling potentially toxic chemicals to actively enter the brain (Thiel and Audus, 2001; Mayhan, 2002; Takeshita et al., 2021). The downregulation of paracellular tight-junction proteins such as claudin-5 (CLDN5), occluding, and ZO-1 by reactive microglia and astrocytes are believed to contribute to the leaky BBB (Morris et al., 2018). Numerous studies demonstrated that increased BBB permeability is observed in a variety of neurological and psychiatric disorders, including stroke, epilepsy, amyotrophic lateral sclerosis, Alzheimer's disease and Parkinson's disease, implying that the compromised BBB plays a role in the pathogenesis and/or severity of brain diseases (Liu et al., 2015; Patel and Frey, 2015; Małkiewicz et al., 2019; Hussain et al., 2021). Thus, therapeutic targets that could minimize the infiltration and invasion of peripheral chemicals or pathogens into the CNS or reduce damage to the NVU that protect the BBB, hold a high promise for treating chronic neurological illnesses and acute CNS traumas. Our present study showed that AN-SG and BA-SG inhibited the inflammatory mediators of NO, IL-6 and TNF-α, which in turn, led to reduced permeability and restored endothelial tight junction, suggesting their the BBB protective effects against cytokine-mediated damage from microglial cells (Haruwaka et al., 2019). This is consistent with the previous studies where AN and BA were shown to protect against BBB damage induced by the production of pro-inflammatory cytokines, and increase ZO-1 expression to reduce BBB permeability (Zhu et al., 2012; Wang et al., 2022).

Abnormal tau phosphorylation accumulation is a distinguishing characteristic of some neurodegenerative diseases, such as Alzheimer's disease (Wolfe, 2012). Tau proteins are often seen as microtubule-associated proteins in the brain. They are widely distributed throughout the neurons of the CNS and play a large part in preserving the stability of microtubules in axons (Buée et al., 2000). Abnormal phosphorylation of tau proteins (p-tau) results in impaired microtubule stability and the production of potentially neurotoxic aggregates (Johnson and Stoothoff, 2004). An increasing number of studies indicate that the sustained neuroinflammatory process involving microglia and astrocytes activation significantly contributes to the progression of tau pathology and neurodegenerative diseases, emphasizing the significance of neuroinflammation as a therapeutic target for neurodegenerative diseases (Laurent et al., 2018). In addition, inhibiting microglial inflammatory mediator production was shown to protect neurons and reduce p-tau in the tau transgenic mouse model. Previous animal studies have demonstrated that AN and BA used individually, can reduce p-tau levels (Serrano et al., 2014; Asai et al., 2015; Gu et al., 2016; Patel et al., 2021; Sonawane et al., 2021). The mechanism of action of AN and BA were both related to the activation of the Nrf2-mediated p62 signaling pathway (Serrano et al., 2014; Gu et al., 2018; Sonawane et al., 2021; Shengkai and Yazhen, 2022). However, the evidence for the potential effect of 6-SG to inhibit p-tau level is lacking. Thus, the strengthened p-tau inhibition by AN-SG maybe is predominately caused by AN, which is potentiated by 6-SG. However, if the Nrf2-mediated p62 signaling pathway plays a role in the combined action warrants further investigation. Overall, our results suggested that AN-SG and BA-SG reduced cytokines such as NO, IL-6, and TNF-α, which can protect the BBB tight junction and the neuron survival and lower the p-tau level. These results provide evidence that AN-SG and BA-SG could provide potential benefits for the treatment of neurodegenerative diseases such as Alzheimer's disease, Parkinson's disease and multiple sclerosis (Laurent et al., 2018; Singh et al., 2020; Shengkai and Yazhen, 2022). Further study to explore the effects of these combinations on other Alzheimer's disease-relevant biomarkers, such as Amyloid beta, which is an early event associated with the onset and progression of neurodegeneration (Roy et al., 2020), is warranted.

Previously, we have established the LPS-stimulated neuroinflammation tri-culture model as a quick and practical tool for quick drug-screening targeting neuroinflammation (Zheng et al., 2021). This model was successfully applied in the current study where promising anti-neuroinflammatory, endothelial tight junction

protective and neuroprotective effects of three herbal bioactive components and their combinations were demonstrated. However, there are several limitations of this study. Firstly, the study focused on the NF-κB nuclear translation pathway as an associated mechanism of AN-SG and BA-SG against neuroinflammation. Other pathways or key gene targets that play major roles in modulating microglia-induced neuroinflammation, such as Nrf-2/HO-1, nucleotide-binding oligomerization domain-like receptor protein three inflammasome, and mitogen-activated protein kinase pathways, were not investigated (Bernhardi, 2009; Song et al., 2017; Chen et al., 2020; Upadhayay and Mehan, 2021). Secondly, the combinations demonstrated an enhanced effect on the biomarkers related to neuroinflammation, endothelial tight junction and neuronal survival in the *in vitro* tri-culture system; these effects were not validated in the whole organism. Thirdly, the effects of the herbal components and their combinations were investigated at only one concentration (25 μM) in this study. Lastly, since synergy quantified needs have a range of doses to get linear dose–effect curves (Foucquier and Guedj, 2015), the consequences can only be described as an enhanced effect. Nonetheless, the enhanced effects of the two herbal combinations against neuroinflammation in our study provide valuable evidence to warrant further investigation of these combinations in the animal and human studies as potential therapy options for neurodegenerative diseases.

5 Conclusion

The present study evaluated the anti-neuroinflammatory effects of AN, BA, 6-SG and two of their combinations, AN-SG and BA-SG in a tri-culture model. Our findings revealed that AN-SG and BA-SG exhibited greater anti-neuroinflammatory activities in the microglia cells compared to their individual components, and in turn produced a greater endothelial tight junction protection and improved neuronal survival. Future study is warranted to further explore the potential of AN-SG and BA-SG as anti-neuroinflammatory and neuroprotective agents for neurodegenerative diseases in animal and clinical studies.

Data availability statement

The raw data supporting the conclusion of this article will be made available by the authors, without undue reservation.

Author contributions

XZ designed the study. TL contributed to the concept of the study. YL conducted the experiments and drafted the original manuscript. DC reviewed the manuscript. The final manuscript is agreed by all authors.

Funding

XZ is supported by the Research Support Program Fellowship, Western Sydney University. TL is supported by Western Sydney University Vice Chancellor's Senior Research Fellowship.

Acknowledgments

Many thanks to Mr Dina Vadassery for technical training and assistance in the laboratory. We appreciate Dr Sindy Kueh for the technical support in confocal microscopy. We are grateful to Dr Jia Li from Macquarie Medical School for the donation of the cell line.

Conflict of interest

The authors declare that the research was conducted in the absence of any commercial or financial relationships that could be construed as a potential conflict of interest.

Publisher's note

Supplementary material

The Supplementary Material for this article can be found online at: https://www.frontiersin.org/articles/10.3389/fphar.2023.1135934/full#supplementary-material

References

Adriani, G., Ma, D., Pavesi, A., Kamm, R. D., and Goh, E. L. (2017). A 3D neurovascular microfluidic model consisting of neurons, astrocytes and cerebral endothelial cells as a blood-brain barrier. *Lab. Chip* 17 (3), 448–459. doi:10.1039/c6lc00638h

Asai, H., Ikezu, S., Tsunoda, S., Medalla, M., Luebke, J., Haydar, T., et al. (2015). Depletion of microglia and inhibition of exosome synthesis halt tau propagation. *Nat. Neurosci.* 18 (11), 1584–1593. doi:10.1038/nn.4132

Benarroch, E. E. (2007). Neurovascular unit dysfunction: A vascular component of alzheimer disease? *Neurology* 68 (20), 1730–1732. doi:10.1212/01.wnl.0000264502.92649.ab

Bernhardi, R. v. (2009). "Neurodegenerative Diseases—MAPK Signalling Pathways in Neuroinflammation," in *Encyclopedia of neuroscience*, 2614–2620. doi:10.1007/978-3-540-29678-2_3820

Bhowmick, S., D'Mello, V., Caruso, D., Wallerstein, A., and Abdul-Muneer, P. M. (2019). Impairment of pericyte-endothelium crosstalk leads to blood-brain barrier dysfunction following traumatic brain injury. *Exp. Neurol.* 317, 260–270. doi:10.1016/j.expneurol.2019.03.014

Block, M. L., and Hong, J. S. (2005). Microglia and inflammation-mediated neurodegeneration: Multiple triggers with a common mechanism. *Prog. Neurobiol.* 76 (2), 77–98. doi:10.1016/j.pneurobio.2005.06.004

Bohl, K. S., and West, J. L. (2000). Nitric oxide-generating polymers reduce platelet adhesion and smooth muscle cell proliferation. *Biomaterials* 21 (22), 2273–2278. doi:10.1016/S0142-9612(00)00153-8

Buée, L., Bussière, T., Buée-Scherrer, V., Delacourte, A., and Hof, P. R. (2000). Tau protein isoforms, phosphorylation and role in neurodegenerative disorders. *Brain Res. Brain Res. Rev.* 33 (1), 95–130. doi:10.1016/s0165-0173(00)00019-9

Calfio, C., Gonzalez, A., Singh, S. K., Rojo, L. E., and Maccioni, R. B. (2020). The emerging role of nutraceuticals and phytochemicals in the prevention and treatment of alzheimer's disease. *J. Alzheimer's Dis.* 77, 33–51. doi:10.3233/JAD-200443

Chen, S., Peng, J., Sherchan, P., Ma, Y., Xiang, S., Yan, F., et al. (2020). TREM2 activation attenuates neuroinflammation and neuronal apoptosis via PI3K/Akt pathway after intracerebral hemorrhage in mice. *J. Neuroinflammation* 17 (1), 168. doi:10.1186/s12974-020-01853-x

Choi, J. G., Moon, M., Kim, H. G., Mook-Jung, I., Chung, S. Y., Kang, T. H., et al. (2011). Gami-Chunghyuldan ameliorates memory impairment and neurodegeneration induced by intrahippocampal Aβ1–42 oligomer injection. *Neurobiol. Learn. Mem.* 96 (2), 306–314. doi:10.1016/j.nlm.2011.06.004

Chuang, W., Zhen, W., Mengmeng, L., Chenli, L., Hanjie, Y., Dongsheng, Z., et al. (2017). "Reducing neuroinflammation in psychiatric disorders: Novel target of phosphodiesterase 4 (PDE4) and developing of the PDE4 inhibitors," in *Mechanisms of neuroinflammation*. doi:10.5772/intechopen.69154

De la Fuente, M. (2008). Role of neuroimmunomodulation in aging. *Neuroimmunomodulation* 15 (4-6), 213–223. doi:10.1159/000156465

El Hassouni, B., Mantini, G., Li Petri, G., Capula, M., Boyd, L., Weinstein, H. N. W., et al. (2019). To combine or not combine: Drug interactions and tools for their analysis. Reflections from the EORTC-PAMM course on preclinical and early-phase clinical pharmacology. *Anticancer Res.* 39 (7), 3303–3309. doi:10.21873/anticanres.13472

Erickson, M. A., Wilson, M. L., and Banks, W. A. (2020). *In vitro* modeling of blood–brain barrier and interface functions in neuroimmune communication. *Fluids Barriers CNS* 17 (1), 26. doi:10.1186/s12987-020-00187-3

Fernández, J. A., Rojo, L., Kuljis, R. O., and Maccioni, R. B. (2008). The damage signals hypothesis of Alzheimer's disease pathogenesis. *J. Alzheimer's Dis.* 14, 329–333. doi:10.3233/JAD-2008-14307

Foucquier, J., and Guedj, M. (2015). Analysis of drug combinations: Current methodological landscape. *Pharmacol. Res. Perspect.* 3 (3), e00149. doi:10.1002/prp2.149

Fumia, A., Cicero, N., Gitto, M., Nicosia, N., and Alesci, A. (2022). Role of nutraceuticals on neurodegenerative diseases: Neuroprotective and immunomodulant activity. *Nat. Prod. Res.* 36 (22), 5916–5933. doi:10.1080/14786419.2021.2020265

Gu, L., Yu, Q., Li, Q., Zhang, L., Lu, H., and Zhang, X. (2018). Andrographolide protects PC12 cells against β-amyloid-induced autophagy-associated cell death through activation of the nrf2-mediated p62 signaling pathway. *Int. J. Mol. Sci.* 19 (9), 2844. doi:10.3390/ijms19092844

Gu, X.-H., Xu, L.-J., Liu, Z.-Q., Wei, B., Yang, Y.-J., Xu, G.-G., et al. (2016). The flavonoid baicalein rescues synaptic plasticity and memory deficits in a mouse model of Alzheimer's disease. *Behav. Brain Res.* 311, 309–321. doi:10.1016/j.bbr.2016.05.052

Guzman-Martinez, L., Maccioni, R. B., Andrade, V., Navarrete, L. P., Pastor, M. G., and Ramos-Escobar, N. (2019). Neuroinflammation as a common feature of neurodegenerative disorders. *Front. Pharmacol.* 10, 1008. doi:10.3389/fphar.2019.01008

Ha, S. K., Moon, E., Ju, M. S., Kim, D. H., Ryu, J. H., Oh, M. S., et al. (2012). 6-Shogaol, a ginger product, modulates neuroinflammation: A new approach to neuroprotection. *Neuropharmacology* 63 (2), 211–223. doi:10.1016/j.neuropharm.2012.03.016

Haruwaka, K., Ikegami, A., Tachibana, Y., Ohno, N., Konishi, H., Hashimoto, A., et al. (2019). Dual microglia effects on blood brain barrier permeability induced by systemic inflammation. *Nat. Commun.* 10 (1), 5816. doi:10.1038/s41467-019-13812-z

Hussain, B., Fang, C., and Chang, J. (2021). Blood-brain barrier breakdown: An emerging biomarker of cognitive impairment in normal aging and dementia. *Front. Neurosci.* 15, 688090. doi:10.3389/fnins.2021.688090

Johnson, G. V., and Stoothoff, W. H. (2004). Tau phosphorylation in neuronal cell function and dysfunction. *J. Cell Sci.* 117 (24), 5721–5729. doi:10.1242/jcs.01558

Jung, Y. J., Tweedie, D., Scerba, M. T., and Greig, N. H. (2019). Neuroinflammation as a factor of neurodegenerative disease: Thalidomide analogs as treatments. *Front. Cell Dev. Biol.* 7, 313. doi:10.3389/fcell.2019.00313

Kempuraj, D., Thangavel, R., Natteru, P. A., Selvakumar, G. P., Saeed, D., Zahoor, H., et al. (2016). Neuroinflammation induces neurodegeneration. *J. Neurol. Neurosurg. Spine* 1 (1), 1003.

Laurent, C., Buée, L., and Blum, D. (2018). Tau and neuroinflammation: What impact for Alzheimer's disease and tauopathies? *Biomed. J.* 41 (1), 21–33. doi:10.1016/j.bj.2018.01.003

Leroi, I., Collins, D., and Marsh, L. (2006). Non-dopaminergic treatment of cognitive impairment and dementia in Parkinson's disease: A review. *J. Neurol. Sci.* 248 (1-2), 104–114. doi:10.1016/j.jns.2006.05.021

Li, X., Wang, T., Zhang, D., Li, H., Shen, H., Ding, X., et al. (2018). Andrographolide ameliorates intracerebral hemorrhage induced secondary brain injury by inhibiting neuroinflammation induction. *Neuropharmacology* 141, 305–315. doi:10.1016/j.neuropharm.2018.09.015

Liebner, S., Dijkhuizen, R. M., Reiss, Y., Plate, K. H., Agalliu, D., and Constantin, G. (2018). Functional morphology of the blood–brain barrier in health and disease. *Acta Neuropathol.* 135 (3), 311–336. doi:10.1007/s00401-018-1815-1

Lin, B. (2011). Polyphenols and neuroprotection against ischemia and neurodegeneration. *Mini Rev. Med. Chem.* 11 (14), 1222–1238. doi:10.2174/13895575111091222

Liu, J., Zhu, J., Xue, J., Qin, Z., Shen, F., Liu, J., et al. (2017). *In silico*-based screen synergistic drug combinations from herb medicines: A case using cistanche tubulosa. *Sci. Rep.* 7 (1), 16364. doi:10.1038/s41598-017-16571-3

Liu, W. Y., Wang, Z. B., Wang, Y., Tong, L. C., Li, Y., Wei, X., et al. (2015). Increasing the permeability of the blood-brain barrier in three different models *in vivo*. *CNS Neurosci. Ther.* 21 (7), 568–574. doi:10.1111/cns.12405

Liy, P. M., Puzi, N. N. A., Jose, S., and Vidyadaran, S. (2021). Nitric oxide modulation in neuroinflammation and the role of mesenchymal stem cells. *Exp. Biol. Med. (Maywood)* 246 (22), 2399–2406. doi:10.1177/1535370221997052

Maccioni, R. B., González, A., Andrade, V., Cortés, N., Tapia, J. P., and Guzmán-Martínez, L. (2018). Alzheimer´s disease in the perspective of neuroimmunology. *Open Neurol. J.* 12, 50–56. doi:10.2174/1874205x01812010050

Maccioni, R. B., Rojo, L. E., Fernández, J. A., and Kuljis, R. O. (2009). The role of neuroimmunomodulation in Alzheimer's disease. *Ann. N. Y. Acad. Sci.* 1153 (1), 240–246. doi:10.1111/j.1749-6632.2008.03972.x

Makkar, R., Behl, T., Bungau, S., Zengin, G., Mehta, V., Kumar, A., et al. (2020). Nutraceuticals in neurological disorders. *Int. J. Mol. Sci.* 21 (12), 4424. doi:10.3390/ijms21124424

Małkiewicz, M. A., Szarmach, A., Sabisz, A., Cubała, W. J., Szurowska, E., and Winklewski, P. J. (2019). Blood-brain barrier permeability and physical exercise. *J. Neuroinflammation* 16 (1), 15. doi:10.1186/s12974-019-1403-x

Mayhan, W. G. (2002). Cellular mechanisms by which tumor necrosis factor-alpha produces disruption of the blood-brain barrier. *Brain Res.* 927 (2), 144–152. doi:10.1016/s0006-8993(01)03348-0

Mecocci, P., Tinarelli, C., Schulz, R. J., and Polidori, M. C. (2014). Nutraceuticals in cognitive impairment and Alzheimer's disease. *Front. Pharmacol.* 5, 147. doi:10.3389/fphar.2014.00147

Mohd Sairazi, N. S., and Sirajudeen, K. N. S. (2020). Natural products and their bioactive compounds: Neuroprotective potentials against neurodegenerative diseases. *Evidence-Based Complementary Altern. Med.* 2020, 6565396. doi:10.1155/2020/6565396

Moncada, S., Palmer, R. M., and Higgs, E. A. (1991). Nitric oxide: Physiology, pathophysiology, and pharmacology. *Pharmacol. Rev.* 43 (2), 109–142.

Montagne, A., Zhao, Z., and Zlokovic, B. V. (2017). Alzheimer's disease: A matter of blood-brain barrier dysfunction? *J. Exp. Med.* 214 (11), 3151–3169. doi:10.1084/jem.20171406

Morales, I., Guzmán-Martínez, L., Cerda-Troncoso, C., Farías, G. A., and Maccioni, R. B. (2014). Neuroinflammation in the pathogenesis of Alzheimer's disease. A rational framework for the search of novel therapeutic approaches. *Front. Cell. Neurosci.* 8, 112. doi:10.3389/fncel.2014.00112

Morris, G., Fernandes, B. S., Puri, B. K., Walker, A. J., Carvalho, A. F., and Berk, M. (2018). Leaky brain in neurological and psychiatric disorders: Drivers and consequences. *Aust. N. Z. J. Psychiatry* 52 (10), 924–948. doi:10.1177/0004867418796955

Nichols, E., Steinmetz, J. D., Vollset, S. E., Fukutaki, K., Chalek, J., Abd-Allah, F., et al. (2022). Estimation of the global prevalence of dementia in 2019 and forecasted prevalence in 2050: An analysis for the global burden of disease study 2019. *Lancet Public Health* 7 (2), e105–e125. doi:10.1016/S2468-2667(21)00249-8

Park, G., Kim, H. G., Ju, M. S., Ha, S. K., Park, Y., Kim, S. Y., et al. (2013). 6-Shogaol, an active compound of ginger, protects dopaminergic neurons in Parkinson's disease models via anti-neuroinflammation. *Acta Pharmacol. Sin.* 34 (9), 1131–1139. doi:10.1038/aps.2013.57

Park, J., Wetzel, I., Marriott, I., Dréau, D., D'Avanzo, C., Kim, D. Y., et al. (2018). A 3D human triculture system modeling neurodegeneration and neuroinflammation in Alzheimer's disease. *Nat. Neurosci.* 21 (7), 941–951. doi:10.1038/s41593-018-0175-4

Patel, J. P., and Frey, B. N. (2015). Disruption in the blood-brain barrier: The missing link between brain and body inflammation in bipolar disorder? *Neural Plast.* 2015, 708306. doi:10.1155/2015/708306

Patel, R., Kaur, K., and Singh, S. (2021). Protective effect of andrographolide against STZ induced Alzheimer's disease in experimental rats: Possible neuromodulation and aβ((1-42)) analysis. *Inflammopharmacology* 29 (4), 1157–1168. doi:10.1007/s10787-021-00843-6

Pluimer, B. R., Colt, M., and Zhao, Z. (2020). G protein-coupled receptors in the mammalian blood-brain barrier. *Front. Cell. Neurosci.* 14, 139. doi:10.3389/fncel.2020.00139

Ronaldson, P. T., and Davis, T. P. (2012). Blood-brain barrier integrity and glial support: Mechanisms that can be targeted for novel therapeutic approaches in stroke. *Curr. Pharm. Des.* 18 (25), 3624–3644. doi:10.2174/138161212802002625

Roy, E. R., Wang, B., Wan, Y. W., Chiu, G., Cole, A., Yin, Z., et al. (2020). Type I interferon response drives neuroinflammation and synapse loss in Alzheimer disease. *J. Clin. Invest.* 130 (4), 1912–1930. doi:10.1172/jci133737

Saha, K., Lajis, N. H., Israf, D. A., Hamzah, A. S., Khozirah, S., Khamis, S., et al. (2004). Evaluation of antioxidant and nitric oxide inhibitory activities of selected Malaysian medicinal plants. *J. Ethnopharmacol.* 92 (2), 263–267. doi:10.1016/j.jep.2004.03.007

Salmina, A. B., Kharitonova, E. V., Gorina, Y. V., Teplyashina, E. A., Malinovskaya, N. A., Khilazheva, E. D., et al. (2021). Blood-brain barrier and neurovascular unit *in vitro* models for studying mitochondria-driven molecular mechanisms of neurodegeneration. *Int. J. Mol. Sci.* 22 (9), 4661. doi:10.3390/ijms22094661

Schmölz, L., Wallert, M., and Lorkowski, S. (2017). Optimized incubation regime for nitric oxide measurements in murine macrophages using the Griess assay. *J. Immunol. Methods* 449, 68–70. doi:10.1016/j.jim.2017.06.012

Schober, J., Polina, J., Walters, F., Scott, N., Lodholz, E., Crider, A., et al. (2021). NNC 26-9100 increases Aβ1-42 phagocytosis, inhibits nitric oxide production and decreases calcium in BV2 microglia cells. *PLoS One* 16 (7), e0254242. doi:10.1371/journal.pone.0254242

Serrano, F. G., Tapia-Rojas, C., Carvajal, F. J., Hancke, J., Cerpa, W., and Inestrosa, N. C. (2014). Andrographolide reduces cognitive impairment in young and mature AβPPswe/PS-1 mice. *Mol. Neurodegener.* 9 (1), 61. doi:10.1186/1750-1326-9-61

Shengkai, D., and Yazhen, S. (2022). Flavonoids from stems and leaves of Scutellaria baicalensis georgi regulate the brain tau hyperphosphorylation at multiple sites induced by composited aβ in rats. *CNS Neurol. Disord. Drug Targets* 21 (4), 367–374. doi:10.2174/1871527320666210827112609

Singh, S. S., Rai, S. N., Birla, H., Zahra, W., Rathore, A. S., and Singh, S. P. (2020). NF-κB-Mediated neuroinflammation in Parkinson's disease and potential therapeutic effect of polyphenols. *Neurotox. Res.* 37 (3), 491–507. doi:10.1007/s12640-019-00147-2

Sonawane, S. K., Uversky, V. N., and Chinnathambi, S. (2021). Baicalein inhibits heparin-induced Tau aggregation by initializing non-toxic Tau oligomer formation. *Cell Commun. Signal.* 19 (1), 16. doi:10.1186/s12964-021-00704-3

Song, L., Pei, L., Yao, S., Wu, Y., and Shang, Y. (2017). NLRP3 inflammasome in neurological diseases, from functions to therapies. *Front. Cell. Neurosci.* 11, 63. doi:10.3389/fncel.2017.00063

Sun, J., Zhang, X., Broderick, M., and Fein, H. (2003). Measurement of nitric oxide production in biological systems by using griess reaction assay. *Sensors* 3 (8), 276–284. doi:10.3390/s30800276

Suzuki, M., Nikaido, T., and Ohmoto, T. (1991). The study of Chinese herbal medicinal prescription with enzyme inhibitory activity. V. The study of hange-shashin-to, kanzo-shashin-to, shokyo-shashin-to with adenosine 3', 5'-cyclic monophosphate phosphodiesterase. *Yakugaku zasshi* 111 (11), 695–701. doi:10.1248/yakushi1947.111.11_695

Takata, F., Nakagawa, S., Matsumoto, J., and Dohgu, S. (2021). Blood-brain barrier dysfunction amplifies the development of neuroinflammation: Understanding of cellular events in brain microvascular endothelial cells for prevention and treatment of BBB dysfunction. *Front. Cell. Neurosci.* 15, 661838. doi:10.3389/fncel.2021.661838

Takeshita, Y., Fujikawa, S., Serizawa, K., Fujisawa, M., Matsuo, K., Nemoto, J., et al. (2021). New BBB model reveals that IL-6 blockade suppressed the BBB disorder, preventing onset of NMOSD. *Neurol. - Neuroimmunol. Neuroinflammation* 8 (6), e1076. doi:10.1212/nxi.0000000000001076

Tanaka, T., Narazaki, M., and Kishimoto, T. (2014). IL-6 in inflammation, immunity, and disease. *Cold Spring Harb. Perspect. Biol.* 6 (10), a016295. doi:10.1101/cshperspect.a016295

Thiel, V. E., and Audus, K. L. (2001). Nitric oxide and blood-brain barrier integrity. *Antioxid. Redox Signal* 3 (2), 273–278. doi:10.1089/152308601300185223

Tsikas, D. (2007). Analysis of nitrite and nitrate in biological fluids by assays based on the Griess reaction: Appraisal of the Griess reaction in the l-arginine/nitric oxide area of research. *J. Chromatogr. B* 851 (1), 51–70. doi:10.1016/j.jchromb.2006.07.054

Upadhayay, S., and Mehan, S. (2021). Targeting Nrf2/HO-1 anti-oxidant signaling pathway in the progression of multiple sclerosis and influences on neurological dysfunctions. *Brain Disord.* 3, 100019. doi:10.1016/j.dscb.2021.100019

Van Bulck, M., Sierra-Magro, A., Alarcon-Gil, J., Perez-Castillo, A., and Morales-Garcia, J. A. (2019). Novel approaches for the treatment of Alzheimer's and Parkinson's disease. *Int. J. Mol. Sci.* 20 (3), 719. doi:10.3390/ijms20030719

Wang, D. P., Kang, K., Sun, J., Lin, Q., Lv, Q. L., and Hai, J. (2022). URB597 and andrographolide improve brain microvascular endothelial cell permeability and apoptosis by reducing oxidative stress and inflammation associated with activation of Nrf2 signaling in oxygen-glucose deprivation. *Oxid. Med. Cell Longev.* 2022, 4139330. doi:10.1155/2022/4139330

Wolfe, M. S. (2012). The role of tau in neurodegenerative diseases and its potential as a therapeutic target. *Sci. (Cairo)* 2012, 796024. doi:10.6064/2012/796024

World Health Organization (2022). Dementia. [Online]. Available at: https://www.who.int/news-room/fact-sheets/detail/dementia.[Accessed].

Wyss-Coray, T., and Mucke, L. (2002). Inflammation in neurodegenerative disease—A double-edged sword. *Neuron* 35 (3), 419–432. doi:10.1016/s0896-6273(02)00794-8

Yang, A., Liu, C., Wu, J., Kou, X., and Shen, R. (2021a). A review on α-mangostin as a potential multi-target-directed ligand for Alzheimer's disease. *Eur. J. Pharmacol.* 897, 173950. doi:10.1016/j.ejphar.2021.173950

Yang, S., Wang, H., Yang, Y., Wang, R., Wang, Y., Wu, C., et al. (2019). Baicalein administered in the subacute phase ameliorates ischemia-reperfusion-induced brain injury by reducing neuroinflammation and neuronal damage. *Biomed. Pharmacother.* 117, 109102. doi:10.1016/j.biopha.2019.109102

Yang, S., Yang, Y., Chen, C., Wang, H., Ai, Q., Lin, M., et al. (2021b). The anti-neuroinflammatory effect of fuzi and ganjiang extraction on LPS-induced BV2 microglia and its intervention function on depression-like behavior of cancer-related fatigue model mice. *Front. Pharmacol.* 12, 670586. doi:10.3389/fphar.2021.670586

Yoon, W. J., Lee, N. H., and Hyun, C. G. (2010). Limonene suppresses lipopolysaccharide-induced production of nitric oxide, prostaglandin E2, and pro-inflammatory cytokines in RAW 264.7 macrophages. *J. Oleo Sci.* 59 (8), 415–421. doi:10.5650/jos.59.415

Yu, X., Ji, C., and Shao, A. (2020). Neurovascular unit dysfunction and neurodegenerative disorders. *Front. Neurosci.* 14, 334. doi:10.3389/fnins.2020.00334

Zarekiani, P., Nogueira Pinto, H., Hol, E. M., Bugiani, M., and de Vries, H. E. (2022). The neurovascular unit in leukodystrophies: Towards solving the puzzle. *Fluids Barriers CNS* 19 (1), 18. doi:10.1186/s12987-022-00316-0

Zhang, H., and Sun, S.-C. (2015). NF-κB in inflammation and renal diseases. *Cell & Biosci.* 5 (1), 63. doi:10.1186/s13578-015-0056-4

Zhang, J., Zheng, Y., Zhao, Y., Zhang, Y., Liu, Y., Ma, F., et al. (2021). Andrographolide ameliorates neuroinflammation in APP/PS1 transgenic mice. *Int. Immunopharmacol.* 96, 107808. doi:10.1016/j.intimp.2021.107808

Zhang, X., Yang, Y., Du, L., Zhang, W., and Du, G. (2017). Baicalein exerts anti-neuroinflammatory effects to protect against rotenone-induced brain injury in rats. *Int. Immunopharmacol.* 50, 38–47. doi:10.1016/j.intimp.2017.06.007

Zheng, Y. F., Zhou, X., Chang, D., Bhuyan, D. J., Zhang, J. P., Yu, W. Z., et al. (2021). A novel tri-culture model for neuroinflammation. *J. Neurochem.* 156 (2), 249–261. doi:10.1111/jnc.15171

Zhu, H., Wang, Z., Xing, Y., Gao, Y., Ma, T., Lou, L., et al. (2012). Baicalin reduces the permeability of the blood-brain barrier during hypoxia *in vitro* by increasing the expression of tight junction proteins in brain microvascular endothelial cells. *J. Ethnopharmacol.* 141 (2), 714–720. doi:10.1016/j.jep.2011.08.063

Zlokovic, B. V. (2005). Neurovascular mechanisms of Alzheimer's neurodegeneration. *Trends Neurosci.* 28 (4), 202–208. doi:10.1016/j.tins.2005.02.001

frontiers | Frontiers in Neuroscience

TYPE Original Research
PUBLISHED 16 February 2023
DOI 10.3389/fnins.2023.1097859

OPEN ACCESS

EDITED BY
Dennis Chang,
Western Sydney University, Australia

REVIEWED BY
Yan Huang,
Beijing Institute of Pharmacology and Toxicology, China
Shiyu Chen,
Chengdu University of Traditional Chinese Medicine, China

*CORRESPONDENCE
Yu Cao
✉ yu.cao-xiyuan@outlook.com
Hao Li
✉ xyhplihao1965@126.com

SPECIALTY SECTION
This article was submitted to Neuropharmacology, a section of the journal Frontiers in Neuroscience

RECEIVED 14 November 2022
ACCEPTED 01 February 2023
PUBLISHED 16 February 2023

CITATION
Wei W, Pei H, Ma L-N, Zheng R, Huang Q-Y, Chang S-r, Cao Y and Li H (2023) Comparison of Yizhiqingxin formula extraction methods and their pharmacodynamic differences. *Front. Neurosci.* 17:1097859. doi: 10.3389/fnins.2023.1097859

Comparison of Yizhiqingxin formula extraction methods and their pharmacodynamic differences

Wei Wei[1,2], Hui Pei[1], Li-Na Ma[1], Rui Zheng[1], Qiao-Yi Huang[1], Su-rui Chang[1], Yu Cao[1]* and Hao Li[2]*

[1]Xiyuan Hospital, China Academy of Chinese Medical Sciences, Beijing, China, [2]Wangjing Hospital, China Academy of Chinese Medical Sciences, Beijing, China

Objectives: This study compared different extraction methods of Yizhiqingxin formula (YQF) and its neuroprotective effects based on pharmacodynamic indices such as learning and memory ability, brain tissue histopathology and morphology, and inflammatory factor expression in a mouse model of Alzheimer's disease (AD).

Methods: The pharmaceutical components of YQF were extracted using three extraction processes, and the components were analyzed by high performance liquid chromatography. Donepezil hydrochloride was used as a positive control drug. Fifty 7–8-month-old 3 × Tg AD mice were randomly divided into three YQF groups (YQF-1, YQF-2, and YQF-3), a donepezil group, and a model group. Ten age-matched C57/BL6 mice were used as normal controls. YQF and Donepezil were administered by gavage at a clinically equivalent dose of 2.6 and 1.3 $mg{\cdot}kg^{-1}{\cdot}d^{-1}$, respectively, with a gavage volume of 0.1 ml/10 g. Control and model groups received equal volumes of distilled water by gavage. After 2 months, the efficacy was evaluated using behavioral experiments, histopathology, immunohistochemistry, and serum assays.

Results: The main components in YQF are ginsenoside Re, ginsenoside Rg1, ginsenoside Rb1, epiberberine, coptisine chloride, palmatine, berberine, and ferulic acid. YQF-3 (alcohol extraction) has the highest content of active compounds, followed by YQF-2 (water extraction and alcohol precipitation method). Compared to the model group, the three YQF groups showed alleviated histopathological changes and improved spatial learning and memory, with the effect in YQF-2 being the most significant. YQF showed protection of hippocampal neurons, most significantly in the YQF-1 group. YQF significantly reduced Aβ pathology and tau hyperphosphorylation, decreased expressions of serum pro-inflammatory factors interleukin-2 and interleukin-6 as well as serum chemokines MCP-1 and MIG.

Conclusion: YQF prepared by three different processes showed differences in pharmacodynamics in an AD mouse model. YQF-2 was significantly better than the other extraction processes in improving memory.

KEYWORDS

Yizhiqingxin formula (YQF), Alzheimer's disease, mice, Chinese medicine, pharmaceutical technology

1. Introduction

Alzheimer's disease (AD), a type of dementia, is a common clinical neurodegenerative disease in the elderly that seriously affects learning and memory functions as well as daily behavioral abilities and brings a heavy burden to families and society. Studies on AD have shown a plethora of genes that can be grouped into a polygenic risk score (Scheltens et al., 2021); however, there is a lack of effective therapeutic drugs that are known to treat AD. Therefore, traditional Chinese medicine (TCM) compounds and their extracts are important in the prevention and treatment of AD with multichannel and multitarget therapeutic characteristics (Pei et al., 2020). The Yizhiqingxin formula (YQF) is based on the TCM theory of dementia "deficiency, stasis, and toxicity," and is composed of *Panax ginseng* C.A.Mey (Renshen), *Coptis chinensis* Franch (Huanglian), and *Ligusticum chuanxiong* S.H.Qiu, Y.Q.Zeng, K.Y.Pan, Y.C.Tang and J.M.Xu (Chuanxiong) in a ratio of 9:5:6. It can significantly improve spatial learning and memory capacity in AD model mice, delay the pathological processes of AD, and exert therapeutic effects by regulating oxidative stress and neuroinflammation, according to basic research (Yang et al., 2019; Ma et al., 2020). It has good potential as a novel drug. To further expand the clinical applications of YQF and develop a safe and effective TCM compound, we designed three compound extraction processes combining the physicochemical characteristics of the medicinal components in the compound, and we selected donepezil hydrochloride, which has definite efficacy in AD, as a control drug for observation. The efficacy of YQF prepared by three different extraction processes was evaluated in the AD mouse model using behavioral and pathological efficacy indexes to evaluate the extraction processes and provide an experimental basis for future studies.

2. Materials and methods

2.1. Animals

In this study, 50 male 3 × Tg AD mice (7–8 months) were used as model mice (No: 14002A), with 10 male wild-type C57/BL6 mice as normal controls. All animals were purchased from Beijing HFK Bioscience Co., Ltd., (Beijing, China). Animal experiments were approved by the Ethics Committee of Xiyuan Hospital of the China Academy of Chinese Medical Sciences (No. 2021XLC032-2). All animals were housed in an specific-pathogen-free animal room at Xiyuan Hospital, Chinese Academy of Traditional Chinese Medicine at 22 ± 3°C with a 12 h/12 h light–dark cycle, 50% ± 10% relative humidity, and *ad libitum* water and food. Animals were acclimatized to their environment for 1 week before experiments.

2.2. Drugs, chemicals, and reagents

YQF consists of *Panax ginseng* C.A.Mey (Renshen), *Coptis chinensis* Franch (Huanglian), and *Ligusticum chuanxiong* S.H.Qiu, Y.Q.Zeng, K.Y.Pan, Y.C.Tang and J.M.Xu (Chuanxiong). These herbs were purchased from Hebei Baicao Kangshen Pharmaceutical Co., Ltd., (Hebei, China). Donepezil hydrochloride (production lot No. 2104113; Shenzhen Anlixin, Shenzhen, China) was purchased from Eisai (Tokyo, Japan). Ginsenosides Rg1 reference substance, purity 99.70% (A0237); ginsenosides Re reference substance, purity 99.52% (A0244); ginsenosides Rd reference substance, purity 98.55% (A0245); ginsenosides Rb1 reference substance, purity 98.58% (A0234); ferulic acid reference substance, purity 99.32% (A0050); provided by Chengdu Desite Biotechnology Co., Ltd., Chengdu, China. Ginsenosides Rh2 reference substance, purity 98% (B21729); Ginsenosides Rg2 reference substance, purity 98% (B21727); epiberberine reference substance, purity 98% (B20108); coptisine chloride reference substance, purity 98% (B21438); palmatine reference substance, purity 98% (B21646);berberine reference substance, purity 98% (B21379); and provided by Shanghai Yuanye Biotechnology Co., Ltd., Shanghai, China.

2.3. Instruments and equipment

The following instruments and equipment were used for experiments: Morris water maze (MWM; ZS-001; Beijing Zhongshidichuang Science and Technology Development Co., Ltd., Beijing, China); fluorescence microscope (Eclipse E100; Nikon, Tokyo, Japan); imaging system (DS-U3; Nikon); flow cytometer (NovoCyte D1040; Hangzhou Essen Pharmaceutical Research Co., Ltd., Hangzhou, China); QBplex® EZPrep plate washer (VM1001; Beijing Kuangbo Biotechnology Co. Ltd., Beijing, China).

2.4. Yizhiqingxin formula extraction processes

YQF-1: raw herbs were firstly decocted for 1.5 h in water in an amount of eight times the weight of materials. Then filtered to get the residue and decocted again for 1 h with six times amount of water. Combined filtrates were concentrated to 384 ml (1.04 g/ml). YQF-2: raw herbs were firstly decocted for 1.5 h in water in an amount of eight times the weight of materials. Then filtered to get the residue and decocted again for 1 h with six times amount of water. Combined filtrates were concentrated to 400 ml and ethanol was added to make the alcohol content to 60% (632 ml). The solution was allowed to stand for 24 h and filtered. Then, ethanol was removed, and the total amount of solution was adjusted to 384 ml (1.04 g/ml). YQF-3: Reflux Extracted twice for 2 h each with 75% ethanol in the amount of six times the volume of raw drugs. Combined filtrates and removed ethanol. Then the solution was adjusted to 384 ml. All extracted solutions (1.04 g/ml) were stored at 4°C and equilibrated to room temperature before administration by gavage. After drying, we got YQF-1 powder 58.2 mg/ml, YQF-2 powder 71 mg/ml, and YQF-3 powder 112.2 mg/ml.

2.5. High-performance liquid chromatography (HPLC) analysis of YQF

The reference standards or YQF powder were precisely weighed and dissolved with methanol solution. Inertsil C18 (150 mm × 4.6 mm, 5 μm) was used as the stationary phase for the

chromatographic separation. The compounds were identified by individual peak retention times compared to reference substances. The detection wavelength of the main components of Panax ginseng C.A.Mey (Renshen) in YQF was 203 nm, with a column temperature at 35°C. The flow rate was 1 ml/min and the total injection volume was 20 μL. The mobile phase consisted of solvent A (acetonitrile) and solvent B (water) with the following gradient elution: 18% A at 0–40 min; 21% A at 40–42 min; 26% A at 42–46 min; 32% A at 46–66 min; 33.5% A at 66–71 min; 38% A at 71–86 min; 65% A at 86–96 min; 85% A at 96–103 min (Guo, 2014). The detection wavelength of the main components of Coptis chinensis Franch (Huanglian) in YQF was 345 nm, with a column temperature at 25°C. The flow rate was 1 mL/min, and the total injection volume was 5 μL. The mobile phase consisted of 70% solvent A (0.05% trifluoroacetic acid) and 30% solvent B (acetonitrile). The detection wavelength of the main components of Ligusticum chuanxiong S.H.Qiu, Y.Q.Zeng, K.Y.Pan, Y.C.Tang and J.M.Xu (Chuanxiong) in YQF was 294 nm, with a column temperature at 30°C. The flow rate was 1 mL/min, and the total injection volume was 5 μL. The mobile phase consisted of 60% solvent A (0.05% trifluoroacetic acid) and 40% solvent B (methanol).

2.6. Drug administration

Mice in the YQF-1, YQF-2, and YQF-3 groups were administered clinically equivalent doses of 2.6 $g \cdot kg^{-1} \cdot d^{-1}$ (Yang et al., 2019), and donepezil mice were administered clinically equivalent doses of 1.3 $mg \cdot d^{-1}$. The control group and the model group received the same volumes of distilled water by gavage. Gavage was administered once a day for 2 months. Two animals in the model group, One animal in the YQF-2 group and two animals in the YQF-3 group died before the end of the experiments.

2.7. Sample collection and preparation

After behavioral experiments, blood and brain tissues were collected. Blood was placed in centrifuge tubes, left for more than 1 h at room temperature, centrifuged (3,000 rpm, 10 min) to collect the serum, and stored at −80°C for examination. Brains were removed, and sagittally cut into left and right hemispheres, fixed in 4% paraformaldehyde, embedded in paraffin, and sectioned.

2.8. Behavioral experiments

MWM was performed after the end of the gavage. The day before MWM testing, each experimental mouse was placed into the pool without a platform for 60 s to adapt to the environment. For training, spatial navigation experiments were performed for five consecutive days; each mouse was trained twice a day for 60 s each using different entry points. The mice were placed in the water facing the wall of the pool, and the time between entering the water and finding the escape platform (with all limbs on the platform for 6 s; escape latency) was recorded using a video tracking system. On day 6, the escape platform was removed for spatial exploration experiments; mice were placed in the water facing the wall of the pool (at the midpoint of the third quadrant), and the number of times the mouse crossed the original platform area within 60 s was recorded, the time in the target quadrant and distance moved in the target quadrant were also recorded to examine memory of the target quadrant where the original platform was located. A quiet environment with a stable light source and a water temperature of 23 ± 1°C were maintained during experiments.

2.9. Histopathological observation of brain tissue

Brain tissues were embedded in paraffin and sectioned. Then sections were processed as follows: Xylene for 20 min, two times; 100% ethanol for 5 min, two times; 75% ethanol for 5 min; and tap water rinsing. Sections were subjected to hematoxylin–eosin (HE) and toluidine blue (Nissl) staining. Hematoxylin–Eosin Staining Kit (G1003; Wuhan Servicebio Technology Co., Ltd., Wuhan, China) was used for HE staining, and Toluidine blue staining solution (G1032; Wuhan Servicebio Technology Co., Ltd.) was used for Nissl staining.

2.10. Multiplex immunoassays for flow cytometry

IL-2, IL-4, IL-6, IL-12p70, IL-17A, IP-10, MCP-1, MCP-3, IFNγ, RANTES, MIG, Eotaxin, and keratinocyte-derived chemokine (KC) were measured using Mouse Group 1 16-plex kit (C261116; Beijing QuantoBio Biotechnology Co., Ltd., Beijing, China) in this experiment. Briefly, 45 μl/well of serum sample and 45 μl/well of mixed capture beads were added in a 96-well plate, shaken and incubated in darkness for 60 min at room temperature, and washed in 100 μl/well washing buffer for three times. Then, 25 μl/well of biotin-conjugated antibodies was added, shaken and incubated in darkness for 30 min at room temperature, followed by three washings in 100 μl/well washing buffer. Next, 25 μl/well of streptavidin-PE was added, shaken and incubated in darkness for 20 min at room temperature. After three times of washing with 100 μl/well washing buffer, 150 μl/well of Reading buffer was added and the fluorescence signals were detected using flow cytometer (NovoCyte D1040; Hangzhou Essen Pharmaceutical Research Co., Ltd., Hangzhou, China). FCAP Array 3.0 software was used to analyze the levels of chemokines and inflammatory factors.

2.11. Immunohistochemistry

After deparaffinized and gradual hydration through graded alcohols, paraffin sections of brain tissue were immersed in EDTA antigen retrieval buffer (pH 6.0) and maintained at a sub-boiling temperature for 9 min, standing for 7 min and then followed by another sub-boiling temperature for 7 min. Sections were washed three times for 5 min each in PBS (pH 7.4). 3% bovine serum albumin was added to block non-specific binding for 30 min. Sections were incubated with the P-tau (Thr212/Ser214) primary antibody (1:200, MN1060; Thermo Fisher Scientific, Waltham, MA,

USA), Aβ primary antibody (1:200, GB11197; Wuhan Servicebio Technology Co., Ltd.), or P-tau (Thr205/Ser202) primary antibody (1:200, GB113883; Wuhan Servicebio Technology Co., Ltd.) overnight at 4°C, washed three times for 5 min each in PBS, and incubated with secondary antibodies (HRP labeled) goat anti-rabbit (1:200, GB23303; Wuhan Servicebio Technology Co., Ltd.) or goat anti-mouse (1: 200, GB23301; Wuhan Servicebio Technology Co., Ltd.) at room temperature for 50 min. After three 5-min washed in PBS, DAB chromogenic agent (G1211; Wuhan Servicebio Technology Co., Ltd.) was added. After nucleus counterstaining and dehydration through graded alcohols, sections were sealed and examined with a microscope.

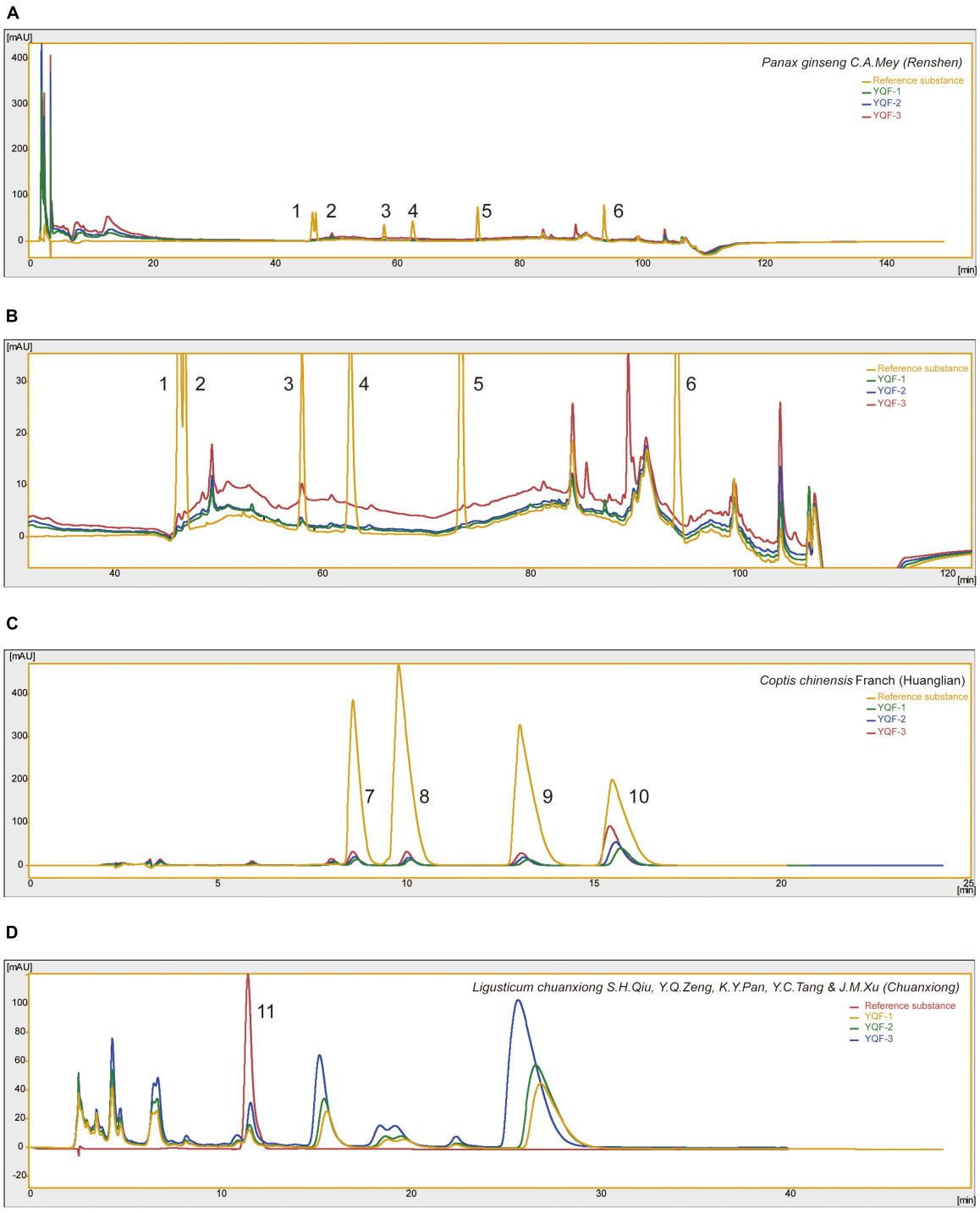

FIGURE 1
The chromatographic profile of Yizhiqingxin formula (YQF). Major compounds of **(A,B)** *Panax ginseng* C. A. Mey (Renshen), **(C)** *Coptis chinensis* Franch (Huanglian) and **(D)** *Ligusticum chuanxiong* S. H. Qiu, Y. Q. Zeng, K. Y. Pan, Y. C. Tang, and J. M. Xu (Chuanxiong) in YQF compared to reference standards, 1: ginsenosides Rg1; 2: ginsenosides Re; 3: ginsenosides Rb1; 4: ginsenosides Rg2; 5: ginsenosides Rd; 6: ginsenosides Rh2; 7: epiberberine; 8: coptisine chloride; 9: palmatine; 10: berberine; 11: ferulic acid.

TABLE 1 Quantification of bioactive components of Yizhiqingxin formula (YQF).

Reference standards	YQF-1 (mg/g)	YQF-2 (mg/g)	YQF-3 (mg/g)
ginsenosides Rg1	10.25	17.33	47.74
ginsenosides Re	–	14.10	38.16
ginsenosides Rb1	11.37	16.81	71.31
ginsenosides Rg2	–	–	–
ginsenosides Rd	–	–	58.92
ginsenosides Rh2	–	–	–
epiberberine	25.99	26.77	51.76
coptisine chloride	23.64	27.87	60.60
palmatine	25.57	35.81	65.74
berberine	115.35	157.08	326.68
ferulic acid	203.92	288.43	826.92

There is a good linear relationship between the concentration of the reference standards and the Peak area (mAU.s), and external standard method was used for quantitative analysis.

2.12. Statistical methods

Data were statistically analyzed using SPSS 22.0 software (IBM Corp., Armonk, NY, USA). Quantitative data were normalized and are expressed as mean ± SEM. Comparison between groups were performed using one-way ANOVA, and Least significance difference (LSD) *post hoc* test. The MWM latency data were analyzed using a repeated-measures analysis of variance. All tests were two-sided with an α of 0.05 and statistical significance threshold of $P < 0.05$.

3. Results

3.1. Bioactive components of YQF

Yizhiqingxin formula (YQF) consist of *Panax ginseng* C.A.Mey (Renshen), *Coptis chinensis* Franch (Huanglian), and *Ligusticum chuanxiong* S.H.Qiu, Y.Q.Zeng, K.Y.Pan, Y.C.Tang and J.M.Xu (Chuanxiong) in a ratio of 9:5:6. High-Performance Liquid Chromatography (HPLC) Analysis of YQF showed the main bioactive components in Figure 1. Specifically speaking, ginsenosides Rg1, ginsenosides Re, ginsenosides Rd, ginsenosides Rh2 in *Panax ginseng* C.A.Mey (Renshen) (Figures 1A, B); epiberberine, coptisine chloride, palmatine, and berberine in *Coptis chinensis* Franch (Huanglian) (Figure 1C); ferulic acid in *Ligusticum chuanxiong* S.H.Qiu, Y.Q.Zeng, K.Y.Pan, Y.C.Tang and J.M.Xu (Chuanxiong) (Figure 1D). Table 1 shows the quantification of bioactive components of YQF. The contents of each component were the most in YQF-3 and the least in YQF-1.

3.2. Effects of YQF on learning and memory ability

There were no significant differences in the swimming speeds of within in each group ($P > 0.05$), and effects on locomotor ability could be excluded. Compared to the control group, the model group showed significantly longer escape latencies ($P = 0.000$) and significantly fewer platform crossings ($P = 0.026$), suggesting impaired spatial learning memory ability in AD mice. The following intra-group comparisons were performed: after 5 days

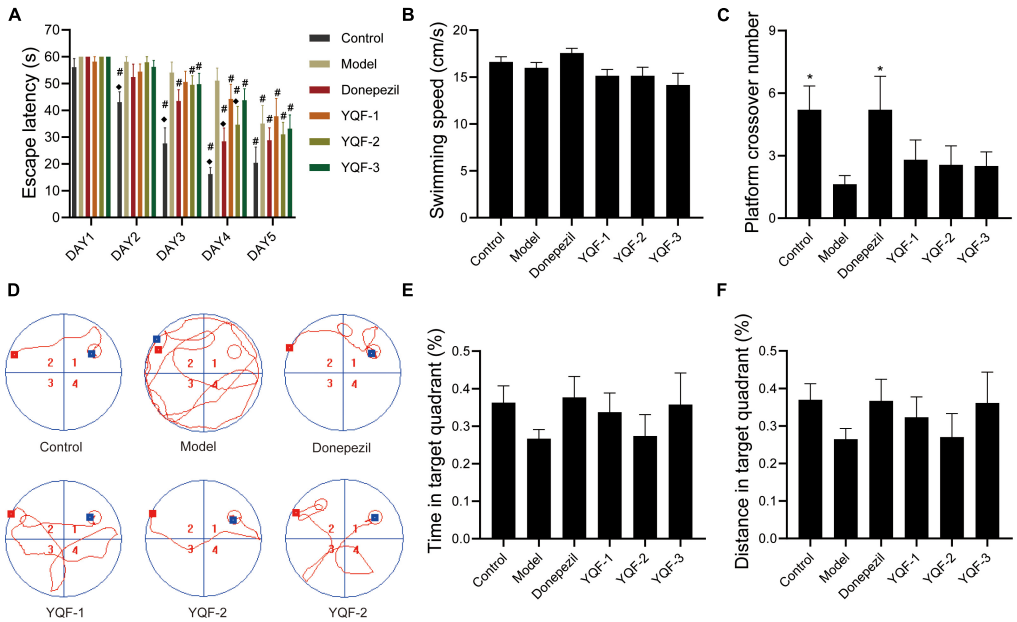

FIGURE 2
Effects on learning and memory ability in Alzheimer's disease (AD) mice; Latency data were analyzed by ANOVA with repeated measures design information, and other data were analyzed by one-way ANOVA, presented as mean ± SEM, $n = 8–10$; $^{*}P < 0.05$, compared to the model group. **(A)** Escape latency, **(B)** swimming speed, **(C)** platform crossover number, **(D)** representative swimming paths, **(E)** time in target quadrant, and **(F)** distance in target quadrant. $^{\blacklozenge}P < 0.05$ for latency data between groups on the same day compared with the model group, and $^{\#}P < 0.05$ for latency data within groups compared with the first day.

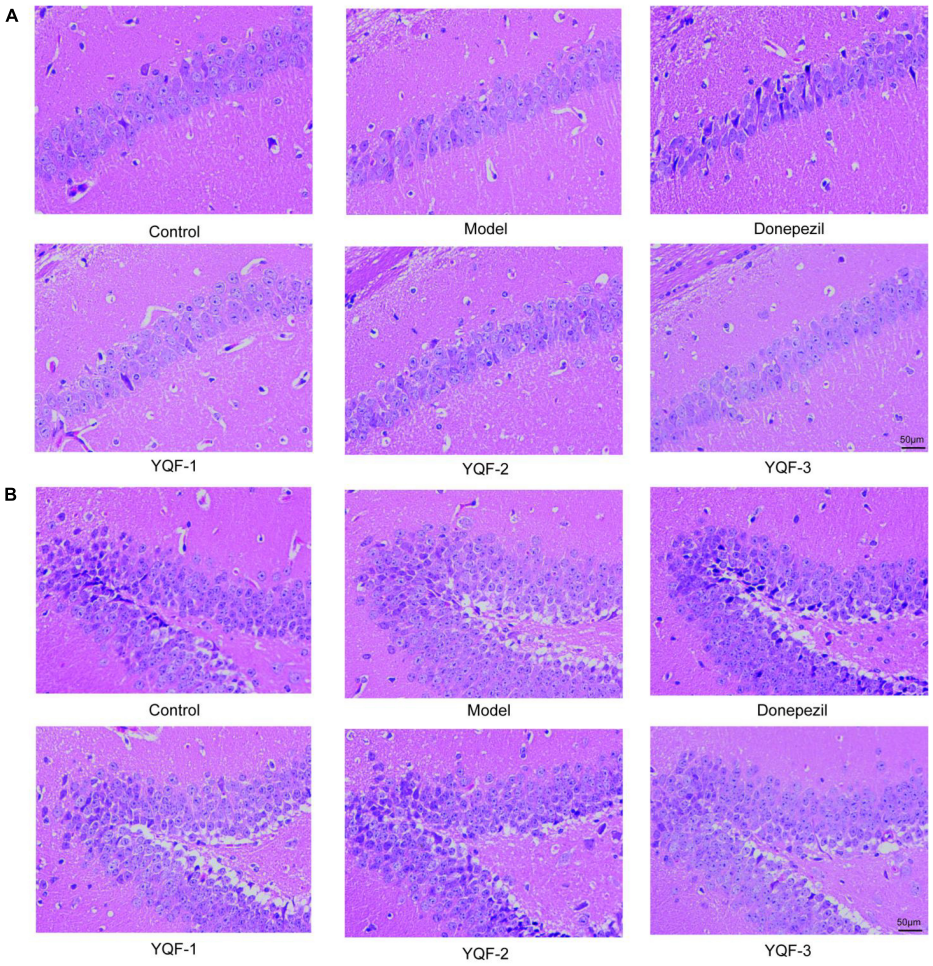

FIGURE 3
Pathological morphology of the hippocampus in each group; Hematoxylin–eosin (HE) staining of the CA1 region **(A)** of the hippocampus and dentate gyrus (DG) region **(B)** in each group, $n = 3$.

of repeated training (twice daily), compared to day 1, escape latency was significantly shorter starting on day 3 in the Donepezil ($P = 0.003$), YQF-2 ($P = 0.014$), and YQF-3 ($P = 0.039$) groups, and day 4 in the YQF-1 group ($P = 0.032$). Escape latency was reduced to different degrees on the training days, suggesting that experimental mice formed a stable spatial reference memory for the fixed platform position. Between-group comparisons showed that the escape latency in the donepezil group was significantly lower on day 4 than that of the model group ($P = 0.003$); on the same day, compared to the model group, escape latencies in YQF-2 group were significantly lower ($P = 0.029$). These results suggested that donepezil and YQF-2 could improve the learning and memory abilities of AD mice. These results are depicted in Figure 2 and Supplementary data 1.

3.3. Histopathological changes of the hippocampus

HE staining was used to observe changes in hippocampal morphology in each group (Figure 3). Compared to the control group, more intensely stained eosinophilic cells were observed in the model group, with a relatively loose cell arrangement, reduced cell number, and unclear or absent nuclei. The donepezil and YQF groups showed different degrees of improvement, with clear cell borders, relatively neat and dense arrangement, clear nucleoli, fewer eosinophilic cells, and more cells with blue-purple cytoplasm, suggesting that the administration of donepezil could reduce neuronal signs of aging and neurodegeneration and repair pathological signs in the hippocampus. The morphologies of the donepezil and YQF-2 groups were clearly different from the other groups.

3.4. Effects of YQF on hippocampal neurons

The effect of YQF on neurons was evaluated using Nissl staining (Figure 4). Morphologically, neurons in the CA1 and dentate gyrus (DG) regions of the hippocampus in the control group were neatly and densely organized, with deep cytoplasmic staining and a high number of Nissl bodies. Neurons in the model group showed relatively lighter blue staining, with a

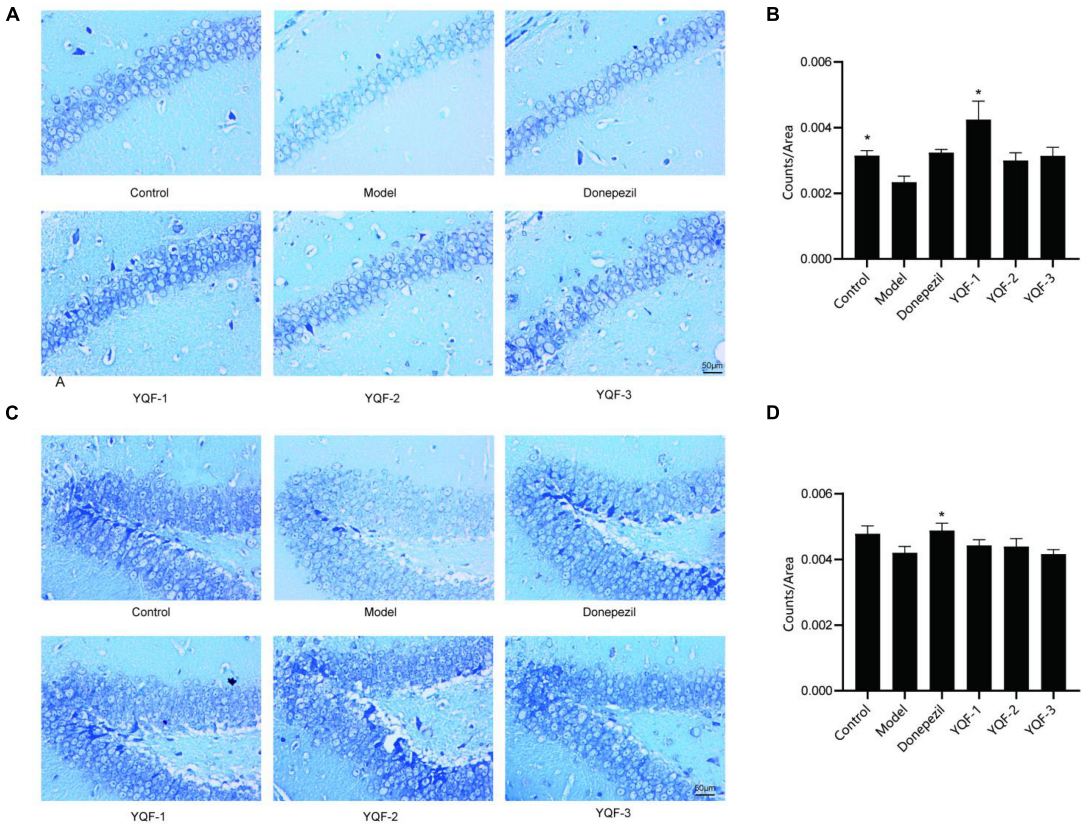

FIGURE 4
Effects on hippocampal neurons in each group; Nissl staining of the CA1 **(A,B)** and dentate gyrus (DG) regions **(C,D)** of the hippocampus in each group. Data were analyzed by one-way ANOVA, presented as mean ± SEM, $n = 3$, $^*P < 0.05$ compared to the model group.

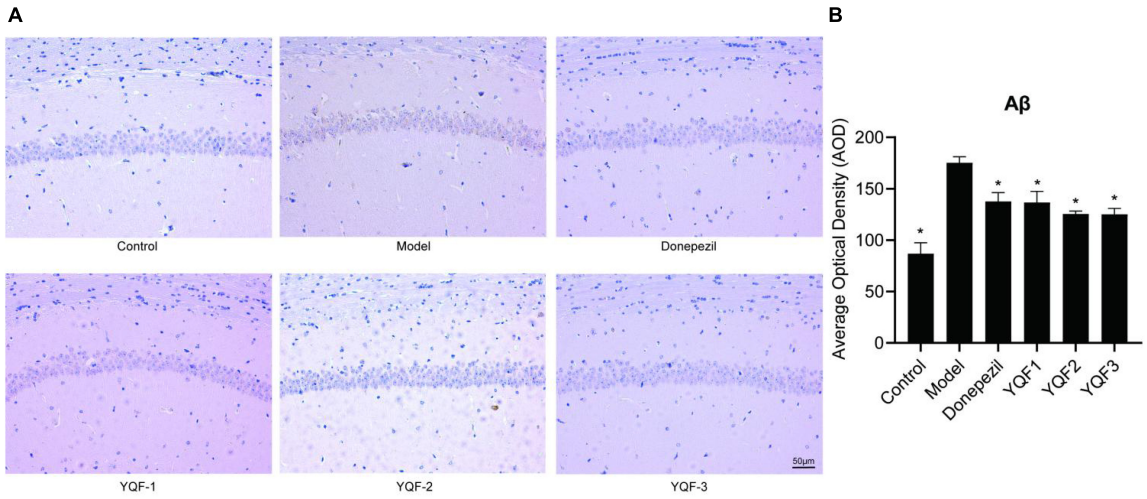

FIGURE 5
Effects on Aβ pathology in the hippocampus in each group; Aβ pathology of the hippocampus CA1 region **(A)** and quantitative analysis **(B)** in each group. Data were analyzed by one-way ANOVA, presented as mean ± SEM, $n = 3$, $^*P < 0.05$ compared to the model group.

reduced number of Nissl bodies and relatively loosely arranged cells. In the YQF groups, there was stronger cytoplasmic staining and neurons were densely arranged. Quantitatively, in the CA1 region of the hippocampus, neuron numbers were significantly higher in the YQF-1 ($P = 0.000$) group compared to the model group, while neuron numbers were significantly higher in the donepezil group ($P = 0.026$) in the DG region of the hippocampus, suggesting that YQF can protect hippocampal neurons to some extent and prevent degenerative necrosis.

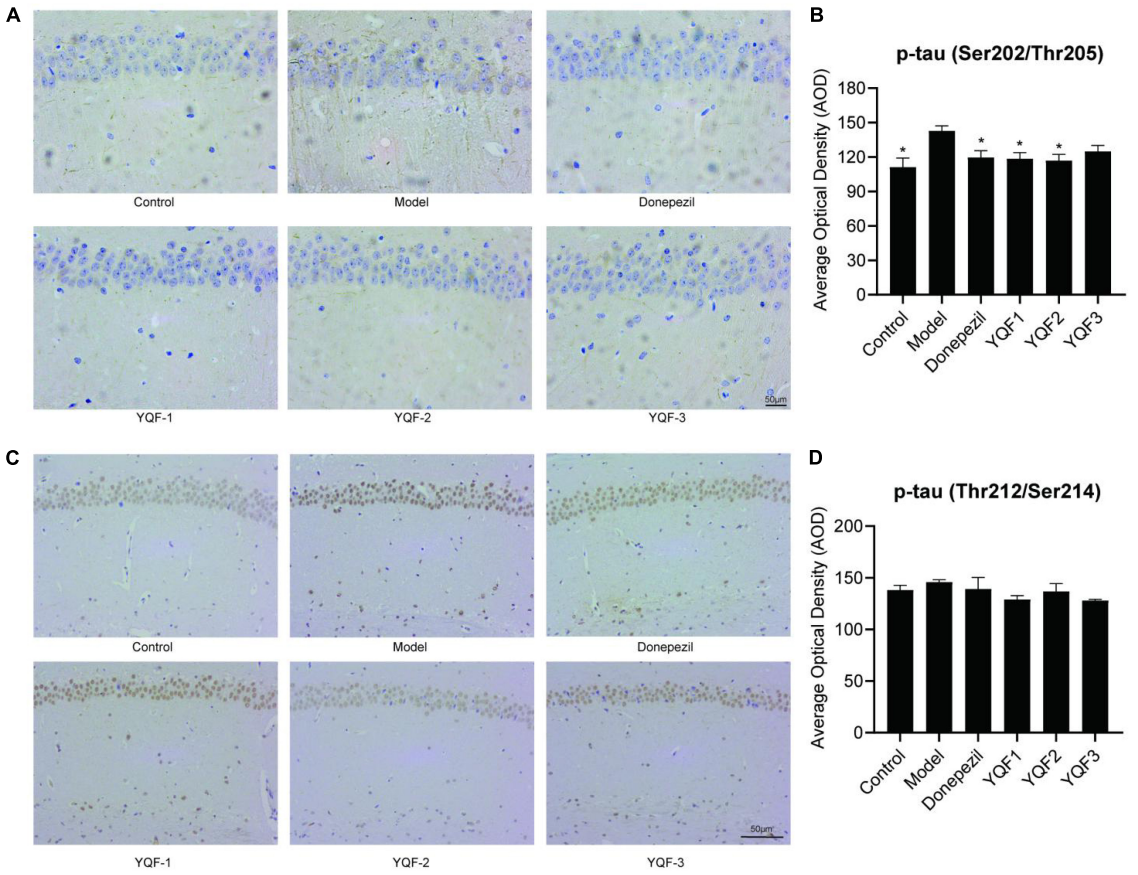

FIGURE 6
Effects on tau protein hyperphosphorylation in the hippocampus in each group; Immunohistochemically labeled p-tau (Ser202/Thr205) **(A,B)** and p-tau (Thr212/Ser214) **(C,D)** in each group. Data were analyzed by one-way ANOVA, presented as mean ± SEM, $n = 3$; *$P < 0.05$, compared to the model group.

3.5. Effects of YQF on Aβ pathology in the hippocampus

Immunohistochemistry was used to evaluate the effects of YQF on Aβ pathology in the CA1 region of the hippocampus. Compared to the control group, there was significantly more Aβ labeling in the CA1 region in model mice, and positive staining in the CA1 region was significantly lower in the donepezil ($P = 0.006$), YQF-1 ($P = 0.005$), YQF-2 ($P = 0.001$), and YQF-3 ($P = 0.001$) groups (Figure 5).

3.6. Effects of YQF on tau protein hyperphosphorylation in the hippocampus

Immunohistochemistry was used to evaluate the effects of YQF on tau hyperphosphorylation in the CA1 region of the hippocampus. Compared to the control group, p-tau labeling (Ser202/Thr205) was significantly higher in the model group and lower in the donepezil ($P = 0.012$), YQF-1 ($P = 0.009$), and YQF-2 ($P = 0.006$) groups (Figures 6A, B). And p-tau (Ser214/Thr212) labeling has the same tendency (Figures 6 C, D).

3.7. Effects of YQF on serum inflammatory factors and chemokines

Serum inflammatory factors and chemokines were evaluated using a high-throughput serum multifactor assay. Regarding the serum inflammatory factors (Figure 7), compared to the control group, serum interleukin IL-2 ($P = 0.000$), IL-6 ($P = 0.000$) were significantly higher in the model group and IL-4 was significantly lower in the model group ($P = 0.043$). The donepezil, YQF-1, YQF-2, and YQF-3 groups showed significantly lower expression of IL-2 and IL-6 ($P = 0.000$), and with significantly higher IL-4 levels in the YQF-1 group ($P = 0.007$).

Regarding the serum chemokines (Figure 8), compared to the control group, Interferon-gamma induced protein 10 (IP-10) ($P = 0.042$), monocyte chemotactic protein (MCP)-1 ($P = 0.000$), monocyte chemotactic protein (MCP)-3 ($P = 0.022$), Interferon gamma (INFγ) ($P = 0.034$), and monokine induced by IFN-γ (MIG) ($P = 0.000$) were significantly higher in the model group, while regulated activation normal T cell expressed and secreted (RANTES), exotaxin, and KC were not significantly different between the control and model groups. The donepezil, YQF-1, YQF-2, and YQF-3 groups showed significantly reduced MCP-1 and MIG levels ($P = 0.000$), suggesting reduced peripheral inflammation levels. Additionally, the YQF-1 group showed

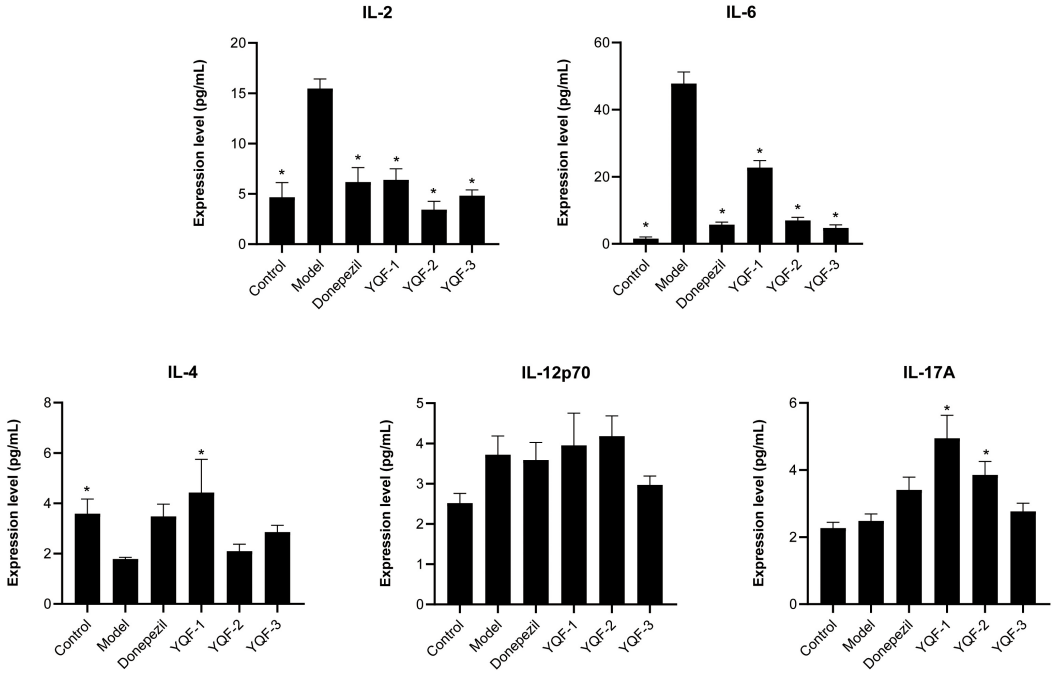

FIGURE 7
Effects on serum inflammatory factors in each group; data were analyzed by one-way ANOVA, presented as mean ± SEM, $n = 6$; *$P < 0.05$, compared to the model group.

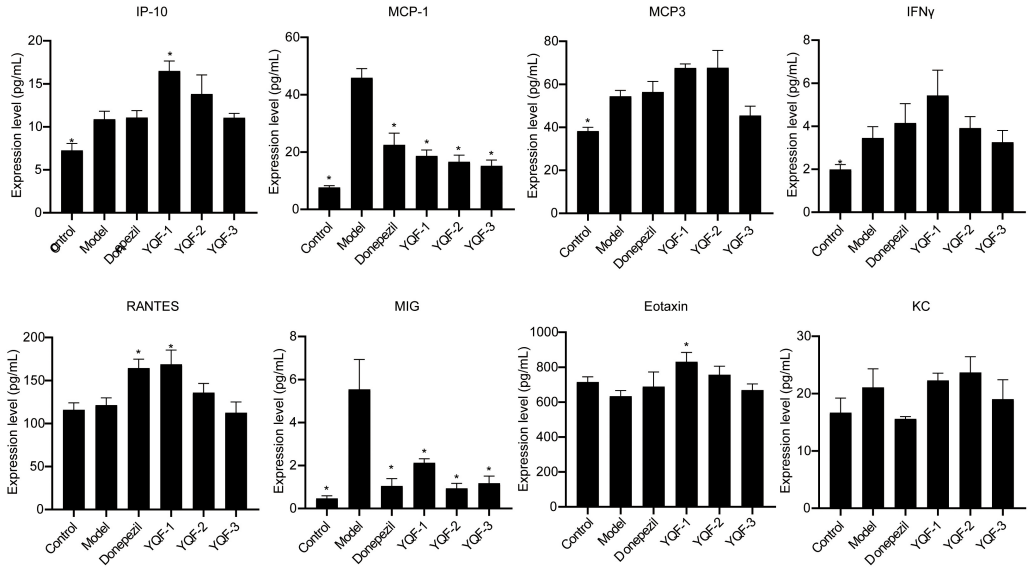

FIGURE 8
Effects on serum chemokines in each group; data were analyzed by one-way ANOVA, presented as mean ± SEM, $n = 6$; *$P < 0.05$, compared to the model group.

significantly higher RANTES ($P = 0.010$), γ-inducible protein (IP)-10 ($P = 0.003$) and Eotaxin levels ($P = 0.005$).

4. Discussion

Patients with AD generally have a long illness duration and poor compliance; therefore, compared to the traditional individual Chinese medicine compound decoction method, the preparations of Chinese medicines based on the established modern Chinese medicine compound extraction processes are stable and convenient to take, which makes them more suitable for "simple, effective, and inexpensive" medicine and long-term use by patients with AD. The development of a Chinese medicine compound with definite efficacy in AD treatment will be beneficial, showing the therapeutic advantages of TCM and meeting the demand for

new drug developments. Previous studies have confirmed that crude extract of YQF can effectively improve spatial learning and memory abilities of aged rats and APP/PS1 model mice, improve histopathological and morphological characteristics in rats, significantly increase acetylcholine and IL-10 levels, reduce the expression of inflammatory factors such as TNF-α and IL-6, and activate the BDNF/TrkB pathway to exert neuroprotective effects, suggesting that it has good clinical prospects in the treatment of AD (Yang et al., 2019; Ma et al., 2020).

The water extraction method is close to the "traditional preparation," with low cost and a simple process, but the scope of its application is small, and many active ingredients with small polarity are not easily extracted, water-soluble components such as polysaccharides, glycosides and alkaloids can be easily extracted. Alcohol precipitation method is a purification and refining method commonly used in water extraction of TCM. By alternating treatment of water and different concentrations of ethanol, alkaloids, glycosides, amino acids, organic acids and other components can be retained, and impurities such as protein, gelatinized starch, lipid-soluble pigment, resin, and some sugars can be removed to further enrich the effective components. Ensure the maximum utilization of raw materials. Ethanol has better solubility, shorter extraction time, and less dissolved water-soluble impurities. Ethanol is a common organic solvent that can increase the extraction rate and is less toxic but flammable. The main active components in *Panax ginseng* C.A.Mey (Renshen) are ginsenosides, and ethanol extraction can reduce the dissolution of other impurities. The main components of *Coptis chinensis* Franch (Huanglian) are alkaloids and flavonoids, which have certain solubility in water. For *Ligusticum chuanxiong* S.H.Qiu, Y.Q.Zeng, K.Y.Pan, Y.C.Tang and J.M.Xu (Chuanxiong), the following two treatment methods can be used: (1) Extracting Chuanxiong with other herbs by decocting; (2) The volatile oil of Chuanxiong was extracted by steam distillation, and the residue of Chuanxiong was extracted by decocting together with other herbs. Considering that there are few kinds of materials containing volatile oil in YQF, and the content of volatile oil in Chuangxiong is low, in order to simplify the technological process, it is proposed to use the decoction method to extract Chuangxiong together with other herbs. In order to complete the preclinical study of the innovative TCM YQF for the treatment of AD, considering the pharmacological effects of each herb in YQF and the physical and chemical properties of the main components, we designed three preparations, namely "water extraction" (YQF-1), "water extraction and alcohol precipitation method" (YQF-2), and "alcohol extraction" (YQF-3). Specific extraction methods were determined by the Preparation Department of Xiyuan Hospital, Chinese Academy of Traditional Chinese Medicine.

The effective components of the three methods were preliminarily explored and quantitatively analyzed by HPLC (**Figure 1**and **Table 1**). The main components in YQF are ginsenoside Re, ginsenoside Rg1, ginsenoside Rb1, epiberberine, coptisine chloride, palmatine, berberine, and ferulic acid. Different extraction processes have a great impact on the content of the effective components of the extracted drugs. The results showed that YQF-3 (alcohol extraction) has the highest content of active compounds, followed by YQF-2 (water extraction and alcohol precipitation method). The YQF-1 (water extraction) has the lowest content of active compounds. The active components of ginseng, protopanaxatriol saponins Re and Rg1, are more polar, while the protopanaxadiol saponin Rb1 contains more glycosyl groups (hydroxyl groups), making aqueous extraction more efficient. Alcohol extraction can increase the extraction rate of ginsenosides to diol-type saponins (Gong et al., 2014). The alkaloids berberine, epiberberine, xanthophylline, and palmatine, which are the main pharmacologically active components of *Coptis chinensis* Franch (Huanglian), are more polar and can be extracted with water or ethanol, but the extraction efficiency is higher in ethanol (Liu et al., 2006). Ferulic acid, a phenolic acid, has a high content in *Ligusticum chuanxiong* S.H.Qiu, Y.Q.Zeng, K.Y.Pan, Y.C.Tang and J.M.Xu (Chuanxiong), its water solubility is poor, but its alcohol solubility is good, and the ethanol extraction rate is relatively high (Yang et al., 2012). Differences in polarity, solubility, and other characteristics of the active ingredients of Chinese herbal medicines have led to slight differences in the compositions and contents of extracts in different solvents, which may be one of the reasons for the differences in the present results.

Ginsenoside Rg1, ginsenoside Re, and coptisine have been detected in the brain of in SAMP8 mice after YQF treatment, showing protective roles (Yang Y. et al., 2017). Impaired learning memory capacity is one of the most significant clinical symptoms of AD, and pathological changes such as Aβ pathology, tau hyperphosphorylation, and inflammation-related indicators can reflect the severity of the disease and are often used as indicators of treatment efficacy. Studies have confirmed that a variety of active ingredients such as ginsenosides, alkaloids, and ferulic acid can play important roles in the prevention and treatment of AD by improving learning and memory and reducing AD pathology and inflammation levels *via* multiple pathways (Sheng et al., 2015; Yang W. T. et al., 2017; Jung et al., 2009; Singh et al., 2021). Ginsenosides negatively regulate β-secretase activity, where Rb1 and Rb2 exhibit a high binding affinity for β-secretase (Choi et al., 2016), while ginsenoside Re activates PPARγ (Cao et al., 2016), ginsenoside Rg1 suppresses PPARγ-regulated BACE1 activity (Chen et al., 2012), and ginsenoside Rd increases sAPPα expression levels (Yan et al., 2017), which ultimately reduces neurotoxic Aβ production. In addition, ginsenoside Rb1 and Rd can inhibit tau protein hyperphosphorylation (Li et al., 2011; Zhao et al., 2013). Berberine reduces Aβ in the brain of AD mice (Ye et al., 2021; Wang Y. Y. et al., 2021), and reduces the tau hyperphosphorylation in the hippocampus of AD mice (He et al., 2017). Ferulic acid also improved Aβ plaque deposition and spatial memory deficits (Wang N. Y. et al., 2021).

It is of great significance for developing safe, effective, quality-controlled and innovative Chinese medicines to screen and evaluate the rationality of the extraction process by pharmacodynamic indicators. To further explore these preparation processes and their efficacy and provide an experimental basis for future translational studies, the present study evaluated three preparations, namely "water extraction" (YQF-1), "water extraction and alcohol precipitation method" (YQF-2), and "alcohol extraction" (YQF-3), in AD treatment. The 3 × Tg AD mice selected for this study are an ideal AD model showing obvious behavioral abnormalities after 6 months of age and age-related Aβ pathology and tau hyperphosphorylation (Oddo et al., 2003; Billings et al., 2005). In the present study, 7–8-month-old AD mice were evaluated for the efficacy of three YQF extraction processes after 2 months of treatment, showing the following results: (1) different degrees of improved spatial learning and memory and histopathological morphology in AD mice, with more significant

effects for YQF-2; (2) different degrees of protective effects on hippocampal neuron morphology, with the most significant effects on CA1 neuron number for YQF-1; (3) the effects of YQF-1, YQF-2 and YQF-3 on Aβ pathology in the CA1 region were both significant (4) reduced hyperphosphorylation of tau Ser202/Thr205 sites, with no effect of YQF-3; (5) reduced expression of serum pro-inflammatory factors IL-2, IL-6 and serum chemokines MCP-1, MIG. Furthermore, YQF-1 not only significantly increased the level of anti-inflammatory factor IL-4 but also increased the expression of pro-inflammatory factor IL-17A. RANTES, IP-10 and Eotaxin were also increased after YQF-1 intervention, but the roles of RANTES, IP-10 and Eotaxin remain controversial in AD.

The present study confirmed the efficacy of YQF as an adjunctive treatment in AD model mice. In general, although the extract contents of the three processes are slightly different, YQF of the three processes can significantly improve the main pathological features of AD, Aβ and hyperphosphorylation of tau protein, and can reduce the level of inflammation in serum. Besides, YQF-2 can significantly improve the learning and memory ability, while YQF-1 and YQF-3 have no significant effect; YQF-1 had a statistically significant protective effect on neurons, and YQF-2 and YQF-3 had the same trend. Limited by the experimental conditions, we only made a rough analysis and quantification of some possible components of YQF. However, the chemical composition of Chinese herbal compounds is complex, there are still many effective components that could not be analyzed in this experiment. Moreover, the number of experimental animals in each group is relatively small, which may also lead to the differences in the above results. In the follow-up studies, more systematic medicinal chemistry and pharmacokinetics studies are needed to optimize the extraction process considering economic costs and the feasibility of industrialization and promotion in addition to comparisons of pharmacodynamics to screen for materials. Different experimental models and efficacy indicators, and expand sample size are also needed to further provide a basis for preclinical research of YQF.

Data availability statement

The raw data supporting the conclusions of this article will be made available by the authors, without undue reservation.

Ethics statement

The animal study was reviewed and approved by the Ethics Committee of the Xiyuan Hospital of the China Academy of Chinese Medical Sciences (No. 2021XLC032-2).

Author contributions

WW performed the experiments and data analysis and wrote the manuscript. RZ, Q-YH, and S-RC assisted in the experiments. HP and L-NM assisted with the data analysis. YC and HL conceived the study, designed the experiments, and assisted in the modification of the manuscript. All authors reviewed and approved the manuscript.

Funding

This study was funded by the Fundamental Research Funds for the Central Public Welfare Research Institutes (ZZ15-YQ-013 and ZZ15-XY-PT-02), and Science and Technology Innovation Project of Chinese Academy of traditional Chinese Medicine (CI2021A01401 and CI2021A04618).

Conflict of interest

The authors declare that the research was conducted in the absence of any commercial or financial relationships that could be construed as a potential conflict of interest.

Publisher's note

Supplementary Material

The Supplementary Material for this article can be found online at: https://www.frontiersin.org/articles/10.3389/fnins.2023.1097859/full#supplementary-material

References

Billings, L. M., Oddo, S., Green, K. N., McGaugh, J. L., and LaFerla, F. M. (2005). Intraneuronal Abeta causes the onset of early Alzheimer's disease-related cognitive deficits in transgenic mice. *Neuron* 45, 675–688. doi: 10.1016/j.neuron.2005.01.040

Cao, G., Su, P., Zhang, S., Guo, L., Zhang, H., Liang, Y., et al. (2016). Ginsenoside Re reduces Aβ production by activating PPARγ to inhibit BACE1 in N2a/APP695 cells. *Eur. J. Pharmacol.* 793, 101–108. doi: 10.1016/j.ejphar.2016.11.006

Chen, L. M., Lin, Z. Y., Zhu, Y. G., Lin, N., Zhang, J., Pan, X. D., et al. (2012). Ginsenoside Rg1 attenuates β-amyloid generation via suppressing PPARγ-regulated BACE1 activity in N2a-APP695 cells. *Eur. J. Pharmacol.* 675, 15–21. doi: 10.1016/j.ejphar.2011.11.039

Choi, R. J., Roy, A., Jung, H. J., Ali, M. Y., Min, B. S., Park, C. H., et al. (2016). BACE1 molecular docking and anti-Alzheimer's disease activities of ginsenosides. *J. Ethnopharmacol.* 190, 219–230. doi: 10.1016/j.jep.2016.06.013

Gong, X., Zhang, Y., Pan, J., and Qu, H. (2014). Optimization of the ethanol recycling reflux extraction process for saponins using a design space approach. *PLoS One* 9:e114300. doi: 10.1371/journal.pone.0114300

Guo, C. (2014). Simultaneous determination of sixteen ginsenosides in Panax ginseng and its preparation by HPLC. *Chin. Traditional Herb. Drugs* 45, 2009–2013.

He, W., Wang, C., Chen, Y., He, Y., and Cai, Z. (2017). Berberine attenuates cognitive impairment and ameliorates tau hyperphosphorylation by limiting the self-perpetuating pathogenic cycle between NF-κB signaling, oxidative stress and neuroinflammation. *Pharmacol. Rep.* 69, 1341–1348. doi: 10.1016/j.pharep.2017.06.006

Jung, H. A., Min, B. S., Yokozawa, T., Lee, J. H., Kim, Y. S., and Choi, J. S. (2009). Anti-Alzheimer and antioxidant activities of Coptidis Rhizoma alkaloids. *Biol. Pharm. Bull.* 32, 1433–1438.

Li, L., Liu, J., Yan, X., Qin, K., Shi, M., Lin, T., et al. (2011). Protective effects of ginsenoside Rd against okadaic acid-induced neurotoxicity in vivo and in vitro. *J. Ethnopharmacol.* 138, 135–141. doi: 10.1016/j.jep.2011.08.068

Liu, B., Li, W., Chang, Y., Dong, W., and Ni, L. (2006). Extraction of berberine from rhizome of Coptis chinensis Franch using supercritical fluid extraction. *J. Pharm. Biomed. Anal.* 41, 1056–1060. doi: 10.1016/j.jpba.2006.01.034

Ma, L., Cao, Y., Wang, F., Li, Z., Wang, Z., Yang, Y., et al. (2020). Yizhi qingxin formula extract ameliorates cognitive decline in aged rats via the brain-derived neurotrophic Factor/Tropomyosin receptor Kinase B pathway. *Front. Pharmacol.* 11:510. doi: 10.3389/fphar.2020.00510

Oddo, S., Caccamo, A., Shepherd, J. D., Murphy, M. P., Golde, T. E., Kayed, R., et al. (2003). Triple-transgenic model of Alzheimer's disease with plaques and tangles: intracellular Abeta and synaptic dysfunction. *Neuron* 39, 409–421. doi: 10.1016/S0896-6273(03)00434-3

Pei, H., Ma, L., Cao, Y., Wang, F., Li, Z., Liu, N., et al. (2020). Traditional Chinese Medicine for Alzheimer's Disease and Other Cognitive Impairment: A Review. *Am. J. Chin. Med.* 48, 487–511.

Scheltens, P., De Strooper, B., Kivipelto, M., Holstege, H., Chételat, G., Teunissen, C. E., et al. (2021). Alzheimer's disease. *Lancet* 397, 1577–1590.

Sheng, C., Peng, W., Xia, Z. A., Wang, Y., Chen, Z., Su, N., et al. (2015). The impact of ginsenosides on cognitive deficits in experimental animal studies of Alzheimer's disease: a systematic review. *BMC Compl. Altern. Med.* 15:386. doi: 10.1186/s12906-015-0894-y

Singh, Y. P., Rai, H., Singh, G., Singh, G. K., Mishra, S., Kumar, S., et al. (2021). A review on ferulic acid and analogs based scaffolds for the management of Alzheimer's disease. *Eur. J. Med. Chem.* 215, 113278. doi: 10.1016/j.ejmech.2021.113278

Wang, N. Y., Li, J. N., Liu, W. L., Huang, Q., Li, W. X., Tan, Y. H., et al. (2021). Ferulic Acid Ameliorates Alzheimer's Disease-like Pathology and Repairs Cognitive Decline by Preventing Capillary Hypofunction in APP/PS1 Mice. *Neurotherapeutics* 18, 1064–1080. doi: 10.1007/s13311-021-01024-7

Wang, Y. Y., Yan, Q., Huang, Z. T., Zou, Q., Li, J., Yuan, M. H., et al. (2021). Ameliorating Ribosylation-Induced Amyloid-β Pathology by Berberine via Inhibiting mTOR/p70S6K Signaling. *J. Alzheimers Dis.* 79, 833–844. doi: 10.3233/JAD-200995

Yan, X., Hu, G., Yan, W., Chen, T., Yang, F., Zhang, X., et al. (2017). Ginsenoside Rd promotes non-amyloidogenic pathway of amyloid precursor protein processing by regulating phosphorylation of estrogen receptor alpha. *Life Sci.* 168, 16–23. doi: 10.1016/j.lfs.2016.11.002

Yang, W. T., Zheng, X. W., Chen, S., Shan, C. S., Xu, Q. Q., Zhu, J. Z., et al. (2017). Chinese herbal medicine for Alzheimer's disease: Clinical evidence and possible mechanism of neurogenesis. *Biochem. Pharmacol.* 141, 143–155.

Yang, X., Wu, X., Hu, L., and Guo, H. (2012). [Effect of different solvents on extraction of effective components from Ligusticum chuanxiong]. *Zhongguo Zhong Yao Za Zhi* 37, 1942–1945.

Yang, Y., Jia, X., Feng, J., Wang, Z., Cao, Y., Liu, J., et al. (2017). Fuzheng quxie decoction ameliorates learning and memory impairment in SAMP8 mice by decreasing tau hyperphosphorylation. *Evid. Based Complement. Alternat. Med.* 2017, 5934254. doi: 10.1155/2017/5934254

Yang, Y., Wang, Z., Cao, Y., Liu, J., Li, P., Li, H., et al. (2019). Yizhiqingxin formula alleviates cognitive deficits and enhances autophagy via mtor signaling pathway modulation in early onset Alzheimer's disease mice. *Front. Pharmacol.* 10:1041. doi: 10.3389/fphar.2019.01041

Ye, C., Liang, Y., Chen, Y., Xiong, Y., She, Y., Zhong, X., et al. (2021). Berberine improves cognitive impairment by simultaneously impacting cerebral blood flow and β-amyloid accumulation in an APP/tau/PS1 mouse model of Alzheimer's disease. *Cells* 10:1161. doi: 10.3390/cells10051161

Zhao, H. H., Di, J., Liu, W. S., Liu, H. L., Lai, H., and Lü, Y. L. (2013). Involvement of GSK3 and PP2A in ginsenoside Rb1's attenuation of aluminum-induced tau hyperphosphorylation. *Behav. Brain Res.* 241, 228–234. doi: 10.1016/j.bbr.2012.11.037

frontiers | Frontiers in Neuroscience

TYPE Review
PUBLISHED 01 March 2023
DOI 10.3389/fnins.2023.1123817

OPEN ACCESS

EDITED BY
Dennis Chang,
Western Sydney University, Australia

REVIEWED BY
Yan Huang,
Beijing Institute of Pharmacology and Toxicology, China
Mehdi Farhoudi,
Tabriz University of Medical Sciences, Iran

*CORRESPONDENCE
Yunling Zhang
✉ yunlingzhang2004@126.com
Wei Shen
✉ 676665709@qq.com

SPECIALTY SECTION
This article was submitted to Neuropharmacology, a section of the journal Frontiers in Neuroscience

RECEIVED 14 December 2022
ACCEPTED 13 February 2023
PUBLISHED 01 March 2023

CITATION
Chi X, Wang L, Liu H, Zhang Y and Shen W (2023) Post-stroke cognitive impairment and synaptic plasticity: A review about the mechanisms and Chinese herbal drugs strategies.
Front. Neurosci. 17:1123817.
doi: 10.3389/fnins.2023.1123817

Post-stroke cognitive impairment and synaptic plasticity: A review about the mechanisms and Chinese herbal drugs strategies

Xiansu Chi[1], Liuding Wang[1], Hongxi Liu[2], Yunling Zhang[1]* and Wei Shen[1]*

[1]Xiyuan Hospital, China Academy of Chinese Medical Sciences, Beijing, China, [2]Graduate School, Beijing University of Chinese Medicine, Beijing, China

Post-stroke cognitive impairment, is a major complication of stroke, characterized by cognitive dysfunction, which directly affects the quality of life. Post-stroke cognitive impairment highlights the causal relationship between stroke and cognitive impairment. The pathological damage of stroke, including the increased release of excitatory amino acids, oxidative stress, inflammatory responses, apoptosis, changed neurotrophic factor levels and gene expression, influence synaptic plasticity. Synaptic plasticity refers to the activity-dependent changes in the strength of synaptic connections and efficiency of synaptic transmission at pre-existing synapses and can be divided into structural synaptic plasticity and functional synaptic plasticity. Changes in synaptic plasticity have been proven to play important roles in the occurrence and treatment of post-stroke cognitive impairment. Evidence has indicated that Chinese herbal drugs have effect of treating post-stroke cognitive impairment. In this review, we overview the influence of pathological damage of stroke on synaptic plasticity, analyze the changes of synaptic plasticity in post-stroke cognitive impairment, and summarize the commonly used Chinese herbal drugs whose active ingredient or extracts can regulate synaptic plasticity. This review will summarize the relationship between post-stroke cognitive impairment and synaptic plasticity, provide new ideas for future exploration of the mechanism of post-stroke cognitive impairment, compile evidence of applying Chinese herbal drugs to treat post-stroke cognitive impairment and lay a foundation for the development of novel formulas for treating post-stroke cognitive impairment.

KEYWORDS

post-stroke cognitive impairment, mechanisms, synaptic plasticity, structural synaptic plasticity, functional synaptic plasticity, Chinese herbal drugs

1. Introduction

Post-stroke cognitive impairment (PSCI), one of the major complications after stroke, occurs in the 3 to 6 months after stroke onset and is characterized by impairment of cognitive function (Mijajlović et al., 2017; Rost et al., 2022). Nowadays, about one-third of stroke survivors manifest considerable cognitive impairment within a few months after stroke (Gorelick et al., 2011). Based on the analysis of the cognitive status of 3,146 patients of stroke

(97%) or transient ischemic attack (3%) from eight countries, Lo et al. found that within 2 to 6 months after stroke, 44% of patients were found overall cognitive impairment and 30–35% of stroke survivors had the impairment in a single cognitive domain (Lo et al., 2019). PSCI can affect quality of life, prevent patients from participating in social activities, and increase the burden on families (Zhang and Bi, 2020).

PSCI highlights the causal relationship between stroke and cognitive impairment. Thus, understanding the complex pathological mechanism between stroke events and cognitive disorders is essential for the development of targeted intervention and treatment strategies. Evidence shows that stroke induces synaptic plasticity impairment, which may be a potential mechanism for PSCI (Joy and Carmichael, 2021). Synaptic plasticity refers to the activity-dependent changes in the strength of synaptic connections and efficiency of synaptic transmission at pre-existing synapses (Mateos-Aparicio and Rodríguez-Moreno, 2020). It can be divided into structural synaptic plasticity and functional synaptic plasticity (**Figure 1**). Structural synaptic plasticity refers to adaptive changes in the synaptic ultrastructure such as number, density, and distribution of synapses, highlighting the strength of synaptic connections (Sadigh-Eteghad et al., 2018). Functional synaptic plasticity refers to the efficacy of synaptic transmission, including long-term potentiation (LTP) and long-term depression (LTD). Synaptic plasticity is closely related to the recovery and improvement of cognitive impairment, the increase in the strength of synaptic connections and efficiency of synaptic transmission directly upregulate the processing and storage of information within the central nervous system, thus improving the cognitive function (Raven et al., 2018).

Currently, there is limited evidence to support the effectiveness of therapeutic strategies in the treatment of PCSI. Considering their overlap with the neuropathological mechanisms of PSCI (Mok et al., 2017), the choice of treatments for PCSI currently relies on the evidence of the drugs used in the treatment of vascular cognitive impairment, vascular dementia, and Alzheimer's disease (Wang et al., 2021). In terms of Western medicine treatment options, donepezil, an acetylcholinesterase inhibitor, is recommended for improving cognitive function and activities of daily living in PSCI patients, with the character of safe and well-tolerated. Meanwhile, galantamine, the cholinesterase inhibitor, is potentially effective for PSCI but is less safe and less tolerated (Whyte et al., 2008). Additionally, the antioxidant drug dimethyl fumarate has been demonstrated to improve learning and memory function in a rat model of PSCI, possibly by reducing apoptosis and autophagy and exerting anti-oxidative effects *via* the Nrf2-ARE (Hou et al., 2020), however, reported side effects include a 30% drop in lymphocyte count after administration and an increased risk of infection, which cannot be ignored (Berkovich and Weiner, 2015). Thus, extensive clinical and mechanistic studies are still needed. Non-pharmacological therapies are also the effective strategy for PSCI, such as enriched environments, physical activity, lifestyle interventions, and acupuncture (Liu et al., 2021; Wang et al., 2021), however, large-scale controlled trials are still lacking. Furthermore, Chinese herbal drugs, as a class of natural medicinal products based on the theory of traditional Chinese medicine, are widely used in Asia and play an important role in improving cognitive function in patients with PSCI. In our previous research, python language data was used to optimize and integrate the medication rules of Chinese herbal drugs in the clinical treatment of PSCI, and 214 Chinese herbal drugs with a total frequency of 1,685 times were found (Shen et al., 2022). However, the mechanism of these Chinese herbal drugs in treating PSCI still needs to be further explored and summarized.

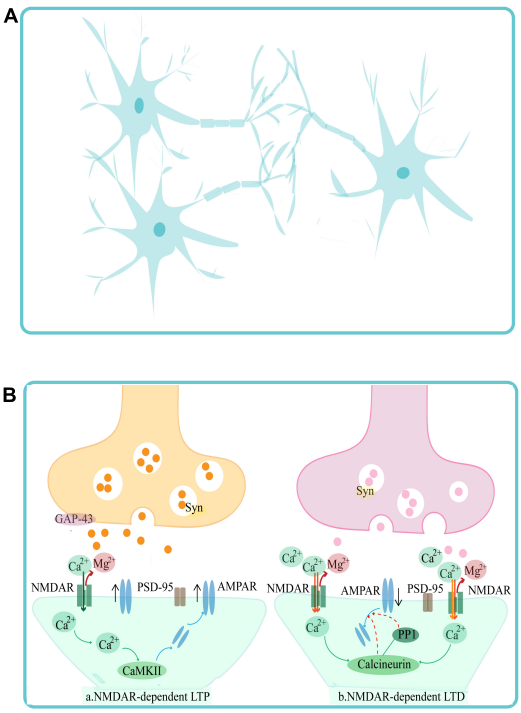

FIGURE 1
Synaptic plasticity can be categorized into structural synaptic plasticity **(A)** and functional synaptic plasticity **(B)**. Structural synaptic plasticity panel **(A)** refers to the number, density, distribution of synapses, and highlights the strength of synaptic connections. Functional synaptic plasticity panel **(B)** refers to the efficiency of synaptic transmission, and includes NMDAR-dependent LTP and NMDAR-dependent LTD. GAP-43, PSD-95, Syn, CaMKII, NMDAR, and AMPAR are synaptic plasticity-related proteins, which play important roles in mediating changes in synaptic morphology, structure, and density and in the function of inter-synaptic information transfer.

Nowadays, strategies that regulate synaptic plasticity have been proven to play an important role in improving cognitive impairment (Bordet et al., 2017), but the specific mechanisms are still unclear. In this review, we overview the influence of pathological damage of stroke on synaptic plasticity, analyze the changes of synaptic plasticity in PSCI, and summarize the applications and the underlying mechanisms of Chinese herbal drugs in the treatment of PSCI from the perspective of synaptic plasticity. This review will provide new ideas for future exploration of the mechanism of PSCI, and compile evidence of applying Chinese herbal drugs to treat PSCI.

2. Pathological damage of stroke influence synaptic plasticity

Stroke is an important cause of PSCI and accompanied with a series of pathological damage (Joy and Carmichael, 2021). During the hyperacute phase of stroke, inadequate perfusion limits the

supply of oxygen and glucose. Subsequently, ATP deficiency leads to abnormal ion pump operation, triggering the depolarization of neurons and glial cells, and abnormal extracellular accumulation of glutamate resulting in excitotoxicity (Karaszewski et al., 2009; Castillo et al., 2016). Excessive glutamate release also leads to the excessive activation of *N*-methyl-D-aspartic acid receptors (NMDAR), increased the inward flow and overload of deficiency calcium (Ca^{2+}), which trigger mitochondrial damage, and a series of oxidative stress responses (Chan, 2001; Iadecola and Anrather, 2011), which are accompanied by inflammatory cytokine release (Taylor and Sansing, 2013). The acute phase in the week following stroke is characterized by neuronal apoptosis and further activation of immune responses (Anrather and Iadecola, 2016). In the subacute phase, alterations in transcriptional growth factor activity and gene expression can impact synaptic plasticity. Approximately 500 different neuronal genes in the peri-infarct region regulate nerve growth factor expression and cytoskeletal rearrangements (Li et al., 2010), influencing the axonal growth and synapse formation. This alteration in plasticity diminishes when entering into the chronic phase and the reduced strength and transmission efficiency of synaptic connections continuously affects brain function (Joy and Carmichael, 2021). A series of pathological damage of stroke, including increased release of excitatory amino acids, oxidative stress, inflammatory responses, apoptosis, changed neurotrophic factor levels and gene expression influence synaptic plasticity (**Figure 2**), and ultimately participate in the development of PSCI. The specific mechanism is as follows.

2.1. Increased release of excitatory amino acid and synaptic plasticity

Glutamate has complex functions in excitatory neurotransmission; in addition to its role as a neurotransmitter, glutamate regulates neuronal survival, neurite growth, and synaptogenesis (Mattson, 2008). However, disturbed clearance of glutamate in the synaptic cleft results in synaptic dysfunction (Postnikova et al., 2021). Glutamate excitotoxicity triggers excessive activation of CDK5, which increases Ca^{2+} influx in neuronal cells, it will promote dendritic retraction, spine loss, increased endoplasmic reticulum mitochondrial Ca^{2+}, and ultimately neuronal death (Toro-Fernández et al., 2021). These changes manifest clinically as a decline in memory, cognition, and general functioning (McGrath et al., 2022). Moreover, disturbed glutamate system after cerebral ischemia injury, has been indicated to participate in the development of cognitive impairment (Nie and Yang, 2017).

2.2. Oxidative stress and synaptic plasticity

Mitochondria maintain energy supplement to neuronal activity, and play an important role in synaptic plasticity and neurotransmitter synthesis. Because of the high oxygen consumption with restricted antioxidant mechanisms, neurons are vulnerable to oxidative stress, thus, protecting the integrity and survival of neurons from oxidative stress damage is vital (Cenini et al., 2019). Chronic oxidative stress can impact synaptic plasticity in various ways, for example, through the loss of dendritic spines, neurons, or brain repair mechanisms, resulting in the loss of synaptic connections and the ability to process information. Moreover, oxidative stress can also affect gene expression (Bello-Medina et al., 2019). The structure and function of neurons are very sensitive to pathological and physiological changes, and oxidative stress responses and decreased antioxidant capacity can significantly impair learning and memory function by reducing the production of new neurons and altering the structure of dendrites in the hippocampus (Huang et al., 2015).

2.3. Inflammatory response and synaptic plasticity

Homeostatic regulation of synaptic function is the key principle of the nervous system, and molecules associated with inflammatory responses are critical in regulating synaptic plasticity. Cytokines are released by resident myeloid cells to maintain synaptic plasticity. When cytokines release is disordered, neuroinflammation can be triggered which negatively influences the brain networks associated with learning and cognition, contributing to neurodegeneration (Rizzo et al., 2018). Pro-inflammatory cytokines, such as interleukin (IL)–1, and tumor necrosis factor (TNF-α), induce the activation of transcription factor NF-κB and initiate the expression of downstream genes related to inflammation, thus inducing an inflammatory response. These above inflammatory response activates the microglia and astrocytes, can down-regulate synaptic plasticity and synaptic scaling in several core brain areas, such as the cortex, striatum, and hippocampus (Yirmiya and Goshen, 2011; Yang et al., 2013). Evidence indicates that low doses of IL-1 facilitate learning processes, whereas mice with genetic impairments or pharmacological blockade of IL-1 signaling and downregulated levels of IL-1 have decreased cognitive and memory functions (Yirmiya and Goshen, 2011). Likewise, high level of TNF-α impair synaptic plasticity in pyramidal neurons by regulating signaling pathways which are modulated by intracellular Ca^{2+} stores and synaptopodin (Maggio and Vlachos, 2018). The inflammatory response is the main cause of secondary injury after ischemic stroke.

2.4. Apoptosis and synaptic plasticity

Protection from cerebral ischemia-reperfusion injury can be achieved by reducing the apoptosis rate of ischemic and hypoxic brain cells, regulating the plasticity of synaptic structures by inhibiting the activity of neuronal apoptosis-related factors, and promoting neuronal regeneration (Xia and Lin, 2021). The apoptosis activated at the end of the synapse or in the synapses, leads to the local functional and morphological changes of the synapse, and even spreads to the cell body, ultimately resulting in neuronal death. Evidence indicates that the activation of the caspase family at the end of the synapse is used to respond various stimuli (Mattson and Duan, 1999). Caspases have important functions in apoptosis, and inflammation. After activation by B-cell lymphoma 2 (Bcl-2), apoptotic protease activating factor 1 (Apaf-1) regulates

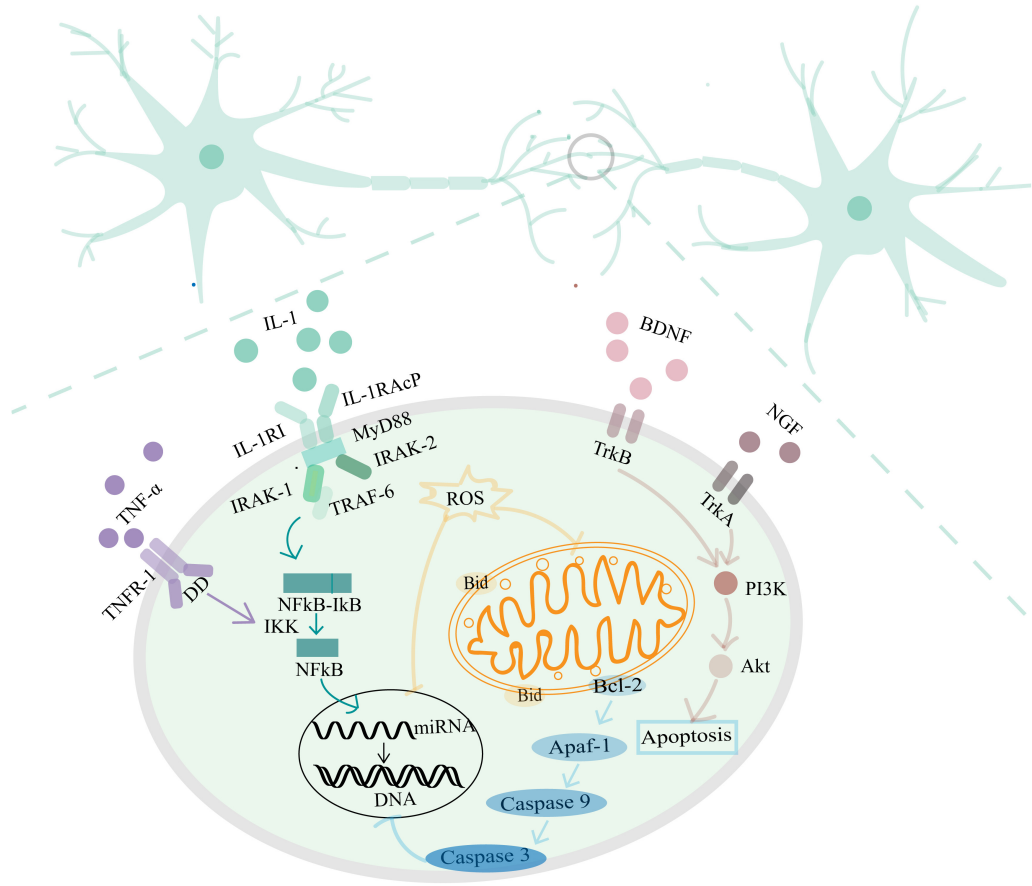

FIGURE 2
The mechanism of the pathological damage of stroke influencing synaptic plasticity.

the level of caspase-3 and caspase-9, resulting in the promotion of apoptosis and even affects DNA expression. Restricted and localized caspase activation within neurons also participates in axon and dendrite pruning, neurite outgrowth, and dendrite branch formation, and LTD (Hollville and Deshmukh, 2018). Finally, the low strength and efficiency of synaptic connections induced by caspase manifests as cognitive impairment.

2.5. Neurotrophic factors and synaptic plasticity

A growing number of publications have focused on the relationship between the expression of neurotrophic factors such as brain-derived neurotrophic factor (BDNF) and the nerve growth factor (NGF) and synaptic plasticity. Expression of BDNF and its receptor tropomyosin-associated kinase B (TrkB) supports the morphology, differentiation and regeneration of neurons, axonal growth, and the functions of synapses after neurological injury (Griesbach et al., 2004). BDNF is the main activity-dependent neurotrophin on which active neuronal organization relies. In a synapse-specific manner, BDNF balances the effects of excitatory and inhibitory transmission (Spedding and Gressens, 2008). NGF and its receptors (P75 and TrkA) can regulate cholinergic neuronal markers, facilitate LTP induction in structural synaptic plasticity, increase neurite outgrowth, and promote synaptic plasticity (Conner et al., 2009). Neurotrophic factors regulate synaptic connections and dendritic morphology, thereby influencing synaptic plasticity and cognitive function.

2.6. Gene expression and synaptic plasticity

The development of synapses and the transmission of synaptic signals are regulated by gene expression, and neuronal genes in the peri-infarct region will influence synaptic plasticity. miRNAs regulate gene expression and interact with 3'-untranslated regions of mRNAs to maintain mRNA stability and promote mRNA translation, thereby regulating synaptic activity, as well as protein synthesis and expression (Hu and Li, 2017). Although the expression of synaptic miRNAs is region-specific, they are core ingredients of dendrites, axons, and dendritic spines and can be detected in synaptoneurosomes (enriched because of dendritic spines), synaptosomes (consisting of axon terminals and adherent postsynaptic densities), and postsynaptic densities (Lugli et al., 2008). Different miRNAs play distinct roles in regulating synaptic plasticity. The inactivation of *Dicer1* in excitatory hippocampal neurons leads to increases in dendritic spine length, neural excitability, and post-tetanic potentiation

(Fiorenza et al., 2016). The knockout of Ncoa3 is accompanied by a reduction in the volume of dendritic spines (Störchel et al., 2015). Substantial evidence indicates that miR-125b, miR-223, miR-137, and miR-146a-5p modulate postsynaptic responses by controlling the abundance of postsynaptic glutamate receptors. Among these, miR-125b controls the expression of the NMDAR subunit GluN2A (Edbauer et al., 2010), whereas miR-223 controls the NMDAR subunit GluN2B and the α-amino-3-hydroxy-5-methyl–4-isoxazole propionic acid receptor (AMPAR) subunit GluA2 (Harraz et al., 2012), miR-137 participates in the decreased expression of the AMPAR subunit GluA1 (Olde Loohuis et al., 2015) and miR146a-5p participates in controlling the number of AMPARs in synapses as well as synaptic transport processes (Chen and Shen, 2013). These miRNAs influence synaptic plasticity, thereby participating in the regulation of cognitive function.

3. Changes of synaptic plasticity in PSCI

Synapses can be regarded as hubs where neurotransmitters are released across the synaptic cleft, and bind to receptors, thereby carrying information from the pre-synaptic neuron to the postsynaptic neuron (Bellot et al., 2014). The strength of synaptic connections and efficiency of synaptic transmission directly affect the processing and storage of information within the central nervous system (Raven et al., 2018).

3.1. Changes of structural synaptic plasticity in PSCI

Alterations in structural synaptic plasticity in the early stage are characterized by the swelling of dendrites and loss of spines (Sigler and Murphy, 2010). The indexes of structural synaptic plasticity such as the dendritic branching, spine density, and mushroom-shaped spines have been confirmed decreased in a mouse model of medial prefrontal cortex ischemia-induced cognitive impairment (Sadigh-Eteghad et al., 2018). With prolonged ischemia duration, clinical evidence indicates that a significant reduction in synaptic density is indicated at 21 ± 8 days after stroke onset (Michiels et al., 2022). Chronic lack of blood supply can also lead to the instantaneous loss of synaptic number (Sigler and Murphy, 2010). The decreased number, density, and distribution of synapses reduce the strength of synaptic connections, which are widely regarded as the basis of learning and memory.

3.2. Changes of functional synaptic plasticity in PSCI

As for the changes of functional synaptic plasticity, on the one hand, postsynaptic depolarization is caused by the voltage-dependent release of magnesium ions, followed by the rapid permeation of Ca^{2+} ions through the NMDAR to activate Ca^{2+}/calmodulin-dependent protein kinase II (CaMKII), resulting in the insertion of AMPARs into the postsynaptic membrane to enhance postsynaptic responses (Malenka and Bear, 2004). The inhibition of ERK and the activation of $GABA_A$ receptor after stroke can reduce the postsynaptic depolarization to decrease hippocampal LTP, thus downregulating the efficacy of synaptic transmission. On the other hand, excessive release of glutamate after stroke finally leads to excessive activation of NMDAR, and then the Ca^{2+} move quickly through the NMDAR. After that the protein phosphatases calcineurin and protein phosphatase 1 are activated and their expression levels are upregulated, resulting in the internalization of AMPARs (Kauer and Malenka, 2007). The above changes are called LTD, which means that the prolonged low-frequency stimulation results in the decrease in synaptic efficiency. The low efficiency of synaptic connections affects the brain's ability to take in and process external information from the outside, eventually manifesting as cognitive impairment.

3.3. Changes of synaptic plasticity-related proteins in PSCI

Synaptic plasticity-related proteins refer to those proteins in axon terminals, pre-synaptic membranes, postsynaptic membranes, and synaptic vesicles, include growth-associated protein 43 (GAP-43), postsynaptic density protein 95 (PSD-95), synaptophysin (SYN) and so on. These proteins not only influence synaptic morphology and structure by participating in synaptogenesis and remodeling, but also participate in the function of inter-synaptic information transfer. Participating in long-term plasticity and memory function, GAP-43, a synaptic protein in growth cones, can be regarded as a marker of axonal growth and of morphologic changes in synapses (Baumgärtel and Mansuy, 2012; Nemes et al., 2017). PSD-95, related to receptors and cytoskeletal elements at synapses, increases the number and size of dendritic spines, enhances the maturation of the pre-synaptic terminal, coordinates synaptic maturation, and stabilizes postsynaptic membranes (El-Husseini et al., 2000). As an abundant phosphoprotein present on the membranes of synaptic vesicles, SYN contributes to the development of synapses and increases neurotransmission and spatial memory (Hao et al., 2017). Levels of synaptic plasticity-related proteins GAP-43, PSD-95, SYN have been confirmed to be decreased in a mouse model of PSCI (Sadigh-Eteghad et al., 2018).

4. Chinese herbal drugs *via* regulating synaptic plasticity to treat PSCI

Because the pathogenesis of PSCI is determined by various factors and their complex interplay, it is necessary to consider developing therapeutic strategies which target the pathological changes of PSCI. Among these, Chinese herbal drugs, as a class of natural medicinal products based on the theory of traditional Chinese medicine, have great potential to improve synaptic plasticity thus improving cognitive function (Bordet et al., 2017). In our previous research, python language data was used to mine the medication rules of Chinese herbal drugs in the treatment of

PSCI and the 38 Chinese herbal drugs that were used more than 10 times were excavated (Shen et al., 2022). After scrutinizing the literature about the mechanism of the above 38 Chinese herbal drugs, we summarized the Chinese herbal drugs that reverse cognitive impairment by improving synaptic plasticity. According to the clinical efficacy of traditional Chinese medicine, we divided twelve Chinese herbal drugs into seven classes:deficiency-tonifying Chinese herbal drugs, blood-activating/stasis-resolving Chinese herbal drugs, sedative Chinese herbal drugs, transforming phlegm and treating cough and asthma Chinese herbal drugs, resuscitation-inducing aromatic Chinese herbal drugs, diaphoretic Chinese herbal drugs and liver-smoothing Chinese herbal drugs. Because of the characteristics of multiple components, the therapeutic mechanisms of in Chinese herbal drugs are complex. The active ingredients of Chinese herbal drugs are not only the material basis of the prescription, but also can be studied to clarify the main mechanism. In order to better elucidate the mechanism and promote the further development and application of the Chinese herbal drugs highlighted above, we have paid particular attention to the active ingredients or extracts.

4.1. Deficiency-tonifying Chinese herbal drugs

Deficiency-tonifying Chinese herbal drugs refer to the drugs that can strengthen the body and improve resistance to disease. The commonly used deficiency-tonifying Chinese herbal drugs in treating PSCI include *Epimedium brevicornum Maxim, Herba Cistanches, Panax ginseng C. A. Mey.,* and *Radix Angelica Sinensis*. The common mechanisms involved are promoting the expression of neurotrophic factors, suppressing oxidative stress, and inhibiting cell apoptosis to regulate synaptic plasticity.

4.1.1. *Epimedium brevicornum Maxim*

The natural medicine *Epimedium brevicornum Maxim* mainly contains flavonoids, polysaccharides lignans, alkaloids, and other active ingredient. Among these, icariin is the most useful and active ingredients, which can alleviate vascular cognitive impairment by regulating expression of neurotrophic factors, preventing oxidative stress, inhibiting neuroinflammatory responses, inhibiting apoptosis of nerve cells, and promoting neuronal regeneration (Jiang and Wu, 2020). Previous research showed that the numbers of neurons in the hippocampal CA1 regions of the icariin medium-dose and high-dose groups were higher than those in the model group, indicating that icariin can alleviate neuronal injury and improve structural synaptic plasticity (He et al., 2022). Furthermore, icariin not only increases the levels of acetylcholine and choline acetyltransferase in central cholinergic neural circuits, but also maintains histone acetylation homeostasis, thereby improving cognitive function (Wang, 2013).

4.1.2. *Herba Cistanches*

In classic works of traditional Chinese medicine, *Herba Cistanches* is commonly considered as an effective ingredient to improve intelligence. Among the various chemical components of *Herba Cistanches*, phenylethanoid glycosides represent the most important identified ingredients to uncover and determine the content of *Herba Cistanches* and to improve cognitive function (Rao et al., 2022). As effective ingredients of phenylethanoid glycosides, verbascoside, and echinacoside play different roles in improving cognition. Verbascoside improves memory impairment by reducing oxidative stress, regulating the mTOR signaling pathway, and inhibiting neuronal cell apoptosis (Li et al., 2019). Echinacoside inhibits the activation of microglia cells and astrocytes, reduces inflammatory responses, and releases anti-inflammatory and neurotrophic factors to enhance memory and learning (Wang et al., 2017; Liang et al., 2019). In addition, echinacoside can inhibit the damage induced by over-release of glutamate by reducing voltage-dependent Ca^{2+} entry and suppressing protein kinase (Lu et al., 2016).

4.1.3. *Panax ginseng C. A. Mey.*

Ginsenoside, consisting of ginsenoside Rg1 and ginsenoside Rd are the main active ingredients in *Panax ginseng C. A. Mey.*, which has a variety of neuroprotective effects and causes cognitive improvement after stroke. After a stroke, ginsenoside Rg1 can reduce the NO activity in neurons (He et al., 2014), and downregulate the expression of aquaporin 4 and protease-activated receptor-1 (Zhou et al., 2014; Xie et al., 2015). Moreover, ginsenoside Rd can inhibit the ASK1-JNK pathway and downregulate the expression of caspase-3 (Wang et al., 2014). These two mechanisms may interplay to reduce the damage to neuronal cells. What's more, ginsenosides can also reduce the damage by free radicals *via* decreased oxidative stress response.

In terms of restoring cognitive function after stroke, accumulating evidence has indicated that Rg1 can also stimulate the differentiation of neural stem cells, increase the secretion of NGF, and induce axonal regeneration (Li et al., 2015). By increasing the expression of vascular endothelial growth factor and BDNF, ginsenoside Rd can activate PI3K-Akt and ERK12 pathways, increase the expression of regulatory transcription factors and genes, and upregulate the expression of GAP-43, thereby improving synaptic plasticity (Liu et al., 2015). Ginsenoside not only plays a role in reducing neuronal cell damage, but also help recover the cognitive function by improving synaptic plasticity.

4.1.4. *Radix Angelica Sinensis*

Radix Angelica Sinensis contains the active ingredient Ligustilide, which promotes recovery from cognitive impairment by alleviating neuronal apoptosis and dendritic injury, increasing BDNF and GABA expression to enhance synaptic efficacy (Feng et al., 2012; Xin et al., 2013).

4.2. Blood-activating/stasis-resolving Chinese herbal drugs

Blood-activating/stasis-resolving Chinese herbal drugs refer to drugs of which the main effects are promoting blood circulation and dissipating blood stasis. Blood-activating/stasis-resolving Chinese herbal drugs include *Ligusticum chuanxiong Hort, Salvia miltiorrhiza Bunge,* and *Carthamus tinctorius L.,* mainly through reducing oxidative stress and inhibiting apoptosis to regulate synaptic plasticity and thereby improve the cognitive function.

4.2.1. *Ligusticum chuanxiong Hort*

The active ingredients of *Ligusticum chuanxiong Hort* include tetramethylpyrazine, ligustilide, ferulic acid, caffeic acid, and chlorogenic acid. Tetramethylpyrazine, one of its effective active ingredients, has antioxidant, anti-inflammatory and anti-apoptotic properties. It can regulate autophagy and prevent mitochondrial damage to maintain the energy supplement of neurons, thus it plays a neuroprotective role and enhance synaptic plasticity to improve cognition function (Lin et al., 2022). Tetramethylpyrazine can reduce the over-activation of microglia and the NF-κB signaling pathway, down-regulate the level of TNF-α, and inhibit caspase-3 expression, thereby preventing neuronal apoptosis and promoting cognitive recovery (Liang et al., 2022; Zhang et al., 2022). In addition, tetramethylpyrazine could increase BDNF levels, regulate the expression of the synapse-associated proteins PSD-95, SYN, GAP-43, and SYP by activating the TrkB/ERK/CREB signaling pathway (Tan et al., 2021), and increases PSD-93 and PSD-95 expression by restoring the normal function of the cAMP/PKA/CREB pathway. Thus, tetramethylpyrazine directly regulates synaptic plasticity to accelerate the recovery of cognitive function (Wu et al., 2013).

Other ingredients of *Ligusticum chuanxiong Hort* also play an important role in the treatment of neurological diseases. For example, ligustilide can prevent oxidative stress, and regulate endoplasmic reticulum stress and autophagy to reduce neurotoxicity, whereas ferulic acid can inhibit microglial activation, prevent oxidative stress, and reverse mitochondrial dysfunction (Zou et al., 2022). Chlorogenic acid can inhibit increases in NO levels, prevent the release of TNF-α, slow down the breakdown of acetylcholine and butyrylcholine in the brain, improve the activity of the mitochondrial complexes I, IV, and V, reduce the mitochondrial glutathione levels, and modulate Ca^{2+} entry into neurons to protect them from glutamate-induced neurotoxicity (Shen et al., 2012; Mikami and Yamazawa, 2015; Singh et al., 2020). Finally, caffeic acid can prevent oxidative neurodegeneration by inhibiting acetylcholinesterase and cholinesterase activities, thereby slowing down the breakdown of acetylcholine and butanylcholine in the brain (Oboh et al., 2013).

4.2.2. *Salvia miltiorrhiza Bunge*

Tanshinone IIA, the most utilized active ingredient of *Salvia miltiorrhiza Bunge,* is regarded as an effective drug candidate with the broad-spectrum potential for the treatment of neuronal damage and cognitive impairment. Tanshinone IIA attenuates neuronal damage by reducing neuroinflammation and oxidative stress, inhibiting cell apoptosis, recovering blood–brain barrier dysfunctions, and even promoting neurogenesis and angiogenesis (Subedi and Gaire, 2021). Moreover, it can attenuate intracellular Ca^{2+} overload induced by excitatory amino acids, and the impairment of LTP (Wang et al., 2011).

4.2.3. *Carthamus tinctorius L.*

Hydroxy saffron yellow A is the main active component of *Carthamus tinctorius L.* and exerts neuroprotective and cognitive regulatory effects (Xing et al., 2016). Hydroxy saffron yellow A can inhibit the release of inflammatory mediators, reduce free radical responses, exert antioxidant effects, and play the anti-apoptotic effects by regulating the PI3K/Akt signaling pathway (Wang et al., 2022). It also regulates hippocampal synaptic plasticity by enhancing the endogenous expression of VEGF, NR1, BDNF, GluN2A, and GluN2B (Zhang et al., 2014), and improving presynaptic neurotransmitter release and postsynaptic AMPA receptor function (Xing et al., 2016). What's more, it can restore the damaged LTP amplitude at CA3-CA1 synapses (Yu et al., 2018).

4.3. Sedative Chinese herbal drugs

4.3.1. *Polygala tenuifolia Willd.*

In *Polygala tenuifolia Willd.*, the main ingredients that play a role in improving cognitive impairment are triterpenoid saponins, and oligosaccharide esters (Hong et al., 2017). As the most utilized ingredient to improve cognitive impairment, tenuigenin inhibits acetylcholinesterase activity to improve the cholinergic system, exerts antioxidant effects by reducing malondialdehyde levels and increasing superoxide dismutase activity, and enhances field excitatory synaptic potential amplitude to improve synaptic plasticity (Huang et al., 2013). DISS and tenuifoliside (A, B, and C), as the active ingredient of oligosaccharide esters, can inhibit NOS hyper-activation, increase CREB phosphorylation, regulate BDNF expression, promote neuronal cell proliferation, and improve synaptic plasticity (Shi et al., 2013).

4.4. Transforming phlegm and treating cough and asthma Chinese herbal drugs

4.4.1. *Ginkgo biloba L.*

The medicinal products derived from the natural medicine *Ginkgo biloba L.* have been widely used to treat neurological diseases. Among them, EGb 761 and ginkgolide have the effect of improving cognitive function. Although it is not a single active ingredient, EGb 761, is the most commonly used extract derived from *Ginkgo biloba L.*, and its main active ingredients are flavonoids (24% flavone glycosides), terpene lactones (6%) terpene lactones, and ginkgolic acid (< 5 ppm) (Nash and Shah, 2015). EGb 761 has been shown to improve mitochondrial function to increase metabolic rates, enhance the connection of neurons in the hippocampus to improve synaptic plasticity, and reduce blood viscosity to ensure the sufficient blood supply to brain regions, thereby alleviating symptoms of cognitive impairment after stroke (Müller et al., 2012).

As an important active ingredient of *Ginkgo biloba L.*, the application of ginkgolide in improving PSCI has attracted increasing attention. Moreover, ginkgolide can reverse oxidative DNA damage in neurons (Hao et al., 2013), promote Bcl-2/Bax expression, which are important oncogenes involved in apoptosis, reduce the expression of activated caspase-3 and decrease intracellular levels of reactive oxygen species, thereby inhibit cell apoptosis and reduce intracellular oxidative stress response (Xia et al., 2014). Ginkgolide could also repair ultrastructure damage of glial cells in the CA1 region of the rat hippocampus, modulate inflammatory responses, support the formation of neurovascular units, nourish neurons and protect synapses (He et al., 2012).

Yinxing Tongzhi tablets are widely used in clinical practice and consist of flavone glycosides and terpene lactones. When combined with western medicine, reports show that Yinxing Tongzhi tablets regulate inflammatory responses by reducing the expression of pro-inflammatory factors such as IL-6 and IL-8, and protect nerve cells by reducing MBP, S100β, and NSE expression (Pan et al., 2018; Yang et al., 2020).

4.5. Resuscitation-inducing aromatic Chinese herbal drugs

4.5.1. *Acorus tatarinowii Schott*

α-asarone and β-asarone are regarded as the main ingredients of *Acorus tatarinowii Schott* that improve cognitive function. α-asarone could restore the metabolic imbalance of free radicals which is closely related to the decline in learning and memory function through reducing the MDA levels in hippocampal brain tissue. Moreover, α-asarone inhibits SOD and NOS activity, downregulates the expression of nNOS proteins, and upregulates nNOS/NO signaling in the hippocampus, thereby increasing synaptic plasticity in the hippocampus (Zhu et al., 2020). Evidence indicates that β-asarone may act *via* the Arc/Arg3.1 and Wnt signaling pathways to regulate synaptogenesis, attenuate the spine density reduction in the hippocampal CA1 region, and increase the expression of the synaptic plasticity-related factor GAP-43 in the hippocampus (Yang et al., 2016; Sun et al., 2020). Furthermore, β-asarone can inhibit phosphorylation of the JNK signaling pathway in hippocampal neurons, upregulate Bcl-2 expression, and downregulate caspase-3 expression, thereby playing an anti-apoptotic role in hippocampal neurons. Using Python software to analyze the prescription of traditional Chinese medicine in the treatment of PSCI, *Acorus tatarinowii Schott* was found to be the most clinically applied natural medicine (Shen et al., 2022).

4.6. Diaphoretic Chinese herbal drugs

4.6.1. *Radix Puerariae*

Puerarin, a major ingredient of *Radix Puerariae,* reduces the brain infarct size after stroke, attenuates apoptosis *via* activation of the PI3K/Akt signaling pathway (Han et al., 2012), abrogates NMDAR expression after stroke and prevents the toxic effect of excitatory amino acids (Zhang et al., 2011). In addition, puerarin can repair neuronal disorders, restore the synaptic microstructure, reduce neuronal oxidative stress (ROS/SOD/MDA) levels, improve endothelial dysfunction, and inhibit apoptosis by upregulating pro-apoptotic factors (Bax) and downregulating anti-apoptotic factors (Bcl-2) (Zhu et al., 2021).

4.7. Liver-smoothing Chinese herbal drugs

4.7.1. *Rhizoma Gastrodiae*

Gastrodin the main active ingredient extracted from *Rhizoma Gastrodiae* has been widely applied in central nervous system disorders, and is a mature, sustainable industrial product used to treat vascular cognitive impairment (Deng et al., 2022). Gastrodin increases the activity of choline acetyltransferase, decreases the activity of acetylcholinesterase and glutamate, and regulates the brain cholinergic system after stroke (Zhang et al., 2008). Gastrodin also exerts antioxidant effects by modulating the total levels of glutathione peroxidase and thiol and attenuates cellular autophagy by inhibiting Ca^{2+}/CaMKII signaling (Li and Zhang, 2015; Chen et al., 2021). In addition, the AMPK/UCP2 signaling pathway is activated by gastrodin to improve mitochondrial structure and energy metabolism to ensure sufficient energy supply for synaptic transmission (Sun et al., 2021). In addition, gastrodin directly affects neuronal cells. On the one hand, it can inhibit apoptosis in hippocampal neurons *via* the Nrf2/Keap1-GPx4 signaling pathway (Li et al., 2022). On the other hand, it can induce neural stem cell differentiation by regulating the cAMP/PKA/CREB signaling pathway (Ma et al., 2020). Furthermore, gastrodin can repair axons in the peripheral nervous system and to promote the growth of functional axons and myelin regeneration, and reconstruct the peripheral neural microvascular network (Deng et al., 2022; Yang et al., 2022).

5. Conclusion

PSCI refers to a disorder of cognitive dysfunction after the occurrence of a stroke and mainly manifests as an impairment in the five core cognitive domains, including executive function, attention, memory, language ability, and visual-spatial ability (Wang et al., 2021). PSCI highlights the potential causal relationship between stroke and cognitive impairment. The pathological damage of stroke including the increased release of excitatory amino acid, oxidative stress, inflammatory responses, apoptosis, changed neurotrophic factor levels and gene expression influence synaptic plasticity. The changes of synaptic plasticity in PSCI include the changes of structural and functional synaptic plasticity. Structural synaptic plasticity highlights the strength of synaptic connections while functional synaptic plasticity refers to the improvement or inhibition of the efficiency of synaptic transmission. What's more, synaptic plasticity-related proteins also reflect the changes of synaptic plasticity. Chinese herbal drugs that integrate their active ingredients or extracts with the mechanism of regulating synaptic plasticity have been proven to play a role in improving cognitive impairment. According to the clinical efficacy in traditional Chinese medicine, the 12 most commonly used Chinese herbal drugs can be divided into seven classes. The above seven classes' drugs both can play anti-oxidative effects to regulate synaptic plasticity. Except for sedative Chinese herbal drugs, the other six classes of drugs can through inhibiting cell apoptosis to regulate synaptic plasticity. Deficiency-tonifying Chinese herbal drugs and sedative Chinese herbal drugs both promote the expression of neurotrophic factors to regulate synaptic plasticity. In addition, *Herba Cistanches, Ligusticum chuanxiong Hort, Salvia miltiorrhiza Bunge and Radix Puerariae* can reduce the damage induced by disturbed glutamate system. *Herba Cistanches, Epimedium brevicornum Maxim, Salvia miltiorrhiza Bunge and Ginkgo biloba L.* regulate inflammatory responses to restore synaptic plasticity,

while *Ginkgo biloba L.* can also reverse DNA damage. In summary, Chinese herbal drugs mainly through anti-oxidative stress effect and inhibition of cell apoptosis to regulate synaptic plasticity thereby treating PSCI, which is consistent with evidence shown in previous studies that oxidative stress and neuronal apoptosis are strongly associated with the development of PSCI (Feng et al., 2013; Zhang et al., 2021). Summarizing the mechanism of Chinese herbal drugs in treating PSCI can guide the selection of drugs and the development the novel formulas.

In this review, we overview the influence of pathological damage of stroke on synaptic plasticity, analyze the important roles of synaptic plasticity changes in PSCI, and summarize those Chinese herbal drugs of which the active ingredient or extracts regulate synaptic plasticity to improve cognitive function. We hope that this review will contribute to the summarize the relationship between PSCI and synaptic plasticity, compile evidence of applying Chinese herbal drugs to treat PSCI, and lay a foundation for the development of novel formulas for treating post-stroke cognitive impairment.

Author contributions

XC conceived and designed the study and drew the figures. LW and HL revised the manuscript. WS and YZ directed the research. All authors contributed to the article and approved the final manuscript.

Funding

This research was supported by the National Natural Science Foundation of China (82205093), Fundamental Research Funds for the Central Public Welfare Research Institutes (ZZ16-YQ-003), Scientific and Technological Innovation Project of China Academy of Chinese Medical Sciences (Nos. CI2021A01310 and CI2021B006), and Innovation Team and Talents Cultivation Program of National Administration of Traditional Chinese Medicine (No. ZYYCXTD-C-202007).

Conflict of interest

The authors declare that the research was conducted in the absence of any commercial or financial relationships that could be construed as a potential conflict of interest.

Publisher's note

References

Anrather, J., and Iadecola, C. (2016). Inflammation and stroke: An overview. *Neurotherapeutics* 13, 661–670. doi: 10.1007/s13311-016-0483-x

Baumgärtel, K., and Mansuy, I. M. (2012). Neural functions of calcineurin in synaptic plasticity and memory. *Learn. Mem.* 19, 375–384. doi: 10.1101/lm.027201.112

Bello-Medina, P. C., Rodríguez-Martínez, E., Prado-Alcalá, R. A., and Rivas-Arancibia, S. (2019). Ozone pollution, oxidative stress, synaptic plasticity, and neurodegeneration. *Neurologia* 37, 277–286. doi: 10.1016/j.nrl.2018.10.003

Bellot, A., Guivernau, B., Tajes, M., Bosch-Morató, M., Valls-Comamala, V., and Muñoz, F. J. (2014). The structure and function of actin cytoskeleton in mature glutamatergic dendritic spines. *Brain Res.* 1573, 1–16. doi: 10.1016/j.brainres.2014.05.024

Berkovich, R., and Weiner, L. P. (2015). Effects of dimethyl fumarate on lymphocyte subsets. *Mult. Scler. Relat. Disord.* 4, 339–341. doi: 10.1016/j.msard.2015.06.002

Bordet, R., Ihl, R., Korczyn, A. D., Lanza, G., Jansa, J., Hoerr, R., et al. (2017). Towards the concept of disease-modifier in post-stroke or vascular cognitive impairment: A consensus report. *BMC Med.* 15:107. doi: 10.1186/s12916-017-0869-6

Castillo, J., Loza, M. I., Mirelman, D., Brea, J., Blanco, M., Sobrino, T., et al. (2016). A novel mechanism of neuroprotection: Blood glutamate grabber. *J. Cereb. Blood Flow Metab.* 36, 292–301. doi: 10.1177/0271678x15606721

Cenini, G., Lloret, A., and Cascella, R. (2019). Oxidative stress in neurodegenerative diseases: From a mitochondrial point of view. *Oxid. Med. Cell Longev.* 2019:2105607. doi: 10.1155/2019/2105607

Chan, P. H. (2001). Reactive oxygen radicals in signaling and damage in the ischemic brain. *J. Cereb. Blood Flow Metab.* 21, 2–14. doi: 10.1097/00004647-200101000-00002

Chen, T. T., Zhou, X., Xu, Y. N., Li, Y., Wu, X. Y., Xiang, Q., et al. (2021). Gastrodin ameliorates learning and memory impairment in rats with vascular dementia by promoting autophagy flux via inhibition of the Ca(2+)/CaMKII signal pathway. *Aging* 13, 9542–9565. doi: 10.18632/aging.202667

Chen, Y. L., and Shen, C. K. (2013). Modulation of mGluR-dependent MAP1B translation and AMPA receptor endocytosis by microRNA miR-146a-5p. *J. Neurosci.* 33, 9013–9020. doi: 10.1523/jneurosci.5210-12.2013

Conner, J. M., Franks, K. M., Titterness, A. K., Russell, K., Merrill, D. A., Christie, B. R., et al. (2009). NGF is essential for hippocampal plasticity and learning. *J. Neurosci.* 29, 10883–10889. doi: 10.1523/jneurosci.2594-09.2009

Deng, C., Chen, H., Meng, Z., and Meng, S. (2022). Gastrodin and vascular dementia: Advances and current perspectives. *Evid. Based Complement. Alternat. Med.* 2022:2563934. doi: 10.1155/2022/2563934

Edbauer, D., Neilson, J. R., Foster, K. A., Wang, C. F., Seeburg, D. P., Batterton, M. N., et al. (2010). Regulation of synaptic structure and function by FMRP-associated microRNAs miR-125b and miR-132. *Neuron* 65, 373–384. doi: 10.1016/j.neuron.2010.01.005

El-Husseini, A. E., Schnell, E., Chetkovich, D. M., Nicoll, R. A., and Bredt, D. S. (2000). PSD-95 involvement in maturation of excitatory synapses. *Science* 290, 1364–1368.

Feng, X., Yang, S., Liu, J., Huang, J., Peng, J., Lin, J., et al. (2013). Electroacupuncture ameliorates cognitive impairment through inhibition of NF-κB-mediated neuronal cell apoptosis in cerebral ischemia-reperfusion injured rats. *Mol. Med. Rep.* 7, 1516–1522. doi: 10.3892/mmr.2013.1392

Feng, Z., Lu, Y., Wu, X., Zhao, P., Li, J., Peng, B., et al. (2012). Ligustilide alleviates brain damage and improves cognitive function in rats of chronic cerebral hypoperfusion. *J. Ethnopharmacol.* 144, 313–321. doi: 10.1016/j.jep.2012.09.014

Fiorenza, A., Lopez-Atalaya, J. P., Rovira, V., Scandaglia, M., Geijo-Barrientos, E., and Barco, A. (2016). Blocking miRNA biogenesis in adult forebrain neurons enhances seizure susceptibility, fear memory, and food intake by increasing neuronal responsiveness. *Cereb. Cortex* 26, 1619–1633. doi: 10.1093/cercor/bhu332

Gorelick, P. B., Scuteri, A., Black, S. E., Decarli, C., Greenberg, S. M., Iadecola, C., et al. (2011). Vascular contributions to cognitive impairment and dementia: A statement for healthcare professionals from the american heart association/american stroke association. *Stroke* 42, 2672–2713. doi: 10.1161/STR.0b013e3182299496

Griesbach, G. S., Hovda, D. A., Molteni, R., Wu, A., and Gomez-Pinilla, F. (2004). Voluntary exercise following traumatic brain injury: Brain-derived neurotrophic factor upregulation and recovery of function. *Neuroscience* 125, 129–139. doi: 10.1016/j.neuroscience.2004.01.030

Han, J. Q., Yu, K. Y., and He, M. (2012). Effects of puerarin on the neurocyte apoptosis and p-Akt (Ser473) expressions in rats with cerebral ischemia/reperfusion injury. *Zhongguo Zhong Xi Yi Jie He Za Zhi* 32, 1069–1072.

Hao, C. Z., Wang, J., and Liao, W. J. (2017). The influence of"preservation from both physique and spirit"on cognitive function, SYN, MAP-2 and pyramidal cells in rats. *Chin. J. Rehabil. Med.* 32, 384–390.

Hao, L., Ren, X. H., Zhao, Y., Xia, C. Y., Guo, C. X., Wang, Y. C., et al. (2013). The effects of Ginkgo Biloba Extract on anti oxidantive DNA damaging and delaying telomere shortening in prefrontal cortex of natural aging rats and its mechanisms. *Pharmacol. Clin. Chin. Mater. Med.* 29, 38–42. doi: 10.13412/j.cnki.zyyl.2013.06.013

Harraz, M. M., Eacker, S. M., Wang, X., Dawson, T. M., and Dawson, V. L. (2012). MicroRNA-223 is neuroprotective by targeting glutamate receptors. *Proc. Natl. Acad. Sci. U. S. A.* 109, 18962–18967. doi: 10.1073/pnas.1121288109

He, G. Y., Zhang, Z. X., Xu, Y., Dong, X. W., and Wang, X. Y. (2012). Effects of Ginkgo biloba extract 50 on inflammatory cytokines and glia cell ultrastructures in the prefrontal cortex and hippocampus of aging rat. *Chin. J. Integr. Trad. Western Med.* 32, 1064–1068.

He, L. J., Yang, B. B., Zhuo, S., Gu, C. Z., Ding, W., Liu, D. Q., et al. (2022). Mechanism of icariin ameliorating neuronal and dendritic damage in ad by regulating RhoA/ROCK signaling pathway. *Chin. J. Exp. Trad. Med. Form.* 28, 90–97. doi: 10.13422/j.cnki.syfjx.20221943

He, Q., Sun, J., Wang, Q., Wang, W., and He, B. (2014). Neuroprotective effects of ginsenoside Rg1 against oxygen-glucose deprivation in cultured hippocampal neurons. *J. Chin. Med. Assoc.* 77, 142–149. doi: 10.1016/j.jcma.2014.01.001

Hollville, E., and Deshmukh, M. (2018). Physiological functions of non-apoptotic caspase activity in the nervous system. *Semin. Cell. Dev. Biol.* 82, 127–136. doi: 10.1016/j.semcdb.2017.11.037

Hong, F., Wang, L., Wu, S. L., Tang, H. C., Sha, O., Wai, M. S. M., et al. (2017). A review of three commonly used herbs which enhance memory and new evidences which show their combination could improve memory in young animals. *Mini Rev. Med. Chem.* 17, 1537–1547. doi: 10.2174/1389557516666160919164352

Hou, X., Xu, H., Chen, W., Zhang, N., Zhao, Z., Fang, X., et al. (2020). Neuroprotective effect of dimethyl fumarate on cognitive impairment induced by ischemic stroke. *Ann. Transl. Med.* 8:375. doi: 10.21037/atm.2020.02.10

Hu, Z., and Li, Z. (2017). miRNAs in synapse development and synaptic plasticity. *Curr. Opin. Neurobiol.* 45, 24–31. doi: 10.1016/j.conb.2017.02.014

Huang, J. N., Wang, C. Y., Wang, X. L., Wu, B. Z., Gu, X. Y., Liu, W. X., et al. (2013). Tenuigenin treatment improves behavioral Y-maze learning by enhancing synaptic plasticity in mice. *Behav. Brain Res.* 246, 111–115. doi: 10.1016/j.bbr.2013.03.001

Huang, T. T., Leu, D., and Zou, Y. (2015). Oxidative stress and redox regulation on hippocampal-dependent cognitive functions. *Arch. Biochem. Biophys.* 576, 2–7. doi: 10.1016/j.abb.2015.03.014

Iadecola, C., and Anrather, J. (2011). The immunology of stroke: From mechanisms to translation. *Nat. Med.* 17, 796–808. doi: 10.1038/nm.2399

Jiang, Y. W., and Wu, M. H. (2020). Research progress on the mechanism of icariin regulating vascular cognitive impairment. *Jiangsu J. Trad. Chin. Med.* 52, 85–89.

Joy, M. T., and Carmichael, S. T. (2021). Encouraging an excitable brain state: Mechanisms of brain repair in stroke. *Nat. Rev. Neurosci.* 22, 38–53. doi: 10.1038/s41583-020-00396-7

Karaszewski, B., Wardlaw, J. M., Marshall, I., Cvoro, V., Wartolowska, K., Haga, K., et al. (2009). Early brain temperature elevation and anaerobic metabolism in human acute ischaemic stroke. *Brain* 132, 955–964. doi: 10.1093/brain/awp010

Kauer, J. A., and Malenka, R. C. (2007). Synaptic plasticity and addiction. *Nat. Rev. Neurosci.* 8, 844–858. doi: 10.1038/nrn2234

Li, M., Zhu, Y., Li, J., Chen, L., Tao, W., Li, X., et al. (2019). Effect and mechanism of verbascoside on hypoxic memory injury in plateau. *Phytother. Res.* 33, 2692–2701. doi: 10.1002/ptr.6443

Li, S., Overman, J. J., Katsman, D., Kozlov, S. V., Donnelly, C. J., Twiss, J. L., et al. (2010). An age-related sprouting transcriptome provides molecular control of axonal sprouting after stroke. *Nat. Neurosci.* 13, 1496–1504. doi: 10.1038/nn.2674

Li, Y. B., Wang, Y., Tang, J. P., Chen, D., and Wang, S. L. (2015). Neuroprotective effects of ginsenoside Rg1-induced neural stem cell transplantation on hypoxic-ischemic encephalopathy. *Neural Regen. Res.* 10, 753–759. doi: 10.4103/1673-5374.156971

Li, Y., and Zhang, Z. (2015). Gastrodin improves cognitive dysfunction and decreases oxidative stress in vascular dementia rats induced by chronic ischemia. *Int. J. Clin. Exp. Pathol.* 8, 14099–14109.

Li, Y., Zhang, E., Yang, H., Chen, Y., Tao, L., Xu, Y., et al. (2022). Gastrodin ameliorates cognitive dysfunction in vascular dementia rats by suppressing ferroptosis via the regulation of the Nrf2/Keap1-GPx4 signaling pathway. *Molecules* 27:6311. doi: 10.3390/molecules27196311

Liang, B., Zhao, K., Ma, X. D., and Li, J. (2022). Experimental study on anti-apoptotic effect and mechanism of ligustrazine on neurons of cerebral ischemia -reperfusion injury rats. *Chin. Arch. Trad. Chin. Med.* 40, 205–209. doi: 10.13193/j.issn.1673-7717.2022.06.047

Liang, Y., Chen, C., Xia, B., Wu, W., Tang, J., Chen, Q., et al. (2019). Neuroprotective effect of echinacoside in subacute mouse model of Parkinson's disease. *Biomed. Res. Int.* 2019:4379639. doi: 10.1155/2019/4379639

Lin, J., Wang, Q., Zhou, S., Xu, S., and Yao, K. (2022). Tetramethylpyrazine: A review on its mechanisms and functions. *Biomed. Pharmacother.* 150:113005. doi: 10.1016/j.biopha.2022.113005

Liu, H. H., Yuan, J., Su, K. Q., Li, R. Q., and Feng, X. D. (2021). Research progress on the relationship between synaptic plasticity and cognitive impairment. *J. Apoplexy Nervous Dis.* 38, 753–755. doi: 10.19845/j.cnki.zfysjjbzz.2021.0203

Liu, X. Y., Zhou, X. Y., Hou, J. C., Zhu, H., Wang, Z., Liu, J. X., et al. (2015). Ginsenoside Rd promotes neurogenesis in rat brain after transient focal cerebral ischemia via activation of PI3K/Akt pathway. *Acta Pharmacol. Sin.* 36, 421–428. doi: 10.1038/aps.2014.156

Lo, J. W., Crawford, J. D., Desmond, D. W., Godefroy, O., Jokinen, H., Mahinrad, S., et al. (2019). Profile of and risk factors for poststroke cognitive impairment in diverse ethnoregional groups. *Neurology* 93, e2257–e2271. doi: 10.1212/wnl.0000000000008612

Lu, C. W., Lin, T. Y., Huang, S. K., and Wang, S. J. (2016). Echinacoside inhibits glutamate release by suppressing voltage-dependent Ca(2+) entry and protein kinase c in rat cerebrocortical nerve terminals. *Int. J. Mol. Sci.* 17:1006. doi: 10.3390/ijms17071006

Lugli, G., Torvik, V. I., Larson, J., and Smalheiser, N. R. (2008). Expression of microRNAs and their precursors in synaptic fractions of adult mouse forebrain. *J. Neurochem.* 106, 650–661. doi: 10.1111/j.1471-4159.2008.05413.x

Ma, C. L., Li, L., Yang, G. M., Zhang, Z. B., Zhao, Y. N., Zeng, X. F., et al. (2020). Neuroprotective effect of gastrodin in methamphetamine-induced apoptosis through regulating cAMP/PKA/CREB pathway in cortical neuron. *Hum. Exp. Toxicol.* 39, 1118–1129. doi: 10.1177/0960327120911438

Maggio, N., and Vlachos, A. (2018). Tumor necrosis factor (TNF) modulates synaptic plasticity in a concentration-dependent manner through intracellular calcium stores. *J. Mol. Med.* 96, 1039–1047. doi: 10.1007/s00109-018-1674-1

Malenka, R. C., and Bear, M. F. (2004). LTP and LTD: An embarrassment of riches. *Neuron* 44, 5–21. doi: 10.1016/j.neuron.2004.09.012

Mateos-Aparicio, P., and Rodríguez-Moreno, A. (2020). Calcium dynamics and synaptic plasticity. *Adv. Exp. Med. Biol.* 1131, 965–984. doi: 10.1007/978-3-030-12457-1_38

Mattson, M. P. (2008). Glutamate and neurotrophic factors in neuronal plasticity and disease. *Ann. N. Y. Acad. Sci.* 1144, 97–112. doi: 10.1196/annals.1418.005

Mattson, M. P., and Duan, W. (1999). "Apoptotic" biochemical cascades in synaptic compartments: Roles in adaptive plasticity and neurodegenerative disorders. *J. Neurosci. Res.* 58, 152–166.

McGrath, T., Baskerville, R., Rogero, M., and Castell, L. (2022). Emerging evidence for the widespread role of glutamatergic dysfunction in neuropsychiatric diseases. *Nutrients* 14:917. doi: 10.3390/nu14050917

Michiels, L., Mertens, N., Thijs, L., Radwan, A., Sunaert, S., Vandenbulcke, M., et al. (2022). Changes in synaptic density in the subacute phase after ischemic stroke: A (11)C-UCB-J PET/MR study. *J. Cereb. Blood Flow Metab.* 42, 303–314. doi: 10.1177/0271678x211047759

Mijajlović, M. D., Pavlović, A., Brainin, M., Heiss, W. D., Quinn, T. J., Ihle-Hansen, H. B., et al. (2017). Post-stroke dementia - a comprehensive review. *BMC Med.* 15:11. doi: 10.1186/s12916-017-0779-7

Mikami, Y., and Yamazawa, T. (2015). Chlorogenic acid, a polyphenol in coffee, protects neurons against glutamate neurotoxicity. *Life Sci.* 139, 69–74. doi: 10.1016/j.lfs.2015.08.005

Mok, V. C., Lam, B. Y., Wong, A., Ko, H., Markus, H. S., and Wong, L. K. (2017). Early-onset and delayed-onset poststroke dementia - revisiting the mechanisms. *Nat. Rev. Neurol.* 13, 148–159. doi: 10.1038/nrneurol.2017.16

Müller, W. E., Heiser, J., and Leuner, K. (2012). Effects of the standardized Ginkgo biloba extract EGb 761§on neuroplasticity. *Int. Psychogeriatr.* 24, S21–S24. doi: 10.1017/s1041610212000592

Nash, K. M., and Shah, Z. A. (2015). Current perspectives on the beneficial role of ginkgo biloba in neurological and cerebrovascular disorders. *Integr. Med. Insights* 10, 1–9. doi: 10.4137/imi.S25054

Nemes, A. D., Ayasoufi, K., Ying, Z., Zhou, Q. G., Suh, H., and Najm, I. M. (2017). Growth associated protein 43 (GAP-43) as a novel target for the diagnosis, treatment and prevention of epileptogenesis. *Sci. Rep.* 7:17702. doi: 10.1038/s41598-017-17377-z

Nie, J., and Yang, X. (2017). Modulation of synaptic plasticity by exercise training as a basis for ischemic stroke rehabilitation. *Cell Mol. Neurobiol.* 37, 5–16. doi: 10.1007/s10571-016-0348-1

Oboh, G., Agunloye, O. M., Akinyemi, A. J., Ademiluyi, A. O., and Adefegha, S. A. (2013). Comparative study on the inhibitory effect of caffeic and chlorogenic acids on key enzymes linked to Alzheimer's disease and some pro-oxidant induced oxidative stress in rats' brain-in vitro. *Neurochem. Res.* 38, 413–419. doi: 10.1007/s11064-012-0935-6

Olde Loohuis, N. F., Ba, W., Stoerchel, P. H., Kos, A., Jager, A., Schratt, G., et al. (2015). MicroRNA-137 controls AMPA-receptor-mediated transmission and mGluR-dependent LTD. *Cell Rep.* 11, 1876–1884. doi: 10.1016/j.celrep.2015.05.040

Pan, W., Zhu, W., Gao, Q., Liao, W., Gao, P., and Liu, T. (2018). Effect of Yin-Xing-Tong-Zhi Tablets on improving vascular cognitive impairment no dementia. *Evid. Based Complement. Alternat. Med.* 2018:6184260. doi: 10.1155/2018/6184260

Postnikova, T. Y., Malkin, S. L., Zakharova, M. V., Smolensky, I. V., Zubareva, O. E., and Zaitsev, A. V. (2021). Ceftriaxone treatment weakens long-term synaptic potentiation in the hippocampus of young rats. *Int. J. Mol. Sci.* 22:8417. doi: 10.3390/ijms22168417

Rao, Z. H., Yang, W. M., Li, X., Huang, P., Hu, Y., Hao, W. J., et al. (2022). Study on the drug components and action mechanism of Cistanche for improving cognitive function. *Chin. J. Ethnomed. Ethnopharm.* 31, 56–60.

Raven, F., Van der Zee, E. A., Meerlo, P., and Havekes, R. (2018). The role of sleep in regulating structural plasticity and synaptic strength: Implications for memory and cognitive function. *Sleep Med. Rev.* 39, 3–11. doi: 10.1016/j.smrv.2017.05.002

Rizzo, F. R., Musella, A., De Vito, F., Fresegna, D., Bullitta, S., Vanni, V., et al. (2018). Tumor Necrosis Factor and Interleukin-1β Modulate Synaptic Plasticity during Neuroinflammation. *Neural Plast.* 2018:8430123. doi: 10.1155/2018/8430123

Rost, N. S., Brodtmann, A., Pase, M. P., van Veluw, S. J., Biffi, A., Duering, M., et al. (2022). Post-stroke cognitive impairment and dementia. *Circ. Res.* 130, 1252–1271. doi: 10.1161/circresaha.122.319951

Sadigh-Eteghad, S., Geranmayeh, M. H., Majdi, A., Salehpour, F., Mahmoudi, J., and Farhoudi, M. (2018). Intranasal cerebrolysin improves cognitive function and structural synaptic plasticity in photothrombotic mouse model of medial prefrontal cortex ischemia. *Neuropeptides* 71, 61–69. doi: 10.1016/j.npep.2018.07.002

Shen, W., Fan, X., Wang, L., and Zhang, Y. (2022). Analysis on medication rules of traditional Chinese medicine in treatment of post stroke cognitive impairment based on Python language. *Chin. Trad. Herbal Drugs* 53, 3093–3102.

Shen, W., Qi, R., Zhang, J., Wang, Z., Wang, H., Hu, C., et al. (2012). Chlorogenic acid inhibits LPS-induced microglial activation and improves survival of dopaminergic neurons. *Brain Res. Bull.* 88, 487–494. doi: 10.1016/j.brainresbull.2012.04.010

Shi, T., Li, Y., Jiang, Y., and Tu, P. (2013). Isolation of flavonoids from the aerial parts of *Polygala tenuifolia* willd. and their antioxidant activities. *J. Chin. Pharm. Sci.* 22, 36–39.

Sigler, A., and Murphy, T. H. (2010). In vivo 2-photon imaging of fine structure in the rodent brain: Before, during, and after stroke. *Stroke* 41, S117–S123. doi: 10.1161/strokeaha.110.594648

Singh, S. S., Rai, S. N., Birla, H., Zahra, W., Rathore, A. S., Dilnashin, H., et al. (2020). Neuroprotective effect of chlorogenic acid on mitochondrial dysfunction-mediated apoptotic death of Da neurons in a parkinsonian mouse model. *Oxid. Med. Cell Longev.* 2020:6571484. doi: 10.1155/2020/6571484

Spedding, M., and Gressens, P. (2008). Neurotrophins and cytokines in neuronal plasticity. *Novartis Found Symp.* 289, 222–233. doi: 10.1002/9780470751251.ch18

Störchel, P. H., Thümmler, J., Siegel, G., Aksoy-Aksel, A., Zampa, F., Sumer, S., et al. (2015). A large-scale functional screen identifies Nova1 and Ncoa3 as regulators of neuronal miRNA function. *EMBO J.* 34, 2237–2254. doi: 10.15252/embj.201490643

Subedi, L., and Gaire, B. P. (2021). Tanshinone IIA: A phytochemical as a promising drug candidate for neurodegenerative diseases. *Pharmacol. Res.* 169:105661. doi: 10.1016/j.phrs.2021.105661

Sun, C., Liu, M., Liu, J., Zhang, T., Zhang, L., Li, H., et al. (2021). Shenmayizhi decoction improves the mitochondrial structure in the brain and ameliorates cognitive impairment in VCI Rats via the AMPK/UCP2 signaling pathway. *Neuropsychiatr. Dis. Treat.* 17, 1937–1951. doi: 10.2147/ndt.S302355

Sun, X. X., Wang, N. N., Li, L., and Rong, H. (2020). Effects of active ingredients of *Acorus tatarindii* on GAP-43 expression in APP/PS1 double transgenic mice. *Med. Innov. China* 17, 21–25.

Tan, Z., Qiu, J., Zhang, Y., Yang, Q., Yin, X., Li, J., et al. (2021). Tetramethylpyrazine alleviates behavioral and psychological symptoms of dementia through facilitating hippocampal synaptic plasticity in rats with chronic cerebral hypoperfusion. *Front. Neurosci.* 15:646537. doi: 10.3389/fnins.2021.646537

Taylor, R. A., and Sansing, L. H. (2013). Microglial responses after ischemic stroke and intracerebral hemorrhage. *Clin. Dev. Immunol.* 2013:746068. doi: 10.1155/2013/746068

Toro-Fernández, L. F., Zuluaga-Monares, J. C., Saldarriaga-Cartagena, A. M., Cardona-Gómez, G. P., and Posada-Duque, R. (2021). Targeting CDK5 in astrocytes promotes calcium homeostasis under excitotoxic conditions. *Front. Cell. Neurosci.* 15:643717. doi: 10.3389/fncel.2021.643717

Wang, B., Zhu, Q., Man, X., Guo, L., and Hao, L. (2014). Ginsenoside Rd inhibits apoptosis following spinal cord ischemia/reperfusion injury. *Neural Regen. Res.* 9, 1678–1687. doi: 10.4103/1673-5374.141802

Wang, J., Chen, L., Li, H., and Yi, X. (2022). Research progress in protective mechanism of hydroxysafflor yellow A against ischemia-reperfusion injury. *Med. Recapitulate* 28, 2739–2745.

Wang, K., Dong, Q., Yu, J. T., and Hu, P. P. (2021). Expert consensus on the management of cognitive impairment after stroke 2021. *Chin. J. Stroke* 16, 376–389.

Wang, N., Ji, S., Zhang, H., Mei, S., Qiao, L., and Jin, X. (2017). Herba cistanches: Anti-aging. *Aging Dis.* 8, 740–759. doi: 10.14336/ad.2017.0720

Wang, W., Zheng, L. L., Wang, F., Hu, Z. L., Wu, W. N., Gu, J., et al. (2011). Tanshinone IIA attenuates neuronal damage and the impairment of long-term potentiation induced by hydrogen peroxide. *J. Ethnopharmacol.* 134, 147–155. doi: 10.1016/j.jep.2010.11.069

Wang, X. (2013). *Research about icariin improving post-stroke cognition of mice by regulating histone acetylation homestasis of cholinergic circuits*. Ph.D thesis. Nanjing: Nanjing University of Chinese Medicine.

Whyte, E. M., Lenze, E. J., Butters, M., Skidmore, E., Koenig, K., Dew, M. A., et al. (2008). An open-label pilot study of acetylcholinesterase inhibitors to promote functional recovery in elderly cognitively impaired stroke patients. *Cerebrovasc. Dis.* 26, 317–321. doi: 10.1159/000149580

Wu, W., Yu, X., Luo, X. P., Yang, S. H., and Zheng, D. (2013). Tetramethylpyrazine protects against scopolamine-induced memory impairments in rats by reversing the cAMP/PKA/CREB pathway. *Behav. Brain Res.* 253, 212–216. doi: 10.1016/j.bbr.2013.07.052

Xia, C. Y., Zhao, Y., Xu, Y., Dong, X. W., Hao, L., Gao, Q., et al. (2014). Ginkgo biloba Extract 50 inhibit beta-amyloid-induced apoptosis in hippocampal neurons. *China J. Trad. Chin. Med. Pharm.* 29, 2030–2034.

Xia, J. Y., and Lin, R. H. (2021). Research progress of acupuncture based on synaptic plasticity in the treatment of cognitive impairment after stroke. *J. Guangdong Pharm. Univ.* 37, 146–150. doi: 10.16809/j.cnki.2096-3653.2021071406

Xie, C. L., Li, J. H., Wang, W. W., Zheng, G. Q., and Wang, L. X. (2015). Neuroprotective effect of ginsenoside-Rg1 on cerebral ischemia/reperfusion injury in rats by downregulating protease-activated receptor-1 expression. *Life Sci.* 121, 145–151. doi: 10.1016/j.lfs.2014.12.002

Xin, J., Zhang, J., Yang, Y., Deng, M., and Xie, X. (2013). Radix *Angelica sinensis* that contains the component Z-ligustilide promotes adult neurogenesis to mediate recovery from cognitive impairment. *Curr. Neurovasc. Res.* 10, 304–315. doi: 10.2174/15672026113109990023

Xing, M., Sun, Q., Wang, Y., Cheng, Y., and Zhang, N. (2016). Hydroxysafflor yellow A increases BDNF and NMDARs in the hippocampus in a vascular dementia rat model. *Brain Res.* 1642, 419–425. doi: 10.1016/j.brainres.2016.04.030

Yang, G., Parkhurst, C. N., Hayes, S., and Gan, W. B. (2013). Peripheral elevation of TNF-α leads to early synaptic abnormalities in the mouse somatosensory cortex in experimental autoimmune encephalomyelitis. *Proc. Natl. Acad. Sci. U S A.* 110, 10306–10311. doi: 10.1073/pnas.1222895110

Yang, H., Li, Q., Li, L., Chen, S., Zhao, Y., Hu, Y., et al. (2022). Gastrodin modified polyurethane conduit promotes nerve repair via optimizing Schwann cells function. *Bioact. Mater.* 8, 355–367. doi: 10.1016/j.bioactmat.2021.06.020

Yang, Q. Q., Xue, W. Z., Zou, R. X., Xu, Y., Du, Y., Wang, S., et al. (2016). β-Asarone rescues Pb-induced impairments of spatial memory and synaptogenesis in rats. *PLoS One* 11:e0167401. doi: 10.1371/journal.pone.0167401

Yang, X., Fan, X., and Yang, X. (2020). Clinical study on Yinxing Tongzhi tablets combined with butylphthalide soft capsules in treatment of vascular mild cognitive impairment. *Drugs Clin.* 35, 1089–1092.

Yirmiya, R., and Goshen, I. (2011). Immune modulation of learning, memory, neural plasticity and neurogenesis. *Brain Behav. Immun.* 25, 181–213. doi: 10.1016/j.bbi.2010.10.015

Yu, L., Duan, Y., Zhao, Z., He, W., Xia, M., Zhang, Q., et al. (2018). Hydroxysafflor yellow A (HSYA) improves learning and memory in cerebral ischemia reperfusion-injured rats via recovering synaptic plasticity in the hippocampus. *Front. Cell. Neurosci.* 12:371. doi: 10.3389/fncel.2018.00371

Zhang, L., Gong, X., Hu, M., Li, Y., Ji, H., and Liu, G. (2008). Anti-vascular dementia effect of gastrodin and its mechanism of action. *Chin. J. Nat. Med.* 6, 130–134.

Zhang, N., Xing, M., Wang, Y., Liang, H., Yang, Z., Shi, F., et al. (2014). Hydroxysafflor yellow A improves learning and memory in a rat model of vascular dementia by increasing VEGF and NR1 in the hippocampus. *Neurosci. Bull.* 30, 417–424. doi: 10.1007/s12264-013-1375-2

Zhang, R., Guo, H. N., Wu, H. Q., Cheng, H. X., and Wang, H. Q. (2011). Effect of puerarin on the expression of NMDA receptor in the hippocampus CA1 region after focal cerebral ischemia in rats. *Sichuan Da Xue Xue Bao Yi Xue Ban* 42, 52–55.

Zhang, X. Y., Ye, H. X., Zheng, Y. J., and Hu, Y. L. (2022). Effects of tetramethylpyrazine on cognitive function and neuroinflammation in lipopolysaccharide-induced mouse model of dementia. *Pharmacol. Clin. Chin. Mater. Med.* 38, 96–101. doi: 10.13412/j.cnki.zyyl.2022.04.007

Zhang, X., and Bi, X. (2020). Post-stroke cognitive impairment: A review focusing on molecular biomarkers. *J. Mol. Neurosci.* 70, 1244–1254. doi: 10.1007/s12031-020-01533-8

Zhang, X., Yuan, M., Yang, S., Chen, X., Wu, J., Wen, M., et al. (2021). Enriched environment improves post-stroke cognitive impairment and inhibits

neuroinflammation and oxidative stress by activating Nrf2-ARE pathway. *Int. J. Neurosci.* 131, 641–649. doi: 10.1080/00207454.2020.1797722

Zhou, Y., Li, H. Q., Lu, L., Fu, D. L., Liu, A. J., Li, J. H., et al. (2014). Ginsenoside Rg1 provides neuroprotection against blood brain barrier disruption and neurological injury in a rat model of cerebral ischemia/reperfusion through downregulation of aquaporin 4 expression. *Phytomedicine* 21, 998–1003. doi: 10.1016/j.phymed.2013.12.005

Zhu, M. J., Mao, Z. H., Guo, H. Y., Zhu, H. Z., and Ding, X. M. (2020). Effects of *Acorus tatarinowii* Schott and alpha asarone on free radicals and nNOS /NO in hippocampus of rats with fatigue movement. *Chin. J. Appl. Physiol.* 36, 306–311. doi: 10.12047/j.cjap.5947.2020.066

Zhu, T., Zhu, M., Qiu, Y., Wu, Z., Huang, N., Wan, G., et al. (2021). Puerarin alleviates vascular cognitive impairment in vascular dementia rats. *Front. Behav. Neurosci.* 15:717008. doi: 10.3389/fnbeh.2021.717008

Zou, M., Xu, S. J., and Dai, Y. (2022). Pharmacological research progress of active ingredients of lligusticum chuanxiong hort for improving neurodegenerative diseases. *Glob. Trad. Chin. Med.* 15, 1497–1502.

frontiers | Frontiers in Neuroscience

TYPE Mini Review
PUBLISHED 07 March 2023
DOI 10.3389/fnins.2023.1158204

OPEN ACCESS

EDITED BY
Jianxun Liu,
Xiyuan Hospital, China Academy of Chinese Medical Sciences, China

REVIEWED BY
Punya Sachdeva,
Amity University, India

*CORRESPONDENCE
Yang Yang
yangyang8821@126.com
Hao Li
xyhplihao1965@126.com

SPECIALTY SECTION
This article was submitted to Neuropharmacology, a section of the journal Frontiers in Neuroscience

RECEIVED 03 February 2023
ACCEPTED 23 February 2023
PUBLISHED 07 March 2023

CITATION
Li Z, Cao Y, Pei H, Ma L, Yang Y and Li H (2023) The contribution of mitochondria-associated endoplasmic reticulum membranes (MAMs) dysfunction in Alzheimer's disease and the potential countermeasure. *Front. Neurosci.* 17:1158204. doi: 10.3389/fnins.2023.1158204

The contribution of mitochondria-associated endoplasmic reticulum membranes (MAMs) dysfunction in Alzheimer's disease and the potential countermeasure

Zehui Li[1], Yu Cao[1], Hui Pei[1], Lina Ma[1], Yang Yang[1]* and Hao Li[1,2]*

[1]Department of Geriatrics, Xiyuan Hospital, China Academy of Chinese Medical Sciences, Beijing, China, [2]Wangjing Hospital, China Academy of Chinese Medical Sciences, Beijing, China

Alzheimer's disease (AD) is the most common neurodegenerative disease. There are many studies targeting extracellular deposits of amyloid β-peptide (Aβ) and intracellular neurofibrillary tangles (NFTs), however, there are no effective treatments to halt the progression. Mitochondria-associated endoplasmic reticulum membranes (MAMs) have long been found to be associated with various pathogenesis hypotheses of AD, such as Aβ deposition, mitochondrial dysfunction, and calcium homeostasis. However, there is a lack of literature summarizing recent advances in the mechanism and treatment studies. Accordingly, this article reviews the latest research involving the roles of MAM structure and tethering proteins in the pathogenesis of AD and summarizes potential strategies targeting MAMs to dissect treatment perspectives for AD.

KEYWORDS

Alzheimer's disease, mitochondria, endoplasmic reticulum, calcium homeostasis, lipid metabolism

Introduction

According to Alzheimer's disease (AD) International, 55 million people worldwide suffer from dementia. The most common type of dementia is AD. The main histopathological characteristics of AD are the accumulation of extracellular deposits of amyloid β-peptide (Aβ) and intracellular neurofibrillary tangles (NFTs). However, there are other biochemical and morphological characteristics present earlier in the course of AD, such as alterations in phospholipid metabolism, the elevation of circulating cholesterol levels, aberrant calcium regulation, reduction of brain glucose levels, and mitochondrial dysfunction. Plaques and tangles have received a lot of attention because they are observable physical entities, however, the other features may be the upstream factors and should not be overlooked (Area-Gomez and Schon, 2017).

Mitochondria-associated endoplasmic reticulum membranes (MAMs) are a special subdomain of the endoplasmic reticulum (ER) that physically and biologically connects mitochondria to ER. ER-mitochondrial communication and MAM functions are increased expressively in AD (Leal et al., 2020). MAMs are generated by the ER side-by-side to

the mitochondrial outer membrane linked by a series of tethering proteins (Degechisa et al., 2022). They are not the collection of membranes but the employment of the proteinaceous tethers (Rowland and Voeltz, 2012), which play a key role in many important metabolic processes including the transfer of calcium, mitochondrial dynamics, lipid synthesis, autophagy, apoptosis, and inflammation. MAM dysfunction is also central to the pathogenic mechanisms of AD, especially in the Aβ generation and deposition, mitochondrial dysfunction, imbalanced calcium homeostasis, abnormal lipids metabolism, and abnormal autophagy. This review highlights abnormal MAM structures and tethering proteins in the pathogenesis of AD from these aspects. In addition, we provide a summary of compounds and drugs that target MAM tethering proteins in AD models.

The role of MAMs in Aβ generation of AD

The Aβ peptide is the main component of the AD hallmark amyloid plaques, which is produced by the proteolysis of amyloid beta-precursor protein (APP) by two enzymes: β-site APP cleaving enzyme 1 (BACE1) and the γ-secretase complex. Many studies have shown that MAMs are the main site of Aβ generation. Schreiner et al. (2015) reported that Aβ may be generated directly in MAMs. APP, BACE1, and γ-secretase have all been found in MAMs (Leal et al., 2020). BACE1 cleaves APP to produce sAPPβ and C99. C99 is delivered to MAMs and cleaved to produce Aβ and APP intracellular domain (AICD) by γ-secretase (Montesinos et al., 2020). In addition, it has been reported that the main pathway for Aβ entering mitochondria is MAMs (Del Prete et al., 2017). Knockdown of mitofusin-2 (Mfn2), which is involved in MAM tethering, leads to decreased contact between mitochondria and ER, resulting in lower γ-secretase activity and decreased concentrations of intracellular and extracellular $A\beta_{40}$ and $A\beta_{42}$ (Leal et al., 2016). This proves that the increase of MAMs may promote mitochondrial Aβ deposition. Axonal generation of Aβ also plays a key role in AD pathology. In AD models, swollen axons contain high levels of BACE1 (Gowrishankar et al., 2017). An average of 37 ± 4% of the total $A\beta_{40}$ secreted from each mouse hippocampal neuron is secreted by axons (Niederst et al., 2015). Bhattacharyya et al. showed that down-regulation of MAM assembly by silencing MAM-resident sigma-1 receptor expression resulted in reduced palmitoylated APP cleavage by BACE1, thereby decreasing Aβ generation in neuronal processes and axons (Bhattacharyya et al., 2021).

The role of MAMs in mitochondria dysfunction of AD

The neuronal activity must depend on the energy produced by mitochondria. Mitochondrial death can be observed before the histopathological features of AD appear. MAMs wrap around the location where mitochondria undergo fissuring by recruiting MAM protein inverted formin 2 (INF2) (Steffen and Koehler, 2018). The mitochondrial outer membrane protein FUNDC1 is a MAM protein that recruits dynamin 1 Like (DNM1L)/dynamin-related protein 1 (DRP1) to drive mitochondrial fission (Wu et al., 2016). In an AD mouse model, alterations in MAMs precede changes in mitochondrial dynamics accompanied by aberrations in mitochondrial membrane potential (MMP) and ATP production (Leal et al., 2020). Moreover, the MAMs control mitochondrial Ca^{2+} intake. Reduced Ca^{2+} intake affects mitochondrial metabolism, leading to mitochondrial dysfunction. Fernandes et al. (2021) found a decrease in close ER-mitochondria contacts, a reduction of Ca^{2+} transfer from ER to mitochondria, and impaired mitochondrial function in APPswe cells. γ-secretase activating protein (GSAP) fluorescence staining showed high colocalization with a MAM marker Facl4. Knockdown of GSAP significantly increased mitochondrial basal respiration and total ATP levels, which suggests that GSAP impairs mitochondria function (Xu et al., 2021). In an AD cell model, increased concentration of unprocessed C99 in the MAM region increased sphingolipid turnover and altered the lipid composition of mitochondrial membranes, which can interfere with the normal activity of the respiratory supercomplexes and thus may contribute to the bioenergetic defects in AD (Pera et al., 2017). Atlastin 2 (ATL2) is a protein associated with ER-mitochondria contacts whose expression was significantly increased both in 3 × Tg mice and AD patients. While, knockout of ATL2 rescued the elevated ER-mitochondria contacts back to normal levels, reduced the abnormally elevated mitochondrial superoxide, and significantly increased the MMP (Han et al., 2021).

The role of MAMs in calcium homeostasis of AD

Calcium signaling in neurons is essential for neurotransmission and the maintenance of synaptic plasticity (Skobeleva et al., 2022). Dysregulation of calcium homeostasis disrupts neuronal and synaptic function in AD (McDaid et al., 2020). Ca^{2+} homeostasis depends on the Sarcoplasmic/endoplasmic reticulum Ca^{2+} ATPase (SERCA) pumps to regulate Ca^{2+} uptake from the cytoplasm to the ER and activated inositol 1,4,5-triphosphate receptors (IP3Rs) and ryanodine receptors (RyRs) to enable Ca^{2+} efflux from the ER (Kawamoto et al., 2012). The IP3R–glucose-regulated protein 75 (Grp75)–voltage-dependent anion channel (VDAC) Ca^{2+} channeling complex was concentrated in MAMs. Up-regulation of this complex results in increased calcium content. The accumulation of mitochondrial calcium could be prohibited by the IP3R inhibitor (Chen et al., 2021b). The RyR is a Ca^{2+}-release channel protein located in the MAMs and sarcoplasmic reticulum. The RyR3 plays a dual character in AD pathology. Deletion of RyR3 in young APP/PS1 mice increases the excitability of hippocampal neuronal networks and accelerates AD progress. However, in aged APP/PS1 mice, the deletion of RyR3 restored network excitability (Liu et al., 2014). In the 5xFAD mouse model of AD, restricting RyR2 open time blocked the excessive activity of CA1 neurons (Yao et al., 2020). A small-molecule SERCA activator can increase ER Ca^{2+} and has shown efficacy in APP/PS1 mice, supporting SERCA activation as a therapeutic strategy for AD (Krajnak and Dahl, 2018).

The role of MAMs in lipid metabolism of AD

Lipid metabolism, especially cholesterol metabolism, has been implicated in the synaptic dysfunction of AD (Petrov et al., 2017). Ceramide and cholesterol have been found to increase in the brains of AD patients, normal aging mice, and neurons exposed to $A\beta_{1-42}$ (Cutler et al., 2004). MAMs are transient lipid rafts that are closely related to cholesterol and phospholipid metabolism (Pera et al., 2020). It has been proven that phospholipid transport between the ER and mitochondria is dependent on membrane integrity including MAMs rather than energy or MMP (Kojima et al., 2016). MAMs are where the enzymatic activities such as acetyl-CoA acetyltransferase 1 (ACAT1) that regulate cholesterol levels reside. ACAT1 gene ablation led to the amelioration of amyloid pathology and cognitive deficits in 3 × Tg AD mice (Bryleva et al., 2010). The concentration of unprocessed C99 at the MAMs is increased in models of AD and cells from AD patients, subsequently associated with the increase in ceramide levels (Pera et al., 2017). GSAP enriched in MAMs regulates lipid homeostasis through the processing of APP (Xu et al., 2021). In a cortical impact mice model of AD, the injured cortex and hippocampus exhibited significant increases in MAM activity, phospholipid synthesis, sphingomyelinase (SMases) activity, and cholesterol turnover (Agrawal et al., 2022). When cholesterol concentrations exceed a certain threshold, SMases are activated and hydrolyze sphingomyelin (SM) to produce ceramides. The cholesterol affinity of APP is involved in limiting APP distribution, conversely, APP senses and balances the membrane cholesterol (DelBove et al., 2019). An increase in MAM-localized C99 triggers the upregulation of SMase activity. The increased cholesterol mobilization observed in AD cells may be an outcome of persistent SMase activity caused by increased MAM-C99, which disrupts cellular lipid homeostasis and causes the alterations in membrane lipid composition commonly happen in AD (Montesinos et al., 2020).

The role of MAMs in abnormal autophagy in AD

Autophagy is a degradation mechanism of cells to remove damaged and senescent organelles and maintain cellular homeostasis. Autophagy plays a vital role in the generation and clearance of Aβ. Abnormal autophagy is involved in the development of AD (Yuan et al., 2022). Activation of autophagy alleviates pathological characters and cognitive deficits in APP/PS1 mice (Yang et al., 2023). The MAMs mark the starting point of autophagosome formation. Mitochondrial fusion protein Mfn2 is a MAM protein responsible for binding the ER and mitochondria. The energy sensor AMP-activated protein kinase (AMPK) interacts with Mfn2 and phosphorylates Mfn2 and induces autophagy (Hu et al., 2021). Autophagy initiation proteins such as autophagy and beclin 1 regulator 1 (AMBRA1) and Beclin 1 are recruited to the MAMs to regulate autophagy, demonstrating that MAM raft-like microdomains play a crucial part in the autophagosome formation (Garofalo et al., 2016). The sigma-1 receptor (Sig-1R) is a receptor with molecular chaperone activity clustered on MAMs. Autophagosome clearance is impaired in Sigma-1 KO cells, possibly due to impaired autophagosome-lysosomal organelle fusion mediated by the complex formed by Sig-1R with STX17 and ATG14. STX17 and ATG14 both appear at the ER-mitochondria contact site (Yang et al., 2019). The combination of vesicle-associated membrane protein-associated protein B (VAPB) and protein tyrosine phosphatase interacting protein 51 (PTPIP51) is identified as one of the MAM tethers. Manipulation of their expression to increase and decrease ER-mitochondrial junctions had significant effects on autophagy (Gomez-Suaga et al., 2017). The decreased expression of MAM tethering protein complexes including VAPB-PTPP51, BAP31-FIS1, and Mfn2-Mfn1 leads to abnormal autophagy, which leads to the decline of cognitive ability (Liu et al., 2022). The role of MAM tethering proteins in several major pathogeneses of AD is summarized in **Figure 1** schematically.

Strategies targeting MAMs for treating AD

The functions of MAMs are mainly exerted by its numerous tethering proteins. The abnormalities of these proteins eventually lead to the pathological processes of AD through multiple mechanisms. The expression of MAM tethering proteins and the tight connection between mitochondria and ER can be one of the hallmarks of AD progression. The regulation of these proteins to improve the corresponding phenotypes can be used as a strategy and target for AD treatment.

Knockdown of MAM protein GSAP reduced Aβ generation and plaque formation in an AD mouse model (He et al., 2010). Imatinib and imatinib methanesulfonate could prevent Aβ formation by inhibiting GSAP (He et al., 2010; Weintraub et al., 2013; Chu et al., 2014). Lithium treatment reduced abnormal IP3R-dependent ER Ca^{2+} signaling and enhanced synaptic plasticity in 3 × Tg AD mice (Wiseman et al., 2023). Xestospongin C can ameliorate the Ca^{2+} overload of primary hippocampal neurons induced by $A\beta_{1-42}$ and improve the cognitive ability of APP/PS1 mice (Wang et al., 2019). Mecobalamin also reduces ER-mitochondrial calcium flux through IP3R and prevents mitochondrial dysfunction (Wang and Xu, 2019). RyR2 instability plays a vital role in the reduction of ER Ca^{2+} content, which alters synaptic transmission and plasticity mechanisms. While Dantrolene stabilizes RyR2 thereby reversing most AD-related phenotypes in AppNL-G-F mice (Nakamura et al., 2021). Compound 12a inhibited Ca^{2+} release and significantly accelerated the cognitive behavior of FAD mice in the Morris water maze test. Moreover, docking simulations testified that 12a could bind to the active site of RyR1 (Dai et al., 2021). A Sig-1R agonist (+) SKF-10,047 could significantly increase mitochondrial movement in cortical neurons of 3 × Tg mice, which might be because it leads to the removal of Sig-1R from MAMs to mitochondria. (+) SKF-10,047 also leads to an increase in the number of mitochondria (Cavendish et al., 2019). Two other Sig-1R agonists ANAVEX2-73 and PRE-084 could prevent mitochondrial respiratory dysfunction in $A\beta_{25-35}$-injected mice (Lahmy et al., 2014). IRE1α inhibitor 4μ8c can reduce ER-mitochondrial association and restore the normal function of MAMs by inhibiting the expression and interaction of IP3R, Grp75, and VDAC1, thereby restoring ATP content and MMP (Chu et al., 2021). Artesunate could reverse

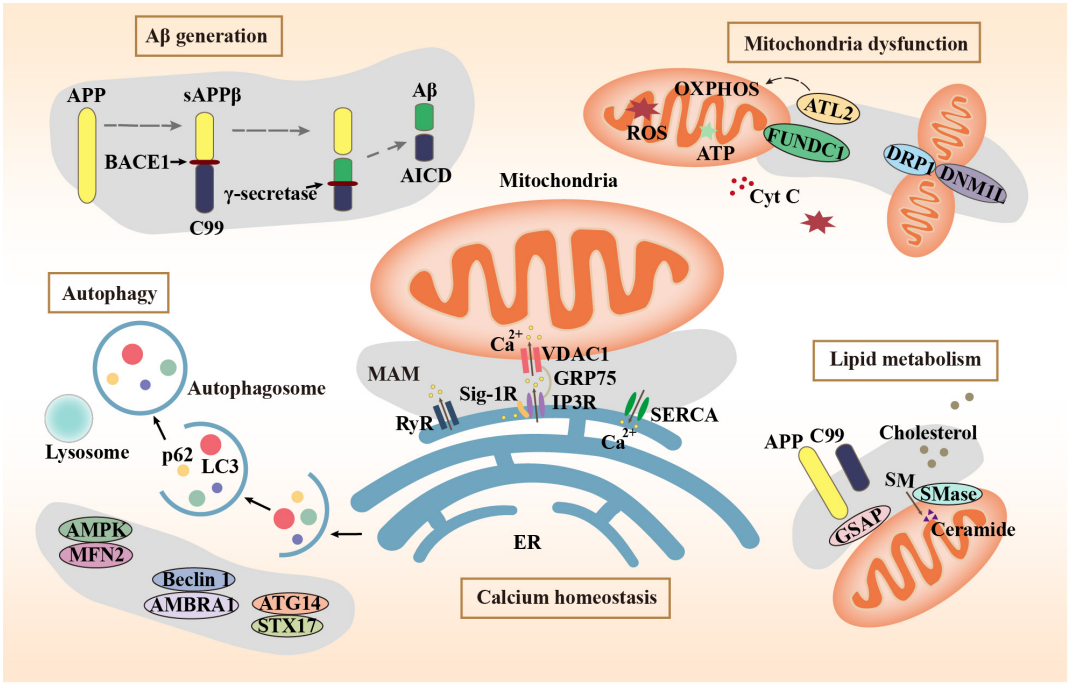

FIGURE 1
Mechanisms related to MAMs in AD.

cognitive impairment in APP/PS1 mice by regulating DRP1 to maintain mitochondrial dynamics (Qin et al., 2022). By increasing the expression of the MAM protein Mfn2, Biochanin A could reverse the imbalance of mitochondrial dynamics and abnormal mitophagy in APP/PS1 mice (Hou et al., 2022). Curcumin restores basal mitochondrial respiration and ATP production in thapsigargin-injured SH-SY5Y cells by targeting Mfn2 (Zhou et al., 2022). Besides, Myricetin, Selenomethionine, Leptin, *Trans*-ferulic acid, Ligustilide, and Albiflorin were also able to regulate Mfn2 and ameliorate mitochondrial dysfunction (Xu et al., 2018, 2019; Zafeer et al., 2019; Cheng et al., 2020; Zhu et al., 2020; Chen et al., 2021a; Yao et al., 2022). Cholesteryl ester produced in MAMs is involved in the pathogenesis of AD. Progesterone reduced the expression of ACAT1 through the ERK1/2 pathway, shortened the abnormally prolonged MAM length, inhibited cholesteryl ester accumulation in the cortex, and improved the cognitive function of APP/PS1 mice (Shi et al., 2021). We summarize potential compounds and drugs that exert anti-AD effects by regulating MAM tethering proteins in **Table 1**.

Discussion

Drug development for AD has continuously been challenged. The most popular AD hypotheses are amyloid cascade, hyperphosphorylation of tau, and mitochondrial cascade. However, numerous studies targeting these hypotheses have not been able to fully elucidate the mechanism of AD or retard its progression. The interaction between different organelles, especially mitochondria and ER in cells has gradually emerged in the study of various diseases (Theurey and Rieusset, 2017; Luan et al., 2021). Cellular dysfunction in the early stage of AD, including Ca^{2+} homeostasis, mitochondrial dysfunction, oxidative stress, and abnormal autophagy, are all associated with MAM function (Tapella et al., 2022).

As for the amyloid cascade, MAMs are the sites where C99 is cleaved to Aβ. Inhibition of MAMs protein expression and function may reduce Aβ production and extracellular deposition. MAMs recruit proteins such as INF2 and DRP1 to participate in mitochondrial fission, thereby affecting MMP and ATP production. Upregulation of some MAM-resident proteins causes enhanced mitochondria-ER contacts, along with mitochondrial damage such as increased mitochondrial superoxide. The MAM has both protein pumps that allow Ca^{2+} to flow from the cytoplasm to the ER and Ca^{2+} to flow from the ER, thus regulating Ca^{2+} homeostasis. Ca^{2+} flux also plays a dual role in AD progression. For instance, excessive Ca^{2+} influx leads to increased ROS production and cell death due to caspase activation; however, attenuated Ca^{2+} signaling may also be detrimental to ATP production (Filadi and Greotti, 2021; Arnst et al., 2022). Modulation of MAM-resident enzymes such as ACAT1 and MAM-C99 content affects cholesterol levels and lipid homeostasis in AD, along with amyloid synthesis and synaptic transmission. MAMs mark the starting point of autophagy. Decreased expressions of MAM tethering proteins, such as Sig-1R, VAPB-PTPP51, and Mfn2-Mfn1, lead to abnormal autophagy. All these indicate that MAM is an important target that should not be ignored in the study of AD pathogenesis.

Although MAMs have been shown to be closely related to the progression of AD, the molecular pathways are still not fully understood. At present, the research targets of AD drugs targeting MAM proteins are still limited. The mechanisms of interest are mainly in Aβ production, mitochondrial function, calcium

TABLE 1 Compounds and drugs targeting MAM tethering proteins for treating AD.

Compound/drug	Target	Mechanism	Model	References
Imatinib	GSAP	Aβ generation	3 × Tg mice N2a-APP695 cells	He et al., 2010; Chu et al., 2014
Imatinib methanesulfonate	GSAP	Aβ generation	LPS-induced inflammation	Weintraub et al., 2013
Lithium	IP3R	Ca^{2+} signaling abnormalities	3 × Tg mice	Wiseman et al., 2023
Xestospongin C	IP3R	Ca^{2+} homeostasis	APP/PS1 mice, $A\beta_{1-42}$-treated primary hippocampal neurons	Wang et al., 2019
Methyl vitamin B12	IP3R	Ca^{2+} homeostasis, mitochondrial dysfunction	Aβ-treated PC12 cells	Wang and Xu, 2019
Dantrolene	RyR2	Ca^{2+} homeostasis	App^{NL-G-F} mice	Nakamura et al., 2021
12a	RyR1	Ca^{2+} homeostasis	FAD mice	Dai et al., 2021
(+) SKF-10,047	Sig-1R	Mitochondrial movement and number	Primary hippocampal neurons from 3 × Tg mice	Cavendish et al., 2019
ANAVEX2-73, PRE-084	Sig-1R	Mitochondrial respiratory dysfunction	$A\beta_{25-35}$-injected mice	Lahmy et al., 2014
4μ8c	IP3R, Grp75, and VDAC1	Mitochondrial dysfunction	Aβ-treated SH-SY5Y cells	Chu et al., 2021
Artesunate	DRP1	Mitochondrial dynamics	APP/PS1 mice	Qin et al., 2022
Biochanin A	Mfn2	Mitochondrial dynamics and mitophagy	APP/PS1 mice	Hou et al., 2022
Curcumin	Mfn2	Mitochondrial dysfunction	Thapsigargin-treated SH-SY5Y cells	Zhou et al., 2022
Myricetin	Mfn2	Mitochondrial dysfunction	N2a-APP695-Swedish cells	Yao et al., 2022
Selenomethionine	Mfn2	Mitochondrial dysfunction	N2a-APP695-Swedish cells, 3 × Tg mice	Chen et al., 2021a
Leptin	Mfn2	Mitochondrial dysfunction	Aβ1-42-treated SH-SY5Y cells	Cheng et al., 2020
Trans-ferulic acid	Mfn2	Mitochondrial dysfunction	Streptozocin injection	Zafeer et al., 2019
Ligustilide	Mfn1, Mfn2	Mitochondrial dysfunction	SAMP8 mice APP/PS1 mice	Xu et al., 2018; Zhu et al., 2020
Albiflorin	Mfn1, Mfn2	Mitochondrial dysfunction	APP/PS1 mice	Xu et al., 2019
Progesterone	ACAT1	Cholesterol metabolism	APP/PS1 mice	Shi et al., 2021

homeostasis, and lipid metabolism. Currently, there are few studies on the interaction between MAMs and tau phosphorylation. Besides, although tethering proteins are the main manifestation of MAM function, the observation of MAM structure should not be ignored despite the technical difficulties in the research of AD treatment strategies. We look forward to new studies to further explore the role of the structure and functions of MAMs in the pathogenesis and treatment of AD.

Author contributions

YY and HL conceived the idea. ZL wrote the manuscript. YC, HP, and LM revised the manuscript. All authors contributed to the work and approved the submitted version.

Funding

This work was supported by the Fundamental Research Funds for the Central Public Welfare Research Institutes (No. ZZ15-YQ-018), the National Natural Science Foundation of China (Nos. 82205103 and 82205233), and the CACMS Innovation Fund (No. CI2021A01401).

Conflict of interest

The authors declare that the research was conducted in the absence of any commercial or financial relationships that could be construed as a potential conflict of interest.

The handling editor declared a shared affiliation with the authors ZL, YC, HP, LM, and YY.

Publisher's note

References

Agrawal, R. R., Larrea, D., Xu, Y., Shi, L., Zirpoli, H., Cummins, L. G., et al. (2022). Alzheimer's-associated upregulation of mitochondria-associated ER membranes after traumatic brain injury. *Cell Mol. Neurobiol.* doi: 10.1007/s10571-022-01299-0 [Epub ahead of print].

Area-Gomez, E., and Schon, E. A. (2017). On the pathogenesis of Alzheimer's disease: the MAM hypothesis. *FASEB J.* 31, 864–867. doi: 10.1096/fj.201601309

Arnst, N., Redolfi, N., Lia, A., Bedetta, M., Greotti, E., and Pizzo, P. (2022). Mitochondrial Ca(2+) signaling and bioenergetics in Alzheimer's disease. *Biomedicines* 10:3025. doi: 10.3390/biomedicines10123025

Bhattacharyya, R., Black, S. E., Lotlikar, M. S., Fenn, R. H., Jorfi, M., Kovacs, D. M., et al. (2021). Axonal generation of amyloid-β from palmitoylated APP in mitochondria-associated endoplasmic reticulum membranes. *Cell Rep.* 35:109134. doi: 10.1016/j.celrep.2021.109134

Bryleva, E. Y., Rogers, M. A., Chang, C. C., Buen, F., Harris, B. T., Rousselet, E., et al. (2010). ACAT1 gene ablation increases 24(S)-hydroxycholesterol content in the brain and ameliorates amyloid pathology in mice with AD. *Proc. Natl. Acad. Sci. U. S. A.* 107, 3081–3086. doi: 10.1073/pnas.0913828107

Cavendish, J. Z., Sarkar, S. N., Colantonio, M. A., Quintana, D. D., Ahmed, N., White, B. A., et al. (2019). Mitochondrial movement and number deficits in embryonic cortical neurons from 3xTg-AD mice. *J. Alzheimers Dis.* 70, 139–151. doi: 10.3233/jad-190143

Chen, C., Chen, Y., Zhang, Z. H., Jia, S. Z., Chen, Y. B., Huang, S. L., et al. (2021a). Selenomethionine improves mitochondrial function by upregulating mitochondrial selenoprotein in a model of Alzheimer's disease. *Front. Aging Neurosci.* 13:750921. doi: 10.3389/fnagi.2021.750921

Chen, L. T., Xu, T. T., Qiu, Y. Q., Liu, N. Y., Ke, X. Y., Fang, L., et al. (2021b). Homocysteine induced a calcium-mediated disruption of mitochondrial function and dynamics in endothelial cells. *J. Biochem. Mol. Toxicol.* 35:e22737. doi: 10.1002/jbt.22737

Cheng, Y., Buchan, M., Vitanova, K., Aitken, L., Gunn-Moore, F. J., Ramsay, R. R., et al. (2020). Neuroprotective actions of leptin facilitated through balancing mitochondrial morphology and improving mitochondrial function. *J. Neurochem.* 155, 191–206. doi: 10.1111/jnc.15003

Chu, B., Li, M., Cao, X., Li, R., Jin, S., Yang, H., et al. (2021). IRE1α-XBP1 affects the mitochondrial function of Aβ25-35-treated SH-SY5Y cells by regulating mitochondria-associated endoplasmic reticulum membranes. *Front. Cell Neurosci.* 15:614556. doi: 10.3389/fncel.2021.614556

Chu, J., Lauretti, E., Craige, C. P., and Praticò, D. (2014). Pharmacological modulation of GSAP reduces amyloid-β levels and tau phosphorylation in a mouse model of Alzheimer's disease with plaques and tangles. *J. Alzheimers Dis.* 41, 729–737. doi: 10.3233/jad-140105

Cutler, R. G., Kelly, J., Storie, K., Pedersen, W. A., Tammara, A., Hatanpaa, K., et al. (2004). Involvement of oxidative stress-induced abnormalities in ceramide and cholesterol metabolism in brain aging and Alzheimer's disease. *Proc. Natl. Acad. Sci. U.S.A.* 101, 2070–2075. doi: 10.1073/pnas.0305799101

Dai, B., Ma, X., Tang, Y., Xu, L., Guo, S., Chen, X., et al. (2021). Design, synthesis, and biological activity of novel semicarbazones as potent Ryanodine receptor1 inhibitors of Alzheimer's disease. *Bioorg. Med. Chem.* 29:115891. doi: 10.1016/j.bmc.2020.115891

Degechisa, S. T., Dabi, Y. T., and Gizaw, S. T. (2022). The mitochondrial associated endoplasmic reticulum membranes: a platform for the pathogenesis of inflammation-mediated metabolic diseases. *Immun. Inflamm. Dis.* 10:e647. doi: 10.1002/iid3.647

Del Prete, D., Suski, J. M., Oulès, B., Debayle, D., Gay, A. S., Lacas-Gervais, S., et al. (2017). Localization and processing of the amyloid-β protein precursor in mitochondria-associated membranes. *J. Alzheimers Dis.* 55, 1549–1570. doi: 10.3233/jad-160953

DelBove, C. E., Strothman, C. E., Lazarenko, R. M., Huang, H., Sanders, C. R., and Zhang, Q. (2019). Reciprocal modulation between amyloid precursor protein and synaptic membrane cholesterol revealed by live cell imaging. *Neurobiol. Dis.* 127, 449–461. doi: 10.1016/j.nbd.2019.03.009

Fernandes, T., Resende, R., Silva, D. F., Marques, A. P., Santos, A. E., Cardoso, S. M., et al. (2021). Structural and functional alterations in mitochondria-associated membranes (MAMs) and in mitochondria activate stress response mechanisms in an *in vitro* model of Alzheimer's disease. *Biomedicines* 9:881. doi: 10.3390/biomedicines9080881

Filadi, R., and Greotti, E. (2021). The yin and yang of mitochondrial Ca(2+) signaling in cell physiology and pathology. *Cell Calcium* 93:102321. doi: 10.1016/j.ceca.2020.102321

Garofalo, T., Matarrese, P., Manganelli, V., Marconi, M., Tinari, A., Gambardella, L., et al. (2016). Evidence for the involvement of lipid rafts localized at the ER-mitochondria associated membranes in autophagosome formation. *Autophagy* 12, 917–935. doi: 10.1080/15548627.2016.1160971

Gomez-Suaga, P., Paillusson, S., Stoica, R., Noble, W., Hanger, D. P., and Miller, C. C. J. (2017). The ER-mitochondria tethering complex VAPB-PTPIP51 regulates autophagy. *Curr. Biol.* 27, 371–385. doi: 10.1016/j.cub.2016.12.038

Gowrishankar, S., Wu, Y., and Ferguson, S. M. (2017). Impaired JIP3-dependent axonal lysosome transport promotes amyloid plaque pathology. *J. Cell Biol.* 216, 3291–3305. doi: 10.1083/jcb.201612148

Han, J., Park, H., Maharana, C., Gwon, A. R., Park, J., Baek, S. H., et al. (2021). Alzheimer's disease-causing presenilin-1 mutations have deleterious effects on mitochondrial function. *Theranostics* 11, 8855–8873. doi: 10.7150/thno.59776

He, G., Luo, W., Li, P., Remmers, C., Netzer, W. J., Hendrick, J., et al. (2010). Gamma-secretase activating protein is a therapeutic target for Alzheimer's disease. *Nature* 467, 95–98. doi: 10.1038/nature09325

Hou, Y., Zhao, W., Yu, H., Zhang, F., Zhang, H. T., and Zhou, Y. (2022). Biochanin A alleviates cognitive impairment and hippocampal mitochondrial damage in ovariectomized APP/PS1 mice. *Phytomedicine* 100:154056. doi: 10.1016/j.phymed.2022.154056

Hu, Y., Chen, H., Zhang, L., Lin, X., Li, X., Zhuang, H., et al. (2021). The AMPK-MFN2 axis regulates MAM dynamics and autophagy induced by energy stresses. *Autophagy* 17, 1142–1156. doi: 10.1080/15548627.2020.1749490

Kawamoto, E. M., Vivar, C., and Camandola, S. (2012). Physiology and pathology of calcium signaling in the brain. *Front. Pharmacol.* 3:61. doi: 10.3389/fphar.2012.00061

Kojima, R., Endo, T., and Tamura, Y. (2016). A phospholipid transfer function of ER-mitochondria encounter structure revealed *in vitro*. *Sci. Rep.* 6:30777. doi: 10.1038/srep30777

Krajnak, K., and Dahl, R. (2018). A new target for Alzheimer's disease: a small molecule SERCA activator is neuroprotective *in vitro* and improves memory and cognition in APP/PS1 mice. *Bioorg. Med. Chem. Lett.* 28, 1591–1594. doi: 10.1016/j.bmcl.2018.03.052

Lahmy, V., Long, R., Morin, D., Villard, V., and Maurice, T. (2014). Mitochondrial protection by the mixed muscarinic/σ1 ligand ANAVEX2-73, a tetrahydrofuran derivative, in Aβ25-35 peptide-injected mice, a nontransgenic Alzheimer's disease model. *Front. Cell Neurosci.* 8:463. doi: 10.3389/fncel.2014.00463

Leal, N. S., Dentoni, G., Schreiner, B., Naia, L., Piras, A., Graff, C., et al. (2020). Amyloid B-peptide increases mitochondria-endoplasmic reticulum contact altering mitochondrial function and autophagosome formation in Alzheimer's disease-related models. *Cells* 9:2552. doi: 10.3390/cells9122552

Leal, N. S., Schreiner, B., Pinho, C. M., Filadi, R., Wiehager, B., Karlström, H., et al. (2016). Mitofusin-2 knockdown increases ER-mitochondria contact and decreases amyloid β-peptide production. *J. Cell Mol. Med.* 20, 1686–1695. doi: 10.1111/jcmm.12863

Liu, J., Supnet, C., Sun, S., Zhang, H., Good, L., Popugaeva, E., et al. (2014). The role of ryanodine receptor type 3 in a mouse model of Alzheimer disease. *Channels* 8, 230–242. doi: 10.4161/chan.27471

Liu, J., Wang, L., Ge, L., Sun, W., Song, Z., Lu, X., et al. (2022). Lanthanum decreased VAPB-PTPP51, BAP31-FIS1, and MFN2-MFN1 expression of mitochondria-associated membranes and induced abnormal autophagy in rat hippocampus. *Food Chem. Toxicol.* 161:112831. doi: 10.1016/j.fct.2022.112831

Luan, Y., Luan, Y., Yuan, R. X., Feng, Q., Chen, X., and Yang, Y. (2021). Structure and function of mitochondria-associated endoplasmic reticulum membranes (MAMs) and their role in cardiovascular diseases. *Oxid. Med. Cell Longev.* 2021:4578809. doi: 10.1155/2021/4578809

McDaid, J., Mustaly-Kalimi, S., and Stutzmann, G. E. (2020). Ca(2+) dyshomeostasis disrupts neuronal and synaptic function in Alzheimer's disease. *Cells* 9:2655. doi: 10.3390/cells9122655

Montesinos, J., Pera, M., Larrea, D., Guardia-Laguarta, C., Agrawal, R. R., Velasco, K. R., et al. (2020). The Alzheimer's disease-associated C99 fragment of APP regulates cellular cholesterol trafficking. *Embo J.* 39:e103791. doi: 10.15252/embj.2019103791

Nakamura, Y., Yamamoto, T., Xu, X., Kobayashi, S., Tanaka, S., Tamitani, M., et al. (2021). Enhancing calmodulin binding to ryanodine receptor is crucial to limit neuronal cell loss in Alzheimer disease. *Sci. Rep.* 11:7289. doi: 10.1038/s41598-021-86822-x

Niederst, E. D., Reyna, S. M., and Goldstein, L. S. (2015). Axonal amyloid precursor protein and its fragments undergo somatodendritic endocytosis and processing. *Mol. Biol. Cell* 26, 205–217. doi: 10.1091/mbc.E14-06-1049

Pera, M., Larrea, D., Guardia-Laguarta, C., Montesinos, J., Velasco, K. R., Agrawal, R. R., et al. (2017). Increased localization of APP-C99 in mitochondria-associated ER membranes causes mitochondrial dysfunction in Alzheimer disease. *Embo J.* 36, 3356–3371. doi: 10.15252/embj.201796797

Pera, M., Montesinos, J., Larrea, D., Agrawal, R. R., Velasco, K. R., Stavrovskaya, I. G., et al. (2020). MAM and C99, key players in the pathogenesis of Alzheimer's disease. *Int. Rev. Neurobiol.* 154, 235–278. doi: 10.1016/bs.irn.2020.03.016

Petrov, A. M., Kasimov, M. R., and Zefirov, A. L. (2017). Cholesterol in the pathogenesis of Alzheimer's, Parkinson's diseases and autism: link to synaptic dysfunction. *Acta Naturae* 9, 26–37.

Qin, Y. R., Ma, C. Q., Jiang, J. H., Wang, D. P., Zhang, Q. Q., Liu, M. R., et al. (2022). Artesunate restores mitochondrial fusion-fission dynamics and alleviates neuronal

injury in Alzheimer's disease models. *J. Neurochem.* 162, 290–304. doi: 10.1111/jnc.15620

Rowland, A. A., and Voeltz, G. K. (2012). Endoplasmic reticulum-mitochondria contacts: function of the junction. *Nat. Rev. Mol. Cell Biol.* 13, 607–625. doi: 10.1038/nrm3440

Schreiner, B., Hedskog, L., Wiehager, B., and Ankarcrona, M. (2015). Amyloid-β peptides are generated in mitochondria-associated endoplasmic reticulum membranes. *J. Alzheimers Dis.* 43, 369–374. doi: 10.3233/jad-132543

Shi, W., Wu, H., Liu, S., Wu, Z., Wu, H., Liu, J., et al. (2021). Progesterone suppresses cholesterol esterification in APP/PS1 mice and a cell model of Alzheimer's disease. *Brain Res. Bull* 173, 162–173. doi: 10.1016/j.brainresbull.2021.05.020

Skobeleva, K., Shalygin, A., Mikhaylova, E., Guzhova, I., Ryazantseva, M., and Kaznacheyeva, E. (2022). The STIM1/2-regulated calcium homeostasis is impaired in hippocampal neurons of the 5xFAD mouse model of Alzheimer's disease. *Int. J. Mol. Sci.* 23:14810. doi: 10.3390/ijms232314810

Steffen, J., and Koehler, C. M. (2018). ER-mitochondria contacts: actin dynamics at the ER control mitochondrial fission via calcium release. *J. Cell Biol.* 217, 15–17. doi: 10.1083/jcb.201711075

Tapella, L., Dematteis, G., Moro, M., Pistolato, B., Tonelli, E., Vanella, V. V., et al. (2022). Protein synthesis inhibition and loss of homeostatic functions in astrocytes from an Alzheimer's disease mouse model: a role for ER-mitochondria interaction. *Cell Death Dis.* 13:878. doi: 10.1038/s41419-022-05324-4

Theurey, P., and Rieusset, J. (2017). Mitochondria-associated membranes response to nutrient availability and role in metabolic diseases. *Trends Endocrinol. Metab.* 28, 32–45. doi: 10.1016/j.tem.2016.09.002

Wang, M., and Xu, T. (2019). Methyl B12 protects PC12 cells against cytotoxicity induced by Aβ(25-35). *J. Cell Biochem.* 120, 11921–11930. doi: 10.1002/jcb.28475

Wang, Z. J., Zhao, F., Wang, C. F., Zhang, X. M., Xiao, Y., Zhou, F., et al. (2019). Xestospongin C, a reversible IP3 receptor antagonist, alleviates the cognitive and pathological impairments in APP/PS1 mice of Alzheimer's disease. *J. Alzheimers Dis.* 72, 1217–1231. doi: 10.3233/jad-190796

Weintraub, M. K., Bisson, C. M., Nouri, J. N., Vinson, B. T., Eimerbrink, M. J., Kranjac, D., et al. (2013). Imatinib methanesulfonate reduces hippocampal amyloid-β and restores cognitive function following repeated endotoxin exposure. *Brain Behav. Immun.* 33, 24–28. doi: 10.1016/j.bbi.2013.05.002

Wiseman, A. L., Briggs, C. A., Peritt, A., Kapecki, N., Peterson, D. A., Shim, S. S., et al. (2023). Lithium provides broad therapeutic benefits in an alzheimer's disease mouse model. *J. Alzheimers Dis.* 91, 273–290. doi: 10.3233/jad-220758

Wu, W., Li, W., Chen, H., Jiang, L., Zhu, R., and Feng, D. (2016). FUNDC1 is a novel mitochondrial-associated-membrane (MAM) protein required for hypoxia-induced mitochondrial fission and mitophagy. *Autophagy* 12, 1675–1676. doi: 10.1080/15548627.2016.1193656

Xu, P., Chang, J. C., Zhou, X., Wang, W., Bamkole, M., Wong, E., et al. (2021). GSAP regulates lipid homeostasis and mitochondrial function associated with Alzheimer's disease. *J. Exp. Med.* 218:e20202446. doi: 10.1084/jem.20202446

Xu, Y. J., Mei, Y., Qu, Z. L., Zhang, S. J., Zhao, W., Fang, J. S., et al. (2018). Ligustilide ameliorates memory deficiency in APP/PS1 transgenic mice via restoring mitochondrial dysfunction. *Biomed. Res. Int.* 2018:4606752. doi: 10.1155/2018/4606752

Xu, Y. J., Mei, Y., Shi, X. Q., Zhang, Y. F., Wang, X. Y., Guan, L., et al. (2019). Albiflorin ameliorates memory deficits in APP/PS1 transgenic mice via ameliorating mitochondrial dysfunction. *Brain Res.* 1719, 113–123. doi: 10.1016/j.brainres.2019.05.037

Yang, C. Z., Wang, S. H., Zhang, R. H., Lin, J. H., Tian, Y. H., Yang, Y. Q., et al. (2023). Neuroprotective effect of astragalin via activating PI3K/Akt-mTOR-mediated autophagy on APP/PS1 mice. *Cell Death Discov.* 9:15. doi: 10.1038/s41420-023-01324-1

Yang, H., Shen, H., Li, J., and Guo, L. W. (2019). SIGMAR1/Sigma-1 receptor ablation impairs autophagosome clearance. *Autophagy* 15, 1539–1557. doi: 10.1080/15548627.2019.1586248

Yao, J., Sun, B., Institoris, A., Zhan, X., Guo, W., Song, Z., et al. (2020). Limiting RyR2 open time prevents Alzheimer's disease-related neuronal hyperactivity and memory loss but not β-amyloid accumulation. *Cell Rep.* 32:108169. doi: 10.1016/j.celrep.2020.108169

Yao, X., Zhang, J., Lu, Y., Deng, Y., Zhao, R., and Xiao, S. (2022). Myricetin restores Aβ-induced mitochondrial impairments in N2a-SW cells. *ACS Chem. Neurosci.* 13, 454–463. doi: 10.1021/acschemneuro.1c00591

Yuan, M., Wang, Y., Huang, Z., Jing, F., Qiao, P., Zou, Q., et al. (2022). Impaired autophagy in amyloid-beta pathology: a traditional review of recent Alzheimer's research. *J. Biomed. Res.* 37, 30–46. doi: 10.7555/jbr.36.20220145

Zafeer, M. F., Firdaus, F., Anis, E., and Mobarak Hossain, M. (2019). Prolong treatment with Trans-ferulic acid mitigates bioenergetics loss and restores mitochondrial dynamics in streptozotocin-induced sporadic dementia of Alzheimer's type. *Neurotoxicology* 73, 246–257. doi: 10.1016/j.neuro.2019.04.006

Zhou, H. Y., Sun, Y. Y., Chang, P., and Huang, H. C. (2022). Curcumin inhibits cell damage and apoptosis caused by thapsigargin-induced endoplasmic reticulum stress involving the recovery of mitochondrial function mediated by mitofusin-2. *Neurotox Res.* 40, 449–460. doi: 10.1007/s12640-022-00481-y

Zhu, W. L., Zheng, J. Y., Cai, W. W., Dai, Z., Li, B. Y., Xu, T. T., et al. (2020). Ligustilide improves aging-induced memory deficit by regulating mitochondrial related inflammation in SAMP8 mice. *Aging* 12, 3175–3189. doi: 10.18632/aging.102793

frontiers | Frontiers in Neuroscience

TYPE Review
PUBLISHED 12 April 2023
DOI 10.3389/fnins.2023.1158228

OPEN ACCESS

EDITED BY
Guibo Sun,
Chinese Academy of Medical Sciences and Peking Union Medical College, China

REVIEWED BY
Kuo Zhang,
Shenyang Pharmaceutical University, China
Vivek Puri,
Chitkara University, Himachal Pradesh, India

*CORRESPONDENCE
Ning Jiang
jennifer-jn@126.com
Wenxia Zhou
zhouwx@bmi.ac.cn

SPECIALTY SECTION
This article was submitted to Neuropharmacology, a section of the journal Frontiers in Neuroscience

RECEIVED 03 February 2023
ACCEPTED 13 March 2023
PUBLISHED 12 April 2023

CITATION
Shen W, Jiang N and Zhou W (2023) What can traditional Chinese medicine do for adult neurogenesis?
Front. Neurosci. 17:1158228.
doi: 10.3389/fnins.2023.1158228

What can traditional Chinese medicine do for adult neurogenesis?

Wei Shen[1,2,3], Ning Jiang[2,3]* and Wenxia Zhou[1,2,3]*

[1]School of Chinese Materia Medica, Tianjin University of Traditional Chinese Medicine, Tianjin, China, [2]Beijing Institute of Pharmacology and Toxicology, Beijing, China, [3]State Key Laboratory of Toxicology and Medical Countermeasures, Beijing, China

Adult neurogenesis plays a crucial role in cognitive function and mood regulation, while aberrant adult neurogenesis contributes to various neurological and psychiatric diseases. With a better understanding of the significance of adult neurogenesis, the demand for improving adult neurogenesis is increasing. More and more research has shown that traditional Chinese medicine (TCM), including TCM prescriptions (TCMPs), Chinese herbal medicine, and bioactive components, has unique advantages in treating neurological and psychiatric diseases by regulating adult neurogenesis at various stages, including proliferation, differentiation, and maturation. In this review, we summarize the progress of TCM in improving adult neurogenesis and the key possible mechanisms by which TCM may benefit it. Finally, we suggest the possible strategies of TCM to improve adult neurogenesis in the treatment of neuropsychiatric disorders.

KEYWORDS

adult neurogenesis, neural stem cells, traditional Chinese medicine, TCM prescriptions, Chinese herbal medicine, bioactive components

1. Introduction

Adult neurogenesis is the process of generating functional neurons from neural stem cells (NSCs) (Ming and Song, 2011), which is involved in learning, memory, and emotion and may also be involved in the remodeling of the central nervous system (Taupin, 2005; Lledo et al., 2006; Toda and Gage, 2018). Adult neurogenesis abnormalities play an important role in a variety of neurodegenerative disorders, such as Alzheimer's disease (AD), Huntington's disease (HD), and Parkinson's disease (PD) (Winner and Winkler, 2015; Horgusluoglu et al., 2017; Berger et al., 2020). In addition, adult neurogenesis is associated with emotional illnesses, such as depression (Sahay and Hen, 2007; Vaidya et al., 2007; Berger et al., 2020) and anxiety (Cheung et al., 2016; Toda and Gage, 2018). Stress (Odaka et al., 2017; Schoenfeld et al., 2017) and stroke (Rahman et al., 2021) are also associated with abnormal adult neurogenesis. Considering the role of adult neurogenesis in the pathophysiology of neurological and psychiatric diseases, restoring neurological function by improving adult neurogenesis is one of the main directions in the field of neuroscience.

A lot of work has gone into finding effective medications to boost adult neurogenesis. Recent progress in adult neurogenesis represents a potentially promising target for the treatment of neurological (Taupin, 2008; Matsuda and Nakashima, 2021) and mental conditions (DeCarolis and Eisch, 2010; Jun et al., 2012). Traditional Chinese medicine (TCM) has been used for centuries in China and other Asian countries, such as Korea and Japan. In recent years, TCM, including TCM prescription drugs (TCMPs), Chinese herbal medicine (CHM), and bioactive

components extracted from TCM, have been found to have great potential for improving adult neurogenesis in the treatment of neuropsychiatric disorders. In this review, we summarize the effects of TCM on regulating adult neurogenesis and their potential mechanisms and provide the basis for TCM targeting adult neurogenesis in the treatment of neuropsychiatric diseases.

2. Adult neurogenesis: From neural stem cells to therapy

2.1. Biological significance of adult neurogenesis

Neurogenesis is the process by which NSCs proliferate and differentiate to produce new neurons (this process can be seen in Figure 1), which is essential for the development of the brain and the establishment of functional connections. The nervous system of adult mammals has long been considered a non-regenerative tissue. However, in 1965, Altman and Das (Altman and Das, 1965) first observed neurogenesis in adult rats, subsequently, in 1998, Eriksson et al (Eriksson et al, 1998) provided evidence for the existence of adult neurogenesis of human. Over the next decade, the evidence for adult human neurogenesis has been refined (Boldrini et al., 2018; Sorrells et al., 2018; Moreno-Jimenez et al., 2021), confirming that adult neurogenesis exists throughout life (Zhou et al., 2022). With the deepening of adult neurogenesis research, it has been confirmed that adult neurogenesis occurs in two regions of the adult brain: the subgranular zone of the hippocampus (SGZ) and the subventricular zone (SVZ) of the lateral ventricles of adult mammals (Gould, 2007).

There is growing evidence that adult neurogenesis is essential for central nervous system (CNS) function. Adult neurogenesis is associated with cognition and emotion (Anacker and Hen, 2017; Alam et al., 2018). Adult neurogenesis is involved in cognition, including memory interference and indexing (Miller and Sahay, 2019), learning (Yau et al., 2015), and forgetting (Akers et al., 2014). Adult neurogenesis is also involved in the regulation of mood (Anacker and Hen, 2017), reduced neurogenesis has been implicated in the pathogenesis of anxiety and depression (Snyder et al., 2011), and increasing adult neurogenesis is sufficient to reduce anxiety and depression-like behaviors (Hill et al., 2015). Meanwhile, researchers have found that adult neurogenesis confers stress resilience (Anacker et al., 2018), and this resilience is necessary for the body to adapt to new environments. In addition, after a brain injury, the new neurons generated by adult neurogenesis are essential for the recovery of neural function (Marques et al., 2019).

It is known that NSCs progress through distinct stages before they become mature neurons, and this process is tightly controlled by cell-intrinsic factors and signals in the neurogenic niche (Johnson et al., 2009; Suh et al., 2009). In short, adult neurogenesis is tightly regulated by cell-intrinsic molecules and extrinsic signaling. Intrinsic signaling involves phosphoinositide 3-kinase (PI3K)/Akt, Notch-Hairy, and enhancer of split (Notch-Hes) signaling, Hedgehog signaling, bone morphogenetic protein signaling, and Wingless/Integrated signaling (Goncalves et al., 2016; Matsubara et al., 2021). Extracellular signaling is mainly from the NSC niche that creates a favorable microenvironment and architecture to sustain NSCs and neurogenesis (Li and Guo, 2021). Such factors as growth factors, neurotrophic factors, and neurotransmitters have also been reported to be part of the regulatory signaling within the hippocampal niche (Goncalves et al., 2016). Importantly, intrinsic and extrinsic signaling crosstalk and act on the CNS to regulate neurogenesis.

As its existence has been questioned in the past, studies have sought to understand how adult neurogenesis affects the human brain in both health and disease. Researchers have also looked at the factors that may affect this process. The above developments greatly promote

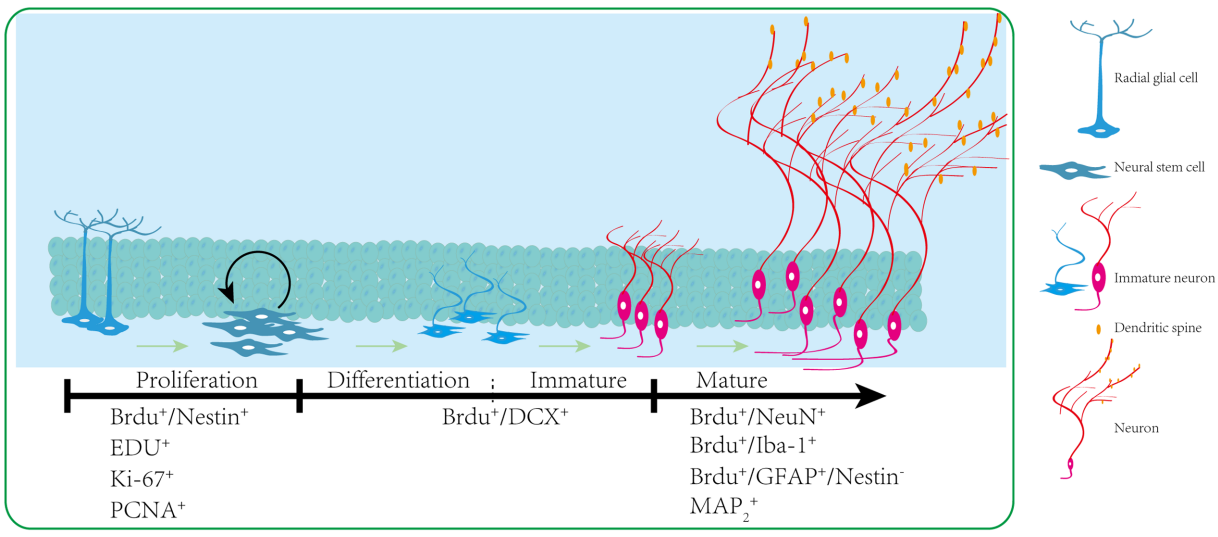

FIGURE 1
Adult hippocampus of the dentate gyrus. Newly formed neurons in the sub-granular zone of the dentate gyrus pass through several consecutive developmental stages. The radial glial cells can generate proliferating NSCs with transient amplifying characteristics. These NSCs can give rise to neuroblasts that subsequently differentiate into dentate granule neurons. The developmental trajectory is accompanied by the subsequent expression of stage-specific molecular markers.

our understanding of adult neurogenesis and how it might be used to enhance CNS performance and for the prevention and treatment of diseases that affect it.

2.2. Adult neurogenesis and neuropsychiatric diseases

With the growing understanding of the role of adult neurogenesis in the regulation of cognitive function, emotion, and brain repair after injury, the study of the relationship between this process and neuropsychiatric diseases has also made progress. Changes in adult neurogenesis were observed in neurological (such as AD, PD, HD, and stroke) and psychiatric (depression and post-stroke depression) diseases, and adult neurogenesis has been found to be involved in the pathological mechanisms of these diseases. Improving adult neurogenesis has been tried as a means of alleviating neurological and psychiatric disorders.

Alterations in adult neurogenesis have been reported in most neurological disorders, including neurodegenerative diseases and stroke. Since adult neurogenesis is involved in the regulation of cognition (Anacker and Hen, 2017), modulating adult neurogenesis may help to improve cognitive deficits in some neuropsychiatric disorders (Berger et al., 2020). In fact, abnormal adult neurogenesis has been observed in neurodegenerative diseases such as AD, HD, PD, and amyotrophic lateral sclerosis (ALS) (Jordan et al., 2006; Vivar, 2015; Horgusluoglu et al., 2017), which manifest as cognitive decline (Winner and Winkler, 2015; Terreros-Roncal et al., 2021). In contrast to the reduction of neurogenesis in neurodegenerative diseases, the proliferation of NSCs and the production of neuroblasts were activated after stroke. These neuroblasts migrate to the infarcted area, contribute to the repair of the infarcted brain, and form glial scar tissue (Koh and Park, 2017). However, based on comparisons between the density of BrdU-stained cells colabeled with a neuronal marker at 2 and 6 weeks post-ischemia about 80% or more of the new neurons died during this time interval (Arvidsson et al., 2002). Meanwhile, the effect of compensatory neurogenesis in repairing and restoring neural function has been limited. Fortunately, exogenous transplantation of NSCs (Hassani et al., 2012) and drugs (Chen et al., 2016) can be beneficial for neurogenesis and contribute to the recovery of brain function (such as motor balance and cognition) after stroke (Jin et al., 2006), and promoting adult neurogenesis has become an important direction for post-stroke recovery treatment (Marques et al., 2019).

Alterations in adult neurogenesis and reduced size of the hippocampus were reported in most psychiatric disorders, including schizophrenia, major depression, addiction, and anxiety, and in a significant subpopulation of patients with depression (Goncalves et al., 2016). Depressive disorders may be caused by impaired adult hippocampal neurogenesis in adults (Miller and Hen, 2015), and the effects of antidepressants have been found to relate to neurogenesis (Santarelli et al., 2003). Currently, medicine uses antidepressants such as fluoxetine, sertraline, and paroxetine, which could improve impaired cognitive, emotional, and motor function by promoting adult neurogenesis (Li et al., 2009).

However, to date, there isno clinical evidence of an isolated impairment of adult hippocampal neurogenesis in the absence of other abnormalities,but numerous studies have reported alterations in adult neurogenesis that are associated with several neurological and psychiatric disorders, providing a link between adult neurogenesis and human disease (Goncalves et al., 2016).

Since neurogenesis is related to a variety of neurological and psychiatric diseases, researchers have begun to try to alleviate diseases by influencing neurogenesis and have made some progress. The amelioration of diseases by neurogenesis mainly includes intracerebral transplantation and endogenous activation of NSCs (Chrostek et al., 2019; Wang J. et al., 2021). Although clinical data or evidence of a causal relationship between adult neurogenesis and disease are still lacking, a growing body of evidence in rodents and non-human primates indicates that improving adult neurogenesis contributes to restoring brain function in neuropsychiatric disorders. On this basis, research was carried out on the treatment of diseases with NSC transplantation or endogenous activation of NSCs. NSC transplantation could improve AD, PD, depression (Bao and Song, 2018), stroke, and other diseases (Boese et al., 2018). Promoting adult neurogenesis through endogenous activation of NSCs may also have good application prospects through lifestyle interventions or drugs. In lifestyle practice, exercise, environmental enrichment, and even dietary factors have been shown to enhance adult neurogenesis in animal models and can effectively alleviate depression and cognitive decline associated with animal models of mental illness (Hueston et al., 2017; Ma C. L. et al., 2017; Gronska-Peski et al., 2021). Adult neurogenesis is improved by medication for the symptoms of depression (Elder et al., 2006; Zeng et al., 2022), AD (Ye et al., 2016; Stazi and Wirths, 2021), and stroke (Chen et al., 2016), with TCM having the greatest effects on the aforementioned adult neurogenesis-related diseases. Together, these findings show that improving adult neurogenesis is indeed one of the most important ways to treat diseases. TCM has a variety of clinical procedures to treat neurological and psychiatric diseases and brain injuries, and these procedures have a proven track record of success. Improving adult neurogenesis may also be one of the key mechanisms underlying these procedures' efficacy.

3. The effects of TCM on adult neurogenesis in neurological and psychiatric diseases

TCM has good clinical effects in the treatment of CNS diseases. Some researchers suggest that adult neurogenesis may be the mechanism of TCM for CNS diseases (Ren and Zuo, 2012; Yang et al., 2017; Wang J. et al., 2021; Feng et al., 2022). Thus, TCM has great potential for targeting adult neurogenesis to improve CNS diseases. Indeed, it has been observed that TCM prescriptions (TCMPs), CHMs, and bioactive components derived from TCM could affect adult neurogenesis and improve cognition, alleviate mood, and restore brain function in the animal model. In addition, different TCM may be involved in the regulation of different stages of adult neurogenesis.

3.1. The effects of TCM prescriptions on adult neurogenesis

In recent years, more and more researchers have focused on TCM's improvement of CNS diseases by targeting adult neurogenesis. Table 1 and Figure 2 show that 28 kinds of TCMPs were reported to

TABLE 1 Effects of TCM prescriptions on neurological conditions and adult neurogenesis.

Prescription	Composition	Animals/cell types	Outcome measurement	Aspects of behaviors/function	References
Buyang Huanwu decoction	Hedysari Radix, Angelicae Sinensis Radix, Paeoniae Rubra Radix, Chuanxiong Rhizoma, Persicae Semen, Carthami Flos, Pheretima.	Male ICR mice were subjected to an acute ischemic stroke by inducing a middle cerebral ischemic/reperfusion (CIR) injury	cerebral cortex:↑MAP-2$^+$/BrdU$^+$ at day 7 and day 14 after stroke.	↑ Brain function, ameliorated the cerebral infarction, and significantly improved the neurological deficits	Wang et al. (2011)
		A rat model of cerebral ischemia by MCAO	Cerebral cortex, SGZ and SVZ:↑BrdU$^+$/MAP2$^+$	Not given	Liu et al. (2013)
		cerebral ischemia/reperfusion (CIR) injury ICR mouse model	SGZ and SVZ: ↑DCX$^+$	↑Locomotor activity and behavior response in a novel open field	Chen H. J. et al. (2015)
		Adult male Sprague–Dawley rats MCAO ischemic	DG: ↑DCX$^+$ ↑GFAP/BrdU-positive cells	↑Learning function but not memory functions by Water maze test	Chen et al. (2020)
		C17.2 neural stem cells	↑BrdU$^+$, nestin$^+$ in the NSCs ↑Tuj1$^+$ and GFAP$^+$	Cell	Chen et al. (2020)
		cerebral ischemia/reperfusion (CIR) injury	cerebral cortex: ↑BrdU$^+$/DCX $^+$, BrdU$^+$/NeuN$^+$	↑Modified neurological severity score (mNSS) and the corner test	Zhuge et al. (2020)
Danggui-Jakyak-San	Paeoniae Radix, Atractylodis Rhizoma, Alismatis Rhizoma, Hoelen, Cnidii Rhizoma, and Angelicae Gigantis Radix.	Male C57BL/6 mice (22–26 g, 7 weeks) bilateral common carotid artery occluded ischemia (BCCAO)	DG: ↑Ki67, DCX$^+$, BrdU$^+$, ↑BrdU$^+$/ NeuN$^+$; ↑BrdU$^+$/DCX$^+$, BrdU$^+$ /GFAP$^+$	↑ Spatial memory in the Morris water maze	Song et al. (2013)
Tongxinluo	Ginseng Radix et Rhizoma, Hirudo，Scorpio, Paeoniae Radix Rubra, Cicadae Periostracum，Eupolyphaga Steleophaga, Scolopendra, Santali Albi Lignum, Dalbergiae Odoriferae Lignum, Olibanum，Ziziphi Spinosae Semen, Borneolum.	male Sprague–Dawley rats receive permanent distal middle cerebral artery occlusion (MCAO)	ipsilateral thalamus:7 days: ↑BrdU$^+$, Nestin+14 days: ↑BrdU$^+$, Nestin$^+$, BrdU$^+$/ Nestin$^+$, BrdU$^+$/NeuN$^+$	↑Neurological function (Bederson scores) without reducing infarction volume (Nissl staining)	Chen L. et al. (2014)
		The MCAO model in the hypertensive rats	SVZ: ↑BrdU$^+$/NeuN$^+$ cells, BrdU$^+$ /DCX$^+$	↑Neurological Function (Bederson scores)	Chen et al. (2016)
Danggui-Shaoyao-San	Angelicae Sinensis Radix, Paeoniae Radix Alba, Smilacis Glabrae Rhizoma, Atractylodis Macrocephalae Rhizoma, Alismatis Rhizoma, Chuanxiong Rhizoma.	Female Sprague–Dawley rats MCAO was induced by intraluminal occlusion for 90 min with a nylon monofilament suture	SVZ: ↑ DCX$^+$, BrdU$^+$/DCX$^+$	Improved Neurological deficits (body posture and sensorimotor integration) motor deficits also improved based on The elevated body swing test	Ren et al. (2015)
Huang-Lian-Jie-Du-Decoction (HLJDD)	Coptidis Rhizoma, Scutellariae Radix, Phellodendri Chinensis Cortex, Gardeniae Fructus.	Male Sprague–Dawley rats, create the permanent middle cerebral artery occlusion (pMACO)	ipsilateral cortex:Alkaloids: ↑BrdU$^+$,BrdU$^+$/MAP2$^+$ iridoids:↑BrdU$^+$,BrdU$^+$/MAP2$^+$ flavonoids:↑BrdU$^+$/ MAP2$^+$、↓BrdU$^+$/GFAP$^+$	↑Bederson scores and motor coordination (Beam walking test)	Zou et al. (2016)
Huatuo Zaizao pill	Chuanxiong Rhizoma, Borneol, Euodiae Fructus, Carthami Flos, angelicae Sinensis Radix.	Male Sprague–Dawley rats with Cerebral I/R model	peri-infarct regions of cortex of rats:↑ EdU$^+$ /NeuN$^+$	↑Cylinder test (assessed forelimb use asymmetry) Beam-walking test (coordination and integration of motor movements) and Adhesive (assess the sensorimotor deficit)	Duan et al. (2017)
Ginseng-Angelica-Shanseng-Pulvis (GASP)	Ginseng Radix et Rhizoma, Angelicae Sinensis Radix, Cinnamomi Cortex.	Male Sprague–Dawley (SD) rats with permanent MCAO	SVZ: 4.6 or 9.2 g/kg:↑Ki67$^+$ SGZ:2.3 g/kg:↓DCX$^+$, ↑DCX$^+$/ NeuN$^+$, GFAP$^+$, Nestin$^+$ 4.6 or 9.2 g/kg:↑DCX$^+$, DCX$^+$/NeuN$^+$, GFAP$^+$, Nestin$^+$	↑Sensorimotor functions (Basket Test and Adhesive Removal Test) and Recognition Memory (novel object recognition test); Cerebral Blood Flow and Infarction Volume	Liu et al. (2019)

(Continued)

TABLE 1 (Continued)

Prescription	Composition	Animals/cell types	Outcome measurement	Aspects of behaviors/function	References
Gualou Guizhi decoction	Trichosanthis Radix, Cinnamomi Ramulus, Paeoniae Radix Alba, Glycyrrhizae Radix, Zingiberis Rhizoma Recens, Jujubae Fructus.	Sprague Dawley rats ; Transient MCAO surgery	SVZ: ↑$BrdU^+$, DCX^+,$BrdU^+$/DCX^+, Striatum: ↑$BrdU^+$/$GFAP^+$	↓ The modified neurological severity score and the balance beam score a lower percentage of foot faults	Han et al. (2018)
Sanhua Decoction (SHD)	Rhei Radix et Rhizoma, Notopterygii Rhizoma et Radix, Magnoliae Officinalis Cortex, Aurantii Fructus Immaturus.	Sprague–Dawley (SD) rats; MCAO	SVZ: ↑$BrdU^+$,$BrdU^+$/DCX^+	↓ Neurological Deficit Scores	Fu et al. (2020)
Yi-nao-jie-yu prescription (YNJYP)	Acanthopanacis Senticosi Radix et Rhizoma Seu Cauls, Curcumae Radix, Schisandrae Chinensis Fructus, Gardeniae Fructus, Salviae Miltiorrhizae Radix Et Rhizoma, Chuanxiong Rhizoma.	Sprague–Dawley rats; Combined MCAO and Depression Model	DG: ↑$BrdU^+$ /$NeuN^+$ DG: ↓$BrdU^+$/$GFAP^+$	↓ The immobility time of forced swim test ↑ increased the sucrose preference	Tian et al. (2018)
Jieyu Anshen granule (JY)	*Bupleuri Radix, Jujubae Fructus, Acori Tatarinowii* Rhizoma, Pinelliae Rhizoma Praeparatum *Cum* Zingibere et Alumine, Atractylodis Macrocephalae Rhizoma, Tritici Levis Fructus, Polygalae Radix, Glycyrrhizae Radix et Rhizoma, Gardeniae Fructus, Lilii Bulbus, Arisaema *Cum* Bile, Curcumae Radix, Dragon's Teeth, Ziziphi Spinosae Semen, Poria, Angelicae Sinensis Radix.	Sprague–Dawley rats:MCAO + CUMS (MCAO, then CUMS for 18 days	DG: ↑ $BrdU^+$/$NeuN^+$	↑Open-field and sucrose preference tests, in beam-walking, cylinder, grip strength, and water maze tests	Du et al. (2020)
modified "Shengyu" decoction (MSD)	Rehmanniae Radix Praeparata, Paeoniae Radix Alba, Chuanxiong Rhizoma, Ginseng Radix et Rhizoma, Angelicae Sinensis Radix, Salviae Miltiorrhizae Radix et Rhizoma, Astragali Radix, Myrrha, Acori Tatarinowii Rhizoma, Curcumae Radix.	Sprague–Dawley rats with TBI	Cortex, CA1, CA3,and DG:↑$BrdU^+$/$Nestin^+$	↑Neurological functions by beam balance and prehensile traction tests	Chen M. M. et al. (2015)
MLC901	Astragali Radix, Salvia Miltiorrhizae Radix, Paeoniae Radix Rubra, Chuanxiong Rhizoma, Angelicae Sinensis Radix, Carthami Flos, Persica Prunus, Polygalae Radix, Acori Tatarinowii Rhizoma.	Male Sprague–Dawley rats with TBI	DG: ↑$BrdU^+$	↑Modified version of object recognition task called the "what-where-when" test	Quintard et al. (2014)
Kami-ondam-tang	Pinelliae Rhizoma, Bambusae Caulis, Aurantii Immaturus Fructus, Poria, Citri Reticulatae Pericarpium, Glycyrrhizae Radix, Polygalae Radix, Scrophulariae Radix, Ginseng Radix, Rehmanniae Radix, Zizyphi Spinosae Semen, Jujubae Fructus, Zingiberis Rhizoma.	Male ICR mice	DG: ↑ DCX^+	↑Step through latency in the retention trial of the passive avoidance task	Hong et al. (2011)
Xiaochaihutang	Bupleuri Radix, Scutellariae Radix, Ginseng, Radix Glycyrrhizae, Zingiberis Rhizoma Recens, Jujubae Fructus.	Kunming mice	DG(HRG): ↑$Ki\text{-}67^+$,DCX^+	↓Immobility duration in Tail suspension test and Forced Swim. the latency in Novelty Suppressed Feeding Test ↑ immobility latency in Forced Swim Test.	Zhang et al. (2015)

(Continued)

TABLE 1 (Continued)

Prescription	Composition	Animals/cell types	Outcome measurement	Aspects of behaviors/function	References
		Mice were injected subcutaneously with CORT (40 mg/kg) dissolved in sesame oil for 35 days.	DG:XCHT (2.3,7,21 g/kg):↑Ki-67 $^{+}$ XCHT (7,21 g/kg):↑Ki-67^{+}, DCX^{+}	↑Weight, the coat state, the escape behavior in open field test and elevated plus maze, immobility time in tail suspension test and forced swimming test.	Zhang et al. (2016)
		Male C57 BL/6 J mice were reared isolated for 8 weeks	DG:XCHT (2.3 g/kg):↑Ki-67 $^{+}$ XCHT (7.0 g/kg):↑Ki-67^{+}, BrdU^{+}, DCX^{+}	↑ Immobility time in TST and FST, OFT and EPM, aggressive behaviors of SI-reared mice.	Ma C. L. et al. (2017) and Ma J. et al. (2017)
Chaihu Shugan San	Bupleuri Radix, Citri Reticulatae Pericarpium, Chuanxiong Rhizoma, Cyperi Rhizoma, Aurantii Fructus, Paeoniae Radix Alba, Glycyrrhizae Radix et Rhizoma.	perimenopausal rats exposed to chronic unpredictable mild stress (CUMS).	DG:2 g/kg CSS:↑ DCX^{+}	↑ The sucrose preference. ↓immobility time of the forced swimming test.	Chen et al. (2018)
		C57BL/6 mice exposed to chronic unpredictable mild stress (CUMS).	DG: ↑BrdU^{+}, NeuN^{+}/BrdU^{+}	↑Sucrose preference ↓immobility time in the TST and FST	Zhang et al. (2021)
Kaixinsan	Ginseng Radix et Rhizoma, Smilacis Glabrae Rhizoma, Polygalae Radix, Acori Tatarinowii Rhizoma.	Cortical and hippocampal neurons, from SD rat embryos at days of 18	KXS2012 in DIV 5 of cortical neurons: ↑synaptic vesicle protein, synaptotagmin KXS2012 in DIV 15 of cortical neurons: ↑the dendritic spine density;↑synaptotagmin expression	↑Sucrose preference; cumulative immobility time of forced swimming test; open field tests	Yan et al. (2016)
		male Sprague–Dawley rats ; CMS rat models of depression	Functional analysis: differentially expressed proteins participate in synaptic plasticity, neurodevelopment, and neurogenesis	↑Sucrose consumption and body weight	Dong et al. (2020)
kami-shoyo-san	Paeoniae Radix; Bupleuri Radix; Atractylodis Macrocephalae Rhizoma; Liriopis Tuber; Angelicae Gigantis Radix; Hoelen; Menthae Folium; Glycyrrhizae Radix; Zingiberis Rhizome.	Sprague–Dawley rats; Immobilization stress for 21 days (Stress group)	DG (KSS 20X):↑ BrdU^{+}	↓Immobility times compared to the control group.	Park et al. (2007)
Jiaweisinisan	Bupleurum, Peony Root, Citrus Aurantium, Medlar, Gardenia, Rehmanniae, Abalone.	a stress damage model was established with 120 μM corticosterone	↑BrdU^{+} ↓BrdU^{+}/TUNEL^{+}	Cell	Wu et al. (2013)
		Wistar rats weighing;6-week Chronic Unpredictable Mild Stress (CUMS) model	DG: ↑BrdU^{+}/DCX^{+}	↑Sucrose preference, locomotion activity level and accuracy of T-maze, as well as increased immobility time	Wang H. Z. et al. (2021) and Wang J. et al. (2021)
Wuling Capsule	*Wuling*	Sprague–Dawley rats were subjected to3-week CMS to induce depression	DG: ↑ BrdU^{+}	↑Sucrose preference	Li et al. (2010)
Kososan	Cyperi Rhizoma, Perillae Herba, Aurantii Nobilis Pericarpium, Glycyrrhizae Radix, Zingiberis Rhizoma	Male C57BL/6 J were exposed to 10 min of social defeat stress from an aggressive CD-1 mouse for 10 consecutive days (days 1–10).	DG: ↑BrdU^{+}/DCX^{+}	↑Social avoidance, depression- and anxiety-like behaviors,	Ito et al. (2017)
Ninjinyoeito	Rehmannia Root, Japanese Angelica Root, Atractylodes Rhizome, Poria Sclerotium, Ginseng, Cinnamon Bark, Polygala Root, Peony Root, Citrus Unshiu Peel, Astragalus Root, Glycyrrhiza, Schisandra Fruit.	C57BL6 mice were administered CORT (100 mg/m) in place of drinking water for 14 days， Animal were weaned with 50 mg/ml CORT for 3 days and then with 25 mg/ml CORT for 3 days to allow for gradual recovery of endogenous corticosterone secretion.	DG: ↑Ki67, DCX^{+}	↓ Immobility and latency to immobility of the tail suspension; ↑ the latency to immobility of the forced swim test; sucrose consumption rate; spontaneous alternations with Y-maze test; spent more time with the novel object	Murata et al. (2018)

(Continued)

TABLE 1 (Continued)

Prescription	Composition	Animals/cell types	Outcome measurement	Aspects of behaviors/function	References
		NPCs from the adult mouse hippocampus;NPCs were cultured for 72 h in the presence of 20 mM CORT	↑$BrdU^+$ in a dose dependent manner	Cell	Murata et al. (2018)
Jie Yu Chu Fan (JYCF) capsule	Gardeniae Fructus, Magnoliae Officinalis Cortex, Pinelliae Rhizome, Forsythiae Fructus.	C57BL/6 mice were subjected to the following mild stressors for 5 weeks (CUMS)	DG: ↑$Ki\text{-}67^+$, $NeuN^+$, $MAP\text{-}2^+$	↑Weight; the number of crossings of open field test; sucrose preference; ↓ immobility time of the forced swim test	Ji et al. (2020)
Zhengtian capsule (ZTC)	Spatholobi Caulis, Angelicae Sinensis Radix, Chuanxiong Rhizoma, Asari Radix Et Rhizoma, Uncariae Ramulus *Cum* Uncis, Paeoniae Radix Alba, Angelica Dahuricae Radix, Rehmanniae Radix, Saposhnikoviae Radix, Notopterygii Rhizoma et Radix, Persicae Semen, Carthami Flos, Angelicae Pubescentis Radix, Ephedrae Herba, Aconiti Lateralis Radix Praeparata,	Kunming (KM) mice were intraperitoneally injected with a single dose of LPS (5 mg/kg)	DG: ↑$BrdU^+$, ↑$GAD67^+$, DCX^+, $BrdU^+/DCX^+$	↑The crossing numbers and the grooming numbers; coordination and balance of exercise	Yang et al. (2020)
Fuzhisan	Ginseng, Baical, Acorus Talarinowi Rhizoma, Glycyrrhizae Radix.	Eight-month-old male SAMP-8	SGZ: ↑$BrdU^+$, $PCAN^+$	↓The average escape latency, ↑The number of crossings of the platform location	Yang et al. (2011)
Yokukansan (YKS)	Atractylodes Lancea Rhizome, Poria Sclerotium, Cnidium Rhizome, Angelica Radix, Uncaria Uncis *Cum* Ramulus, Bupleurum Radix, Glycyrrhizae Radix	Male SAMP8 mice at 5 months of age	DG: ↑ $BrdU^+$	↓The escape latency and the swimming path length	Azuma et al. (2018)
Herbal formula PM012	Lycii Fructus, Rehmanniae Radix, Corni Fructus, Dioscoreae Radix, Hoelen, Alismatis Radix, Mountain Cortex Radices.	3xTg mice carrying a mutant APP (KM670/671NL), a human mutant PS1 (M146V) knock-in and tau (P301L) transgenes [B6;129-Psen1tm1Mpm Tg(APPSwe,tauP301L)1Lfa/J] mice	CA1 and DG: PM012 (100 mg): ↑$BrdU^+/NeuN^+$. PM012 (400 mg):↑DCX^+, $BrdU^+/NeuN^+$	↓ Escape latencies, increased time spent in the target zone during probe tests.	Ye et al. (2016)
Jowiseungchungtang (JWS)	Coicis Semen, Castaneae Semen, Raphani Semen, Longanae Arillus, Liriopis Tuber, Platycodi Radix, Acori Gramineri Rhizoma, Thujae Semen, Zizyphi Semen, Massa Medicata Fermentata, Ephedrae Herba, Schisandrae Fructus, Amomi Semen, Polygalae Radix.	5XFAD mice have mutations in the *APP* SweK670N/M671L, LonV717I, and FloI716V) and *PSEN1* (M146L and L286V) genes regulated by the Thy1 promoter.	DG: ↑$Ki\text{-}67^+$, DCX^+	Not given	Shin et al. (2018)
Shenzao jiannao oral liquid (SZJN)	Ginseng Radix et Rhizoma，Ziziphi Spinosae Semen， Celastrus Orbiculatus Thunb，Epimedii Folium，Rehmanniae Radix，Gastrodiae Rhizoma，Chrysanthemi Flos，Zingiberis Rhizoma，Glycyrrhizae Radix et Rhizoma.	Kunming mice (half-male and half-female); AD mouse model caused by a combination of Aβ42 and scopolamine	DG: ↑$BrdU^+$, $Nestin^+$ cortex and DG: ↑$NeuN^+$	↑ The learning and memory abilities of Morris water maze test	Xiao et al. (2020)
		NSCs were obtained from hippocampal tissues of neonatal C57BL/6 mice ; transfect NSCs with APP695swe and GFP genes	32 mg/ml of SZJN promote NSCs proliferation	Cell	Xiao et al. (2020)

improve abnormal adult neurogenesis, which may be related to neurological and psychiatric diseases. Besides, two kinds of TCMPs were also reported to improve adult neurogenesis under normal physiological conditions.

Traditional Chinese medicine prescriptions could improve neurological diseases, some of which were found to be related to adult neurogenesis. At present, it has been reported that the major neurological diseases improved by TCMPs mainly include AD, stroke, and traumatic brain injury (TBI), and these diseases are all related to abnormalities of neurogenesis. From a functional perspective, promoting adult neurogenesis plays an important role in structural plasticity and network maintenance in AD (Mu and Gage,

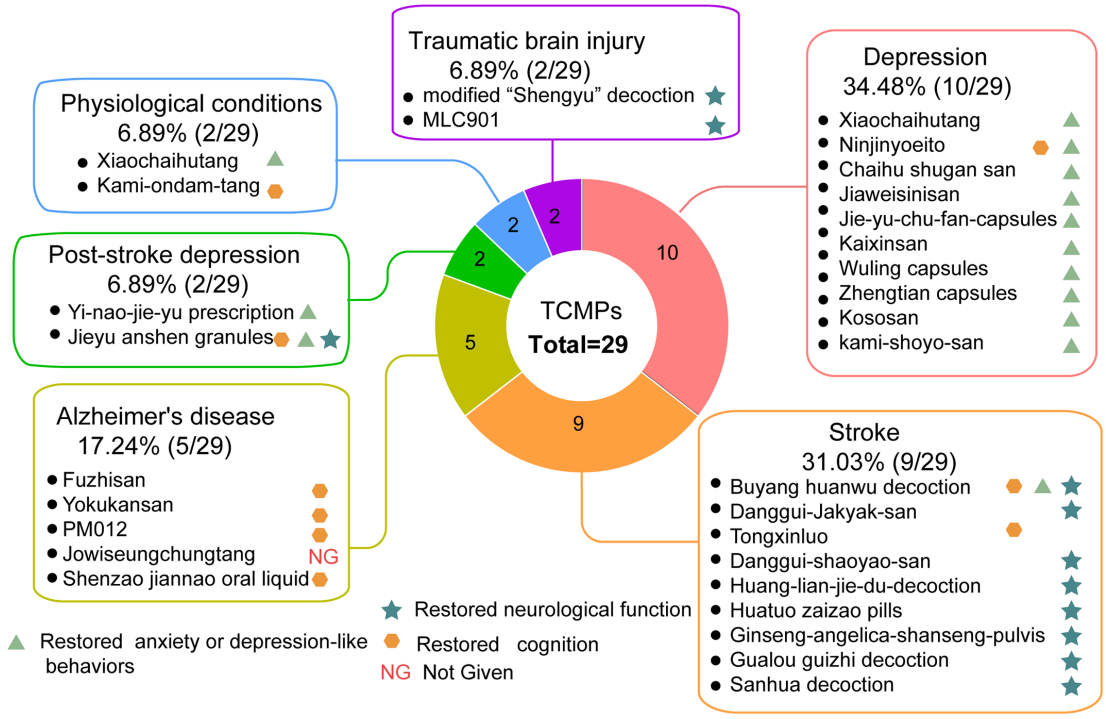

FIGURE 2
Pie chart of TCMPs improving adult neurogenesis and brain function, *n*=29. Xiaochaihutang improves adult neurogenesis in stroke and physiological conditions, so it was counted in two cases for two situations.

2011). Currently, five types of TCMPs are being used in the treatment of AD; four of them improved the cognitive function in AD, and one reduced amyloid-β (Aβ) aggregation and Aβ-mediated pathology. Different TCMPs may improve the behavioral or pathological abnormalities of AD by acting at different stages of neurogenesis. Fuzhisan (Yang et al., 2011) and yokukansan (Azuma et al., 2018) acted at the proliferation level, Shenzao Jiannao oral liquid acted at the proliferation and maturation stages (Xiao et al., 2020), and herbal formula PM012 acted at the differentiation and maturation stages (Ye et al., 2016). Moreover, Jowiseungchungtang (Shin et al., 2018) inhibited Aβ-mediated pathology in an AD animal model (5XFAD) and restored adult neurogenesis in the proliferation and differentiation stages. Nine types of TCMPs have been shown to be effective in treating stroke, which is another common neurological disease. Seven of these TCMPs increased post-stroke brain function, and two of them improved both brain function and cognition after stroke. The above-mentioned nine TCMPs improved the restoration of brain function after stroke by promoting neurogenesis proliferation, differentiation, and maturation. Danggui Shaoyao San (Ren et al., 2015), Huatuo zaizao pill (Duan et al., 2017), and Sanhua decoction (Fu et al., 2020) acted at the differentiation stage. Tongxinluo (Chen L. et al., 2014; Chen et al., 2016) and Gualou Guizhi decoction (Han et al., 2018) all had an effect on the proliferation and differentiation levels. Huang-Lian-Jie-Du decoction (Zou et al., 2016) and Danggui jakyak San (Song et al., 2013) targeted the stages of proliferation, differentiation, and maturation of neurogenesis. Significantly, Buyang Huanwu decoction (Wang et al., 2011; Liu et al., 2013; Chen H. J. et al., 2015; Chen et al., 2020; Zhuge et al., 2020) and Ginseng Angelica shansheng pulvis (Liu et al., 2019) not only improved post-stroke brain function but also improved cognition, which may be related to the action of these two TCMPs on the proliferation, differentiation, and maturation stages of neurogenesis. In addition, after TBI, modified "Shengyu" decoction (Chen M. M. et al., 2015) improved neurological function, and MLC901 (Quintard et al., 2014) restored cognitive function, which may be related to the fact that these two TCMPs promoted the proliferation of the NCS (Figure 2).

The most important psychiatric disorder improved by TCMPs is depression. Depression is associated with impairments in adult neurogenesis in the dentate gyrus, while the effects of antidepressants are mediated by increased neurogenesis. Increasing adult hippocampal neurogenesis could reduce anxiety and depression-like behaviors (Hill et al., 2015; Tunc-Ozcan et al., 2019). At present, a total of ten TCMPs alleviated the mental symptoms of depression, with nine of them significantly improving anxiety and depression-like mood after depression; one TCMP not only alleviated mood but also improved cognition. The aforementioned TCMPs that improve cognition and mood in depression may act on different stages of neurogenesis. Kami-shoyo-san (Park et al., 2007), Kososan (Ito et al., 2017), and Wuling capsules (Li et al., 2010) promoted the proliferation stage; Jiaweisinisan promoted the differentiation stage (Wang H. Z. et al., 2021); Kaixinsan promoted the maturation stage (Yan et al., 2016; Dong et al., 2020); Jie Yu Chu fan capsules (Ji et al., 2020), Xiaochaihutang (Zhang et al., 2015, 2016; Ma J. et al., 2017) and Zhengtian capsules (Yang et al., 2020) promoted the proliferation and differentiation stages; Chaihu-Shugan-San (Chen et al., 2018; Zhang et al., 2021) promoted the differentiation and maturation stages. In addition to reducing depressive symptoms, Ninjinyoeito (Murata

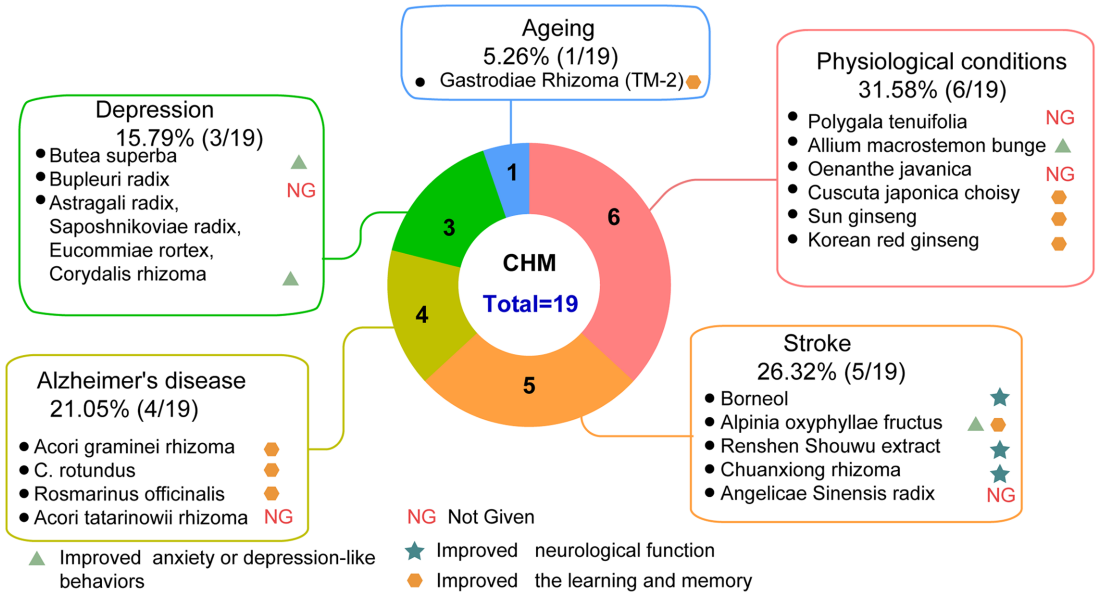

FIGURE 3
The effect of Chinese herbal medicine on adult neurogenesis and brain function, *n*=19.

et al., 2018) also improved cognitive performance, which may be connected to promoting the proliferation and differentiation stages of neurogenesis. Meanwhile, Kososan (Ito et al., 2017) improved mood, but it simply tended to advance the stage of proliferation. In addition, post-stroke depression (PSD) is a significant social and public health issue, and antidepressant preventive and curative treatments are worth investigating (Villa et al., 2018). TCMs not only ameliorated depression by affecting neurogenesis but also alleviated the symptoms of PSD by promoting the maturation of neurogenesis. Both Yi-nao-jie-yu (Tian et al., 2018) and Jieyu Anshen granules (Du et al., 2020) relieved the mood after PSD, restored brain function, and improved cognitive function; this may be related to the fact that these two TCMPs promoted NSC maturation.

In addition, under physiological conditions, Kami-ondam-tang (Hong et al., 2011) is good for cognition, and Xiaochaihutang (Zhang et al., 2015) is beneficial for emotion, which may be related to the fact that these TCMPs are able to promote the differentiation of neural stem cells.

The application of each of the above 29 types of TCMPs is based on the theory of TCM and has been consistently enhanced through the process of practice. As a result, neurogenesis has been improved in a variety of situations. It is evident that each TCMP contains several different herbs, but identifying which ones are the most important may be difficult to explain. Future research will focus on those factors that support adult neurogenesis and have either antagonistic or synergistic effects.

3.2. The effects of Chinese herbal medicine on adult neurogenesis

According to the "jun-chen-zuo-shi" principle of TCM, each CHM in a TCMP is essential and has a specific function (Zhang et al., 2014). The advancement of modern pharmacology has made it easier to further study the active components in TCM that promote adult neurogenesis. Therefore, the effects of CHMs on adult neurogenesis have been widely studied. Table 2 and Figure 3 summarizes the impact of CHMs on adult neurogenesis under different pathological and physiological situations.

The main neurological diseases that CHMs could improve are AD and stroke, and this improvement in neurological symptoms may be related to neurogenesis. Four CHMs promoted neurogenesis in AD animal models, and three of them improved the cognition of AD animals, but they had different effects on neurogenesis. Acori graminei rhizoma mainly acted on proliferation and differentiation (Ma et al., 2015), Rosmarinus officinalis mainly acted on differentiation (Mirza et al., 2021), and Cyperus rotundus mainly acted on maturation (Shakerin et al., 2020). In addition, Acori tatarinowii rhizoma (Mao et al., 2015) promoted the proliferation and maturation of neurogenesis in AD animal models, but its effect on cognition has not been shown. Five CHMs have improved brain function after an ischemic stroke. The restored brain function after stroke may be related to chuanxiong rhizome-stimulated differentiation (Wang et al., 2020), Borneol (Zhang X. G. et al., 2017), and Renshen Shouwu extract stimulated maturation (Li et al., 2020). Meanwhile, Alpiniae oxyphyllae fructus improved cognition and mood after stroke, which may be related to its promotion of cell proliferation, differentiation, and maturation (He et al., 2020).

Three reports indicate that CHMs improved the neurogenesis of depression Butea superba (Mizuki et al., 2014); Astragali radix, Saposhnikoviae radix, Eucommiae cortex, and Corydalis rhizoma (Sun et al., 2016) all have the potential to lessen depression, and one of the possible mechanisms is the promotion of the proliferation of neurogenesis. In addition, Bupleuri radix is a key component in a number of oriental herbal medicines used to treat stress and other psychiatric illnesses, and these seem to have proliferative effects (Seo et al., 2013).

TABLE 2 Effects of CHMs on neurological conditions and adult neurogenesis.

Herbs	Extraction method	Animals/cell types	Outcome measurement	Aspects of behaviors/ function	References
Polygalae Radix	EtOH extract	Adult male Sprague–Dawley rats	CA1:↑ $BrdU^+$. ↑ $Nestin^+/BrdU^+$, $Tuj1^+/BrdU^+$	Not GIVEN	Park et al. (2008)
		HiB5(rat neuronal precursor cells)	↑Promoted the neurite outgrowth	Cell	Park et al. (2008)
Allium macrostemon Bunge (AM-W)	Water extract	Male ICR mice	CA1:100 mg/kg: ↑ DCX^+, $NeuN^+/BrdU^+$ 200 mg/kg: ↑ $BrdU^+$,DCX^+,$NeuN^+/BrdU^+$	↓The immobility duration of the forced swimming test ↓the immobility duration of the tail suspension test	Lee et al. (2010)
Sun ginseng	EtOH extract	Male ICR mice	DG: 20 mg/kg: ↑ $BrdU^+$,DCX^+	↑ The step-through latency	Lee et al. (2013)
Oenanthe javanica	EtOH extract	male Wistar rats	DG: ↑ DCX^+, $Ki\text{-}67^+$	Not GIVEN	Chen B. H. et al. (2015)
Acori tatarinowii Rhizoma	EtOH extract	C57BL/6 mice	DG:↑$BrdU^+$、$Ki67^+$ ↑$Tbr2^+/BrdU^+$ ↑DCX+/Ki67+, DCX+/Ki67 ↑$BrdU^+/NeuN^+$	Not GIVEN	Mao et al. (2015)
		NPCs from hippocampal of C57BL/6 mice	↑EDU^+	Cell	Mao et al. (2015)
Cuscutae Semen	Water extract	Male ICR mice	DG: 10 mg/kg/day: ↑ $BrdU^+/NeuN^+$ 50 mg/kg/day:↑$Ki\text{-}67^+$, DCX^+, $BrdU^+/NeuN^+$ 100 mg/kg/day:↑$Ki\text{-}67^+$, DCX^+, $BrdU^+/DCX^+$, $BrdU^+/NeuN^+$	↑ Time exploring the novel object	Moon et al. (2016)
Korean red ginseng		C57BL/6 mice	DG: ↑$BrdU^+$, $BrdU^+/DCX^+$	↑ The learning and memory abilities of Morris water maze test	Ryu et al. (2020)
Astragali Radix, Saposhnikoviae Radix, Eucommiae Cortex, Corydalis Rhizoma	Water extract	The mouse NSC line (mNSC 9,601)	↑ cell proliferation (MTS assay)	Cell	Sun et al. (2016)
		BALB/c mice; chronic mild stress (CMS) was used in mice for 14 days to establish a depression-like mouse model.	DG: ↑$BrdU^+$	↑ The body weight gain ↓ the duration of immobility in the FST	Sun et al. (2016)
Bupleuri Radix	Water extract	Oxidative stress induced by serum deprivation in SH-SY5Y cells	↑ $BrdU^+$	Cell	Seo et al. (2013)
Butea superba (BS)	EtOH extract	72 male ddY mice were obtained at the age of 7 weeks old, The UCMS group received various unpredictable stressful stimuli for 7 weeks	DG↑ DCX^+	↑The sucrose intake ↓the immobility times (tail suspension test)	Mizuki et al. (2014)
Acori graminei Rhizoma (AGR)	Water extract, volatile oil fraction, or defatted decoction fraction of AGR	Alzheimer disease-like symptoms induced by Amyloid Beta (Aß) 1–42 intra-hippocampal injection for 7 days	DG↑ DCX^+, $Nestin^+$	↑Spatial memory (Morris water maze)	Ma et al. (2015)
Rhizoma Acori tatarinowii		aged C57BL/6 mice (age at 18–23 months);8-month-old middle-aged APP/PS1 mice	DG aged mice: ↑ $BrdU^+$,$BrdU^+/NeuN^+$ APP/PS1:↑$BrdU^+$,$Ki67^+$,$BrdU^+/NeuN^+$	Not given	Mao et al. (2015)
C. rotundus	EtOH extract	Wistar rats received 5 ug/ul Aβ1-42 into CA1 bilaterally for AD	DG: ↑$NeuN^+$	↑Spatial memory (Morris water maze test)	Shakerin et al. (2020)
Gastrodiae Rhizoma (TM-2)	EtOH extract	C57BL/6 mice, The D-gal groups were subcutaneously injected with 200 mg/kg D-gal daily for 8 weeks to establish the aging model.	DG:↑$BrdU^+$,DCX^+	↑Spatial memory (Morris water maze test); Burrowing and nesting behaviors	Hsu et al. (2021)
Rosmarinus officinalis	EtOH extract	BALB/c male mice; Aβ1-42 peptide (dilution 1 μg per μl) was injected into the CA1 area of the hippocampus for AD	Hippocampus(mRNA):↑$Ki67^+$;DCX^+; $NeuN^+$	↑Spatial memory (Morris water maze test) and object recognition memory (NOR test) exhibit anti-anxiety effects (the elevated plus maze test)	Mirza et al. (2021)
Borneol	Borneol was dissolved in 5% Tween 80 and given to mice by gavage	C57BL/6 mice, with Focal Cerebral Ischemia–Reperfusion Model	Infarct zone:↑$NeuN^+$ ↓$GFAP^+$	↑ Neurological score and global score	Zhang X. et al. (2017) and Zhang X. G. et al. (2017)

(Continued)

TABLE 2 (Continued)

Herbs	Extraction method	Animals/cell types	Outcome measurement	Aspects of behaviors/ function	References
Alpiniae Oxyphyllae Fructus	EtOH extract	C17.2 cells exposed to 4-h OGD plus 20-h reoxygenation	*p*-coumaric acid:↑$BrdU^+$/$Ki67^+$ ↑$BrdU^+$/$SOX2^+$	Cell	He et al. (2020)
		Sprague–Dawley (S.D.) rats were subjected to MCAO to induce cerebral ischemia animal model	DG and SVZ: *p*-coumaric acid:↑$BrdU^+$/$Ki67^+$, $BrdU^+$/DCX^+, $BrdU^+$/$NeuN^+$in the	↑ Body Weight; spatial learning/ memory (Morris water maze test) and recognition capacity (NOR test), ↓anxiety (open-field test)	He et al. (2020)
Renshen Shouwu extract	EtOH extract	Sprague–Dawley rats with Middle cerebral artery occlusion (MCAO) surgery	Penumbra: ↑$NeuN^+$/$BrdU^+$	↑Neurological function (the Zea Longa' method)	Li et al. (2020)
Chuanxiong Rhizoma	EtOH extract	Wistar rats was induction of microsphere-induced cerebral embolism (ME) FOR ischemia	DG: ↑DCX^+	↑Neurological score after operation at 1, and 3 days, respectively	Wang et al. (2020)
Angelicae Sinensis Radix	Water extract	Sprague–Dawley rats; global cerebral ischemia (GCI) was induced in the rats using the 4-vessel occlusion (4-VO) method	ASD-0.5 g, and ASD-1 g: SGZ: ↑$BrdU^+$ and $BrdU^+$/$NeuN^+$ SGZ: ↑$Ki67^+$ and $Ki67^+$/$nestin^+$ CA1: ↑$MAP\text{-}2^+$/$NeuN^+$	Not GIVEN	Cheng et al. (2021)

Six CHMs promote neurogenesis under physiological conditions, and three of these improved learning and memory, with one CHM alleviating emotion and two others promoting neurogenesis (however, their effects on cognition and emotion were not demonstrated). The following three CHMs have been shown to improve learning and memory. Their potential mechanisms may involve sun ginseng, which promotes NSC proliferation and survival (Lee et al., 2013), Korean red ginseng, which promotes NSC differentiation (Ryu et al., 2020), and Cuscuta japonica Choisy, which promotes NSC proliferation, differentiation, and maturation (Moon et al., 2016). Allium macrostemon Bunge (Lee et al., 2010) was beneficial to antidepressant-like activity and promoted the proliferation, differentiation, and maturation of neurogenesis. In addition, Oenanthe javanica encouraged neurogenesis proliferation and differentiation (Chen B. H. et al., 2015), and the root of Polygala tenuifolia encouraged neurogenesis proliferation and maturation (Park et al., 2008), although their effects on cognition and emotion under physiological situations were not demonstrated. In Asia, certain CHMs, such as Korean red ginseng, are used as both medicine and food.

3.3. The effects of bioactive components on adult neurogenesis

The bioactive components were extracted from CHMs due to their structural diversity and biological activities, which make them important sources of clinical drugs. Although there are fewer components in CHMs than in TCMPs, it is still very difficult to determine which components are effective. Therefore, the separation and extraction of bioactive components from CHMs for research provide a more stable outcome and may be conducive to the study of pharmacological mechanisms. The destiny of NSCs may be influenced by bioactive components (Zhang Z. et al., 2018), and bioactive components' support of adult neurogenesis has attracted extensive attention. Table 3 and Figure 4A show the 17 kinds of bioactive components that were reported to improve adult neurogenesis in connection to physiological or pathological conditions. The effects of bioactive components on adult neurogenesis have been studied at the cellular and animal levels (Table 3).

At present, *in vivo* experiments have shown that bioactive components are being used to treat neurologic diseases such as stroke, PD, multiple sclerosis, and aging. Five bioactive components improved symptoms after stroke, promoting neurogenesis. Cornel iridoid glycoside (Yao et al., 2009) restored brain function, which may be related to NSC proliferation. Learning and memory after stroke were improved by salvianolic acid B (Zhuang et al., 2012) and Gastrodin (Xiao et al., 2021). This improvement may have been caused by the stimulation of neurogenesis. Astragaloside IV (Chen et al., 2019; Li et al., 2021) not only restored brain function after stroke but also improved cognition, which may have the potential to encourage NSC proliferation, differentiation, and maturation. Baicalin also performed well in regulating proteins in energy metabolism, but had a relatively weak effect in the regulation of proteins in neurogenesis and apoptosis, according to results from proteomics to explore the various protein expression modes in mouse brains after stroke (Zhang et al., 2009). Magnesium lithospermate B (Zhang Z. et al., 2018) improved the cognitive function of PD animal models, which may be connected to NSC growth promotion. Scutellarin (Wang et al., 2016) alleviated behavioral deficits in a mouse model of multiple sclerosis, possibly by inhibiting NSC apoptosis and promoting NSC differentiation into myelin-producing oligodendrocytes. *Lycium barbarum* polysaccharides (LBP) (Chen W. et al., 2014) prevented cognitive and memory deficits, in addition to decreasing cell proliferation and neuroblast differentiation, in scopolamine-treated rats. Ginsenoside Rg1 prevented cognitive impairment in a rat model of aging (Zhu et al., 2014). This may be related to its ability to protect NSCs/NPCs and promote differentiation. Depression is the primary psychiatric illness alleviated by the bioactive components. Five bioactive components improved the symptoms of depression, with four of them relieving depression-like mood. This may be related to the fact that these four bioactive components can affect the neurogenesis of depression in model mice. Curcumin promoted

TABLE 3 The bioactive components of neurological conditions and adult neurogenesis.

Bioactive components	Source	Animals/cell types	Outcome measurement	Aspects of behaviors/function	References
In vivo					
Baicalin	Scutellariae Radix	KunMing mice; MCAO model	Baicalin performed well in regulating proteins in energy metabolism but had a relatively weak effect in the regulation of proteins in neurogenesis and apoptosis	↑Nissl's bodies	Zhang et al. (2009)
Cornel iridoid glycoside (CIG)	Corni Fructus	Sprague–Dawley rats; The middle cerebral artery occlusion was induced for MCAO	CIG (60 and 180 mg/kg/day):↑ $BrdU^+$, $Nestin^+$ in the ischemic ipsilateral SVZ 14–28 days after MACO,	↑ Neurological function (Modified neurological severity score)	Yao et al. (2009)
Salvianolic acid B	Salviae Miltiorrhizae Radix et Rhizoma	Wistar rats were subjected to transient forebrain ischemia	DG: 50 mg/kg Sal B ↑$BrdU^+$	↑ The learning and memory ability (Morris water-maze)	Zhuang et al. (2012)
Gastrodin	Gastrodiae Rhizoma	C57BL/6 J mice with *cerebral ischemia*	DG: Day15: ↑$BrdU^+$, DCX^+ in the dentate gyrus. Day29:↑$BrdU^+$/$NeuN^+$ cells,	↑Spatial memory (Morris water-maze)	Xiao et al. (2021)
Astragaloside IV	Astragali Radix	Sprague–Dawley rats; middle *cerebral artery occlusion/ reperfusion model*	Peri-ischemic regions: ↑$BrdU^+$/$NeuN^+$ and $BrdU^+$/$GFAP^+$	↑ *Neurological function recovery* (modified neurological severity score) ↓infarct volume (toluidine blue solution)	Li et al. (2021)
		Sprague–Dawley (SD) rats with Cerebral Ischemia–Reperfusion Model	SVZ and DG: ↑$BrdU^+$/$SOX2^+$, $BrdU^+$/DCX^+, $BrdU^+$/$NeuN^+$-positive staining cells ↑$BrdU^+$/$GFAP^+$	↑Spatial memory (Morris water-maze test), and Motor Function (the rotarod test) Recovery	Chen et al. (2019)
Baicalin	Scutellariae Radix	Sprague–Dawley rats ; corticosterone groups at a dose of 40 mg/kg daily for 14 days to induce stress.	DG: ↑DCX^+	Not given	Jiang et al. (2013)
		C57BL/6 N mice were exposed to chronic CORT treatment (70 μg/ml/day, 30 days). APPL2 Tg mice (male, 8 weeks)	↑$BrdU^+$、$BrdU^+$/$NeuN^+$in DG region; ↑$BrdU^+$/$NeuN^+$ cells in the GCL areas;6.7 mg/kg/day:↑$BrdU^+$/DCX^+, density of neuronal progenitors at both dorsal and ventral SVZ regions	↓The CORT-Induced Depressive- and Anxiety-Like Behaviors (tests including splash, tail suspension test, forced swim test, open field test, and novelty suppressed feeding)	Gao et al. (2018)
		Male ICR mice CUMS for 6 weeks	DG: ↑DCX^+, $BrdU^+$/$NeuN^+$ the SGZ	↑ Sucrose consumption, the number of crossings in open filed test and ↓the immobility time in tail suspension test	Zhang et al. (2019)
Curcumin	Xiaoyao-san	Sprague–Dawley (SD) rats, stress was administered once per day over a period of 20 days	DG:(at 10 and 20 mg/kg): ↑$BrdU^+$	Not given	Xu et al. (2007)
2,3,5,4′-Tetrahydroxystilbene-2-O-beta-D-glucoside (THSG)	Polygoni Multiflori Caulis	C57BL/6 mice chronic restraint stress for 28 days	Hippocampus: (40 mg/ml): ↑DCX^+	Depressive-like behaviors in CRS mice as measured by the tail suspension test, forced swimming test, and open-field test.	Jiang et al. (2018)
Helicid	Helicia nilagirica	Sprague–Dawley (SD) rats; Chronic Unpredictable Mild Stress for 12 weeks	CA1 and DG: ↑$BrdU^+$ in the	↑body weight; sucrose consumption, distance and number of crossings in the open-field test (OFT), ↓the immobility times in the forced swimming test (FST) and improved spatial memory in the Morris water maze (MWM);	Li et al. (2019)
Fuzi polysaccharide-1	Aconiti Lateralis Radix Praeparata	Male C57BL/6 J mice	DG: A single injection of FPS (10–400 mg/kg):↑$BrdU^+$ in the DG; FPS (100 mg/kg,7 Days):↑$NeuN^+$/$BrdU^+$、the proportion of $NeuN^+$/$BrdU^+$ cells to the total number of $BrdU^+$	↓ Immobility in the forced swim test, and latency in the novelty suppressed-feeding test.	Yan et al. (2010)

(Continued)

TABLE 3 (Continued)

Bioactive components	Source	Animals/cell types	Outcome measurement	Aspects of behaviors/function	References
Magnesium lithospermate B	*Salviae Miltiorrhizae Radix et Rhizoma*	PD rat model	↑Ki67$^+$, Thy1$^+$, in DG region ↑MAP2$^+$ and PSD95 in hippocampal region	↑Spatial memory (Morris water maze)	Zhang J. H. et al. (2018), Zhang R. et al. (2018), Zhang Z. et al. (2018)
L. barbarum polysaccharides (LBP)	Lycii Fructus	Sprague–Dawley rats; Scopolamine-Treated Rats pumps 440 mg/ml of SCO solution were subcutaneously embedded in abdominal wall SCO release (0.25 ml/h) was maintained for 28 days	DG: ↑Ki67$^+$, DCX$^+$	↑ Time exploring the novel object or location in the recognition tasks ↓ escape latency in the water maze.	Chen W. et al. (2014)
		Sprague–Dawley rats received daily i.p. injection with 40 mg/kg dextromethorphan for 14 days	DG: ↑DCX$^+$, ↑DCX$^+$/BrdU$^+$	Alleviated DXM-induced depression-like (forced swim test) and social anxiety-like behaviors (social interaction test)	Po et al. (2017)
		Sprague–Dawley rats	↑Ki-67$^+$	Not given	Wang et al. (2015)
Scutellarin	*Erigeron breviscapus* Hand-Mazz	C57BL/6 mice were exposed to cuprizone (8 mg/day) *via* food intake (0.2% cuprizone in standard rodent chow) for 6 weeks	SVZ: ↑Sox2$^+$, Nestin$^+$	↓ The motor deficit (rotarod test)	Wang et al. (2016)
Aromatic (ar-) turmerone	Curcumae Longae Rhizoma	Spontaneously breathing male Wistar rats ； single intracerebroventricular injection of 3 mg ar-turmerone at a concentration of 1 mg/μl.	SVZ: ↑DCX$^+$ in	Not given	Hucklenbroich et al. (2014)
Scorpion venom heat-resistant peptide	Scorpio	C57BL/6 male mic	SGZ and OB: ↑BrdU$^+$, BrdU$^+$/NeuN$^+$,PSA-NCAM$^+$ SGZ and SVZ: ↑GFAP$^+$/ Nestin$^+$ radial glia-like precursors	Not given	Wang et al. (2014)
Schisandrin A and B	Schisandrae Chinensis Fructus	Kunming White mice	DG: Sch A:↑GFAP$^+$, NeuN$^+$ Sch B: ↑PHH3$^+$, GFAP$^+$, NeuN$^+$	Not given	Cai et al. (2020)
Koumine	Gelsemium elegans Benth	Both male and female c57BL/6 J mice	SGZ: ↓DCX$^+$, BrdU$^+$, BrdU$^+$/DCX$^+$ in the	Prenatal KM:↓cognitive and memory (Morris water maze, Y-maze test, and novel object recognition test), long-term potentiation Prenatal KM offspring: ↑Anxiety-like behavior (the open field test and elevated plus maze test)	Yang et al. (2021)
In vitro					
Salvianolic acid B	Salviae Miltiorrhizae Radix et Rhizoma	Primary neurospheres were from the cerebral cortex of 13.5-day-embryonic Wistar rats	Promoting NSPCs proliferation. ↑Nestin and Notch-1	Cell	Zhuang et al. (2012)
Magnesium lithospermate B	Salviae Miltiorrhizae Radix et Rhizoma	NSCs were from the hippocampal of newborn mice. Wide type newborn C57BL/6 mice (P1 age)	Increasing effect reached the maximum around the concentration of 10 μg/ml, and maintained its effect on proliferation of NSCs at 50 and 100 μg/ml	Cell	Zhang J. H. et al. (2018), Zhang R. et al. (2018), Zhang Z. et al. (2018)
Angelica polysaccharide	Angelicae Sinensis Radix	NSCs	ASP increased the cell proliferation, and proliferation viability of ASP treated NSCs was dose-dependent (0–160 ug/mL).	Cell	Cheng et al. (2019)
Astragaloside IV	Astragali Radix	Neural progenitor cell line C17.2 cells (1 × 104 cells/ml).	↑ BrdU$^+$, the diameters of neurosphere, and cell viability	Cell	Chen et al. (2019)

(Continued)

TABLE 3 (Continued)

Bioactive components	Source	Animals/cell types	Outcome measurement	Aspects of behaviors/function	References
Saikosaponins-d	Bupleuri Radix	Primary NPCs were isolated from the hippocampus of newborn C57BL/6 J mice	Dose dependent decrease in cell viability in NPCs. NPCs were incubated with SSd (2, 4 μM) for 24 h:↓Edu^+, $Ki67^+$	Cell	Qin et al. (2019)
Tetramethylpyrazine	Chuanxiong Rhizoma	SH-SY5Y human neuroblastoma cells	Western blot analysis showed that MAP2 and tau started to increase from 5 days and 3 days, respectively, after treatment with TMP	Cell	Yan et al. (2014)
Musk ketone	Musk	Brain tissues from neonatal rats were aseptically obtained for NSC Establishment of oxygen–glucose deprivation (OGD) cell model *in vitro*	Treated with 0.9 lM or 1.8 lM musk ketone: ↑$BrdU^+$/$Tju\text{-}1^+$ and $BrdU^+$/$vimentin^+$ cells	Cell	Zhou et al. (2020)
Epimedium flavonoids	Epimedii Folium	Hippocampi from neonatal 1-day rats were isolated and mechanically triturated	10, 50 mg/ml: ↑axons' lengths 100 mg/ml: ↑average migration distances、axons' lengths 200 mg/ml:↑neurospheres	Cell	Yao et al. (2010)
Aromatic (ar-) turmerone	Curcumae longae Rhizoma	NSCs were cultured from fetal rat cortex at embryonic day 14.5	1.56 μg/ml: ↑$BrdU^+$ 3.125 μg/ml:↑cell number, $BrdU^+$ 6.25 μg/ml:↑cell numbers, $BrdU^+$, $Ki67^+$, $SOX2^+$	Cell	Hucklenbroich et al. (2014)

proliferation (Xu et al., 2007), 2,3,5,4 '-Tetrahydroxystilbene-2-*O*-beta-D-glucoside (Jiang et al., 2018), and LBP (Po et al., 2017) promoted differentiation, and baicalin promoted proliferation, differentiation, and maturation (Jiang et al., 2013; Gao et al., 2018; Zhang et al., 2019). Meanwhile, Helicid (Li et al., 2019) not only relieved post-depression mood but also improved cognition, which may be associated with boosting NSC proliferation. Also, under physiological conditions, bioactive components promoted neurogenesis. For example, Fuzi polysaccharide-1 (Yan et al., 2010) improved mood, which may have been connected to its support of proliferation and maturation. The effect of LBP promoted proliferation (Wang et al., 2015), aromatic Turmerone (Hucklenbroich et al., 2014), and schisandrin A and B (Cai et al., 2020) promoted differentiation, scorpion venom heat resistant peptide promoted proliferation and differentiation (Wang et al., 2014), but the effects above five bioactive components on the behaviors of mice have not been reported.

In vitro, bioactive components mainly promoted the proliferation and differentiation of NSCs. Magnesium lithospermate B (Zhang Z. et al., 2018), angelica polysaccharide (Cheng et al., 2019), and astragaloside IV (Chen et al., 2019) all promoted the proliferation of stem cells; tetramethylpyrazine (Yan et al., 2014) and musk ketone promoted differentiation, while salvianolic acid B (Zhuang et al., 2012) and aromatic turmerone (Hucklenbroich et al., 2014) regulated both proliferation and differentiation. In addition, Epimedium flavonoids promoted axon growth, which is essential for stem cell maturation (Yao et al., 2010). Unfortunately, when pregnant rats were exposed to koumine (Zhou et al., 2020), which was isolated from Gelsemium elegans Benth, the offspring of both male and female c57BL/6 J mice showed a marked reduction in neurogenesis in the hippocampal DG. In addition, the offspring presented cognitive deficits and increased anxiety-like behavior (Yang et al., 2021). Similarly, Saikosaponin-d replicated cell viability and reduced cell growth (Qin et al., 2019).

The structural classification of the aforementioned bioactive components can be seen in Figure 4B. The indicated bioactive components are mainly concentrated in saponin (28.57%), phenylpropanoid (19.05%), and polysaccharide (14.29%), in addition to terpenoids (9.52%), organic acids (9.52%), amino acids (4.76%), alkaloids (4.76%), flavonoids (4.76%), and bioactive substances (4.76%).

As people pay more attention to the role of neurogenesis in diseases, how to improve diseases through drugs that affect neurogenesis has become a hot subject in neuroscience in recent years. TCM has outstanding clinical efficacy in the treatment of neurogenesis-related diseases and is an important source of drugs that affect neurogenesis. TCMPs have a large amount of clinical practice data, such as Xiaochaihutang (Chen et al., 2009) and Buyang Huanwu decoction (Lee et al., 2020). Some herbs, such as medlar, ginseng, and licorice can be used as both medicine and food. Surprisingly, 9 of the 21 CHMs (47.6%) were shown to enhance adult neurogenesis under physiological conditions. When it comes to the different stages of neurogenesis, TCM may regulate more than just the one biological process of adult neurogenesis mentioned above. Figure 5 shows how TCM regulates and plays a vital role in the multi-stage process of adult neurogenesis.

As shown in Figure 6, there are currently 19 CHMs that are almost present in 26 TCMPs (89.66% of the total number of TCMPs), and further analysis found that 20 CHMs contain 17 types of bioactive compounds (80.95% of the total number of bioactive compounds), which have a high potential for use before clinical application, such as baicalin, which was isolated from the root of Scutellaria baicalensis and has a great neuroprotective

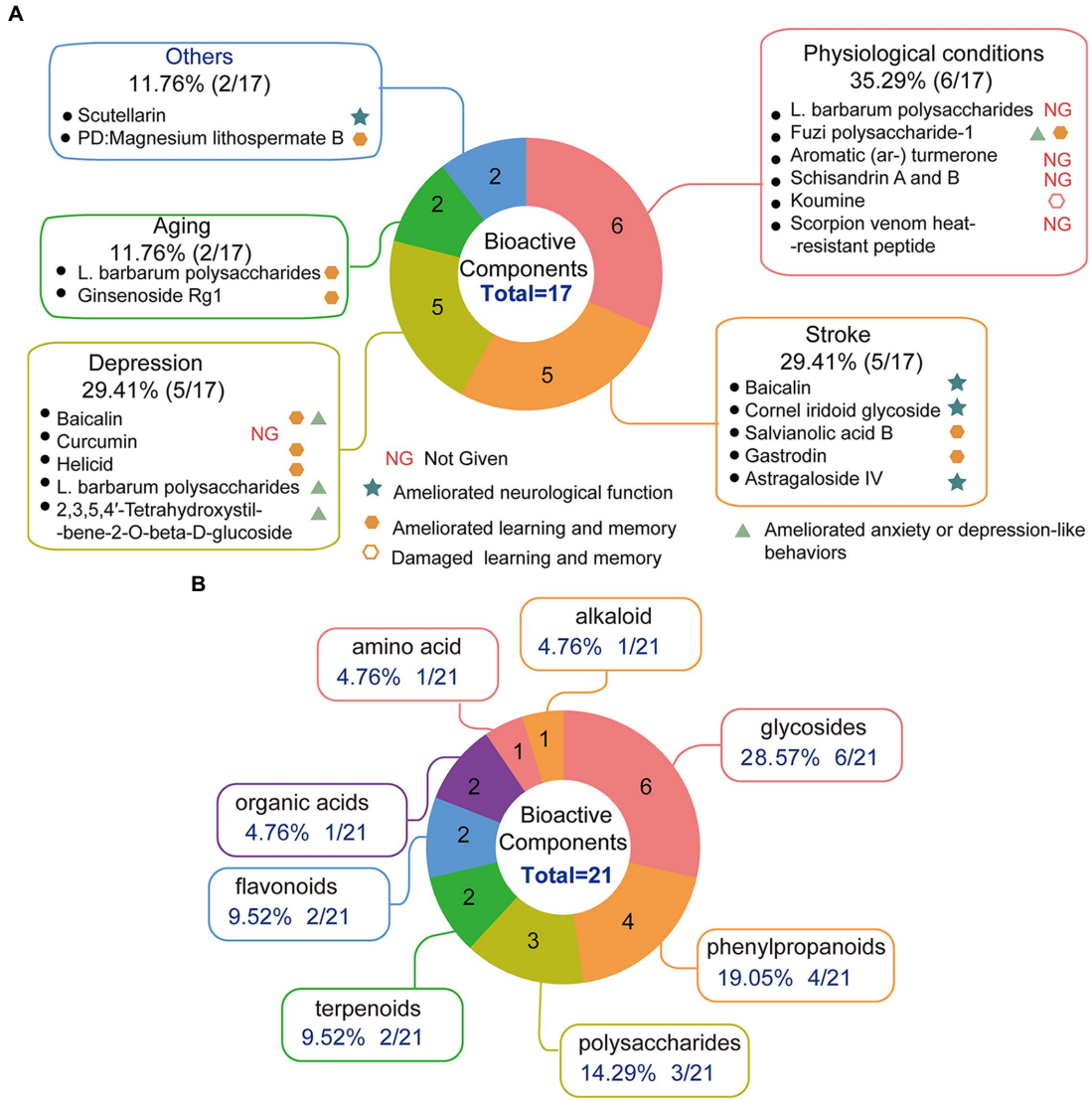

FIGURE 4
The effect of bioactive components on adult neurogenesis. **(A)** Pie chart of bioactive components improving adult neurogenesis and brain function, *n*=17, *L. barbarum* polysaccharides improves adult neurogenesis in aging, depression, and physiological conditions, so it was counted in three cases for three situations; baicalin improves adult neurogenesis in depression and stroke conditions, so it was counted in two cases for two situations. **(B)** Pie chart of bioactive components according to the chemical composition that promotes adult neurogenesis (animal) or contributes to the proliferation and differentiation of NSCs, *n*=21.

effect. More importantly, baicalin has shown highly promising results in two clinical trials (chiCTR180016727 and ChiCTR180016727) on mental health. If we can fully explore the mechanism of its influence on neurogenesis, its clinical application will advance even further.

4. Mechanism of TCM on adult neurogenesis

4.1. Increase of neurotrophic factor

Neurotrophic factors play a central role in NSC proliferation, migration, and differentiation. Their existence is crucial for maintaining neuronal function, structural integrity, and adult neurogenesis throughout life. Many TCMs (Figure 7A) show the ability to promote the secretion of neurotrophic factors, thereby enhancing hippocampal adult neurogenesis (Zhang et al., 2014).

There are many TCMs that promote adult neurogenesis while simultaneously regulating BDNF, including Huatuo Zaizao pill (Duan et al., 2017), Shenzao jiannao oral liquid (Xiao et al., 2020), Danshen-Chuanxiong-Honghua (Zhang X. et al., 2017), and Allium macrostemon Bunge (Lee et al., 2010): these not only promote the proliferation of NSCs, but also enhance BDNF expression. Both Zhengtian capsules (Yang et al., 2020) and Oenanthe javanica ethanol extract (Chen B. H. et al., 2015) promote the proliferation and differentiation of hippocampal NSCs, while BDNF expression is also increased. PM012 promotes BDNF expression and NSC differentiation and maturation (Ye et al., 2016). In addition to the aqueous extract of gardenia, Fructus

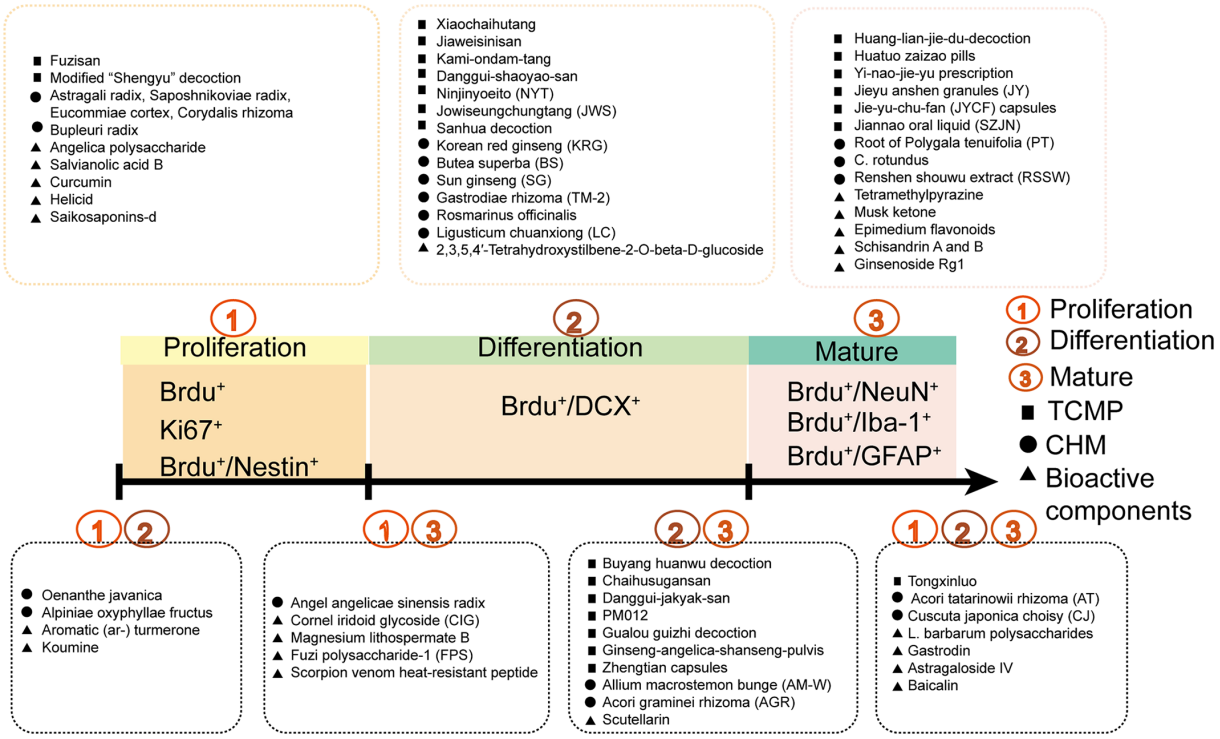

FIGURE 5
The influence of TCMPs, CHMs, and bioactive components on adult neurogenesis at different stages.

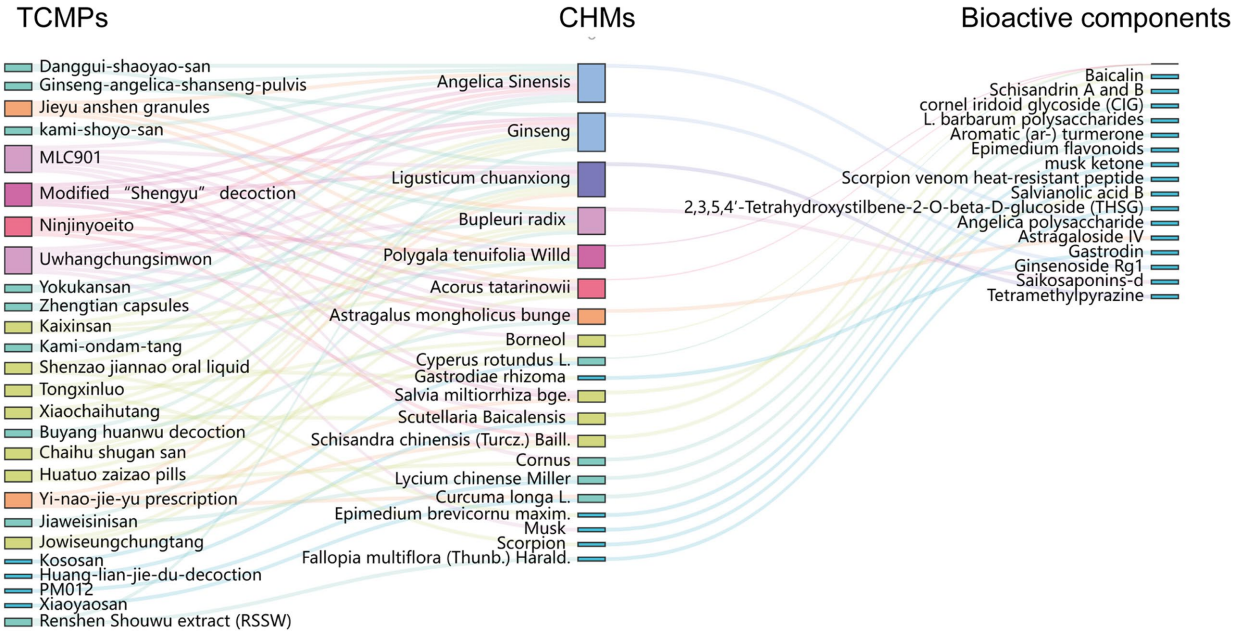

FIGURE 6
TCMPs and CHMs are commonly used to enhance adult neurogenesis and a network of its bioactive components.

aurantii, and Magnolia officinalis also increase BDNF expression in the hippocampus of rats with chronic unpredictable mild stress and affect NSC differentiation and maturation (Xing et al., 2015). As a result, BDNF may be the target of traditional Chinese medicine to regulate neurogenesis. Thus, some researchers believe that the beneficial effect of Jieyu Chufan capsules (Ji et al., 2020) and curcumin (Xu et al., 2007) on depressed mice involves enhancing adult neurogenesis by boosting BDNF expression (Ji

et al., 2020). Buyang Huanwu decoction promotes recovery from cerebral ischemia, and its mechanism may be related to the increased expression of VEGF and BDNF proteins for the differentiation and maturation of NSCs (Zhuge et al., 2020). PMC-12 (Park et al., 2016) and Xiaobuxin decoction (An et al., 2008) have beneficial effects on maturation through an increase in BDNF and p-CREB expression (An et al., 2008). Further research confirms that P-coumaric acid's effects on BDNF/TrkB/Akt activation and NSC proliferation are eliminated when coupled with the BDNF/TrkB-specific inhibitor ANA12 (He et al., 2020). Meanwhile, K252a is an antagonist of Trk, an upstream molecule of BDNF signal transduction. TrkB inhibition blocks the transmission of the BDNF signal pathway. Although Fuzi polysaccharide-1 (Yan et al., 2010) promotes proliferation Chaihu Shugan San improves differentiation (Chen et al., 2018), and Ginseng and Polygala tenuifolia aqueous extracts (Jiang et al., 2021) enhance NSC differentiation and maturation, K252a may disrupt the function of the aforementioned TCMs on adult neurogenesis. In addition, administering Scorpion venom heat resistant peptide (SVHRP) promotes astrocytes to release BDNF and promotes the growth of axons of immature neurons. However, blocking BDNF with anti-BDNF antibodies can eliminate these SVHRP-dependent neurotrophic effects (Wang et al., 2014).

In addition to regulating BNDF to enhance adult neurogenesis, TCM can also control other neurotrophic factors to enhance adult neurogenesis. In TBI rats, "Shengyu" decoction can increase the expression of glial cell line-derived neurotrophic factor (GDNF) and nerve growth factor (NGF) for the proliferation of NSCs (Chen M. M. et al., 2015). Huatuo Zaizao extract can boost the production of newly formed neurons, and increase the levels of VEGF and BDNF (Zheng et al., 2014), in addition to BDNF, NGF, TrkB, TrkA, which are all upregulated by *Xiaoyao pills* (Fang et al., 2020). Additionally, Angelica sinensis (Oliv.) Diels not only promotes the proliferation and maturation of hippocampal NSCs, but can also upregulate the expression of BDNF, GDNF, and vascular endothelial growth factor A (VEGF-A) in the hippocampus in chronic cerebral ischemia models (Cheng et al., 2021).

4.2. Increase of neurotransmitters

Depression is associated with decreased adult neurogenesis and abnormal monoammonia levels (Lanni et al., 2009; Jiang et al., 2022). Importantly, monoamine neurotransmitters function to increase neurogenesis (Cameron et al., 1998). A 5-Hydroxytryptamine (5-HT) reuptake inhibitor like fluoxetine not only has an obvious antidepressant effect but can also greatly improve adult neurogenesis in depression models. The antidepressant effects of Jie Yu Chu fan capsules in depressed mice can enhance adult neurogenesis by increasing the levels of norepinephrine (NE) and dopamine (DA) (Ji et al., 2020). Jieyu Anshen granules improving the neurological and cognitive functions of PSD model mice may be related to increases in the levels of NE, DA, and 5-HT (Du et al., 2020). Curcumin increased hippocampal adult neurogenesis, which may be related to curcumin increasing 5-HT (1a) mRNA in the hippocampal subregion after stress (Xu et al., 2007). The mechanism by which the above TCMs may influence neurogenesis by affecting neurotransmitters is shown in Figure 7B.

4.2.1. Inflammation reduction

Pro-inflammatory factors IL-1β, IL-6, and NF-κB produced by activated microglia or astrocytes may impact different phases of adult neurogenesis (Ekdahl et al., 2009; Czeh et al., 2011). TCMs (Figure 7C) may alleviate abnormal adult neurogenesis by reducing glial cell activation and inflammatory factors.

One strategy for TCM to increase adult neurogenesis is to inhibit microglial activation. The influence of α-Asarone on neurogenesis may be correlated with a decline in the proportion of activated microglia, a reduction in microglial numbers, and the maintenance of velocity (Cai et al., 2016). Kososan extract can prevent the avoidance behavior of socially failed mice, which is partially mediated by the downregulation of hippocampal neuroinflammation, possibly through the regulation of increased anti-inflammatory microglia and adult hippocampal neurogenesis (Ito et al., 2017). Erinacine A and erinacine S promote hippocampal adult neurogenesis in AD mice, which may lessen glial cell activation (Tzeng et al., 2018).

Another strategy for TCM to increase adult neurogenesis at different stages is to inhibit the release of proinflammatory cytokines (TNF-α, IL-1β, and IL-6) by microglia. In the proliferation stage, ZTC increases NSC proliferation and inhibits the expression level of NF-kB in a dose-dependent manner (Yang et al., 2020). Under the differentiation stage, Ligusticum chuanxiong (LC) significantly increased DCX in the hippocampal DG of adult rats 14 days after cerebral ischemia. Meanwhile, LC reduces IL-1β and TNF-α (Wang et al., 2020). THSG, the main active compound of the traditional Chinese herb *Polygonum multiflorum*, can lower TNF-α, IL-1β, and IL-6 (Jiang et al., 2018). At the maturation stage, Xiaoyao pills increase newly formed neurons and significantly decrease the levels of IL-6 and TNF-α (Fang et al., 2020). Treatment with Polygoni multiflori radix extract can greatly increase the number of new neurons after an ischemic stroke. This may be accomplished by blocking the TLR4/NF-κB/NLRP3 inflammatory signaling pathway after an ischemic stroke in rats (Li et al., 2020). Moreover, Jieyu Anshen granules (Du et al., 2020), Hericium erinaceus mycelium (HEM), and an isolated diterpenoid derivative known as erinacine A (Tsai et al., 2019) all support the development of new neurons and can reduce TNF-α and IL-1 β, which are linked to the regulation of adult neurogenesis (Du et al., 2020).

Traditional Chinese medicine can inhibit both microglia activation and the release of proinflammatory factors. Andrographolide (Lu et al., 2019) inhibits chronic stress-induced abnormalities in adult hippocampal neurogenesis by reversing microglia-mediated pro-inflammatory cytokine production. Nuclear transcription factor NF-κB level decreased, and LPS-induced IL-1β level was changed by ALWPS-regulated FAK signal. Moreover, ALWPS significantly inhibited the LPS-induced migration of BV2 microglia. Oral administration of ALWPS to C57BL/6 J mice injected with LPS can greatly improve short- and long-term memory. More importantly, oral treatment of ALWPS significantly reduced microglia activation in the hippocampus and cortex (Lee et al., 2018).

Additionally, TCM may regulate astrocyte anti-inflammation and increase NSC proliferation. Ilexonin A can enhance NSC proliferation by activating astrocytes and decreasing TNF-α and IL-1 β (Xu et al., 2020). Ginsenoside Rg1 decreased astrocyte activation and increased hippocampal cell proliferation by reducing IL-1β, IL-6, and TNF-α (Zhu et al., 2014).

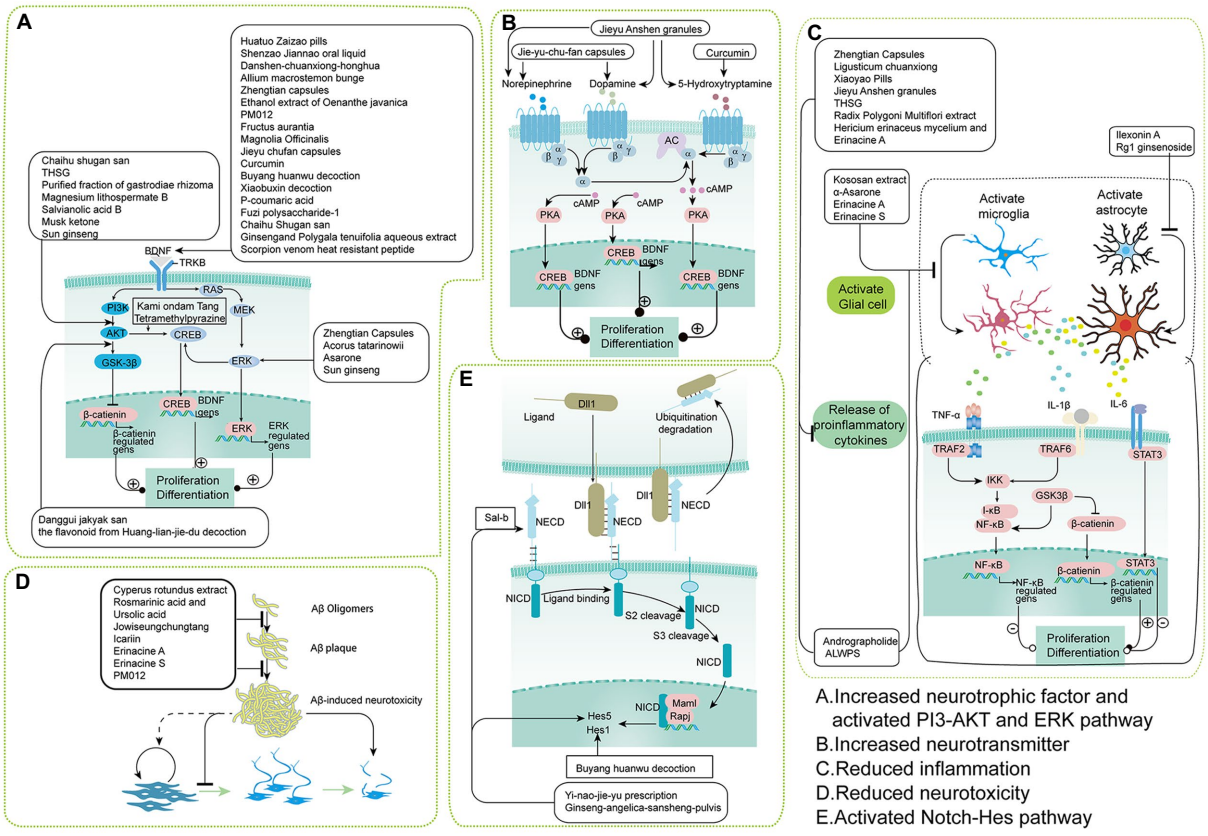

FIGURE 7
Mechanisms of TCMPs, CHMs, and bioactive components on adult neurogenesis. **(A)** TCM could increase neurotrophic factors or activate the PI3-AKT and ERK pathways for adult neurogenesis. **(B)** TCM could increase neurotransmitters for adult neurogenesis. **(C)** TCMs could reduce inflammation for adult neurogenesis. **(D)** TCM could reduce neurotoxicity for adult neurogenesis. **(E)** TCM could activate the Notch-Hes pathway for adult neurogenesis.

4.2.2. Reduction of neurotoxicity

In the past few years, impaired adult hippocampal neurogenesis has emerged as a hallmark of AD pathophysiology along with Aβ and tau hyperphosphorylation-induced neurotoxicity, and further research has shown that Aβ-induced neurotoxicity is associated with altered neurogenesis and memory formation (Abshenas et al., 2020; Amber et al., 2020). Although Aβ causes a temporary increase in the number of neurons in younger mice, it also causes a drop in the NSC pool, which results in a lower rate of adult neurogenesis in older animals (Lopez-Toledano et al., 2010). In the existing animal model of AD, mice with Aβ intraperitoneal injections or transgenic Aβ accumulation can severely impair adult neurogenesis, and TCMs (Figure 7D) improved this situation. On the one hand, TCMs such as Cyperus rotundus extract (Shakerin et al., 2020), rosmarinic acid, and ursolic acid (Mirza et al., 2021) repaired the spatial memory damage induced by Aβ1-42 and increased adult neurogenesis. On the other hand, the transgene-induced aggregation of Aβ was also associated with an aberrant reduction of adult neurogenesis. In this situation, TCMs reduced Aβ deposition in the brain and enhanced hippocampal adult neurogenesis in AD animal models with different genetic backgrounds. For instance, Jowiseungchungtang inhibited the aggregation of Aβ and the pathology induced by Aβ in AD model mice (five family AD variants) and improved adult hippocampal adult neurogenesis *in vivo* (Shin et al., 2018), Icariin reduced Aβ in the brain of Tg2576 mice and enhanced adult hippocampal neurogenesis (Li et al., 2015), erinacine A and erinacine S inhibited the growth and reduced the load of Aβ plaque and promoted adult hippocampal neurogenesis in APPswe/PS1ΔE9 transgenic mice (Tzeng et al., 2018), and PM012 significantly reduced Aβ deposition and increased adult neurogenesis in 3xTG AD mice (Ye et al., 2016).

4.2.3. Activation of PI3-AKT and ERK pathways

The ERK and PI3K / Akt pathways may regulate different stages of adult neurogenesis, including the growth, differentiation, maturation, and survival of NSCs (Shioda et al., 2009; Mellios et al., 2018). TCMs (Figure 7A) could affect adult neurogenesis by regulating the ERK and PI3K / Akt pathways of NSCs.

Salvianolic acid B maintains self-renewal and promotes the proliferation of NSCs *via* the PI3K / Akt signaling pathway, which is confirmed by PI3 (LY294002) inhibition eliminating this effect (Zhuang et al., 2012). Meanwhile, THSG (a primary active compound of the traditional Chinese herb *Polygonum multiflorum*) (Jiang et al., 2018) and the purified fraction of *Gastrodiae rhizoma* (Hsu et al., 2021) stimulate adult neurogenesis and regulate the PI3K/Akt pathway. Moreover, magnesium lithospermate B (Zhang Z. et al., 2018) and musk ketone (Zhou et al., 2020) promote the proliferation and differentiation of NSCs through the activation of the PI3K/Akt signaling pathway. Akti-1/2, an Akt inhibitor, also blocks the effect of musk ketone on NSCs. This suggests that Muscone promotes NSC proliferation and differentiation by

activating the PI3K/Akt signaling pathway (Zhou et al., 2020). Chaihu Shugan San increases the levels of pPI3k/PI3K and pAkt/Akt in the hippocampus of stressed mice and restores the newly formed neurons. The two main active ingredients in Chaihu Shugan San, quercetin and luteolin, were then discovered to have a good docking fraction with the PI3K protein using molecular docking technology. This further confirmed that the PI3K/Akt pathway is how CSS participates in the treatment of MDD (Zhang et al., 2021).

Chaihu Shugan San not only boosted the PI3K/Akt pathway in stressed mice but also reduced the level of p-GSK3β/GSK3β to promote adult neurogenesis (Zhang et al., 2021). Danggui Jakyak San increases Akt/GSK3 β/β- Catenin signal transduction, which may be one of the mechanisms through which it promotes adult neurogenesis (Song et al., 2013). Similarly, raising p-Akt and p-GSK-3β is thought to play a factor in how alkaloids in Huanglian Jiedu decoction encourage NSC proliferation. Flavonoid treatment promotes the differentiation of cortical precursor cells into neurons rather than glial cells, which could be attributed to the upregulation of Akt and GSK-3β (Zou et al., 2016). In addition, Saikosaponin-d (SSD) inhibits cell viability and proliferation of hippocampal NPCs in a concentration-dependent manner. Subsequent research indicates that SSD suppresses adult neurogenesis and NPC proliferation *via* the GSK3 β/β- Catenin signaling pathway (Qin et al., 2019).

Traditional Chinese medicine could aid the PI3K/Akt/CREB pathway in NSC differentiation. Kami-ondam-tang greatly enhanced the expression of p-Akt and p-CREB in the hippocampal CA1 region and dentate gyrus, and, at the same time, the number of DCX-positive cells in the dentate gyrus increased significantly. These results suggest that Kami-ondam-tang improves cognitive ability by upregulating Akt/CREB/BDNF signaling and adult neurogenesis (Hong et al., 2011). Tetramethylpyrazine induces the release of BDNF from bone marrow mesenchymal stem cells by activating the PI3K/Akt/CREB pathway for neural differentiation. This effect could be reversed by the PI3K inhibitor LY294002 (Chen et al., 2021).

Traditional Chinese medicine could also influence NSC during development and survival *via* the Akt pathway. Baicalin induces neuronal development, matures them *via* the Akt/Foxg1 pathway, and sustains them to have an antidepressant effect (Zhang et al., 2019). By the activation of PI3K/Akt/BAD, Buyang Huanwu decoction (BHD) stimulates neurogenesis in apoptosis, proliferation, differentiation, maturation, and eventually the recovery of the function of learning and memory (Chen et al., 2020).

Another type of kinase that influences NSC proliferation, differentiation, and survival is extracellularly regulated protein kinases (ERK) (Rai et al., 2019). TCM promotes the proliferation of NSCs through ERK. Acorus tatarinowii and its components, α- asarone and β- asarone, promote NPC proliferation *in vitro*. Subsequent research has shown that Acorus tatarinowii and asarone activated ERK but did not activate the Akt pathway; FR180204 inhibited ERK activity and effectively blocked the promoting effect of Acorus tatarinowii or asarone on the proliferation of NPC (Mao et al., 2015). In contrast to Acorus tatarinowii, Sun ginseng increases p-ERK and p-Akt levels in addition to NSC proliferation and survival, which may be the method through which memory is enhanced (Lee et al., 2013). In addition, Zhengtian capsules promote the proliferation of hippocampal NSCs and the protein levels of phosphorylated ERK1/2 and CREB (Yang et al., 2020).

4.2.4. Activation of the Notch-Hes pathway

Activation of the Notch signaling pathway enhances the production of Hes1 and Hes5, which promote stem cell proliferation and inhibit neuronal differentiation (Mendes-da-Silva et al., 2015; Zhang R. et al., 2018; Ohtsuka and Kageyama, 2021). TCM may influence adult neurogenesis by regulating stem cell proliferation and differentiation *via* the Notch1/Hes pathway (Figure 7E). Zhuang et al. (2012) screened 45 bioactive components from TCM, which were widely used in the treatment of stroke in China, and evaluated their effect on the proliferation of neural stem/progenitor cells. The results showed that Sal-b promoted NSC self-renewal along with an increase in Notch1 gene expression. The Buyang Huanwu decoction increased the expression of Hes1 and promoted NSCs to differentiate into astrocytes (Chen et al., 2020). More importantly, TCMs regulate neurogenesis under different pathological conditions through the Notch1/Hes5 pathway, which may have a time effect from the Yi-nao-jie-yu prescription (Tian et al., 2018) and a dosage effect from the Ginseng-Angelica-Sansheng-pulvis combination (Liu et al., 2019).

5. Toxic and side effects

There are only a few clinical reports on the toxicity and adverse effects of TCMs regulating adult neurogenesis, whether used alone or in combination. The side effects of TCMs, including MLC901 (Kumar et al., 2020), curcumin (Asher and Spelman, 2013; Fan et al., 2013), and Polygala tenuifolia (Zhao X. et al., 2020), are largely gastrointestinal, such as nausea, vomiting, and diarrhea. The majority of side effects are mild and temporary, and after discontinuing the medication, these symptoms will gradually subside. There are also a few reports on the side effects of TCMs in other systems. Pseudoaldosteronism caused by Yokukansan (Ishida et al., 2020; Katsuki et al., 2021) causes hypertension, hypokalemia, and muscular weakness, which may lead to death. Therefore, patients must be aware of the risks when considering taking Yokukansan (Ishida et al., 2020). Curcumin may chelate dietary trace elements, and long-term supplementation of curcumin aggravates iron deficiency (Chin et al., 2014). Clinicians should pay attention to any side effects that could increase the number and function of myeloid-derived suppressor cells when using angelica polysaccharide as an immune enhancer (Shen et al., 2022). Cornus officinalis extract has shown good results in treating drug-resistant asthma, but it may cause allergic contact dermatitis (Mirsadraee et al., 2018).

The toxic and adverse effects of combining TCMs with Western medicine have also been documented and require special attention. TCMs may affect the activity of the cytochrome P450 (CYP) enzyme system, which may enhance therapeutic effects but could also lead to increased side effects. For the treatment of epilepsy, Gastrodiae rhizoma might lengthen the plasma half-life and concentration of carbamazepine and its metabolite (carbamazepine-10, 11-epoxide). However, it could also be accompanied by an expansion of the neurological signs of toxicity (Yip et al., 2020). Ginkgo stimulates both CYP3A4 and CYP2C9 and alters the AUC and Cmax of conventional medications like midazolam, tolbutamide, lopinavir, and nifedipine. Ginsenosides Re increased CYP2C9, which reduced the anticoagulant activity of warfarin (Suroowan and Mahomoodally, 2019). In addition, Glycyrrhizae radix et rhizoma replaces serum-bound cardiovascular medications and reduces the disease-treating effects of diltiazem, nifedipine, and verapamil (Suroowan and Mahomoodally, 2019).

Individuals who took ginger and aprepitant together experienced more severe acute nausea than those who took only aprepitant (Zick et al., 2009). Despite the limited and contradictory results about curcumin enhancing the function of doxorubicin-induced cardiac toxicity, it is necessary to conduct carefully designed research to evaluate the safety and effectiveness of the new formulation of this compound during cancer treatment (Armandeh et al., 2022).

It should be noted that ingesting an excessive amount of TCMs, even "medicine food homologous," will produce adverse reactions. For example, Korean red ginseng (KRG) is very popular as a dietary supplement, but its excessive intake can cause "shanghuo," which is closely related to the acceleration of the TCA cycle and the increase of AMPK activity (Zhao T. et al., 2020). At a regular dose, Morinda officinalis has not been associated with any significant negative effects in clinical trials, but in some cases, doses greater than 1 g/kg have been linked to irritability, insomnia, and unpleasant feelings (Zhang J. H. et al., 2018). Excessive intake of curcumin may have adverse effects on the kidney, heart, liver, blood, and immune system, which is a reminder that there is still much research to be done before curcumin can be effectively used and transformed (Liu et al., 2022). High doses of baicalin improve the antioxidant system in rat liver, but at the same time, they also lead to the reduction of trace minerals, thereby decreasing the activity of some metal-containing enzymes and having negative health implications (Gao et al., 2003).

Based on the aforementioned reports, TCMs that regulate adult neurogenesis should be used with caution in clinical applications due to their toxicity and side effects. Regarding the effectiveness, toxicity, and side effects of TCMs on adult neurogenesis, quality control and reliability of TCMs are also important determining factors. Genuine traditional Chinese materia medica, processing, safety, compatibility with other medications, and dosage of TCMs used for different medical conditions should all be taken into consideration. It is also necessary to keep researching the scientific and ethical principles of TCM clinical trials on adult neurogenesis. All of these techniques can effectively protect the subjects' rights, interests, and safety while also improving the development of TCMs on adult neurogenesis to prevent and treat nervous system disorders.

6. Conclusion and future work

Many studies have shown that adult neurogenesis plays an important role in the regulation of neurological and psychotic disorders. A better understanding of the effects and mechanisms that regulate adult neurogenesis will identify disease pathologies that drive cognitive and emotional impairments, thereby providing an avenue for the development of effective therapeutic strategies. Here, we have focused on the role of adult neurogenesis in neuropsychiatric disorders, especially the characteristics and mechanisms of the ameliorative effects of TCM resulting from its regulation of adult neurogenesis. This review provides recent evidence on the regulation of adult neurogenesis by TCM.

Extensive studies have made significant progress in the regulation of adult neurogenesis thanks to TCM, but there are still many questions and thus further studies are needed. (1) Although adult neurogenesis has been shown to exist in animals, there is insufficient evidence to date to adequately support its existence in adult humans. It is crucial for future research to explore the dynamic changes and the functional role of adult neurogenesis in the normal human brain and alterations in neuropsychiatric disorders. More accurate approaches, cell markers, and human imaging protocols that can efficiently study adult neurogenesis are the greatest necessities in this field. (2) Although many promising results have been achieved by using TCM to regulate adult neurogenesis in various animal models and in *in vitro* cell cultures, no clinical trials have been conducted so far. One limitation that hinders the clinical trials of drugs on adult neurogenesis is the lack of an *in situ* method to monitor and calculate adult neurogenesis. However, greater efforts should be made to conduct clinical research to further verify the efficacy of TCM in improving adult neurogenesis in humans. (3) The discovery of effective ingredients from TCM to improve adult neurogenesis holds great promise, but current studies on the exact targets and the pathways involved are far from sufficient. The study of the exact pharmacological targets of TCM for improving adult neurogenesis should be further conducted in the future. With the aid of new methods such as bioinformatics, it would be clarified, and then more effective agents could be designed and developed accordingly.

Although adult neurogenesis *per se* has not yet yielded a clinically approved compound for any indication, the target remains of interest and is under investigation for drug development. TCM is a great treasure that provides abundant sources for drug discovery to modulate adult neurogenesis. We believe that the future development of medications from TCM that can improve adult neurogenesis would bring us one step closer to its application in the treatment of human diseases.

Author contributions

WS reviewed the databases and analyzed the information on subjects. NJ and WZ designed this review and worked on the manuscript revision. WS and NJ wrote the draft and modified this article. WZ revised this article and replied to the reviewers in the modification phase. All authors contributed to the article and approved the submitted version.

Funding

This work was supported by the National Key R&D Program of China (Grant No. 2022YFC3500304).

Conflict of interest

The authors declare that the research was conducted in the absence of any commercial or financial relationships that could be construed as a potential conflict of interest.

Publisher's note

References

Abshenas, R., Artimani, T., Shahidi, S., Ranjbar, A., Komaki, A., Salehi, I., et al. (2020). Treadmill exercise enhances the promoting effects of preconditioned stem cells on memory and neurogenesis in Aβ-induced neurotoxicity in the rats. *Life Sci.* 249:117482. doi: 10.1016/j.lfs.2020.117482

Akers, K. G., Martinez-Canabal, A., Restivo, L., Yiu, A. P., De Cristofaro, A., Hsiang, H. L., et al. (2014). Hippocampal neurogenesis regulates forgetting during adulthood and infancy. *Science* 344, 598–602. doi: 10.1126/science.1248903

Alam, M. J., Kitamura, T., Saitoh, Y., Ohkawa, N., Kondo, T., and Inokuchi, K. (2018). Adult neurogenesis conserves hippocampal memory capacity. *J. Neurosci.* 38, 6854–6863. doi: 10.1523/JNEUROSCI.2976-17.2018

Altman, J., and Das, G. D. (1965). Autoradiographic and histological evidence of postnatal hippocampal neurogenesis in rats. *J. Comp. Neurol.* 124, 319–335. doi: 10.1002/cne.901240303

Amber, S., Sumera, M. F. J., Asif, M., Hassan, D., Ahmed, T., and Zahid, S. (2020). Amyloid-beta induced neurotoxicity impairs cognition and adult hippocampal neurogenesis in a mouse model for Alzheimer's disease. *Curr. Alzheimer Res.* 17, 1033–1042. doi: 10.2174/1567205017666201224162730

An, L., Zhang, Y. Z., Yu, N. J., Liu, X. M., Zhao, N., Yuan, L., et al. (2008). The total flavonoids extracted from Xiaobuxin-Tang up-regulate the decreased hippocampal neurogenesis and neurotrophic molecules expression in chronically stressed rats. *Prog. Neuro-Psychopharmacol. Biol. Psychiatry* 32, 1484–1490. doi: 10.1016/j.pnpbp.2008.05.005

Anacker, C., and Hen, R. (2017). Adult hippocampal neurogenesis and cognitive flexibility - linking memory and mood. *Nat. Rev. Neurosci.* 18, 335–346. doi: 10.1038/nrn.2017.45

Anacker, C., Luna, V. M., Stevens, G. S., Millette, A., Shores, R., Jimenez, J. C., et al. (2018). Hippocampal neurogenesis confers stress resilience by inhibiting the ventral dentate gyrus. *Nature* 559, 98–102. doi: 10.1038/s41586-018-0262-4

Armandeh, M., Bameri, B., Samadi, M., Heidari, S., Foroumadi, R., and Abdollahi, M. (2022). A systematic review of nonclinical studies on the effect of Curcumin in chemotherapy- induced Cardiotoxicity. *Curr. Pharm. Des.* 28, 1843–1853. doi: 10.2174/1381612828666220513125312

Arvidsson, A., Collin, T., Kirik, D., Kokaia, Z., and Lindvall, O. (2002). Neuronal replacement from endogenous precursors in the adult brain after stroke. *Nat. Med.* 8, 963–970. doi: 10.1038/nm747

Asher, G. N., and Spelman, K. (2013). Clinical utility of curcumin extract. *Altern. Ther. Health Med.* 19, 20–22. doi: 10.1016/j.hermed.2012.11.003

Azuma, K., Toyama, T., Katano, M., Kajimoto, K., Hayashi, S., Suzuki, A., et al. (2018). Yokukansan ameliorates hippocampus-dependent learning impairment in senescence-accelerated mouse. *Biol. Pharm. Bull.* 41, 1593–1599. doi: 10.1248/bpb.b18-00359

Bao, H., and Song, J. (2018). Treating brain disorders by targeting adult neural stem cells. *Trends Mol. Med.* 24, 991–1006. doi: 10.1016/j.molmed.2018.10.001

Berger, T., Lee, H., Young, A. H., Aarsland, D., and Thuret, S. (2020). Adult hippocampal neurogenesis in major depressive disorder and Alzheimer's disease. *Trends Mol. Med.* 26, 803–818. doi: 10.1016/j.molmed.2020.03.010

Boese, A. C., Le, Q. E., Pham, D., Hamblin, M. H., and Lee, J. P. (2018). Neural stem cell therapy for subacute and chronic ischemic stroke. *Stem Cell Res Ther* 9:154. doi: 10.1186/s13287-018-0913-2

Boldrini, M., Fulmore, C. A., Tartt, A. N., Simeon, L. R., Pavlova, I., Poposka, V., et al. (2018). Human hippocampal neurogenesis persists throughout aging. *Cell Stem Cell* 22, 589–599.e5. doi: 10.1016/j.stem.2018.03.015

Cai, Q., Li, Y., Mao, J., and Pei, G. (2016). Neurogenesis-promoting natural product α-Asarone modulates morphological dynamics of activated microglia. *Front. Cell. Neurosci.* 10:280. doi: 10.3389/fncel.2016.00280

Cai, N. N., Wang, Z. Z., Zhu, X. C., Jiang, Y., Zhu, W. Q., Yang, R., et al. (2020). Schisandrin a and B enhance the dentate gyrus neurogenesis in mouse hippocampus. *J. Chem. Neuroanat.* 105:101751. doi: 10.1016/j.jchemneu.2020.101751

Cameron, H. A., Hazel, T. G., and McKay, R. D. (1998). Regulation of neurogenesis by growth factors and neurotransmitters. *J. Neurobiol.* 36, 287–306. doi: 10.1002/(SICI)1097-4695(199808)36:2<287::AID-NEU13>3.0.CO;2-B

Chen, B., An, J., Guo, Y. S., Tang, J., Zhao, J. J., Zhang, R., et al. (2021). Tetramethylpyrazine induces the release of BDNF from BM-MSCs through activation of the PI3K/AKT/CREB pathway. *Cell Biol. Int.* 45, 2429–2442. doi: 10.1002/cbin.11687

Chen, X., Chen, H., He, Y., Fu, S., Liu, H., Wang, Q., et al. (2020). Proteomics-guided study on Buyang Huanwu decoction for its Neuroprotective and neurogenic mechanisms for transient ischemic stroke: involvements of EGFR/PI3K/Akt/bad/14-3-3 and Jak2/Stat3/Cyclin D1 Signaling cascades. *Mol. Neurobiol.* 57, 4305–4321. doi: 10.1007/s12035-020-02016-y

Chen, F. P., Chen, F. J., Maw-Shiou, J., Hui-Lin, T., Wang, J. R., and Shinn-Jang, H. (2009). Modern use of Chinese herbal formulae from Shang-Han Lun. *Chin Med J* 122, 1889–1894.

Chen, W., Cheng, X., Chen, J., Yi, X., Nie, D., Sun, X., et al. (2014). *Lycium barbarum* polysaccharides prevent memory and neurogenesis impairments in scopolamine-treated rats. *PLoS One* 9:e88076. doi: 10.1371/journal.pone.0088076

Chen, X. Q., Li, C. F., Chen, S. J., Liang, W. N., Wang, M., Wang, S. S., et al. (2018). The antidepressant-like effects of Chaihu Shugan san: dependent on the hippocampal BDNF-TrkB-ERK/Akt signaling activation in perimenopausal depression-like rats. *Biomed. Pharmacother.* 105, 45–52. doi: 10.1016/j.biopha.2018.04.035

Chen, B. H., Park, J. H., Cho, J. H., Kim, I. H., Shin, B. N., Ahn, J. H., et al. (2015). Ethanol extract of *Oenanthe javanica* increases cell proliferation and neuroblast differentiation in the adolescent rat dentate gyrus. *Neural Regen. Res.* 10, 271–276. doi: 10.4103/1673-5374.152382

Chen, H. J., Shen, Y. C., Shiao, Y. J., Liou, K. T., Hsu, W. H., Hsieh, P. H., et al. (2015). Multiplex brain proteomic analysis revealed the molecular therapeutic effects of Buyang Huanwu decoction on cerebral ischemic stroke mice. *PLoS One* 10:e0140823. doi: 10.1371/journal.pone.0140823

Chen, L., Wang, X., Chen, X., Xing, S., Zhang, J., Li, J., et al. (2014). Tongxinluo attenuates neuronal loss and enhances neurogenesis and angiogenesis in the ipsilateral thalamus and improves neurological outcome after focal cortical infarction in hypertensive rats. *Restor. Neurol. Neurosci.* 32, 533–546. doi: 10.3233/RNN-140403

Chen, L., Wang, X., Zhang, J., Dang, C., Liu, G., Liang, Z., et al. (2016). Tongxinluo enhances neurogenesis and angiogenesis in Peri-infarct area and subventricular zone and promotes functional recovery after focal cerebral ischemic infarction in hypertensive rats. *Evid. Based Complement. Alternat. Med.* 2016:8549590. doi: 10.1155/2016/8549590

Chen, X., Wu, H., Chen, H., Wang, Q., Xie, X. J., and Shen, J. (2019). Astragaloside VI promotes neural stem cell proliferation and enhances neurological function recovery in transient cerebral ischemic injury via activating EGFR/MAPK Signaling cascades. *Mol. Neurobiol.* 56, 3053–3067. doi: 10.1007/s12035-018-1294-3

Chen, M. M., Zhao, G. W., He, P., Jiang, Z. L., Xi, X., Xu, S. H., et al. (2015). Improvement in the neural stem cell proliferation in rats treated with modified "Shengyu" decoction may contribute to the neurorestoration. *J. Ethnopharmacol.* 165, 9–19. doi: 10.1016/j.jep.2015.02.037

Cheng, C. Y., Huang, H. C., Kao, S. T., and Lee, Y. C. (2021). Angelica sinensis extract promotes neuronal survival by enhancing p38 MAPK-mediated hippocampal neurogenesis and dendritic growth in the chronic phase of transient global cerebral ischemia in rats. *J. Ethnopharmacol.* 278:114301. doi: 10.1016/j.jep.2021.114301

Cheng, X., Yao, H., Xiang, Y., Chen, L., Xiao, M., Wang, Z., et al. (2019). Effect of Angelica polysaccharide on brain senescence of nestin-GFP mice induced by D-galactose. *Neurochem. Int.* 122, 149–156. doi: 10.1016/j.neuint.2018.09.003

Cheung, J. S., Chan, J. N., Lau, B. W., and Ngai, S. P. (2016). Purposeful activity in psychiatric rehabilitation: is neurogenesis a key player? *Hong Kong J. Occup. Ther.* 27, 42–47. doi: 10.1016/j.hkjot.2016.04.002

Chin, D., Huebbe, P., Frank, J., Rimbach, G., and Pallauf, K. (2014). Curcumin may impair iron status when fed to mice for six months. *Redox Biol.* 2, 563–569. doi: 10.1016/j.redox.2014.01.018

Chrostek, M. R., Fellows, E. G., Crane, A. T., Grande, A. W., and Low, W. C. (2019). Efficacy of stem cell-based therapies for stroke. *Brain Res.* 1722:146362. doi: 10.1016/j.brainres.2019.146362

Czeh, M., Gressens, P., and Kaindl, A. M. (2011). The yin and yang of microglia. *Dev. Neurosci.* 33, 199–209. doi: 10.1159/000328989

DeCarolis, N. A., and Eisch, A. J. (2010). Hippocampal neurogenesis as a target for the treatment of mental illne ss: a critical evaluation. *Neuropharmacology* 58, 884–893. doi: 10.1016/j.neuropharm.2009.12.013

Dong, X. Z., Wang, D. X., Zhang, T. Y., Liu, X., Liu, P., and Hu, Y. (2020). Identification of protein targets for the antidepressant effects of Kai-Xin-san in Chinese medicine using isobaric tags for relative and absolute quantitation. *Neural Regen. Res.* 15, 302–310. doi: 10.4103/1673-5374.265555

Du, Y., Ruan, J., Zhang, L., and Fu, F. (2020). Jieyu Anshen granule, a Chinese herbal formulation, exerts effects on Poststroke depression in rats. *Evid. Based Complement. Alternat. Med.* 2020:7469068. doi: 10.1155/2020/7469068

Duan, S., Wang, T., Zhang, J., Li, M., Lu, C., Wang, L., et al. (2017). Huatuo Zaizao pill promotes functional recovery and neurogenesis after cerebral ischemia-reperfusion in rats. *BMC Complement. Altern. Med.* 17:19. doi: 10.1186/s12906-016-1516-z

Ekdahl, C. T., Kokaia, Z., and Lindvall, O. (2009). Brain inflammation and adult neurogenesis: the dual role of microglia. *Neuroscience* 158, 1021–1029. doi: 10.1016/j.neuroscience.2008.06.052

Elder, G. A., De Gasperi, R., and Gama Sosa, M. A. (2006). Research update: neurogenesis in adult brain and neuropsychiatric disorders. *Mt. Sinai J. Med.* 73, 931–940.

Eriksson, P. S., Perfilieva, E., Bjork-Eriksson, T., Alborn, A. M., Nordborg, C., Peterson, D. A., et al. (1998). Neurogenesis in the adult human hippocampus. *Nat. Med.* 4, 1313–1317. doi: 10.1038/3305

Fan, X., Zhang, C., Liu, D. B., Yan, J., and Liang, H. P. (2013). The clinical applications of curcumin: current state and the future. *Curr. Pharm. Des.* 19, 2011–2031. doi: 10.2174/138161213805289255

Fang, Y., Shi, B., Liu, X., Luo, J., Rao, Z., Liu, R., et al. (2020). Xiaoyao pills attenuate inflammation and nerve injury induced by lipopolysaccharide in hippocampal neurons in vitro. *Neural Plast.* 2020:8841332. doi: 10.1155/2020/8841332

Feng, L., Xing, H., and Zhang, K. (2022). The therapeutic potential of traditional Chinese medicine in depression: targeting adult hippocampal neurogenesis. *Phytomedicine* 98:153980. doi: 10.1016/j.phymed.2022.153980

Fu, D. L., Li, J. H., Shi, Y. H., Zhang, X. L., Lin, Y., and Zheng, G. Q. (2020). Sanhua decoction, a classic herbal prescription, exerts Neuroprotection through regulating phosphorylated tau level and promoting adult endogenous neurogenesis after cerebral ischemia/reperfusion injury. *Front. Physiol.* 11:57. doi: 10.3389/fphys.2020.00057

Gao, C., Du, Q., Li, W., Deng, R., Wang, Q., Xu, A., et al. (2018). Baicalin modulates APPL2/glucocorticoid receptor Signaling Cascade, promotes neurogenesis, and attenuates emotional and olfactory dysfunctions in chronic Corticosterone-induced depression. *Mol. Neurobiol.* 55, 9334–9348. doi: 10.1007/s12035-018-1042-8

Gao, Z., Xu, H., Chen, X., and Chen, H. (2003). Antioxidant status and mineral contents in tissues of rutin and baicalin fed rats. *Life Sci.* 73, 1599–1607. doi: 10.1016/S0024-3205(03)00487-9

Goncalves, J. T., Schafer, S. T., and Gage, F. H. (2016). Adult neurogenesis in the hippocampus: from stem cells to behavior. *Cells* 167, 897–914. doi: 10.1016/j.cell.2016.10.021

Gould, E. (2007). How widespread is adult neurogenesis in mammals? *Nat. Rev. Neurosci.* 8, 481–488. doi: 10.1038/nrn2147

Gronska-Peski, M., Goncalves, J. T., and Hebert, J. M. (2021). Enriched environment promotes adult hippocampal neurogenesis through FGFRs. *J. Neurosci.* 41, 2899–2910. doi: 10.1523/JNEUROSCI.2286-20.2021

Han, J., Zhang, J. Z., Zhong, Z. F., Li, Z. F., Pang, W. S., Hu, J., et al. (2018). Gualou Guizhi decoction promotes neurological functional recovery and neurogenesis following focal cerebral ischemia/reperfusion. *Neural Regen. Res.* 13, 1408–1416. doi: 10.4103/1673-5374.235296

Hassani, Z., O'Reilly, J., Pearse, Y., Stroemer, P., Tang, E., Sinden, J., et al. (2012). Human neural progenitor cell engraftment increases neurogenesis and microglial recruitment in the brain of rats with stroke. *PLoS One* 7:e50444. doi: 10.1371/journal.pone.0050444

He, Y., Chen, S., Tsoi, B., Qi, S., Gu, B., Wang, Z., et al. (2020). Alpinia oxyphylla Miq. And its active compound P-Coumaric acid promote brain-derived Neurotrophic factor Signaling for inducing hippocampal neurogenesis and improving post-cerebral ischemic spatial cognitive functions. Front cell. *Dev. Biol.* 8:577790. doi: 10.3389/fcell.2020.577790

Hill, A. S., Sahay, A., and Hen, R. (2015). Increasing adult hippocampal neurogenesis is sufficient to reduce anxiety and depression-like behaviors. *Neuropsychopharmacology* 40, 2368–2378. doi: 10.1038/npp.2015.85

Hong, J. G., Kim, D. H., Park, S. J., Kim, J. M., Cai, M., Liu, X., et al. (2011). The memory-enhancing effects of kami-ondam-tang in mice. *J. Ethnopharmacol.* 137, 251–256. doi: 10.1016/j.jep.2011.05.014

Horgusluoglu, E., Nudelman, K., Nho, K., and Saykin, A. J. (2017). Adult neurogenesis and neurodegenerative diseases: a systems biology perspective. *Am. J. Med. Genet. B Neuropsychiatr. Genet.* 174, 93–112. doi: 10.1002/ajmg.b.32429

Hsu, W. H., Huang, N. K., Shiao, Y. J., Lu, C. K., Chao, Y. M., Huang, Y. J., et al. (2021). Gastrodiae rhizoma attenuates brain aging via promoting neuritogenesis and neurodifferentiation. *Phytomedicine* 87:153576. doi: 10.1016/j.phymed.2021.153576

Hucklenbroich, J., Klein, R., Neumaier, B., Graf, R., Fink, G. R., Schroeter, M., et al. (2014). Aromatic-turmerone induces neural stem cell proliferation in vitro and in vivo. *Stem Cell Res Ther* 5:100. doi: 10.1186/scrt500

Hueston, C. M., Cryan, J. F., and Nolan, Y. M. (2017). Stress and adolescent hippocampal neurogenesis: diet and exercise as cognitive modulators. *Transl. Psychiatry* 7:e1081. doi: 10.1038/tp.2017.48

Ishida, T., Kawada, K., Morisawa, S., Jobu, K., Morita, Y., and Miyamura, M. (2020). Risk factors for Pseudoaldosteronism with Yokukansan use: analysis using the Japanese adverse drug report (JADER) database. *Biol. Pharm. Bull.* 43, 1570–1576. doi: 10.1248/bpb.b20-00424

Ito, N., Hirose, E., Ishida, T., Hori, A., Nagai, T., Kobayashi, Y., et al. (2017). Kososan, a Kampo medicine, prevents a social avoidance behavior and attenuates neuroinflammation in socially defeated mice. *J. Neuroinflammation* 14:98. doi: 10.1186/s12974-017-0876-8

Ji, M., Niu, S., Mi, H., Jang, P., Li, Y., and Hu, W. (2020). Antidepressant functions of Jie Yu Chu Fan capsule in promoting hippocampal nerve cell neurogenesis in a mouse model of chronic unpredictable mild stress. *Ann Transl Med* 8:1020. doi: 10.21037/atm-20-5599

Jiang, C. Y., Qin, X. Y., Yuan, M. M., Lu, G. J., and Cheng, Y. (2018). 2,3,5,4'-Tetrahydroxystilbene-2-O-beta-D-glucoside reverses stress-induced depression via inflammatory and oxidative stress pathways. *Oxidative Med. Cell. Longev.* 2018:9501427. doi: 10.1155/2018/9501427

Jiang, N., Wang, H., Li, C., Zeng, G., Lv, J., Wang, Q., et al. (2021). The antidepressant-like effects of the water extract of Panax ginseng and *Polygala tenuifolia* are mediated via the BDNF-TrkB signaling pathway and neurogenesis in the hippocampus. *J. Ethnopharmacol.* 267:113625. doi: 10.1016/j.jep.2020.113625

Jiang, X., Xu, J., Zou, D., Yang, L., and Wang, Y. (2013). Baicalin influences the dendritic morphology of newborn neurons in the hippocampus of chronically stressed rats. *Neural Regen. Res.* 8, 496–505. doi: 10.3969/j.issn.1673-5374.2013.06.002

Jiang, Y., Zou, D., Li, Y., Gu, S., Dong, J., Ma, X., et al. (2022). Monoamine neurotransmitters control basic emotions and affect major depressive disorders. *Pharmaceuticals (Basel)* 15, 1–19. doi: 10.3390/ph15101203

Jin, K., Wang, X., Xie, L., Mao, X. O., Zhu, W., Wang, Y., et al. (2006). Evidence for stroke-induced neurogenesis in the human brain. *Proc. Natl. Acad. Sci. U. S. A.* 103, 13198–13202. doi: 10.1073/pnas.0603512103

Johnson, M. A., Ables, J. L., and Eisch, A. J. (2009). Cell-intrinsic signals that regulate adult neurogenesis in vivo: insights from inducible approaches. *BMB Rep.* 42, 245–259. doi: 10.5483/BMBRep.2009.42.5.245

Jordan, J. D., Ming, G. L., and Song, H. (2006). Adult neurogenesis as a potential therapy for neurodegenerative diseases. *Discov. Med.* 6, 144–147. doi: 10.1517/14712598.6.9.879

Jun, H., Hussaini, M. Q., Rigby, M. J., and Jang, M.-H. (2012). Functional role of adult hippocampal neurogenesis as a therapeutic str ategy for mental disorders. *Neural Plast.*:854285. doi: 10.1155/2012/854285

Katsuki, M., Kawamura, S., Kashiwagi, K., and Koh, A. (2021). Medication overuse headache successfully treated by Japanese herbal Kampo medicine. *Yokukansan. Cureus* 13:e18326. doi: 10.7759/cureus.18326

Koh, S. H., and Park, H. H. (2017). Neurogenesis in stroke recovery. *Transl. Stroke Res.* 8, 3–13. doi: 10.1007/s12975-016-0460-z

Kumar, R., Abu Bakar, A., Thanabalan, J., Paramasvaran, S., Toh, C. J., Jaffar, A., et al. (2020). Safety and use of MLC601/MLC901 (NeuroAiD(TM)) in primary Intracerebral Hemorrhage: a cohort study from the NeuroAiD safe treatment registry. *Brain Sci.* 10, 1–9. doi: 10.3390/brainsci10080499

Lanni, C., Govoni, S., Lucchelli, A., and Boselli, C. (2009). Depression and antidepressants: molecular and cellular aspects. *Cell. Mol. Life Sci.* 66, 2985–3008. doi: 10.1007/s00018-009-0055-x

Lee, J. Y., Joo, B., Nam, J. H., Nam, H. Y., Lee, W., Nam, Y., et al. (2018). An aqueous extract of herbal medicine ALWPs enhances cognitive performance and inhibits LPS-induced Neuroinflammation via FAK/NF-κB signaling pathways. *Front. Aging Neurosci.* 10:269. doi: 10.3389/fnagi.2018.00269

Lee, C. H., Kim, J. M., Kim, D. H., Park, S. J., Liu, X., Cai, M., et al. (2013). Effects of Sun ginseng on memory enhancement and hippocampal neurogenesis. *Phytother. Res.* 27, 1293–1299. doi: 10.1002/ptr.4873

Lee, S., Kim, D. H., Lee, C. H., Jung, J. W., Seo, Y. T., Jang, Y. P., et al. (2010). Antidepressant-like activity of the aqueous extract of Allium macrostemon in mice. *J. Ethnopharmacol.* 131, 386–395. doi: 10.1016/j.jep.2010.07.015

Lee, Y. S., Woo, S. C., Kim, S. Y., and Park, J. Y. (2020). Understanding the multi-herbal composition of Buyang Huanwu decoction: a review for better clinical use. *J. Ethnopharmacol.* 255:112765. doi: 10.1016/j.jep.2020.112765

Li, W. L., Cai, H. H., Wang, B., Chen, L., Zhou, Q. G., Luo, C. X., et al. (2009). Chronic fluoxetine treatment improves ischemia-induced spatial cognitive deficits through increasing hippocampal neurogenesis after stroke. *J. Neurosci. Res.* 87, 112–122. doi: 10.1002/jnr.21829

Li, F., Dong, H. X., Gong, Q. H., Wu, Q., Jin, F., and Shi, J. S. (2015). Icariin decreases both APP and Aβ levels and increases neurogenesis in the brain of Tg2576 mice. *Neuroscience* 304, 29–35. doi: 10.1016/j.neuroscience.2015.06.010

Li, L., Gan, H., Jin, H., Fang, Y., Yang, Y., Zhang, J., et al. (2021). Astragaloside IV promotes microglia/macrophages M2 polarization and enhances neurogenesis and angiogenesis through PPARγ pathway after cerebral ischemia/reperfusion injury in rats. *Int. Immunopharmacol.* 92:107335. doi: 10.1016/j.intimp.2020.107335

Li, Y., and Guo, W. (2021). Neural stem cell niche and adult neurogenesis. *Neuroscientist* 27, 235–245. doi: 10.1177/1073858420939034

Li, D. Q., Li, X. J., Duan, J. F., and Cai, W. (2010). Wuling capsule promotes hippocampal neurogenesis by improving expression of connexin 43 in rats exposed to chronic unpredictable mild stress. *Zhong Xi Yi Jie He Xue Bao* 8, 662–669. doi: 10.3736/jcim20100710

Li, Y., Liang, W., Guo, C., Chen, X., Huang, Y., Wang, H., et al. (2020). Renshen Shouwu extract enhances neurogenesis and angiogenesis via inhibition of TLR4/NF-κB/NLRP3 signaling pathway following ischemic stroke in rats. *J. Ethnopharmacol.* 253:112616. doi: 10.1016/j.jep.2020.112616

Li, X. Y., Qi, W. W., Zhang, Y. X., Jiang, S. Y., Yang, B., Xiong, L., et al. (2019). Helicid ameliorates learning and cognitive ability and activities cAMP/PKA/CREB Signaling in chronic unpredictable mild stress rats. *Biol. Pharm. Bull.* 42, 1146–1154. doi: 10.1248/bpb.b19-00012

Liu, B., Cai, G., Yi, J., and Chen, X. (2013). Buyang Huanwu decoction regulates neural stem cell behavior in ischemic brain. *Neural Regen. Res.* 8, 2336–2342. doi: 10.3969/j.issn.1673-5374.2013.25.004

Liu, S., Liu, J., He, L., Liu, L., Cheng, B., Zhou, F., et al. (2022). A comprehensive review on the benefits and problems of Curcumin with respect to human health. *Molecules* 27, 1–27. doi: 10.3390/molecules27144400

Liu, B., Zhang, Q., Ke, C., Xia, Z., Luo, C., Li, Y., et al. (2019). Ginseng-Angelica-Sansheng-Pulvis boosts neurogenesis against focal cerebral ischemia-induced neurological deficiency. *Front. Neurosci.* 13:515. doi: 10.3389/fnins.2019.00515

Lledo, P. M., Alonso, M., and Grubb, M. S. (2006). Adult neurogenesis and functional plasticity in neuronal circuits. *Nat. Rev. Neurosci.* 7, 179–193. doi: 10.1038/nrn1867

Lopez-Toledano, M. A., Ali Faghihi, M., Patel, N. S., and Wahlestedt, C. (2010). Adult neurogenesis: a potential tool for early diagnosis in Alzheimer's disease? *J. Alzheimers Dis.* 20, 395–408. doi: 10.3233/JAD-2010-1388

Lu, J., Ma, Y., Wu, J., Huang, H., Wang, X., Chen, Z., et al. (2019). A review for the neuroprotective effects of andrographolide in the central nervous system. *Biomed. Pharmacother.* 117:109078. doi: 10.1016/j.biopha.2019.109078

Ma, C. L., Ma, X. T., Wang, J. J., Liu, H., Chen, Y. F., and Yang, Y. (2017). Physical exercise induces hippocampal neurogenesis and prevents cognitive decline. *Behav. Brain Res.* 317, 332–339. doi: 10.1016/j.bbr.2016.09.067

Ma, Y., Tian, S., Sun, L., Yao, S., Liang, Z., Li, S., et al. (2015). The effect of acori graminei rhizoma and extract fractions on spatial memory and hippocampal neurogenesis in amyloid beta 1-42 injected mice. *CNS Neurol. Disord. Drug Targets* 14, 411–420. doi: 10.2174/1871527314666150225124348

Ma, J., Wang, F., Yang, J., Dong, Y., Su, G., Zhang, K., et al. (2017). Xiaochaihutang attenuates depressive/anxiety-like behaviors of social isolation-reared mice by regulating monoaminergic system, neurogenesis and BDNF expression. *J. Ethnopharmacol.* 208, 94–104. doi: 10.1016/j.jep.2017.07.005

Mao, J., Huang, S., Liu, S., Feng, X. L., Yu, M., Liu, J., et al. (2015). A herbal medicine for Alzheimer's disease and its active constituents promote neural progenitor proliferation. *Aging Cell* 14, 784–796. doi: 10.1111/acel.12356

Marques, B. L., Carvalho, G. A., Freitas, E. M. M., Chiareli, R. A., Barbosa, T. G., Di Araujo, A. G. P., et al. (2019). The role of neurogenesis in neurorepair after ischemic stroke. *Semin. Cell Dev. Biol.* 95, 98–110. doi: 10.1016/j.semcdb.2018.12.003

Matsubara, S., Matsuda, T., and Nakashima, K. (2021). Regulation of adult mammalian neural stem cells and neurogenesis by cell extrinsic and intrinsic factors. *Cells* 10, 1–15. doi: 10.3390/cells10051145

Matsuda, T., and Nakashima, K. (2021). Natural and forced neurogenesis in the adult brain: mechanisms and the ir possible application to treat neurological disorders. *Neurosci. Res.* 166, 1–11. doi: 10.1016/j.neures.2020.05.011

Mellios, N., Feldman, D. A., Sheridan, S. D., Ip, J. P. K., Kwok, S., Amoah, S. K., et al. (2018). MeCP2-regulated miRNAs control early human neurogenesis through differential effects on ERK and AKT signaling. *Mol. Psychiatry* 23, 1051–1065. doi: 10.1038/mp.2017.86

Mendes-da-Silva, C., Lemes, S. F., Baliani Tda, S., Versutti, M. D., and Torsoni, M. A. (2015). Increased expression of Hes5 protein in notch signaling pathway in the hippocampus of mice offspring of dams fed a high-fat diet during pregnancy and suckling. *Int. J. Dev. Neurosci.* 40, 35–42. doi: 10.1016/j.ijdevneu.2014.11.005

Miller, B. R., and Hen, R. (2015). The current state of the neurogenic theory of depression and anxiety. *Curr. Opin. Neurobiol.* 30, 51–58. doi: 10.1016/j.conb.2014.08.012

Miller, S. M., and Sahay, A. (2019). Functions of adult-born neurons in hippocampal memory interference and indexing. *Nat. Neurosci.* 22, 1565–1575. doi: 10.1038/s41593-019-0484-2

Ming, G. L., and Song, H. (2011). Adult neurogenesis in the mammalian brain: significant answers and significant questions. *Neuron* 70, 687–702. doi: 10.1016/j.neuron.2011.05.001

Mirsadraee, M., Tavakoli, A., Ghorani, V., and Ghaffari, S. (2018). Effects of *Rosmarinus officinalis* and *Platanus orientalis* extracts on asthmatic subjects resistant to routine treatments. *Avicenna J. Phytomed.* 8, 399–407. doi: 10.22038/AJP.2018.25278.1925

Mirza, F. J., Amber, S., Sumera, H. D., Ahmed, T., and Zahid, S. (2021). Rosmarinic acid and ursolic acid alleviate deficits in cognition, synaptic regulation and adult hippocampal neurogenesis in an Aβ(1-42)-induced mouse model of Alzheimer's disease. *Phytomedicine* 83:153490. doi: 10.1016/j.phymed.2021.153490

Mizuki, D., Matsumoto, K., Tanaka, K., Thi Le, X., Fujiwara, H., Ishikawa, T., et al. (2014). Antidepressant-like effect of *Butea superba* in mice exposed to chronic mild stress and its possible mechanism of action. *J. Ethnopharmacol.* 156, 16–25. doi: 10.1016/j.jep.2014.08.014

Moon, M., Jeong, H. U., Choi, J. G., Jeon, S. G., Song, E. J., Hong, S. P., et al. (2016). Memory-enhancing effects of *Cuscuta japonica* Choisy via enhancement of adult hippocampal neurogenesis in mice. *Behav. Brain Res.* 311, 173–182. doi: 10.1016/j.bbr.2016.05.031

Moreno-Jimenez, E. P., Terreros-Roncal, J., Flor-Garcia, M., Rabano, A., and Llorens-Martin, M. (2021). Evidences for adult hippocampal neurogenesis in humans. *J. Neurosci.* 41, 2541–2553. doi: 10.1523/JNEUROSCI.0675-20.2020

Mu, Y., and Gage, F. H. (2011). Adult hippocampal neurogenesis and its role in Alzheimer's disease. *Mol. Neurodegener.* 6:85. doi: 10.1186/1750-1326-6-85

Murata, K., Fujita, N., Takahashi, R., and Inui, A. (2018). Ninjinyoeito improves behavioral abnormalities and hippocampal neurogenesis in the corticosterone model of depression. *Front. Pharmacol.* 9:1216. doi: 10.3389/fphar.2018.01216

Odaka, H., Adachi, N., and Numakawa, T. (2017). Impact of glucocorticoid on neurogenesis. *Neural Regen. Res.* 12, 1028–1035. doi: 10.4103/1673-5374.211174

Ohtsuka, T., and Kageyama, R. (2021). Hes1 overexpression leads to expansion of embryonic neural stem cell pool and stem cell reservoir in the postnatal brain. *Development* 148, 1–15. doi: 10.1242/dev.189191

Park, H. R., Kim, J. Y., Lee, Y., Chun, H. J., Choi, Y. W., Shin, H. K., et al. (2016). PMC-12, a traditional herbal medicine, enhances learning memory and hippocampal neurogenesis in mice. *Neurosci. Lett.* 617, 254–263. doi: 10.1016/j.neulet.2016.02.036

Park, S. W., Kim, Y. K., Lee, J. G., Kim, S. H., Kim, J. M., Yoon, J. S., et al. (2007). Antidepressant-like effects of the traditional Chinese medicine kami-shoyo-san in rats. *Psychiatry Clin. Neurosci.* 61, 401–406. doi: 10.1111/j.1440-1819.2007.01676.x

Park, H. J., Lee, K., Heo, H., Lee, M., Kim, J. W., Whang, W. W., et al. (2008). Effects of *Polygala tenuifolia* root extract on proliferation of neural stem cells in the hippocampal CA1 region. *Phytother. Res.* 22, 1324–1329. doi: 10.1002/ptr.2488

Po, K. K., Leung, J. W., Chan, J. N., Fung, T. K., Sánchez-Vidaña, D. I., Sin, E. L., et al. (2017). Protective effect of Lycium Barbarum polysaccharides on dextromethorphan-induced mood impairment and neurogenesis suppression. *Brain Res. Bull.* 134, 10–17. doi: 10.1016/j.brainresbull.2017.06.014

Qin, T., Fu, X., Yu, J., Zhang, R., Deng, X., Fu, Q., et al. (2019). Modification of GSK3β/β-catenin signaling on saikosaponins-d-induced inhibition of neural progenitor cell proliferation and adult neurogenesis. *Toxicology* 424:152233. doi: 10.1016/j.tox.2019.06.004

Quintard, H., Lorivel, T., Gandin, C., Lazdunski, M., and Heurteaux, C. (2014). MLC901, a traditional Chinese medicine induces neuroprotective and neuroregenerative benefits after traumatic brain injury in rats. *Neuroscience* 277, 72–86. doi: 10.1016/j.neuroscience.2014.06.047

Rahman, A. A., Amruta, N., Pinteaux, E., and Bix, G. J. (2021). Neurogenesis after stroke: a therapeutic perspective. *Transl. Stroke Res.* 12, 1–14. doi: 10.1007/s12975-020-00841-w

Rai, S. N., Dilnashin, H., Birla, H., Singh, S. S., Zahra, W., Rathore, A. S., et al. (2019). The role of PI3K/Akt and ERK in neurodegenerative disorders. *Neurotox. Res.* 35, 775–795. doi: 10.1007/s12640-019-0003-y

Ren, C., Wang, B., Li, N., Jin, K., and Ji, X. (2015). Herbal formula Danggui-Shaoyao-san promotes neurogenesis and angiogenesis in rat following middle cerebral artery occlusion. *Aging Dis.* 6, 245–253. doi: 10.14336/AD.2014.1126

Ren, Z. L., and Zuo, P. P. (2012). Neural regeneration: role of traditional Chinese medicine in neurological diseases treatment. *J. Pharmacol. Sci.* 120, 139–145. doi: 10.1254/jphs.12R06CP

Ryu, S., Jeon, H., Kim, H. Y., Koo, S., and Kim, S. (2020). Korean red ginseng promotes hippocampal neurogenesis in mice. *Neural Regen. Res.* 15, 887–893. doi: 10.4103/1673-5374.268905

Sahay, A., and Hen, R. (2007). Adult hippocampal neurogenesis in depression. *Nat. Neurosci.* 10, 1110–1115. doi: 10.1038/nn1969

Santarelli, L., Saxe, M., Gross, C., Surget, A., Battaglia, F., Dulawa, S., et al. (2003). Requirement of hippocampal neurogenesis for the behavioral effects of antidepressants. *Science* 301, 805–809. doi: 10.1126/science.1083328

Schoenfeld, T. J., McCausland, H. C., Morris, H. D., Padmanaban, V., and Cameron, H. A. (2017). Stress and loss of adult neurogenesis differentially reduce hippocampal volume. *Biol. Psychiatry* 82, 914–923. doi: 10.1016/j.biopsych.2017.05.013

Seo, M. K., Cho, H. Y., Lee, C. H., Koo, K. A., Park, Y. K., Lee, J. G., et al. (2013). Antioxidant and proliferative activities of Bupleuri radix extract against serum deprivation in SH-SY5Y cells. *Psychiatry Investig.* 10, 81–88. doi: 10.4306/pi.2013.10.1.81

Shakerin, Z., Esfandiari, E., Razavi, S., Alaei, H., Ghanadian, M., and Dashti, G. (2020). Effects of *Cyperus rotundus* extract on spatial memory impairment and neuronal differentiation in rat model of Alzheimer's disease. *Adv. Biomed. Res.* 9:17. doi: 10.4103/abr.abr_173_19

Shen, J., Zhang, M., Zhang, K., Qin, Y., Liu, M., Liang, S., et al. (2022). Effect of angelica polysaccharide on mouse myeloid-derived suppressor cells. *Front. Immunol.* 13:989230. doi: 10.3389/fimmu.2022.989230

Shin, S. J., Jeong, Y. O., Jeon, S. G., Kim, S., Lee, S. K., Nam, Y., et al. (2018). Jowiseungchungtang inhibits amyloid-β aggregation and amyloid-β-mediated pathology in 5XFAD mice. *Int. J. Mol. Sci.* 19:4026. doi: 10.3390/ijms19124026

Shioda, N., Han, F., and Fukunaga, K. (2009). Role of Akt and ERK signaling in the neurogenesis following brain ischemia. *Int. Rev. Neurobiol.* 85, 375–387. doi: 10.1016/S0074-7742(09)85026-5

Snyder, J. S., Soumier, A., Brewer, M., Pickel, J., and Cameron, H. A. (2011). Adult hippocampal neurogenesis buffers stress responses and depressive behaviour. *Nature* 476, 458–461. doi: 10.1038/nature10287

Song, M. D., Kim, D. H., Kim, J. M., Lee, H. E., Park, S. J., Ryu, J. H., et al. (2013). Danggui-Jakyak-san ameliorates memory impairment and increase neurogenesis induced by transient forebrain ischemia in mice. *BMC Complement. Altern. Med.* 13:324. doi: 10.1186/1472-6882-13-324

Sorrells, S. F., Paredes, M. F., Cebrian-Silla, A., Sandoval, K., Qi, D., Kelley, K. W., et al. (2018). Human hippocampal neurogenesis drops sharply in children to undetectable levels in adults. *Nature* 555, 377–381. doi: 10.1038/nature25975

Stazi, M., and Wirths, O. (2021). Chronic memantine treatment ameliorates behavioral deficits, neuron loss, and impaired neurogenesis in a model of Alzheimer's disease. *Mol. Neurobiol.* 58, 204–216. doi: 10.1007/s12035-020-02120-z

Suh, H., Deng, W., and Gage, F. H. (2009). Signaling in adult neurogenesis. *Annu. Rev. Cell Dev. Biol.* 25, 253–275. doi: 10.1146/annurev.cellbio.042308.113256

Sun, G. G., Shih, J. H., Chiou, S. H., Hong, C. J., Lu, S. W., and Pao, L. H. (2016). Chinese herbal medicines promote hippocampal neuroproliferation, reduce stress hormone levels, inhibit apoptosis, and improve behavior in chronically stressed mice. *J. Ethnopharmacol.* 193, 159–168. doi: 10.1016/j.jep.2016.07.025

Suroowan, S., and Mahomoodally, M. F. (2019). Herbal medicine of the 21st century: a focus on the chemistry, pharmacokinetics and toxicity of five widely advocated phytotherapies. *Curr. Top. Med. Chem.* 19, 2718–2738. doi: 10.2174/1568026619666191112121330

Taupin, P. (2005). Adult neurogenesis in the mammalian central nervous system: functionality and potential clinical interest. *Med. Sci. Monit.* 11, Ra247–Ra252. doi: 10.1016/j.lfs.2005.02.003

Taupin, P. (2008). Adult neurogenesis pharmacology in neurological diseases and disorders. *Expert. Rev. Neurother.* 8, 311–320. doi: 10.1586/14737175.8.2.311

Terreros-Roncal, J., Moreno-Jimenez, E. P., Flor-Garcia, M., Rodriguez-Moreno, C. B., Trinchero, M. F., Cafini, F., et al. (2021). Impact of neurodegenerative diseases on human adult hippocampal neurogenesis. *Science* 374, 1106–1113. doi: 10.1126/science.abl5163

Tian, H., Li, X., Tang, Q., Zhang, W., Li, Q., Sun, X., et al. (2018). Yi-nao-jie-yu prescription exerts a positive effect on neurogenesis by regulating notch signals in the hippocampus of post-stroke depression rats. *Front. Psych.* 9:483. doi: 10.3389/fpsyt.2018.00483

Toda, T., and Gage, F. H. (2018). Review: adult neurogenesis contributes to hippocampal plasticity. *Cell Tissue Res.* 373, 693–709. doi: 10.1007/s00441-017-2735-4

Tsai, Y. C., Lin, Y. C., Huang, C. C., Villaflores, O. B., Wu, T. Y., Huang, S. M., et al. (2019). Hericium erinaceus mycelium and its isolated compound, Erinacine a, ameliorate high-fat high-sucrose diet-induced metabolic dysfunction and spatial learning deficits in aging mice. *J. Med. Food* 22, 469–478. doi: 10.1089/jmf.2018.4288

Tunc-Ozcan, E., Peng, C. Y., Zhu, Y., Dunlop, S. R., Contractor, A., and Kessler, J. A. (2019). Activating newborn neurons suppresses depression and anxiety-like behaviors. *Nat. Commun.* 10:3768. doi: 10.1038/s41467-019-11641-8

Tzeng, T. T., Chen, C. C., Chen, C. C., Tsay, H. J., Lee, L. Y., Chen, W. P., et al. (2018). The cyanthin diterpenoid and sesterterpene constituents of Hericium erinaceus mycelium ameliorate Alzheimer's disease-related pathologies in APP/PS1 transgenic mice. *Int. J. Mol. Sci.* 19, 1–22. doi: 10.3390/ijms19020598

Vaidya, V. A., Fernandes, K., and Jha, S. (2007). Regulation of adult hippocampal neurogenesis: relevance to depression. *Expert. Rev. Neurother.* 7, 853–864. doi: 10.1586/14737175.7.7.853

Villa, R. F., Ferrari, F., and Moretti, A. (2018). Post-stroke depression: mechanisms and pharmacological treatment. *Pharmacol. Ther.* 184, 131–144. doi: 10.1016/j.pharmthera.2017.11.005

Vivar, C. (2015). Adult hippocampal neurogenesis, aging and neurodegenerative diseases: possible strategies to prevent cognitive impairment. *Curr. Top. Med. Chem.* 15, 2175–2192. doi: 10.2174/1568026615666150610141524

Wang, J., Hu, J., Chen, X., Lei, X., Feng, H., Wan, F., et al. (2021). Traditional Chinese medicine monomers: novel strategy for endogenous neural stem cells activation after stroke. *Front. Cell. Neurosci.* 15:628115. doi: 10.3389/fncel.2021.628115

Wang, H., Lau, B. W., Wang, N. L., Wang, S. Y., Lu, Q. J., Chang, R. C., et al. (2015). *Lycium barbarum* polysaccharides promotes in vivo proliferation of adult rat retinal progenitor cells. *Neural Regen. Res.* 10, 1976–1981. doi: 10.4103/1673-5374.172315

Wang, H. W., Liou, K. T., Wang, Y. H., Lu, C. K., Lin, Y. L., Lee, I. J., et al. (2011). Deciphering the neuroprotective mechanisms of Bu-yang Huan-wu decoction by an integrative neurofunctional and genomic approach in ischemic stroke mice. *J. Ethnopharmacol.* 138, 22–33. doi: 10.1016/j.jep.2011.06.033

Wang, W. W., Lu, L., Bao, T. H., Zhang, H. M., Yuan, J., Miao, W., et al. (2016). Scutellarin alleviates behavioral deficits in a mouse model of multiple sclerosis, possibly through protecting neural stem cells. *J. Mol. Neurosci.* 58, 210–220. doi: 10.1007/s12031-015-0660-0

Wang, H. Z., Luo, W. L., Zeng, N. X., Li, H. Z., Li, L., Yan, C., et al. (2021). Cerebrospinal fluid proteomics reveal potential protein targets of JiaWeiSiNiSan in preventing chronic psychological stress damage. *Pharm. Biol.* 59, 1065–1076. doi: 10.1080/13880209.2021.1954666

Wang, T., Wang, S. W., Zhang, Y., Wu, X. F., Peng, Y., Cao, Z., et al. (2014). Scorpion venom heat-resistant peptide (SVHRP) enhances neurogenesis and neurite outgrowth of immature neurons in adult mice by up-regulating brain-derived neurotrophic factor (BDNF). *PLoS One* 9:e109977. doi: 10.1371/journal.pone.0110617

Wang, M., Yao, M., Liu, J., Takagi, N., Yang, B., Zhang, M., et al. (2020). Ligusticum chuanxiong exerts neuroprotection by promoting adult neurogenesis and inhibiting inflammation in the hippocampus of ME cerebral ischemia rats. *J. Ethnopharmacol.* 249:112385. doi: 10.1016/j.jep.2019.112385

Winner, B., and Winkler, J. (2015). Adult neurogenesis in neurodegenerative diseases. *Cold Spring Harb. Perspect. Biol.* 7:a021287. doi: 10.1101/cshperspect.a021287

Wu, L., Ran, C., Liu, S., Liao, L., Chen, Y., Guo, H., et al. (2013). Jiaweisinisan facilitates neurogenesis in the hippocampus after stress damage. *Neural. Regen. Res.* 8, 1091–1102. doi: 10.3969/j.issn.1673-5374.2013.12.004

Xiao, H., Jiang, Q., Qiu, H., Wu, K., Ma, X., Yang, J., et al. (2021). Gastrodin promotes hippocampal neurogenesis via PDE9-cGMP-PKG pathway in mice following cerebral ischemia. *Neurochem. Int.* 150:105171. doi: 10.1016/j.neuint.2021.105171

Xiao, H., Li, H., Song, H., Kong, L., Yan, X., Li, Y., et al. (2020). Shenzao jiannao oral liquid, an herbal formula, ameliorates cognitive impairments by rescuing neuronal death and triggering endogenous neurogenesis in AD-like mice induced by a combination of Aβ42 and scopolamine. *J. Ethnopharmacol.* 259:112957. doi: 10.1016/j.jep.2020.112957

Xing, H., Zhang, K., Zhang, R., Shi, H., Bi, K., and Chen, X. (2015). Antidepressant-like effect of the water extract of the fixed combination of Gardenia jasminoides, Citrus aurantium and Magnolia officinalis in a rat model of chronic unpredictable mild stress. *Phytomedicine* 22, 1178–1185. doi: 10.1016/j.phymed.2015.09.004

Xu, Y., Ku, B., Cui, L., Li, X., Barish, P. A., Foster, T. C., et al. (2007). Curcumin reverses impaired hippocampal neurogenesis and increases serotonin receptor 1A mRNA and brain-derived neurotrophic factor expression in chronically stressed rats. *Brain Res.* 1162, 9–18. doi: 10.1016/j.brainres.2007.05.071

Xu, A. L., Zheng, G. Y., Ye, H. Y., Chen, X. D., and Jiang, Q. (2020). Characterization of astrocytes and microglial cells in the hippocampal CA1 region after transient focal cerebral ischemia in rats treated with Ilexonin a. *Neural Regen. Res.* 15, 78–85. doi: 10.4103/1673-5374.264465

Yan, L., Hu, Q., Mak, M. S., Lou, J., Xu, S. L., Bi, C. W., et al. (2016). A Chinese herbal decoction, reformulated from Kai-Xin-san, relieves the depression-like symptoms in stressed rats and induces neurogenesis in cultured neurons. *Sci. Rep.* 6:30014. doi: 10.1038/srep30014

Yan, H. C., Qu, H. D., Sun, L. R., Li, S. J., Cao, X., Fang, Y. Y., et al. (2010). Fuzi polysaccharide-1 produces antidepressant-like effects in mice. *Int. J. Neuropsychopharmacol.* 13, 623–633. doi: 10.1017/S1461145709990733

Yan, Y., Zhao, J., Cao, C., Jia, Z., Zhou, N., Han, S., et al. (2014). Tetramethylpyrazine promotes SH-SY5Y cell differentiation into neurons through epigenetic regulation of topoisomerase IIβ. *Neuroscience* 278, 179–193. doi: 10.1016/j.neuroscience.2014.08.010

Yang, L., Wang, Y., Li, N., Xu, B., Duan, J., Yuan, C., et al. (2020). The anti-depression-like effects of Zhengtian capsule via induction of neurogenesis and the neurotrophic signaling pathway. *Front. Pharmacol.* 11:1338. doi: 10.3389/fphar.2020.01338

Yang, H., Wen, S. R., Zhang, G. W., Wang, T. G., Hu, F. X., Li, X. L., et al. (2011). Effects of Chinese herbal medicine Fuzhisan on autologous neural stem cells in the brain of SAMP-8 mice. *Exp. Gerontol.* 46, 628–636. doi: 10.1016/j.exger.2010.12.004

Yang, Z. H., Zhang, G. M., Chen, C. Y., He, J., and Chen, C. J. (2021). Prenatal exposure to koumine results in cognitive deficits and increased anxiety-like behavior in mice offspring. *J. Chem. Neuroanat.* 111:101888. doi: 10.1016/j.jchemneu.2020.101888

Yang, W. T., Zheng, X. W., Chen, S., Shan, C. S., Xu, Q. Q., Zhu, J. Z., et al. (2017). Chinese herbal medicine for Alzheimer's disease: clinical evidence and possible mechanism of neurogenesis. *Biochem. Pharmacol.* 141, 143–155. doi: 10.1016/j.bcp.2017.07.002

Yao, R., Zhang, L., Li, X., and Li, L. (2010). Effects of epimedium flavonoids on proliferation and differentiation of neural stem cells in vitro. *Neurol. Res.* 32, 736–742. doi: 10.1179/174313209X459183

Yao, R. Q., Zhang, L., Wang, W., and Li, L. (2009). Cornel iridoid glycoside promotes neurogenesis and angiogenesis and improves neurological function after focal cerebral ischemia in rats. *Brain Res. Bull.* 79, 69–76. doi: 10.1016/j.brainresbull.2008.12.010

Yau, S. Y., Li, A., and So, K. F. (2015). Involvement of adult hippocampal neurogenesis in learning and forgetting. *Neural Plast.* 2015:717958. doi: 10.1155/2015/717958

Ye, M., Chung, H. S., An, Y. H., Lim, S. J., Choi, W., Yu, A. R., et al. (2016). Standardized herbal formula PM012 decreases cognitive impairment and promotes neurogenesis in the 3xTg AD mouse model of Alzheimer's disease. *Mol. Neurobiol.* 53, 5401–5412. doi: 10.1007/s12035-015-9458-x

Yip, K. L., Zhou, X., Chook, P., Leung, P. C., Schachter, S., Mok, V. C. T., et al. (2020). Herb-drug interaction of gastrodiae rhizoma on carbamazepine: a pharmacokinetic study in rats. *Epilepsy Res.* 165:106376. doi: 10.1016/j.eplepsyres.2020.106376

Zeng, J., Ji, Y., Luan, F., Hu, J., Rui, Y., Liu, Y., et al. (2022). Xiaoyaosan ethylacetate fraction alleviates depression-like behaviors in CUMS mice by promoting hippocampal neurogenesis via modulating the IGF-1Rbeta/PI3K/Akt signaling pathway. *J. Ethnopharmacol.* 288:115005. doi: 10.1016/j.jep.2022.115005

Zhang, R., Engler, A., and Taylor, V. (2018). Notch: an interactive player in neurogenesis and disease. *Cell Tissue Res.* 371, 73–89. doi: 10.1007/s00441-017-2641-9

Zhang, S., Lu, Y., Chen, W., Shi, W., Zhao, Q., Zhao, J., et al. (2021). Network pharmacology and experimental evidence: PI3K/AKT signaling pathway is involved in the antidepressive roles of Chaihu Shugan san. *Drug Des. Devel. Ther.* 15, 3425–3441. doi: 10.2147/DDDT.S315060

Zhang, R., Ma, Z., Liu, K., Li, Y., Liu, D., Xu, L., et al. (2019). Baicalin exerts antidepressant effects through Akt/FOXG1 pathway promoting neuronal differentiation and survival. *Life Sci.* 221, 241–248. doi: 10.1016/j.lfs.2019.02.033

Zhang, X. G., Shan, C., Zhu, J. Z., Bao, X. Y., Tong, Q., Wu, X. F., et al. (2017). Additive neuroprotective effect of borneol with mesenchymal stem cells on ischemic stroke in mice. *Front. Physiol.* 8:1133. doi: 10.3389/fphys.2017.01133

Zhang, E., Shen, J., and So, K. F. (2014). Chinese traditional medicine and adult neurogenesis in the hippocampus. *J. Tradit. Complement. Med.* 4, 77–81. doi: 10.4103/2225-4110.130372

Zhang, Z., Wang, Z., Rui, W., and Wu, S. (2018). Magnesium lithospermate B promotes proliferation and differentiation of neural stem cells in vitro and enhances neurogenesis in vivo. *Tissue Cell* 53, 8–14. doi: 10.1016/j.tice.2018.05.012

Zhang, K., Wang, F., Yang, J. Y., Wang, L. J., Pang, H. H., Su, G. Y., et al. (2015). Analysis of main constituents and mechanisms underlying antidepressant-like effects of Xiaochaihutang in mice. *J. Ethnopharmacol.* 175, 48–57. doi: 10.1016/j.jep.2015.08.031

Zhang, Z., Wu, R., Li, P., Liu, F., Zhang, W., Zhang, P., et al. (2009). Baicalin administration is effective in positive regulation of twenty-four ischemia/reperfusion-related proteins identified by a proteomic study. *Neurochem. Int.* 54, 488–496. doi: 10.1016/j.neuint.2009.02.005

Zhang, J. H., Xin, H. L., Xu, Y. M., Shen, Y., He, Y. Q., Hsien, Y., et al. (2018). Morinda officinalis how – A comprehensive review of traditional uses, phytochemistry and pharmacology. *J. Ethnopharmacol.* 213, 230–255. doi: 10.1016/j.jep.2017.10.028

Zhang, K., Yang, J., Wang, F., Pan, X., Liu, J., Wang, L., et al. (2016). Antidepressant-like effects of Xiaochaihutang in a neuroendocrine mouse model of anxiety/depression. *J. Ethnopharmacol.* 194, 674–683. doi: 10.1016/j.jep.2016.10.028

Zhang, X., Zheng, W., Wang, T., Ren, P., Wang, F., Ma, X., et al. (2017). Danshen-Chuanxiong-Honghua ameliorates cerebral impairment and improves spatial cognitive deficits after transient focal ischemia and identification of active compounds. *Front. Pharmacol.* 8:452. doi: 10.3389/fphar.2017.00452

Zhao, X., Cui, Y., Wu, P., Zhao, P., Zhou, Q., Zhang, Z., et al. (2020). Polygalae radix: a review of its traditional uses, phytochemistry, pharmacology, toxicology, and pharmacokinetics. *Fitoterapia* 147:104759. doi: 10.1016/j.fitote.2020.104759

Zhao, T., Yang, Z., Mei, X., Xu, L., and Fan, Y. (2020). Metabolic disturbance in Korean red ginseng-induced "Shanghuo" (excessive heat). *J. Ethnopharmacol.* 253:112604. doi: 10.1016/j.jep.2020.112604

Zheng, Y. Q., Li, L., Liu, J. X., Yao, M. J., Liu, S. B., Hu, Y., et al. (2014). Study on effect of huatuo zaizao extractum on focal cerebral ischemia/reperfusion neurogenesis in rats and its mechanisms. *Zhongguo Zhong Yao Za Zhi* 39, 891–895. doi: 10.4268/cjcmm20140526

Zhou, Z., Dun, L., Wei, B., Gan, Y., Liao, Z., Lin, X., et al. (2020). Musk ketone induces neural stem cell proliferation and differentiation in cerebral ischemia via activation of the PI3K/Akt Signaling pathway. *Neuroscience* 435, 1–9. doi: 10.1016/j.neuroscience.2020.02.031

Zhou, Y., Su, Y., Li, S., Kennedy, B. C., Zhang, D. Y., Bond, A. M., et al. (2022). Molecular landscapes of human hippocampal immature neurons across lifespan. *Nature* 607, 527–533. doi: 10.1038/s41586-022-04912-w

Zhu, J., Mu, X., Zeng, J., Xu, C., Liu, J., Zhang, M., et al. (2014). Ginsenoside Rg1 prevents cognitive impairment and hippocampus senescence in a rat model of D-galactose-induced aging. *PLoS One* 9:e101291. doi: 10.1371/journal.pone.0101291

Zhuang, P., Zhang, Y., Cui, G., Bian, Y., Zhang, M., Zhang, J., et al. (2012). Direct stimulation of adult neural stem/progenitor cells in vitro and neurogenesis in vivo by salvianolic acid B. *PLoS One* 7:e35636. doi: 10.1371/journal.pone.0035636

Zhuge, L., Fang, Y., Jin, H., Li, L., Yang, Y., Hu, X., et al. (2020). Chinese medicine Buyang Huanwu decoction promotes neurogenesis and angiogenesis in ischemic stroke rats by upregulating miR-199a-5p expression. *Zhejiang Da Xue Xue Bao Yi Xue Ban* 49, 687–696. doi: 10.3785/j.issn.1008-9292.2020.12.03

Zick, S. M., Ruffin, M. T., Lee, J., Normolle, D. P., Siden, R., Alrawi, S., et al. (2009). Phase II trial of encapsulated ginger as a treatment for chemotherapy-induced nausea and vomiting. *Support Care Cancer* 17, 563–572. doi: 10.1007/s00520-008-0528-8

Zou, H., Long, J., Zhang, Q., Zhao, H., Bian, B., Wang, Y., et al. (2016). Induced cortical neurogenesis after focal cerebral ischemia--three active components from Huang-Lian-Jie-Du decoction. *J. Ethnopharmacol.* 178, 115–124. doi: 10.1016/j.jep.2015.12.001

frontiers | Frontiers in Neuroscience

TYPE Original Research
PUBLISHED 20 April 2023
DOI 10.3389/fnins.2023.1134176

OPEN ACCESS

EDITED BY
Guibo Sun,
Chinese Academy of Medical Sciences and Peking Union Medical College, China

REVIEWED BY
Guoqi Zhu,
Anhui University of Chinese Medicine, China
Baiyan Liu,
Hunan University of Chinese Medicine, China

*CORRESPONDENCE
Zhiyong Xiao
✉ zy-xiao@163.com
Wenxia Zhou
✉ zhouwx@bmi.ac.cn

†These authors have contributed equally to this work and share first authorship

SPECIALTY SECTION
This article was submitted to Neuropharmacology, a section of the journal Frontiers in Neuroscience

RECEIVED 30 December 2022
ACCEPTED 28 March 2023
PUBLISHED 20 April 2023

CITATION
Huang Y, Wang J, Liu F, Wang C, Xiao Z and Zhou W (2023) Liuwei Dihuang formula ameliorates chronic stress-induced emotional and cognitive impairments in mice by elevating hippocampal O-GlcNAc modification.
Front. Neurosci. 17:1134176.
doi: 10.3389/fnins.2023.1134176

Liuwei Dihuang formula ameliorates chronic stress-induced emotional and cognitive impairments in mice by elevating hippocampal O-GlcNAc modification

Yan Huang[1,2,3†], Jianhui Wang[2,3†], Feng Liu[2,3], Chenran Wang[2,3], Zhiyong Xiao[2,3*] and Wenxia Zhou[1,2,3*]

[1]Nanjing University of Chinese Medicine, Nanjing, China, [2]Beijing Institute of Pharmacology and Toxicology, Beijing, China, [3]State Key Laboratory of Toxicology and Medical Countermeasures, Beijing, China

A substantial body of evidence has indicated that intracerebral O-linked N-acetyl-β-D-glucosamine (O-GlcNAc), a generalized post-translational modification, was emerging as an effective regulator of stress-induced emotional and cognitive impairments. Our previous studies showed that the Liuwei Dihuang formula (LW) significantly improved the emotional and cognitive dysfunctions in various types of stress mouse models. In the current study, we sought to determine the effects of LW on intracerebral O-GlcNAc levels in chronic unpredictable mild stress (CUMS) mice. The dynamic behavioral tests showed that anxiety- and depression-like behaviors and object recognition memory of CUMS mice were improved in a dose-dependent manner after LW treatment. Moreover, linear discriminate analysis (LEfSe) of genera abundance revealed a significant difference in microbiome among the study groups. LW showed a great impact on the relative abundance of these gut microbiota in CUMS mice and reinstated them to control mouse levels. We found that LW potentially altered the Uridine diphosphate-N-acetylglucosamine (UDP-GlcNAc) biosynthesis process, and the abundance of O-GlcNAcase (OGA) and O-GlcNAc transferase (OGT) in CUMS mice, which was inferred using PICRUSt analysis. We further verified advantageous changes in hippocampal O-GlcNAc modification of CUMS mice following LW administration, as well as changes in the levels of OGA and OGT. In summary, LW intervention increased the levels of hippocampal O-GlcNAc modification and ameliorated the emotional and cognitive impairments induced by chronic stress in CUMS mice. LW therefore could be considered a potential prophylactic and therapeutic agent for chronic stress.

KEYWORDS

O-GlcNAc, Liuwei Dihuang formula, gut microbiota, O-GlcNAcase, O-GlcNAc transferase

Introduction

Mounting evidence has proposed that the dynamic form of intracellular post-translational modification (PTM) of proteins, O-linked N-acetylglucosamine (O-GlcNAc), as a sensor of stress pathways in organismal cells and tissues (Fehl and Hanover, 2022). The O-GlcNAcylation is regulated by the "writer" O-GlcNAc transferase (OGT) and the "eraser" O-GlcNAcase (OGA), which catalyze the addition and hydrolyzation of the GlcNAc moiety to the proteins, respectively (Chatham et al., 2021). To date, this dynamic PTM has been shown to participate in the pathogenesis and pathological process of various stress-related diseases, ranging from tumors (Hanover et al., 2018) to diabetes (Hegyi et al., 2020) and neurodegeneration (Yin et al., 2022). Hence, a developing hypothesis is that any abnormal physiological state with changed stress levels has an O-GlcNAc component (Yang and Suh, 2014). O-GlcNAc cycling is essential in the central nervous system, which has a higher level of OGT than peripheral tissues (Okuyama and Marshall, 2003). The catalytic deficiency of O-GlcNAc transferase was reported to contribute to X-linked intellectual disability, which directly reveals the key role of O-GlcNAc events in the nervous system (Pravata et al., 2019; Meek et al., 2021). Increasing global levels of O-GlcNAc by modulating OGT and OGA activity induced neuroprotection (Yuzwa et al., 2012) and slowed neurodegeneration (Wang et al., 2016a). The O-GlcNAc deficiency or depletion, using a conditional knockout mouse model, led to diminishing the pool of adult neural stem/progenitor cells and consequently aberrant adult neurogenesis *in vivo* (Chen et al., 2021). Reduced neuron-specific O-GlcNAc in the hippocampus elicited a decrease in synaptic protein expression and alteration in excitatory synaptic function (Wheatley et al., 2019). These evidence reveals an essential role for O-GlcNAc in the function of the neuronal system.

Due to the regulatory function of O-GlcNAc in synapse underlying memory formation, alterations in O-GlcNAc levels affected cognitive capability. Increasing the global O-GlcNAc of type 2 diabetes mellitus subjects was positively correlated with better memory function (Huang R. et al., 2019). Sleep deprivation cognitive impairment was facilitated by a reduction in cerebral O-GlcNAc levels (Lee et al., 2020). The catalytically inactive OGA elicited defects in habituation behaviors, demonstrating the requisite of O-GlcNAc for cognitive function (Muha et al., 2020). Due to the strong association between impaired glucose metabolism and depressive disorder (Elias et al., 2022), the altered O-GlcNAc flux is also involved in emotional behaviors. The OGA heterozygous rodents exhibited antidepressant-like behaviors, by chronically elevating cerebral O-GlcNAc levels (Cho et al., 2020). While abnormal levels of O-GlcNAc in mice of cognitive impairment caused by the pathologies of Alzheimer's disease (Kim et al., 2022), hyperglycemia (Shi et al., 2021), and sleep deprivation (Kim et al., 2021) have been demonstrated, however, the role of O-GlcNAc in contributing to changed emotional and cognitive phenotypes under chronic stress conditions has been largely overlooked and unknown.

Previous research has found that the hormones in the hypothalamus pituitary adrenal axis, neuronal remodeling, intracerebral metabolism, and gut microbiome were strongly associated with chronic stress-induced behavioral disturbances (Bollinger et al., 2022; Morella et al., 2022; Zhou R. et al., 2022; Huang et al., 2023). Additionally, emerging evidence has implicated that O-GlcNAc modification might serve as a stress sensor (Liu Y. et al., 2020). Moreover, the OGT secreted from *Legionella*, *Photorhabdus,* and *Clostridium perfringens* could promote the host's protein O-GlcNAcylation to modify cellular processes (Guttenberg et al., 2012; Lu et al., 2015). The *cp*OGA, a promiscuous microbial OGA, could remove O-GlcNAc from TGF-beta activated kinase 1 binding protein 1 (Pathak et al., 2012). In addition, gut bacterial secreted OGAs could protect rodents from ulcerative colitis by hydrolyzing O-GlcNAcylated proteins in the host (He et al., 2021). According to current studies, gut microbiota might affect the level of intracerebral O-GlcNAc through short-chain fatty acids (SCFAs), bile acids, and gut-brain-liver interaction (Cuervo-Zanatta et al., 2022; Hurley et al., 2022; Wang T. Y. et al., 2022). These studies revealed that in addition to being regulated by the host's hydrolase and transferase, the O-GlcNAcylated proteins in the host might be also controlled by bacterial-secreted OGTs and OGAs. However, it remains an open question whether manipulating gut microbial communities could regulate the levels of the host's protein O-GlcNAcylation and subsequent physiological functions.

Liuwei Dihuang formula (LW) is a classical traditional Chinese medicine consisting of six herbs (Zhou et al., 2016). In recent years, numerous studies have indicated that LW displayed ameliorative effects on the impairments of cognitive function induced by D-galactose (Liu B. et al., 2022), β-amyloid (Sangha et al., 2012), and senescence (Huang et al., 2012). Moreover, further studies demonstrate that the active fraction and monomers of LW could also alleviate cognitive dysfunction via diverse mechanisms, including hippocampal transcriptome (Wang et al., 2017b), N-glycan (Wang et al., 2017a), neuroendocrine-immune system (Wang et al., 2016c), as well as intestinal microbiome (Wang et al., 2019; Huang et al., 2022). While the crosstalk between gut microbiota and O-GlcNAcylation has been previously described (He et al., 2021), the ameliorative effect of LW on emotional and cognitive dysfunction associated with O-GlcNAc modification has yet to be explored. In this study, a chronic unpredictable mild stress (CUMS) mouse model was used to observe the effects of LW administration on the emotional and cognitive impairments, the alterations of community diversity and composition of gut microbiota, as well as on the O-GlcNAc-related biosynthesis pathways and enzymes, aiming to understand whether the amelioration of emotional and cognitive impairments by LW is related to the regulations of gut microbiota and hippocampal O-GlcNAc modifications.

Materials and methods

Animals and treatment

One hundred adult Male C57BL/6J mice (6–7 weeks-old) were used in the present study, which was purchased from SiPeiFu (Beijing) Biotechnology Co., Ltd. (Beijing, China) and maintained under specific pathogen-free conditions at the Laboratory Animal Center, Academy of Military Medicine Sciences. Behavioral experiments were conducted after 1 week of adaptive feeding. The

mice were fed and drank freely and individually housed at room temperature (25 ± 1°C) with 55 ± 5% humidity and a 12 h light/dark cycle (lights on 7:00–19:00).

The experiment was assigned into two time periods of 14 and 28 days (**Figure 1**), each of which was subdivided into five groups, control group, chronic unpredictable mild stress (CUMS) group, low dose group (0.7 g/kg), middle dose group (1.4 g/kg), and high dose group (2.8 g/kg). All mice were randomly divided into five groups of 10 mice each. There was no stress or medication treatment in the control group. The CUMS group was given intragastric administration of normal saline. The other three groups were given different doses of the Liuwei Dihuang formula (0.7 g/kg, 1.4 g/kg, 2.8 g/kg). The LW (20071816, National Medicine Permission Number Z19993068, Beijing, China) was purchased from Beijing Tongrentang Technology Development Co., Ltd. The animal feeding environment and experimental program are following the relevant regulations of the Beijing Institute of Pharmacology and Toxicology and are approved by the Institute of Animal Care and Use Committee (IACUC) of the National Beijing Center for Drug Safety Evaluation and Research (NBCDSER).

Chronic unpredictable mild stress

The modeling method of CUMS model is based on previous literature (Chevalier et al., 2020) with some modifications. In this study, 14 stress conditions were adopted, which were the following: food deprivation for 24 h, water deprivation for 24 h, cage tilt 45° for 24 h, daytime darkness for 12 h, overnight light for 12 h, wet padding for 24 h, no padding for 24 h, tail clamping for 2 min, restraint for 2 h, swimming at 4°C for 5 min, noise for 1 h (100 dB), foot shock for 1 h (1 mA, 5 s/min), tail suspension 30 min, cage vibration 1 h (220 r/min). Any two random combinations of stress styles per day.

Behavioral assessments

Open field test (OFT)

The open-field test was used to measure activity and anxiety-like behaviors (Zhou L. et al., 2020). Thirty minutes before the test, the mice were put into the behavioral room for environmental adaptation, and then put into the center of the open field box of 40 cm × 40 cm × 40 cm (XR-XZ301, Shanghai Xinxin Information Technology Co., Ltd) and allowed to roam freely for 10 min. The whole experiment was recorded by the camera system (ANY-maze, Global Biotech Inc., USA), and the distance of the mouse movement in the central region within 10 min was recorded.

Elevated plus-maze test (EPM)

Each mouse was placed in the central position of the elevated cross maze (central area 5 cm × 5 cm, open arm 35 cm × 35 cm, closed arm 35 cm × 35 cm, and the height from the ground 76 cm, XR-XG201, Shanghai Xinxin Information Technology Co., Ltd.), and started facing the open arm area. Each mouse was tested for 5 min and recorded using animal behavior video (ANY-maze, Global Biotech Inc., USA) analysis software. The open-arm exploration time was used as an indicator of anxiety (Dong et al., 2020).

Sucrose preference test (SPT)

Before the formal start of the experiment (Liu et al., 2018a), the baseline of mice was tested first. The mice with a sucrose water preference rate of more than 80% were selected to ensure that the sugar water baseline of each group of mice was consistent, and then the SPT was conducted. The drinking bottle and squirrel cage specially used in the SPT was selected, and the water was first adapted to pure water for 24 h and then 2% sucrose water for 24 h under the same experimental environment. After the acclimation, all mice were deprived of water for 24 h, and a bottle of sucrose water and another bottle of pure water were placed above each mouse cage for 24 h test. After 12 h of testing, the positions of the two bottles of water were switched to exclude the effect of positional preference. The experiment was the same as the above details.

Novel object recognition test (NOR)

The novel object recognition test (Bevins and Besheer, 2006) was divided into three stages. The mice were put into a room 30 min before each stage for environmental adaptation. In the first stage of adaptation (days 1–2), mice were put into the testing box (XR-XX117, Shanghai Jilang Software Technology Co., Ltd) and allowed to freely explore for 20 min. After that, the box was wiped with 75% ethanol to avoid odor interference with the next mouse. In the second stage of learning (day 3), put two identical objects A and B into the box, and then put the mice on the side of the box wall away from the object, respectively. Each mouse was free to explore in the box for 16 min and recorded the total time T_A, T_B of exploring the two objects. In the third stage of the test period (1 and 24 h after stage II), one end of the box was the original object A, and the other end replaced object B with a new object C. The test lasted for 4 min, and the total time (T_A and T_C) of the mice exploring the original object A and the novel object C was recorded. The mice whose total exploration time of the two objects was less than 5 s were excluded. The preference index (PI) was used to evaluate the cognitive behavior of mice. The higher PI = $T_C/(T_A + T_C)$, the better the recognition and memory ability of mice.

Western blot (WB)

Total protein was extracted from the hippocampus in RIPA lysis (C1053, APPLYGEN, China) buffer containing a protease inhibitor and supplemented with phosphatase inhibitors (11836170001, Roche, Germany), and centrifuged at 12,000 × g for 5 min at 4°C. The protein was quantified by the BCA protein assay kit. Protein lysates were cleared of insoluble material through centrifugation. Proteins were wet transferred to 0.2 μm pore size, hydrophobic PVDF transfer membranes (ISEQ00010, Millipore, Germany), which were blocked using 5% non-fat milk in 1% TBST buffer for 1 h at room temperature. The membranes were incubated overnight using the following primary antibodies: O-GlcNAc (CTD110.6, 1:1000 dilution) Mouse mAb (12938S, CST, USA), GAPDH (1:5000 dilution) Mouse McAb (60004-1, Proteintech, China). All primary antibodies were used in 5% BSA (CZ1006, czkwbio, China). Membranes were washed in 1%TBST (T1082, Solarbio, China) and incubated with the following appropriate secondary antibodies: goat anti-mouse HRP. The secondary antibodies were used at a 1:5,000 and 1:10000 dilution in 5% BSA. Protein bands were visualized following exposure of the membranes to ECL (RM0021, ABclonal, China) and quantified by densitometry analysis using Image software.

Enzyme-linked immunosorbent assay (ELISA)

The protein extracted from the hippocampus was brought to room temperature for ELISA. The manufacturer's protocol for OGT (ml940027, Enzyme-linked Biotechnology, Shanghai, China) and OGA ELISA kit (ml950023, Enzyme-linked Biotechnology, Shanghai, China) was followed. Samples were visualized using an Enspire^{TM} multilabel reader 2,300 (Perkin Elmer, Finland) at the 450 nm wavelength. The concentrations of OGT and OGA in the sample were calculated according to the standard curve, and the ratio of OGT to OGA is calculated.

Mouse fecal collection and 16s rRNA sequencing

Fresh fecal samples (approximately 5–6 granules) from each mouse were collected and stored at −80°C for testing after the CUMS. Mouse fecal microbial genomic DNA was extracted according to the E.Z.N.A.® soil DNA kit (Omega Bio-Tek, Norcross, USA) instructions, and the quality of DNA extraction was detected using 1% agarose gel electrophoresis. PCR products from the same sample were mixed and then recovered using 2% agarose Gel. AxyPrep DNA Gel Extraction Kit (Axygen Biosciences, Union City, USA) was used to purify the recovered products. The recovered products were detected by 2% agarose gel electrophoresis and quantified by Quantus Fluorometer (Promega, USA). Use NEXTFLEX Rapid DNA-Seq Kit to build libraries. Sequencing was performed using Illumina's Miseq PE300/NovaSeq PE250 platform (Shanghai Majorbio Bio-pharm Technology Co., Ltd., China).

To study microbial diversity in the environment, the richness and diversity of the microbial community can be reflected by Alpha diversity analysis (Rogers et al., 2016; Zverev et al., 2021) in a single sample. Alpha diversity refers to the diversity in a specific region or ecosystem. Metrics in this study include sobs, chao, Shannon, and Simpson. By comparing species diversity in different habitats or microbial communities, Beta diversity analysis was conducted to explore the similarity or differences in community composition among different groups (Mohamed et al., 2021; Shen et al., 2021). Principal co-ordinates analysis (PCoA) is a non-binding data dimension reduction analysis method, which can be used to study the similarity or differences of sample community composition, PCoA was mapped based on the selected distance matrix, and was used to find out the potential principal components that affected the differences in sample community composition by dimensionality reduction. The differential gut microbiota obtain from the analysis of community composition (Ji et al., 2017) is based on data tables in the tax_summary_a folder and is graphed using R language tools. According to the results of taxonomic analysis, the species composition of different groups (or samples) at various taxonomic levels (such as domain, kingdom, phylum, class, order, family, genus, species, OTU, etc.) can be known. To evaluate the metabolic potential of the microbial community after LW intervention, the 16S rRNA sequence reading was clustered into operational taxonomic units (OTUs) using the closed reference method in QIIME2 software. Import the generated OTU table into PICRUSt (Langille et al., 2013; Tang et al., 2018; Ijoma et al., 2021), and use the Kyoto Encyclopedia of Genes and Genome (KEGG) database to predict the functional gene content of various microbial communities represented in the Greengenes 16S rRNA gene sequence database. In addition, for Pathway, PICRUSt was used to obtain information on three levels of metabolic pathways and the abundance tables of each level.

Statistical analysis

GraphPad Prism 9.0 was used for graphing and statistical analyses. Student's *t*-test was used for a two-group comparison of parametric data. One-way ANOVA with Dunnett's or Tukey's correction was used for multi-group non-parametric analyses. The behavioral data were combined by the *z*-score (Penny et al., 2019). A lower *z*-score signified an increase in behavioral deficits. The community richness of microbiota was analyzed by sobs and Chao, and the diversity of microbiota was analyzed by Shannon and Simpson. The microbial similarity was analyzed by principal coordinate analysis (PCoA). The effect sizes of the differentially abundant gut genus were analyzed by linear discriminant analysis (LDA) effect size (LEfSe) analysis ($|\text{LDA}| > 2$ and P-value < 0.05). Profiling of the predicted microorganisms was analyzed by phylogenetic investigation of communities by reconstruction of unobserved states (PICRUSt) method (Langille et al., 2013). The microbial data analysis was performed using the online platform Majorbio Cloud Platform.[1] Data are depicted as mean ± S.D., with $P < 0.05$ considered statistically significant.

Results

LW ameliorates emotional and cognitive impairments of CUMS mice

To investigate whether LW administration alleviates emotional and cognitive impairments induced by CUMS for 14 days in mice, the CUMS mice were fed with LW for 2 weeks. In the open field test and elevated plus-maze test, CUMS-14D mice exhibited significantly decreased center distance (**Figure 2A1**) and open arm time (**Figure 2A2**) than control mice. There were no group differences in sucrose preference rate (**Figure 2A3**), preference index (**Figure 2A4**), and *z*-score (**Figure 2A5**). However, the effects of LW (0.7, 1.4, 2.8 g/kg) on improving emotional and cognitive impairments were not obtained on day 14 of CUMS. These results indicate that the anxiety-like behavior appeared following 14-day CUMS but was unrelieved by administering three doses of LW.

For the 28-day CUMS, there were no group differences in the center distance (**Figure 2B1**) and open arm time (**Figure 2B2**). To examine depression in these mice, we employed the sucrose preference test (**Figure 2B3**). The CUMS-28D group exhibited a lower sucrose preference rate than the control group. Furthermore, administration of LW (0.7, 1.4, 2.8 g/kg) increased this rate in CUMS-28D mice. The results of the novel object recognition test (NOR) revealed a significantly decreased preferential index in CUMS-28D mice, and treatment with LW (0.7 g/kg) significantly improved

1 www.majorbio.com

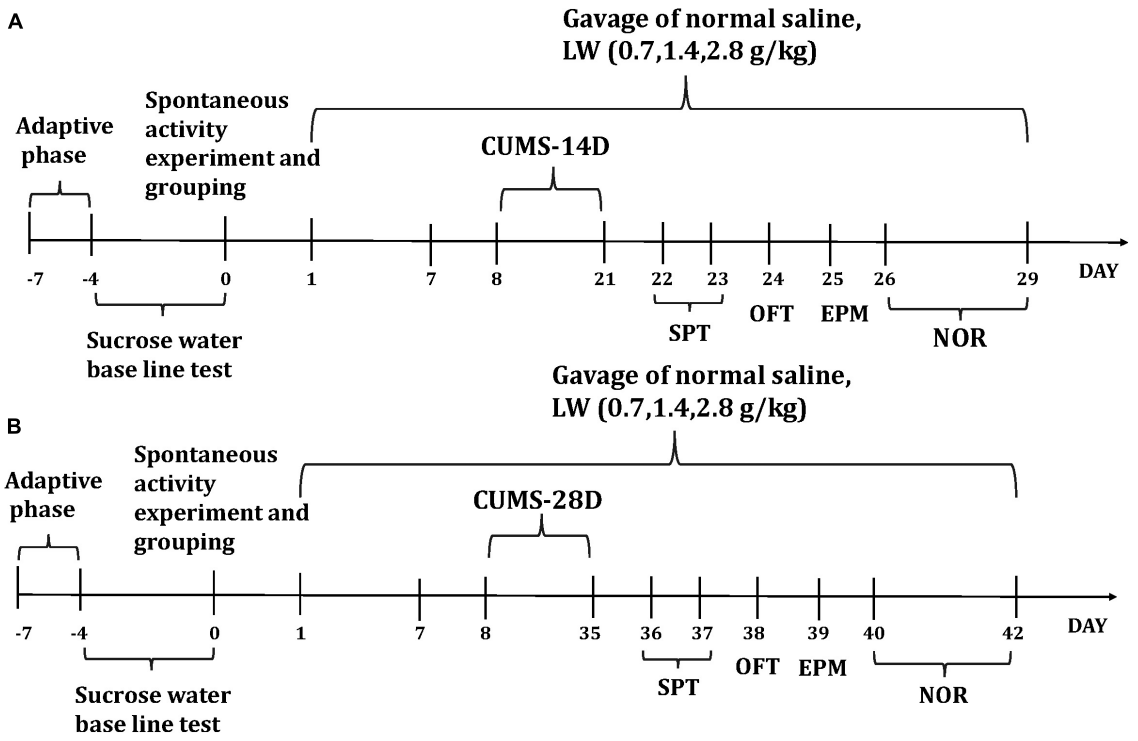

FIGURE 1
The experimental timeline and the effects of CUMS on mice. The dosage and days of intragastric administration and the specific time arrangement of each behavior after the end of CUMS-14D **(A)**, CUMS-28D **(B)**.

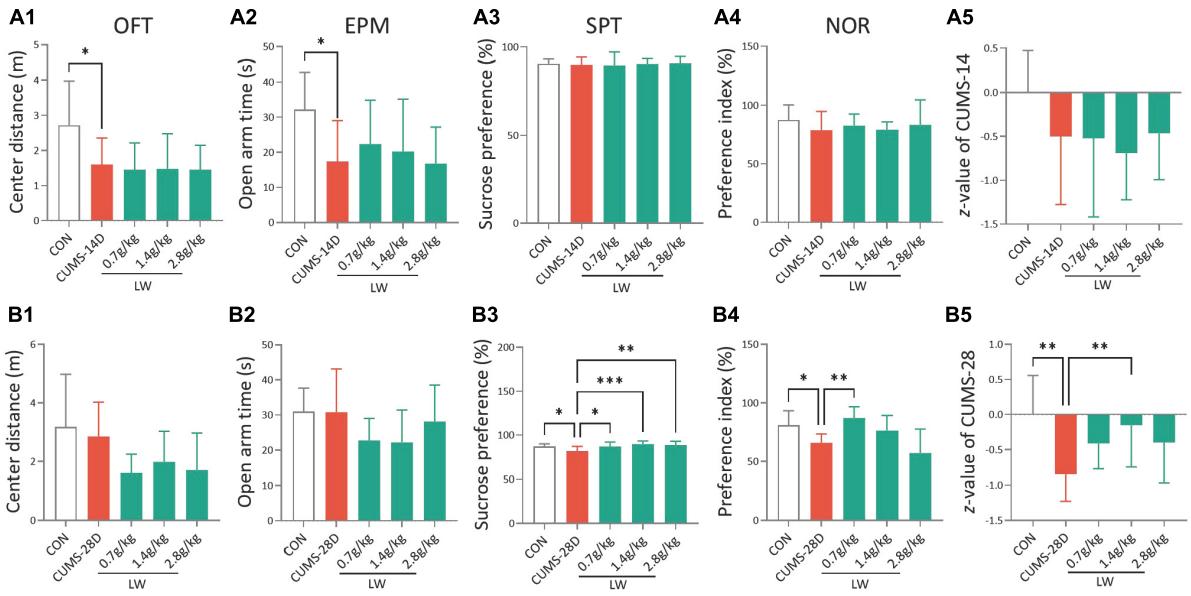

FIGURE 2
Liuwei Dihuang formula (LW) ameliorates the emotional and cognitive impairments of CUMS mice. Intragastric administration was started 7 days in advance and behavioral tests were performed after chronic stress. The distance in the center zone **(A1)** in the OFT, open arm time **(A2)** in the EPM, sucrose preference rate **(A3)** in SPT, preference index **(A4)** in the NOR test, and emotion and cognition z-score **(A5)** of mice on day 14 of CUMS. The center distance **(B1)**, open arm time **(B2)**, sucrose preference rate **(B3)**, preference index **(B4)**, and z-score **(B5)** of mice on day 28 of CUMS. $^{*}P < 0.05$, $^{**}P < 0.01$, $^{***}P < 0.001$ were one-way ANOVA followed by Dunnett's *post-hoc* test. The values are mean ± S.D., $n = 10$.

the preferential index (Figure 2B4). The emotion-cognition phenotype evaluated by the composite *z*-score analysis showed a higher stress response of CUMS-28D mice in comparison to the control group, while 1.4 g/kg LW normalized the *z*-score in the CUMS group (Figure 2B5). These results indicated that the depression-like behavior and cognitive impairment

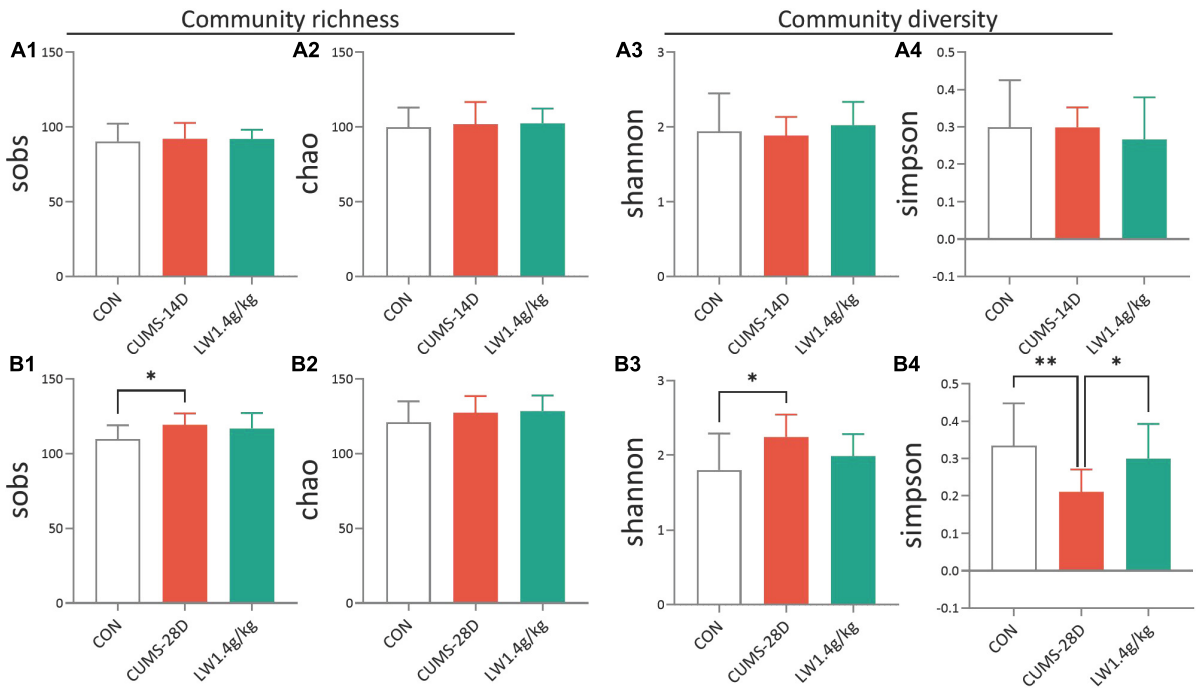

FIGURE 3
Liuwei Dihuang formula increases the community diversity of gut microbiota in CUMS mice. Mice to be sampled were placed in a clean cage covered with sterile filter paper after behavioral tests, and fecal samples were collected immediately after the mice defecated. This was used to detect gut microbiota. Different mouse samples should be replaced with new filter paper. The community richness of mice on days 14 **(A1,A2)** and 28 **(B1,B2)** of CUMS were analyzed by sobs and chao. The community diversity of mice on days 14 **(A3,A4)** and 28 **(B3,B4)** of CUMS were analyzed by Shannon and Simpson. $^{*}P < 0.05$, $^{**}P < 0.01$ were one-way ANOVA followed by Dunnett's *post-hoc* test. The values are mean ± S.D., $n = 10$.

appeared following 28-day CUMS and were relieved by administering 1.4 g/kg of LW.

LW reshapes community diversity and composition of gut microbiota in CUMS mice

Our previous studies have described that active fractions of LW restored cognitive deficits of adult senescence-accelerated mice by modifications of gut microbiota (Wang et al., 2016b, 2019). Hence, we next examined whether LW (1.4 g/kg) intervention protection against CUMS-induced cognitive deficits was related to gut microbiome alterations. The composition and diversity of gut microbiota composition and diversity were analyzed by 16S sequencing. The results of alpha diversity analysis showed that there were no group differences in sobs (**Figure 3A1**) and chao (**Figure 3A2**) (richness of microbiota), or Shannon (**Figure 3A3**) and Simpson (**Figure 3A4**) (diversity of microbiota) on day 14 of CUMS, as shown in **Supplementary Table 1**. The CUMS-28D group exhibited higher sobs and Shannon, and a lower Simpson than the control group (**Figures 3B1–B4**), as shown in **Supplementary Table 2**. Moreover, the administration of LW normalized these indexes in CUMS-28D mice. These results showed that the prominently disordered microbiota richness and diversity were observed following 28-day CUMS. In terms of community diversity, we mainly tested Shannon and Simpson, LW administration improved the Shannon of CUMS mice and showed a trend of ameliorating the Simpson of CUMS mice.

To analyze the dynamical similarities and differences of the gut microbiome in each group, principal coordinate analysis (PCoA) were performed. PCoA plot and score showed that there was no obvious separation between the three communities, control, CUMS-14D, and LW (**Figures 4A1, A2** and **Supplementary Tables 3, 4**). In contrast, there was a significant separation of PCoA scores among groups on day 28 of CUMS (**Figures 4B1, B2** and **Supplementary Tables 5, 6**). These data indicated that LW facilitated beneficial alterations in the structure of the gut microbial community, and the patterns of microbiota in the LW-treated group were more similar to the control group than the CUMS-28D group.

To investigate the gut microbiota variations in response to LW intervention, we first compared the microbial composition at the phylum level (**Figures 5A1, A2** and **Supplementary Tables 7, 8**). On day 14 of CUMS, the relative abundance of *Bacteroidota* phylum was significantly lower in CUMS-14D mice compared with control mice (52.51 vs. 40.75%), while the relative abundance of *Firmicutes* in the model group was significantly higher than that of the control group (43.38 vs. 54.65%), which were significantly restored by the LW intervention (**Figure 5B1** and **Supplementary Table 9**). Conversely, CUMS-28D mice exhibited significantly increased *Bacteroidota* phylum (52.93 vs. 54.78%) and decreased *Firmicutes* phylum (38.79 vs. 32.60%) than control mice (**Figure 5B2** and **Supplementary Table 10**). Next, we performed linear discriminant analysis (LDA) effect size (LEfSe) analysis

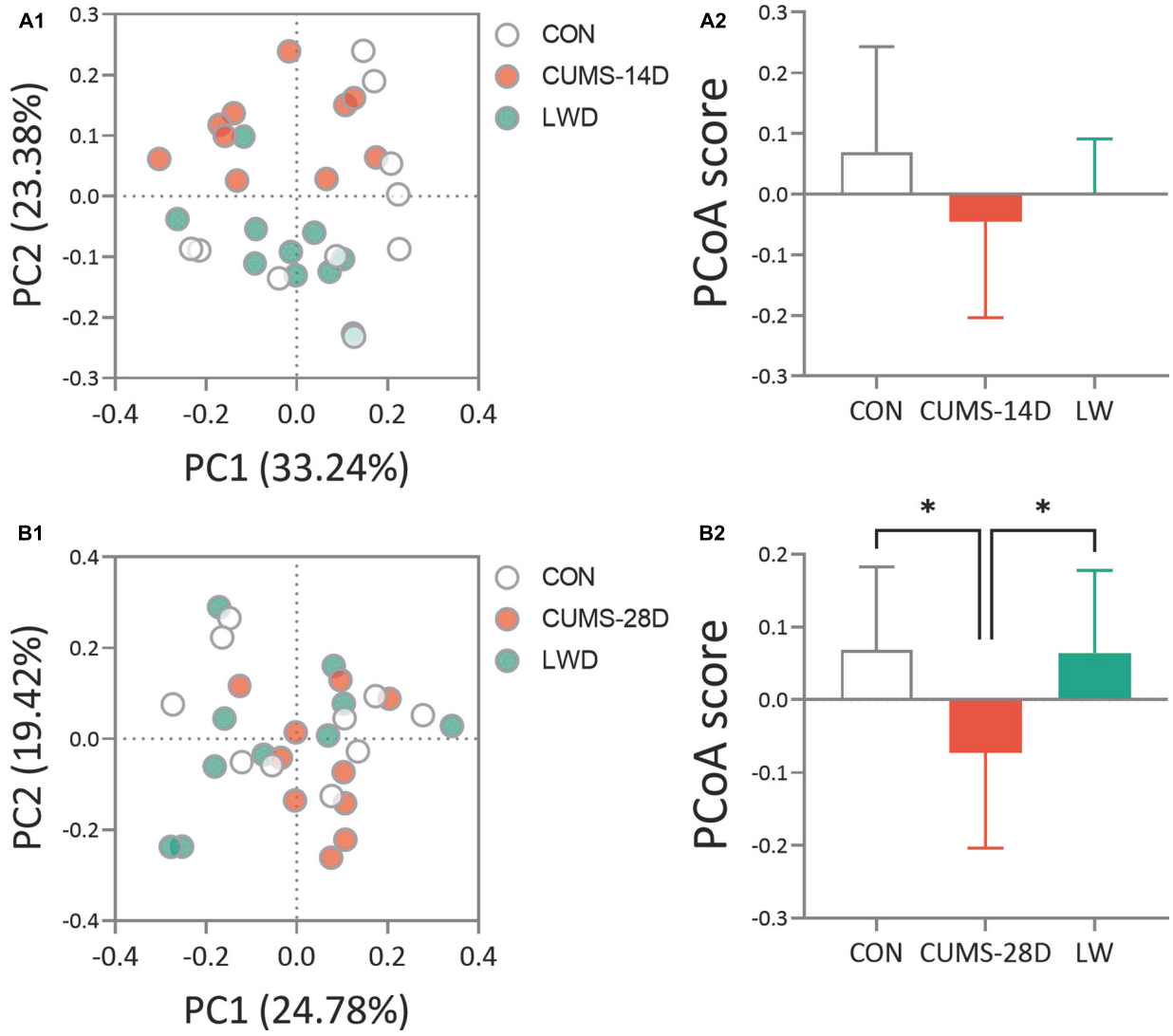

FIGURE 4
Liuwei Dihuang formula restored the beta diversity of gut microbiota in CUMS mice. After the basic collection of mouse feces, DNA extraction, and PCR amplification were performed to process the constructed Illumina Miseq sequencing data. Principle coordinate analysis (PCoA) plots were calculated by the Bray-Curtis similarity methods based on the microbial genus of CUMS-14D **(A1)**, CUMS-28D **(B1)** mice. Characterization of gut microbiota composition in CUMS-14D **(A2)**, CUMS-28D **(B2)** mice based on PCoA scores. *$P < 0.05$ was one-way ANOVA followed by Dunnett's *post-hoc* test. The values are mean ± S.D., n = 10.

(| LDA| > 2 and *P*-value < 0.05) to detect the dominant gut genus significantly affected by CUMS and LW treatment (Figure 5C and Supplementary Table 11). The relative abundances of the 7 genera, including *Rumi.* (*Ruminococcus_torques_group*, LDA = 2.63, $P = 0.03$), *Aero.* (*Aerococcus*, LDA = 2.45, $P = 0.01$), *Prev.* (*Prevotellaceae_NK3B31_group*, LDA = 2.82, $P = 0.04$), *Euba.* (*Eubacterium_nodatum_group*, LDA = 2.53, $P = 0.01$), *Desu.* (*Desulfovibrio*, LDA = 3.24, $P = 0.02$), *Stap.* (*Staphylococcus*, LDA = 4.17, $P = 0.04$), and *Para.* (*Parabacteroides*, LDA = 3.38, $P = 0.01$), were different in the control group. Moreover, 4 genera, including *Rike.* (*Rikenellaceae_RC9_gut_group*, LDA = 3.98, $P = 0.0003$), *Allo.* (*Allobaculum*, LDA = 4.13, $P = 0.0005$), *Dubo.* (*Dubosiella*, LDA = 3.38, $P = 0.01$), and *Eryt.* (*Erythrobacter*, LDA = 3.57, $P = 0.04$), were different in the CUMS group. When comparing the LW group with the control and CUMS group, 4 genera, including *Sacc.* (*Candidatus_Saccharimonas*, LDA = 2.68, $P = 0.03$), *Acti.* (*Candidatus_Actinomarina*, LDA = 3.55, $P = 0.04$), *Muci.* (*Mucispirillum*, LDA = 3.27, $P = 0.02$), and *Heli.* (*Helicobacter*, LDA = 4.14, $P = 0.01$), were revealed as characteristic gut genera.

LW altered the O-GlcNAc-related biosynthesis pathways and enzymes of CUMS mice

To better understand the role of the gut microorganisms in CUMS and the potential underlying mechanism for LW ameliorating emotional and cognitive impairments, we then predicted functional pathway by the phylogenetic investigation of communities by reconstruction of unobserved states (PICRUSt)

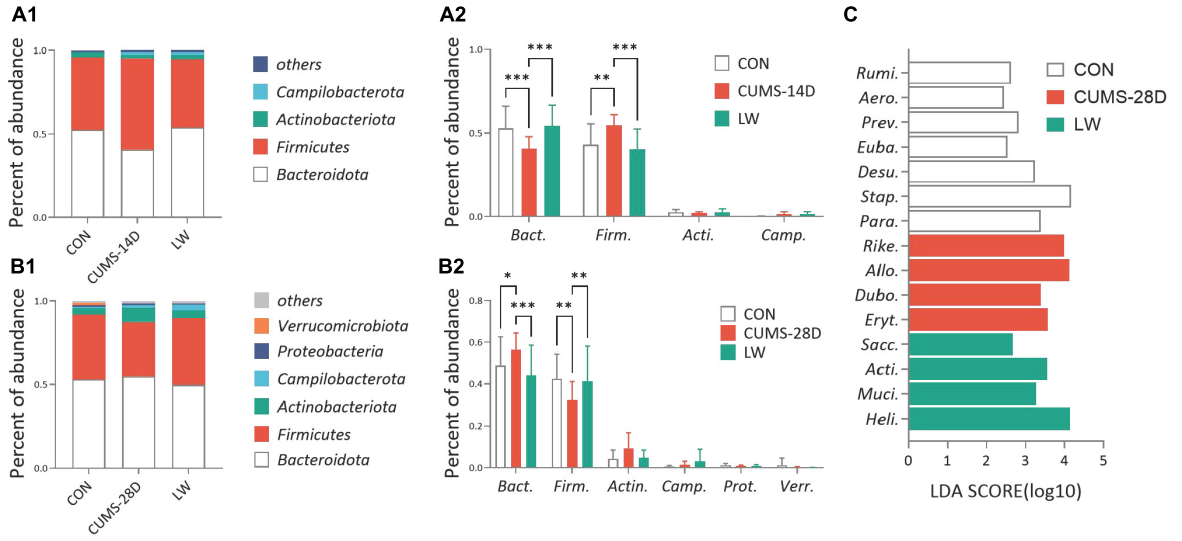

FIGURE 5
Liuwei Dihuang formula reversed the relative abundances of the predominant bacterial taxon of gut microbiota in CUMS mice. The average abundance of the predominant bacterial phylum (with relative abundance >1% in at least one sample) in CUMS-14D **(A1)** and -28D **(B1)** mice. Gut microbiota variations at the phylum level in CUMS-14D **(A2)** and -28D **(B2)** mice. **(C)** The linear discriminant analysis (LDA) effect size (LEfSe) classifying the most differentially abundant taxa at the genus level in CUMS-28D mice (| LDA| > 2 and *P*-value < 0.05 were shown). $^{*}P < 0.05$, $^{**}P < 0.01$, $^{***}P < 0.001$ were one-way ANOVA followed by Dunnett's *post-hoc* test. The values are mean ± S.D., $n = 10$.

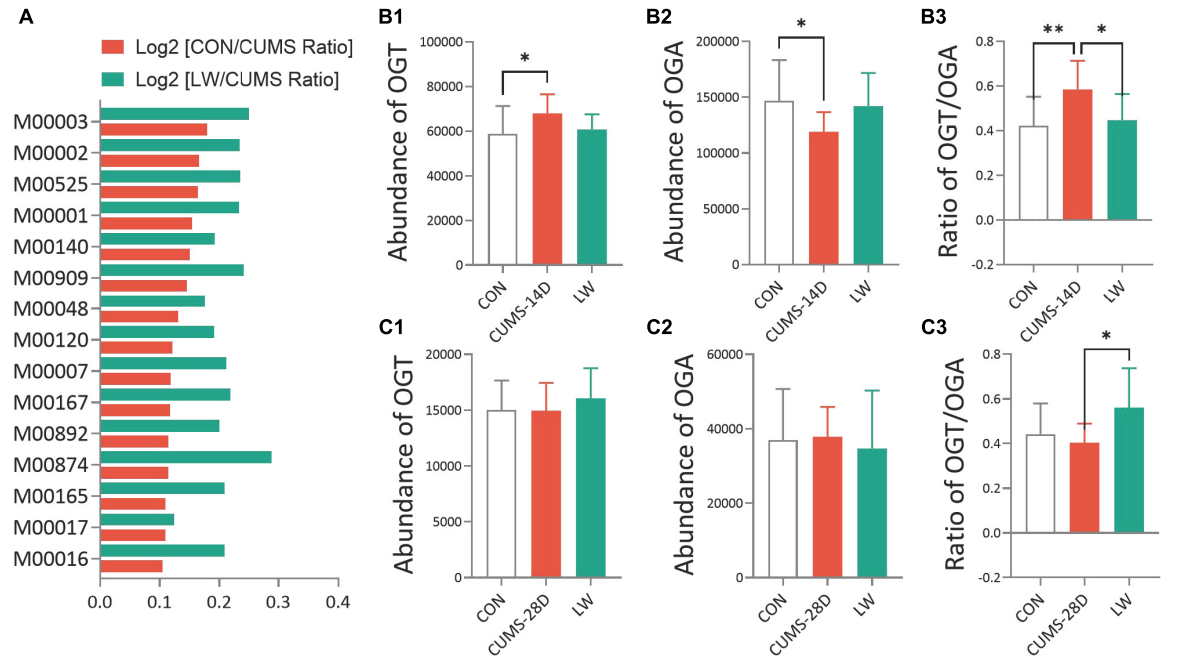

FIGURE 6
Liuwei Dihuang formula altered the O-GlcNAc-related biosynthesis pathways and enzymes of gut microbiota in CUMS mice. PICRUSt was used to standardize the OTU abundance table, that is, to remove the influence of the copy number of the 16S marker gene in the genome. Then, COG and KEGG functional annotations of OTU were carried out according to the corresponding green-gene id of each OTU, and annotation information of OTU at COG and KEGG functional levels and abundance information of each function in different samples were obtained. **(A)** The functional prediction of KEGG pathways using the phylogenetic investigation of communities by reconstruction of unobserved states (PICRUSt) based on OTUs of CUMS mice. Distribution of relative abundances of OGT **(B1,B2)**, OGA **(C1,C2)**, and the ratio of OGT/OGA **(B3,C3)** in CUMS-14D and -28D mice. $^{*}P < 0.05$, $^{**}P < 0.01$ were one-way ANOVA followed by Dunnett's *post-hoc* test. The values are mean ± S.D., $n = 10$.

method (Figure 6A and Supplementary Table 12). The discrepancy in pathways relating to O-GlcNAc-related biosynthesis based on the KEGG database was observed when comparing the CUMS group to control and LW groups, including glycolysis (M00001 and M00002) (Nie et al., 2020), gluconeogenesis (M00003) (Misra et al., 2016), and UDP-N-acetyl-D-glucosamine

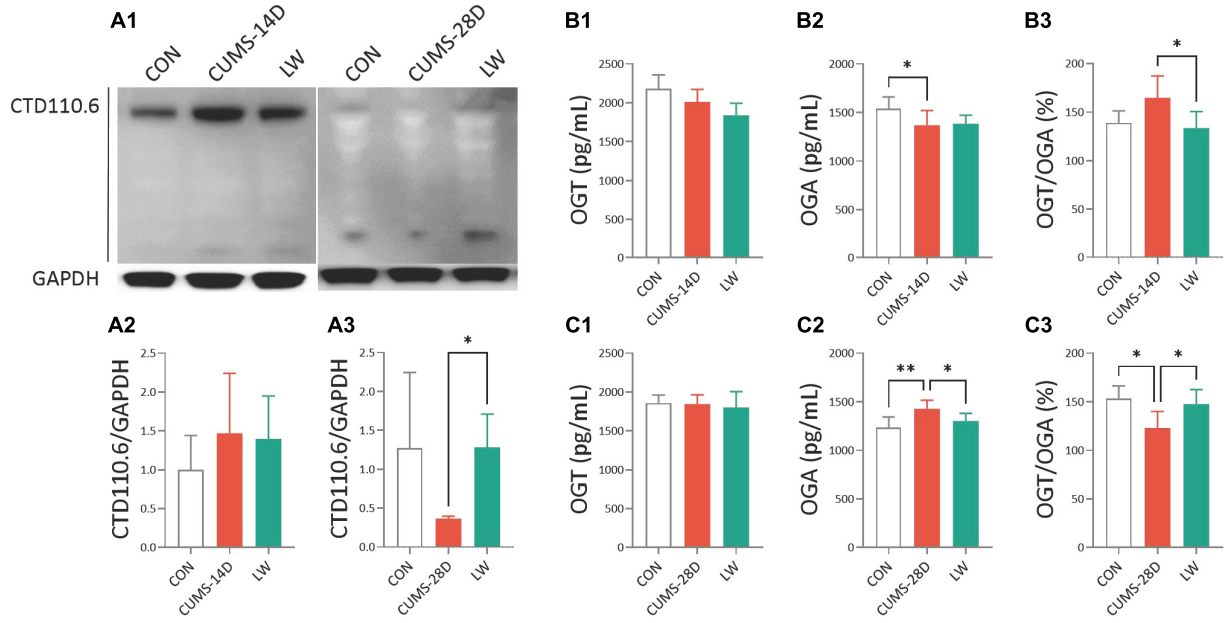

FIGURE 7
Liuwei Dihuang formula elevated hippocampal O-GlcNAc modification of CUMS mice. After behavioral tests, the mice were sacrificed, the hippocampus was isolated from the brain tissue and hippocampus protein was extracted. **(A1)** Representative Western blot of O-GlcNAc from whole hippocampal lysates of CUMS mice. Quantification of hippocampal O-GlcNAc modification levels in CUMS-14D **(A2)** and -28D **(A3)** mice, represented as mean optical intensity normalized to GAPDH. The concentrations of OGT **(B1,C1)**, OGA **(B2,C2)**, and the ratio of OGT/OGA **(B3,C3)** in the hippocampus of CUMS-14D and -28D mice were obtained by ELISA. $^{*}P < 0.05$, $^{**}P < 0.01$ were one-way ANOVA followed by Dunnett's *post-hoc* test. The values are mean ± S.D., $n = 10$.

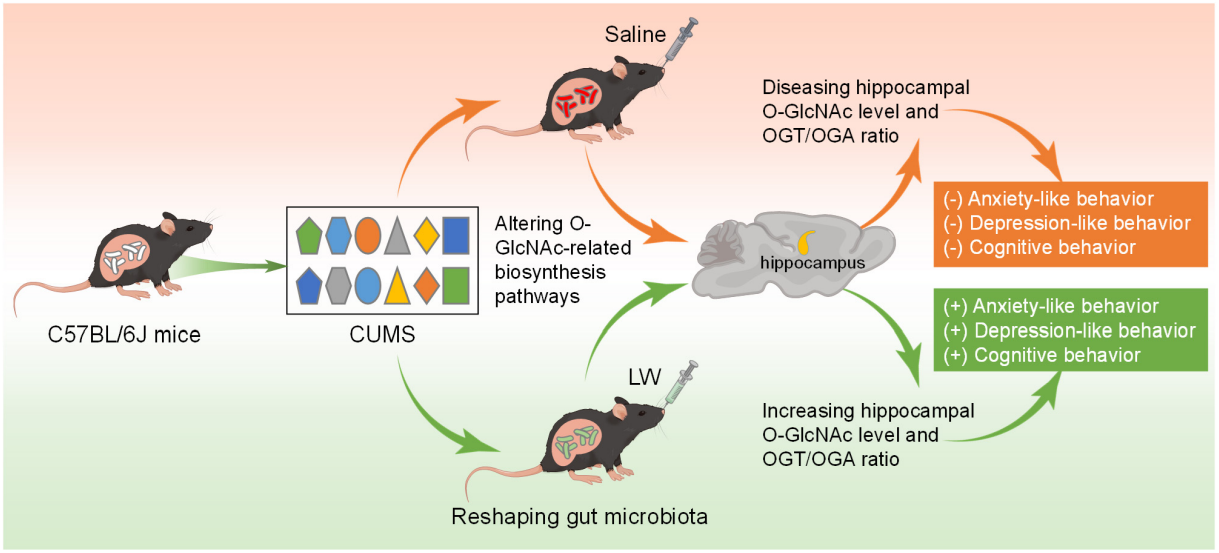

FIGURE 8
Sketch map for the mechanisms of LW on CUMS induced emotional disorders and cognitive impairment. LW decreases the ratio of OGT/OGA levels in CUMS-14D mice but increases the hippocampal ratio of OGT/OGA in CUMS-28D mice. LW intervention increased the levels of hippocampal O-GlcNAc modification and ameliorated the emotional and cognitive impairments induced by chronic stress in CUMS mice.

biosynthesis (M00909 and M00892) (Umapathi et al., 2021). Then, the O-GlcNAc-related enzymes of the gut microorganisms after LW treatment were predicted (Figures 6B1–C3 and Supplementary Tables 13, 14). CUMS-14D mice exhibited a significantly increased abundance of OGT (Figure 6B1) and decreased abundance of OGA (Figure 6B2) than control mice. For the 28-day CUMS, there were no group differences in the abundance of OGT (Figure 6C1) and OGA (Figure 6C2). The ratio of OGT and OGA was positively associated with the level of O-GlcNAc modification. On day 14 of CUMS, the ratio of OGT and OGA was significantly higher in CUMS-14D mice compared with control mice and significantly decreased with LW administration

(Figure 6B3). Within the 28-day CUMS, the ratio of OGT and OGA was no significant change but significantly increased by LW administration (Figure 6C3). The predictive functional analysis partly indicated that O-GlcNAc modification was one of the possible mechanisms of LW ameliorating stress-induced emotional and cognitive impairments.

LW increased the hippocampal O-GlcNAc level and OGT/OGA ratio in CUMS mice

To further examine the effect of LW on O-GlcNAc modification in CUMS mice, Western blot and ELISA were performed on whole hippocampal lysates (Figure 7). The uncropped blots can be found in Supplementary Material 1. There was also a trend to higher O-GlcNAc levels in the hippocampus of CUMS-14D mice (Figures 7A1, A2), and lower O-GlcNAc in CUMS-28D mice (Figures 7A1, A3), although the differences here were not statistically significant. LW treatment significantly increased hippocampal O-GlcNAc modification of CUMS-28D mice. There were no group differences in hippocampal OGT concentration in CUMS-14D (Figure 7B1) and -28D mice (Figure 7C1). For the 14-day CUMS, the hippocampal OGA concentration was observably decreased in CUMS group (Figure 7B2), and the ratio of OGT and OGA was significantly decreased by LW administration (Figure 7B3). For the 28-day CUMS, the hippocampal OGA concentration in CUMS group was significantly increased beyond the control group, while LW normalized this concentration in the CUMS group (Figure 7C2). The ratio of OGT and OGA was significantly decreased in the CUMS group and increased significantly with LW administration, which was consistent with the results of Western blot (Figure 7C3). Although there was no direct evidence that bacterial OGA or OGT could enter the brain, we found that there was a significantly positive correlation between the O-GlcNAc-related enzymes analyzed by PICRUSt and these assayed by ELISA (Supplementary Figure 1). These results indicated that LW intervention potentially decreased hippocampal OGA concentration and increased O-GlcNAc level by modifying the gut microbiota of CUMS mice.

Discussion

Our previous studies have revealed that LW and its active fractions improved cognitive and emotional dysfunctions in various animal models by modulating hippocampal neurogenesis, neurogenic microenvironment, neuroendocrine immunomodulation network, long-term potentiation, hippocampal transcriptome, and intestinal microbiome (Wang et al., 2016c, 2017b, 2019; Wei et al., 2021; Huang et al., 2022). Nevertheless, the role of O-GlcNAc modification in LW ameliorating emotional and cognitive function in CUMS mice, and the specific enzymes involved has generally received scant attention. Here, our results showed that anxiety-like behavior was present approximately at early-CUMS phase (day 14 of CUMS), and depression-like behavior and memory impairment were present on day 28 of CUMS. The administration of LW led to emotional and cognitive improvements in CUMS mice. Mechanistically, LW potentially modified the UDP-GlcNAc biosynthesis process, OGA and OGT levels by modulating the gut microbiome. Moreover, LW intervention increased hippocampal O-GlcNAc modification by elevating the ratio of OGT/OGA in the CUMS mice. These data revealed a significant role of O-GlcNAc modification in behavioral amelioration by LW intervention, which introduced a new mechanistic insight into the improved CUMS effects of LW on emotion and cognition (Figure 8).

To the best of our knowledge, the changes in anxiety-like behavior during the CUMS process were inconsistent in various studies. We have found that CUMS-14D center time was significantly different between the control group and the model group in OFT (Zhou X. D. et al., 2020). However, some literature also reported that there was no difference (Olave et al., 2022). And likewise, there are inconsistent results on day 28 of CUMS. There was significantly increased, decreased, or invariant total distance in the model group compared with the control group (Jeong et al., 2022; Wang C. et al., 2022; Zhou H. et al., 2022). Regarding the center time in OFT, there were also two opposite outcomes (Jeong et al., 2022; Wu et al., 2022; Zhou H. et al., 2022). Moreover, the center distance was not significantly different in OFT on days 28, 42, and 49 of CUMS (Liu et al., 2018c; Jiang et al., 2022; Wang G. et al., 2022), which was consistent with this study. We considered that the different experimental environments and conditions, and animal strains were the main possible reasons for the inconsistent results. And the indicators selected in this study were also relatively simple. In the further study, we will prolong the stress duration and repeat the experimental observation results to explore the deep mechanism of anxiety-like behavior appearing in CUMS-14D and disappearing in CUMS-28D.

Generally, stress can be divided into two forms: acute stress and chronic stress. Human studies have identified both acute and chronic stress as major risk factors for neuropsychiatric disorders, such as cognitive dysfunction (Zhang et al., 2021), major depressive disorder (Bernardo et al., 2022), anxiety disorder (Lopes Sakamoto et al., 2019), and Alzheimer's disease (Muñoz-Mayorga et al., 2020). Recent studies over the span of the last decade showed the significant role of gut homeostasis in maintaining the host's health during the stress process (Cruz-Pereira et al., 2020; Dawud et al., 2022). In this study, we focused on the dynamic changes in the distribution and composition of the gut microflora during chronic stress. We found that the dominant gut constituents in the LW-treated group were *Candidatus_Saccharimonas*, *Candidatus_Actinomarina*, *Mucispirillum*, and *Helicobacter* at the genus level. The *Candidatus Saccharimonas* microflora could be significantly elevated (Liu B. et al., 2022), and be related to inflammatory-related diseases (Cruz et al., 2020). Moreover, *Candidatus Saccharimonas* was a known short-chain fatty acid (SCFA) producer, and its increased abundance affected intestinal pH (Yao et al., 2022). The relative abundance of *Candidatus Actinomarina* was down-regulation in the chronic colitis model (Wu et al., 2020). Many studies have discovered that *Mucispirillum*, a Gram-negative, is highly connected with obesity, infection, inflammatory bowel disease, as well as stress (Anderson and Paschos, 2019; Herp et al., 2021). For example, the studies showed that the high abundance of

Mucispirillum was associated with *Porphyromonas gingivalis*-and anesthesia/surgery-induced cognitive impairments (Chi et al., 2021; Lian et al., 2021). In addition, the elevated the relative abundance of *Mucispirillum* was correlated negatively with cognitive function in Alzheimer's disease transgenic mice (Liu J. et al., 2020) and senile dementia mice (Gao et al., 2018). The *Helicobacter* is an endotoxin-producing microbe, which have a closely associated with ischemic stroke-induced cognitive impairment (Lv et al., 2022), and is implicated in the development of numerous cognitive-related disorders. For instance, increased *Helicobacter* was detected in chronic psychosocial stress, Parkinson's disease and Alzheimer's disease models (Cryan et al., 2019; Luo S. et al., 2022). All of these results suggested that the *Candidatus_Saccharimonas*, *Candidatus_Actinomarina*, *Mucispirillum*, and *Helicobacter* were essential for the improved effects of LW on CUMS mice.

To furtherly investigate the mechanisms underlying potential biological pathways of CUMS-induced emotional and cognitive impairments, PICRUSt based on the KEGG database was executed. Finally, we found that glycolysis, gluconeogenesis, and UDP-N-acetyl-D-glucosamine biosynthesis, which were particularly relevant to O-GlcNAc modification (Misra et al., 2016; Nie et al., 2020; Umapathi et al., 2021), might be the principal pathways in the differential flora. Hence, we assume that O-GlcNAc modification might play a significant role in CUMS. Various types of research have proved that dynamic protein O-GlcNAc modification is an intracellular signaling mechanism triggered by numerous stressors, including pressure-overload hypertrophy (Zhu et al., 2021), trauma-hemorrhage (Zou et al., 2007), cardiac injury (Jones et al., 2008), as well as a stress response (Fahie et al., 2022). As a stress receptor, O-GlcNAcylated p65 rapidly upregulated RNA binding motif protein 3 (Liu Y. et al., 2022) and interleukin-6 level (Hu et al., 2022) to maintain glucose metabolism and decrease apoptosis in the skeletal muscle of mice under acute cold exposure. Acute exercise stress significantly increased the O-GlcNAc level for cellular adaptation to oxidative stress, and this effect persists for at least 4 h (Peternelj et al., 2015). Additionally, etoposide (apoptotic agent), hydrogen peroxide, and glucose deprivation-induced a dynamic time-dependent O-GlcNAcylation in NCI-H1299 cells and Balb/c mice, and mutations at the S549 site (a major site of O-GlcNAcylation) of sirtuin 1 led to cell death (Han et al., 2017). The corticosterone release was mainly triggered by stress-induced activation of the hypothalamic-pituitary-adrenal (HPA) axis in rodents (Maggio and Segal, 2019). Corticosterone exposure for 60 h increased global O-GlcNac levels in female placentae (Pantaleon et al., 2017). Treatment of C2C12 with dexamethasone (a corticosteroid) for 48 h increased the O-GlcNAcylation level and concomitantly decreased protein phosphorylation level by reducing OGA expression at mRNA and protein levels (Massaccesi et al., 2016). Conversely, the long-term dexamethasone exposure (subcutaneously administered for 7 days) increased OGA expression concomitant with a decrease in OGT expression at protein levels (Liu et al., 2018b). In decoding the characteristic of O-GlcNAc in the stress process, the raising O-GlcNAc levels during acute stress was generally described as a cytoprotection effect, while the decreasing O-GlcNAc levels had cytotoxic effects, which is consistent with our present results. Our data have shown decreased OGA expression, increased ratio of OGT/OGA, and an increasing trend of O-GlcNAc levels in the hippocampus of mice at early-CUMS process. By contrast, hippocampal OGT/OGA and O-GlcNAc levels were decreased and the OGA level was increased at day 28 of CUMS. All of these results suggest that O-GlcNAc modification might be essential for relief from stress response in the CUMS process.

O-GlcNAc modification signaling serves as a sensor stress and nutrient to be involved in numerous manipulation of biological processes, which include gut microbiota (Dennis et al., 2006). The previous study has demonstrated O-GlcNAc down-regulation and dysfunction in patients with inflammatory bowel disease (Ma J. et al., 2022). Deficiency of OGT expression resulted in a damaged epithelial barrier and gut inflammation in mice, which were partially rescued by an OGA inhibitor (Zhao et al., 2020; Ma J. et al., 2022). Additionally, since bacteria-derived OGT and OGA have a similar catalytic domain as that of humans, they could modify host protein O-GlcNAc modification (He et al., 2021). However, there is currently no direct evidence to support bacterial OGA or OGT existed in the host's brain. To the best of our knowledge, we did not find any direct or indirect correlation among these bacteria (*Candidatus_Saccharimonas, Candidatus_Actinomarina, Mucispirillum,* and *Helicobacter*) and OGA/OGT and O-GlcNAc. But we found a couple of flora that were associated with SCFAs (Wang et al., 2020; Gu et al., 2021; Liu Q. et al., 2021; Luo L. et al., 2022), glucose metabolism (Gao et al., 2020; Li L. et al., 2022; Luo L. et al., 2022; Ma Q. et al., 2022), glycolysis (Feichtinger et al., 2017; Zhou et al., 2021; Li L. et al., 2022), bile acids (Alizadeh and Raufman, 2022; Jian et al., 2022; Yin et al., 2022; Yuan et al., 2022) and other aspects. The intracerebral glucose metabolism and glycolysis, which produced the major donor substrate for O-GlcNAcylation (Liu X. et al., 2021), were regulated directly by intestinal microbiota and their metabolites. For instance, SCFAs were involved in the dysregulation of intracerebral glucose metabolism that occurs in the initial stages of Alzheimer's disease (Zhang et al., 2022). Moreover, propionate promoted glycolysis in astrocytes of Alzheimer's mice (Cuervo-Zanatta et al., 2022). Therefore, SCFAs could protect against brain-related diseases by preventing glucose metabolism (Rekha et al., 2022). In addition, bile acids synthesized in the gut could regulate cellular glucose metabolism in the brain (Hurley et al., 2022). Intestinal signals, which are transported to the brain, could also inhibit glucose synthesis via vagal afferent nerves (Xu et al., 2018; Bai et al., 2019). These results preliminarily showed that gut microbiota is one of the possible regulation manners in intracerebral O-GlcNAc modification. Recently, we found that the oligosaccharide fraction derived from LW reshaped gut microbiota and modified OGA abundance in the senescence-accelerated mouse (Wang et al., 2019). Hence, we sought to investigate whether LW administration changed O-GlcNAc modification of CUMS mice by gut microbiota, and the results confirmed our assumption. Here, in our work, we did observe LW treatment significantly elevated hippocampal O-GlcNAc levels in CUMS mice. Due to the O-GlcNAc modification being directly mediated by OGT and OGA, we next assayed the effect of LW on them. These preliminary results indicated that LW administration might improve the CUMS-induced emotional and cognitive impairments by increasing the levels of hippocampal O-GlcNAc and reducing OGA through gut microbiota. Currently, few researchers have

investigated the effects of LW on O-GlcNAc. Our study represented the basis for future pharmacological research of LW and opened new perspectives in the discovery of prophylactic and therapeutic agents for chronic stress.

Our results further showed that LW decreases the ratio of OGT/OGA levels in CUMS-14D mice but increases the hippocampal ratio of OGT/OGA in CUMS-28D mice. It has been reported that changes in cell O-GlcNAc levels are affected by systemic physiological and pathological factors (Chatham et al., 2021). It has been proposed that OGT and OGA work together to form a "buffer" system to maintain the normal level of O-GlcNAcylation (Yang and Qian, 2017). LW-treated diseases were mainly connected with the restoration of the neuroendocrine immunomodulation (NIM) network (Huang Y. et al., 2019). The balance of the NIM network plays a key role in maintaining the physiological function of the body; thus, any imbalance in the NIM network is considered to be closely associated with diseases and the aging process (Besedovsky and Sorkin, 1977; Besedovsky and del Rey, 2002; Wang et al., 2018). It has been found that LW can rebalance the hypothalamic-pituitary-adrenal (HPA) and hypothalamic-pituitary-gonadal (HPG) axes and regulate the disturbance of the immune system and gut microbiota (Cheng et al., 2020). Our preliminary experimental results show that LW plays an integral role in regulating the balance of the NIM network by bidirectionally regulating the communication and interaction between the neuroendocrine and immune systems (Zhou et al., 2016). So LW plays a wide range of pharmacological roles by regulating and restoring NIM balance. The NIM network is interfered with by various pathological factors. The results of this study suggest that LW may balance NIM by regulating the change of O-GlcNAc levels.

There are still several limitations of this research. Firstly, in our work, we chiefly focus on the O-GlcNAc modification and did not devote attention to other types of protein glycosylation. The primary reasons are as follows. In recent years, over 5 thousand O-GlcNAcylated proteins have been identified (Ma et al., 2021) and implicated in multiple adaptive cellular processes (Ma J. et al., 2022). The latest authoritative research has revealed that O-GlcNAcylation effectively prevents cognitive declines (Xie et al., 2016), neurogenesis (Chen et al., 2021), and neural stem cell fate switch (White et al., 2020). The therapeutic effects of several traditional medicines might be related to normalizing the O-GlcNAc-modification (Diwu et al., 2013; Shi et al., 2021; Wu et al., 2021). The above advances in O-GlcNAc research enlighten our research future and idea in this work. Meanwhile, to the best of our knowledge, no other research is dealing with the effect of LW on O-GlcNAc modification so far. Secondly, to copiously uncover the specific O-GlcNAcylated protein involved in the physiological process of LW improving emotional and cognitive impairments, O-GlcNAcomic profiling was necessary. However, due to limited experimental conditions and resources, we did not complete the O-GlcNAcomic profiling in this study, which will be our future research priority. Thirdly, LW consists of 6 herbs: Dihuang (the prepared root of *Rehmannia glutinosa*), Shanyao (rhizome of *Dioscorea opposita*), Shanzhuyu (fruit of *Cornus officinalis*), Mudanpi (root bark of *Paeonia suffruticosa*), Zexie (rhizome of *Alisma plantago-aquatica*), and Fuling (sclerotia of *Poria cocos*). The composition and monomers of LW are detailed in this review (Zhou et al., 2016). Based on previous studies in our laboratory, the activity and active site of LW-AFC were mainly composed of polysaccharides, glycosides, and oligosaccharides (Huang Y. et al., 2019). We have done many studies on the principal component contribution of LW (Wang et al., 2016d, 2017a, 2016c; Huang Y. et al., 2019; Zeng et al., 2019; Cheng et al., 2020; Wei et al., 2021; Huang et al., 2022). We did not experimentally confirm the probable pharmacological effects of primarily active fractions or monomers in LW on O-GlcNAc modification, such as stachyose, paeoniflorin, morroniside, etc (Cheng et al., 2020). Although our insights provided a new perspective on the pharmacologic mechanisms of LW ameliorating stress-induced emotional and cognitive impairments, more precise and scientific experimental evidence is persuasive and integrity.

Conclusion

Collectively, this study confirmed the capability of LW to ameliorate emotional and cognitive function, modulate gut microbial diversity and composition, and restored O-GlcNAc-related biological processes in CUMS mice. Moreover, this study, for the first time, demonstrated that the increased ratio of OGT/OGA and O-GlcNAc levels in the hippocampus induced by LW administration was one of the possible mechanisms of LW on CUMS mice, which deserves further investigation.

Data availability statement

The datasets presented in this study can be found in online repositories. The names of the repository/repositories and accession number(s) can be found in the article/**Supplementary material**.

Ethics statement

This animal study was reviewed and approved by the Institute of Animal Care and Use Committee (IACUC) of the National Beijing Center for Drug Safety Evaluation and Research (NBCDSER).

Author contributions

WZ, ZX, and JW conceived the study, participated in its design and coordination, and helped to draft the manuscript. YH carried out the behavioral tests and wrote and revised the manuscript. FL and CW participated in the behavioral tests, biochemical analyses, and 16s rRNA analysis. All authors confirmed the final manuscript.

Funding

This work was supported by the National Natural Science Foundation of China (82174006), National Key R&D Program

of China (Grant No. 2022YFC3500304), and the Beijing Municipal Natural Science Foundation (7222292).

Conflict of interest

The authors declare that the research was conducted in the absence of any commercial or financial relationships that could be construed as a potential conflict of interest.

Publisher's note

All claims expressed in this article are solely those of the authors and do not necessarily represent those of their affiliated organizations, or those of the publisher, the editors and the reviewers. Any product that may be evaluated in this article, or claim that may be made by its manufacturer, is not guaranteed or endorsed by the publisher.

Supplementary material

The Supplementary Material for this article can be found online at: https://www.frontiersin.org/articles/10.3389/fnins.2023.1134176/full#supplementary-material

SUPPLEMENTARY FIGURE 1
(A) Correlation analysis (Pearson's correlation) between the standardized abundance of OGT analyzed by PICRUSt and standardized hippocampal OGT concentration assayed by ELISA. **(B)** Correlation analysis between the abundance of OGA and hippocampal OGA. $n = 5–6$.

References

Alizadeh, M., and Raufman, J. P. (2022). Gastrointestinal neoplasia: Carcinogenic interaction between bile acids and *Helicobacter pylori* in the stomach. *J. Clin. Invest.* 132:e160194. doi: 10.1172/JCI160194

Anderson, S. T., and Paschos, G. K. (2019). The role for the microbiome in the regulation of the circadian clock and metabolism. *Nutr. Epigenom.* 14, 231–248.

Bai, L., Mesgarzadeh, S., Ramesh, K. S., Huey, E. L., Liu, Y., Gray, L. A., et al. (2019). Genetic identification of vagal sensory neurons that control feeding. *Cell* 179, 1129–1143.e23. doi: 10.1016/j.cell.2019.10.031

Bernardo, A., Lee, P., Marcotte, M., Mian, M. Y., Rezvanian, S., Sharmin, D., et al. (2022). Symptomatic and neurotrophic effects of GABAA receptor positive allosteric modulation in a mouse model of chronic stress. *Neuropsychopharmacology* 47, 1608–1619. doi: 10.1038/s41386-022-01360-y

Besedovsky, H., and Sorkin, E. (1977). Network of immuneneuroendocrine interactions. *Clin. Exp. Immunol.* 27, 1–12.

Besedovsky, H. O., and del Rey, A. (2002). Introduction: Immuneneuroendocrine network. *Front. Horm. Res.* 29, 1–14. doi: 10.1159/000061055

Bevins, R., and Besheer, J. (2006). Object recognition in rats and mice: A one-trial non-matching-to-sample learning task to study 'recognition memory'. *Nat. Protoc.* 1, 1306–1311. doi: 10.1038/nprot.2006.205

Bollinger, J. L., Dadosky, D. T., Flurer, J. K., Rainer, I. L., Woodburn, S. C., and Wohleb, E. S. (2022). Microglial P2Y12 mediates chronic stress-induced synapse loss in the prefrontal cortex and associated behavioral consequences. *Neuropsychopharmacology*. doi: 10.1038/s41386-022-01519-7 [Epub ahead of print].

Chatham, J. C., Zhang, J., and Wende, A. R. (2021). Role of O-linked N-acetylglucosamine protein modification in cellular (patho)physiology. *Physiol. Rev.* 101, 427–493. doi: 10.1152/physrev.00043.2019

Chen, J., Dong, X., Cheng, X., Zhu, Q., Zhang, J., Li, Q., et al. (2021). Ogt controls neural stem/progenitor cell pool and adult neurogenesis through modulating Notch signaling. *Cell Rep.* 34, 108905. doi: 10.1016/j.celrep.2021.108905

Cheng, X., Huang, Y., Zhang, Y., and Zhou, W. (2020). LW-AFC, a new formula from the traditional Chinese medicine Liuwei Dihuang decoction, as a promising therapy for Alzheimer's disease: Pharmacological effects and mechanisms. *Adv. Pharmacol.* 87, 159–177. doi: 10.1016/bs.apha.2019.10.005

Chevalier, G., Siopi, E., Guenin-Macé, L., Pascal, M., Laval, T., Rifflet, A., et al. (2020). Effect of gut microbiota on depressive-like behaviors in mice is mediated by the endocannabinoid system. *Nat. Commun.* 11:6363. doi: 10.1038/s41467-020-19931-2

Chi, L., Cheng, X., Lin, L., Yang, T., Sun, J., Feng, Y., et al. (2021). Porphyromonas gingivalis-induced cognitive impairment is associated with gut dysbiosis, neuroinflammation, and glymphatic dysfunction. *Front. Cell Infect. Microbiol.* 11:755925. doi: 10.3389/fcimb.2021.755925

Cho, Y., Hwang, H., Rahman, M. A., Chung, C., and Rhim, H. (2020). Elevated O-GlcNAcylation induces an antidepressant-like phenotype and decreased inhibitory transmission in medial prefrontal cortex. *Sci. Rep.* 10:6924. doi: 10.1038/s41598-020-63819-6

Cruz, B., Conceição, L. L. D., Mendes, T. A. O., Ferreira, C., Gonçalves, R. V., and Peluzio, M. (2020). Use of the synbiotic VSL#3 and yacon-based concentrate attenuates intestinal damage and reduces the abundance of Candidatus Saccharimonas in a colitis-associated carcinogenesis model. *Food Res. Int.* 137:109721.

Cruz-Pereira, J. S., Rea, K., Nolan, Y. M., O'Leary, O. F., Dinan, T. G., and Cryan, J. F. (2020). Depression's Unholy trinity: Dysregulated stress, immunity, and the microbiome. *Annu. Rev. Psychol.* 71, 49–78. doi: 10.1146/annurev-psych-122216-011613

Cryan, J. F., O'Riordan, K. J., Cowan, C. S. M., Sandhu, K. V., Bastiaanssen, T. F. S., Boehme, M., et al. (2019). The microbiota-gut-brain axis. *Physiol. Rev.* 99, 1877–2013.

Cuervo-Zanatta, D., Syeda, T., Sánchez-Valle, V., Irene-Fierro, M., Torres-Aguilar, P., Torres-Ramos, M. A., et al. (2022). Dietary fiber modulates the release of gut bacterial products preventing cognitive decline in an Alzheimer's mouse model. *Cell Mol. Neurobiol.* doi: 10.1007/s10571-022-01268-7 [Epub ahead of print].

Dawud, L. M., Holbrook, E. M., and Lowry, C. A. (2022). Evolutionary aspects of diverse microbial exposures and mental health: Focus on "old friends" and stress resilience. *Curr. Top Behav. Neurosci.* doi: 10.1007/7854_2022_385 [Epub ahead of print].

Dennis, R. J., Taylor, E. J., Macauley, M. S., Stubbs, K. A., Turkenburg, J. P., Hart, S. J., et al. (2006). Structure and mechanism of a bacterial beta-glucosaminidase having O-GlcNAcase activity. *Nat. Struct. Mol. Biol.* 13, 365–371. doi: 10.1038/nsmb1079

Diwu, Y., Tian, J., and Shi, J. (2013). Effect of xixin decoction on O-linked N-acetylglucosamine glycosylation of tau proteins in rat brain with sporadic Alzheimer disease. *J. Tradit. Chin. Med.* 33, 367–372. doi: 10.1016/s0254-6272(13)60180-6

Dong, Y., Li, S., Lu, Y., Li, X., Liao, Y., Peng, Z., et al. (2020). Stress-induced NLRP3 inflammasome activation negatively regulates fear memory in mice. *J. Neuroinflammation* 17:205. doi: 10.1186/s12974-020-01842-0

Elias, G. J. B., Germann, J., Boutet, A., Pancholi, A., Beyn, M. E., Bhatia, K., et al. (2022). Structuro-functional surrogates of response to subcallosal cingulate deep brain stimulation for depression. *Brain* 145, 362–377. doi: 10.1093/brain/awab284

Fahie, K. M. M., Papanicolaou, K. N., and Zachara, N. E. (2022). Integration of O-GlcNAc into stress response pathways. *Cells* 11:3509. doi: 10.3390/cells11213509

Fehl, C., and Hanover, J. A. (2022). Tools, tactics and objectives to interrogate cellular roles of O-GlcNAc in disease. *Nat. Chem. Biol.* 18, 8–17. doi: 10.1038/s41589-021-00903-6

Feichtinger, R. G., Neureiter, D., Skaria, T., Wessler, S., Cover, T. L., Mayr, J. A., et al. (2017). Oxidative phosphorylation system in gastric carcinomas and gastritis. *Oxid. Med. Cell. Longev.* 2017:1320241.

Gao, L., Li, J., Zhou, Y., Huang, X., Qin, X., and Du, G. (2018). Effects of baicalein on cortical proinflammatory cytokines and the intestinal microbiome in senescence accelerated mouse prone 8. *ACS Chem. Neurosci.* 9, 1714–1724. doi: 10.1021/acschemneuro.8b00074

Gao, S., Song, D., Liu, Y., Yan, H., and Chen, X. (2020). *Helicobacter pylori* CagA protein attenuates 5-Fu sensitivity of gastric cancer cells through upregulating cellular glucose metabolism. *Onco Targets Ther.* 13, 6339–6349. doi: 10.2147/OTT.S230875

Gu, J., Sun, R., Wang, Q., Liu, F., Tang, D., and Chang, X. (2021). Standardized *Astragalus mongholicus* bunge-curcuma aromatica salisb. extract efficiently suppresses

colon cancer progression through gut microbiota modification in CT26-bearing mice. *Front. Pharmacol.* 12:714322. doi: 10.3389/fphar.2021.714322

Guttenberg, G., Hornei, S., Jank, T., Schwan, C., Lü, W., Einsle, O., et al. (2012). Molecular characteristics of *Clostridium perfringens* TpeL toxin and consequences of mono-O-GlcNAcylation of Ras in living cells. *J. Biol. Chem.* 287, 24929–24940. doi: 10.1074/jbc.M112.347773

Han, C., Gu, Y., Shan, H., Mi, W., Sun, J., Shi, M., et al. (2017). O-GlcNAcylation of SIRT1 enhances its deacetylase activity and promotes cytoprotection under stress. *Nat. Commun.* 8:1491. doi: 10.1038/s41467-017-01654-6

Hanover, J. A., Chen, W., and Bond, M. R. (2018). O-GlcNAc in cancer: An Oncometabolism-fueled vicious cycle. *J. Bioenerg. Biomembr.* 50, 155–173. doi: 10.1007/s10863-018-9751-2

He, X., Gao, J., Peng, L., Hu, T., Wan, Y., Zhou, M., et al. (2021). Bacterial O-GlcNAcase genes abundance decreases in ulcerative colitis patients and its administration ameliorates colitis in mice. *Gut* 70, 1872–1883. doi: 10.1136/gutjnl-2020-322468

Hegyi, B., Borst, J. M., Bailey, L. R. J., Shen, E. Y., Lucena, A. J., Navedo, M. F., et al. (2020). Hyperglycemia regulates cardiac K(+) channels via O-GlcNAc-CaMKII and NOX2-ROS-PKC pathways. *Basic Res. Cardiol.* 115:71. doi: 10.1007/s00395-020-00834-8

Herp, S., Durai Raj, A. C., Salvado Silva, M., Woelfel, S., and Stecher, B. (2021). The human symbiont *Mucispirillum schaedleri*: Causality in health and disease. *Med. Microbiol. Immunol.* 210, 173–179. doi: 10.1007/s00430-021-00702-9

Hu, Y., Liu, Y., Yang, Y., Lv, H., Lian, S., Xu, B., et al. (2022). OGT upregulates myogenic IL-6 by mediating O-GlcNAcylation of p65 in mouse skeletal muscle under cold exposure. *J. Cell Physiol.* 237, 1341–1352. doi: 10.1002/jcp.30612

Huang, H. S., Lin, Y. E., Panyod, S., Chen, R. A., Lin, Y. C., Chai, L. M. X., et al. (2023). Anti-depressive-like and cognitive impairment alleviation effects of Gastrodia elata Blume water extract is related to gut microbiome remodeling in ApoE(−/−) mice exposed to unpredictable chronic mild stress. *J. Ethnopharmacol.* 302(Pt B), 115872. doi: 10.1016/j.jep.2022.115872

Huang, R., Tian, S., Han, J., Cai, R., Lin, H., Guo, D., et al. (2019). Increased ratio of global O-GlcNAcylation to tau phosphorylation at Thr212 site is associated with better memory function in patients with type 2 diabetes. *Front. Physiol.* 10:110. doi: 10.3389/fphys.2019.00110

Huang, Y., Li, D., Cheng, B., Liu, G., Zhang, Y. X., and Zhou, W. X. (2019). Active fraction combination from Liuwei Dihuang decoction (LW-AFC) ameliorates corticosterone-induced long-term potentiation (LTP) impairment in mice in vivo. *J. Ethnopharmacol.* 236, 147–154. doi: 10.1016/j.jep.2019.03.002

Huang, Y., Li, D., Wang, C., Sun, N., and Zhou, W. X. (2022). Stachyose alleviates corticosterone-induced long-term potentiation impairment via the gut-brain axis. *Front. Pharmacol.* 13:799244. doi: 10.3389/fphar.2022.799244

Huang, Y., Zhang, H., Yang, S., Qiao, H., Zhou, W., and Zhang, Y. (2012). Liuwei Dihuang decoction facilitates the induction of long-term potentiation (LTP) in senescence accelerated mouse/prone 8 (SAMP8) hippocampal slices by inhibiting voltage-dependent calcium channels (VDCCs) and promoting N-methyl-d-aspartate receptor (n.d.) receptors. *J. Ethnopharmacol.* 140, 384–390. doi: 10.1016/j.jep.2012.01.030

Hurley, M. J., Bates, R., Macnaughtan, J., and Schapira, A. H. V. (2022). Bile acids and neurological disease. *Pharmacol. Ther.* 240:108311.

Ijoma, G. N., Nkuna, R., Mutungwazi, A., Rashama, C., and Matambo, T. S. (2021). Applying PICRUSt and 16S rRNA functional characterisation to predicting co-digestion strategies of various animal manures for biogas production. *Sci. Rep.* 11:19913. doi: 10.1038/s41598-021-99389-4

Jeong, H. R., Kim, J. M., Lee, U., Kang, J. Y., Park, S. K., Lee, H. L., et al. (2022). Leaves of Cedrela sinensis attenuate chronic unpredictable mild stress-induced depression-like behavior via regulation of hormonal and inflammatory imbalance. *Antioxidants* 11:2448. doi: 10.3390/antiox11122448

Ji, P., Rhoads, W. J., Edwards, M. A., and Pruden, A. (2017). Impact of water heater temperature setting and water use frequency on the building plumbing microbiome. *ISME J.* 11, 1318–1330. doi: 10.1038/ismej.2017.14

Jian, J., Nie, M. T., Xiang, B., Qian, H., Yin, C., Zhang, X., et al. (2022). Rifaximin ameliorates non-alcoholic steatohepatitis in mice through regulating gut microbiome-related bile acids. *Front. Pharmacol.* 13:841132. doi: 10.3389/fphar.2022.841132

Jiang, Q., Li, C. R., Zeng, W. F., Xu, H. J., Li, J. M., Zhang, T., et al. (2022). Inhibition of connexin 36 attenuates HMGB1-mediated depressive-like behaviors induced by chronic unpredictable mild stress. *Brain Behav.* 12:e2470. doi: 10.1002/brb3.2470

Jones, S. P., Zachara, N. E., Ngoh, G. A., Hill, B. G., Teshima, Y., Bhatnagar, A., et al. (2008). Cardioprotection by N-acetylglucosamine linkage to cellular proteins. *Circulation* 117, 1172–1182. doi: 10.1161/CIRCULATIONAHA.107.730515

Kim, J., Kang, S., and Chang, K. A. (2022). Effect of cx-DHED on abnormal glucose transporter expression induced by AD pathologies in the 5xFAD mouse model. *Int. J. Mol. Sci.* 23:10602. doi: 10.3390/ijms231810602

Kim, S. M., Zhang, S., Park, J., Sung, H. J., Tran, T. T., Chung, C., et al. (2021). REM sleep deprivation impairs learning and memory by decreasing brain O-GlcNAc cycling in mouse. *Neurotherapeutics* 18, 2504–2517. doi: 10.1007/s13311-021-01094-7

Langille, M. G., Zaneveld, J., Caporaso, J. G., McDonald, D., Knights, D., Reyes, J. A., et al. (2013). Predictive functional profiling of microbial communities using 16S rRNA marker gene sequences. *Nat. Biotechnol.* 31, 814–821.

Lee, Y., Park, J., Kim, S. M., Nam, K., Lee, W., Cho, H., et al. (2020). Sleep deprivation impairs learning and memory by decreasing protein O-GlcNAcylation in the brain of adult zebrafish. *FASEB J.* 34, 853–864. doi: 10.1096/fj.201901399RR

Li, C., Lu, C., Gong, L., Liu, J., Kan, C., Zheng, H., et al. (2022). SHP2/SPI1axis promotes glycolysis and the inflammatory response of macrophages in *Helicobacter pylori*-induced pediatric gastritis. *Helicobacter* 27:e12895. doi: 10.1111/hel.12895

Li, L., Ma, C., Hurilebagen, Yuan, H., Hu, R., Wang, W., et al. (2022). Effects of lactoferrin on intestinal flora of metabolic disorder mice. *BMC Microbiol.* 22:181. doi: 10.1186/s12866-022-02588-w

Lian, X., Zhu, Q., Sun, L., and Cheng, Y. (2021). Effect of anesthesia/surgery on gut microbiota and fecal metabolites and their relationship with cognitive dysfunction. *Front. Syst. Neurosci.* 15:655695. doi: 10.3389/fnsys.2021.655695

Liu, B., Chen, B., Yi, J., Long, H., Wen, H., Tian, F., et al. (2022). Liuwei Dihuang decoction alleviates cognitive dysfunction in mice with D-galactose-induced aging by regulating lipid metabolism and oxidative stress via the microbiota-gut-brain Axis. *Front. Neurosci.* 16:949298. doi: 10.3389/fnins.2022.949298

Liu, H., Zhang, B., Li, F., Liu, L., Yang, T., Zhang, H., et al. (2022). Effects of heat stress on growth performance, carcass traits, serum metabolism, and intestinal microflora of meat rabbits. *Front. Microbiol.* 13:998095. doi: 10.3389/fmicb.2022.998095

Liu, J., Yu, C., Li, R., Liu, K., Jin, G., Ge, R., et al. (2020). High-altitude Tibetan fermented milk ameliorated cognitive dysfunction by modified gut microbiota in Alzheimer's disease transgenic mice. *Food Funct.* 11, 5308–5319. doi: 10.1039/c9fo03007g

Liu, M., Yin, C., Zhu, L., Zhu, X., Xu, C., Luo, C., et al. (2018a). Sucrose preference test for measurement of stress-induced anhedonia in mice. *Nat. Protoc.* 13, 1686–1698.

Liu, W., Xue, X., Xia, J., Liu, J., and Qi, Z. (2018c). Swimming exercise reverses CUMS-induced changes in depression-like behaviors and hippocampal plasticity-related proteins. *J. Affect. Disord.* 227, 126–135. doi: 10.1016/j.jad.2017.10.019

Liu, W., Wang, H., Xue, X., Xia, J., Liu, J., Qi, Z., et al. (2018b). OGT-related mitochondrial motility is associated with sex differences and exercise effects in depression induced by prenatal exposure to glucocorticoids. *J. Affect. Disord.* 226, 203–215.

Liu, Q., Xi, Y., Wang, Q., Liu, J., Li, P., Meng, X., et al. (2021). Mannan oligosaccharide attenuates cognitive and behavioral disorders in the 5xFAD Alzheimer's disease mouse model via regulating the gut microbiota-brain axis. *Brain Behav. Immun.* 95, 330–343. doi: 10.1016/j.jad.2017.09.053

Liu, X., Blaženović, I., Contreras, A. J., Pham, T. M., Tabuloc, C. A., Li, Y. H., et al. (2021). Hexosamine biosynthetic pathway and O-GlcNAc-processing enzymes regulate daily rhythms in protein O-GlcNAcylation. *Nat. Commun.* 12:4173. doi: 10.1038/s41467-021-24301-7

Liu, Y., Chen, Q., Zhang, N., Zhang, K., Dou, T., Cao, Y., et al. (2020). Proteomic profiling and genome-wide mapping of O-GlcNAc chromatin-associated proteins reveal an O-GlcNAc-regulated genotoxic stress response. *Nat. Commun.* 11:5898. doi: 10.1038/s41467-020-19579-y

Liu, Y., Shi, H., Hu, Y., Yao, R., Liu, P., Yang, Y., et al. (2022). RNA binding motif protein 3 (RBM3) promotes protein kinase B (AKT) activation to enhance glucose metabolism and reduce apoptosis in skeletal muscle of mice under acute cold exposure. *Cell Stress Chaperones* 27, 603–618. doi: 10.1007/s12192-022-01297-7

Lopes Sakamoto, F., Metzker Pereira Ribeiro, R., Amador Bueno, A., and Oliveira Santos, H. (2019). Psychotropic effects of (L)-theanine and its clinical properties: From the management of anxiety and stress to a potential use in schizophrenia. *Pharmacol. Res.* 147:104395. doi: 10.1016/j.phrs.2019.104395

Lu, Q., Li, S., and Shao, F. (2015). Sweet talk: Protein glycosylation in bacterial interaction with the host. *Trends Microbiol.* 23, 630–641.

Luo, L., Luo, J., Cai, Y., Fu, M., Li, W., Shi, L., et al. (2022). Inulin-type fructans change the gut microbiota and prevent the development of diabetic nephropathy. *Pharmacol. Res.* 183, 106367. doi: 10.1016/j.phrs.2022.106367

Luo, S., Zhang, X., Huang, S., Feng, X., Zhang, X., and Xiang, D. (2022). A monomeric polysaccharide from Polygonatum sibiricum improves cognitive functions in a model of Alzheimer's disease by reshaping the gut microbiota. *Int. J. Biol. Macromol.* 213, 404–415. doi: 10.1016/j.ijbiomac.2022.05.185

Lv, H., Wang, S., Tian, M., Wang, L., Gao, J., Zhao, Q., et al. (2022). Exercise preconditioning ameliorates cognitive impairment in mice with ischemic stroke by alleviating inflammation and modulating gut microbiota. *Mediators Inflamm.* 2022:2124230. doi: 10.1155/2022/2124230

Ma, J., Hou, C., and Wu, C. (2022). Demystifying the O-GlcNAc code: A systems view. *Chem. Rev.* 122, 15822–15864. doi: 10.1021/acs.chemrev.1c01006

Ma, J., Li, Y., Hou, C., and Wu, C. (2021). O-GlcNAcAtlas: A database of experimentally identified O-GlcNAc sites and proteins. *Glycobiology* 31, 719–723. doi: 10.1093/glycob/cwab003

Ma, Q., Zhai, R., Xie, X., Chen, T., Zhang, Z., Liu, H., et al. (2022). Hypoglycemic effects of lycium barbarum polysaccharide in type 2 diabetes mellitus mice via modulating gut microbiota. *Front. Nutr.* 9:916271. doi: 10.3389/fnut.2022.916271

Maggio, N., and Segal, M. (2019). "Chapter 8 – Stress, corticosterone, and hippocampal plasticity," in *Stress: Physiology, biochemistry, and pathology*, ed. G. Fink (Cambridge, MA: Academic Press), 93–104.

Massaccesi, L., Goi, G., Tringali, C., Barassi, A., Venerando, B., and Papini, N. (2016). Dexamethasone-induced skeletal muscle atrophy increases O-GlcNAcylation in C2C12 Cells. *J. Cell Biochem.* 117, 1833–1842. doi: 10.1002/jcb.25483

Meek, R. W., Blaza, J. N., Busmann, J. A., Alteen, M. G., Vocadlo, D. J., and Davies, G. J. (2021). Cryo-EM structure provides insights into the dimer arrangement of the O-linked β-N-acetylglucosamine transferase OGT. *Nat. Commun.* 12:6508.

Misra, J., Kim, D. K., Jung, Y. S., Kim, H. B., Kim, Y. H., Yoo, E. K., et al. (2016). O-GlcNAcylation of orphan nuclear receptor estrogen-related receptor γ promotes hepatic gluconeogenesis. *Diabetes* 65, 2835–2848. doi: 10.2337/db15-1523

Mohamed, T. M., Sun, W., Bumbie, G. Z., Elokil, A. A., Mohammed, K. A. F., Zebin, R., et al. (2021). Feeding *Bacillus subtilis* ATCC19659 to broiler chickens enhances growth performance and immune function by modulating intestinal morphology and cecum microbiota. *Front. Microbiol.* 12:798350. doi: 10.3389/fmicb.2021.798350

Morella, I. M., Brambilla, R., and Morè, L. (2022). Emerging roles of brain metabolism in cognitive impairment and neuropsychiatric disorders. *Neurosci. Biobehav. Rev.* 142:104892.

Muha, V., Fenckova, M., Ferenbach, A. T., Catinozzi, M., Eidhof, I., Storkebaum, E., et al. (2020). O-GlcNAcase contributes to cognitive function in *Drosophila*. *J. Biol. Chem.* 295, 8636–8646. doi: 10.1074/jbc.RA119.010312

Muñoz-Mayorga, D., Rissman, R. A., and Morales, T. (2020). Reproductive status impact on tau phosphorylation induced by chronic stress. *Neurobiol. Stress* 13:100241. doi: 10.1016/j.ynstr.2020.100241

Nie, H., Ju, H., Fan, J., Shi, X., Cheng, Y., Cang, X., et al. (2020). O-GlcNAcylation of PGK1 coordinates glycolysis and TCA cycle to promote tumor growth. *Nat. Commun.* 11:36. doi: 10.1038/s41467-019-13601-8

Okuyama, R., and Marshall, S. (2003). UDP-N-acetylglucosaminyl transferase (OGT) in brain tissue: Temperature sensitivity and subcellular distribution of cytosolic and nuclear enzyme. *J. Neurochem.* 86, 1271–1280. doi: 10.1046/j.1471-4159.2003.01939.x

Olave, F. A., Aguayo, F. I., Román-Albasini, L., Corrales, W. A., Silva, J. P., González, P. I., et al. (2022). Chronic restraint stress produces sex-specific behavioral and molecular outcomes in the dorsal and ventral rat hippocampus. *Neurobiol. Stress* 17:100440. doi: 10.1016/j.ynstr.2022.100440

Pantaleon, M., Steane, S. E., McMahon, K., Cuffe, J. S. M., and Moritz, K. M. (2017). Placental O-GlcNAc-transferase expression and interactions with the glucocorticoid receptor are sex specific and regulated by maternal corticosterone exposure in mice. *Sci. Rep.* 7:2017. doi: 10.1038/s41598-017-01666-8

Pathak, S., Borodkin, V. S., Albarbarawi, O., Campbell, D. G., Ibrahim, A., and van Aalten, D. M. (2012). O-GlcNAcylation of TAB1 modulates TAK1-mediated cytokine release. *EMBO J.* 31, 1394–1404.

Penny, T. R., Sutherland, A. E., Mihelakis, J. G., Paton, M. C. B., Pham, Y., Lee, J., et al. (2019). Human umbilical cord therapy improves long-term behavioral outcomes following neonatal hypoxic ischemic brain injury. *Front. Physiol.* 10:283. doi: 10.3389/fphys.2019.00283

Peternelj, T. T., Marsh, S. A., Strobel, N. A., Matsumoto, A., Briskey, D., Dalbo, V. J., et al. (2015). Glutathione depletion and acute exercise increase O-GlcNAc protein modification in rat skeletal muscle. *Mol. Cell Biochem.* 400, 265–275. doi: 10.1007/s11010-014-2283-0

Pravata, V. M., Muha, V., Gundogdu, M., Ferenbach, A. T., Kakade, P. S., Vandadi, V., et al. (2019). Catalytic deficiency of O-GlcNAc transferase leads to X-linked intellectual disability. *Proc. Natl. Acad. Sci. U.S.A.* 116, 14961–14970. doi: 10.1073/pnas.1900065116

Rekha, K., Venkidasamy, B., Samynathan, R., Nagella, P., Rebezov, M., Khayrullin, M., et al. (2022). Short-chain fatty acid: An updated review on signaling, metabolism, and therapeutic effects. *Crit. Rev. Food Sci. Nutr.* doi: 10.1080/10408398.2022.2124231 [Epub ahead of print].

Rogers, M. B., Firek, B., Shi, M., Yeh, A., Brower-Sinning, R., Aveson, V., et al. (2016). Disruption of the microbiota across multiple body sites in critically ill children. *Microbiome* 4:66. doi: 10.1186/s40168-016-0211-0

Sangha, J. S., Sun, X., Wally, O. S., Zhang, K., Ji, X., Wang, Z., et al. (2012). Liuwei Dihuang (LWDH), a traditional Chinese medicinal formula, protects against β-amyloid toxicity in transgenic *Caenorhabditis elegans*. *PLoS One* 7:e43990. doi: 10.1371/journal.pone.0043990

Shen, M. C., Zhang, Y. Z., Bo, G. D., Yang, B., Wang, P., Ding, Z. Y., et al. (2021). Microbial Responses to the Reduction of Chemical Fertilizers in the rhizosphere soil of flue-cured tobacco. *Front. Bioeng. Biotechnol.* 9:812316. doi: 10.3389/fbioe.2021.812316

Shi, J. J., Liu, H. F., Hu, T., Gao, X., Zhang, Y. B., Li, W. R., et al. (2021). Danggui-Shaoyao-San improves cognitive impairment through inhibiting O-GlcNAc-modification of estrogen α receptor in female db/db mice. *J. Ethnopharmacol.* 281:114562.

Tang, R., Wei, Y., Li, Y., Chen, W., Chen, H., Wang, Q., et al. (2018). Gut microbial profile is altered in primary biliary cholangitis and partially restored after UDCA therapy. *Gut* 67, 534–541. doi: 10.1136/gutjnl-2016-313332

Umapathi, P., Mesubi, O. O., Banerjee, P. S., Abrol, N., Wang, Q., Luczak, E. D., et al. (2021). Excessive O-GlcNAcylation causes heart failure and sudden death. *Circulation* 143, 1687–1703.

Wang, A. C., Jensen, E. H., Rexach, J. E., Vinters, H. V., and Hsieh-Wilson, L. C. (2016a). Loss of O-GlcNAc glycosylation in forebrain excitatory neurons induces neurodegeneration. *Proc. Natl. Acad. Sci. U.S.A.* 113, 15120–15125. doi: 10.1073/pnas.1606899113

Wang, J. H., Lei, X., Cheng, X. R., Zhang, X. R., Liu, G., Cheng, J. P., et al. (2016c). LW-AFC, a new formula derived from Liuwei Dihuang decoction, ameliorates behavioral and pathological deterioration via modulating the neuroendocrine-immune system in PrP-hAβPPswe/PS1(ΔE9) transgenic mice. *Alzheimers Res. Ther.* 8:57.

Wang, J., Ye, F., Cheng, X., Zhang, X., Liu, F., Liu, G., et al. (2016b). The effects of LW-AFC on intestinal microbiome in senescence-accelerated mouse prone 8 strain, a mouse model of Alzheimer's disease. *J. Alzheimers Dis.* 53, 907–919. doi: 10.3233/JAD-160138

Wang, J. H., Lei, X., Cheng, X. R., Zhang, X. R., Liu, G., Cheng, J. P., et al. (2016d). LW-AFC, a new formula derived from Liuwei Dihuang decoction, ameliorates behavioral and pathological deterioration via modulating the neuroendocrine-immune system in PrP-hAβPPswe/PS1ΔE9 transgenic mice. *Alzheimers Res. Ther.* 8:57.

Wang, B., Kong, Q., Li, X., Zhao, J., Zhang, H., Chen, W., et al. (2020). A high-fat diet increases gut microbiota biodiversity and energy expenditure due to nutrient difference. *Nutrients* 12:3197.

Wang, C., Zhu, M. H., Sun, N., Shen, W., Jiang, N., Zhao, Q. S., et al. (2022). Isorhynchophylline ameliorates stress-induced emotional disorder and cognitive impairment with modulation of NMDA receptors. *Front. Neurosci.* 16:1071068. doi: 10.3389/fnins.2022.1071068

Wang, G., An, T., Lei, C., Zhu, X., Yang, L., Zhang, L., et al. (2022). Antidepressant-like effect of ginsenoside Rb1 on potentiating synaptic plasticity via the miR-134-mediated BDNF signaling pathway in a mouse model of chronic stress-induced depression. *J. Ginseng. Res.* 46, 376–386. doi: 10.1016/j.jgr.2021.03.005

Wang, J., Liu, Y., Cheng, X., Zhang, X., Liu, F., Liu, G., et al. (2017b). The Effects of LW-AFC on the hippocampal transcriptome in senescence-accelerated mouse prone 8 strain, a mouse model of Alzheimer's disease. *J. Alzheimers Dis.* 57, 227–240. doi: 10.3233/JAD-161079

Wang, J., Cheng, X., Zeng, J., Yuan, J., Wang, Z., Zhou, W., et al. (2017a). LW-AFC effects on n-glycan profile in senescence-accelerated mouse prone 8 strain, a mouse model of Alzheimer's disease. *Aging Dis.* 8, 101–114. doi: 10.14336/AD.2016.0522

Wang, J., Zhang, X., Cheng, X., Cheng, J., Liu, F., Xu, Y., et al. (2017c). LW-AFC, a new formula derived from Liuwei Dihuang decoction, ameliorates cognitive deterioration and modulates neuroendocrine-immune system in SAMP8 mouse. *Curr. Alzheimer Res.* 14, 221–238. doi: 10.2174/1567205013666160603001637

Wang, J., Lei, X., Xie, Z., Zhang, X., Cheng, X., Zhou, W., et al. (2019). CA-30, an oligosaccharide fraction derived from Liuwei Dihuang decoction, ameliorates cognitive deterioration via the intestinal microbiome in the senescence-accelerated mouse prone 8 strain. *Aging* 11, 3463–3486. doi: 10.18632/aging.101990

Wang, T., Han, L., Zhang, X., Wu, R., Cheng, X., Zhou, W., et al. (2018). Knowledge-based neuroendocrine immunomodulation (NIM) molecular network construction and its application. *Molecules* 23:1312. doi: 10.3390/molecules23061312

Wang, T. Y., Tao, S. Y., Wu, Y. X., An, T., Lv, B. H., Liu, J. X., et al. (2022). Quinoa reduces high-fat diet-induced obesity in mice via potential microbiota-gut-brain-liver interaction mechanisms. *Microbiol. Spectr.* 10:e0032922. doi: 10.1128/spectrum.00329-22

Wei, M., Feng, S., Zhang, L., Wang, C., Chu, S., Shi, T., et al. (2021). Active fraction combination from Liuwei Dihuang decoction improves adult hippocampal neurogenesis and neurogenic microenvironment in cranially irradiated mice. *Front. Pharmacol.* 12:717719. doi: 10.3389/fphar.2021.717719

Wheatley, E. G., Albarran, E., White, C. W. III, Bieri, G., Sanchez-Diaz, C., Pratt, K., et al. (2019). Neuronal O-GlcNAcylation improves cognitive function in the aged mouse brain. *Curr. Biol.* 29, 3359–3369.e4. doi: 10.1016/j.cub.2019.08.003

White, C. W. III, Fan, X., Maynard, J. C., Wheatley, E. G., Bieri, G., Couthouis, J., et al. (2020). Age-related loss of neural stem cell O-GlcNAc promotes a glial fate switch through STAT3 activation. *Proc. Natl. Acad. Sci. U.S.A.* 117, 22214–22224. doi: 10.1073/pnas.2007439117

Wu, F., Shao, Q., Cheng, Z., Xiong, X., Fang, K., Zhao, Y., et al. (2021). Traditional herbal formula Wu-Mei-Wan alleviates TNBS-induced colitis in mice by inhibiting necroptosis through increasing RIPK3 O-GlcNAcylation. *Chin. Med.* 16:78. doi: 10.1186/s13020-021-00493-4

Wu, J., Wei, Z., Cheng, P., Qian, C., Xu, F., Yang, Y., et al. (2020). Rhein modulates host purine metabolism in intestine through gut microbiota and ameliorates experimental colitis. *Theranostics* 10, 10665–10679. doi: 10.7150/thno.43528

Wu, X., Gu, J., Zou, Z., Yu, M., Zhang, C., Xiao, Q., et al. (2022). Suppressive effects of isofraxidin on depressive-like behaviors induced by chronic unpredictable mild stress in mice. *Brain Sci.* 12:1376. doi: 10.3390/brainsci12101376

Xie, S., Jin, N., Gu, J., Shi, J., Sun, J., Chu, D., et al. (2016). O-GlcNAcylation of protein kinase A catalytic subunits enhances its activity: A mechanism linked to learning and memory deficits in Alzheimer's disease. *Aging Cell* 15, 455–464. doi: 10.1111/acel.12449

Xu, F., Yang, J., Negishi, H., Sun, Y., Li, D., Zhang, X., et al. (2018). Silibinin decreases hepatic glucose production through the activation of gut-brain-liver axis in diabetic rats. *Food Funct.* 9, 4926–4935. doi: 10.1039/c8fo00565f

Yang, X., and Qian, K. (2017). Protein O-GlcNAcylation: Emerging mechanisms and functions. *Nat. Rev. Mol. Cell. Biol.* 18, 452–465. doi: 10.1038/nrm.2017.22

Yang, Y. R., and Suh, P. G. (2014). O-GlcNAcylation in cellular functions and human diseases. *Adv. Biol. Regul.* 54, 68–73.

Yao, B., Pan, B., Tian, T., Su, X., Zhang, S., Li, H., et al. (2022). Baihu renshen decoction ameliorates type 2 diabetes mellitus in rats through affecting gut microbiota enhancing gut permeability and inhibiting TLR4/NF-κB-mediated inflammatory response. *Front. Cell Infect. Microbiol.* 12:1051962. doi: 10.3389/fcimb.2022.1051962

Yin, X., Li, Y., Fan, X., Huang, F., Qiu, Y., Zhao, C., et al. (2022). SIRT1 deficiency increases O-GlcNAcylation of tau, mediating synaptic tauopathy. *Mol. Psychiatry.* 27, 4323–4334. doi: 10.1038/s41380-022-01689-2

Yuan, J., Qin, S., Hu, S., Liu, Z., Song, Y., and Li, L. (2022). Restoration of cefixime-induced gut microbiota changes by a prebiotic blend in a mouse model. *Appl. Microbiol. Biotechnol.* 106, 5197–5209. doi: 10.1007/s00253-022-12044-4

Yuzwa, S. A., Shan, X., Macauley, M. S., Clark, T., Skorobogatko, Y., Vosseller, K., et al. (2012). Increasing O-GlcNAc slows neurodegeneration and stabilizes tau against aggregation. *Nat. Chem. Biol.* 8, 393–399. doi: 10.1038/nchembio.797

Zeng, J., Cheng, B., Huang, Y., Zhang, X., Wang, C., Sun, N., et al. (2019). Active fraction combination from Liuwei Dihuang decoction (LW-AFC) alleviated the LPS-induced long-term potentiation impairment and glial cells activation in hippocampus of mice by modulating immune responses. *Evid. Based Complement. Alternat. Med.* 2019:3040972. doi: 10.1155/2019/3040972

Zhang, T., Wu, X., Yuan, H., Huang, S., and Park, S. (2022). Mitigation of memory impairment with fermented fucoidan and λ-carrageenan supplementation through modulating the gut microbiota and their metagenome function in hippocampal amyloid-β infused rats. *Cells* 11:2301.

Zhang, Y., Li, J. T., Wang, H., Niu, W. P., Zhang, C. C., Zhang, Y., et al. (2021). Role of trace amine-associated receptor 1 in the medial prefrontal cortex in chronic social stress-induced cognitive deficits in mice. *Pharmacol. Res.* 167:105571. doi: 10.1016/j.phrs.2021.105571

Zhao, M., Ren, K., Xiong, X., Cheng, M., Zhang, Z., Huang, Z., et al. (2020). Protein O-GlcNAc modification links dietary and gut microbial cues to the differentiation of enteroendocrine L cells. *Cell Rep.* 32:108013. doi: 10.1016/j.celrep.2020.108013

Zhou, H., Zhu, J., Jia, J., Xiang, W., Peng, H., Zhang, Y., et al. (2022). The antidepressant effect of nucleus accumbens deep brain stimulation is mediated by parvalbumin-positive interneurons in the dorsal dentate gyrus. *Neurobiol. Stress* 21:100492. doi: 10.1016/j.ynstr.2022.100492

Zhou, L., Wu, Z., Wang, G., Xiao, L., Wang, H., Sun, L., et al. (2020). Long-term maternal separation potentiates depressive-like behaviours and neuroinflammation in adult male C57/BL6J mice. *Pharmacol. Biochem. Behav.* 196:172953. doi: 10.1016/j.pbb.2020.172953

Zhou, R., Wang, Z., Zhou, B., Yu, Z., Wu, C., Hou, J., et al. (2022). Estrogen receptors mediate the antidepressant effects of aerobic exercise: A possible new mechanism. *Front. Aging Neurosci.* 14:1040828. doi: 10.3389/fnagi.2022.1040828

Zhou, W., Cheng, X., and Zhang, Y. (2016). Effect of Liuwei Dihuang decoction, a traditional Chinese medicinal prescription, on the neuroendocrine immunomodulation network. *Pharmacol. Ther.* 162, 170–178.

Zhou, X. D., Yang, X. J., Zheng, Y., Qin, Z. S., Sha, W., Chen, G., et al. (2020). Jie-Yu Pill, a proprietary herbal medicine, ameliorates mood disorder-like behavior and cognitive impairment in estrogen-deprived mice exposed to chronic unpredictable mild stress: Implication for a potential therapy of menopause syndrome. *Front. Psychiatry* 11:579995. doi: 10.3389/fpsyt.2020.579995

Zhou, Y., Chen, S., Yang, F., Zhang, Y., Xiong, L., Zhao, J., et al. (2021). Rabeprazole suppresses cell proliferation in gastric epithelial cells by targeting STAT3-mediated glycolysis. *Biochem. Pharmacol.* 188:114525. doi: 10.1016/j.bcp.2021.114525

Zhu, W. Z., Ledee, D., and Olson, A. K. (2021). Temporal regulation of protein O-GlcNAc levels during pressure-overload cardiac hypertrophy. *Physiol. Rep.* 9:e14965. doi: 10.14814/phy2.14965

Zou, L., Yang, S., Hu, S., Chaudry, I. H., Marchase, R. B., and Chatham, J. C. (2007). The protective effects of PUGNAc on cardiac function after trauma-hemorrhage are mediated via increased protein O-GlcNAc levels. *Shock* 27, 402–408. doi: 10.1097/01.shk.0000245031.31859.29

Zverev, A. O., Kichko, A. A., Pinaev, A. G., Provorov, N. A., and Andronov, E. E. (2021). Diversity indices of plant communities and their rhizosphere microbiomes: An attempt to find the connection. *Microorganisms* 9:2339. doi: 10.3390/microorganisms9112339

frontiers | Frontiers in Pharmacology

TYPE Review
PUBLISHED 21 April 2023
DOI 10.3389/fphar.2023.1151196

OPEN ACCESS

EDITED BY
Jianxun Liu,
China Academy of Chinese Medical Sciences, China

REVIEWED BY
Yuxiang Fei,
China Pharmaceutical University, China
Macarena Hernández,
Complutense University of Madrid, Spain

*CORRESPONDENCE
Ke Du,
dkktztg@163.com

†These authors have contributed equally to this work

RECEIVED 25 January 2023
ACCEPTED 07 April 2023
PUBLISHED 21 April 2023

CITATION
Long J-X, Tian M-Z, Chen X-Y, Yu H-H, Ding H, Liu F and Du K (2023), The role of NLRP3 inflammasome-mediated pyroptosis in ischemic stroke and the intervention of traditional Chinese medicine.
Front. Pharmacol. 14:1151196.
doi: 10.3389/fphar.2023.1151196

The role of NLRP3 inflammasome-mediated pyroptosis in ischemic stroke and the intervention of traditional Chinese medicine

Jia-Xin Long[1†], Meng-Zhi Tian[1†], Xiao-Yi Chen[1], Huang-He Yu[1], Huang Ding[2], Fang Liu[1] and Ke Du[1*]

[1]School of Pharmacy, Hunan University of Chinese Medicine, Changsha, China, [2]College of Integrated Traditional Chinese Medicine and Western Medicine, Hunan University of Chinese Medicine, Changsha, China

Ischemic stroke (IS) is the second leading cause of death and disability in the world. Pyroptosis, a form of programmed cell death initiated by caspases, participates in the occurrence and development of IS. Because it can increase cell membrane permeability, mediate the release of inflammatory factors, and aggravate inflammation, inhibiting this process can significantly reduce the pathological injury of IS. The nucleotide binding oligomerization domain-like receptor family pyrin domain protein 3 (NLRP3) is a multiprotein complex whose activation is the core link of pyroptosis. In recent years, studies have reported that traditional Chinese medicine (TCM) could regulate pyroptosis mediated by NLRP3 inflammasome through multi-channel and multi-target networks and thus exert the effect against IS. This article reviews 107 papers published in recent years in PubMed, Chinese National Knowledge Infrastructure (CNKI), and WanFang Data in recent years. It has found that the activation factors of NLRP3 inflammasome include ROS, mitochondrial dysfunction, K^+, Ca^{2+}, lysosome rupture, and trans-Golgi breakdown. TLR4/NF-κB/NLRP3, ROS/TXNIP/NLRP3, AMPK/Nrf2/NLRP3, DRP1/NLRP3, TAK1/JNK/NLRP3 signaling pathways regulate the initiation and assembly of the NLRP3 inflammasome, subsequently induce pyroptosis, affecting the occurrence and development of IS. TCM can affect the above signaling pathways and regulate the pyroptosis mediated by NLRP3 inflammasome, so as to play a protective role against IS, which provides a new entry point for discussing the pathological mechanism of IS and a theoretical basis for developing TCM treasure house.

KEYWORDS

ischemic stroke (IS), pyroptosis, NLRP3, pathways, traditional Chinese medicine (TCM)

Introduction

An analysis of global disease systems in *Lancet Neurology* shows that ischemic stroke (IS) is the second leading cause of mortality and disability worldwide, and the economic costs of its treatment and post-stroke care are substantial (GBD, 2016 Stroke Collaborators, 2019). IS is a clinical syndrome of neurological damage caused by

cerebral blood supply disorder, brain tissue hypoxia, sugar deficiency, and tissue necrosis (Zhao et al., 2022). In recent years, a new type of programmed cell death called pyroptosis, which is closely related to inflammation, has been discovered (Tang et al., 2019). The 2002 Nobel Prize in Physiology or Medicine and the Nobel Prize in Chemistry in 2004 were awarded to scientists who have made pioneering contributions in the field of pyroptosis. The research indicates that pyroptosis has the characteristics of both apoptosis and necrosis, showing that the nuclear morphology is complete and the cell membrane is broken, leading to the release of cell contents and causing inflammation (Wang et al., 2017). Nucleotide-binding oligomerization domain-like receptor protein 3 (NLRP3) inflammasome is the key protein of pyroptosis and closely participates in the process of pyroptosis (Huang et al., 2021). Recent studies have found that pyroptosis mediated by NLRP3 inflammasome participates in the pathological process of IS (Fu et al., 2020; McKenzie et al., 2020). Kind of literature suggests that acupuncture, traditional Chinese medicine monomer, traditional Chinese medicine compound, and Chinese patent medicine can regulate NLRP3 inflammasome-mediated pyroptosis related signaling pathways to play a neuroprotective role in IS (Wang M et al., 2020; Ran et al., 2021; Chen et al., 2022). This article will elucidate the activation mechanism of NLRP3 inflammasome in the central nervous system (CNS), and review the research on the intervention of traditional Chinese medicine on NLRP3 inflammasome.

NLRP3 inflammasome in central nervous system and activation mechanism

The NLRP3 inflammasome is a multi-protein complex composed of NLRP3, ASC and pro-cassase-1, which plays an important role in the classical pyroptosis pathway (Lu et al., 2020). In 2004, *Immunity* first reported that NLRP3 inflammasomes are the basic molecules related to auto-inflammation (Agostini et al., 2004). In 2018, *Nature* further reported the activation mechanism of NLRP3 inflammasome, that is, the disbanded trans-Golgi network activated inflammasome by inducing the transport and aggregation of NLRP3 through phospholipid PtdIns4P (Chen and Chen, 2018). The activation of the NLRP3 inflammasome produces caspase-1. Subsequently, caspase-1 cleaves and splits gasdermin D (GSDMD) and pro-interleukin-1β (pro-IL-1β), pro-interleukin-18 (pro-IL-18), forming GSDMD-N and IL-1β, IL-18 (Chen et al., 2018; Alishahi et al., 2019). Then GSDMD-N acts on phospholipid molecules on the cell membrane to form pores, leading to cell osmotic swelling, cell membrane rupture and pyroptosis, simultaneously IL-1β and IL-18 are released out, which expands the local inflammatory response (Chen S et al., 2018). NLRP3 widely exists in neurons, microglia and cerebral vascular endothelial cells. The activation of NLRP3 inflammasome proceeds in two steps. The first step is priming. The second step is the assembly of inflammasome, which is a step of many studies on activation. Multiple upstream signals can induce the formation of the inflammasome by activating the oligomerization of NLRP3 protein.

Priming of NLRP3 inflammasome

Damage-associated molecular patterns (DAMPs) and pathogen-associated molecular pattern ligands (PAMPs) generated by cerebral ischemia and hypoxia cross the blood-brain barrier (BBB) into the CNS and activate the Toll-like receptor 4 (TLR4) on the surface of neurons, microglia, and astrocyte cell membranes (Shi et al., 2019). TLR4 is a transmembrane receptor protein involved in innate immune response (Li L et al., 2021), which can detect the danger signals of the extracellular environment. TLR4 initiates a signaling cascade to produce inflammatory cytokines (TNF, IL-12, IL-12, IL-6, IL-8, IL-1β, etc.). The key signal ligand downstream of TLR4 is myeloid differentiation factor 88 (MyD88). TLR4 and MyD88 promote the activation of tumor necrosis factor receptor-associated factor 6 (TRAF6) and activate the downstream transcriptional regulator nuclear factor κB (NF-κB) (Mitchell et al., 2018). NF-κB activation increases the transcription of NLRP3 inflammasome related protein coding gene (Jin et al., 2019), thereby activating caspase-1 and isolating the N and C ends of GSDMD to induce pyroptosis (Mohamadi et al., 2018) (Figure 1).

Ye et al. (2019) established an adult male C57BL/6J wild-type mouse middle cerebral occlusion/reperfusion (MCAO/R) *in vivo*. Immunofluorescence staining and western blot showed that the expression of NLRP3 inflammasome and their related proteins in neurons and microglia was activated. Subsequently, an *in vitro* oxygen-glucose deprivation/reperfusion (OGD/R) model was established in HT22 and BV2 cells. Results showed TLR4/NF-κB was significantly upregulated, NLRP3 inflammasomes were activated and M1 microglia/macrophages were polarized (Ye et al., 2019). Liu et al. (2021) used the TLR4 inhibitor TAK242 to reverse prove that the TLR4/NF-KB/NLRP3 pathway was activated in OGD/R BV2 cells. Wang K et al. (2020) detected pyroptosis in the ischemic cortex by dUTP nick end labeling (TUNEL) measurement and lactate dehydrogenase (LDH) release, and detected NLRP3 inflammasome assembly and inflammatory cytokine secretion by enzyme-linked immunosorbent assay (ELISA) and western blot. Confirming the activation of the TLR4/NF-κB/NLRP3 pathway induced by MCAO. While inhibiting NF-κB/NLRP3 protects neurons from OGD-induced pyroptosis (Kang et al., 2021). The above research shows that pyroptosis mediated by TLR4/NF-κB/NLRP3 pathway has a negative regulatory effect on IS, and targeted inhibition of this pathway plays a protective role.

Assembly of NLRP3 inflammasome

NLRP3 inflammasome assembly induced by reactive oxygen species (ROS)

All known PAMPs and DAMPs trigger the production of ROS, which can then induce the assembly of the NLRP3 inflammasome. High levels of ROS promote the dissociation of the oxidation-reduction sensitive signal complex TXNIP, which is translocated from the nucleus to the cytoplasm (Luo et al., 2022). TXNIP binds to the NLRP3 receptor domain (mainly LRR domain), thus inducing the activation of NLRP3 inflammasome (Chen D et al., 2018). *In vivo* experiments show that ROS drives TXNIP overexpression in MCAO rats and MCAO/R C57BL/6 mice, then TXNIP aggravates brain

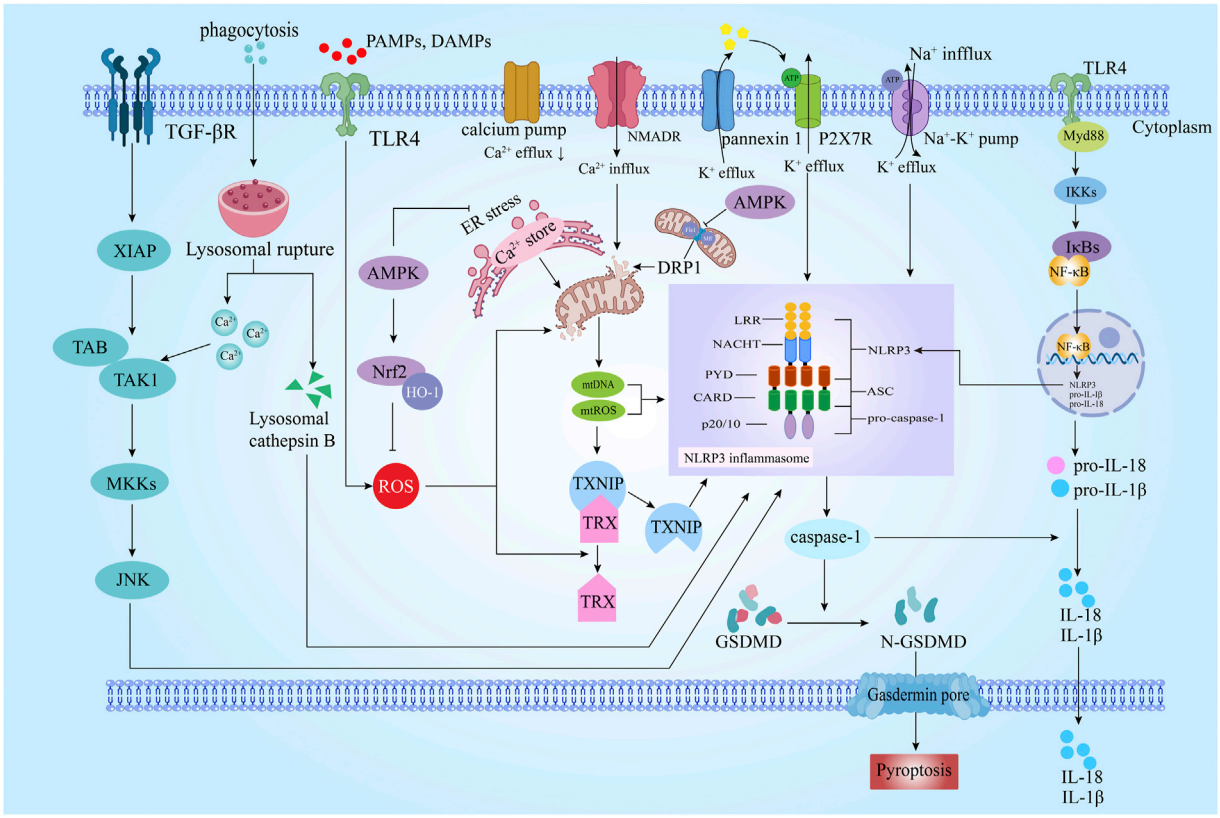

FIGURE 1
Schematic diagram of the molecular mechanism of pyroptosis in ischemic stroke (IS). Pyroptosis is a kind of programmed cell death process mediated by nucleotide-binding oligmerization domain-like receptor protein 3 (NLRP3) inflammasome and activated by Caspase-1) . It has the characteristics of both apoptosis and necrosis NLRP3. The initiation of the NLRP3 inflammasome involves a series of signaling pathways, such as TLR4/NF-κB/NLRP3, ROS/TXNIP/NLRP3, AMPK/NLRP3, DRP1/NLRP3, TAK1/JNK/NLRP3. TGFβ: transforming growth factor-β; XIAP: X-linked inhibitor of apoptosis protein; TAK1: transforming growth factor-beta activated kinase 1; TAB: transforming growth factor-β activated kinase 1 binding protein; MKKs: mitogen-activated protein kinase kinase; JNK: c-JunN-terminalkinase; DAMPs: damage associated molecular pattern; PAMPs: pathogen associated molecular patterns; ROS: Reactive oxygen species; AMPK: AMP-activated protein kinase; Nrf2: nuclear factor erythroid 2-related factor 2; HO-1: Heme Oxygenase-1; ER: endoplasmic reticulum; TXNIP: TRX-interacting protein; TRX: thioredoxin; mtROS: mitochondrial ROS; mtDNA: mitochondrial DNA; DRP1: dynamin-related protein 1; NMDAR: Nmethyl-D-aspartate receptor; ASC: apoptosis-associated speck-like protein containing acaspase recruitment domain; LRR: leucine-rich repeats; NACHT: nucleotidebinding and oligomerization; PYD: pyrin domain; CARD: Caspaseact ivat ing recruitment do main; caspase-1: cysteinyl aspartate specific proteinase-1; TLR4: toll-like receptor 4; MyD88: myeloid differentiation factor 88; IKKs: IkappaB kinases; IκBs: I kappaBs; NF-κB: nuclear factor kappa B; GSDMD: Gasdermin D.

damage through redox imbalance, subsequently activates NLRP3 inflammasome, caspase-1, and causes the release of IL-1β (Cao et al., 2016; Zeng et al., 2021; Yao et al., 2022). *In vitro* experiments show that ROS/TXNIP/NLRP3 signaling pathway activation induces pyroptosis in OGD/R and OGD primary cortical neurons (Yao et al., 2022). Knockdown of TXNIP significantly decreased the expression of NLRP3 in OGD-induced neurons (Liu et al., 2020). The above results suggest that ROS/TXNIP mediated activation of NLRP3 inflammasome is a key factor in IS.

The AMP-activated protein kinase (AMPK)/NF-E2 related factor 2 (Nrf2) pathway suppresses the assembly of NLRP3 inflammasome through anti-ROS. AMPK is phosphorylated and activated in response to an increase in the intracellular AMP/ADP ratio during ischemia and glycogen deprivation (Gu et al., 2018). AMPK directly phosphorylates the Nrf2 with an endogenous neuroprotective effect (Joo et al., 2016; Yu H et al., 2020). The activated Nrf2 translocates from the cytoplasm to the nucleus and binds to the antioxidant response element (ARE) (Fuse and Kobayashi, 2017). Hou et al. (2018) intraperitoneally injected tert-butylhydroquinone (tBHQ) to activate Nrf2. Western blot and qRT-PCR results showed that NLRP3 inflammasome and downstream caspase-1, IL-18, and IL-1β were significantly reduced, whereas Nrf2 knockout produced the opposite result. Transfection of Nrf2 into mice with inflammation had the same effect (Liu et al., 2017). When MCAO rats were treated with AMPK inhibitor dorsomorphin, immunofluorescence and western blot results showed that microglia/macrophages were activated, p-AMPK and Nrf2 were decreased, and NLRP3 was upregulated (Yu J et al., 2020). This is consistent with the result of knocking out Nrf2 (Liu et al., 2017), indicating that Nrf2 could inhibit the expression of NLRP3 (Liu et al., 2017). The downregulation of Nrf2 can also promote the pyroptosis of vascular endothelial cells induced by NLRP3 (Hu et al., 2018). The above experimental results suggest that up-regulating the

expression of AMPK or Nrf2 can significantly improve pyroptosis, promote neural function recovery and improve IS (Qiu et al., 2016).

NLRP3 inflammasome assembly induced by mitochondrial dysfunction

Mitochondrial dysfunction is an important feature of IS pathophysiology (Hasan et al., 2021). DRP1 is a protein related to mitochondrion division which was originally mainly distributed in the cytoplasm of cells. It was recruited by some signals and translocated to the outer membrane of mitochondria to form helical oligomers, which caused mitochondrion division and aggravated mitochondrial dysfunction (Duan et al., 2020). Phosphorylation of DRP1 reduces mitochondrial fission by regulating its translocation via AMPK (Hu et al., 2017). After activation, DRP1 combines with Fission1 (Fis1) and mitochondrial fission factor (Mff) to mediate the metabolic disorder of cells and inhibit glutathione in mitochondria to weaken the ability of free radical scavenging, further increase mitochondrial reactive oxygen species (mtROS), thus up-regulating the level of NLRP3 protein and producing IL-1β, cause pyroptosis, and eventually cause ischemic damage to neurons (Park et al., 2018; Kleele et al., 2021). Knockout of DRP1 can improve the function of mitochondria and reduce the level of NLRP3 protein to reduce pyroptosis (Zhong et al., 2022). It was found that in MCAO/R rats and OGD SH-SY5Y cells, DRP1 translocated mitochondria, resulting in the mitochondrial division, mitochondrial dysfunction, and then produced a large number of ROS, activated NLRP3 inflammasome, and induced pyroptosis (Guo et al., 2018; Hu et al., 2020). Inhibition of the DRP1 phosphorylation cannot only protect the integrity of mitochondria, but also reduce the activation of NLRP3 inflammasome and reduce pyroptosis (Zhou et al., 2011; Carneiro et al., 2012). Therefore, downregulation of the DRP1/NLRP3 pathway can effectively improve mitochondrial damage, inhibit pyroptosis and play a neuroprotective role.

NLRP3 inflammasome assembly induced by ionic steady-state imbalance

Intracellular K^+ efflux is a key factor in the activation of NLRP3 inflammasome (Muñoz-Planillo et al., 2013). K^+ efflux leads to the interaction between the inactive NLRP3 positive motif and the negative PIP on the Golgi membrane, which causes the local accumulation of NLRP3 and provides sufficient conditions for the activation of NLRP3 inflammasomes. The researchers found that NLRP3 inflammasomes could be activated without decreasing the intracellular K^+ concentration in the early stage of crystal stimulation, indicating that the activation of NLRP3 activation signal was not dependent on K^+ efflux, which denied the necessity of K^+ efflux for the activation of NLRP3 inflammasomes (Zhang et al., 2018). Therefore, the reduction of intracellular K^+ concentration provides sufficient and unnecessary conditions for the activation of NLRP3 inflammasomes. Both ATP synthesis and Na^+- K^+-ATPase activity are reduced during IS, leading to an increase in Na^+ influx and K^+ efflux, thus reducing the intracellular K^+ (Zhu et al., 2022). ATP released by necrotic cells binds to the P2X4 receptor, causing the receptor to open, leading to K^+ efflux. In addition, the necrotic cells passively release K^+, resulting in high extracellular K^+. K^+ activates the pannexin 1 channel on the cell membrane, further releasing ATP. Previous studies have revealed that P2X7R triggers the second stage of assembly and activation of NLRP3 inflammasomes (Albalawi et al., 2017), which can activate NLRP3 inflammasomes in astrocytes and participate in the pathogenesis of IS (Ye et al., 2017).

Ca^{2+} influx is another important factor independent of the activation of NLRP3 inflammasomes induced by K^+ efflux (Katsnelson et al., 2015). Ca^{2+} influx is another important factor in NLRP3 inflammasome activation. There are four main ways to cause cytoplasm Ca^{2+} overload in IS. The first is that the N-methyl-D-aspartate receptor (NMDAR) of the postsynaptic membrane is overexcited, which mediates the opening of its coupled calcium channel, and a large amount of extracellular Ca^{2+} influx (Ludhiadch et al., 2022). The second is the release of Ca^{2+} from the endoplasmic reticulum cavity to the cytoplasm caused by endoplasmic reticulum stress (ERS) (Groenendyk et al., 2021). The third is that Ca^{2+} in lysosomes is released to the cytoplasm through the non-selective cation channel TRPML (Weber and Schilling, 2014). The last one is that the permeability of plasma membrane-related calcium pump is reduced due to the lack of ATP activity, leading to the reduction of Ca^{2+} transfer to the outside cell (Hu and Song, 2017). At present, there are two opinions about the Ga^{2+} in the activation of NLRP3 inflammasome. One is that Ca^{2+} is directly involved in the activation of the NLRP3 inflammasome, because the increase of Ca^{2+} can promote the interaction between NLRP3 and ASC (Lee et al., 2012). Another opinion is that the increase of the excessive release of Ca^{2+} from the endoplasmic reticulum (ER) leads to an overload of mitochondrial Ca^{2+}, leading to mitochondrial dysfunction and activation of NLRP3 inflammasome (Murakami et al., 2012). No matter whether Ca^{2+} directly or indirectly activates the NLRP3 inflammasome, it is clear that Ca^{2+} overload induces pyroptosis in IS (Wang L et al., 2020). Interestingly, *Science* published a research article related to the mechanism of Ca^{2+} activating pyroptosis in 2018. It was found that Ca^{2+} influx through the GSDMD pore was used as a signal for cells to start membrane repair, and ESCRT complexes required for transport were recruited to repair damaged membrane systems. Since the inhibition of ESCRT-III could significantly improve pyroptosis, this article provides new insight into the endogenous mechanism of pyroptosis (Rühl et al., 2018).

NLRP3 inflammasome assembly induced by lysosome rupture

The lysosomal membrane loses its stability, integrity and permeability, and lysosome membrane permeabilization (LMP) occurs after IS, leading to the release of cathepsin B and Ca^{2+} (Bruchard et al., 2013; Repnik et al., 2014). Various cathepsins play a role in pro-synthesis and NLRP3 activation (Orlowski et al., 2015). It is reported that the release of lysosomal cathepsin B is IL-1β release required in *Nature* (Duewell et al., 2010). Pharmacological inhibition of cathepsin activity or genomic deletion of various cathepsin can significantly reduce the signal transduction of NLRP3 inflammasome. For example, cathepsin B inhibitor CA-074-Me could partially inhibit the activation of NLRP3 inflammasome (Bruchard et al., 2013). However, there are also studies showing that gene deletion or knockdown of cathepsin B has little effect on NLRP3 inflammasome activation (Orlowski et al., 2015). Therefore, whether lysosomal cathepsin B is

a sufficient and necessary condition for the activation of NLRP3 inflammasome is controversial. Ca^{2+} released by lysosome rupture is activated by NLRP3 inflammasomes via transforming growth factor-beta activated kinase 1 (TAK1)/c-Jun NH2 terminal kinase (JNK) pathway. Ga^{2+}-CaMKII promotes the binding of TAK to TAK 1 binding protein (transforming growth factor-β activated kinase 1 binding protein, TAB), so that phosphorylation of TAK1 activates downstream MAPK kinase (MAPK kinase, MAPKK) MKK4/7, and subsequently MKK4/7 specifically activates JNK (Hirata et al., 2017). JNK promotes the activation of the NLRP3 inflammasome by regulating ASC oligomerization (Hara et al., 2013). Zhang and colleagues confirmed that TAK1/JNK pathway is involved in the pathogenesis of IS in MCAO/R rats and OGD/R primary cortical neurons (Zhang Z et al., 2022). CNS extracellular pathological signal molecule lysophosphatidic acid (LPA) induced PC12 pyroptosis is related to JNK (Choi and Chun, 2013; Li and Zhang, 2020). In addition, lysosome rupture will also trigger a significant reduction of cytoplasmic K^+ before NLRP3 inflammasome assembly and caspase-1 production, and is not related to NLRP3 inflammasome assembly and accumulation (Muñoz-Planillo et al., 2013). This indicates that lysosome rupture activates plasma membrane cation channel, which is a key early signal of NLRP3 inflammasome assembly (Katsnelson et al., 2015). Some studies have also shown that under certain experimental conditions, the effect of lysosome rupture on activating NLRP3 inflammasome signal may be very low. Therefore, lysosome rupture determines whether to activate or inhibit NLRP3 inflammasomes according to different cell environments.

The intervention of traditional Chinese medicine on NLRP3 inflammasome-mediated pyroptosis in ischemic stroke

Modern pharmacological studies have found that most of the traditional Chinese medicine aims to prevent and treat IS by inhibiting the activation of NLRP3 inflammasomes and caspase-1, and by regulating its upstream related signal pathways, such as TLR4/NF-κB, ROS/TXNIP, AMPK/Nrf2 or DRP1/NLRP3 to inhibit the occurrence of pyroptosis. At the same time, it is also found that the same monomer or compound prescription can regulate and control the above multiple pathways to improve NLRP3-mediated pyroptosis. Thus, the influence of traditional Chinese medicine on pyroptosis anti-IS is characterized by multiple pathways.

Acupuncture

Acupuncture is recommended by the World Health Organization (WHO) as an alternative strategy for IS treatment and nursing. Acupuncture can effectively improve IS by promoting nerve regeneration, improving blood flow in the infarct area, fighting apoptosis, and regulating neurochemicals (Chavez et al., 2017; Xu et al., 2018). In recent years, studies have found that acupuncture plays a neuroprotective role by inhibiting NLRP3 inflammasome-mediated pyroptosis (Zhang T et al., 2021; Chen et al., 2022). For example, acupuncture can protect MCAO rats by up-regulating the expression of SIRT1, inhibiting the activation of NLRP3 inflammasome and down-regulating the expression of IL-18 (Zhou et al., 2022). Xu et al. (2020) treated the MCAO/R rats with electroacupuncture at the four points of Zusanli, Sanyinjiao, Chize, and Hegu, and found that the infarction volume of the electroacupuncture group was reduced compared with the model group, and caspase-1 mRNA was lower. Liu et al. (2019) intervened in MCAO/R rats with eye acupuncture. Intervention of MCAO/R rats with eye acupuncture has no significant difference from that of the NLRP3 inflammasome inhibitor glibenclamide group. Both of them can inhibit the expression of P2X7R, NLRP3, pro-capase-1, ASC, caspase-1 protein in rats, indicating that eye acupuncture can inhibit the occurrence of pyroptosis. The results show that eye-acupuncture could inhibit the expression of P2X7R, NLRP3, pro-caspase-1, ASC, and caspase-1 proteins in rats, which is consistent with the trend of the group using NLRP3 inflammasome inhibitor glibenclamide, indicating that eye acupuncture could inhibit the occurrence of pyroptosis. miRNA-mediated pyroptosis is also involved in the development of IS. For example, the level of miR-223 in the cortex around the infarction of MCAO rats treated with electroacupuncture increased, while the level of NLRP3, caspase-1, IL-1β and IL-18 decreased (Sha et al., 2019). To sum up, acupuncture can regulate IS with multiple targets, which may become a new treatment tragedy for IS. However, a minority of the above studies have not carried out specific signal pathway studies, so the protective mechanism of acupuncture on neuronal damage after IS still needs to be confirmed by further research (Table 1).

Traditional Chinese medicine monomer

Traditional Chinese medicine monomer is an active ingredient extracted from traditional Chinese medicine. These traditional Chinese medicine monomers are mainly extracted by alcohol, supplemented by ultrasonic cracking (Wang et al., 2014; Yue. et al., 2016). Some TCM monomers have been approved by the China Medical Products Administration (NMPA) for the treatment of IS. In recent years, it has been found that many traditional Chinese medicine monomer can play an anti-pyroptosis role by regulating the signal pathway upstream of NLRP3 inflammasome. Mulberroside A is considered to be the main active ingredient of Cortex Mori, which shows extensive benefits in the routine oral water administration route (Wang et al., 2011). Mulberroside A can inhibit TLR4/NF-κB induced by OGD/R cortical neurons (Wang CP et al., 2014). Artesunate (ART), a derivative of artemisinin (Chen et al., 2021), can reduce the score of neurological deficits induced by MCAO/R rats, improve brain edema, and reduce the volume of cerebral infarction. Its mechanism is related to down-regulating TLR4/NF-κB/NLRP3 pathway (Ran et al., 2021). Carthamin yellow (CY) is a flavonoid compound isolated from safflower, it is considered that CY improves blood circulation and alleviates pain. Thus, CY is used for the treatment of cerebrovascular disease (Lu QY et al., 2019). Its protection mechanism is the same as that of ART (Guo et al., 2021). Curcumin is a natural polyphenolic compound in *Curcuma longa*. Curcumin can reduce NF-κB/NLRP3 signal pathway to inhibit LPS-ATP-induced primary microglial pyroptosis (Ran et al., 2021). In addition to affecting NLRP3 inflammasomes through TLR4/NF-κB pathway, traditional

TABLE 1 Advance in treatment of traditional Chinese medicine against IS by drug intervention pyroptosis.

Treatment	Traditional Chinese medicine	Model	Pathways	References
acupuncture	acupuncture	MCAO/R rats	SIRT1/NLRP3	Zhou et al. (2022)
	electroacupuncture	MCAO/R rats	not clear	Xu et al. (2020)
	eye acupuncture	MCAO/R rats	not clear	Liu et al. (2019)
effective components	Artesunate (ART)	MCAO/R rats	TLR4/NF-κB/NLRP3	Chen et al. (2021)
	Mulberroside A	OGD/R rat cortical neurons	TLR4/NF-κB/NLRP3	Wang et al. (2014)
	Carthamin yellow (CY)	MCAO/R rats	TLR4/NF-κB/NLRP3	Guo et al. (2021)
	Curcumin	MCAO/R rats, LPS with ATP induced-microglia pyroptosis, glutamate induced-SH-SY5Y cells neurotoxicity	TLR4/NF-κB/NLRP3, ROS/TXNIP/NLRP3	Li et al. (2015), Ran et al. (2021)
	Umbelliferone (UMB)	MCAO/R rats	ROS/TXNIP/NLRP3	Wang et al. (2015)
	Ginsenoside Rd (Rd)	MCAO/R rats, OGD/R cortical neuron	ROS/TXNIP/NLRP3	Yao et al. (2022)
	Irisin	MCAO mice, OGD PC12 cells	ROS/NLRP3, AMPK/NLRP3	Li et al. (2017), Peng et al. (2017)
	Ruscogenin	OGD/R-injured mouse brain microvascular endothelial cells (bEnd.3)	ROS/NLRP3, AMPK/NLRP3	Cao et al. (2016)
	Z-Guggulsterone (Z-GS)	MCAO rats; OGD cortical neuron	ROS/NLRP3, AMPK/NLRP3	Liu et al. (2020)
	Sinomenine (SINO)	MCAO mice OGDastrocyte/microglia cells	AMPK/NLRP3	Qiu et al. (2016)
	Astragalode IV (AS-IV)	MCAO rats, OGD/R SH-SY5Y cells	AMPK/NLRP3	Xiao et al. (2021)
	Resveratrol (Res)	LPS- and ATP-induced N9 microglial cells	AMPK/NLRP3	Tufekci et al. (2021)
	Hispidulin	MCAO/Rrats, OGD/R primary cerebral astrocytes cells	AMPK/NLRP3	An et al. (2019)
	Chrysophanol	tMCAO mice	NLRP3	Zhang et al. (2014)
	Quercetin	ECs	ROS/TXNIP/NLRP3	Wu et al. (2014)
	luteolin	ECs	ROS/TXNIP/NLRP3	Wu et al. (2014)
	epigallocatechin gallate	ECs	ROS/TXNIP/NLRP3	Wu et al. (2014)
compound prescription	Dihydromyricetin (DHM) Angelica sinensis and Cinnamomum cassia (AC)	ECs pMCAO rats, LPS-induced BV2 cells pyroptosis	Nrf2/NLRP3 TLR4/NF-κB/NLRP3	Hu et al. (2018) Luo et al. (2021)
	Renshen Shouwu (RSSW)	MCAO rats	TLR4/NF-κB/NLRP3	Li et al. (2020)
	Taohong Siwu decoction (THSWD)	MCAO/R rats	DRP1/NLRP3, TLR4/NF-KB/NLRP3, JNK/p38MAPK	Wang M et al., 2020; Zhou (2021)
	Panax ginseng and Angelica sinensis (CPA)	tMCAO rats; OGD/R BV2microglia cells	DRP1/NLRP3	Hu et al. (2020)
	Qingkailing injection (QKL)	MCAO/R rats	AMPK/NLRP3	Ma et al. (2019)
	Naoxinqing Capsule	MCAO/R rats	not clear	Dongyu et al. (2020)
	Shennaofuyuan Decoction (SNFYD)	OGD PC12 cells	not clear	Li (2019)

Chinese medicine monomer can also regulate ROS/TXNIP/NLRP3 pathway to prevent pyroptosis. Curcumin (10 μmol L^{-1}) inhibits the activation of the TXNIP/NLRP3 pathway by up-regulating AMPK activity in human neuroblastoma SH-SY5Y cells of human neuroblastoma and reducing ROS produced by endoplasmic reticulum stress (Li et al., 2015). Umbelliferone (UMB), a natural antioxidant belonging to coumarin derivatives, is able to cross the blood-brain barrier and protect neuronal cells

from death. UMB (15 and 30 mg/kg) pretreatment for 7 days significantly upregulates peroxisome proliferator-activated receptor (PPAR-γ) with an antioxidant effect in MCAO/R rats, and inhibits ROS, thereby reducing the expression of TXNIP to inhibit NLRP3 inflammasome (Wang X et al., 2015). Ginsenoside Rd (Rd), a monomer component of Panax ginseng and Panax notoginseng, is reported to confer neuroprotection in brain injury models. Rd activates the Nrf2 pathway by up-regulating miR-139-5p, and downregulates ROS/TXNIP/NLRP3 induced by MCAO rats and OGD cortical neurons (Yao et al., 2022). Ruscogenin, an important steroid sapogenin derived from Ophiopogon japonicus, has been shown to inhibit cerebral ischemic injury. In the mouse brain microvascular endothelial cells (bEnd.3) and OGD/R primary cortical neuron, ROS was significantly inhibited by the administration of Ruscogenin (Cao et al., 2016). Z-Guggulsterone (Z-GS), an active component derived from myrrh. MCAO rats were treated with different doses of Z-GS. Morphological results showed that Z-GS significantly alleviated neurological deficits, infarct volume and histopathological damage in MCAO rats. It was related to TXNIP and NLRP3 by immunohistochemistry and immunofluorescence staining. The author conducted *in vitro* experiments to verify the mechanism, it was found that Z-GS treatment scarcely changed the expressions of NLRP3 in siRNA-TXNIP pretreated cells compared with the siRNA-TXNIP alone treatment group, suggesting that the neuroprotective effect of Z-GS was dependent on TXNIP-NLRP3 axis (Liu et al., 2020). Traditional Chinese medicine monomer can also upregulate AMPK/Nrf2 and inhibit NLRP3 inflammasome. *In vitro* and *in vivo* experimental studies showed that AMPK/Nrf2 pathway could be downregulated and NLPR3 inflammasome activated in MCAO/R rats or mice, OGD/R or LPS-ATP SH-SY5Y cells, microglial, and astrocytes. When intervening with an alkaloid extracted from Sinomenium acutum, the expression of AMPK was upregulated, and NLRP3 inflammasome was suppressed (Qiu et al., 2016). Astragaloside IV (AS-IV) is the main effective component of Astragalus membranaceus, and is widely used in the prevention and treatment of cerebrovascular diseases (Li S et al., 2021). Xiao et al. (2021) established MCAO/R rat *in vivo*, OGD/R SH-SY5Y cell *in vitro*, they enhanced NLRP3, caspase-1, IL-1β, GSDMD and GSDMD-N protein levels, indicating that NLRP3/caspase-1/GSDMD pathway is activated to promote pyroptosis. AS-IV increased the protein levels of Nrf2 and promoted the transfer of Nrf2 to the nucleus, accelerating Nrf2 activation. It shows that AS-IV inhibits NLRP3-mediated pyroptosis by activating Nrf2 (Xiao et al., 2021). Resveratrol (Res), which is a natural polyphenolic compound, inhibits LPS- and ATP-activated NLRP3 inflammasome and protects microglial cells upon pyroptosis. Mechanismly, it inhibits NF-κB and activates AMPK/Sirt1 pathways (Tufekci et al., 2021). Hispidulin is a flavonoid present in many Chinese herbal medicines (Kut et al., 2022). When MCAO rats were treated with different doses of hispidulin, hispidulin exerted its neuroprotective effects *in vivo* and *in vitro* by suppressing NLRP3-mediated pyroptosis by modulating the AMPK/GSK3β signaling pathway (An et al., 2019). Particularly revealing was that the AMPK inhibitor Compound C (An et al., 2019) or the Nrf2 inhibitor ML385 (Xiao et al., 2021), some of the effects of the drugs are offset, indicating that the traditional Chinese medicine monomers play an anti-pyroptosis effect through AMPK/Nrf2/NLRP3 pathway. Chrysophanol, the main active ingredient from Dahuang (Radix Et Rhizoma Rhei), Heshouwu (Radix Polygoni Multiflori) and Huzhang (Rhizoma Et Radix Polygoni Cuspidwi), can inhibit the activation of NLRP3 induced by transient MCAO (tMCAO) in mice, but the specific pathway mediated by it is not clear at present, which needs to be further explored (Zhang et al., 2014).

Moreover, endothelial cells (ECs) pyroptosis plays an important role in IS. Wang et al. (2021) confirmed that IS can induce pyroptosis of microvascular endothelial cells (ECs) and aggravate the ischemia-reperfusion injury. When MCC950, a specific drug targeting NLRP3, is used to interfere with ECs in OGD, the results show that endothelial NLRP3 is inhibited, indicating that endothelial NLRP3 inflammasome-mediated pyroptosis is also an effective target (Bellut et al., 2021). Some TCM monomers can target ECs pyroptosis. For example, quercetin, luteolin, and epigallocatechin gallate inhibit TXNIP/NLRP3 by reducing ROS in ECs (Wu et al., 2014). Dihydromyricetin (DHM) pretreated vascular ECs, reduced the release of IL-1β related to pyroptosis, significantly decreased the levels of intracellular ROS, and promoted the activation of Nrf2. When the knockdown of Nrf2 by siRNA, the inhibitory effect of DHM on ECs pyroptosis was counteracted. Therefore, DHM plays an anti-pyroptosis role by activating the Nrf2/NLRP3 pathway of vascular ECs (Hu Q et al., 2018) (Table 1).

Compound prescription and Chinese patent medicine

Due to the occurrence and development of IS is a multi-path and multi-target collaborative process. In the process of treatment, the most effective way is to inhibit or block all the relevant pathways corresponding to the onset of IS. Compound prescription and Chinese patent medicine contain many kinds of effective ingredients of traditional Chinese medicine, which are the most widely used forms of traditional Chinese medicine in clinical practice. At present, studies have confirmed that they can exert neuroprotective effects by affecting pyroptosis. For example, Naoxinqing Capsule, a traditional Chinese patent drug, can effectively inhibit the protein expression of NLRP3, ASC, caspase-1, IL-18 and IL-1β in MCAO/R rats and protect the cerebrovascular function when administered continuously for 21 days at the dose of 100 mg/(kg · d). When OGD PC12 cells were cultured with Shennaofuyuan Decoction (SNFYD) drug-containing serum, the expression level of IL-18 and IL-1β were significantly decreased, suggesting that SNFYD can inhibit neuronal pyroptosis (Li, 2019). Luo et al. (2021) showed for the first time that the expression of TLR4, NLRP3, ASC and caspase-1 was downregulated in a dose-dependent manner after three doses of Angelica Cinnamomum (AC) extract were given to pMCAO rats for 7 days. In LPS-induced BV2 cells, cerebrospinal fluid containing AC extract inhibited the secretion of pro-inflammatory cytokines, and its intervention effect was similar to that of TLR4 siRNA treatment. It suggests that AC may play a neuroprotective role by inhibiting the formation of NLRP3 inflammasome through TLR4/NF-κB. Renshen Shouwu

(RSSW), composed of Ginseng (Root of *Panax ginseng C.A. Mey*) and fleece flower root (*Polygonum multiflorum Thunb.*), is a patented Traditional Chinese Medicine included in Chinese Pharmacopoeia. RSSW (50 mg/kg, 100 mg/kg) was administered to MCAO rats. Western blot showed that RSSW significantly downregulated TLR4/NF-κB/NLRP3 signaling pathway (Li. et al., 2020). Taohong Siwu Decoction (THSWD) can also regulate TLR4/NF-κB/NLRP3 (Wang M et al., 2020). THSWD originated from the traditional Chinese medicine book *Yizong Jinjian* of the Qing Dynasty, which is composed of *Prunus persica* (L.) *Batsch*, *Carthamus tinctorius L*, *Angelica sinensis* (Oliv.) Diels, *Rehmannia glutinosa* (Gaertn.) DC., *Ligusticum chuanxiong* Hort, *Paeonia lactiflora* Pall. Also, previous report has investigated the major constituents of THSWD by UPLCQ-TOF-MS. A total of 95 components have been identififfied, including aromatic acids, flflavonoids, polysaccharides, volatile oils, monoterpene glycosides, aromatic cyanoglycosides (Dong et al., 2019). They are the basis of THSWD inhibitors of pyroptosis (Ye et al., 2020; Yin et al., 2020). Unlike RSSW, THSWD can reduce the expression of TXNIP, p38MAPK and JNK. In addition, THSWD has been found to inhibit MCAO/R rats pyroptosis via DRP1/NLRP3 pathway (Zhou, 2021). These again illustrate the characteristics of multi-component and multi-target action of traditional Chinese medicine. Panax ginseng and Angelica sinensis (CPA) treatment ameliorated MCAO-induced cerebral damage and neurological dysfunction by inhibiting NLRP3 inflammasome activation and microglial pyroptosis. Its inhibitory effect was comparable to that of MCC950, a well-known inhibitor of NLRP3 inflammasome. Further *in vitro* study revealed that the key active ingredients of Panax ginseng and Angelica sinensis inhibited OGD/R-induced NLRP3 inflammasome activation and pyroptosis by inhibiting DRP1-mediated mitochondrial fission (Hu et al., 2020). Qingkailing (QKL) injection, a patented Chinese medicine approved by the China Food and Drug Administration, has been widely used in clinical practice to treat cerebral ischemia in China. Rats in the QKL group received intraperitoneal injections of 3 mL/kg QKL, QKL relieved IS and suppressed the inflammatory response by inhibiting AMPK-mediated activation of the NLRP3 inflammasome (Ma et al., 2019) (Table 1).

Conclusion and perspectives

Pyroptosis is a form of death characterized by cell swelling, membrane rupture, and inflammatory cytokine release. It can be caused by NLRP3 inflammasome that assembly after activation of secreted IL-1β and IL-18. NLRP3 inflammasome play an important role in the development of IS. Most *in vitro* and *in vivo* studies in our review have confirmed that inhibition of NLRP3 inflammasome can improve neural function and reduce the volume of cerebral infarction to a large extent. However, a study from *Stroke* showing that the injury degree of IS has nothing to do with NLRP3 inflammasome (Lemarchand et al., 2019). We speculate that this may be related to experimental modeling, because in this report, C57BL/6 mice were modeled with $FeCl_3$, which is different from the MCAO and OGD models we summarized previously. A variety of signal molecules lead to early pathological changes through corresponding signaling pathways after IS, subsequently activating NLRP3 inflammasome-mediated pyroptosis. These signal-mediated pathological changes include ROS damage, mitochondrial dysfunction, ion imbalance, lysosomal rupture, and trans-Golgi disintegration. The activation of NLRP3 inflammasome consists of two steps, namely, the activation and assembly of NLRP3 inflammasome. The signaling pathway involved in the activation step is TLR4/NF-κB/NLRP3. The signaling pathways involved in the assembly include ROS/TXNIP/NLRP3, AMPK/Nrf2/NLRP3, DRP1/NLRP3, and TAK1/JNK/NLRP3. Current pharmacological studies show that traditional Chinese medicine can inhibit NLRP3 inflammasome by regulating the above signal pathways, thus inhibiting pyroptosis and achieving the purpose of alleviating the process of IS, showing the characteristics of multi-target and multi-channel treatment of traditional Chinese medicine. This provides a positive signal for exploring the role of traditional Chinese medicine in pyroptosis (Table 1).

We believe that there are still some challenges in the research of anti-IS effect of traditional Chinese medicine based on pyroptosis. 1) Strengthen the research of compound prescription and Chinese patent medicine. Our previous summaries found that compared with traditional Chinese medicine monomer, the compound prescription and Chinese patent medicine, as a common clinical form of traditional Chinese medicine, has less research reports, which is not conducive to providing scientific basis for the clinical application of the compound. In the future, bioinformatics methods can be used to identify the potential effective components and target of action of the compound prescription and Chinese patent medicine, structural pharmacology methods such as molecular docking technology can be used to further reveal the binding sites of monomer components, and methods such as gene knockout or inhibition of key proteins can be used to verify the target of action of monomer components. Adopt modern pharmacological methods to carry out simultaneous component research and comparative study with compound prescription, so as to clarify the material basis of drug function. 2) The IS body model is diversified. Most of the models summarized in this review are MACO or MCAO/R models. However, studies have shown that the selection of models may have an impact on the role of NLRP3-mediated pyroptosis in IS (Lemarchand et al., 2019). Therefore, different models can be used for comparative study in future studies, and mutual verification can fully illustrate the empirical conclusions. 3) To explore the potential of non-classical pyroptosis in the study of IS pathological mechanism. Previous studies have shown that the expression of caspase-11 protein upregulated in OGD microglial cells, which indicates that there is activation of non-classical pyrolytic pathway in the process of IS (Fradejas et al., 2010). However, there is no *in vivo* experiment to show the relationship between non-classical pyrolytic pathway and IS. Moreover, there is little research on non-classical pyroptosis pathway in traditional Chinese medicine.

To sum up, NLPR3 inflammasome may be the switch molecular target of the upstream channel of the mechanism of pyroptosis in IS. Deeply exploring the relevant molecular mechanism of NLRP3 inflammaasome affecting pyroptosis, summarizing the relationship between NLRP3 mediated-pyroptosis signal pathway and IS, and the research status of TCM prevention and treatment, clarifying the specific mechanism of TCM, provide new ideas for TCM treatment of IS, and provide theoretical basis for TCM to effectively and economically serve human health.

Author contributions

J-XL and M-ZT contributed equally to this manuscript. J-XL designed the review. J-XL and M-ZT were in charge of searching all the relative papers. H-HY, HD, FL, and KD gave their valuable and professional suggestions and guide in organizing and drafting this manuscript. X-YC and KD revised the manuscript.

Funding

This work was supported by State Key Laboratory Open Program of China (GTZK201711), Hunan Provincial Natural Science Foundation of China (2020JJ9050), Double-class Discipline Pharmacy Open Fund of China (2018YX03), Hunan Provincial Department of Education Postgraduate Innovation and Entrepreneurship Training Program Project of China (CX20220794), Innovation and Entrepreneurship Training Program for College Students of Hunan Provincial Department of Education of China (S202210541074), First-class undergraduate courses in Hunan Province of China (2021(28)-371) and Research project of educational reform in universities in Hunan Province of China (HNJG-2022-0134).

Conflict of interest

The authors declare that the research was conducted in the absence of any commercial or financial relationships that could be construed as a potential conflict of interest.

Publisher's note

All claims expressed in this article are solely those of the authors and do not necessarily represent those of their affiliated organizations, or those of the publisher, the editors and the reviewers. Any product that may be evaluated in this article, or claim that may be made by its manufacturer, is not guaranteed or endorsed by the publisher.

References

Agostini, L., Martinon, F., Burns, K., McDermott, M. F., Hawkins, P. N., and Tschopp, J. (2004). NALP3 forms an IL-1beta-processing inflammasome with increased activity in Muckle-Wells autoinflammatory disorder. *Immunity* 20 (3), 319–325. doi:10.1016/s1074-7613(04)00046-9

Albalawi, F., Lu, W., Beckel, J. M., Lim, J. C., McCaughey, S. A., and Mitchell, C. H. (2017). The P2X7 receptor primes IL-1β and the NLRP3 inflammasome in astrocytes exposed to mechanical strain. *Front. Cell. Neurosci.* 11, 227. doi:10.3389/fncel.2017.00227

Alishahi, M., Farzaneh, M., Ghaedrahmati, F., Nejabatdoust, A., Sarkaki, A., and Khoshnam, S. E. (2019). NLRP3 inflammasome in ischemic stroke: As possible therapeutic target. *Int. J. Stroke* 14 (6), 574–591. doi:10.1177/1747493019841242

An, P., Xie, J., Qiu, S., Liu, Y., Wang, J., Xiu, X., et al. (2019). Hispidulin exhibits neuroprotective activities against cerebral ischemia reperfusion injury through suppressing NLRP3-mediated pyroptosis. *Life Sci.* 232, 116599–599. doi:10.1016/j.lfs.2019.116599

Bellut, M., Papp, L., Bieber, M., Kraft, P., Stoll, G., and Schuhmann, M. K. (2021). NLPR3 inflammasome inhibition alleviates hypoxic endothelial cell death *in vitro* and protects blood-brain barrier integrity in murine stroke. *Cell Death Dis.* 13 (1), 20. doi:10.1038/s41419-021-04379-z

Bruchard, M., Mignot, G., Derangère, V., Chalmin, F., Chevriaux, A., Végran, F., et al. (2013). Chemotherapy-triggered cathepsin B release in myeloid-derived suppressor cells activates the Nlrp3 inflammasome and promotes tumor growth. *Nat. Med.* 19 (1), 57–64. doi:10.1038/nm.2999

Cao, G., Jiang, N., Hu, Y., Zhang, Y., Wang, G., Yin, M., et al. (2016). Ruscogenin attenuates cerebral ischemia-induced blood-brain barrier dysfunction by suppressing TXNIP/NLRP3 inflammasome activation and the MAPK pathway. *Int. J. Mol. Sci.* 17 (9), 1418. doi:10.3390/ijms17091418

Carneiro, L., Allard, C., Guissard, C., Fioramonti, X., Tourrel-Cuzin, C., Bailbé, D., et al. (2012). Importance of mitochondrial dynamin-related protein 1 in hypothalamic glucose sensitivity in rats. *Antioxid. Redox Signal* 17 (3), 433–444. doi:10.1089/ars.2011.4254

Chavez, L. M., Huang, S. S., MacDonald, I., Lin, J. G., Lee, Y. C., and Chen, Y. H. (2017). Mechanisms of acupuncture therapy in ischemic stroke rehabilitation: A literature review of basic studies. *Int. J. Mol. Sci.* 18 (11), 2270. doi:10.3390/ijms18112270

Chen, D., Dixon, B. J., Doycheva, D. M., Li, B., Zhang, Y., Hu, Q., et al. (2018). IRE1α inhibition decreased TXNIP/NLRP3 inflammasome activation through miR-17-5p after neonatal hypoxic-ischemic brain injury in rats. *J. Neuroinflammation* 15 (1), 32. doi:10.1186/s12974-018-1077-9

Chen, J., and Chen, Z. J. (2018). PtdIns4P on dispersed trans-Golgi network mediates NLRP3 inflammasome activation. *Nature* 564 (7734), 71–76. doi:10.1038/s41586-018-0761-3

Chen S, S., Mei, S., Luo, Y., Wu, H., Zhang, J., and Zhu, J. (2018). Gasdermin family: A promising therapeutic target for stroke. *Transl. stroke Res.* 9 (6), 555–563. doi:10.1007/s12975-018-0666-3

Chen, Y., Hao, C., Chen, W., Cheng, W., Li, P., Shen, J., et al. (2022). Anti-depressant effects of acupuncture: The insights from NLRP3 mediated pyroptosis and inflammation. *Neurosci. Lett.* 785, 136787. doi:10.1016/j.neulet.2022.136787

Chen, Y., Wu, J., Zhu, J., Yang, G., Tian, J., Zhao, Y., et al. (2021). Artesunate provides neuroprotection against cerebral ischemia-reperfusion injury via the TLR-4/NF-κB pathway in rats. *Biol. Pharm. Bull.* 44 (3), 350–356. doi:10.1248/bpb.b20-00604

Choi, J. W., and Chun, J. (2013). Lysophospholipids and their receptors in the central nervous system. *Biochim. Biophys. Acta* 1831 (1), 20–32. doi:10.1016/j.bbalip.2012.07.015

Dong, W., Zhu, Q., Yang, B., Qin, Q., Wang, Y., Xia, X., et al. (2019). Polychlorinated biphenyl quinone induces caspase 1-mediated pyroptosis through induction of pro-inflammatory HMGB1-TLR4-NLRP3-GSDMD signal Axis. *Chem. Res. Toxicol.* 32 (6), 1051–1057. doi:10.1021/acs.chemrestox.8b00376

Dongyu, M., Li, H., Guan, L., Jiang, C., Zhang, H., Cui, X., et al. (2020). Protective mechanism of Naoxinqing Capsule in rat models of cerebral ischemia/reperfusion injury. *Chin. J. Tissue Eng. Res.* 24 (2), 215–222.

Duan, C., Kuang, L., Xiang, X., Zhang, J., Zhu, Y., Wu, Y., et al. (2020). Drp1 regulates mitochondrial dysfunction and dysregulated metabolism in ischemic injury via Clec16a-BAX-and GSH- pathways. *Cell Death Dis.* 11 (4), 251. doi:10.1038/s41419-020-2461-9

Duewell, P., Kono, H., Rayner, K. J., Sirois, C. M., Vladimer, G., Bauernfeind, F. G., et al. (2010). NLRP3 inflammasomes are required for atherogenesis and activated by cholesterol crystals. *Nature* 464 (7293), 1357–1361. doi:10.1038/nature08938

Fradejas, N., Pastor, M. D., Burgos, M., Beyaert, R., Tranque, P., and Calvo, S. (2010). Caspase-11 mediates ischemia-induced astrocyte death: Involvement of endoplasmic reticulum stress and C/EBP homologous protein. *J. Neurosci. Res.* 88 (5), 1094–1105. doi:10.1002/jnr.22280

Fu, C., Zhang, X., Lu, Y., Wang, F., Xu, Z., Liu, S., et al. (2020). Geniposide inhibits NLRP3 inflammasome activation via autophagy in BV-2 microglial cells exposed to oxygen-glucose deprivation/reoxygenation. *Int. Immunopharmacol.* 84, 106547. doi:10.1016/j.intimp.2020.106547

Fuse, Y., and Kobayashi, M. (2017). Conservation of the keap1-nrf2 system: An evolutionary journey through stressful space and time. *Molecules* 22 (3), 436. doi:10.3390/molecules22030436

GBD 2016 Stroke Collaborators (2019). Global, regional, and national burden of stroke, 1990-2016: A systematic analysis for the global burden of disease study 2016. *Lancet Neurol.* 18 (5), 439–458. doi:10.1016/s1474-4422(19)30034-1

Groenendyk, J., Agellon, L. B., and Michalak, M. (2021). Calcium signaling and endoplasmic reticulum stress. *Int. Rev. Cell Mol. Biol.* 363, 1–20. doi:10.1016/bs.ircmb.2021.03.003

Gu, C., Li, T., Jiang, S., Yang, Z., Lv, J., Yi, W., et al. (2018). AMP-activated protein kinase sparks the fire of cardioprotection against myocardial ischemia and cardiac ageing. *Ageing Res. Rev.* 47, 168–175. doi:10.1016/j.arr.2018.08.002

Guo, H., Zhu, L., Tang, P., Chen, D., Li, Y., Li, J., et al. (2021). Carthamin yellow improves cerebral ischemia-reperfusion injury by attenuating inflammation and ferroptosis in rats. *Int. J. Mol. Med.* 47 (4), 52. doi:10.3892/ijmm.2021.4885

Guo, M., Wang, X., Zhao, Y., Yang, Q., Ding, H., Dong, Q., et al. (2018). Ketogenic diet improves brain ischemic tolerance and inhibits NLRP3 inflammasome activation by preventing drp1-mediated mitochondrial fission and endoplasmic reticulum stress. *Front. Mol. Neurosci.* 11, 86. doi:10.3389/fnmol.2018.00086

Hara, H., Tsuchiya, K., Kawamura, I., Fang, R., Hernandez-Cuellar, E., Shen, Y., et al. (2013). Phosphorylation of the adaptor ASC acts as a molecular switch that controls the formation of speck-like aggregates and inflammasome activity. *Nat. Immunol.* 14 (12), 1247–1255. doi:10.1038/ni.2749

Hasan, T. F., Hasan, H., and Kelley, R. E. (2021). Overview of acute ischemic stroke evaluation and management. *Biomedicines* 9 (10), 1486. doi:10.3390/biomedicines9101486

Hirata, Y., Takahashi, M., Morishita, T., Noguchi, T., and Matsuzawa, A. (2017). Post-translational modifications of the TAK1-TAB complex. *Int. J. Mol. Sci.* 18 (1), 205. doi:10.3390/ijms18010205

Hou, Y., Wang, Y., He, Q., Li, L., Xie, H., Zhao, Y., et al. (2018). Nrf2 inhibits NLRP3 inflammasome activation through regulating Trx1/TXNIP complex in cerebral ischemia reperfusion injury. *Behav. Brain Res.* 336, 32–39. doi:10.1016/j.bbr.2017.06.027

Hu, C., Huang, Y., and Li, L. (2017). Drp1-Dependent mitochondrial fission plays critical roles in physiological and pathological progresses in mammals. *Int. J. Mol. Sci.* 18 (1), 144. doi:10.3390/ijms18010144

Hu, H. J., and Song, M. (2017). Disrupted ionic homeostasis in ischemic stroke and new therapeutic targets. *J. Stroke Cerebrovasc. Dis.* 26 (12), 2706–2719. doi:10.1016/j.jstrokecerebrovasdis.2017.09.011

Hu, J., Zeng, C., Wei, J., Duan, F., Liu, S., Zhao, Y., et al. (2020). The combination of Panax ginseng and Angelica sinensis alleviates ischemia brain injury by suppressing NLRP3 inflammasome activation and microglial pyroptosis. *Phytomedicine* 76, 153251. doi:10.1016/j.phymed.2020.153251

Hu, Q., Zhang, T., Yi, L., Zhou, X., and Mi, M. (2018). Dihydromyricetin inhibits NLRP3 inflammasome-dependent pyroptosis by activating the Nrf2 signaling pathway in vascular endothelial cells. *Biofactors* 44 (2), 123–136. doi:10.1002/biof.1395

Huang, Y., Xu, W., and Zhou, R. (2021). NLRP3 inflammasome activation and cell death. *Cell Mol. Immunol.* 18 (9), 2114–2127. doi:10.1038/s41423-021-00740-6

Jin, X., Liu, M. Y., Zhang, D. F., Zhong, X., Du, K., Qian, P., et al. (2019). Baicalin mitigates cognitive impairment and protects neurons from microglia-mediated neuroinflammation via suppressing NLRP3 inflammasomes and TLR4/NF-κB signaling pathway. *CNS Neurosci. Ther.* 25 (5), 575–590. doi:10.1111/cns.13086

Joo, M. S., Kim, W. D., Lee, K. Y., Kim, J. H., Koo, J. H., and Kim, S. G. (2016). AMPK facilitates nuclear accumulation of Nrf2 by phosphorylating at serine 550. *Mol. Cell Biol.* 36 (14), 1931–1942. doi:10.1128/mcb.00118-16

Kang, C., Lu, Z., Zhu, G., Chen, Y., and Wu, Y. (2021). Knockdown of TRIM22 relieves oxygen-glucose deprivation/reoxygenation-induced apoptosis and inflammation through inhibition of NF-κB/NLRP3 Axis. *Cell Mol. Neurobiol.* 41 (2), 341–351. doi:10.1007/s10571-020-00855-w

Katsnelson, M. A., Rucker, L. G., Russo, H. M., and Dubyak, G. R. (2015). K^+ efflux agonists induce NLRP3 inflammasome activation independently of Ca^{2+} signaling. *J. Immunol.* 194 (8), 3937–3952. doi:10.4049/jimmunol.1402658

Kleele, T., Rey, T., Winter, J., Zaganelli, S., Mahecic, D., Perreten Lambert, H., et al. (2021). Distinct fission signatures predict mitochondrial degradation or biogenesis. *Nature* 593 (7859), 435–439. doi:10.1038/s41586-021-03510-6

Kut, K., Bartosz, G., Soszyński, M., and Sadowska-Bartosz, I. (2022). Antioxidant properties of hispidulin. *Nat. Prod. Res.* 36 (24), 6401–6404. doi:10.1080/14786419.2022.2032050

Lee, G. S., Subramanian, N., Kim, A. I., Aksentijevich, I., Goldbach-Mansky, R., Sacks, D. B., et al. (2012). The calcium-sensing receptor regulates the NLRP3 inflammasome through Ca^{2+} and cAMP. *Nature* 492 (7427), 123–127. doi:10.1038/nature11588

Lemarchand, E., Barrington, J., Chenery, A., Haley, M., Coutts, G., Allen, J. E., et al. (2019). Extent of ischemic brain injury after thrombotic stroke is independent of the NLRP3 (NACHT, LRR and PYD domains-containing protein 3) inflammasome. *Stroke* 50 (5), 1232–1239. doi:10.1161/strokeaha.118.023620

Li, L., Acioglu, C., Heary, R. F., and Elkabes, S. (2021). Role of astroglial toll-like receptors (TLRs) in central nervous system infections, injury and neurodegenerative diseases. *Brain Behav. Immun.* 91, 740–755. doi:10.1016/j.bbi.2020.10.007

Li, S., Dou, B., Shu, S., Wei, L., Zhu, S., Ke, Z., et al. (2021). Suppressing NK cells by astragaloside IV protects against acute ischemic stroke in mice via inhibiting STAT3. *Front. Pharmacol.* 12, 802047. doi:10.3389/fphar.2021.802047

Li, X. (2019). *The protective effect of shennaofuyuan decoction on PC12 cells in hypoxia and glucose deprivation based on the mechanism of pyroptosis. Changsha (hunan Province in China)*. Hunan: Hunan University of Chinese Medicine.

Li, Y., Li, J., Li, S., Li, Y., Wang, X., Liu, B., et al. (2015). Curcumin attenuates glutamate neurotoxicity in the hippocampus by suppression of ER stress-associated TXNIP/NLRP3 inflammasome activation in a manner dependent on AMPK. *Toxicol. Appl. Pharmacol.* 286 (1), 53–63. doi:10.1016/j.taap.2015.03.010

Li, Y., Liang, W., Guo, C., Chen, X., Huang, Y., Wang, H., et al. (2020). Renshen Shouwu extract enhances neurogenesis and angiogenesis via inhibition of TLR4/NF-κB/NLRP3 signaling pathway following ischemic stroke in rats. *J. Ethnopharmacol.* 253, 112616. doi:10.1016/j.jep.2020.112616

Li, Y., and Zhang, Z. (2020). LPA induced pyroptosis of PC12 cells by JNK phosphorylation. *Stroke Nerv. Dis.* 27 (3), 283–292. (in Chinese).

Liu, J., Ma, W., Zang, C. H., Wang, G. D., Zhang, S. J., Wu, H. J., et al. (2021). Salidroside inhibits NLRP3 inflammasome activation and apoptosis in microglia induced by cerebral ischemia/reperfusion injury by inhibiting the TLR4/NF-κB signaling pathway. *Ann. Transl. Med.* 9 (22), 1694. doi:10.21037/atm-21-5752

Liu, T., Wang, W., Liu, M., Ma, Y., Mu, F., Feng, X., et al. (2020). Z-Guggulsterone alleviated oxidative stress and inflammation through inhibiting the TXNIP/NLRP3 axis in ischemic stroke. *Int. Immunopharmacol.* 89, 107094. doi:10.1016/j.intimp.2020.107094

Liu, X., Zhang, X., Ding, Y., Zhou, W., Tao, L., Lu, P., et al. (2017). Nuclear factor E2-related factor-2 negatively regulates NLRP3 inflammasome activity by inhibiting reactive oxygen species-induced NLRP3 priming. *Antioxid. Redox Signal* 26 (1), 28–43. doi:10.1089/ars.2015.6615

Liu, Y. L., Ma, X. D., and Song, C. Q. (2019). Study on mechanism of anti-pyroptosis effect of eye on CIRI rats. *Chin. J. Immunol.* 35 (24), 2964–2970. (in Chinese).

Lu, F., Lan, Z., Xin, Z., He, C., Guo, Z., Xia, X., et al. (2020). Emerging insights into molecular mechanisms underlying pyroptosis and functions of inflammasomes in diseases. *J. Cell Physiol.* 235 (4), 3207–3221. doi:10.1002/jcp.29268

Lu, Q. Y., Ma, J. Q., Duan, Y. Y., Sun, Y., Yu, S., Li, B., et al. (2019). Carthamin yellow protects the heart against ischemia/reperfusion injury with reduced reactive oxygen species release and inflammatory response. *J. Cardiovasc Pharmacol.* 74 (3), 228–234. doi:10.1097/fjc.0000000000000710

Ludhiadch, A., Sharma, R., Muriki, A., and Munshi, A. (2022). Role of calcium homeostasis in ischemic stroke: A review. *CNS Neurol. Disord. Drug Targets.* 21 (1), 52–61. doi:10.2174/1871527320666210212141232

Luo, C., Chen, Q., Liu, B., Wang, S., Yu, H., Guan, X., et al. (2021). The extracts of Angelica sinensis and Cinnamomum cassia from oriental medicinal foods regulate inflammatory and autophagic pathways against neural injury after ischemic stroke. *Oxid. Med. Cell Longev.* 2021, 9663208. doi:10.1155/2021/9663208

Luo, T., Zhou, X., Qin, M., Lin, Y., Lin, J., Chen, G., et al. (2022). Corilagin restrains NLRP3 inflammasome activation and pyroptosis through the ROS/TXNIP/NLRP3 pathway to prevent inflammation. *Oxid. Med. Cell Longev.* 2022, 1652244. doi:10.1155/2022/1652244

Ma, C., Wang, X., Xu, T., Yu, X., Zhang, S., Liu, S., et al. (2019). Qingkailing injection ameliorates cerebral ischemia-reperfusion injury and modulates the AMPK/NLRP3 Inflammasome Signalling pathway. *BMC Complement. Altern. Med.* 19 (1), 320. doi:10.1186/s12906-019-2703-5

McKenzie, B. A., Dixit, V. M., and Power, C. (2020). Fiery cell death: Pyroptosis in the central nervous system. *Trends Neurosci.* 43 (1), 55–73. doi:10.1016/j.tins.2019.11.005

Mitchell, J., Kim, S. J., Seelmann, A., Veit, B., Shepard, B., Im, E., et al. (2018). Src family kinase tyrosine phosphorylates Toll-like receptor 4 to dissociate MyD88 and Mal/Tirap, suppressing LPS-induced inflammatory responses. *Biochem. Pharmacol.* 147, 119–127. doi:10.1016/j.bcp.2017.11.015

Mohamadi, Y., Mousavi, M., Khanbabaei, H., Salarinia, R., Javankiani, S., Hassanzadeh, G., et al. (2018). The role of inflammasome complex in ischemia-reperfusion injury. *J. Cell Biochem.* 2018, 27368. doi:10.1002/jcb.27368

Muñoz-Planillo, R., Kuffa, P., Martínez-Colón, G., Smith, B. L., Rajendiran, T. M., and Núñez, G. (2013). K^+ efflux is the common trigger of NLRP3 inflammasome activation by bacterial toxins and particulate matter. *Immunity* 38 (6), 1142–1153. doi:10.1016/j.immuni.2013.05.016

Murakami, T., Ockinger, J., Yu, J., Byles, V., McColl, A., Hofer, A. M., et al. (2012). Critical role for calcium mobilization in activation of the NLRP3 inflammasome. *Proc. Natl. Acad. Sci. U. S. A.* 109 (28), 11282–11287. doi:10.1073/pnas.1117765109

Orlowski, G. M., Colbert, J. D., Sharma, S., Bogyo, M., Robertson, S. A., and Rock, K. L. (2015). Multiple cathepsins promote pro-IL-1β synthesis and NLRP3-mediated IL-1β activation. *J. Immunol.* 195 (4), 1685–1697. doi:10.4049/jimmunol.1500509

Park, H. S., Liu, G., Liu, Q., and Zhou, Y. (2018). Swine influenza virus induces RIPK1/DRP1-mediated interleukin-1 beta production. *Viruses* 10 (8), 419. doi:10.3390/v10080419

Qiu, J., Wang, M., Zhang, J., Cai, Q., Lu, D., Li, Y., et al. (2016). The neuroprotection of Sinomenine against ischemic stroke in mice by suppressing NLRP3 inflammasome via AMPK signaling. *Int. Immunopharmacol.* 40, 492–500. doi:10.1016/j.intimp.2016.09.024

Ran, Y., Su, W., Gao, F., Ding, Z., Yang, S., Ye, L., et al. (2021). Curcumin ameliorates white matter injury after ischemic stroke by inhibiting microglia/macrophage pyroptosis through NF-κB suppression and NLRP3 inflammasome inhibition. *Oxid. Med. Cell Longev.* 2021, 1552127. doi:10.1155/2021/1552127

Repnik, U., Hafner Česen, M., and Turk, B. (2014). Lysosomal membrane permeabilization in cell death: Concepts and challenges. *Mitochondrion* 19, 49–57. doi:10.1016/j.mito.2014.06.006

Rühl, S., Shkarina, K., Demarco, B., Heilig, R., Santos, J. C., and Broz, P. (2018). ESCRT-dependent membrane repair negatively regulates pyroptosis downstream of GSDMD activation. *Science* 362 (6417), 956–960. doi:10.1126/science.aar7607

Sha, R., Zhang, B., Han, X., Peng, J., Zheng, C., Zhang, F., et al. (2019). Electroacupuncture alleviates ischemic brain injury by inhibiting the miR-223/NLRP3 pathway. *Med. Sci. Monit. Int. Med. J. Exp. Clin. Res.* 25, 4723–4733. doi:10.12659/msm.917213

Shi, K., Tian, D. C., Li, Z. G., Ducruet, A. F., Lawton, M. T., and Shi, F. D. (2019). Global brain inflammation in stroke. *Lancet Neurol.* 18 (11), 1058–1066. doi:10.1016/s1474-4422(19)30078-x

Tang, D., Kang, R., Berghe, T. V., Vandenabeele, P., and Kroemer, G. (2019). The molecular machinery of regulated cell death. *Cell Res.* 29 (5), 347–364. doi:10.1038/s41422-019-0164-5

Tufekci, K. U., Eltutan, B. I., Isci, K. B., and Genc, S. (2021). Resveratrol inhibits NLRP3 inflammasome-induced pyroptosis and miR-155 expression in microglia through Sirt1/AMPK pathway. *Neurotox. Res.* 39 (6), 1812–1829. doi:10.1007/s12640-021-00435-w

Wang, C. P., Wang, Y., Wang, X., Zhang, X., Ye, J. F., Hu, L. S., et al. (2011). Mulberroside a possesses potent uricosuric and nephroprotective effects in hyperuricemic mice. *Planta Med.* 77 (8), 786–794. doi:10.1055/s-0030-1250599

Wang, C. P., Zhang, L. Z., Li, G. C., Shi, Y. W., Li, J. L., Zhang, X. C., et al. (2014). Mulberroside A protects against ischemic impairment in primary culture of rat cortical neurons after oxygen-glucose deprivation followed by reperfusion. *J. Neurosci. Res.* 92 (7), 944–954. doi:10.1002/jnr.23374

Wang, K., Ru, J., Zhang, H., Chen, J., Lin, X., Lin, Z., et al. (2020). Melatonin enhances the therapeutic effect of plasma exosomes against cerebral ischemia-induced pyroptosis through the TLR4/NF-κB pathway. *Front. Neurosci.* 14, 848. doi:10.3389/fnins.2020.00848

Wang, L., Negro, R., and Wu, H. (2020). TRPM2, linking oxidative stress and Ca^{2+} permeation to NLRP3 inflammasome activation. *Curr. Opin. Immunol.* 62, 131–135. doi:10.1016/j.coi.2020.01.005

Wang, M., Liu, Z., Hu, S., Duan, X., Zhang, Y., Peng, C., et al. (2020). Taohong siwu decoction ameliorates ischemic stroke injury via suppressing pyroptosis. *Front. Pharmacol.* 11, 590453. doi:10.3389/fphar.2020.590453

Wang, X., Li, R., Wang, X., Fu, Q., and Ma, S. (2015). Umbelliferone ameliorates cerebral ischemia-reperfusion injury via upregulating the PPAR gamma expression and suppressing TXNIP/NLRP3 inflammasome. *Neurosci. Lett.* 600, 182–187. doi:10.1016/j.neulet.2015.06.016

Wang, Y., Gao, W., Shi, X., Ding, J., Liu, W., He, H., et al. (2017). Chemotherapy drugs induce pyroptosis through caspase-3 cleavage of a gasdermin. *Nature* 547 (7661), 99–103. doi:10.1038/nature22393

Wang, Y., Guan, X., Gao, C. L., Ruan, W., Zhao, S., Kai, G., et al. (2021). Medioresinol as a novel PGC-1α activator prevents pyroptosis of endothelial cells in ischemic stroke through PPARα-GOT1 axis. *Pharmacol. Res.* 169, 105640. doi:10.1016/j.phrs.2021.105640

Weber, K., and Schilling, J. D. (2014). Lysosomes integrate metabolic-inflammatory cross-talk in primary macrophage inflammasome activation. *J. Biol. Chem.* 289 (13), 9158–9171. doi:10.1074/jbc.M113.531202

Wu, J., Xu, X., Li, Y., Kou, J., Huang, F., Liu, B., et al. (2014). Quercetin, luteolin and epigallocatechin gallate alleviate TXNIP and NLRP3-mediated inflammation and apoptosis with regulation of AMPK in endothelial cells. *Eur. J. Pharmacol.* 745, 59–68. doi:10.1016/j.ejphar.2014.09.046

Xiao, L., Dai, Z., Tang, W., Liu, C., and Tang, B. (2021). Astragaloside IV alleviates cerebral ischemia-reperfusion injury through NLRP3 inflammasome-mediated pyroptosis inhibition via activating Nrf2. *Oxid. Med. Cell Longev.* 2021, 9925561. doi:10.1155/2021/9925561

Xu, H. X., Zhou, G. P., Dong, M. M., Li, Y. L., Yang, L., and Zhan, Z. L. (2020). Effect of electroacupuncture on caspase-1 in hippocampus of rats with cerebral ischemia-reperfusion injury. *Mod. Traditional Chin. Med. Materia Materia-World Sci. Technol.* 22 (2), 446–451.

Xu, Y., Lin, S., Jiang, C., Ye, X., Tao, J., Wilfried, S., et al. (2018). Synergistic effect of acupuncture and mirror therapy on post-stroke upper limb dysfunction: A study protocol for a randomized controlled trial. *Trials* 19 (1), 303. doi:10.1186/s13063-018-2585-8

Yao, Y., Hu, S., Zhang, C., Zhou, Q., Wang, H., Yang, Y., et al. (2022). Ginsenoside Rd attenuates cerebral ischemia/reperfusion injury by exerting an anti-pyroptotic effect via the miR-139-5p/FoxO1/Keap1/Nrf2 axis. *Int. Immunopharmacol.* 105, 108582. doi:10.1016/j.intimp.2022.108582

Ye, J. X., Wang, M., Wang, R. Y., Liu, H. T., Qi, Y. D., Fu, J. H., et al. (2020). Hydroxysafflor yellow A inhibits hypoxia/reoxygenation-induced cardiomyocyte injury via regulating the AMPK/NLRP3 inflammasome pathway. *Int. Immunopharmacol.* 82, 106316. doi:10.1016/j.intimp.2020.106316

Ye, X., Shen, T., Hu, J., Zhang, L., Zhang, Y., Bao, L., et al. (2017). Purinergic 2X7 receptor/NLRP3 pathway triggers neuronal apoptosis after ischemic stroke in the mouse. *Exp. Neurol.* 292, 46–55. doi:10.1016/j.expneurol.2017.03.002

Ye, Y., Jin, T., Zhang, X., Zeng, Z., Ye, B., Wang, J., et al. (2019). Meisoindigo protects against focal cerebral ischemia-reperfusion injury by inhibiting NLRP3 inflammasome activation and regulating microglia/macrophage polarization via TLR4/NF-κB signaling pathway. *Front. Cell. Neurosci.* 13, 553. doi:10.3389/fncel.2019.00553

Yin, N., Gao, Q., Tao, W., Chen, J., Bi, J., Ding, F., et al. (2020). Paeoniflorin relieves LPS-induced inflammatory pain in mice by inhibiting NLRP3 inflammasome activation via transient receptor potential vanilloid 1. *J. Leukoc. Biol.* 108 (1), 229–241. doi:10.1002/jlb.3ma0220-355r

Yu, H., Wu, Z., Wang, X., Gao, C., Liu, R., Kang, F., et al. (2020). Protective effects of combined treatment with mild hypothermia and edaravone against cerebral ischemia/reperfusion injury via oxidative stress and Nrf2 pathway regulation. *Int. J. Oncol.* 57 (2), 500–508. doi:10.3892/ijo.2020.5077

Yu, J., Wang, W. N., Matei, N., Li, X., Pang, J. W., Mo, J., et al. (2020). Ezetimibe attenuates oxidative stress and neuroinflammation via the AMPK/Nrf2/TXNIP pathway after MCAO in rats. *Oxid. Med. Cell Longev.* 2020, 4717258. doi:10.1155/2020/4717258

Yue, G. G-L., Jiang, L., Kwok, H-F., Lee, J. K-M., Chan, K-M., Fung, K-P., et al. (2016). Turmeric ethanolic extract possesses stronger inhibitory activities on colon tumour growth than curcumin – the importance of turmerones. *J. Funct. Foods* 22, 565–577. doi:10.1016/j.jff.2016.02.011

Zeng, C., Liu, Z., Chen, Y., Shang, X., Xia, Z., and He, Q. (2021). The effect of asiaticoside on Nrf2/TXNIP/NLRP3 pathway and microglia activation in rats with cerebral ischemia-reperfusion injury. *Stroke Nerv. Dis.* 28, 288–294.

Zhang, N., Zhang, X., Liu, X., Wang, H., Xue, J., Yu, J., et al. (2014). Chrysophanol inhibits NALP3 inflammasome activation and ameliorates cerebral ischemia/reperfusion in mice. *Mediat. Inflamm.* 2014, 370530. doi:10.1155/2014/370530

Zhang, T., Guan, B., Tan, S., Zhu, H., Ren, D., Li, R., et al. (2021). Bushen huoxue acupuncture inhibits NLRP1 inflammasome-mediated neuronal pyroptosis in SAMP8 mouse model of alzheimer's disease. *Neuropsychiatr. Dis. Treat.* 17, 339–346. doi:10.2147/ndt.S279304

Zhang, Y., Rong, H., Zhang, F. X., Wu, K., Mu, L., Meng, J., et al. (2018). A membrane potential- and calpain-dependent reversal of caspase-1 inhibition regulates canonical NLRP3 inflammasome. *Cell Rep.* 24 (9), 2356–2369. doi:10.1016/j.celrep.2018.07.098

Zhang, Z., Ma, T., Fu, Z., Feng, Y., Wang, Z., Tian, S., et al. (2022). TBC1Domain Family Member 25 deficiency aggravates cerebral ischemia-reperfusion injury via TAK1-JNK/p38 pathway. *J. Neurochem.* 160 (3), 392–411. doi:10.1111/jnc.15546

Zhao, Y., Zhang, X., Chen, X., and Wei, Y. (2022). Neuronal injuries in cerebral infarction and ischemic stroke: From mechanisms to treatment (Review). *Int. J. Mol. Med.* 49 (2), 15. doi:10.3892/ijmm.2021.5070

Zhong, L., Ren, X., Ai, Y., and Liu, Z. (2022). SS-31 improves cognitive function in sepsis-associated encephalopathy by inhibiting the drp1-NLRP3 inflammasome activation. *Neuromolecular Med.* 2022, 8730. doi:10.1007/s12017-022-08730-1

Zhou, D., Zhang, L., Mao, L., Cao, J., and Gao, J. (2022). Biological mechanism on SIRT1/NLRP3/IL-18 signaling pathway of acupuncture for treatment of ischemic stroke with center poststroke pain. *Comput. Intell. Neurosci.* 2022, 8958742. doi:10.1155/2022/8958742

Zhou, R., Yazdi, A. S., Menu, P., and Tschopp, J. (2011). A role for mitochondria in NLRP3 inflammasome activation. *Nature* 469 (7329), 221–225. doi:10.1038/nature09663

Zhou, Y. (2021). *Study on the effect and mechanism of Taohong Siwu decoction on pyroptosis after acute cerebral infarction based on DRP1/NLRP3 pathway*. Beijing(China): Beijing University of Chinese Medicine.

Zhu, M., Sun, H., Cao, L., Wu, Z., Leng, B., and Bian, J. (2022). Role of Na^+/K^+-ATPase in ischemic stroke: In-depth perspectives from physiology to pharmacology. *J. Mol. Med. Berl.* 100 (3), 395–410. doi:10.1007/s00109-021-02143-6

frontiers | Frontiers in Neuroscience

TYPE Original Research
PUBLISHED 04 May 2023
DOI 10.3389/fnins.2023.1059496

OPEN ACCESS

EDITED BY
Dennis Chang,
Western Sydney University, Australia

REVIEWED BY
Pengda Liu,
University of North Carolina at Chapel Hill, United States
Anurag Kumar Singh,
Alabama State University, United States
Elena Mitroshina,
Lobachevsky State University of Nizhny Novgorod, Russia
Md Abdul Hannan,
Bangladesh Agricultural University, Bangladesh

*CORRESPONDENCE
Yu Cao
✉ yu.cao-xiyuan@outlook.com
Hao Li
✉ xyhplihao1965@126.com

†These authors have contributed equally to this work and share first authorship

RECEIVED 01 October 2022
ACCEPTED 12 April 2023
PUBLISHED 04 May 2023

CITATION
Wei W, Yao J-x, Zhang T-t, Wen J-y, Zhang Z, Luo Y-m, Cao Y and Li H (2023) Network pharmacology reveals that Berberine may function against Alzheimer's disease via the AKT signaling pathway.
Front. Neurosci. 17:1059496.
doi: 10.3389/fnins.2023.1059496

Network pharmacology reveals that Berberine may function against Alzheimer's disease via the AKT signaling pathway

Wei Wei[1,2†], Jiu-xiu Yao[3†], Ting-ting Zhang[1], Jia-yu Wen[2], Zhen Zhang[2], Yi-miao Luo[2], Yu Cao[2*] and Hao Li[1*]

[1]Wangjing Hospital, China Academy of Chinese Medical Science, Beijing, China, [2]Institute of Geriatrics, Xiyuan Hospital, China Academy of Chinese Medical Science, Beijing, China, [3]College of First Clinical Medicine, Shandong University of Traditional Chinese Medicine, Jinan, Shandong, China

Objective: To investigate the mechanism underlying the effects of berberine (BBR) in the treatment of Alzheimer's disease (AD).

Methods: 3×Tg AD mice were treated with BBR for 3months, then the open field test (OFT), the novel object recognition test (NOR) and the Morris water maze (MWM) test were performed to assess behavioral performance. Hematoxylin–eosin (HE) staining, Nissl staining were used to examine histopathological changes. The pharmacological and molecular properties of BBR were obtained from the TCMSP database. BBR-associated AD targets were identified using the PharmMapper (PM), the comparative toxicogenomics database (CTD), DisGeNet and the human gene database (GeneCards). Core networks and BBR targets for the treatment of AD were identified using PPI network and functional enrichment analyses. AutoDock software was used to model the interaction between BBR and potential targets. Finally, RT-qPCR, western blotting were used to validate the expression of core targets.

Results: Behavioral experiments, HE staining and Nissl staining have shown that BBR can improve memory task performance and neuronal damage in the hippocampus of AD mice. 117 BBR-associated targets for the treatment of AD were identified, and 43 genes were used for downstream functional enrichment analysis in combination with the results of protein–protein interaction (PPI) network analysis. 2,230 biological processes (BP) terms, 67 cell components (CC) terms, 243 molecular function (MF) terms and 118 KEGG terms were identified. *ALB*, *EGFR*, *CASP3* and five targets in the PI3K-AKT signaling pathway including *AKT1*, *HSP90AA1*, *SRC*, *HRAS*, *IGF1* were selected by PPI network analysis, validated by molecular docking analysis and RT-q PCR as core targets for further analysis. *Akt1* mRNA expression levels were significantly decreased in AD mice and significantly increased after BBR treatment ($p<0.05$). Besides, AKT and ERK phosphorylation decreased in the model group, and BBR significantly increased their phosphorylation levels.

Conclusion: *AKT1*, *HSP90AA1*, *SRC*, *HRAS*, *IGF1* and *ALB*, *EGFR*, *CASP3* were core targets of BBR in the treatment of AD. BBR may exert a neuroprotective effect by modulating the ERK and AKT signaling pathways.

KEYWORDS

Berberine, Alzheimer's disease, AKT, pharmacology, neuroprotective effect

Introduction

Alzheimer's disease International (ADI) estimates that approximately 50 million people worldwide have dementia and that this number will triple by 2050, placing a great burden on families and society. Despite the urgent need, the development of new drugs faces significant challenges. Currently, only cholinesterase inhibitors and N-methyl-D-aspartate receptor antagonists have been approved for cognitive enhancement, although tremendous progress has been made in the understanding of the molecular mechanisms (Scheltens et al., 2021). In addition to the classical targets related to Aβ and tau protein hyperphosphorylation, lysosomal pathways, autophagy, apoptosis, transcription factor EB (TFEB), and TREM2 are also potential therapeutic pathways and targets for Alzheimer's disease (AD) (Singh et al., 2019a; Rai et al., 2021). Multi-target effect of Traditional Chinese medicine (TCM) has been attributed with unique benefits in the treatment of AD. Pharmacological data show that various formulas, extracts and compounds can alleviate symptoms and improve the quality of life of AD patients (Alexiou et al., 2019; Pei et al., 2020).

Recently, Berberine (BBR) has attracted much interest due to its pharmacological effects in the treatment and/or management of AD (Singh et al., 2019b, 2021a). BBR is an isoquinoline alkaloid and the main active component of several well-known herbs used in TCM, such as *Coptis chinensis* Franch (Huanglian) and *Phellodendron sinii* Y.C. Wu (Huangbo). Previous data suggest that BBR is a promising therapeutic agent for the treatment of bacterial diarrhea, cardiovascular and metabolic diseases (Jiang et al., 2011; Feng et al., 2019; Xu et al., 2021). BBR has therapeutic potential in the treatment of AD by targeting amyloid beta plaques, neurofibrillary tangles, neuroinflammation, and oxidative stress (Zhu and Qian, 2006; Jiang et al., 2015). However, the molecular basis of these effects has not been elucidated.

To further explore the therapeutic potential and efficacy basis of BBR in AD, we used network pharmacology to investigate the mechanisms underlying the multiple effects of BBR in this work. Network pharmacology is an emerging field of pharmacology that can be used to study drug action and interaction with targets (Berger and Iyengar, 2009). The dose of BBR used in our experiments was based on a previous research report (Kong et al., 2004). The workflow of this study is presented in Figure 1. This study may provide the basis for the development of BBR applications in the prevention and treatment of AD.

Materials and methods

Animals

Twenty 11–12 months 3 × Tg AD female mice (No: 14002A) were randomly divided in 2 groups: the 3 × Tg AD model group and the BBR group (50 mg•kg^{-1}•d^{-1}). Ten age-matched wild-type female C57 mice were used as controls. All animals were purchased from Beijing HFK Bioscience Co., Ltd. All animals were caged in SPF barrier-protected facilities with a temperature of (22 ± 3) °C, relative humidity of (50 ± 10) % and automatic light cycles (12 h light/dark). Food and water were freely available. This experiment started after 1 week of adaptive feeding. All experiments were carried out according to animal care guidelines and were approved by the Ethics Committee of the Xiyuan Hospital of the China Academy of Chinese Medical Sciences (No. 2022XLC020-2). Each mouse was fed 0.1 ml/10 g body weight by gavage for 3 months, and the BBR group received the corresponding drug, while the 3 × Tg AD model group and the control group received equal amounts of distilled water. The final numbers of animals in the control group, model group and BBR group were 9, 9 and 7, respectively due to mishandling.

Chemical reagents

Berberine at ≥98% purity (LDSW220209-1) was supplied by Shaanxi Langde Biotechnology Co., Ltd., and the HE staining kit was purchased from Servicebio (G1003).

Behavioral experiments

The open field test (OFT) was performed by placing the mice in a box (40 cm L × 40 cm W × 40 cm H). The test area in the box was divided into 16 squares (10 × 10 cm) by the computer software and the four innermost squares were defined as the central area. During 5 min OFT test, total distance (cm), total movement (s), speed (cm / s), distance in the center (cm), and time in the center (s) were calculated.

Twenty-four hours after OFT test, a novel object recognition test (NOR) was performed. This test consisted of an exposure phase to a familiar object, followed by a phase of exposure to a novel object the next day. Each phase lasted 10 min. During the exposure phase to a familiar object, mice were placed in the same box with two identical objects in two parallel corners. 24 h later, one of the two objects was replaced by a novel one. The preference index (PI) and the recognition index (RI) were recorded. PI was defined as the time spent exploring two objects during the exposure phase to a familiar object, while RI was calculated as follows: $T_{novel}/(T_{novel} + T_{familiar})$. Notes: T_{novel} and $T_{familiar}$ indicate the time spent with the novel and familiar objects during the exposure phase to the novel object.

Next, the Morris water maze (MWM) test was used to assess spatial memory of mice. The facility consists of a white tank (diameter 120 cm, height 50 cm), an automatic camera, and a computer analysis system. The pool was divided into four quadrants with specific markers, respectively, and a cylindrical escape platform (diameter 10 cm, height 15 cm) was placed in the first quadrant 1 cm beneath the water filled with nontoxic white dye. For training, spatial navigation experiments were performed for five consecutive days; each mouse was trained four trials per day for 90 s each using different entry points. The mice were placed in the water facing the wall of the pool, and the time between entering the water and finding the escape platform (with all limbs on the platform for 6 s; escape latency) was recorded using a video tracking system. On day 6, the escape platform was removed for spatial exploration experiments; mice were placed in the water facing the wall of the pool (at the midpoint of the third quadrant), and the number of times the mouse crossed the original platform area within 90 s was recorded, the time in the target quadrant and distance moved in the target quadrant were also recorded to examine memory of the target quadrant where the original platform was located. A quiet environment with a stable light

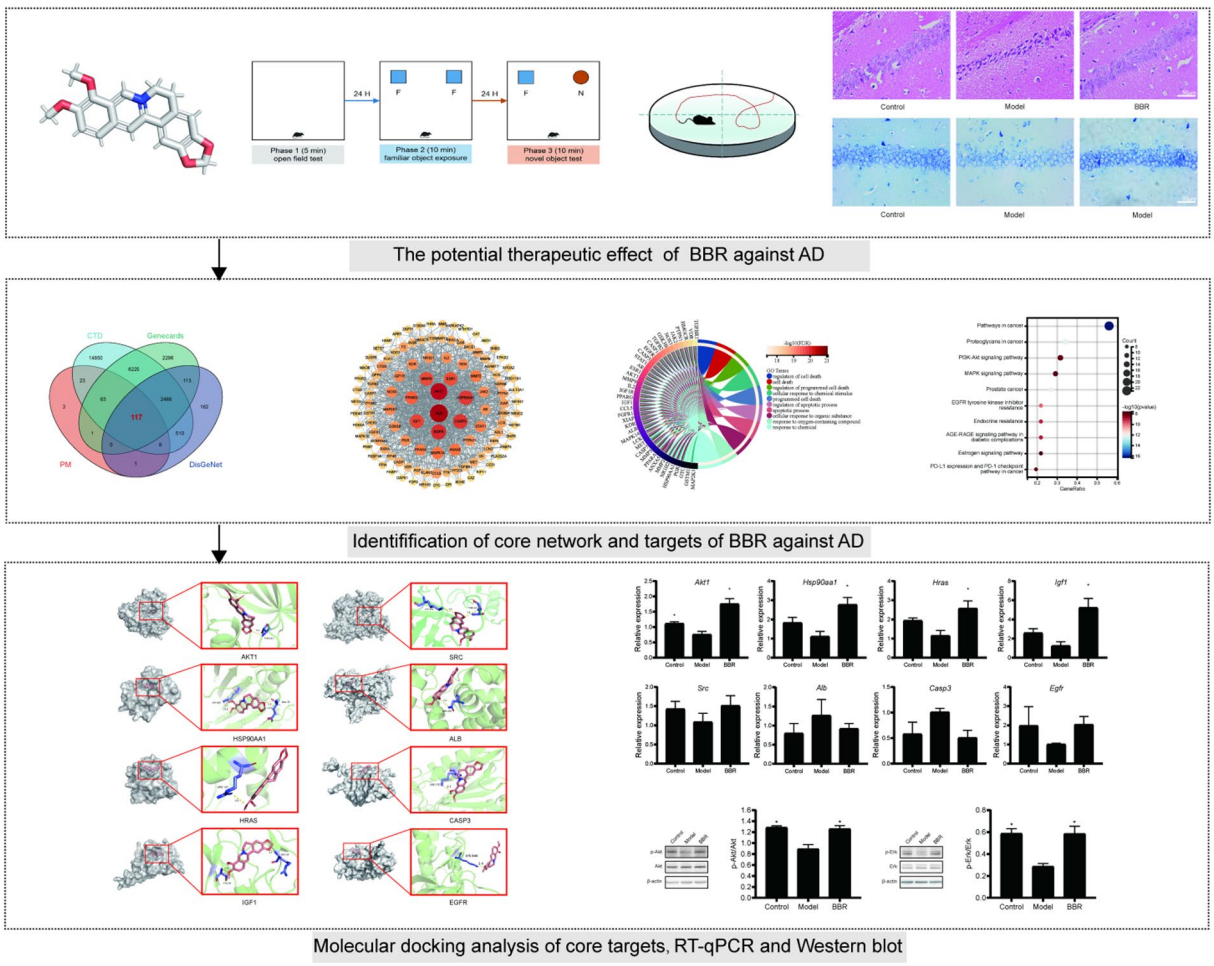

FIGURE 1
Workflow of the study.

source and a water temperature of 23 ± 1°C were maintained during experiments.

Tissue preparation

After the behavioral experiments, the brains were quickly removed. For each group, half of the brains were fixed in 4% paraformaldehyde, and the other half were snap frozen in liquid nitrogen and stored at −80° C for further analysis.

Histomorphological observation of brain tissue

Brain tissues were embedded in paraffin and sectioned. Then sections were processed as follows: Xylene for 20 min, two times; 100% ethanol for 5 min, two times; 75% ethanol for 5 min; and tap water rinsing. Sections were subjected to hematoxylin–eosin (HE) and toluidine blue (Nissl) staining. Hematoxylin–Eosin Staining Kit (G1003; Wuhan Servicebio Technology Co., Ltd., Wuhan, China) was used for HE staining, and Toluidine blue staining solution (G1032; Wuhan Servicebio Technology Co., Ltd.) was used for Nissl staining. Sections were finally sealed with neutral gum and examined under an upright optical microscope (NIKON ECLIPSE E100) for image acquisition.

Data on the pharmacological and molecular properties of BBR

MOL001454 (CAS, 2086-83-1) was found by searching for the chemical name "berberine" in the traditional Chinese medicine systems pharmacology database (TCMSP),[1] and absorption, distribution, metabolism, and excretion (ADME) parameters for BBR were also obtained. The molecular structure of BBR was downloaded from the PubChem database[2] and dealed with PyMOL2.4.0 software.

1 https://tcmsp-e.com/tcmsp.php
2 https://pubchem.ncbi.nlm.nih.gov/compound/2353

Identification and collection of potential targets of BBR

Potential BBR targets were identified and collected using the PharmMapper platform,[3] which is an integrated pharmacophore matching platform including targets extracted from TargetBank, DrugBank, BindingDB, and PDTD database and over 7,000 receptor-based pharmacophore models (Liu et al., 2010; Wang et al., 2017). All predicted targets were imported in EXCEL to establish the BBR target database.

BBR-associated targets of Alzheimer's disease

The comparative toxicogenomics database (CTD),[4] DisGeNet[5] (Piñero et al., 2015, 2017, 2020, 2021) and the human gene database (GeneCards)[6] were used to identify AD targets with the keyword 'Alzheimer's disease'. Then, BBR-associated targets of AD were generated by intersecting BBR targets with the above targets of Alzheimer's disease.

Network construction and analysis of the protein–protein interaction

BBR-associated targets of AD were imported into STRING,[7] and protein–protein interaction (PPI) data were exported under the condition that the minimum required interaction score was 0.700. We then built a network diagram using the Cytoscape 3.7.2 software. In addition, the MCODE and cytoHubba plug-ins were used to screen important PPI network modules.

Functional enrichment analysis

The biological process (BP), molecular function (MF), and cellular component (CC) are three important parts of gene ontology (GO). GO and Kyoto Encyclopedia of Genes and Genomes (KEGG) pathway analysis were used for functional enrichment analysis. The R 3.6.3 software was used for statistical analysis and visualization; the ggplot2 package 3.3.3 and the clusterProfiler package 3.14 were used. Significant terms were identified under the condition that false discovery rate (FDR) was <0.05. The top terms identified were visualized in a diagram.

Molecular docking verification

The molecular structure of BBR was downloaded from TCMSP, while the crystal structures of target proteins were obtained from the Protein Data Bank (PDB) database.[8] PyMOL 2.4.0 software,[9] Auto Dock Tools 1.5.7 software were used for pre-docking molecular processing to obtain PDBQT file. The Auto Dock Vina software 1.1.2[10] was then used for molecular docking and calculation of the affinity score. A lower affinity score indicates stronger binding. The results of molecular docking were visualized by PyMOL2.4.0 software. We calculated the RMSD (Root Mean Square Deviation) using PyMOL2.4.0 to verify the reliability, and RMSD <2A was considered reliable.

RT-qPCR analysis

An RNA extraction kit (Servicebio, G3640-50 T) was used to extract total RNA from brain tissue. ReverTra Ace qPCR RT Master Mix (TOYOBO, FSQ-201) was used for reverse transcription to generate cDNA templates and then real-time PCR was performed under the following conditions: 95° C for 10 min, followed by 40 cycles of 95 ° C for 15 s and 60 ° C for 60 s. Real-time PCR was performed using Applied Biosystem 7,500 Real-Time PCR System, and the relative expression of mRNA was calculated using the $2^{-\Delta\Delta Ct}$ method. The primer sequences of all target genes are shown in Table 1.

Western blotting

Brain tissues were lysed on ice in lysis buffer and then centrifuged at 12,000 rpm for 20 min at 4°C. The protein content was determined using the bicinchoninic acid (BCA) method (G2026, Servicebio, Wuhan, China). The extracted proteins were subjected to SDS-PAGE electrophoresis, transferred to 0.45 μm polyvinylidene difluoride membranes (Millipore, Bedford, MA), and then blocked with 5% BSA in TBST for 60 min. The membranes were subsequently incubated with primary antibodie. The primary antibodies were listed as follows: Erk 1/2 (diluted 1:2000, rabbit, Cell Signaling Technology, Cat# 4695), p-Erk 1/2 (diluted 1:2000, rabbit, Cell Signaling Technology, Cat# 4370), Akt (diluted 1:5000, rabbit, proteintech, Cat No. 10176-2-AP), p-Akt (diluted 1:5000, Mouse, proteintech, Cat No: 66444-1-Ig), or β–actin (diluted 1:10000, Mouse, proteintech, Cat No: 66009-1-Ig) overnight at 4°C. The membrane was incubated with the HRP conjugated secondary antibodies, goat anti-mouse (diluted 1:10000, Abbkine, China) or goat anti-rabbit IgG (diluted 1:10000, Abbkine, China) for 90 min after the membrane had been washed with TBST 4 times for 10 min each. The blots of proteins of interest were visualized using sensitive ECL western HRP substrate (# 17046, ZENBIO, Chengdu, China). Quantitative analysis of protein bands were performed using ImageJ software.

Statistical analysis

Data were statistically analyzed using SPSS 22.0 software (IBM Corp., Armonk, NY, USA). Quantitative data were expressed as mean with standard error of mean (SEM). Comparison between two groups were performed using *t* test. The MWM latency data were analyzed

3 http://lilab-ecust.cn/pharmmapper/
4 http://ctdbase.org/about/
5 https://www.disgenet.org/
6 https://www.genecards.org/
7 https://string-db.org/
8 https://www.rcsb.org/
9 https://pymol.org/2/
10 http://vina.scripps.edu/

TABLE 1 Primer sequences of all target genes.

Gene	Forward Primer (5′-3′)	Reverse Primer (5′-3′)
Hsp90	TTTACTCTGCCTATTTGGTTGCTG	CACAAAGAGAGTAATGGGATAGCC
Akt1	TTTGGGAAGGTGATTCTGGTG	CAGGACACGGTTCTCAGTAAGC
Src	AGATCACTAGACGGGAATCAGAGC	GCACCTTTTGTGGTCTCACTCTC
Hras	AGTACAGGGAGCAGATCAAGCG	TGGCTGATGTTTCAATGTAGGG
Igf1	GACCGCACCTGCAATAAAGATAC	CCTGTGGGCTTGTTGAAGTAAA
Alb	AACAAGAGCCCGAAAGAAACG	CTGGCAACTTCATGCAAATAGTG
Casp3	TGGAATGTCATCTCGCTCTGGT	GAAGAGTTTCGGCTTTCCAGTC
Egfr	CCGAAACTACGTGGTGACAGAT	TGCCATTACAAACTTTGCGAC
Gapdh	CCTCGTCCCGTAGACAAAATG	TGAGGTCAATGAAGGGGTCGT

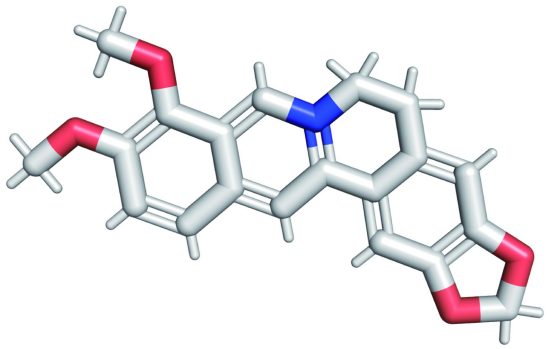

FIGURE 2
The molecular structure of BBR. The red structure in the figure represents the oxygen atom and the blue structure represents the hydrogen atom.

using a repeated-measures analysis of variance. All tests were two-sided with an α of 0.05 and statistical significance threshold of $p < 0.05$.

Results

Evaluation of druggability of BBR

The pharmacological and molecular properties of BBR were obtained from TCMSP (Ru et al., 2014) and are as follows: molecular weight (MW) = 336.39, oral bioavailability (OB) = 36.86%, drug-likeness (DL) = 0.78, blood brain barrier (BBB) = 0.57, half-life (HL) = 6.57. BBR half-life ($t_{1/2}$) is in the mid-elimination group. The molecular structure of BBR ($C_{20}H_{18}NO_4$) is shown in Figure 2. BBR is believed to be more druggable in the 180–500 Dalton MW range. It is a promising therapeutic agent that can act in the central nervous system and is characterized by high OR (≥20%) (Xu et al., 2012), high DL (≥0.18) (Tao et al., 2013), and strong penetration (BBB > 0.3)(Tattersall et al., 1975).

BBR improves the performance of memory and recognition tasks in AD mice

The sequence of behavioral experiments is shown in Figure 3A. During the OFT test, the BBR group differed significantly from the model group in speed ($t = 3.59$, $p = 0.003$), total move time ($t = 3.07$, $p = 0.008$), time in the center ($t = 2.27$, $p = 0.039$), total distance ($t = 3.59$, $p = 0.003$), and distance in the center ($t = 2.46$, $p = 0.0273$), indicating differences in overall activity or anxiety-like behavior (Figures 3B–F). During the novel object recognition test, neither the control group nor the BBR group differed significantly from the model group in the preference index (PI) ($p > 0.05$, Figure 3G). After 3 months of BBR administration, mice in the BBR group spent significantly more time with the novel object in the NOR test as indicated by a significantly higher recognition index ($t = -2.47$, $p = 0.028$) in the NOR test (Figure 3H).

The MWM test consists of a navigation test and an exploratory experiment, which can be used to evaluate the learning memory ability of mice. In the navigation test, as shown in Figure 3I, the escape latency of all mice gradually decreased with the increasing number of training sessions, indicating that their ability to locate the platform was enhanced. The escape latency of mice in the BBR group was diminished compared to the model group and exhibited a significant difference on day 1 ($p = 0.003$), day 2 ($p = 0.011$) and day 5 ($p = 0.007$). There were no significant differences in the speed of swimming among the groups ($p > 0.05$, Figure 3J), and effects on locomotor ability could be excluded. In addition, compared to the model group, mice in the BBR group had a significantly higher number of platform crossings in the exploratory experiment on day 6 ($p = 0.039$, Figure 3K).

These results suggest that BBR alleviated the tense, manic, and anxious behaviors of AD mice and improves recognition and memory performance, although more studies are necessary to clarify the mechanisms involved. See details in Supplementary data S1.

BBR ameliorates neuronal damage in the hippocampus

The size, density and arrangement of neurons in the hippocampus may indicate neuronal damage. Using HE staining, chromatin in the nucleus and ribosomes in the cytoplasm were stained blue-violet, while components in the cytoplasm and extracellular matrix were stained red, and the degree of staining may reflect the functional properties of hippocampal neurons. Under normal conditions, the cytoplasm is only slightly stained, but it becomes overstained when cellular senescence or neurodegenerative alterations occur. The hippocampal neurons of control mice were dense and neatly organized, with full nuclei and clear boundaries, whereas the neurons of model mice were overstained

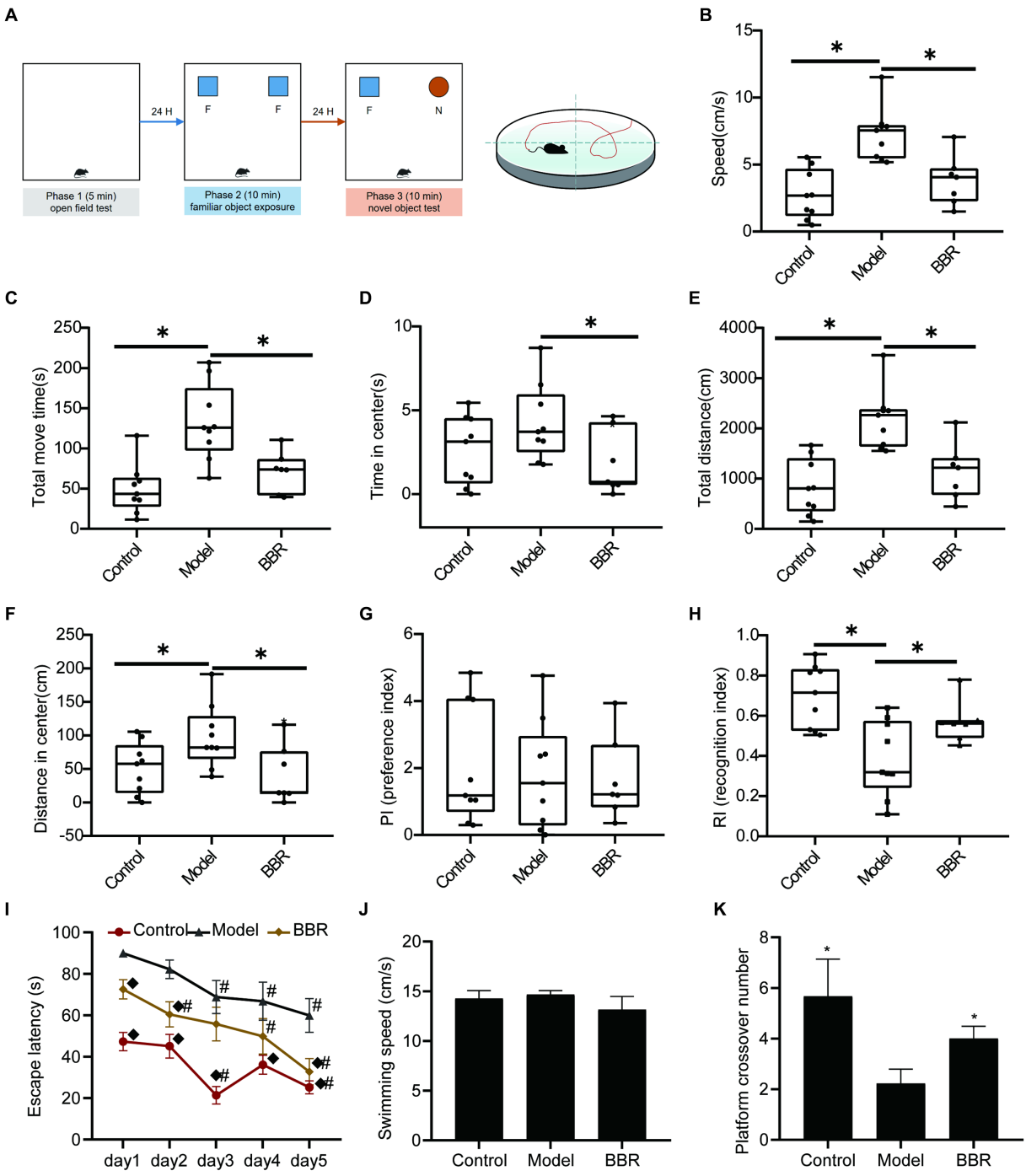

FIGURE 3
BBR improves recognition and memory task performance in AD mice. **(A)** Workflow of behavioral experiments; **(B)** Speed (cm/s), **(C)** Total move time (S), **(D)** Time in center (s), **(E)** Total distance (CM), and **(F)** Distance in center (cm) during OFT test; PI **(G)** and RI **(H)** of NOR test; Escape latency **(I)**; Swimming speed **(J)** and Platform crossover number **(K)** during the MWM test, n=7–9, *p<0.05, compared with model group; ◆p<0.05 for latency data between groups on the same day compared with the model group; #p<0.05 for latency data within groups compared with the first day.

and loosely arranged, with cytoplasmic deformation and swelling. In the model mice, BBR treatment was able to reverse this phenotype and the neuronal morphology resembled that of controls (Figure 4A).

Neurons in the model group showed relatively lighter blue staining, with a reduced number of Nissl bodies. Besides, in the BBR groups, there was stronger cytoplasmic staining and neurons were densely arranged (Figure 4B). Quantitatively, in the CA1 region of the hippocampus, neuron numbers were significantly higher in the BBR ($t = -4.07$, $p = 0.015$) group compared to the model group (Figure 4C), suggesting that BBR can protect hippocampal neurons to some extent and prevent degenerative necrosis.

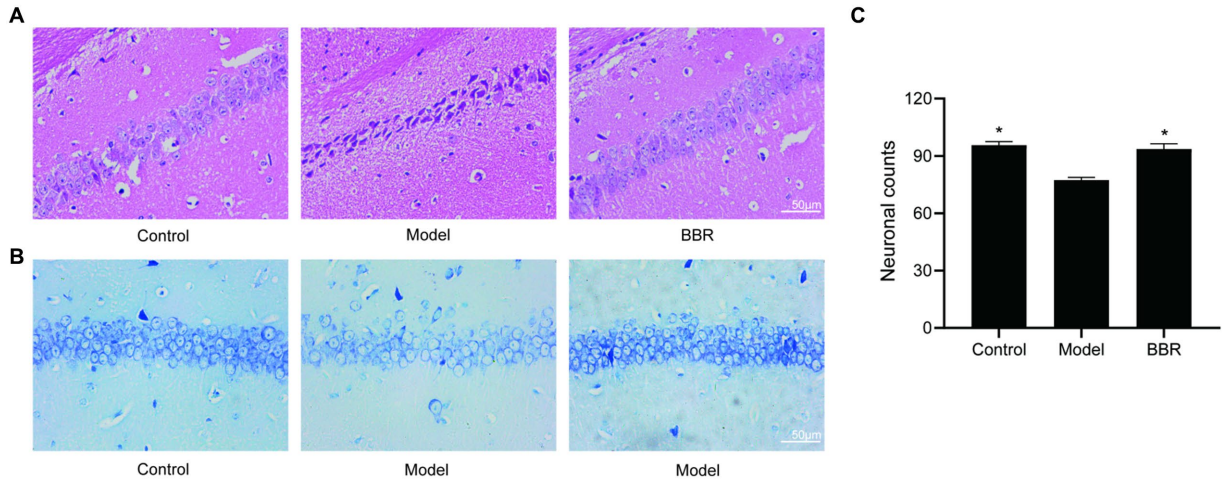

FIGURE 4
BBR ameliorated neuronal damage in the hippocampus. **(A)** HE staining and Nissl staining **(B)** and its quantitative analysis **(C)** of the CA1 region. Data were analyzed by *t* test between two groups, presented as mean±SEM, $n=3$, $^*p<0.05$ compared to the model group.

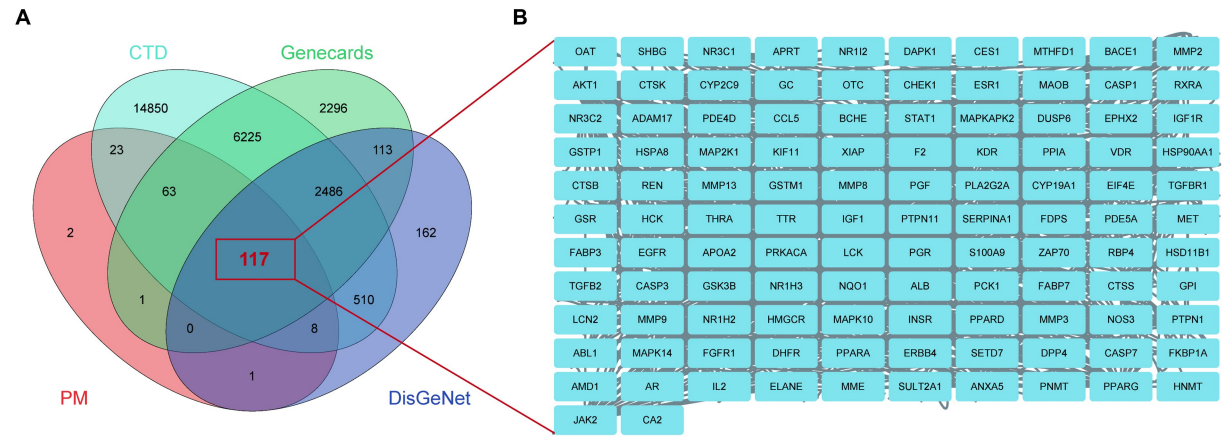

FIGURE 5
BBR-associated targets of Alzheimer's disease. **(A)** BBR-associated targets of AD from the intersection between BBR-targets and targets of AD, zoom in to show the specific target in **(B)**.

Identification of BBR-associated targets of Alzheimer's disease

Using the keyword 'Alzheimer's disease', 215 potential BBR targets were obtained from the PM database, 24,282 AD targets from the CTD database, 3,397 AD targets from the DisGeNet database and 11,301 AD targets from GeneCards. 117 BBR-associated AD targets were generated from the intersection of these three databases using a Venn plot (Figure 5A). The names of these targets are shown in Figure 5B. See detailed gene information in Supplementary data S2.

Identification of the core networks and targets of BBR in AD pathology

Proteins interact with each other to participate in various aspects of life processes such as biological signaling, regulation of gene expression, energy and material metabolism, and cell cycle regulation. By detecting the interrelationship between target proteins, the possible pathways of action of drugs can be predicted and provide directions for in-depth research. In this study, PPI analysis between BBR-associated AD targets was performed to explore underlying mechanisms using STRING and the results are shown in Supplementary data S3. The PPI network is visualized in Figure 6A. The results of MCODE (Figure 6B) and cytoHubba are shown in Supplementary data S4. Combining the data obtained from the above algorithms, we obtained 43 genes for downstream functional enrichment analysis. In total, 2,230 BP terms, 67 CC terms, 243 MF terms ($p<0.01$ and FDR<0.01) and 118 KEGG terms ($p<0.05$ and FDR<0.01) (Supplementary data S5) were obtained. The top terms for each category are shown in Figure 6C: regulation of cell death, cell death, regulation of programmed cell death, cellular response to chemical stimulus, programmed cell death, regulation of apoptotic process, apoptotic process, cellular response to organic substance, response to oxygen-containing compound, response to

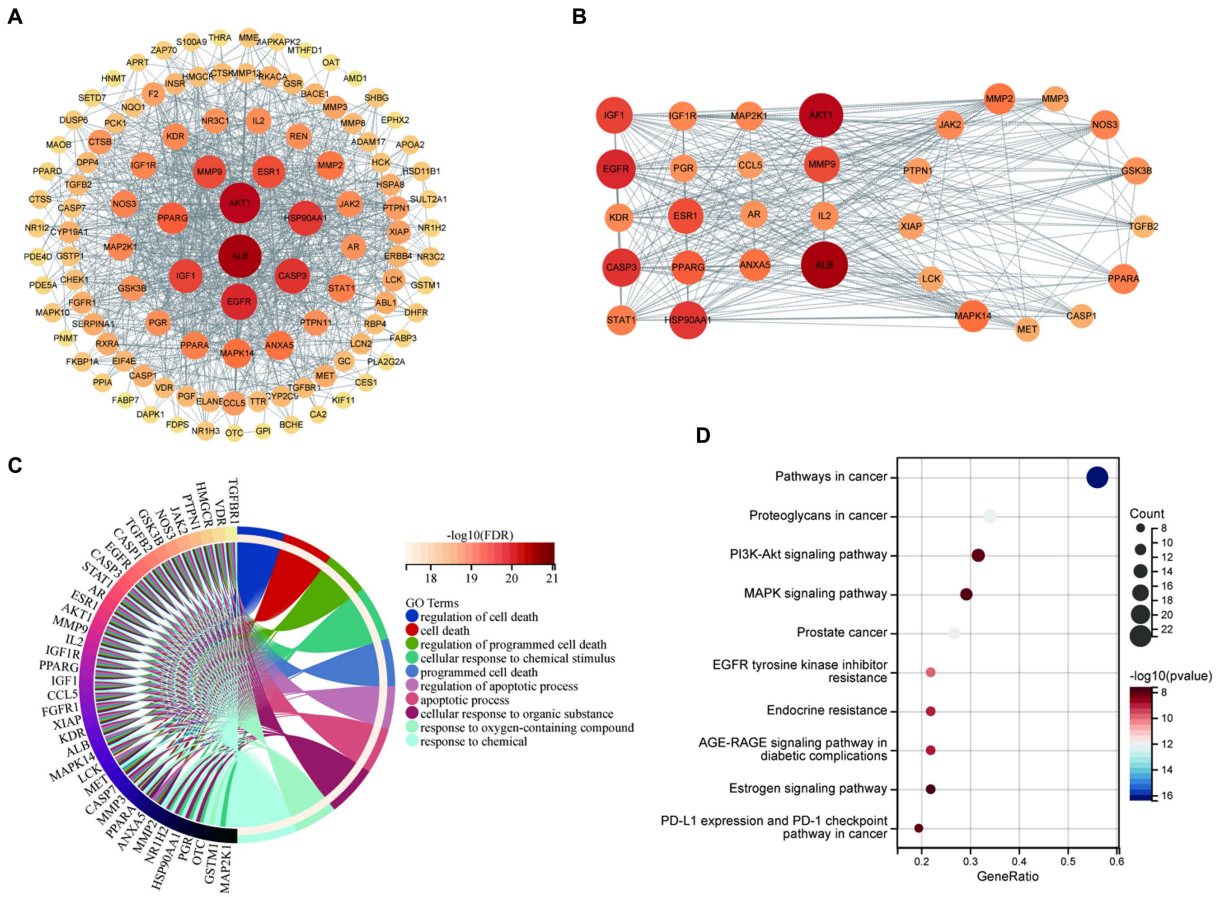

FIGURE 6
Core BBR targets in AD and GO/KEGG analysis. **(A)** PPI network of 117 BBR-associated targets of AD; **(B)** representative clusters extracted using MCODE; **(C)** GO analysis of all the targets identified above; **(D)** KEGG analysis of all the targets identified above.

chemical in BP enrichment analysis Furthermore, Pathways in cancer, Proteoglycans in cancer, PI3K-AKT signaling pathway, MAPK signaling pathway, Prostate cancer, EGFR tyrosine kinase inhibitor resistance, Endocrine resistance, AGE-RAGE signaling pathway in diabetic complications, Estrogen signaling pathway, PD-L1 expression and PD-1 checkpoint pathway in cancer involved in BBR treatment for AD based on KEGG pathway analysis (Figure 6D). Importantly, *ALB*, *EGFR*, *CASP3* and five members of the PI3K-Akt signaling pathway including *AKT1*, *HSP90AA1*, *SRC*, *HRA*, and *IGF1* were identified as core BBR targets in AD for further study.

Molecular docking analysis of core targets

To validate the core targets of BBR in AD, semi-flexible molecular docking was performed using Auto Dock Vina software. A lower affinity score indicates a stronger binding force. The crystal structures of the target proteins are listed below: AKT1 (PDB: 4ejn), HSP90AA1 (PDB: 3t0h), SRC (PDB: 1fmk), HRAS (PDB: 2ce2), IGF1 (PDB: 1wqj), ALB (PDB: 6hn1), CASP3 (PDB: 2dko), EGFR (PDB: 8a27). After molecular docking and interaction analysis, BBR was found to bind in a stable conformation to its targets as indicated by the low affinity scores: −10.2 kcal/mol (AKT1), −6.5 kcal/mol (HSP90AA1), −9.6 kcal/mol (SRC), −5.2 kcal/mol (HRAS), −7.8 kcal/mol (IGF1), −8.4 kcal/mol (ALB), −6.6 kcal/mol (CASP3) and −9.5 kcal/mol (EGFR). All RMSD values were less than 2A, suggesting the molecular docking results are reliable (Table 2). Docking of core targets and BBR is shown in Figure 7.

TABLE 2 Molecular docking results of core targets and BBR.

Target name	PDB	Affinity (kcal/mol)	RMSD (A)
AKT1	4ejn	−10.2	0.001
HSP90AA1	3t0h	−6.5	0.000
SRC	1fmk	−9.6	0.000
HRAS	2ce2	−5.2	0.001
IGF1	1wqj	−7.8	0.000
ALB	6hn1	−8.4	0.000
CASP3	2dko	−6.6	0.001
EGFR	8a27	−9.5	0.000

PDB, Protein Data Bank; RMSD, Root Mean Square Deviation.

BBR acts through the AKT pathway

Relative expression changes of the core targets were detected by RT-qPCR (Figure 8A). The level of *Akt1* mRNA was significantly reduced in AD mice ($t = 2.96$, $p = 0.025$). A similar

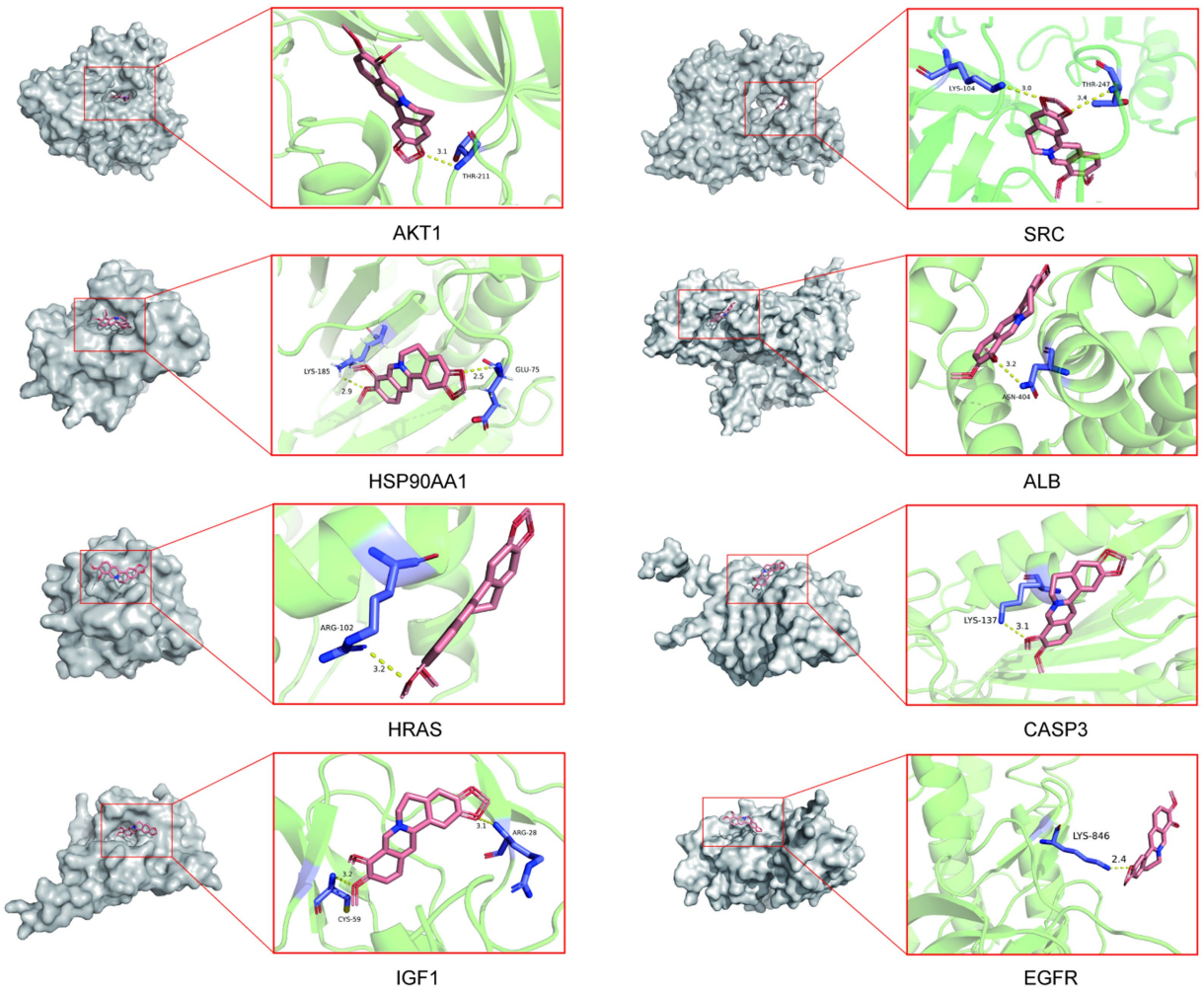

FIGURE 7
Molecular docking results of core protein targets with BBR. The dotted line represents hydrogen bond interaction.

trend was observed for *Hsp90aa1*, *Hras*, *Igf1*, and *Src* mRNA levels, but none of them was statistically significant ($p > 0.05$). Among the core targets, *Akt1* ($t = -5.01$, $p = 0.002$), *Hsp90aa1* ($t = -3.66$, $p = 0.011$), *Hras* ($t = -2.99$, $p = 0.024$) and *Igf1* ($t = 3.75$, $p = 0.019$) mRNA levels were significantly increased after BBR treatment, while *Src*, *Egfr* mRNA levels showed a similar trend but lacked statistical significance ($p > 0.05$). *Alb*, *Casp3* mRNA levels showed the opposite trend. These results suggest that *Akt1*, *Hsp90aa1*, *Hras*, *Igf1* could play important roles in BBR treatment of AD.

Then, we explored whether BBR affects protein phosphorylation of AKT as well as ERK by western blotting at the protein assay level. As shown in Figures 8B,C, AKT ($t = 4.489$, $p = 0.004$) and ERK ($t = 5.645$, $p = 0.001$) phosphorylation decreased in the model group, and BBR significantly increased AKT ($t = -3.721$, $p = 0.010$) and ERK ($t' = -4.126$, $p = 0.014$) phosphorylation levels.

Discussion

The molecular characteristics and physicochemical properties of BBR indicate good druggability (Kumar et al., 2015). The properties of BBR suggest that it may be able to cross the blood–brain barrier (BBB) thus facilitating direct binding to potential targets within the central nervous system (Peng et al., 2004; Jiang et al., 2015). After intravenous administration, BBR is quickly removed from the plasma ($t_{1/2\beta} = 1.13$ h) and sharply increased in the hippocampus ($t_{1/2\alpha} = 0.215$ h) with a delayed clearance rate ($t_{1/2\beta} = 12.0$ h), indicating that it has the potential to act instantly through BBB, and can be stored in the hippocampus, affecting memory and recognition performance (Wang et al., 2005).

Several *in vitro* and *in vivo* experiments have revealed that BBR elicits neuroprotective effects in AD models as indicated by the following lines of data: ① BBR reduces Aβ levels by modulating APP processing and ameliorates Aβ pathology *by* inhibiting the mTOR/p70S6K signaling pathway (Asai et al., 2007; Durairajan et al., 2012; Panahi et al., 2013; Wang et al., 2021); ② it inhibits tau hyperphosphorylation at Thr205 and Thr231 in the hippocampus *via* the GSK3β/PGC-1α (Yang and Wang, 2022) or NF-κB signaling pathways (He et al., 2017); ③ it reduces the production of pro-inflammatory cytokines in activated microglial cells and modulates mitochondrial bioenergetics (He et al., 2017; Wong et al., 2021); ④ it reduces lactate dehydrogenase release and reactive oxygen species (ROS) generation (Chen et al., 2015), as well as the relative

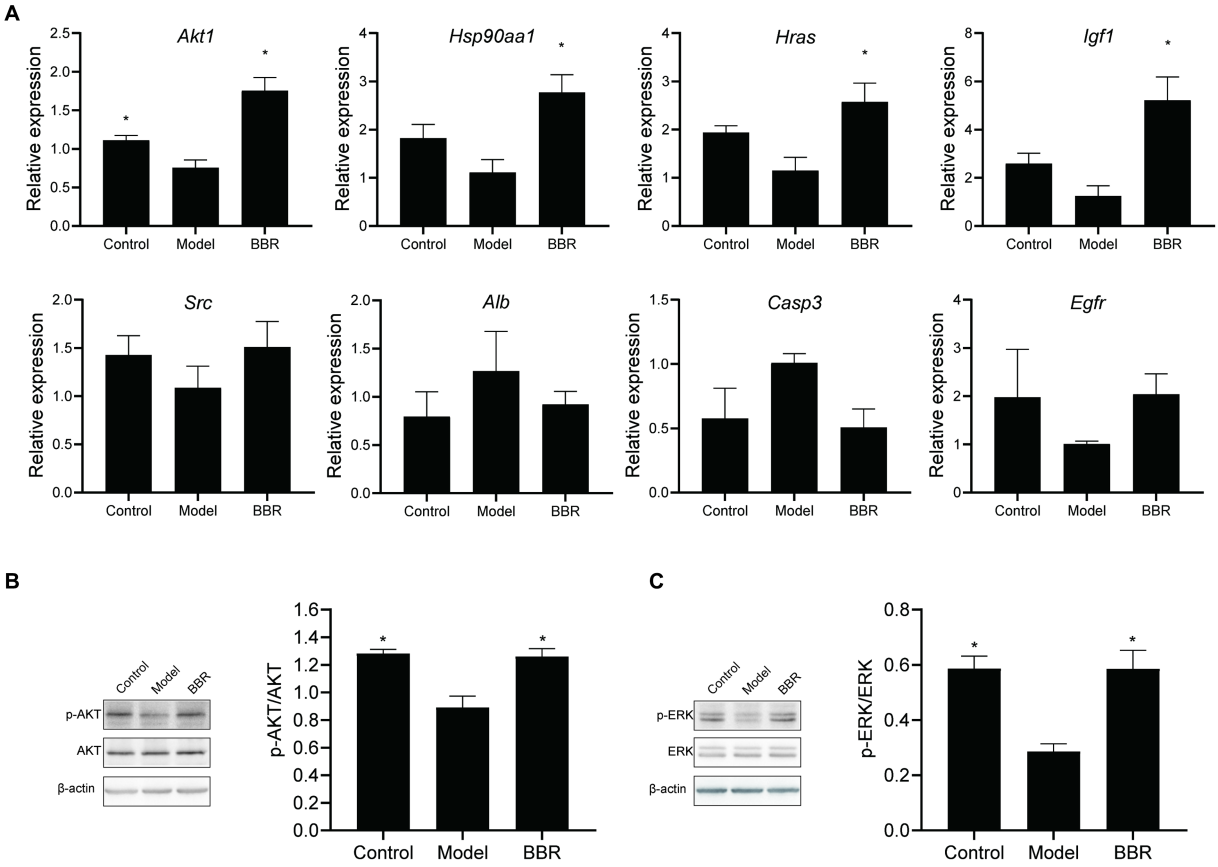

FIGURE 8
BBR acts through the AKT pathway. **(A)** Relative expression changes of the core targets; **(B)** BBR increased AKT phosphorylation; **(C)** BBR increased ERK phosphorylation. Data were analyzed by *t* test between two groups, presented as mean±SEM, $n=4$, $^*p<0.05$ compared to the model group.

mRNA expression of endoplasmic reticulum (ER) stress related pathway genes (Xuan et al., 2020); ⑤ it rescues synaptic damage by activating LKB1/AMPK signaling in AD mice (Cai et al., 2019); ⑥ it promotes the formation of brain microvessels by enhancing CD31, VEGF, N-cadherin, Ang-1 and inhibits neuronal apoptosis (Ye et al., 2021). Consistent with a previous study (Ye et al., 2021), our work shows that BBR improves memory and recognition performance in AD mice. Furthermore, we show that BBR also ameliorates neuronal damage in the hippocampus. These results suggest that BBR plays a potential therapeutic role in AD by protecting hippocampal neurons. However, the specific targets and mechanisms involved in this protective effect are currently poorly understood and more basic and clinical studies will be needed to confirm these results. In addition, BBR, together with epiberberine, coptisine, palmatine, and gatrorrhizine are the main active constituents of *Coptis chinensis* Franch (Huanglian), participating in the prevention and treatment of AD (Meng et al., 2018; Wang et al., 2020). Among them, BBR is the component with the highest content. Due to the similarity of physicochemical properties of these substances, the purification and separation process of BBR by conventional methods such as acid-water and ethanol inevitably incorporates other impurities, and it is difficult to achieve 100% purity (Sun et al., 2014). Although most of the commercially purchased BBR products can reach a purity of 98% or more, there are still less than 2% impurities that may have undeniable influence on the study results. Thus, HPLC purification to remove contaminants would need to be performed to ensure activities observe are not from these impurities in a more in-depth study in the future.

Network pharmacology is considered the next paradigm in drug discovery because it allows to analyze the "herb-compound-protein/gene-disease" interaction network from a systems biology perspective. Therefore, we investigated the targets of the action of BBR in AD using network pharmacology. 117 BBR-associated targets of AD were identified, of which 43 targets were selected for downstream functional analysis by protein–protein interaction analysis using MCODE and cytoHubba. The PI3K-AKT signaling pathway and MAPK signaling pathway are members of the most significant terms identified. *ALB, EGFR, CASP3* and five targets that are members of the PI3K-AKT pathway, including *AKT1, HSP90AA1, SRC, HRAS, IGF1* were extracted as core targets of BBR in AD.

AKT, which functions downstream of PI3K, is the core component of the PI3K-AKT pathway. Many cytokines or growth factors induce phosphorylation of tyrosine residues by binding to the RTK membrane receptor. The regulatory subunit of PI3K, P85, binds to phosphorylated tyrosine residues through its SH2 domain, which in turn recruits the catalytic subunit P110 to form the active PI3K enzyme. Activated PI3K further acts on PDK1, PIP3, to promote AKT phosphorylation (Thorpe et al., 2015; Long et al., 2021). AKT, also known as protein kinase B (PKB), is a serine/threonine kinase participating in the PI3K-Akt pathway. AKT1/PKBα is encoded by *AKT1*, which is composed of three isoforms that contain a conserved plekstrin homology domain, a central fragment, and a regulatory

domain (Hanada et al., 2004). Thr308 and Ser473 are essential phosphorylation sites for AKT activation (Wei et al., 2019). HSP90AA1, SRC, HRAS, and IGF1 are members of the PI3K-AKT pathway. The heat shock protein (Hsp) 90 encoded by HSP90AA is a molecular chaperone involved in protein folding that regulates the activity of AKT (Jhaveri and Modi, 2015). In the brain, Hsp90 is involved in synaptic plasticity (Chen et al., 2014) as well as in the targeting of tau for proteosomal degradation (Dickey et al., 2007), regulate Aβ processing (Blair et al., 2014). Hsp90 usually forms a protein complex with other co-chaperones Hsp70, Hsp60, Hsp23, acting as the core of the complex to promote the activation or stabilize the conformation of the target protein. Inhibitors of Hsp90 bind to the regulatory site of Hsp90 and act on it. There are two possible pathways: one occurs by inducing a cytoprotective heat shock response, and the other acts by directing the degradation of pathogenic proteins. In AD, Hsp90 expression is downregulated, and after administration of Hsp90 inhibitor, Aβ-induced neurotoxicity could be prevented by increasing the level of Hsp70 and Hsp90 (Ansar et al., 2007; Gezen-Ak et al., 2013; Ou et al., 2014). The SRC protein-tyrosine kinase family mainly consists of 11 members, including SRC, FYN, and YES, three closely related group I enzymes (Brown and Cooper, 1996). Members of the SRC kinase family are controlled by cytokine receptors, G-protein coupled receptors, etc., participating in pathways that regulate survival, proliferation, and regulation of gene expression through AKT or MAPKs (Thomas and Brugge, 1997; Roskoski, 2015). Recently, FYN was shown to have several functions in the central nervous system (CNS), and FYN dysfunction has been implicated in the pathological processes leading to AD (Nygaard, 2018). Rho GTPases, including HRAS, have significant therapeutic potential in the treatment of neurodegenerative diseases, as they have been implicated in nearly all stages of brain development (Zamboni et al., 2018; Schmidt et al., 2022). IGF1 may have a therapeutic effect in neurodegenerative disorders by enhancing hippocampal neurogenesis (Morel et al., 2017) and promoting neuronal survival through the PI3K / AKT and MAPK pathways (Vincent et al., 2004; Bronzi et al., 2010). Extracellular-signalregulated protein kinase (ERK), as one of the MAPK signaling subfamilies, is usually downstream of the AKT pathway. Phosphorylation of ERK1/2 protein activates the ERK pathway and plays an important role in regulating cell growth and differentiation (Kumar et al., 2023).

The *ALB* gene encodes the most abundant protein in the blood, which is albumin. Higher levels of albumin in the cerebrospinal fluid (CSF) of AD patients respond to damage to the BBB (Lin et al., 2021). It can differentiate AD patients from controls together with hub genes including *JUN*, *SLC2A1*, *TFRC*, and *NFE2L2* (Wang et al., 2022). *EGFR* is a potential therapeutic target for AD (Tsuji et al., 2021; Zhang et al., 2022).The protein encoded by *CASP3* gene is a cysteine-aspartic acid protease that plays an important role in the execution-phase of cell apoptosis in AD, and the PI3K/AKT signaling pathway is the most important intracellular factor involved in regulation of cellular apoptosis (Khezri et al., 2023). In addition, it can be activated upstream by the presence of extracellular factors and then act downstream on tau protein (Avila, 2010). However, interactions obtained using STRING for PPI analysis are not specific for brain, which may interfere with the specificity of the targets and the subsequent validation results.

To validate identified core targets, we performed molecular docking analysis using AutoDock Vina (Trott and Olson, 2010), a computational method for predicting bound conformations and binding affinity. The results showed strong binding between BBR and the identified core targets. This suggests to us that BBR may play a role by altering the function of these proteins through compound binding. Furthermore, we determined the relative expression changes of the main targets in AD mice by RT-qPCR, and found that *Akt1, Hsp90aa1, Hras*, and *Igf1* mRNA levels were significantly altered after BBR treatment. In addition, our results confirm that BBR significantly increased AKT and ERK phosphorylation levels. Phosphorylated AKT activates a range of downstream pathways, including the P53 pathway, regulating protein translation, cell cycle, apoptosis. Activation of PI3K/AKT signaling protects neurons from Aβ-induced neurotoxicity (Do et al., 2014), inhibits the formation of pathogenic neurogenic fiber tangles (NFT) (Kitagishi et al., 2014), and regulates synaptic plasticity (Spinelli et al., 2019), playing an important regulatory role in AD. Phosphorylation of ERK1/2 protein activates the ERK pathway, and accumulation of intra-neuronal (Aβ1–42) causes the significant reduction in phosphorylation of ERK1/2 protein, affecting neuronal viability (Cruz et al., 2018; Kumar et al., 2023). Taken together, these results suggest that the ERK and AKT signaling pathways are crucial pathways to mediate the therapeutic effects of BBR in AD mice.

BBR can have multiple effects in the treatment of AD, and this is important because of the complex pathological changes and symptoms at different stages of AD. Given the low water solubility and limited gastrointestinal absorption of BBR, nanotechnological modifications of BBR and its use in combination with other drugs may be useful to improve both bioavailability and therapeutic efficacy (Singh A. et al., 2021; Singh et al., 2021b; Behl et al., 2022). More in-depth studies are needed in the future.

Conclusion

AKT1, *HSP90AA1*, *SRC*, *HRAS*, *IGF1*, and *ALB*, *EGFR*, *CASP3* were core targets of BBR in the treatment of AD. BBR can exert a neuroprotective effect by modulating the ERK and AKT signaling pathways.

Data availability statement

The original contributions presented in the study are included in the article/Supplementary material, further inquiries can be directed to the corresponding authors.

Ethics statement

The animal study was reviewed and approved by the Ethics Committee of Xiyuan Hospital of China Academy of Chinese Medical Sciences.

Author contributions

WW and J-xY performed experiments and data analysis and wrote the manuscript. T-tZ, J-yW, ZZ, and Y-mL assisted in the experiments. YC and HL assisted with ideas and modification of the manuscript. All authors reviewed and approved the manuscript.

Funding

This study was funded National Key R&D Program of China (2022YFC3501400), and the Fundamental Research Funds for the Central public welfare research institutes (ZZ15-YQ-013 and ZZ15-XY-PT-02), and science and technology innovation project of Chinese Academy of traditional Chinese Medicine (CI2021A01401 and CI2021A04618).

Conflict of interest

The authors declare that the research was conducted in the absence of any commercial or financial relationships that could be construed as a potential conflict of interest.

Publisher's note

Supplementary material

The Supplementary material for this article can be found online at: https://www.frontiersin.org/articles/10.3389/fnins.2023.1059496/full#supplementary-material

References

Alexiou, A., Kamal, M. A., and Ashraf, G. M. (2019). Editorial: the Alzheimer's disease challenge. *Front. Neurosci.* 13:768. doi: 10.3389/fnins.2019.00768

Ansar, S., Burlison, J. A., Hadden, M. K., Yu, X. M., Desino, K. E., Bean, J., et al. (2007). A non-toxic Hsp90 inhibitor protects neurons from Abeta-induced toxicity. *Bioorg. Med. Chem. Lett.* 17, 1984–1990. doi: 10.1016/j.bmcl.2007.01.017

Asai, M., Iwata, N., Yoshikawa, A., Aizaki, Y., Ishiura, S., Saido, T. C., et al. (2007). Berberine alters the processing of Alzheimer's amyloid precursor protein to decrease Abeta secretion. *Biochem. Biophys. Res. Commun.* 352, 498–502. doi: 10.1016/j.bbrc.2006.11.043

Avila, J. (2010). Alzheimer disease: caspases first. *Nat. Rev. Neurol.* 6, 587–588. doi: 10.1038/nrneurol.2010.157

Behl, T., Singh, S., Sharma, N., Zahoor, I., Albarrati, A., Albratty, M., et al. (2022). Expatiating the pharmacological and Nanotechnological aspects of the alkaloidal drug Berberine: current and future trends. *Molecules* 27:3705. doi: 10.3390/molecules27123705

Berger, S. I., and Iyengar, R. (2009). Network analyses in systems pharmacology. *Bioinformatics* 25, 2466–2472. doi: 10.1093/bioinformatics/btp465

Blair, L. J., Sabbagh, J. J., and Dickey, C. A. (2014). Targeting Hsp90 and its co-chaperones to treat Alzheimer's disease. *Expert Opin. Ther. Targets* 18, 1219–1232. doi: 10.1517/14728222.2014.943185

Bronzi, D., Bramanti, V., Tomassoni, D., Laureanti, F., Grasso, S., Volsi, G. L., et al. (2010). Neural markers expression in rat bone marrow mesenchymal stem cell cultures treated with neurosteroids. *Neurochem. Res.* 35, 2154–2160. doi: 10.1007/s11064-010-0283-3

Brown, M. T., and Cooper, J. A. (1996). Regulation, substrates and functions of SRC. *Biochim. Biophys. Acta* 1287, 121–149. doi: 10.1016/0304-419x(96)00003-0

Cai, Z. Y., Wang, C. L., Lu, T. T., and Yang, W. M. (2019). Berberine alleviates amyloid-beta pathogenesis via activating LKB1/AMPK signaling in the brain of APP/PS1 transgenic mice. *Curr. Mol. Med.* 19, 342–348. doi: 10.2174/1566524019666190315164120

Chen, M., Tan, M., Jing, M., Liu, A., Liu, Q., Wen, S., et al. (2015). Berberine protects homocysteic acid-induced HT-22 cell death: involvement of Akt pathway. *Metabolic Brain Disease* 30, 137–142. doi: 10.1007/s11011-014-9580-x

Chen, Y., Wang, B., Liu, D., Li, J. J., Xue, Y., Sakata, K., et al. (2014). Hsp90 chaperone inhibitor 17-AAG attenuates Aβ-induced synaptic toxicity and memory impairment. *J. Neurosci.* 34, 2464–2470. doi: 10.1523/JNEUROSCI.0151-13.2014

Cruz, E., Kumar, S., Yuan, L., Arikkath, J., and Batra, S. K. (2018). Intracellular amyloid beta expression leads to dysregulation of the mitogen-activated protein kinase and bone morphogenetic protein-2 signaling axis. *PLoS One* 13:e0191696. doi: 10.1371/journal.pone.0191696

Dickey, C. A., Kamal, A., Lundgren, K., Klosak, N., Bailey, R. M., Dunmore, J., et al. (2007). The high-affinity HSP90-CHIP complex recognizes and selectively degrades phosphorylated tau client proteins. *J. Clin. Invest.* 117, 648–658. doi: 10.1172/JCI29715

Do, T. D., Economou, N. J., Chamas, A., Buratto, S. K., Shea, J. E., and Bowers, M. T. (2014). Interactions between amyloid-β and tau fragments promote aberrant aggregates: implications for amyloid toxicity. *J. Phys. Chem. B* 118, 11220–11230. doi: 10.1021/jp506258g

Durairajan, S. S., Liu, L. F., Lu, J. H., Chen, L. L., Yuan, Q., Chung, S. K., et al. (2012). Berberine ameliorates β-amyloid pathology, gliosis, and cognitive impairment in an Alzheimer's disease transgenic mouse model. *Neurobiol. Aging* 33, 2903–2919. doi: 10.1016/j.neurobiolaging.2012.02.016

Feng, X., Sureda, A., Jafari, S., Memariani, Z., Tewari, D., Annunziata, G., et al. (2019). Berberine in cardiovascular and metabolic diseases: from mechanisms to therapeutics. *Theranostics* 9, 1923–1951. doi: 10.7150/thno.30787

Gezen-Ak, D., Dursun, E., Hanağası, H., Bilgiç, B., Lohman, E., Araz, Ö. S., et al. (2013). BDNF, TNFα, HSP90, CFH, and IL-10 serum levels in patients with early or late onset Alzheimer's disease or mild cognitive impairment. *J. Alzheimers Dis.* 37, 185–195. doi: 10.3233/JAD-130497

Hanada, M., Feng, J., and Hemmings, B. A. (2004). Structure, regulation and function of PKB/AKT—a major therapeutic target. *Biochim. Biophys. Acta* 1697, 3–16. doi: 10.1016/j.bbapap.2003.11.009

He, W., Wang, C., Chen, Y., He, Y., and Cai, Z. (2017). Berberine attenuates cognitive impairment and ameliorates tau hyperphosphorylation by limiting the self-perpetuating pathogenic cycle between NF-κB signaling, oxidative stress and neuroinflammation. *Pharmacol. Rep.* 69, 1341–1348. doi: 10.1016/j.pharep.2017.06.006

Jhaveri, K., and Modi, S. (2015). Ganetespib: research and clinical development. *Onco. Targets. Ther.* 8, 1849–1858. doi: 10.2147/OTT.S65804

Jiang, W., Li, S., and Li, X. (2015). Therapeutic potential of berberine against neurodegenerative diseases. *Sci. China Life Sci.* 58, 564–569. doi: 10.1007/s11427-015-4829-0

Jiang, Q., Liu, P., Wu, X., Liu, W., Shen, X., Lan, T., et al. (2011). Berberine attenuates lipopolysaccharide-induced extracelluar matrix accumulation and inflammation in rat mesangial cells: involvement of NF-κB signaling pathway. *Mol. Cell. Endocrinol.* 331, 34–40. doi: 10.1016/j.mce.2010.07.023

Khezri, M. R., Ghasemnejad-Berenji, M., and Moloodsouri, D. (2023). The PI3K/AKT signaling pathway and Caspase-3 in Alzheimer's disease: which one is the beginner? *J. Alzheimers Dis.* 92, 391–393. doi: 10.3233/JAD-221157

Kitagishi, Y., Nakanishi, A., Ogura, Y., and Matsuda, S. (2014). Dietary regulation of PI3K/AKT/GSK-3β pathway in Alzheimer's disease. *Alzheimers Res. Ther.* 6:35. doi: 10.1186/alzrt265

Kong, W., Wei, J., Abidi, P., Lin, M., Inaba, S., Li, C., et al. (2004). Berberine is a novel cholesterol-lowering drug working through a unique mechanism distinct from statins. *Nat. Med.* 10, 1344–1351. doi: 10.1038/nm1135

Kumar, H., Chakrabarti, A., Sarma, P., Modi, M., Banerjee, D., Radotra, B. D., et al. (2023). Novel therapeutic mechanism of action of metformin and its nanoformulation in Alzheimer's disease and role of AKT/ERK/GSK pathway. *Eur. J. Pharm. Sci.* 181:106348. doi: 10.1016/j.ejps.2022.106348

Kumar, A., Ekavali, C. K., Mukherjee, M., Pottabathini, R., and Dhull, D. K. (2015). Current knowledge and pharmacological profile of berberine: an update. *Eur. J. Pharmacol.* 761, 288–297. doi: 10.1016/j.ejphar.2015.05.068

Lin, Z., Sur, S., Liu, P., Li, Y., Jiang, D., Hou, X., et al. (2021). Blood-brain barrier breakdown in relationship to Alzheimer and vascular disease. *Ann. Neurol.* 90, 227–238. doi: 10.1002/ana.26134

Liu, X., Ouyang, S., Yu, B., Liu, Y., Huang, K., Gong, J., et al. (2010). PharmMapper server: a web server for potential drug target identification using pharmacophore mapping approach. *Nucleic Acids Res.* 38, W609–W614. doi: 10.1093/nar/gkq300

Long, H. Z., Cheng, Y., Zhou, Z. W., Luo, H. Y., Wen, D. D., and Gao, L. C. (2021). PI3K/AKT signal pathway: a target of natural products in the prevention and treatment of Alzheimer's disease and Parkinson's disease. *Front. Pharmacol.* 12:648636. doi: 10.3389/fphar.2021.648636

Meng, F. C., Wu, Z. F., Yin, Z. Q., Lin, L. G., Wang, R., and Zhang, Q. W. (2018). Coptidis rhizoma and its main bioactive components: recent advances in chemical investigation, quality evaluation and pharmacological activity. *Chin. Med.* 13:13. doi: 10.1186/s13020-018-0171-3

Morel, G. R., León, M. L., Uriarte, M., Reggiani, P. C., and Goya, R. G. (2017). Therapeutic potential of IGF-I on hippocampal neurogenesis and function during aging. *Neurogenesis (Austin)* 4:e1259709. doi: 10.1080/23262133.2016.1259709

Nygaard, H. B. (2018). Targeting Fyn kinase in Alzheimer's disease. *Biol. Psychiatry* 83, 369–376. doi: 10.1016/j.biopsych.2017.06.004

Ou, J. R., Tan, M. S., Xie, A. M., Yu, J. T., and Tan, L. (2014). Heat shock protein 90 in Alzheimer's disease. *Biomed. Res. Int.* 2014:796869. doi: 10.1155/2014/796869

Panahi, N., Mahmoudian, M., Mortazavi, P., and Hashjin, G. S. (2013). Effects of berberine on β-secretase activity in a rabbit model of Alzheimer's disease. *Arch. Med. Sci.* 9, 146–150. doi: 10.5114/aoms.2013.33354

Pei, H., Ma, L., Cao, Y., Wang, F., Li, Z., Liu, N., et al. (2020). Traditional Chinese medicine for Alzheimer's disease and other cognitive impairment: a review. *Am. J. Chin. Med.* 48, 487–511. doi: 10.1142/S0192415X20500251

Peng, W. H., Wu, C. R., Chen, C. S., Chen, C. F., Leu, Z. C., and Hsieh, M. T. (2004). Anxiolytic effect of berberine on exploratory activity of the mouse in two experimental anxiety models: interaction with drugs acting at 5-HT receptors. *Life Sci.* 75, 2451–2462. doi: 10.1016/j.lfs.2004.04.032

Piñero, J., Bravo, À., Queralt-Rosinach, N., Gutiérrez-Sacristán, A., Deu-Pons, J., Centeno, E., et al. (2017). DisGeNET: a comprehensive platform integrating information on human disease-associated genes and variants. *Nucleic Acids Res.* 45, D833–D839. doi: 10.1093/nar/gkw943

Piñero, J., Queralt-Rosinach, N., Bravo, À., Deu-Pons, J., Bauer-Mehren, A., Baron, M., et al. (2015). DisGeNET: a discovery platform for the dynamical exploration of human diseases and their genes. *Database (Oxford)* 2015:bav028. doi: 10.1093/database/bav028

Piñero, J., Ramírez-Anguita, J. M., Saüch-Pitarch, J., Ronzano, F., Centeno, E., Sanz, F., et al. (2020). The DisGeNET knowledge platform for disease genomics: 2019 update. *Nucleic Acids Res.* 48, D845–D855. doi: 10.1093/nar/gkz1021

Piñero, J., Saüch, J., Sanz, F., and Furlong, L. I. (2021). The DisGeNET cytoscape app: exploring and visualizing disease genomics data. *Comput. Struct. Biotechnol. J.* 19, 2960–2967. doi: 10.1016/j.csbj.2021.05.015

Rai, S. N., Tiwari, N., Singh, P., Mishra, D., Singh, A. K., Hooshmandi, E., et al. (2021). Therapeutic potential of vital transcription factors in Alzheimer's and Parkinson's disease with particular emphasis on transcription factor EB mediated autophagy. *Front. Neurosci.* 15:777347. doi: 10.3389/fnins.2021.777347

Roskoski, R. Jr. (2015). Src protein-tyrosine kinase structure, mechanism, and small molecule inhibitors. *Pharmacol. Res.* 94, 9–25. doi: 10.1016/j.phrs.2015.01.003

Ru, J., Li, P., Wang, J., Zhou, W., Li, B., Huang, C., et al. (2014). TCMSP: a database of systems pharmacology for drug discovery from herbal medicines. *J. Cheminform.* 6:13. doi: 10.1186/1758-2946-6-13

Scheltens, P., De Strooper, B., Kivipelto, M., Holstege, H., Chételat, G., Teunissen, C. E., et al. (2021). Alzheimer's disease. *Lancet* 397, 1577–1590. doi: 10.1016/S0140-6736(20)32205-4

Schmidt, S. I., Blaabjerg, M., Freude, K., and Meyer, M. (2022). RhoA signaling in neurodegenerative diseases. *Cells* 11:1520. doi: 10.3390/cells11091520

Singh, A., Dhaneshwar, S., and Mazumder, A. (2021). Investigating neuroprotective potential of Berberine, Levetiracetam and their combination in the Management of Alzheimer's disease utilizing drug repurposing strategy. *Curr. Rev. Clin. Exp. Pharmacol.* 18, 182–190. doi: 10.2174/2772432816666210910104306

Singh, A. K., Mishra, G., Maurya, A., Awasthi, R., Kumari, K., Thakur, A., et al. (2019a). Role of TREM2 in Alzheimer's disease and its consequences on β- amyloid, tau and neurofibrillary tangles. *Curr. Alzheimer Res.* 16, 1216–1229. doi: 10.2174/1567205016666190903102822

Singh, A. K., Rai, S. N., Maurya, A., Mishra, G., Awasthi, R., Shakya, A., et al. (2021a). Therapeutic potential of Phytoconstituents in Management of Alzheimer's disease. *Evid. Based Complement. Alternat. Med.* 2021:5578574. doi: 10.1155/2021/5578574

Singh, A. K., Singh, S. K., Nandi, M. K., Mishra, G., Maurya, A., Rai, A., et al. (2019b). Berberine: a plant-derived alkaloid with therapeutic potential to combat Alzheimer's disease. *Cent. Nerv. Syst. Agents Med. Chem.* 19, 154–170. doi: 10.2174/1871524919666190820160053

Singh, A. K., Singh, S. S., Rathore, A. S., Singh, S. P., Mishra, G., Awasthi, R., et al. (2021b). Lipid-coated MCM-41 mesoporous silica nanoparticles loaded with Berberine improved inhibition of acetylcholine esterase and amyloid formation. *ACS Biomater. Sci. Eng.* 7, 3737–3753. doi: 10.1021/acsbiomaterials.1c00514

Spinelli, M., Fusco, S., and Grassi, C. (2019). Brain insulin resistance and hippocampal plasticity: mechanisms and biomarkers of cognitive decline. *Front. Neurosci.* 13:788. doi: 10.3389/fnins.2019.00788

Sun, C., Li, J., Wang, X., Duan, W., Zhang, T., and Ito, Y. (2014). Preparative separation of quaternary ammonium alkaloids from Coptis chinensis Franch by pH-zone-refining counter-current chromatography. *J. Chromatogr.* 1370, 156–161. doi: 10.1016/j.chroma.2014.10.043

Tao, W., Xu, X., Wang, X., Li, B., Wang, Y., Li, Y., et al. (2013). Network pharmacology-based prediction of the active ingredients and potential targets of Chinese herbal Radix Curcumae formula for application to cardiovascular disease. *J. Ethnopharmacol.* 145, 1–10. doi: 10.1016/j.jep.2012.09.051

Tattersall, M. H., Sodergren, J. E., Dengupta, S. K., Trites, D. H., Modest, E. J., and Frei, E. 3rd. (1975). Pharmacokinetics of actinoymcin D in patients with malignant melanoma. *Clin. Pharmacol. Ther.* 17, 701–708. doi: 10.1002/cpt1975176701

Thomas, S. M., and Brugge, J. S. (1997). Cellular functions regulated by Src family kinases. *Annu. Rev. Cell Dev. Biol.* 13, 513–609. doi: 10.1146/annurev.cellbio.13.1.513

Thorpe, L. M., Yuzugullu, H., and Zhao, J. J. (2015). PI3K in cancer: divergent roles of isoforms, modes of activation and therapeutic targeting. *Nat. Rev. Cancer* 15, 7–24. doi: 10.1038/nrc3860

Trott, O., and Olson, A. J. (2010). AutoDock Vina: improving the speed and accuracy of docking with a new scoring function, efficient optimization, and multithreading. *J. Comput. Chem.* 31, 455–461. doi: 10.1002/jcc.21334

Tsuji, S., Hase, T., Yachie-Kinoshita, A., Nishino, T., Ghosh, S., Kikuchi, M., et al. (2021). Artificial intelligence-based computational framework for drug-target prioritization and inference of novel repositionable drugs for Alzheimer's disease. *Alzheimers Res. Ther.* 13:92. doi: 10.1186/s13195-021-00826-3

Vincent, A. M., Mobley, B. C., Hiller, A., and Feldman, E. L. (2004). IGF-I prevents glutamate-induced motor neuron programmed cell death. *Neurobiol. Dis.* 16, 407–416. doi: 10.1016/j.nbd.2004.03.001

Wang, Y., Chen, G., and Shao, W. (2022). Identification of Ferroptosis-related genes in Alzheimer's disease based on Bioinformatic analysis. *Front. Neurosci.* 16:823741. doi: 10.3389/fnins.2022.823741

Wang, X., Shen, Y., Wang, S., Li, S., Zhang, W., Liu, X., et al. (2017). PharmMapper 2017 update: a web server for potential drug target identification with a comprehensive target pharmacophore database. *Nucleic Acids Res.* 45, W356–W360. doi: 10.1093/nar/gkx374

Wang, X., Wang, R., Xing, D., Su, H., Ma, C., Ding, Y., et al. (2005). Kinetic difference of berberine between hippocampus and plasma in rat after intravenous administration of Coptidis rhizoma extract. *Life Sci.* 77, 3058–3067. doi: 10.1016/j.lfs.2005.02.033

Wang, Y. Y., Yan, Q., Huang, Z. T., Zou, Q., Li, J., Yuan, M. H., et al. (2021). Ameliorating Ribosylation-induced amyloid-β pathology by Berberine via inhibiting mTOR/p70S6K signaling. *J. Alzheimers Dis.* 79, 833–844. doi: 10.3233/JAD-200995

Wang, Z., Yang, Y., Liu, M., Wei, Y., Liu, J., Pei, H., et al. (2020). Rhizoma Coptidis for Alzheimer's disease and vascular dementia: a literature review. *Curr. Vasc. Pharmacol.* 18, 358–368. doi: 10.2174/1570161117666190710151545

Wei, Y., Zhou, J., Yu, H., and Jin, X. (2019). AKT phosphorylation sites of Ser473 and Thr308 regulate AKT degradation. *Biosci. Biotechnol. Biochem.* 83, 429–435. doi: 10.1080/09168451.2018.1549974

Wong, L. R., Tan, E. A., Lim, M. E. J., Shen, W., Lian, X. L., Wang, Y., et al. (2021). Functional effects of berberine in modulating mitochondrial dysfunction and inflammatory response in the respective amyloidogenic cells and activated microglial cells–*in vitro* models simulating Alzheimer's disease pathology. *Life Sci.* 282:119824. doi: 10.1016/j.lfs.2021.119824

Xu, X., Yi, H., Wu, J., Kuang, T., Zhang, J., Li, Q., et al. (2021). Therapeutic effect of berberine on metabolic diseases: both pharmacological data and clinical evidence. *Biomed. Pharmacother.* 133:110984. doi: 10.1016/j.biopha.2020.110984

Xu, X., Zhang, W., Huang, C., Li, Y., Yu, H., Wang, Y., et al. (2012). A novel chemometric method for the prediction of human oral bioavailability. *Int. J. Mol. Sci.* 13, 6964–6982. doi: 10.3390/ijms13066964

Xuan, W. T., Wang, H., Zhou, P., Ye, T., Gao, H. W., Ye, S., et al. (2020). Berberine ameliorates rats model of combined Alzheimer's disease and type 2 diabetes mellitus via the suppression of endoplasmic reticulum stress. *3 Biotech* 10:359. doi: 10.1007/s13205-020-02354-7

Yang, M., and Wang, J. (2022). Berberine ameliorates cognitive disorder via GSK3β/PGC-1α signaling in APP/PS1 mice. *J. Nutr. Sci. Vitaminol.* 68, 228–235. doi: 10.3177/jnsv.68.228

Ye, C., Liang, Y., Chen, Y., Xiong, Y., She, Y., Zhong, X., et al. (2021). Berberine improves cognitive impairment by simultaneously impacting cerebral blood flow and β-amyloid accumulation in an APP/tau/PS1 mouse model of Alzheimer's disease. *Cells* 10:1161. doi: 10.3390/cells10051161

Zamboni, V., Jones, R., Umbach, A., Ammoni, A., Passafaro, M., Hirsch, E., et al. (2018). Rho GTPases in intellectual disability: from genetics to therapeutic opportunities. *Int. J. Mol. Sci.* 19:1821. doi: 10.3390/ijms19061821

Zhang, T., Wei, W., Chang, S., Liu, N., and Li, H. (2022). Integrated network pharmacology and comprehensive bioinformatics identifying the mechanisms and molecular targets of Yizhiqingxin formula for treatment of comorbidity with Alzheimer's disease and depression. *Front. Pharmacol.* 13:853375. doi: 10.3389/fphar.2022.853375

Zhu, F., and Qian, C. (2006). Berberine chloride can ameliorate the spatial memory impairment and increase the expression of interleukin-1beta and inducible nitric oxide synthase in the rat model of Alzheimer's disease. *BMC Neurosci.* 7:78. doi: 10.1186/1471-2202-7-78

frontiers | Frontiers in Neuroscience

TYPE Review
PUBLISHED 05 May 2023
DOI 10.3389/fnins.2023.1136266

OPEN ACCESS

EDITED BY
Jianxun Liu,
China Academy of Chinese Medical Sciences, China

REVIEWED BY
Zequn Yin,
Hefei University of Technology, China
Ke-Yang Chen,
Wenzhou Medical University, China

*CORRESPONDENCE
Shijing Huang
✉ hsjgam2878@163.com
Manman Xu
✉ xummjournal@163.com
Juhua Pan
✉ journal5739@163.com

†These authors have contributed equally to this work and share first authorship

RECEIVED 02 January 2023
ACCEPTED 19 April 2023
PUBLISHED 05 May 2023

CITATION
Zhai W, Zhang T, Jin Y, Huang S, Xu M and Pan J (2023) The fibroblast growth factor system in cognitive disorders and dementia. *Front. Neurosci.* 17:1136266. doi: 10.3389/fnins.2023.1136266

The fibroblast growth factor system in cognitive disorders and dementia

Wujianwen Zhai†, Tong Zhang†, Yujing Jin, Shijing Huang*, Manman Xu* and Juhua Pan*

Traditional Chinese Medicine Research and Development Center, Guang' Anmen Hospital, China Academy of Chinese Medical Sciences, Beijing, China

Cognitive impairment is the core precursor to dementia and other cognitive disorders. Current hypotheses suggest that they share a common pathological basis, such as inflammation, restricted neurogenesis, neuroendocrine disorders, and the destruction of neurovascular units. Fibroblast growth factors (FGFs) are cell growth factors that play essential roles in various pathophysiological processes via paracrine or autocrine pathways. This system consists of FGFs and their receptors (FGFRs), which may hold tremendous potential to become a new biological marker in the diagnosis of dementia and other cognitive disorders, and serve as a potential target for drug development against dementia and cognitive function impairment. Here, we review the available evidence detailing the relevant pathways mediated by multiple FGFs and FGFRs, and recent studies examining their role in the pathogenesis and treatment of cognitive disorders and dementia.

KEYWORDS

fibroblast growth factor, fibroblast growth factor receptor, dementia, cognitive disorders, Alzheimer's disease, neurodegenerative diseases

1. Introduction

Dementia which occurs in the late stages of the cognitive disorders is one of the most prevalent mental illnesses, particularly among the elderly (Bennett and Thomas, 2014). The primary clinical manifestation of cognitive disorders is a decline in cognitive function, accompanied by disordered thinking, memory deficits, sensory disturbances, and poor concentration, which are risk factors and precursor symptoms of dementia, including Alzheimer's disease (AD; Anderson, 2019), vascular dementia (VaD; Dichgans and Leys, 2017), and Huntington's disease (HD; Papoutsi et al., 2014; van der Flier et al., 2018; Iadecola et al., 2019). Recent research has shown that the pathogenesis of those diseases is associated with various pathological mechanisms, including neuroinflammation (Byers and Yaffe, 2011; Leng and Edison, 2021), oxidative stress (Luca and Luca, 2019; Manduca et al., 2020), immune dysregulation (Hayley et al., 2021), disruption of neurotransmitters (Singh, 2009), synaptic plasticity injury (Byers and Yaffe, 2011; Skaper et al., 2017), and neuroendocrine disorders (Manduca et al., 2020). FGFs are cell growth factors involved in multiple critical pathophysiologic processes in the human body via paracrine and autocrine pathways such as embryonic development and angiogenesis, neurogenesis, wound healing, and glucolipid metabolism, which need to bind fibroblast growth factors receptor (FGFR) to produce physiological effects (Hui et al., 2018). Some researchers believe that FGFs have the potential to become a novel biological marker for the diagnosis and prognosis of neurodegenerative diseases, and these results may also indicate new targets for treatment (Galvez-Contreras et al., 2016). This review focuses on

how the FGF-FGFR system changes and affects the pathogenesis and treatment of cognitive disorders and other dementia. We hypothesized that maintaining a dynamic balance in the FGF-FGFR system would be beneficial for nerve repair and neuroprotection to reduce the clinical symptoms and risk of cognitive disorders.

2. Fibroblast growth factors in cognitive disorders and dementia

Patients with cognitive impairment without meeting the diagnostic criteria for dementia tend to be diagnosed by clinicians as mild cognitive impairment (MCI), while patients with concomitant cerebrovascular pathological changes or whose cognitive deficit occurs secondary to cerebrovascular disease can be diagnosed as vascular cognitive impairment. Cognitive impairment can be classified as 'functional' or 'non-functional' depending on the presence or absence of neurodegenerative changes (Ball et al., 2020). For the former, only cognitive, memory, and emotional impairments occur, which are less likely to deteriorate into dementia; for the latter, the subjective cognitive decline is accompanied by structural changes in the brain and eventually degenerates into dementia.

The pathological changes of dementia are, on the one hand, neurodegenerative changes due to senescence, such as AD, HD, frontotemporal dementia, and Parkinson's disease dementia; on the other hand, dementia is also closely associated with cerebrovascular injury, metabolic disorder, intracranial infections, intracranial tumors, hypoxic–ischemic brain injury, which secondary to stroke, atherosclerosis, chronic renal insufficiency, diabetes, hyperlipidemia, hypertension, and other diseases. These suggest a mixed pathology for dementia. Cellular senescence apoptosis and abnormal autophagy, inflammation, oxidative stress, vascular damage, and metabolic dysfunction interact to induce neuropathic protein accumulation and morphological changes in the brain, which are further disordered in a vicious cycle of neurodegenerative disease (Gonzales et al., 2022).

The FGF-FGFR system consists of seven receptors and 22 ligands that are required to bind to their corresponding receptors via acetyl heparan sulfate (HS) cofactor or α/β-Klotho (α/β-KL) transmembrane proteins to exert their physiological effects (Beenken and Mohammadi, 2009; Xie et al., 2020). The 22 FGFs can be divided into different subgroups based on sequence homology and developmental characteristics. For example, FGF-15/19, FGF-21, and FGF-23 are members of a particular FGF type called endocrine FGFs, which require KL proteins to bind to their receptors because of their low affinity for HS (Belov and Mohammadi, 2013; Owen et al., 2015; Hui et al., 2018cc Deng et al., 2019; Chen K. et al., 2022). Except for homologous factor subfamily (FGF-11/12/13/14) and endocrine FGF subfamily, other FGFs all belong to paracrine subfamilies, including FGF-1, FGF-2, FGF-9, and FGF-17 (Deng et al., 2019). Abnormal FGF expression levels have been observed by researchers in patients with dementia and other cognitive disorders (Stopa et al., 1990; Mashayekhi et al., 2010; Hensel et al., 2016; Liang et al., 2021). Moreover, the effects of FGFs on neuromodulation and cognitive improvement have been validated in literature (Lee et al., 2011; Taliyan et al., 2019). Fibroblast growth factors in cognitive disorders and dementia is summarized in Table 1.

2.1. Paracrine fibroblast growth factors

2.1.1. FGF-1

Fibroblast growth factor-1 (FGF-1), also known as acidic fibroblast growth factor (aFGF), is secreted by meningeal cells in the ventricles of the third ventricle and is widespread in multiple tissues, including the hippocampus, pituitary gland, heart, and kidney (Beenken and Mohammadi, 2009; Mashayekhi et al., 2010). FGF-1 can modulate physiological activities such as embryonic development, angiogenesis, cell proliferation and differentiation, and adult hippocampal neurogenesis (AHN) by activating different FGFRs (Lee et al., 2011; Tsai et al., 2015; Gasser et al., 2017; Sun et al., 2021). Although there remains a paucity of studies investigating the specific role of FGF-1 in the pathological mechanisms of cognitive impairment, several lines of evidence have shown that dysregulation of FGF-1 expression is closely associated with dementia, especially Alzheimer's disease (Takami et al., 1998; Yamagata et al., 2004).

AHN refers to the process by which neural stem cells in the hippocampus undergo symmetric or asymmetric division into neuroblasts, gradually migrate to specific regions after cell proliferation and then differentiate into new neurons and other resident brain cells. Thus, AHN is the fundamental physiological basis for neuroplasticity. After binding to FGFR-1, FGF-1 has a significant reparatory effect on damaged neurons in the cortex and hippocampus, reducing inflammatory factors secreted by microglial (MG) activation, thereby promoting neurogenesis and vascular regeneration (Tsai et al., 2015). However, there is no one-to-one correspondence between the FGFs and FGFRs. For instance, FGF-1 secreted by activated astrocytes (ASTs) induces neuroinflammation instead of neuroprotection if by binding to FGFR-2 (Lee et al., 2011). The neurovascular unit (NVU) is a microstructure composed of neurons, neuroglia, the BBB, and the extracellular matrix, and plays an essential role in maintaining nerve function. The BBB is an essential barrier, that protects the stability of the neural microenvironment and is the core of NVU coupling, providing protection against leakage of neurotoxic substances from the blood into the cerebral parenchyma. The BBB consists of cerebral microvascular endothelial cells and is connected to astrocytes, pericytes, perivascular macrophages, and basement membranes, which are hyperpermeable in depressed patients, triggering inflammation of the central nervous system (CNS) and endothelial damage to cerebral microvessels, further exacerbating neuronal injury. At the same time, FGF-1 could repair the BBB by upregulating the expression of tight junction proteins and adherens junction proteins via activating p-PI3K, PI3K, p-Akt, and Akt to suppress RhoA but activate Rac1 (Wu et al., 2017). Preliminary observations suggest that FGF-1 expression is reduced in neurons of the internal olfactory cortex in patients with AD, which inhibits the expression of calcium-binding proteins and induces overexpression of the N-methyl-D-aspartic acid receptor (NMDAR), resulting in the disruption of calcium homeostasis and glutamate-mediated excitotoxicity (Thorns and Masliah, 1999; Thorns et al., 2001). Several recent studies reported a significant increase in FGF-1 levels in both plasma and cerebrospinal fluid in AD (Mashayekhi et al., 2010; Liang et al., 2021), suggesting that there may be differences in local concentrations of FGF-1, but this remains to be verified further.

Glucose is the primary energy source of the brain (Mergenthaler et al., 2013). In addition to providing energy for neural activity, glucose indirectly regulates the transmission of signals that affect

TABLE 1 The expressions and prospects of the FGF/FGFR system in cognitive disorders and dementia.

Members	Receptors	Sample	Trends	Main effects	Prospects	References
FGF-1	FGFR-1b,1c	Cortex homogenate (AD)	↑	Reduced inflammation and oxidative stress, repaired BBB, suppressed excitotoxicity, improved insulin sensitivity	AD, VaD, MCI, VCI	Takami et al. (1998), Thorns et al. (2001), Yamagata et al. (2004), Mashayekhi et al. (2010), Tsai et al. (2015), Wu et al. (2017), and Liang et al. (2021)
	FGFR-2b,2c	Serum (AD)	↓			
	FGFR-3b,3c	CSF (AD)	↓			
	FGFR-4					
FGF-2	FGFR-1b,1c	Cortex homogenate (AD)	↑	Promoted neurogenesis, inhibited neurotoxicity, extended neurons life-span, induced angiogenesis, inhibited inflammation	AD, VaD, HD	Jin et al. (2005), Duff et al. (2010), Wang et al. (2016), Tyebji and Hannan (2017), Liu M. et al. (2018), and Ilieva et al. (2019)
	FGFR-2c					
	FGFR-3c	Serum (AD)	↓			
	FGFR-4					
FGF-9	FGFR-2c	Hippocampus homogenate (AD)	↑	Promoted neuronal development, inhibited oxidative stress, suppressed apoptosis, promoted neurogenesis	AD, HD	Nakamura et al. (1998), Chuang et al. (2015), and Yusuf et al. (2019, 2021a,b)
	FGFR-3b,3c	Serum (HD)	↓			
FGF-17	β-KL/FGFR-2	N/A	N/A	Supported oligodendrocyte precursor cell growth, inhibited FGF-19 pathway	MCI	Liu S. et al. (2018) and Iram et al. (2022)
	FGFR-3c					
FGF-15/19	β-KL/FGFR-4	N/A	N/A	Inhibited HPA axis hyperexcitability, reduced insulin resistance, regulated neurotransmitter homeostasis, promoted neurogenesis, regulated bile acid metabolism	AD, MCI	Marcelin et al. (2014), McMillin et al. (2015), Perry et al. (2015), Mertens et al. (2017), Liu S. et al. (2018), and Li et al. (2020)
FGF-21	β-KL/FGFR-1	Serum (AD)	↓	Improved BBB integrity, repair cerebrovascular endothelium, inhibited inflammation, promoted neurogenesis, suppressed apoptosis, maintained neurotransmitter homeostasis, regulated lipid metabolism and glucose metabolism, enhanced insulin sensitivity	AD, VaD	Sa-Nguanmoo et al. (2016), Kuroda et al. (2017), Chen et al. (2018), Zheng et al. (2019), Jiang et al. (2020), and Wang et al. (2020)
	PPAR-γ					
FGF-23	α-KL/FGFR-1c	Serum (MCI)	↑	Regulated phosphate homeostasis and glucose metabolism, promoted neurogenesis	MCI	Liu et al. (2011), Drew et al. (2014), and Drew and Weiner (2014)
	FGFR-2c					
	FGFR-3c					

AD, Alzheimer's disease; BBB, blood–brain barrier; CSF, cerebrospinal fluid; FGF, fibroblast growth factor; FGFR, fibroblast growth factor receptor; HD, Huntington's dementia; MCI, mild cognitive impairment; VCI, vascular cognitive impairment; VaD, vascular dementia; α/β-KL, α/β-klotho protein.

neural function (Dienel, 2012; Hossain et al., 2020). Cerebral glucose metabolism plays a crucial role in the physiological mechanisms of cognitive function and the pathomechanisms of dementia. Therefore, cerebral insulin resistance can trigger oxidative stress, mitochondrial dysfunction, inflammation, and autophagy by inducing severe dysfunction of extracellular glucose transport and intracellular glucose metabolism disorders, leading to neurodegeneration (Chen and Zhong, 2013; Butterfield and Halliwell, 2019). Notably, patients with AD or MCI exhibit a dramatic decline in cerebral glucose metabolism due to insulin resistance (Chen and Zhong, 2013; Butterfield and Halliwell, 2019). Researchers have also found that patients with dementia have significant insulin resistance in their hippocampi (Wijesekara et al., 2018; Hamer et al., 2019), suggesting that dysregulation of brain insulin signaling pathways may play an important role in cognitive dysfunction. Exogenous FGF-1 has been shown to reduce blood glucose concentrations and increase insulin sensitivity (Holmes, 2014; Suh et al., 2014; Gasser et al., 2017; Tennant et al., 2019) via modulating the Wnt/β-catenin (Sun et al., 2021) and AMPK pathways (Chen Q. et al., 2022). Thus, FGF-1 could indirectly ameliorate cognitive impairment by attenuating insulin resistance in local brain regions. The potential therapeutic mechanisms of FGF-1 are shown in Figure 1.

2.1.2. FGF-2

FGF-2, also known as basic fibroblast growth factor (bFGF), was the first fibroblast growth factor to ever be identified. In the CNS, FGF-2 is primarily produced by ASTs and distributed throughout the cortex, hippocampus, and hypothalamus. Physiological concentrations of FGF-2 have been reported to promote proliferation, differentiation, migration, and maturation of neural stem cells and neuroglia, maintain cortical synaptic connectivity, stimulate neurogenesis, inhibit neuroinflammation, and exert tremendous neuroprotective and neurotrophic effects (Numakawa et al., 2015; Wu et al., 2017). The expression levels of FGF-2 are elevated in a compensatory manner in dementia (Stopa et al., 1990; Tennakoon et al., 2022), whereas the artificial modulation of FGF-2 levels improves cognitive function in rodents (Kiyota et al., 2011; Feng et al., 2012; Numakawa et al., 2015). In addition, FGF-2 has been shown to be a significant therapeutic target for certain anti-dementia medications, such as memantine (Namba et al., 2010).

Hippocampal neuronal cells are critical for the regulation of memory, learning, cognition, emotion, and other functions. FGF-2 has been proposed to stimulate the growth of neuronal synapses and regulate tight junction proteins in vascular endothelial cells via activating the PI3K/AKT pathway to promote AHN and protect the BBB (Wang et al., 2016; Ilieva et al., 2019). Neuroglia cells are a crucial component of the NVU, as they maintain the stability of the physiological functions of the neurons in the brain and consist of ASTs, MG, and oligodendrocytes (OLs). In HD, FGF-2 could promote the proliferation and recruitment of neuronal cells and inhibit the neurotoxicity produced by polyglutamine protein aggregation, which would prolong the lifespan of neurons (Jin et al., 2005; Duff et al., 2010; Tyebji and Hannan, 2017). ASTs, which have both an anti-inflammatory resting state and a pro-inflammatory reactive state, are the most abundant and largest neuroglia in the CNS and play a key role in neurotransmitter regulation and energy provision. In cognitive disorders, the density and number of resting ASTs decrease with the aggravation of symptoms, which leads to a decline in neurotrophic factors and nerve growth factors secreted by ASTs, while the number of reactive ASTs, which produce large amounts of inflammatory factors and neurotoxins is raised (Wang et al., 2017; Lu et al., 2020). Excessive activation of GSK-3β can induce hyperphosphorylation of tau. Furthermore, spatial memory deficits and cognitive decline in AD

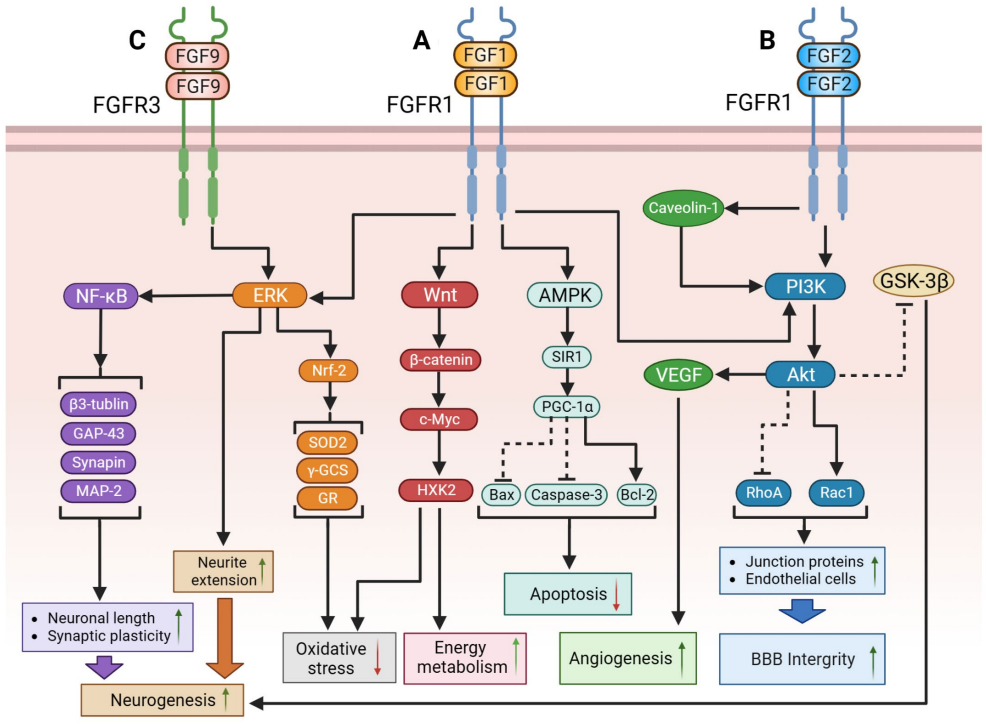

FIGURE 1
The potential therapeutic mechanism of paracrine FGFs (FGF-1, FGF-2, FGF-9). **(A)** FGF-1might regulate the following signaling pathways to improve cognition function: (1) FGF-1 activates PI3K/Akt pathway to suppress RhoA but activate Rac1, causing the upregulation of BBB integrity; (2) FGF-1 activates ERK pathway to extend neurite for promoting neurogenesis; (3) FGF-1 activates Wnt/β-catenin/c-Myc/ HXK2 pathway to improve mitochondrial energy metabolism and suppress oxidative stress; (4) FGF-1 exert the activation of the AMPK/SIRT1/PGC-1α pathway to modulate the apoptosis. **(B)** (1) FGF-2 might inhibit GSK-3β through PI3K/AKT pathway to promote adult hippocampal neurogenesis; FGF-2 could also repair blood–brain barrier integrity through the activation of PI3K/Akt/Rac1axis, but inhibiting RhoA; (2) Additionally, protect astrocytes and induce angiogenesis to improve cerebral blood supply by upregulating the Caveolin-1/PI3K/AKT/VEGF pathway. **(C)** FGF-9 might activate ERK/Nrf-2pathway to suppress oxidative stress and activate the ERK/NF-κB pathway to improve hippocampal neurogenesis. The solid black lines and arrows indicate the activation of the signaling pathway, and the dashed black lines and T-arrows indicate the inhibition of the signaling pathway. FGF, fibroblast growth factor; PI3K, phosphatidylinositol-3-hydroxy kinase; AKT, protein kinase B; Rac1, rac family small GTPase 1; RhoA, ras homolog family member A; BBB, blood–brain barrier; ERK, extracellular signal-regulated kinase; HXK2, hexokinase 2; AMPK, adenosine monophosphate activated protein kinase; SIR1, sirtuin1; PGC-1α, peroxisome proliferator-activated receptors-γ coactivator 1-α; GSK-3β, glycogen synthase kinase-3β; VEGF, vascular endothelial growth factor; Nrf-2, nuclear factor erythroid-like 2; SOD2, superoxide dismutase 2; γ-GCS, gamma-glutamylcysteine synthetase; GR, glutathione reductase; NF-κB, nuclear factor kappa-B; MAP-2, microtubule-associated protein-2; GAP-43, growth association protein-43.

could be ameliorated by FGF-2 through a simultaneous decrease in amyloid-β (Aβ) and microtubule-associated protein tau while increasing the number of resting ASTs in the hippocampal dentate gyrus (Katsouri et al., 2015). A possible explanation for this result is that exogenous FGF-2 may suppress the over-activated GSK-3β-related pathway and strengthened neurogenesis (Hong et al., 2016). It could activate p-GSK-3β and GSK-3β, triggering tau hyperphosphorylation to aggravate cognitive decline, but could also inhibit GSK-3β via activating the Akt pathway to promote hippocampal neurogenesis. We assumed that these mixed results might attribute to different molecular weight isoforms of FGF-2 activating different downstream pathways. Moreover, FGF-2 could protect ASTs from ischemia–reperfusion injury, a common pathological basis of VaD, and induce angiogenesis to ameliorate chronic cerebral hypoperfusion by upregulating the Caveolin-1/PI3K/AKT/vascular endothelial growth factor (VEGF) signaling pathway (Liu M. et al., 2018).

Neuroinflammation is a critical pathological mechanism that disrupts NVU homeostasis. The levels of multiple pro-inflammatory factors observed in both the blood and cerebrospinal fluid of patients with dementia were higher than those in healthy individuals (Shen et al., 2019). For example, MG is an integral type of neuroglia for maintaining the AHN process with a pro-inflammatory phenotype M1 and an anti-inflammatory phenotype M2. Activation of M1 induces neuroinflammation, which inhibits FGF-2 expression and activates downstream ERK pathway in the hippocampal region, thereby restraining the AHN process. In contrast, exogenous FGF-2 could effectively inhibit interleukin-1β (IL-1β), interleukin-6 (IL-6), tumor growth factor-α (TNF-α) and other pro-inflammatory factors produced by M1-type MG in an attempt to improve depressive-like behaviors (Tang et al., 2017). FGF-2 may also enhance the activation of M2-type MG and its phagocytosis of Aβ, thereby promoting neurogenesis in dementia (Kiyota et al., 2011). OLs are crucial for the modulation of the cerebrovascular system and the maintenance of white matter structure and function, while FGF-2 can promoted proliferation, maturation, differentiation, and migration of OLs and suppress their apoptosis (Miyamoto et al., 2014). White matter hyperintensities (WMH) are the imaging features of white matter lesions, with several studies suggesting a clinically relevant link between WMH burden and cognitive decline in MCI and AD (Garnier-Crussard et al., 2022; Kamal et al., 2022). Researchers have also found that senescent oligodendrocyte precursor cells (OPCs) were the primary neuroglial cell expressed in neuritic plaques, which could induce cell senescence in AD, causing cognitive decline (Zhang et al., 2019). Therefore, modulation of neuroglial cells (OLs, ASTs, and MG) via the FGF-2 pathway may play a role in the treatment of cerebral white matter lesions and VaD via angiotensin-converting enzyme II (Wakayama et al., 2021). The current application of FGF-2 is mainly in synthetic recombinant human-derived FGF-2 which has several limitations such as short half-life in the blood, inability to completely cross the BBB, or side effects on the vascular system (Bogousslavsky et al., 2002). However, novel synthetic compounds such as SUN11602 have been proposed, which mimic the structure of FGF-2, and could potentially avoid the aforementioned defects and exert neuroprotective effects of FGF-2 to a certain extent (Ogino et al., 2014; Ardizzone et al., 2022).

In recent decades, several researchers have observed opposing trends in the changes of FGF-2 in serum and brain tissue in dementia. For example, Katsouri et al. (2015) found that the concentration of FGF-2 in the frontal cortical homogenates of patients with AD was decreased, rather than increased, contrary to previous studies (Stopa et al., 1990). Additionally, the original hypothesis assumed that FGF-2 attracts neurons into plaques in AD (Cummings et al., 1993); however, recent studies have argued that FGF-2 confers neuroprotective effects (Feng et al., 2012; Katsouri et al., 2015). We speculate that discrepancies could be explained with the following reasons: (1) Numerous cells in the peripheral system, such as blood cells, bone marrow stromal cells, and smooth muscle cells, can also secrete FGF-2. Therefore, serum FGF-2 levels might be affected by other systemic diseases in ways that truly reflect the level of FGF-2 in the CNS. (2) Subjects in the discussed studies were not receiving uniform treatment, which may increase the uptake of FGF-2 into damaged neuronal cells, resulting in a relative decrease in serum FGF-2 levels. (3) An increase in serum FGF-2 levels could also be a result of compensatory secretion to repair nerve injury. (4) There are at least six different molecular weight isoforms of FGF-2 (Chlebova et al., 2009), which may have different physiological roles, but routine detection could be unable to show the differences between the isomers (Jiang et al., 2007; Chen X. et al., 2019). Therefore, despite ample evidence supporting the key role of FGF-2 in cognitive impairment and dementia, it still fails to become an independent clinical diagnosis or assessment indicator. These points made above are also the common challenges we face during the study of the FGF family members. The potential therapeutic mechanisms of FGF-2 are shown in Figure 1.

2.1.3. FGF-9

FGF-9 is synthesized by neurons of the CNS which binds to FGFR-2, FGFR-3, but not FGFR1 and FGFR4, playing a prominent role in angiogenesis, neurogenesis, cellular differentiation and cardiac development (Hecht et al., 1995; Reuss and von Bohlen und Halbach, 2003; Wang S. et al., 2018). Nakamura et al. (1998) found that high levels of FGF-9 expression in the hippocampus of patients with AD promoted the activation of the pro-inflammatory phenotype of ASTs around senile plaques, thereby exacerbating cognitive impairment. Alternatively the expression level in the CNS of FGF-9 may decrease in patients with HD. Previous results of Chuang et al. (2015) which have identified prominent FGF-9 and FGFR-3 expression in primary neuron-enriched cultures, suggesting the FGF-9 effects are cell-type specific in brain, may be a likely explanation for the different expression trends of FGF-9 in AD and HD.

It has been shown that exogenous FGF-9 may promote neuronal development and synaptic growth in striatal cell models of HD in response to anti-oxidant and anti-apoptotic effects via extracellular signaling that modulates the ERK/NF-κB pathway (Yusuf et al., 2019, 2021a,b), which provides a novel insight into the treatment of cognitive decline due to HD. FGF-9 activates Nrf-2 to upregulate transcription factors (SOD2, γ-GCS, and GR) for suppressing oxidative stress, through the activation of the ERK pathway. Additionally, FGF-9 could also activate the ERK/NF-κB pathway to upregulate β-tubulin, MAP-2, GAP-43, and synapsin to improve the neuronal length and synaptic plasticity. These studies suggest that FGF-9 overexpression in AD might be a compensatory mechanism for neuroprotection.

In addition, a negative correlation was found between FGF-9 and adiponectin (ADPN). ADPN is a pleiotropic adipocyte-secreting

hormone with neurotrophic effects. Animals knocked out of the ADPN gene could present depressive-like behavior and cognitive deficits (You et al., 2021). Researchers have found that the Chinese herbal extract carnosic acid could simultaneously reduce FGF-9 levels and raise ADPN levels both in mice's serum and hippocampal tissues, thereby ameliorating depression-like symptoms (Azhar et al., 2021; Wang et al., 2021). Interestingly, Carnosic acid could also alleviate AD-induced cognitive decline by inhibiting neuroinflammation, ameliorating cholinergic deficits, and enhancing energy metabolism (Chen Y. et al., 2022; Yi-Bin et al., 2022). We supposed that FGF-9 may also participate in carnosic acid's anti-dementia mechanism of action, but it requires further study. The potential therapeutic mechanisms of FGF-9 are shown in Figure 1.

2.1.4. FGF-17

FGF-17 is mainly expressed in the cerebrospinal fluid, plasma, and cortical neurons. It binds mainly to FGFR-3 to regulate downstream signaling, fulfilling vital roles in embryonic development, cell proliferation, and early neurogenesis, which declines during senescence (Hoshikawa et al., 1998; Machado et al., 2015; Han et al., 2019; Sathyan et al., 2020; Iram et al., 2022). Iram et al. (2022) recently observed that the growth of OPCs was suppressed after blocking the FGF-17/FGFR-3 pathway, which impaired hippocampal function in mice and provoked cognitive impairments and memory loss. Furthermore, they proved that exogenous injection of FGF-17 could enhance cognitive and memory performance in older mice. This finding is contrary to a previous study by Scearce-Levie et al. (2008) which found that young mice did not show obvious symptoms of cognitive impairment after knocking out the FGF-17 gene. These differences can be attributed to the fact that the subjects were in different physiological states that were influenced by their age. Besides, FGF-17 has been found to bind to the β-KL/FGFR-2 homodimer in the hypothalamus and show antagonize FGF-15/19, which blocked the insulin signaling pathway regulated by FGF-15/19 and triggered a decrease in glucose tolerance (Liu S. et al., 2018). The following may indicate that FGF-17 exerts distinct effects when bound to different receptors separately in the hippocampus or hypothalamus. Therefore, the therapeutic potential and side effects of FGF-17 remain to be studied over a long period of time. The potential therapeutic mechanisms of FGF-17 are shown in Figure 2.

2.2. Endocrine fibroblast growth factors

FGF-19, FGF-21, and FGF-23 are members of the same subgroup, have low affinity for HS, and require the activation of corresponding receptors by binding to the KL transmembrane protein, which causes them to diffuse into the bloodstream and exert hormone-like regulatory effects readily. Therefore, they are also known as endocrine-FGFs. FGF-19 from intestinal epithelial cells and hepatocytes could restrain the synthesis of primary bile acids and alter the ratio of primary to secondary bile acids, thus indirectly regulating lipid metabolism and bile acid signaling (Owen et al., 2015; Al-Aqil et al., 2018). FGF-21, produced mainly by hepatocytes and adipocytes, is a vital regulator for maintaining the homeostasis of lipid, glucose, and energy metabolism (Kharitonenkov et al., 2005; Owen et al., 2015). FGF-23, synthesized in osteoblasts and osteocytes, is highly expressed in the kidney and parathyroid glands and regulates the dynamic balance of phosphate, calcium, and vitamin D metabolism (Cunningham et al., 2011; Vervloet, 2019). The above three FGFs have been shown to affect metabolism in the CNS and have a relationship with cognitive disorders and dementia (Hsuchou et al., 2013; Hensel et al., 2016; Li, 2019; Jiang et al., 2020).

2.2.1. FGF-15/19

Researchers often refer to FGF-19 as FGF15/19, since FGF-19 in both humans and rats is expressed in mice as the homologous protein FGF-15. This protein is synthesized primarily in the enterocyte at the end of the ileum via the farnesoid X receptor (FXR) -related pathway and is expressed in the small intestine, liver, gallbladder, kidney, brain, and other tissues (Rysz et al., 2015). In tissues with rich β-KL, for example, the liver, FGF-15/19 binds to β-Kloth and activates FGFR-1, FGFR-2, FGFR-3, and FGFR-4, whereas, in tissues relatively deficient in β-KL like the brain, FGF-15/19 only binds to FGFR-4 (Nakamura et al., 2011). FGF-15/19 could stimulate the development of the heart and brain in the embryonic stage, regulate the production and circulation of bile acids (BAs) and promote glucolipid metabolism mainly in the liver at maturity; recently, it has also been found to have an insulin-like effect in the CNS, with the potential to tune sleep, cognition, and sensory functions (Hsuchou et al., 2013; Giacomini et al., 2016).

Due to the significant neuromodulatory, protective and nutritional effects of insulin on the brain, insulin resistance in the brain might exacerbate Aβ deposition, tau hyperphosphorylation, and vascular inflammation, causing cognitive impairments in AD and VaD (Hotamisligil, 2006; Kellar and Craft, 2020). Hypothalamic–pituitary–adrenal (HPA) axis hyperfunction is prevalent in dementia and other cognitive disorders, which might be the reason for higher adrenocorticotropic hormone (ACTH) and glucocorticoid (GC) levels, resulting in insulin resistance. Perry et al. (2015) have shown that intracerebroventricular injection of exogenous FGF-19 may improve insulin sensitivity by reducing serum ACTH and GC levels through inhibition of the HPA axis. This effect may arise from the inhibition of agouti-related protein/neuropeptide-Y (AGRP/NPY) neurons and the activation of the ERK1/2 pathway in the hypothalamus (Marcelin et al., 2014; Liu S. et al., 2018). In addition, recent studies have identified a link between the HPA axis dysfunction and cognitive decline in MCI and AD (Csernansky et al., 2006; Canet et al., 2019). Researchers have observed that the HPA axis dysfunction might emerge in the early stages of cognitive deficits, leading to structural damage in the hippocampus and cortex and NVU destabilization through the elevation of cortisol and norepinephrine (NE) levels with concomitant glucocorticoid receptor disruption and neurotoxicity (Popp et al., 2015; Canet et al., 2019). This finding was supported by Csernansky et al. (2006), Lara et al. (2013), and Wang L. Y. et al. (2018). Thus, the FGF-15/19 pathway might become a novel therapeutic target to maintain HPA axis function for drug discovery.

Furthermore, FGF-15/19 could affect NVU homeostasis by modulating BA production and circulation. The FXR for BA is found in neurons and ASTs in the hypothalamus and hippocampus of both humans and rodents (Mano et al., 2004; Huang et al., 2016; He et al., 2021), while physiological concentrations of BA can penetrate the BBB and suppress hyperexcitability of the HPA axis by activating glucocorticoid receptors in the hypothalamus and protect NVU by activating the BDNF–TrkB pathway (McMillin et al., 2015; Mertens et al., 2017; Li et al., 2020). Brain-derived neurotrophic factor (BDNF)

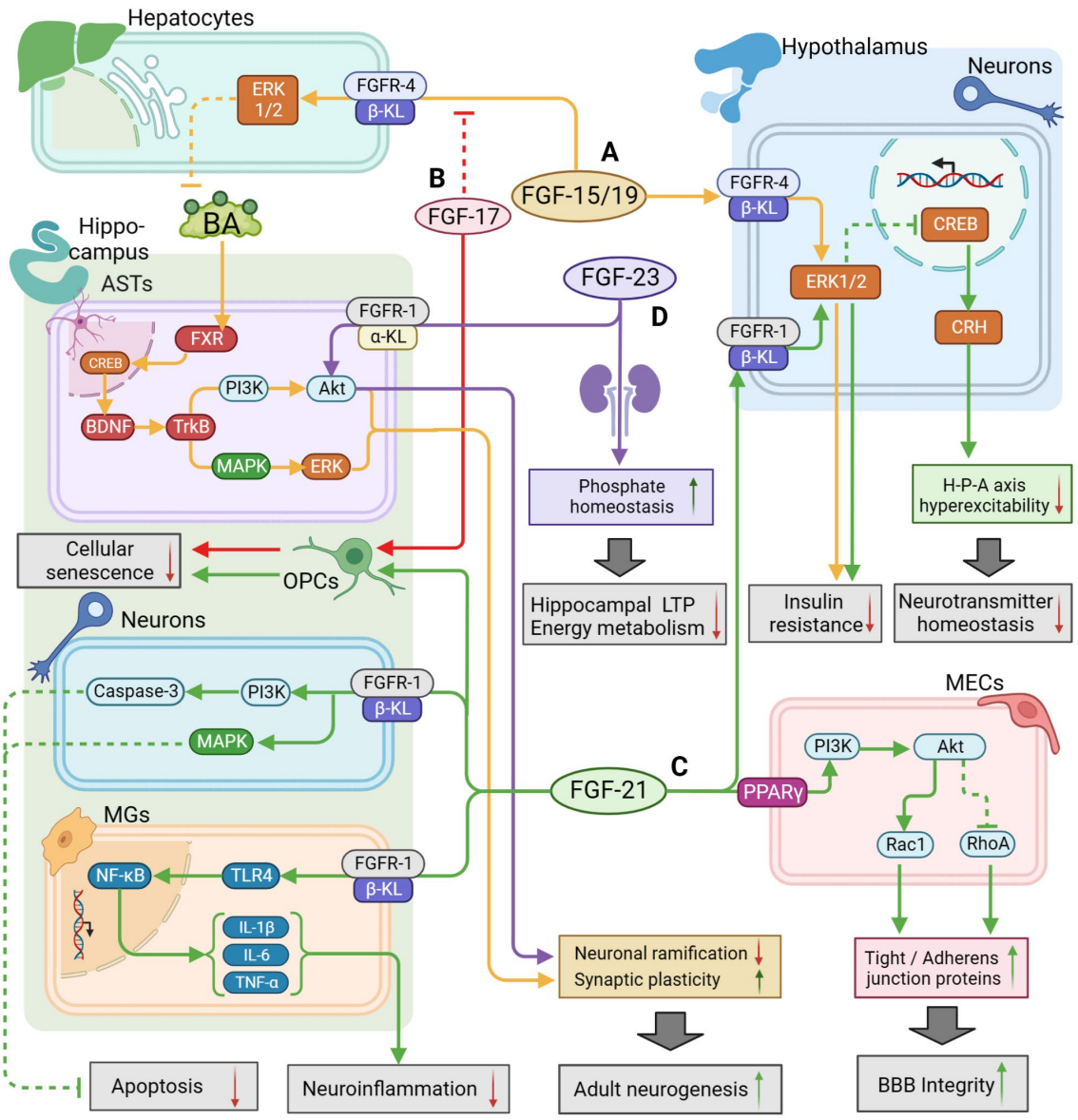

FIGURE 2
The potential therapeutic mechanism of endocrine FGFs (FGF15/19, FGF21, FGF23) and FGF17. **(A)** FGF-15/19/FGFR4/β-KL might activate the ERK1/2 pathway in hepatocytes to regulate BA metabolism for activating BDNF/TrkB/PI3K pathway and BDNF/TrkB/MAPK pathway in hippocampal ASTs, leading to improvement of adult neurogenesis; FGF15/19 could also penetrate the BBB to inhibit insulin resistance by activating the ERK1/2 pathway in hypothalamus. **(B)** FGF-17 could enhance the growth of OPCs to defer cell aging and suppress FGF-15/19 pathway as a competitive inhibitor. **(C)** FGF-21 could enhance BBB integrity by activating PI3K/Akt pathway in MECs, and reduce neuroinflammation through the suppression of TLR4/ NF-κB pathway in MGs; FGF-21 could also inhibit apoptosis by activating PI3K/Caspase-3 pathway and MAPK pathway in neurons; FGF-21 could also regulate HPA axis function by activating ERK/CREB pathway to maintain neurotransmitter balance; Additionally, FGF-21 might defer OPCs aging for repairing cognitive function. **(D)** FGF-23/FGFR-1/α-KL might directly activate the AKT pathway to inhibit neuronal ramification but maintain synaptic plasticity; FGF-23 expressed in the kidney could also indirectly regulate phosphate homeostasis to promote LTP and mitochondrial energy metabolism for improvement of cognitive function. The solid arrows indicate the activation of the signaling pathway, and the dashed T-arrows indicate the inhibition of the signaling pathway. The yellow lines represent the FGF-15/19 pathway, the red lines represent the FGF-17 pathway, the green lines represent the FGF-21 pathway and the purple lines represent the FGF-23 pathway. FGF, fibroblast growth factor; BA, bile acid; FXR, farnesoid X receptor; GR, glucocorticoid receptors; KL, klotho protein; BBB, blood–brain barrier; BDNF, Brain Derived Neurotrophic Factor; PI3K, phosphatidylinositol-3-hydroxy kinase; Akt, protein kinase B; TrkB, tyrosine kinase receptor B; ERK, extracellular signal-regulated kinase; MAPK, mitogen-activated protein kinase; CREB, cAMP-response element binding protein; TLR4, toll like receptor-4; NF-κB, nuclear factor kappa-B; OPCs, oligodendrocyte precursor cells; ASTs, astrocytes; MECs, microvascular endothelial cells; LTP, long-time potentiation.

is widely distributed in the CNS, especially in the cerebral cortex and hippocampus, with a significant role in the survival and maintenance of neurons. BDNF regulates synaptic plasticity via the autocrine pathway and modulates the presynaptic gamma-aminobutyric acid system via the paracrine pathway. BAs regulated by FGF-15/19 could enter hippocampal astrocytes and bind to FXR binding to promote BDNF synthesis, activate TrkB/PI3K/AKT pathway and TrkB/MAPK/ERK pathway, thus promoting hippocampal neurogenesis. Al-Aqil et al. (2018) observed that a high dosage of GC could elevate BA levels and downregulate FGF-15 expression in the serum and liver of mice.

A recent metabolomics study identified that the serum concentrations of cholic acid (CA) and lithocholic acid (LCA) were significantly lower in patients with AD than in normal individuals (Pan et al., 2017). In contrast, the levels of CA, lithocholic acid, deoxycholic acid (DCA), chenodeoxycholic acid (CDCA), taurodeoxycholic acid (TDCA), and glycinodeoxycholic acid (GDCA) in serum, cerebrospinal fluid, and brain tissue have increased observably (MahmoudianDehkordi et al., 2019; Baloni et al., 2020). Changes in the ratio of secondary to primary BA have also been shown to be in close correlation with cognitive decline. For instance, the proportion changes of GDCA to CA shows a positive relationship with the amount of Aβ deposition in the cerebrospinal fluid in animal models of AD, while the proportion of TDCA and GDCA to CA is negatively correlated with glucose levels in the prefrontal cortex and hippocampus volume (MahmoudianDehkordi et al., 2019; Nho et al., 2019). Meanwhile, mounting evidence suggests that anti-dementia effects could be achieved with some common medicines used to treat gallstones, sclerosing cholangitis, sloughy hepatitis, and other cholestatic diseases. For example, tauroursodeoxycholic acid (TUDCA) has been insulin resistance shown to possess antidepressant efficacy and effectively inhibit Aβ deposition in AD (Lo et al., 2013; Lu et al., 2018; Cheng et al., 2019); Additionally, obeticholic acid, a synthetic FXR agonist that was developed based on the structure of CDCA, has been shown to enhance memory and cognition by maintaining BBB permeability and retarding neuronal degeneration (Gee et al., 2022). These findings suggest that modulation of BA-related pathways has the potential to be a new approach to improve mood and cognitive function and defer neuronal degeneration. In physiological conditions, FGF-15/19 activates the ERK1/2 pathway to inhibit cholesterol 7α-hydroxylase from preventing BA synthesis in order to bring BA concentration into equilibrium. In cases of dementia, disrupted endogenous glucocorticoids in the serum or disordered gut microbiota could restrict FGF-15/19 synthesis following FXR activation and counterbalance the inhibitory effect of FGF-15/19 on BA, thereby perturbing the balance of blood and tissue concentrations of BA. As a result, excessive BA would enter the CNS through circulation and cross the BBB, producing cytotoxicity, lysing the membranes of neuronal and endothelial cells, further disrupting NVU homeostasis. The following would aggravate the structural damage or lead to dysfunction in the hippocampus, hypothalamus, and other key regions, which would create a vicious cycle of cognitive impairment and morphological damage. Thus, FGF-15/19 may have an indirect regulatory role in the pathological changes seen in dementia by regulating glucose metabolism, HPA axis function, and BA homeostasis in critical brain regions. Although there is still a lack of direct evidence for changes in FGF-15/19 levels in dementia or other cognitive disorders, the above studies suggest a promising new therapeutic method for modulating BA synthesis, metabolism, and component ratios through the FGF-15/19 pathway to improve cognitive function. The potential therapeutic mechanisms of FGF-15/19 are shown in Figure 2.

2.2.2. FGF-21

Fibroblast growth factor 21 (FGF-21) is primarily synthesized in the liver and adipose tissue, which is distributed throughout the bone, muscle, heart, kidney, and brain. FGF-21 is regulated by peroxisome proliferator-activated receptor-α (PPAR-α) and binds mainly to PPAR-γ, FGFR-1, and other receptors (Kuroda et al., 2017). FGF-21 has been proven to enhance glucose tolerance and insulin sensitivity, inhibit lipid synthesis and exert anti-inflammatory, antioxidant, and anti-apoptotic effects (Hui et al., 2018; Dolegowska et al., 2019). It could also penetrate the BBB to bind to FGFR-1 in the CNS and exert potent neuroprotective effects (Kuroda et al., 2017; Jiang et al., 2020). Researchers have currently identified that FGF-21 exerts neuroprotective effects through the following five significant pathways. (1) Protection of the BBB integrity: the FGF-21/β-KL/FGFR-1 pathway is automatically activated after cerebral microvascular injury or focal ischemia to mitigate neural and vascular endothelial damage. In addition, FGF-21 protects BBB integrity through the activation of PPAR-γ/PI3K/AKT/Rac1 pathway in cerebral microvascular endothelial cells and upregulation of tight junction proteins and adherent junction proteins expressions (Chen et al., 2018; Jiang et al., 2020). (2) Inhibition of neuroinflammation: FGF-21 could inhibit the pro-inflammatory phenotype of MG and NF-κB signaling pathway by suppressing the expression of pro-inflammatory factors such as IL-1β, IL-6, and TNF-α, in a way that nerve cells are protected from the damage caused by inflammation (Wang et al., 2020). (3) Promotion of neurogenesis: FGF-21 could activate PI3K/Caspase-3 signaling pathway and alleviate the apoptosis of neuronal cells (Zheng et al., 2019). In addition, FGF-21 may enhance hippocampal synaptic plasticity, increase dendritic spine density, promote restoration of mitochondrial function in the brain tissue, and inhibit apoptosis (Sa-Nguanmoo et al., 2016). Furthermore, since OPCs are widely distributed in the CNS, OLs differentiated from OPCs could be a crucial link between neural regeneration and myelin restoration. More specially, Kuroda et al. (2017) showed that the regulation of OPCs proliferation and differentiation by the FGF-21/β-KL/FGFR-1 pathway would be beneficial for neuroprotection. (4) Neurotransmitter regulation: FGF-21 could activate the HPA axis through the ERK/CREB pathway and induce the expression of corticotropin-releasing hormone (CRH) and ACTH, thereby regulating the secretion of serum corticosterone (Kuroda et al., 2017).

Researchers have gradually identified a close link between lipid metabolism disorders and dementia, especially AD. Disturbed lipid metabolism leads to aberrant levels and types of lipids such as fats, cholesterol, fatty acids, lipoproteins, and phospholipids. These abnormal changes affect the gut microbiota, brain-gut peptides, and neurotransmitter signaling and cause BBB disruption, mitochondrial dysfunction, oxidative stress, and inflammation, which eventually combine to cause a decline in synaptic plasticity and cognitive impairment (Kao et al., 2020). Lipidomics is a novel technique for researching the mechanism of lipid metabolism, which Akyol et al. (2021) have utilized to compare the biochemical profiles of brain tissues from patients with different degrees of AD. They found that different subgenera of lipids in AD were significantly disturbed, including neutral lipids, glycerolipids, glycerophospholipids, and sphingolipids (Akyol et al., 2021).

Interestingly, serum FGF-21 levels were reduced in both animal models and patients of AD but increased following cognitive improvement (Tournissac et al., 2019; Conte et al., 2021). Recombinant human FGF-21 could reduce the concentrations of total cholesterol, low-density lipoprotein, and high-density lipoprotein, inhibit neuroinflammation, and correct cognitive decline in cognitive impairment caused by hyperlipidaemia (Wang Q. et al., 2018). This

result may be attributed to the capacity of FGF21 to regulate the lipolytic signaling pathway, or insulin signaling pathway, in hepatocytes (Gimeno and Moller, 2014). Researchers also found that the administration of exogenous FGF-21 suppressed the expression of β-site amyloid precursor protein cleaving enzyme1 (Bace1), reduced Aβ deposition, and improved manifestations of dementia by inhibiting neuroinflammation through the TLR4/NF-κB signaling pathway, which could also restrain apoptosis via the MAPK signaling pathway (Amiri et al., 2018; Chen S. et al., 2019; Taliyan et al., 2019). These suggest a correlation between FGF-21 and AD, which makes it a potential biomarker for exploring new biomarkers, developing new drug targets, and providing new directions for in-depth exploration of AD metabolic mechanisms. Besides, since FGF21 could improve neuronal metabolism and energy supply in the CNS, enhance neuronal plasticity, and repair cerebrovascular endothelium to relieve symptoms of cognitive impairment, developing new drugs based on FGF-21 might be the most suitable choice to explore a new therapy for VaD. The potential therapeutic mechanisms of FGF-21 are shown in Figure 2.

2.2.3. FGF-23

FGF-23 is a bone-released endocrine growth factor and a member of the FGF-19 subgroup. FGF-23 is synthesized by osteoblasts and osteoclasts that are distributed primarily in the kidney, cortex, hippocampus, hypothalamus, thyroid gland, and bone, but also to a small degree in the spleen, liver, and other tissues (Hensel et al., 2016; Kuro-O, 2021; Ursem et al., 2021). FGF-23 primarily binds to α-KL/FGFR-1 to exert physiological effects, including regulating phosphate homeostasis and glucose metabolism, promoting neurogenesis, and maintaining emotional and cognitive functions (Beenken and Mohammadi, 2009; Kuro-O, 2021). FGF-23 overexpression in the serum may induce impaired hippocampal long-time potentiation (LTP) and reduce hippocampal adenosine-triphosphate (ATP) content with cognitive and memory decline, especially in people with chronic kidney disease (Liu et al., 2011; Drew et al., 2014; Drew and Weiner, 2014). Although Zhu et al. (2018) arrived at the opposite conclusion as they observed no significant differences between the levels of serum FGF-23 in individuals with mild cognitive impairment and healthy individuals, however, they assayed FGF-23 in a different way compared to previous experiments, which may explain the discrepancy in the results. The difference might also be attributed to the fact that FGF-23, like FGF-21, is affected by sex, and it is also possible that FGF-23 levels in the cerebrospinal fluid and blood are different. FGF-23 knockout mice also exhibited cognitive impairment in several *in vivo* studies, which may be associated with dysregulation of phosphate homeostasis and cytotoxicity (Laszczyk et al., 2019). As for the *in vitro* studies, the FGF-23/α-KL/FGFR-1 pathway was shown to increase hippocampal neuronal synaptic density but inhibits neuronal ramification via activating the downstream Akt signaling pathway, leading to memory deficits (Hensel et al., 2016; Zhu et al., 2018). These difference between animal and cellular experiments suggest that FGF-23 may have bidirectional modulatory effects on cognitive function.

On the other hand, intracranial atherosclerosis may trigger endothelial injury in blood vessels, induce neuroinflammation, and thus damage the structure and function of key brain regions where emotion and cognition are regulated, such as the hippocampus (Castello et al., 2022). In the vascular system, FGF-23 could bind directly to FGFR-2 or FGFR-3 without α-KL to induce vascular calcification (Vervloet, 2019). Thus, FGF-23 is highly associated with atherosclerosis and is a significant risk factor for atherosclerosis and stroke (Fakhri et al., 2014; Chang et al., 2020; Zheng et al., 2020). In other words, FGF-23 may indirectly trigger cognitive impairment by aggravating cerebrovascular damage. The potential therapeutic mechanisms of FGF-23 are shown in Figure 2.

3. Fibroblast growth factor receptors in cognitive disorders and dementia

The four main fractions of the transmembrane receptor tyrosine kinase FGFR, including FGFR-1, FGFR-2, FGFR-3, and FGFR-4, can mediate the signaling of FGFs via HS or KL-dependent pathways. Although all FGFRs are widely distributed in the CNS, existing evidence suggests that the main receptor that has been observed to change significantly in cognitive disorders is FGFR-1 (Goswami et al., 2013).

3.1. FGFRs

FGFR-1 is predominantly expressed in the hippocampus, and mediates downstream pathways by inhibiting neuroinflammation and maintaining LTP to protect learning and cognitive abilities (Rajendran et al., 2021). FGF-2, FGF-9, and FGF-22 can bind directly to FGFR-1 in the CNS. For example, the BBB protective effect on the BBB exhibited by FGF-2 is achieved by activating FGFR-1 (Lin et al., 2018), whereas the involvement of β-KL is required for binding FGF-21 and FGF-23 to FGFR-1, as mentioned above. Alternatively, dramatic AHN restriction, diminished amplitude of LTP, and hypomnesia could be observed in FGFR-1 knockout mice, and these changes were reversed with FGFR-1 agonists (Zhao et al., 2007; Pereda-Pérez et al., 2019). A compensatory increase in FGFR-3 expression can be observed in ASTs in the vicinity of "senile plaques" in AD patients (Ferrer and Martí, 1998). Moreover, FGF-2 binding to FGFR-3 could activate the anti-inflammatory phenotype of MG, inhibit excitatory toxicity, and exert neuroprotective effects through regulation of the ERK1/2 signaling pathway (Noda et al., 2014). Although the expression of FGFR-4 is low in the CNS and mainly concentrated in specific brain areas, especially the hypothalamus, FGF-15/19 could only inhibit the HPA axis and exert insulin-like effects by specifically binding to FGFR-4 due to the relatively low number of β-KL in the hypothalamus. Experiments by Ryan et al. (2013) showed that FGF-15/19/β-KL/FGFR-4 in the hypothalamus plays an integral role in regulating glucose metabolism throughout the body. As previously mentioned, abnormal glucose metabolism is strongly associated with the development of cognitive impairment and dementia. FGFRs demonstrate high homology and overlapping recognizability, which means there is no corresponding relationship between FGFRs and FGFs. Thus, it is difficult to study the changes in FGFRs. However, the future progressive exploration of the correspondence between FGFs and FGFRs and their downstream pathways will have profound implications for the study and application of the FGFs/FGFRs system in the field of neuroscience.

3.2. Co-receptor KL protein

Endocrine FGFs have a poor affinity to HS, and all have to form different homodimers by binding the co-receptor KL protein to the corresponding FGFR to activate the downstream pathways, such as FGF-19/β-KL/FGFR-4, FGF-21/β-KL/FGFR-1, or FGF-23/α-KL/FGFR-1. Subsequently, endocrine FGFs exert beneficial cognitive effects by inhibiting the HPA axis activation, suppressing neuroinflammation, facilitating BA metabolism, enhancing insulin sensitivity, and promoting neurogenesis. KL is divided into three categories according to the protein-coding genes, namely low molecular weight α-KL, high molecular weight β-KL, and γ-KL (Massó et al., 2015; Zhou et al., 2015). The α-KL can be further divided into transmembrane (m-KL), free, and secretory type, with the latter two referred to as soluble KL (s-KL), which is one of the hot spots in current dementia research. Researchers have only observed γ-KL in brown adipose tissue and eyeballs and have not yet found an association with the FGFs/FGFRs system (Zhang et al., 2017; Ma et al., 2021). Although much evidence suggests that α-KL has essential effects on cognition and memory, these studies have focused on s-KL rather than m-KL as a ligand for FGF-23 (Cararo-Lopes et al., 2017; Li et al., 2017; Zhao et al., 2020; Tank et al., 2021). These two α-KL have different structural features and physiological roles. However, recent studies have also identified, that hydrolyzed m-KL is a significant source of s-KL (Chen et al., 2007). β-KL protein is mainly distributed in the liver, gallbladder, kidney, brain, and other tissues, synthesized by ependymal cells in the hippocampus in CNS, and excreted into the cerebrospinal fluid, where it can exert antioxidant, anti-inflammatory, and neuroprotective effects (Paroni et al., 2019). These effects may be attributed directly to inhibiting neuroinflammation, reducing oxidative stress, and correcting vascular endothelial dysfunction or indirectly by activating pathways related to endocrine FGFs (Gold et al., 2013).

4. Discussion

FGFs and their receptors constitute a complex network of endocrine functions, and the dynamic balance between FGFs and their receptors may be a critical link that our understanding of cognitive regulation. When the FGFs/FGFRs system is out of balance, pathological changes such as disturbance of glucose metabolism disorder, neuroinflammation, hyperfunction of the HPA axis, disruption of the BBB, reduced neuroplasticity, inhibition of neurogenesis, and apoptosis may occur in the body, which in turn can affect the structure and function of the cerebral cortex, hippocampus, hypothalamus, pituitary gland, and other tissues, resulting in cognitive decline. Therefore, maintaining the stability of the FGF-FGFR system might have the potential to be a new therapeutic strategy for retarding neurodegeneration and improving cognitive function. Endocrine FGFs could be distributed through the blood circulation to multiple organs throughout the body, so they can exert a comprehensive neuroprotective effect by intervening in multiple systems. Besides, The physiological characteristics of endocrine FGFs allow them to penetrate the BBB to act on the brain parenchyma and exert neuroprotective effects easier than paracrine FGFs, including FGF-1, FGF-2, and FGF-9, via multiple metabolic pathways.

In recent years, FGFs-based drugs have been widely used in the clinical treatment of wound healing, osteoarthritis, malignancies, hepatitis, diabetes, cardiovascular disease and cerebrovascular disease (Zhang and Li, 2016; Sanyal et al., 2019; Abou-Alfa et al., 2020; Chen K. et al., 2022; Subbiah et al., 2022). Although the relevance of the FGF-FGFR system to neurodegenerative diseases has been identified, the application of FGF-based drugs remains *in vivo* and *in vivo* experiments which are still far from clinical application for treating cognitive disorders. Moreover, the use of FGFs as biomarkers for detecting neurodegenerative diseases is also limited by many factors. Although researchers are still unable to elucidate the specific mechanisms of the FGFs/FGFRs system, they have noted the trends and therapeutic potential of multiple FGFs in various diseases and have discovered or developed drugs, such as synthetic human recombinant FGFs (Bogousslavsky et al., 2002), synthetic analogs of FGFs (Sanyal et al., 2019; Ardizzone et al., 2022), molecular inhibitors or agonists of FGFs/FGFRs (Bahleda et al., 2020; van Brummelen et al., 2020; Subbiah et al., 2022), or extracts of natural herbal medicines (Hong et al., 2016; Yuan et al., 2019; Cheng et al., 2021; Wang et al., 2021) that could effectively modulate this system. In the current literature review, we found that the difficulties faced by previous studies on the application of FGFs/FGFRs systems in treatment and diagnose mainly focus on the following four aspects (Figure 3): (1) Different FGFs isoforms: some FGFs have different molecular weight isoforms with different physiological effects, but their individual microscopic expression changes cannot be reflected by the overall changes, for example, High molecular weight (HMW) FGF-2 and Light molecular weight (LMW) FGF-2 (Chlebova et al., 2009; Katsouri et al., 2015; Chen X. et al., 2019). (2) Inhomogeneous space distribution of FGFs: the spatial distribution of FGFs in serum, cerebrospinal fluid and brain parenchyma is inhomogeneous, because some FGFs cannot completely penetrate the BBB. The following may obscure particular properties of FGFs in various tissues under pathological state, and render the statistical assessment their heterogeneity inaccurate (Katsouri et al., 2015; Liu et al., 2017; Chang et al., 2018; Tennakoon et al., 2022). (3) Correspondence between FGFs and FGFRs: single FGF could bind to different FGFRs in different microenvironments and regulate different signaling pathways, thus exerting distinct physiological or pathological effects, due to the overlapping recognition of FGFRs and discrepancy in expression sites (Lee et al., 2011; Noda et al., 2014; Lin et al., 2018; Vervloet, 2019). (4) Competitive inhibition between FGFs: FGFs are highly homologous, and subtypes with similar physiological structures may compete with one another for the same receptors, thereby inhibiting the regulation of downstream signaling pathways such as FGF-17 and FGF-15/19 (Liu S. et al., 2018), FGF-2 and FGF-9 (Aurbach et al., 2015).

5. Conclusion

In summary, despite the induced cell proliferation, survival and differentiation, angiogenesis promotion, inflammation inhibition, immune and metabolic modulation, and antioxidant effects possessed by the FGF/FGFR system have been applied in the treatment of tumors, trauma, and renal, hepatic, and cardiovascular diseases, there is still a substantial unexplored gap area, especially for the modulatory

10.3389/fnins.2023.1136266

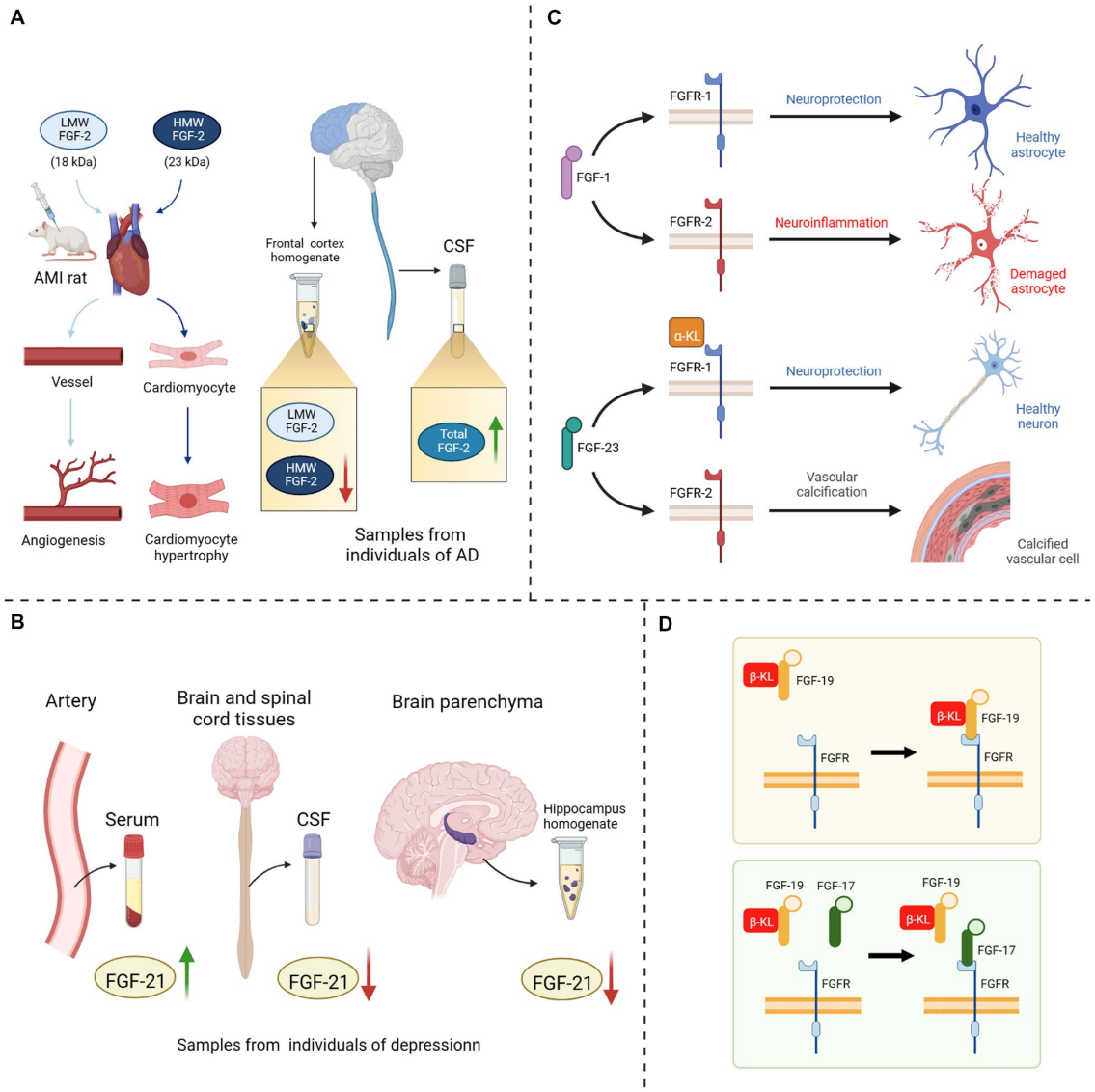

FIGURE 3
Four potential explanations for the hampered FGF in-depth study. **(A)** Different isoforms of FGF-2: injection of HMW FGF-2 into AMI rats could induce cardiomyocyte hypertrophy, whereas injection of LMW FGF-2 only promoted angiogenesis in rat heart; A decrease in HMW FGF-2 expression could be detected in the anterior cortical homogenate of AD patients, while the expression level of LMW FGF-2 remained unchanged, and the level of total FGF-2 in the CSF was significantly increased. **(B)** Inhomogeneous space distribution of FGF21: the expression level of FGF-21 was elevated in the serum of depressed patients, while decreased in both CSF and hippocampus homogenate. **(C)** Correspondence between FGFs and FGFRs: when FGF-1 bound to FGFR-1, it could exert neuroprotective effects, while binding to FGFR-2 could provoke neuroinflammation; The binding of FGF-23 to α-KL/FGFR-1 protects neuronal cells, on the contrary it directly binds to FGFR-2 to induce vascular calcification. **(D)** Competitive inhibition between FGF17 and FGF19: FGF-17 could bind to the β-KL/FGFR-2 homodimer and shown antagonism against FGF-19. LMW, light molecular weight; HMW, high molecular weight; AMI, acute myocardial infarction; CSF, cerebrospinal fluid; AD, Alzheimer's disease; FGF, fibroblast growth factor; FGFR, fibroblast growth factor receptor; α/β-KL, α/β-klotho protein.

effects and diagnostic value of central nervous system diseases and psychiatric disorders. Considering the extensive range of actions and the many targets of the FGF/FGFR system intervention, we should also be aware of the potential risk associated with its long-term or high-dose use, such as adverse effects, resistance, and addiction, when used to treat cognitive or mood disorders. Here, we propose to conduct more clinical and basic studies in combination with new technologies to investigate the structural and functional characteristics of the FGFs/FGFRs system and its specific mechanism in cognitive disorders and dementia to find new biomarkers and therapeutic approaches for these diseases.

Author contributions

WZ and TZ conceived the topic and drafted the manuscript. YJ helped WZ to draw the figures. SH, MX, and JP revised the draft. All authors contributed to the article and approved the submitted version.

Funding

This research was supported by National Natural Science Foundation of China (NSFC-81573790, NSFC-81603443, and NSFC-82204922) and the Fundamental Research Funds for the Central public welfare research institutes of China (no. ZZ15-XY-LCQ-04).

Acknowledgments

We would like to thank Editage (www.editage.cn) for English language editing and BioRender (www.biorender.com) for Excellent drawing tool. All the figures in the text are created with BioRender.com.

Conflict of interest

The authors declare that the research was conducted in the absence of any commercial or financial relationships that could be construed as a potential conflict of interest.

Publisher's note

All claims expressed in this article are solely those of the authors and do not necessarily represent those of their affiliated organizations, or those of the publisher, the editors and the reviewers. Any product that may be evaluated in this article, or claim that may be made by its manufacturer, is not guaranteed or endorsed by the publisher.

References

Abou-Alfa, G. K., Sahai, V., Hollebecque, A., Vaccaro, G., Melisi, D., Al-Rajabi, R., et al. (2020). Pemigatinib for previously treated, locally advanced or metastatic cholangiocarcinoma: a multicentre, open-label, phase 2 study. *Lancet Oncol.* 21, 671–684. doi: 10.1016/S1470-2045(20)30109-1

Akyol, S., Ugur, Z., Yilmaz, A., Ustun, I., Gorti, S. K. K., Oh, K., et al. (2021). Lipid profiling of Alzheimer's disease brain highlights enrichment in glycerol(phospho)lipid, and sphingolipid metabolism. *Cells* 10:2591. doi: 10.3390/cells10102591

Al-Aqil, F. A., Monte, M. J., Peleteiro-Vigil, A., Briz, O., Rosales, R., González, R., et al. (2018). Interaction of glucocorticoids with FXR/FGF19/FGF21-mediated ileum-liver crosstalk. Biochimica et biophysica acta. *Mol Basis Dis* 1864, 2927–2937. doi: 10.1016/j.bbadis.2018.06.003

Amiri, M., Braidy, N., and Aminzadeh, M. (2018). Protective effects of fibroblast growth factor 21 against amyloid-Beta-induced toxicity in SH-SY5Y cells. *Neurotox. Res.* 34, 574–583. doi: 10.1007/s12640-018-9914-2

Anderson, N. D. (2019). State of the science on mild cognitive impairment (MCI). *CNS Spectr.* 24, 78–87. doi: 10.1017/S1092852918001347

Ardizzone, A., Bova, V., Casili, G., Filippone, A., Campolo, M., Lanza, M., et al. (2022). SUN11602, a bFGF mimetic, modulated neuroinflammation, apoptosis and calcium-binding proteins in an in vivo model of MPTP-induced nigrostriatal degeneration. *J. Neuroinflammation* 19:107. doi: 10.1186/s12974-022-02457-3

Aurbach, E. L., Inui, E. G., Turner, C. A., Hagenauer, M. H., Prater, K. E., Li, J. Z., et al. (2015). Fibroblast growth factor 9 is a novel modulator of negative affect. *Proc. Natl. Acad. Sci. U. S. A.* 112, 11953–11958. doi: 10.1073/pnas.1510456112

Azhar, M., Zeng, G., Ahmed, A., Dar Farooq, A., Choudhary, M. I., De-Jiang, J., et al. (2021). Carnosic acid ameliorates depressive-like symptoms along with the modulation of FGF9 in the hippocampus of middle carotid artery occlusion-induced Sprague Dawley rats. *Phytother. Res.* 35, 384–391. doi: 10.1002/ptr.6810

Bahleda, R., Meric-Bernstam, F., Goyal, L., Tran, B., He, Y., Yamamiya, I., et al. (2020). Phase I, first-in-human study of futibatinib, a highly selective, irreversible FGFR1-4 inhibitor in patients with advanced solid tumors. *Ann. Oncol.* 31, 1405–1412. doi: 10.1016/j.annonc.2020.06.018

Ball, H. A., McWhirter, L., Ballard, C., Bhome, R., Blackburn, D. J., Edwards, M. J., et al. (2020). Functional cognitive disorder: dementia's blind spot. Brain: a. *J. Neurol.* 143, 2895–2903. doi: 10.1093/brain/awaa224

Baloni, P., Funk, C. C., Yan, J., Yurkovich, J. T., Kueider-Paisley, A., Nho, K., et al. (2020). Metabolic network analysis reveals altered bile acid synthesis and metabolism in Alzheimer's disease. *Cell Rep Med* 1:100138. doi: 10.1016/j.xcrm.2020.100138

Beenken, A., and Mohammadi, M. (2009). The FGF family: biology, pathophysiology and therapy. *Nat. Rev. Drug Discov.* 8, 235–253. doi: 10.1038/nrd2792

Belov, A. A., and Mohammadi, M. (2013). Molecular mechanisms of fibroblast growth factor signaling in physiology and pathology. *Cold Spring Harb. Perspect. Biol.* 5:a015958. doi: 10.1101/cshperspect.a015958

Bennett, S., and Thomas, A. J. (2014). Depression and dementia: cause, consequence or coincidence? *Maturitas* 79, c–190. doi: 10.1016/j.maturitas.2014.05.009

Bogousslavsky, J., Victor, S. J., Salinas, E. O., Pallay, A., Donnan, G. A., Fieschi, C., et al. (2002). Fiblast (trafermin) in acute stroke: results of the European-Australian phase II/III safety and efficacy trial. *Cerebrovasc. Dis.* 14, 239–251. doi: 10.1159/000065683

Butterfield, D. A., and Halliwell, B. (2019). Oxidative stress, dysfunctional glucose metabolism and Alzheimer disease. *Nat. Rev. Neurosci.* 20, 148–160. c

Byers, A. L., and Yaffe, K. (2011). Depression and risk of developing dementia. *Nat. Rev. Neurol.* 7, 323–331. doi: 10.1038/nrneurol.2011.60

Canet, G., Hernandez, C., Zussy, C., Chevallier, N., Desrumaux, C., and Givalois, L. (2019). Is AD a stress-related disorder? Focus on the HPA Axis and its promising therapeutic targets. *Front. Aging Neurosci.* 11:269. doi: 10.3389/fnagi.2019.00269

Cararo-Lopes, M. M., Mazucanti, C. H. Y., Scavone, C., Kawamoto, E. M., and Berwick, D. C. (2017). The relevance of α-KLOTHO to the central nervous system: some key questions. *Ageing Res. Rev.* 36, 137–148. doi: 10.1016/j.arr.2017.03.003

Castello, J. P., Pasi, M., Kubiszewski, P., Abramson, J. R., Charidimou, A., Kourkoulis, C., et al. (2022). Cerebral small vessel disease and depression among intracerebral hemorrhage survivors. *Stroke* 53, 523–531. doi: 10.1161/STROKEAHA.121.035488

Chang, H. H., Chen, P. S., Cheng, Y. W., Wang, T. Y., Yang, Y. K., and Lu, R. B. (2018). FGF21 is associated with metabolic effects and treatment response in depressed bipolar II disorder patients treated with valproate. *Int. J. Neuropsychopharmacol.* 21, 319–324. doi: 10.1093/ijnp/pyx093

Chang, Y., Kim, J., Woo, H. G., Ryu, D. R., Oh, H. J., and Song, T. J. (2020). Plasma fibroblast growth factor 23 concentration is associated with intracranial cerebral atherosclerosis in acute ischemic stroke patients. *J. Clin. Neurol.* 16, 29–36. doi: 10.3988/jcn.2020.16.1.29

Chen, Q., Chen, X., Jia, Z., Du, Y., Zhang, S., Xu, W., et al. (2022). ΔnFGF1 protects-cells against high glucose-induced apoptosis via the AMPK/SIRT1/PGC-1 Axis. *Oxid. Med. Cell. Longev.* 2022:1231970. doi: 10.1155/2022/1231970

Chen, S., Chen, S. T., Sun, Y., Xu, Z., Wang, Y., Yao, S. Y., et al. (2019). Fibroblast growth factor 21 ameliorates neurodegeneration in rat and cellular models of Alzheimer's disease. *Redox Biol.* 22:101133. doi: 10.1016/j.redox.2019.101133

Chen, J., Hu, J., Liu, H., Xiong, Y., Zou, Y., Huang, W., et al. (2018). FGF21 protects the blood-brain barrier by upregulating PPARgamma via FGFR1/beta-klotho after traumatic brain injury. *J. Neurotrauma* 35, 2091–2103. doi: 10.1089/neu.2017.5271

Chen, X., Li, Z., Cheng, Y., Kardami, E., and Loh, Y. P. (2019). Low and high molecular weight FGF-2 have differential effects on astrocyte proliferation, but are both protective against Aβ-induced cytotoxicity. *Front. Mol. Neurosci.* 12:328. doi: 10.3389/fnmol.2019.00328

Chen, C.-D., Podvin, S., Gillespie, E., Leeman, S. E., and Abraham, C. R. (2007). Insulin stimulates the cleavage and release of the extracellular domain of klotho by ADAM10 and ADAM17. *Proc. Natl. Acad. Sci. U. S. A.* 104, 19796–19801. doi: 10.1073/pnas.0709805104

Chen, K., Rao, Z., Dong, S., Chen, Y., Wang, X., Luo, Y., et al. (2022). Roles of the fibroblast growth factor signal transduction system in tissue injury repair. *Burns Trauma* 10:tkac005. doi: 10.1093/burnst/tkac005

Chen, Y., Wang, Y., Qin, Q., Zhang, Y., Xie, L., Xiao, J., et al. (2022). Carnosic acid ameliorated Aβ-mediated (amyloid-β peptide) toxicity, cholinergic dysfunction and mitochondrial defect in of Alzheimer's model. *Food Funct.* 13, 4624–4640. doi: 10.1039/d1fo02965g

Chen, Z., and Zhong, C. (2013). Decoding Alzheimer's disease from perturbed cerebral glucose metabolism: implications for diagnostic and therapeutic strategies. *Prog. Neurobiol.* 108, 21–43. doi: 10.1016/j.pneurobio.2013.06.004

Cheng, J., Chen, M., Wan, H.-Q., Chen, X.-Q., Li, C.-F., Zhu, J.-X., et al. (2021). Paeoniflorin exerts antidepressant-like effects through enhancing neuronal FGF-2 by microglial inactivation. *J. Ethnopharmacol.* 274:114046. doi: 10.1016/j.jep.2021.114046

Cheng, L., Huang, C., and Chen, Z. (2019). Tauroursodeoxycholic acid ameliorates lipopolysaccharide-induced depression like behavior in mice via the inhibition of Neuroinflammation and Oxido-Nitrosative stress. *Pharmacology* 103, 93–100. doi: 10.1159/000494139

Chlebova, K., Bryja, V., Dvorak, P., Kozubik, A., Wilcox, W. R., and Krejci, P. (2009). High molecular weight FGF2: the biology of a nuclear growth factor. *Cell. Mol. Life Sci.* 66, c. doi: 10.1007/s00018-008-8440-4

Chuang, J.-I., Huang, J.-Y., Tsai, S.-J., Sun, H. S., Yang, S.-H., Chuang, P.-C., et al. (2015). FGF9-induced changes in cellular redox status and HO-1 upregulation are FGFR-dependent and proceed through both ERK and AKT to induce CREB and Nrf2 activation. *Free Radic. Biol. Med.* 89, 274–286. doi: 10.1016/j.freeradbiomed.2015.08.011

Conte, M., Sabbatinelli, J., Chiariello, A., Martucci, M., Santoro, A., Monti, D., et al. (2021). Disease-specific plasma levels of mitokines FGF21, GDF15, and Humanin in type II diabetes and Alzheimer's disease in comparison with healthy aging. *GeroScience* 43, 985–1001. doi: 10.1007/s11357-020-00287-w

Csernansky, J. G., Dong, H., Fagan, A. M., Wang, L., Xiong, C., Holtzman, D. M., et al. (2006). Plasma cortisol and progression of dementia in subjects with Alzheimer-type dementia. *Am. J. Psychiatry* 163, 2164–2169. doi: 10.1176/ajp.2006.163.12.2164

Cummings, B. J., Su, J. H., and Cotman, C. W. (1993). Neuritic involvement within bFGF immunopositive plaques of Alzheimer's disease. *Exp. Neurol.* 124, 315–325.

Cunningham, J., Locatelli, F., and Rodriguez, M. (2011). Secondary hyperparathyroidism: pathogenesis, disease progression, and therapeutic options. *Clin. J. Am. Soc. Nephrol.* 6, 913–921. doi: 10.2215/CJN.06040710

Deng, Z., Deng, S., Zhang, M. R., and Tang, M. M. (2019). Fibroblast growth factors in depression. *Front. Pharmacol.* 10:60. doi: 10.3389/fphar.2019.00060

Dichgans, M., and Leys, D. (2017). Vascular Cognitive Impairment. *Circ. Res.* 120, 573–591. doi: 10.1161/CIRCRESAHA.116.308426

Dienel, G. A. (2012). Fueling and imaging brain activation. *ASN Neuro* 4:e00093. doi: 10.1042/AN20120021

Dolegowska, K., Marchelek-Mysliwiec, M., Nowosiad-Magda, M., Slawinski, M., and Dolegowska, B. (2019). FGF19 subfamily members: FGF19 and FGF21. *J. Physiol. Biochem.* 75, 229–240. doi: 10.1007/s13105-019-00675-7

Drew, D. A., Tighiouart, H., Scott, T. M., Lou, K. V., Fan, L., Shaffi, K., et al. (2014). FGF-23 and cognitive performance in hemodialysis patients. Hemodialysis international. *Int Symp Home Hemodial* 18, 78–86. doi: 10.1111/hdi.12100

Drew, D. A., and Weiner, D. E. (2014). Cognitive impairment in chronic kidney disease: keep vascular disease in mind. *Kidney Int.* 85, 505–507. doi: 10.1038/ki.2013.437

Duff, K., Paulsen, J., Mills, J., Beglinger, L. J., Moser, D. J., Smith, M. M., et al. (2010). Mild cognitive impairment in prediagnosed Huntington disease. *Neurology* 75, 500–507. doi: 10.1212/WNL.0b013e3181eccfa2

Fakhri, H., Ricken, R., Adli, M., Fajol, A., Walter, M., Föller, M., et al. (2014). Impact of lithium treatment on FGF-23 serum concentrations in depressive patients. *J. Clin. Psychopharmacol.* 34, 745–747. doi: 10.1097/JCP.0000000000000163

Feng, C., Zhang, C., Shao, X., Liu, Q., Qian, Y., Feng, L., et al. (2012). Enhancement of nose-to-brain delivery of basic fibroblast growth factor for improving rat memory impairments induced by co-injection of β-amyloid and ibotenic acid into the bilateral hippocampus. *Int. J. Pharm.* 423, 226–234. doi: 10.1016/j.ijpharm.2011.12.008

Ferrer, I., and Martí, E. (1998). Distribution of fibroblast growth factor receptor-1 (FGFR-1) and FGFR-3 in the hippocampus of patients with Alzheimer's disease. *Neurosci. Lett.* 240, 139–142.

Galvez-Contreras, A. Y., Campos-Ordonez, T., Lopez-Virgen, V., Gomez-Plascencia, J., Ramos-Zuniga, R., and Gonzalez-Perez, O. (2016). Growth factors as clinical biomarkers of prognosis and diagnosis in psychiatric disorders. *Cytokine Growth Factor Rev.* 32, 85–96. doi: 10.1016/j.cytogfr.2016.08.004

Garnier-Crussard, A., Bougacha, S., Wirth, M., Dautricourt, S., Sherif, S., Landeau, B., et al. (2022). White matter hyperintensity topography in Alzheimer's disease and links to cognition. *Alzheimers Dement.* 18, 422–433. doi: 10.1002/alz.12410

Gasser, E., Moutos, C. P., Downes, M., and Evans, R. M. (2017). FGF1-a new weapon to control type 2 diabetes mellitus. *Nat. Rev. Endocrinol.* 13, 599–609. doi: 10.1038/nrendo.2017.78

Gee, L. M. V., Barron-Millar, B., Leslie, J., Richardson, C., Zaki, M. Y. W., Luli, S., et al. (2022). Anti-Cholestatic therapy with Obeticholic acid improves short-term memory in bile duct ligated mice. *Am. J. Pathol.* 193, 11–26. doi: 10.1016/j.ajpath.2022.09.005

Giacomini, A., Chiodelli, P., Matarazzo, S., Rusnati, M., Presta, M., and Ronca, R. (2016). Blocking the FGF/FGFR system as a two-compartment antiangiogenic/antitumor approach in cancer therapy. *Pharmacol. Res.* cc. doi: 10.1016/j.phrs.2016.03.024

Gimeno, R. E., and Moller, D. E. (2014). FGF21-based pharmacotherapy--potential utility for metabolic disorders. *Trends Endocrinol. Metab.* 25, 303–311. doi: 10.1016/j.tem.2014.03.001

Gold, P. W., Licinio, J., and Pavlatou, M. G. (2013). Pathological parainflammation and endoplasmic reticulum stress in depression: potential translational targets through the CNS insulin, klotho and PPAR-gamma systems. *Mol. Psychiatry* 18, 154–165. doi: 10.1038/mp.2012.167

Gonzales, M. M., Garbarino, V. R., Pollet, E., Palavicini, J. P., Kellogg, D. L., Kraig, E., et al. (2022). Biological aging processes underlying cognitive decline and neurodegenerative disease. *J. Clin. Invest.* 132:e158453. doi: 10.1172/JCI158453

Goswami, D. B., Jernigan, C. S., Chandran, A., Iyo, A. H., May, W. L., Austin, M. C., et al. (2013). Gene expression analysis of novel genes in the prefrontal cortex of major depressive disorder subjects. *Prog. Neuropsychopharmacol. Biol. Psychiatry* 43, 126–133. doi: 10.1016/j.pnpbp.2012.12.010

Hamer, J. A., Testani, D., Mansur, R. B., Lee, Y., Subramaniapillai, M., and McIntyre, R. S. (2019). Brain insulin resistance: a treatment target for cognitive impairment and anhedonia in depression. *Exp. Neurol.* 315, 1–8. doi: 10.1016/j.expneurol.2019.01.016

Han, K.-H., Kim, M.-H., Jeong, G.-J., Kim, A.-K., Chang, J. W., and Kim, D.-I. (2019). FGF-17 from hypoxic human Wharton's jelly-derived mesenchymal stem cells is responsible for maintenance of cell proliferation at late passages. *Int J Stem Cells* 12, 279–290. doi: 10.15283/ijsc18042

Hayley, S., Hakim, A. M., and Albert, P. R. (2021). Depression, dementia and immune dysregulation. *Brain* 144, 746–760. doi: 10.1093/brain/awaa405

He, H., Chen, Z., Chen, D., Lu, X., Huang, C., and Chen, J. (2021). Identification of the expression of farnesoid X receptor in astrocytes. *Neuroreport* 32, 1216–1222. doi: 10.1097/WNR.0000000000001717

Hecht, D., Zimmerman, N., Bedford, M., Avivi, A., and Yayon, A. (1995). Identification of fibroblast growth factor 9 (FGF9) as a high affinity, heparin dependent ligand for FGF receptors 3 and 2 but not for FGF receptors 1 and 4. *Growth Factors* 12, 223–233.

Hensel, N., Schön, A., Konen, T., Lübben, V., Förthmann, B., Baron, O., et al. (2016). Fibroblast growth factor 23 signaling in hippocampal cells: impact on neuronal morphology and synaptic density. *J. Neurochem.* 137, 756–769. doi: 10.1111/jnc.13585

Holmes, D. (2014). Therapy: FGF1 restores blood glucose levels and insulin sensitivity in diabetic mice. *Nat. Rev. Endocrinol.* 10:576. doi: 10.1038/nrendo.2014.129

Hong, X.-P., Chen, T., Yin, N.-N., Han, Y.-M., Yuan, F., Duan, Y.-J., et al. (2016). Puerarin ameliorates D-galactose induced enhanced hippocampal neurogenesis and tau hyperphosphorylation in rat brain. *J. Alzheimers Dis.* 51, 605–617. doi: 10.3233/JAD-150566

Hoshikawa, M., Ohbayashi, N., Yonamine, A., Konishi, M., Ozaki, K., Fukui, S., et al. (1998). Structure and expression of a novel fibroblast growth factor, FGF-17, preferentially expressed in the embryonic brain. *Biochem. Biophys. Res. Commun.* 244, 187–191.

Hossain, M. S., Oomura, Y., Fujino, T., and Akashi, K. (2020). Glucose signaling in the brain and periphery to memory. *Neurosci. Biobehav. Rev.* 110, 100–113. doi: 10.1016/j.neubiorev.2019.03.018

Hotamisligil, G. S. (2006). Inflammation and metabolic disorders. *Nature* 444, 860–867. doi: 10.1038/nature05485

Hsuchou, H., Pan, W., and Kastin, A. J. (2013). Fibroblast growth factor 19 entry into brain. *Fluids Barriers CNS* 10:32. doi: 10.1186/2045-8118-10-32

Huang, C., Wang, J., Hu, W., Wang, C., Lu, X., Tong, L., et al. (2016). Identification of functional farnesoid X receptors in brain neurons. *FEBS Lett.* 590, 3233–3242. doi: 10.1002/1873-3468.12373

Hui, Q., Jin, Z., Li, X., Liu, C., and Wang, X. (2018). FGF family: from drug development to clinical application. *Int. J. Mol. Sci.* 19:1875. doi: 10.3390/ijms19071875

Iadecola, C., Duering, M., Hachinski, V., Joutel, A., Pendlebury, S. T., Schneider, J. A., et al. (2019). Vascular cognitive impairment and dementia: JACC scientific expert panel. *J. Am. Coll. Cardiol.* 73, 3326–3344. doi: 10.1016/j.jacc.2019.04.034

Ilieva, M., Nielsen, T. T., Michel, T., and Pankratova, S. (2019). FGF2 and dual agonist of NCAM and FGF receptor 1, Enreptin, rescue neurite outgrowth loss in hippocampal neurons expressing mutated huntingtin proteins. *J. Neural Transm.* 126, 1493–1500. doi: 10.1007/s00702-019-02073-1

Iram, T., Kern, F., Kaur, A., Myneni, S., Morningstar, A. R., Shin, H., et al. (2022). Young CSF restores oligodendrogenesis and memory in aged mice via Fgf17. *Nature* 605, 509–515. doi: 10.1038/s41586-022-04722-0

Jiang, Z.-S., Jeyaraman, M., Wen, G.-B., Fandrich, R. R., Dixon, I. M. C., Cattini, P. A., et al. (2007). High-but not low-molecular weight FGF-2 causes cardiac hypertrophy in vivo; possible involvement of cardiotrophin-1. *J. Mol. Cell. Cardiol.* 42, 222–233. doi: 10.1016/j.yjmcc.2006.09.002

Jiang, Y., Lin, L., Liu, N., Wang, Q., Yuan, J., Li, Y., et al. (2020). FGF21 protects against aggravated blood-brain barrier disruption after ischemic focal stroke in diabetic db/db male mice via cerebrovascular PPARgamma activation. *Int. J. Mol. Sci.* 21:824. doi: 10.3390/ijms21030824

Jin, K., LaFevre-Bernt, M., Sun, Y., Chen, S., Gafni, J., Crippen, D., et al. (2005). FGF-2 promotes neurogenesis and neuroprotection and prolongs survival in a transgenic mouse model of Huntington's disease. *Proc. Natl. Acad. Sci. U. S. A.* 102, 18189–18194. doi: 10.1073/pnas.0506375102

Kamal, F., Morrison, C., Maranzano, J., Zeighami, Y., and Dadar, M. (2022). Topographical differences in white matter hyperintensity burden and cognition in aging, MCI, and AD. *GeroScience.* 45, 1–16. doi: 10.1007/s11357-022-00665-6

Kao, Y.-C., Ho, P.-C., Tu, Y.-K., Jou, I. M., and Tsai, K.-J. (2020). Lipids and Alzheimer's disease. *Int. J. Mol. Sci.* 21:1505. doi: 10.3390/ijms21041505

Katsouri, L., Ashraf, A., Birch, A. M., Lee, K. K. L., Mirzaei, N., and Sastre, M. (2015). Systemic administration of fibroblast growth factor-2 (FGF2) reduces BACE1 expression and amyloid pathology in APP23 mice. *Neurobiol. Aging* 36, 821–831. doi: 10.1016/j.neurobiolaging.2014.10.004

Kellar, D., and Craft, S. (2020). Brain insulin resistance in Alzheimer's disease and related disorders: mechanisms and therapeutic approaches. *Lancet Neurol.* 19, 758–766. doi: 10.1016/S1474-4422(20)30231-3

Kharitonenkov, A., Shiyanova, T. L., Koester, A., Ford, A. M., Micanovic, R., Galbreath, E. J., et al. (2005). FGF-21 as a novel metabolic regulator. *J. Clin. Invest.* 115, 1627–1635. doi: 10.1172/JCI23606

Kiyota, T., Ingraham, K. L., Jacobsen, M. T., Xiong, H., and Ikezu, T. (2011). FGF2 gene transfer restores hippocampal functions in mouse models of Alzheimer's disease and has therapeutic implications for neurocognitive disorders. *Proc. Natl. Acad. Sci. U. S. A.* 108, E1339–E1348. doi: 10.1073/pnas.1102349108

Kuroda, M., Muramatsu, R., Maedera, N., Koyama, Y., Hamaguchi, M., Fujimura, H., et al. (2017). Peripherally derived FGF21 promotes remyelination in the central nervous system. *J. Clin. Invest.* 127, 3496–3509. doi: 10.1172/JCI94337

Kuro-O, M. (2021). Aging and FGF23-klotho system. *Vitam. Horm.* 115, 317–332. doi: 10.1016/bs.vh.2020.12.013

Lara, V. P., Caramelli, P., Teixeira, A. L., Barbosa, M. T., Carmona, K. C., Carvalho, M. G., et al. (2013). High cortisol levels are associated with cognitive impairment no-dementia (CIND) and dementia. *Clin Chim Acta Int J Clin Chem* 423, 18–22. doi: 10.1016/j.cca.2013.04.013

Laszczyk, A. M., Nettles, D., Pollock, T. A., Fox, S., Garcia, M. L., Wang, J., et al. (2019). FGF-23 deficiency impairs hippocampal-dependent cognitive function. *ENeuro* 6, e0469–18. doi: 10.1523/ENEURO.0469-18.2019

Lee, M., Kang, Y., Suk, K., Schwab, C., Yu, S., and McGeer, P. L. (2011). Acidic fibroblast growth factor (FGF) potentiates glial-mediated neurotoxicity by activating FGFR2 IIIb protein. *J. Biol. Chem.* 286, 41230–41245. doi: 10.1074/jbc.M111.270470

Leng, F., and Edison, P. (2021). Neuroinflammation and microglial activation in Alzheimer disease: where do we go from here? Nature reviews. *Neurology* 17, 157–172. doi: 10.1038/s41582-020-00435-y

Li, X. (2019). The FGF metabolic axis. *Front. Med.* 13, 511–530. doi: 10.1007/s11684-019-0711-y

Li, Q., Vo, H. T., Wang, J., Fox-Quick, S., Dobrunz, L. E., and King, G. D. (2017). Klotho regulates CA1 hippocampal synaptic plasticity. *Neuroscience* 347, 123–133. doi: 10.1016/j.neuroscience.2017.02.006

Li, C., Wang, X., Yan, J., Cheng, F., Ma, X., Chen, C., et al. (2020). Cholic acid protects in vitro neurovascular units against oxygen and glucose deprivation-induced injury through the BDNF-TrkB signaling pathway. *Oxid. Med. Cell. Longev.* 2020:1201624. doi: 10.1155/2020/1201624

Liang, C.-S., Tsai, C.-L., Lin, G.-Y., Lee, J.-T., Lin, Y.-K., Chu, C.-S., et al. (2021). Better identification of cognitive decline with Interleukin-2 than with amyloid and tau protein biomarkers in amnestic mild cognitive impairment. *Front. Aging Neurosci.* 13:670115. doi: 10.3389/fnagi.2021.670115

Lin, L., Wang, Q., Qian, K., Cao, Z., Xiao, J., Wang, X., et al. (2018). bFGF protects against oxygen glucose deprivation/Reoxygenation-induced endothelial monolayer permeability via S1PR1-dependent mechanisms. *Mol. Neurobiol.* 55, 3131–3142. doi: 10.1007/s12035-017-0544-0

Liu, P., Chen, L., Bai, X., Karaplis, A., Miao, D., and Gu, N. (2011). Impairment of spatial learning and memory in transgenic mice overexpressing human fibroblast growth factor-23. *Brain Res.* 1412, 9–17. doi: 10.1016/j.brainres.2011.07.028

Liu, S., Marcelin, G., Blouet, C., Jeong, J. H., Jo, Y.-H., Schwartz, G. J., et al. (2018). A gut-brain axis regulating glucose metabolism mediated by bile acids and competitive fibroblast growth factor actions at the hypothalamus. *Molec Metab* 8, 37–50. doi: 10.1016/j.molmet.2017.12.003

Liu, Y., Wang, M., Tan, X., Wang, X., Yang, X., Xiao, J., et al. (2017). Negative correlation between cerebrospinal fluid FGF21 levels and BDI scores in male Chinese subjects. *Psychiatry Res.* 252, 111–113. doi: 10.1016/j.psychres.2017.01.075

Liu, M., Wu, Y., Liu, Y., Chen, Z., He, S., Zhang, H., et al. (2018). Basic fibroblast growth factor protects astrocytes against ischemia/reperfusion injury by upregulating the Caveolin-1/VEGF signaling pathway. *J. Mol. Neurosci.* 64, 211–223. doi: 10.1007/s12031-017-1023-9

Lo, A. C., Callaerts-Vegh, Z., Nunes, A. F., Rodrigues, C. M. P., and D'Hooge, R. (2013). Tauroursodeoxycholic acid (TUDCA) supplementation prevents cognitive impairment and amyloid deposition in APP/PS1 mice. *Neurobiol. Dis.* 50, 21–29. doi: 10.1016/j.nbd.2012.09.003

Lu, Y., Sareddy, G. R., Wang, J., Zhang, Q., Tang, F.-L., Pratap, U. P., et al. (2020). Neuron-derived estrogen is critical for astrocyte activation and neuroprotection of the ischemic brain. *J. Neurosci.* 40, 7355–7374. doi: 10.1523/JNEUROSCI.0115-20.2020

Lu, X., Yang, R.-R., Zhang, J.-L., Wang, P., Gong, Y., Hu, W.-F., et al. (2018). Tauroursodeoxycholic acid produces antidepressant-like effects in a chronic unpredictable stress model of depression via attenuation of neuroinflammation, oxido-nitrosative stress, and endoplasmic reticulum stress. *Fundam. Clin. Pharmacol.* 32, 363–377. doi: 10.1111/fcp.12367

Luca, M., and Luca, A. (2019). Oxidative stress-related endothelial damage in vascular depression and vascular cognitive impairment: beneficial effects of aerobic physical exercise. *Oxid. Med. Cell. Longev.* 2019:8067045. doi: 10.1155/2019/8067045

Ma, Z., Li, J., Jiang, H., and Chu, Y. (2021). Expression of α-klotho is downregulated and associated with oxidative stress in the Lens in Streptozotocin-induced diabetic rats. *Curr. Eye Res.* 46, 482–489. doi: 10.1080/02713683.2020.1805768

Machado, M. F., Caixeta, E. S., Sudiman, J., Gilchrist, R. B., Thompson, J. G., Lima, P. F., et al. (2015). Fibroblast growth factor 17 and bone morphogenetic protein 15 enhance cumulus expansion and improve quality of in vitro-produced embryos in cattle. *Theriogenology* 84, 390–398. doi: 10.1016/j.theriogenology.2015.03.031

MahmoudianDehkordi, S., Arnold, M., Nho, K., Ahmad, S., Jia, W., Xie, G., et al. (2019). Altered bile acid profile associates with cognitive impairment in Alzheimer's disease-an emerging role for gut microbiome. *Alzheimers Dement.* 15, 76–92. doi: 10.1016/j.jalz.2018.07.217

Manduca, J. D., Thériault, R.-K., and Perreault, M. L. (2020). Glycogen synthase kinase-3: the missing link to aberrant circuit function in disorders of cognitive dysfunction? *Pharmacol. Res.* 157:104819. doi: 10.1016/j.phrs.2020.104819

Mano, N., Goto, T., Uchida, M., Nishimura, K., Ando, M., Kobayashi, N., et al. (2004). Presence of protein-bound unconjugated bile acids in the cytoplasmic fraction of rat brain. *J. Lipid Res.* 45, 295–300. doi: 10.1194/jlr.M300369-JLR200

Marcelin, G., Jo, Y.-H., Li, X., Schwartz, G. J., Zhang, Y., Dun, N. J., et al. (2014). Central action of FGF19 reduces hypothalamic AGRP/NPY neuron activity and improves glucose metabolism. *Molec metab* 3, 19–28. doi: 10.1016/j.molmet.2013.10.002

Mashayekhi, F., Hadavi, M., Vaziri, H. R., and Naji, M. (2010). Increased acidic fibroblast growth factor concentrations in the serum and cerebrospinal fluid of patients with Alzheimer's disease. *J. Clin. Neurosci.* 17, 357–359. doi: 10.1016/j.jocn.2009.05.037

Massó, A., Sánchez, A., Gimenez-Llort, L., Lizcano, J. M., Cañete, M., García, B., et al. (2015). Secreted and transmembrane αKlotho isoforms have different Spatio-temporal profiles in the brain during aging and Alzheimer's disease progression. *PLoS One* 10:e0143623. doi: 10.1371/journal.pone.0143623

McMillin, M., Frampton, G., Quinn, M., Divan, A., Grant, S., Patel, N., et al. (2015). Suppression of the HPA Axis during cholestasis can be attributed to hypothalamic bile acid signaling. *Mol. Endocrinol.* 29, 1720–1730. doi: 10.1210/me.2015-1087

Mergenthaler, P., Lindauer, U., Dienel, G. A., and Meisel, A. (2013). Sugar for the brain: the role of glucose in physiological and pathological brain function. *Trends Neurosci.* 36, 587–597. doi: 10.1016/j.tins.2013.07.001

Mertens, K. L., Kalsbeek, A., Soeters, M. R., and Eggink, H. M. (2017). Bile acid signaling pathways from the enterohepatic circulation to the central nervous system. *Front. Neurosci.* 11:617. doi: 10.3389/fnins.2017.00617

Miyamoto, N., Pham, L.-D. D., Seo, J. H., Kim, K.-W., Lo, E. H., and Arai, K. (2014). Crosstalk between cerebral endothelium and oligodendrocyte. *Cell. Mol. Life Sci.* 71, 1055–1066. doi: 10.1007/s00018-013-1488-9

Nakamura, S., Arima, K., Haga, S., Aizawa, T., Motoi, Y., Otsuka, M., et al. (1998). Fibroblast growth factor (FGF)-9 immunoreactivity in senile plaques. *Brain Res.* 814, 222–225.

Nakamura, M., Uehara, Y., Asada, M., Honda, E., Nagai, N., Kimata, K., et al. (2011). Sulfated glycosaminoglycans are required for specific and sensitive fibroblast growth factor (FGF) 19 signaling via FGF receptor 4 and betaKlotho. *J. Biol. Chem.* 286, 26418–26423. doi: 10.1074/jbc.M111.251140

Namba, T., Yabe, T., Gonda, Y., Ichikawa, N., Sanagi, T., Arikawa-Hirasawa, E., et al. (2010). Pigment epithelium-derived factor up-regulation induced by memantine, an N-methyl-D-aspartate receptor antagonist, is involved in increased proliferation of hippocampal progenitor cells. *Neuroscience* 167, 372–383. doi: 10.1016/j.neuroscience.2010.01.033

Nho, K., Kueider-Paisley, A., MahmoudianDehkordi, S., Arnold, M., Risacher, S. L., Louie, G., et al. (2019). Altered bile acid profile in mild cognitive impairment and Alzheimer's disease: relationship to neuroimaging and CSF biomarkers. *Alzheimers Dement.* 15, 232–244. doi: 10.1016/j.jalz.2018.08.012

Noda, M., Takii, K., Parajuli, B., Kawanokuchi, J., Sonobe, Y., Takeuchi, H., et al. (2014). FGF-2 released from degenerating neurons exerts microglial-induced neuroprotection via FGFR3-ERK signaling pathway. *J. Neuroinflammation* 11:76. doi: 10.1186/1742-2094-11-76

Numakawa, T., Nakajima, S., Yamamoto, N., Ooshima, Y., Odaka, H., Hashido, K., et al. (2015). Basic fibroblast growth factor induces miR-134 upregulation in astrocyte for cell maturation. *Biochem. Biophys. Res. Commun.* 456, 465–470. doi: 10.1016/j.bbrc.2014.11.108

Ogino, R., Murayama, N., Noshita, T., Takemoto, N., Toba, T., Oka, T., et al. (2014). SUN11602 has basic fibroblast growth factor-like activity and attenuates neuronal damage and cognitive deficits in a rat model of Alzheimer's disease induced by amyloid β and excitatory amino acids. *Brain Res.* 1585, 159–166. doi: 10.1016/j.brainres.2014.08.023

Owen, B. M., Mangelsdorf, D. J., and Kliewer, S. A. (2015). Tissue-specific actions of the metabolic hormones FGF15/19 and FGF21. *Trends Endocrinol. Metab.* 26, 22–29. doi: 10.1016/j.tem.2014.10.002

Pan, X., Elliott, C. T., McGuinness, B., Passmore, P., Kehoe, P. G., Hölscher, C., et al. (2017). Metabolomic profiling of bile acids in clinical and experimental samples of Alzheimer's disease. *Metabolites* 7:28. doi: 10.3390/metabo7020028

Papoutsi, M., Labuschagne, I., Tabrizi, S. J., and Stout, J. C. (2014). The cognitive burden in Huntington's disease: pathology, phenotype, and mechanisms of compensation. *Mov. Disord.* 29, 673–683. doi: 10.1002/mds.25864

Paroni, G., Panza, F., De Cosmo, S., Greco, A., Seripa, D., and Mazzoccoli, G. (2019). Klotho at the edge of Alzheimer's disease and senile depression. *Mol. Neurobiol.* 56, 1908–1920. doi: 10.1007/s12035-018-1200-z

Pereda-Pérez, I., Valencia, A., Baliyan, S., Núñez, Á., Sanz-García, A., Zamora, B., et al. (2019). Systemic administration of a fibroblast growth factor receptor 1 agonist rescues

the cognitive deficit in aged socially isolated rats. *Neurobiol. Aging* 78, 155–165. doi: 10.1016/j.neurobiolaging.2019.02.011

Perry, R. J., Lee, S., Ma, L., Zhang, D., Schlessinger, J., and Shulman, G. I. (2015). FGF1 and FGF19 reverse diabetes by suppression of the hypothalamic-pituitary-adrenal axis. *Nat. Commun.* 6:6980. doi: 10.1038/ncomms7980

Popp, J., Wolfsgruber, S., Heuser, I., Peters, O., Hüll, M., Schröder, J., et al. (2015). Cerebrospinal fluid cortisol and clinical disease progression in MCI and dementia of Alzheimer's type. *Neurobiol. Aging* 36, 601–607. doi: 10.1016/j.neurobiolaging.2014.10.031

Rajendran, R., Rajendran, V., Giraldo-Velasquez, M., Megalofonou, F. F., Gurski, F., Stadelmann, C., et al. (2021). Oligodendrocyte-specific deletion of FGFR1 reduces cerebellar inflammation and neurodegeneration in MOG35-55-induced EAE. *Int. J. Mol. Sci.* 22:9495. doi: 10.3390/ijms22179495

Reuss, B., and von Bohlen und Halbach, O. (2003). Fibroblast growth factors and their receptors in the central nervous system. *Cell Tissue Res.* 313, 139–157. doi: 10.1007/s00441-003-0756-7

Ryan, K. K., Kohli, R., Gutierrez-Aguilar, R., Gaitonde, S. G., Woods, S. C., and Seeley, R. J. (2013). Fibroblast growth factor-19 action in the brain reduces food intake and body weight and improves glucose tolerance in male rats. *Endocrinology* 154, 9–15. doi: 10.1210/en.2012-1891

Rysz, J., Gluba-Brzózka, A., Mikhailidis, D. P., and Banach, M. (2015). Fibroblast growth factor 19-targeted therapies for the treatment of metabolic disease. *Expert Opin. Investig. Drugs* 24, 603–610. doi: 10.1517/13543784.2015.1006357

Sa-Nguanmoo, P., Tanajak, P., Kerdphoo, S., Satjaritanun, P., Wang, X., Liang, G., et al. (2016). FGF21 improves cognition by restored synaptic plasticity, dendritic spine density, brain mitochondrial function and cell apoptosis in obese-insulin resistant male rats. *Horm. Behav.* 85, 86–95. doi: 10.1016/j.yhbeh.2016.08.006

Sanyal, A., Charles, E. D., Neuschwander-Tetri, B. A., Loomba, R., Harrison, S. A., Abdelmalek, M. F., et al. (2019). Pegbelfermin (BMS-986036), a PEGylated fibroblast growth factor 21 analogue, in patients with non-alcoholic steatohepatitis: a randomised, double-blind, placebo-controlled, phase 2a trial. *Lancet* 392, 2705–2717. doi: 10.1016/S0140-6736(18)31785-9

Sathyan, S., Ayers, E., Gao, T., Weiss, E. F., Milman, S., Verghese, J., et al. (2020). Plasma proteomic profile of age, health span, and all-cause mortality in older adults. *Aging Cell* 19:e13250. doi: 10.1111/acel.13250

Scearce-Levie, K., Roberson, E. D., Gerstein, H., Cholfin, J. A., Mandiyan, V. S., Shah, N. M., et al. (2008). Abnormal social behaviors in mice lacking Fgf17. *Genes Brain Behav.* 7, 344–354. doi: 10.1111/j.1601-183X.2007.00357.x

Shen, X.-N., Niu, L.-D., Wang, Y.-J., Cao, X.-P., Liu, Q., Tan, L., et al. (2019). Inflammatory markers in Alzheimer's disease and mild cognitive impairment: a meta-analysis and systematic review of 170 studies. *J. Neurol. Neurosurg. Psychiatry* 90, 590–598. doi: 10.1136/jnnp-2018-319148

Singh, S. M. (2009). Depression and dementia. *Br. J. Psychiatry* 194:287. doi: 10.1192/bjp.194.3.287

Skaper, S. D., Facci, L., Zusso, M., and Giusti, P. (2017). Synaptic plasticity, dementia and Alzheimer disease. *CNS Neurol. Disord. Drug Targets* 16, 220–233. doi: 10.2174/1871527316666170113120853

Stopa, E. G., Gonzalez, A. M., Chorsky, R., Corona, R. J., Alvarez, J., Bird, E. D., et al. (1990). Basic fibroblast growth factor in Alzheimer's disease. *Biochem. Biophys. Res. Commun.* 171, 690–696.

Subbiah, V., Iannotti, N. O., Gutierrez, M., Smith, D. C., Féliz, L., Lihou, C. F., et al. (2022). FIGHT-101, a first-in-human study of potent and selective FGFR 1-3 inhibitor pemigatinib in pan-cancer patients with FGF/FGFR alterations and advanced malignancies. *Ann. Oncol.* 33, 522–533. doi: 10.1016/j.annonc.2022.02.001

Suh, J. M., Jonker, J. W., Ahmadian, M., Goetz, R., Lackey, D., Osborn, O., et al. (2014). Endocrinization of FGF1 produces a neomorphic and potent insulin sensitizer. *Nature* 513, 436–439. doi: 10.1038/nature13540

Sun, J., Huang, X., Niu, C., Wang, X., Li, W., Liu, M., et al. (2021). aFGF alleviates diabetic endothelial dysfunction by decreasing oxidative stress via Wnt/β-catenin-mediated upregulation of HXK2. *Redox Biol.* 39:101811. doi: 10.1016/j.redox.2020.101811

Takami, K., Matsuo, A., Terai, K., Walker, D. G., McGeer, E. G., and McGeer, P. L. (1998). Fibroblast growth factor receptor-1 expression in the cortex and hippocampus in Alzheimer's disease. *Brain Res.* 802, 89–97.

Taliyan, R., Chandran, S. K., and Kakoty, V. (2019). Therapeutic approaches to Alzheimer's type of dementia: a focus on FGF21 mediated neuroprotection. *Curr. Pharm. Des.* 25, 2555–2568. doi: 10.2174/1381612825666190716101411

Tang, M.-M., Lin, W.-J., Zhang, J.-T., Zhao, Y.-W., and Li, Y.-C. (2017). Exogenous FGF2 reverses depressive-like behaviors and restores the suppressed FGF2-ERK1/2 signaling and the impaired hippocampal neurogenesis induced by neuroinflammation. *Brain Behav. Immun.* 66, 322–331. doi: 10.1016/j.bbi.2017.05.013

Tank, R., Ward, J., Celis-Morales, C., Smith, D. J., Flegal, K. E., and Lyall, D. M. (2021). Testing for interactions between APOE and klotho genotypes on cognitive, dementia, and brain imaging metrics in UK biobank. *J. Alzheimers Dis.* 83, 51–55. doi: 10.3233/JAD-210181

Tennakoon, A., Katharesan, V., Musgrave, I. F., Koblar, S. A., Faull, R. L. M., Curtis, M. A., et al. (2022). Normal aging, motor neurone disease, and Alzheimer's disease are characterized by cortical changes in inflammatory cytokines. *J. Neurosci. Res.* 100, 653–669. doi: 10.1002/jnr.24996

Tennant, K. G., Lindsley, S. R., Kirigiti, M. A., True, C., and Kievit, P. (2019). Central and peripheral Administration of Fibroblast Growth Factor 1 improves pancreatic islet insulin secretion in diabetic mouse models. *Diabetes* 68, 1462–1472. doi: 10.2337/db18-1175

Thorns, V., Licastro, F., and Masliah, E. (2001). Locally reduced levels of acidic FGF lead to decreased expression of 28-kda calbindin and contribute to the selective vulnerability of the neurons in the entorhinal cortex in Alzheimer's disease. *Neuropathology* 21, 203–211. doi: 10.1046/j.1440-1789.2001.00399.x

Thorns, V., and Masliah, E. (1999). Evidence for neuroprotective effects of acidic fibroblast growth factor in Alzheimer disease. *J. Neuropathol. Exp. Neurol.* 58, 296–306.

Tournissac, M., Bourassa, P., Martinez-Cano, R. D., Vu, T.-M., Hébert, S. S., Planel, E., et al. (2019). Repeated cold exposures protect a mouse model of Alzheimer's disease against cold-induced tau phosphorylation. *Molec Metab* 22, 110–120. doi: 10.1016/j.molmet.2019.01.008

Tsai, M. J., Tsai, S. K., Huang, M. C., Liou, D. Y., Huang, S. L., Hsieh, W. H., et al. (2015). Acidic FGF promotes neurite outgrowth of cortical neurons and improves neuroprotective effect in a cerebral ischemic rat model. *Neuroscience* 305, 238–247. doi: 10.1016/j.neuroscience.2015.07.074

Tyebji, S., and Hannan, A. J. (2017). Synaptopathic mechanisms of neurodegeneration and dementia: insights from Huntington's disease. *Prog. Neurobiol.* 153, 18–45. doi: 10.1016/j.pneurobio.2017.03.008

Ursem, S. R., Diepenbroek, C., Bacic, V., Unmehopa, U. A., Eggels, L., Maya-Monteiro, C. M., et al. (2021). Localization of fibroblast growth factor 23 protein in the rat hypothalamus. *Eur. J. Neurosci.* 54, 5261–5271. doi: 10.1111/ejn.15375

van Brummelen, E. M. J., Levchenko, E., Dómine, M., Fennell, D. A., Kindler, H. L., Viteri, S., et al. (2020). A phase Ib study of GSK3052230, an FGF ligand trap in combination with pemetrexed and cisplatin in patients with malignant pleural mesothelioma. *Invest. New Drugs* 38, 457–467. doi: 10.1007/s10637-019-00783-7

van der Flier, W. M., Skoog, I., Schneider, J. A., Pantoni, L., Mok, V., Chen, C. L. H., et al. (2018). Vascular cognitive impairment. *Nat. Rev. Dis. Primers.* 4:18003. doi: 10.1038/nrdp.2018.3

Vervloet, M. (2019). Renal and extrarenal effects of fibroblast growth factor 23. *Nat. Rev. Nephrol.* 15, 109–120. doi: 10.1038/s41581-018-0087-2

Wakayama, K., Shimamura, M., Yoshida, S., Hayashi, H., Ju, N., Nakagami, H., et al. (2021). Prevention of vascular dementia via immunotherapeutic blockade of renin-angiotensin system in a rat model. *Brain Res.* 1772:147667. doi: 10.1016/j.brainres.2021.147667

Wang, Z.-G., Cheng, Y., Yu, X.-C., Ye, L.-B., Xia, Q.-H., Johnson, N. R., et al. (2016). bFGF protects against blood-brain barrier damage through junction protein regulation via PI3K-Akt-Rac1 pathway following traumatic brain injury. *Mol. Neurobiol.* 53, 7298–7311. doi: 10.1007/s12035-015-9583-6

Wang, Q., Jie, W., Liu, J.-H., Yang, J.-M., and Gao, T.-M. (2017). An astroglial basis of major depressive disorder? An overview. *Glia* 65, 1227–1250. doi: 10.1002/glia.23143

Wang, S., Li, Y., Jiang, C., and Tian, H. (2018). Fibroblast growth factor 9 subfamily and the heart. *Appl. Microbiol. Biotechnol.* 102, 605–613. doi: 10.1007/s00253-017-8652-3

Wang, L. Y., Raskind, M. A., Wilkinson, C. W., Shofer, J. B., Sikkema, C., Szot, P., et al. (2018). Associations between CSF cortisol and CSF norepinephrine in cognitively normal controls and patients with amnestic MCI and AD dementia. *Int. J. Geriatr. Psychiatry* 33, 763–768. doi: 10.1002/gps.4856

Wang, X.-Q., Tang, Y.-H., Zeng, G.-R., Wu, L.-F., Zhou, Y.-J., Cheng, Z.-N., et al. (2021). Carnosic acid alleviates depression-like behaviors on chronic mild stressed mice via PPAR-γ-dependent regulation of ADPN/FGF9 pathway. *Psychopharmacology (Berl)* 238, 501–516. doi: 10.1007/s00213-020-05699-2

Wang, Q., Yuan, J., Yu, Z., Lin, L., Jiang, Y., Cao, Z., et al. (2018). FGF21 attenuates high-fat diet-induced cognitive impairment via metabolic regulation and anti-inflammation of obese mice. *Mol. Neurobiol.* 55, 4702–4717. doi: 10.1007/s12035-017-0663-7

Wang, X., Zhu, L., Hu, J., Guo, R., Ye, S., Liu, F., et al. (2020). FGF21 attenuated LPS-induced depressive-like behavior via inhibiting the inflammatory pathway. *Front. Pharmacol.* 11:154. doi: 10.3389/fphar.2020.00154

Wijesekara, N., Gonçalves, R. A., De Felice, F. G., and Fraser, P. E. (2018). Impaired peripheral glucose homeostasis and Alzheimer's disease. *Neuropharmacology* 136, 172–181. doi: 10.1016/j.neuropharm.2017.11.027

Wu, F. C. Z., Tang, C., Zhang, J., Cheng, L., Zuo, H., Zhang, H., et al. (2017). Acid fibroblast growth factor preserves blood-brain barrier integrity by activating the PI3K-Akt-Rac1 pathway and inhibiting RhoA following traumatic brain injury. *Am. J. Transl. Res.* 9, 910–925.

Xie, Y., Su, N., Yang, J., Tan, Q., Huang, S., Jin, M., et al. (2020). FGF/FGFR signaling in health and disease. *Signal Transduct. Target. Ther.* 5:181. doi: 10.1038/s41392-020-00222-7

Yamagata, H., Chen, Y., Akatsu, H., Kamino, K., Ito, J.-I., Yokoyama, S., et al. (2004). Promoter polymorphism in fibroblast growth factor 1 gene increases risk of definite Alzheimer's disease. *Biochem. Biophys. Res. Commun.* 321, 320–323. doi: 10.1016/j.bbrc.2004.06.142

Yi-Bin, W., Xiang, L., Bing, Y., Qi, Z., Fei-Tong, J., Minghong, W., et al. (2022). Inhibition of the CEBPβ-NFκB interaction by nanocarrier-packaged Carnosic acid ameliorates glia-mediated neuroinflammation and improves cognitive function in an Alzheimer's disease model. *Cell Death Dis.* 13:318. doi: 10.1038/s41419-022-04765-1

You, J., Sun, L., Wang, J., Sun, F., Wang, W., Wang, D., et al. (2021). Role of adiponectin-notch pathway in cognitive dysfunction associated with depression and in the therapeutic effect of physical exercise. *Aging Cell* 20:e13387. doi: 10.1111/acel.13387

Yuan, H., Ni, X., Zheng, M., Han, X., Song, Y., and Yu, M. (2019). Effect of catalpol on behavior and neurodevelopment in an ADHD rat model. *Biomed. Pharmacother.* 118:109033. doi: 10.1016/j.biopha.2019.109033

Yusuf, I. O., Chen, H.-M., Cheng, P.-H., Chang, C.-Y., Tsai, S.-J., Chuang, J.-I., et al. (2019). Fibroblast growth factor 9 activates anti-oxidative functions of Nrf2 through ERK signalling in striatal cell models of Huntington's disease. *Free Radic. Biol. Med.* 130, 256–266. doi: 10.1016/j.freeradbiomed.2018.10.455

Yusuf, I. O., Chen, H.-M., Cheng, P.-H., Chang, C.-Y., Tsai, S.-J., Chuang, J.-I., et al. (2021a). FGF9 induces neurite outgrowth upon ERK signaling in knock-in striatal Huntington's disease cells. *Life Sci.* 267:118952. doi: 10.1016/j.lfs.2020.118952

Yusuf, I. O., Chen, H.-M., Cheng, P.-H., Chang, C.-Y., Tsai, S.-J., Chuang, J.-I., et al. (2021b). Fibroblast growth factor 9 stimulates neuronal length through NF-kB signaling in striatal cell Huntington's disease models. *Mol. Neurobiol.* 58, 2396–2406. doi: 10.1007/s12035-020-02220-w

Zhang, P., Kishimoto, Y., Grammatikakis, I., Gottimukkala, K., Cutler, R. G., Zhang, S., et al. (2019). Senolytic therapy alleviates Aβ-associated oligodendrocyte progenitor cell senescence and cognitive deficits in an Alzheimer's disease model. *Nat. Neurosci.* 22, 719–728. doi: 10.1038/s41593-019-0372-9

Zhang, J., and Li, Y. (2016). Therapeutic uses of FGFs. *Semin. Cell Dev. Biol.* 53, 144–154. doi: 10.1016/j.semcdb.2015.09.007

Zhang, Y., Wang, L., Wu, Z., Yu, X., Du, X., and Li, X. (2017). The expressions of klotho family genes in human ocular tissues and in anterior Lens capsules of age-related cataract. *Curr. Eye Res.* 42, 871–875. doi: 10.1080/02713683.2016.1259421

Zhao, M., Li, D., Shimazu, K., Zhou, Y.-X., Lu, B., and Deng, C.-X. (2007). Fibroblast growth factor receptor-1 is required for long-term potentiation, memory consolidation, and neurogenesis. *Biol. Psychiatry* 62, 381–390. doi: 10.1016/j.biopsych.2006.10.019

Zhao, Y., Zeng, C.-Y., Li, X.-H., Yang, T.-T., Kuang, X., and Du, J.-R. (2020). Klotho overexpression improves amyloid-β clearance and cognition in the APP/PS1 mouse model of Alzheimer's disease. *Aging Cell* 19:e13239. doi: 10.1111/acel.13239

Zheng, K., Lin, L., Cui, P., Liu, T., Chen, L., Yang, C., et al. (2020). Association of Fibroblast Growth Factor 23 with ischemic stroke and its subtypes: a Mendelian randomization study. *Front. Genet.* 11:608517. doi: 10.3389/fgene.2020.608517

Zheng, W., Matei, N., Pang, J., Luo, X., Song, Z., Tang, J., et al. (2019). Delayed recanalization at 3 days after permanent MCAO attenuates neuronal apoptosis through FGF21/FGFR1/PI3K/Caspase-3 pathway in rats. *Exp. Neurol.* 320:113007. doi: 10.1016/j.expneurol.2019.113007

Zhou, X., Chen, K., Lei, H., and Sun, Z. (2015). Klotho gene deficiency causes salt-sensitive hypertension via monocyte chemotactic protein-1/CC chemokine receptor 2-mediated inflammation. *J. Am. Soc. Nephrol.* 26, 121–132. doi: 10.1681/ASN.2013101033

Zhu, B., Jin, L.-N., Shen, J.-Q., Liu, J.-F., Jiang, R.-Y., Yang, L., et al. (2018). Differential expression of serum biomarkers in hemodialysis patients with mild cognitive decline: a prospective single-center cohort study. *Sci. Rep.* 8:12250. doi: 10.1038/s41598-018-29760-5

Glossary

ACTH	Adrenocorticotropic hormone
AD	Alzheimer's disease
ADPN	Adiponectin
aFGF	Acidic fibroblast growth factor
AGRP/NPY	Agouti-related protein/neuropeptide-Y
AHN	Adult hippocampal neurogenesis
AKT	Protein kinase B
AMI	Acute myocardial infarction
AMPK	Adenosine monophosphate activated protein kinase
AST	Astrocytes
ATP	Adenosine-triphosphate
Aβ	Amyloid-β
BA	Bile acid
BBB	Blood–brain barrier
BDNF	Brain-derived neurotrophic factor
bFGF	Basic fibroblast growth factor
CA	Cholic acid
CDCA	Chenodesoxycholic acid
CNS	Central nervous system
CREB	cAMP-response element binding protein
CSF	Cerebral spinal fluid
DCA	Deoxycholic acid
ERK	Extracellular signal-regulated kinase
FGF-1	Fibroblast growth factor-1
FGF-2	Fibroblast growth factor-2
FGF-9	Fibroblast growth factor-9
FGF-15/19	Fibroblast growth factor-15/19
FGF-17	Fibroblast growth factor-17
FGF-21	Fibroblast growth factor-21
FGF-23	Fibroblast growth factor-23
FGFR-1	Fibroblast growth factor receptor-1
FGFR-2	Fibroblast growth factor receptor-2
FGFR-3	Fibroblast growth factor receptor-3
FGFR-4	Fibroblast growth factor receptor-4
FGFRs	Fibroblast growth factor receptors
FGFs	Fibroblast growth factors
FXR	Farnesoid X receptor
GAP-43	Growth association protein-43
GC	Glucocorticoid
GDCA	Glycinodeoxycholic acid
GR	Glutathione reductase
GSK-3β	Glycogen synthase kinase-3β
HD	Huntington's disease
HMW	High molecular weight
HPA	Hypothalamic–pituitary–adrenal

HS	Heparan sulfate
HXK2	Hexokinase 2
IL-6	Interleukin-6
IL-β	Interleukin-1β
LCA	Lithocholic acid
LMW	Light molecular weight
LTP	Long-time potentiation
MAP-2	Microtubule-associated protein-2
MAPK	Mitogen-activated protein kinase
MCI	Mild cognitive impairment
MG	Microglial
m-KL	Membrane Klotho
NE	Norepinephrine
NF-κB	Nuclear factor kappa-B
NMDAR	N-methyl-D-aspartic acid receptor
Nrf-2	Nuclear factor erythroid-like 2
NVU	Neurovascular unit
OL	Oligodendrocyte
OPC	Oligodendrocyte precursor cell
PGC-1α	Peroxisome proliferator-activated receptors-γ coactivator 1-α
PI3K	Phosphatidylinositol-3-hydroxy kinase
PPAR-α	Peroxisome proliferator-activated receptor-α
PPAR-γ	Peroxisome proliferator-activated receptor-γ
Rac1	Rac family small GTPase 1
RhoA	Ras homolog family member A
SIR1	Sirtuin1
s-KL	Soluble Klotho
SOD2	Superoxide dismutase 2
TDCA	Taurodeoxycholic acid
TLR4	Toll like receptor-4
TNF-α	Tumor growth factor-α
TrkB	Tyrosine kinase receptor B
TUDCA	Tauroursodeoxycholic acid
VaD	Vascular dementia
VEGF	Vascular endothelial growth factor
WMH	White matter hyperintensities
α/β/γ-KL	α/β/γ-Klotho protein
γ-GCS	Gamma-glutamylcysteine synthetase

frontiers | Frontiers in Neuroscience

TYPE Methods
PUBLISHED 18 May 2023
DOI 10.3389/fnins.2023.1156037

OPEN ACCESS

EDITED BY
Dennis Chang,
Western Sydney University, Australia

REVIEWED BY
Wang Xue Rui,
Hefei University of Technology, China
Mengli Chang,
China Academy of Chinese Medical Sciences, China

*CORRESPONDENCE
Guojie Xu
✉ guojiexu@bucm.edu.cn

RECEIVED 01 February 2023
ACCEPTED 20 April 2023
PUBLISHED 18 May 2023

CITATION
Wang X, Liu Y, Kang N and Xu G (2023) Wide identification of chemical constituents in fermented licorice and explore its efficacy of anti-neurodegeneration by combining quasi-targeted metabolomics and in-depth bioinformatics.
Front. Neurosci. 17:1156037.
doi: 10.3389/fnins.2023.1156037

Wide identification of chemical constituents in fermented licorice and explore its efficacy of anti-neurodegeneration by combining quasi-targeted metabolomics and in-depth bioinformatics

Xiaotong Wang, Ying Liu, Nianxin Kang and Guojie Xu*

School of Life Sciences, Beijing University of Chinese Medicine, Beijing, China

Licorice (Gan-Cao in Chinese) is one of the most famous herbal medicines around the world. The fermentation of probiotics and herbs can change the chemical constituents and significantly improve the efficacy. However, it is still unknown whether licorice fermented with probiotics would produce beneficial therapeutic effects. This study aimed to comprehensively analyze the chemical constituents in fermented licorice via quasi-targeted metabolomics, predict the potential efficacy of fermentation products via diverse bioinformatic methods, and further verify the efficacy of fermentation products through *in vitro* and *in vivo* experiments. As a result, 1,435 compounds were identified totally. Among them, 424 natural medicinal products were classified with potentially important bioactivities, including 11 anthocyanins, 10 chalcones and dihydrochalcones, 25 flavanones, 45 flavones and flavonols, 117 flavonoids, 34 isoflavonoids, 21 phenols and its derivatives, 20 phenylpropanoids and polyketides, 96 terpenoids and 25 coumarins and derivatives. Interestingly, bioinformatic prediction showed that the targets of some important compounds were related to neurodegeneration, oxidoreductase activity and response to stress. *In vitro* and *in vivo* tests further verified that fermented licorice had excellent effects of DPPH clearance, anti-oxidation, anti-neurodegeneration, and anti-stress. Thus, this study would provide a reference method for related research and the development of fermented licorice-related products.

KEYWORDS

licorice, natural medicinal products, probiotics, quasi-targeted metabolomics, bioinformatics

1. Introduction

Licorice (Gan-Cao in Chinese), mainly derived from the root and rhizome of *Glycyrrhiza* species, is one of the most famous herbal medicines. Licorice has been widely used to treat various chronic diseases in Asia for thousands of years. And now, licorice is also used as an additive in cosmetics, food, and animal husbandry. With the increasing demand of licorice,

G. uralensis is widely cultivated in China, with an annual production of over 5,000 tons (Shibata, 2000; Hosseinzadeh and Nassiri-Asl, 2015; Pastorino et al., 2018; Jalali et al., 2021).

Licorice contains a wide variety of chemical compounds, mainly including triterpenoids and flavonoids, which has a wide range of biological activities, including anti-inflammation, anti-virus, anti-tumor (Asl and Hosseinzadeh, 2008; Abraham and Florentine, 2021; Heidari et al., 2021; Sharifi-Rad et al., 2021; Wahab et al., 2021). Some studies also reported that licorice had the efficacy of preventing severe acute respiratory syndrome (SARS) (Fiore et al., 2008) and coronavirus disease (COVID-19) (Boozari and Hosseinzadeh, 2021; Brendler et al., 2021; Jalali et al., 2021; Liana and Phanumartwiwath, 2022).

Probiotics, defined as good bacteria in the human body, is one of the hotspots in current study. It had shown that probiotics had a wide range of biological activities, including maintaining the structural balance of intestinal flora, improving immunity and inhibiting inflammation (Sarao and Arora, 2017; Suez et al., 2019; Wieërs et al., 2019; Yu et al., 2020; Żółkiewicz et al., 2020). The latest research showed that the co-fermentation of probiotics and herbs could change the composition of ingredients and significantly improve the efficacy (Xiao et al., 2017; Han and Kim, 2020). However, it is still unknown whether licorice co-fermented with probiotics would produce beneficial therapeutic effects.

Quasi-targeted metabolomics is a novel metabolomic detection technology that combines the advantages of high throughput of non-targeted metabolomics with the advantages of high accuracy and sensitivity of targeted metabolomics, which is based on the SCIEX QTRAP® 6500+ mass spectrometer with triple quadrupole - linear ion trap composite and uses Multiple Reaction Monitoring (MRM) to accurately determine and quantify large amounts of metabolites in biological samples (Cao et al., 2022; Wang et al., 2022).

This study aimed to comprehensively analyze the chemical constituents in fermented licorice via quasi-targeted metabolomics, predict the potential functions of fermentation products via diverse bioinformatic methods, and further verify the therapeutic function of fermentation products through *in vitro* and *in vivo* experiments, so as to provide an important basis for the development of fermented licorice-related products.

2. Materials and methods

2.1. Licorice fermentation process

10 mg/mL licorice extract was fermented with 50 mg/mL probiotic complex (including *Lactobacillus plantarum* LP-115, *Streptococcus thermophilus* ST-21, *Lactobacillus casei* LC-11, *Bifidobacterium breve* BB-03, *Bifidobacterium infantis* BI-26, *Bifidobacterium lactis* BI-04, *Lactobacillus rhamnosus* GG, *Lactobacillus rhamnosus* HN001, Lactobacillus gratus LG-36, *Lactobacillus reuteri* 1E1, *Lactobacillus rhamnosus* LR-32, *Lactobacillus paracasei* LPC-37, *Bifidobacterium longum* BL-05, *Lactobacillus bulgaricus* LB-87, *Bifidobacterium lactis* HN019) in anaerobic medium at 37°C for 12 h.

2.2. Sample preparation

1 mL sample was lyophilized and suspended with 100 μL 80% methanol. The sample was incubated on ice for 5 min, centrifugated at 15,000 g, 4°C for 15 min. Supernatant of sample was diluted to final concentration of 53% methanol. The sample was subsequently centrifuged at 15,000 g at 4°C for 15 min and the supernatant was used for the LC–MS/MS analysis. An equal volume sample was taken from each experimental sample and mixed as a QC sample, and the blank sample was replaced by a 53% methanol aqueous solution (Want et al., 2006; Barri and Dragsted, 2013).

2.3. HPLC–MS/MS analysis

Xselect HSS T3 (2.5 μm, 2.1 × 150 mm) was kept at a flow rate of 0.4 mL/min for both the positive and negative polarity mode. Eluent A was 0.1% Formic acid-water and eluent B was 0.1% Formic acid-acetonitrile. The solvent gradient was set as follows: 2% B, 2 min; 2–100% B, 15.0 min; 100% B, 17.0 min; 100–2% B, 17.1 min; 2% B (Luo et al., 2015). LC–MS/MS analyses were performed using an ExionLC™ AD system (SCIEX) coupled with aQTRAP® 6500+ mass spectrometer (SCIEX). Positive polarity mode was set as follows: Curtain Gas of 35 psi, Collision Gas of Medium, IonSpray Voltage of 5,500 V, Temperature of 550°C, Ion Source Gas of 1:60, Ion Source Gas of 2:60º Negative polarity mode was set as follows: Curtain Gas of 35 psi, Collision Gas of Medium, IonSpray Voltage of −4,500 V, Temperature of 550°C, Ion Source Gas of 1:60, Ion Source Gas of 2:60 (Want et al., 2010; Dunn et al., 2011).

2.4. Chemical compound identification and quantification

MRM (Multiple Reaction Monitoring) were used to detect the signals of compounds based on in-house database. The Q1, Q3, RT (retention time), DP (declustering potential) and CE (collision energy) were used for compound identification. The Q3 were used for quantification (Wen et al., 2017).

2.5. Data analysis

Metabolites were annotated using the KEGG database,[1] HMDB database[2] and Lipidmaps database.[3] BATMAN[4] (Liu et al., 2016) and ToppGene[5] (Chen et al., 2007, 2009a,b) were used for annotation of targets.

2.6. *In vitro* and *in vivo* test

DPPH clearance test was performed as follows: 200 μL of the sample was mixed with 200 μL DPPH (0.04 mg/mL) solution at room temperature for 30 min, and centrifuged at 5,000 r/min for 10 min. The supernatant was taken to measure the absorbance value at 517 nm, vitamin C was used as a positive control. The formula for calculating

1 http://www.genome.jp/kegg/
2 http://www.hmdb.ca/
3 http://www.lipidmaps.org
4 http://bionet.ncpsb.org.cn/batman-tcm/
5 https://toppgene.cchmc.org/

the DPPH clearance is: 1−(*A*1−*A*2)/*A*0*100%, where *A*0 is the absorbance value of mixed solution containing 400 μL absolute ethanol and 400 μL DPPH at 517 nm; A1 is the absorbance value of mixed solution containing 800 μL sample and 800 μL DPPH at 517 nm; A2 is the absorbance value of mixed solution containing 800 μL sample and 800 μL absolute ethanol at 517 nm.

The reducing ability test was performed as follows: 100 μL sample was mixed with 250 μL of phosphoric acid buffer of 0.2 mol/L (pH = 6.6) and then 250 μL of 1% potassium ferricyanide at 50°C for 20 min, 250 μL of 10% trichloroacetic acid was added to terminate the reaction. The sample was subsequently centrifugated at 5,000 r/min for 10 min. 500 μL of supernatant was collected and mixed with 500 μL of distilled water and 100 μL FeCl3, and allowed to stand for 10 min. The absorbance value was detected at 700 nm. Vitamin C as a positive control; The relative reduction capacity calculation formula is: absorbance of sample at 700 nm/absorbance of vitamin C at 700 nm * 100%.

Galactose-induced neurodegenerative *Caenorhabditis elegans* model was used to study the efficacy of fermented licorice (Cui et al., 2006; Caldwell et al., 2020). The control group was treated with 400 mM galactose, the other group was treated with 400 mM galactose containing different concentrations of fermented licorice, the number of swings of each *C. elegans* in 20 s was recorded. The heat stress capacity of *C. elegans* was detected as follows: *C. elegans* were treated with heat stress at 35°C, the number of survival *C. elegans* was counted every 2 h and further calculated.

3. Results and discussion

3.1. Comprehensive identification of chemical constituents of fermented licorice based on quasi-targeted metabolomics

The chemical ingredients of licorice are very complex, containing thousands of natural products, and similarly, there are hundreds of metabolites of probiotics. Current technologies are difficult to analyze such a large number of metabolites at one time. In order to comprehensively analyze the chemical constituents of probiotic fermented licorice, we used a triple quadrupole-linear ion trap complex SCIEX QTRAP® 6500+ mass spectrometer combined with multiple reaction monitoring mode (MRM) to accurately analyze the metabolites in probiotic fermented licorice. The results showed that the chromatographic peaks had good shape regardless of the positive ion or negative ion mode, and the quality control evaluation showed a good correlation, with an R2 value of 0.992 (close to 1), indicating that the conditions of liquid phase and mass spectrometry were stable and reliable (Figure 1). Qualitative identification results showed that we had identified 1,435 compounds in total, including compounds in licorice and many possible metabolites of probiotics (Supplementary Dataset S1).

Liquid chromatography coupled with mass spectrometry (LC/MS) was commonly used to analyze the chemical constituents of licorice (Montoro et al., 2011, Xu et al., 2013, Cheng et al., 2021, Shang et al., 2022a,b). Compared with previous studies, we firstly established the method to accurately identify the most chemicals in licorice-related researches via quasi-targeted metabolomics, which provided a reference method for related research.

3.2. Annotation of identified compounds

In order to understand the functional properties and classification of different compounds, we annotated the pathways and classifications of the identified compounds by using databases including Human Metabolome Database (HMDB), Kyoto Encyclopedia of Genes and Genomes (KEGG) and LIPID MAPS.

HMDB annotation results showed that 1 compound belonged to organosulfur compounds, 11 compounds belonged to Lignans, neolignans and related compounds, 13 compounds belonged to alkaloids and derivatives, 16 compounds belonged to organic nitrogen compounds, 59 compounds belonged to nucleosides, nucleotides, and analogs, 84 compounds belonged to benzenoids, 114 compounds belonged to organoheterocyclic compounds, 116 compounds belonged to organic oxygen compounds, 151 compounds belonged to lipids and lipid-like molecules, 166 compounds belonged to phenylpropanoids and polyketides, and 200 compounds belonged to organic acids and derivatives (Figure 2A).

KEGG annotation results showed that 5 compounds were involved in cellular processes pathway, 34 compounds were involved in environmental information processing pathway, 21 compounds were involved in genetic information processing pathway, 663 compounds were involved in metabolism pathway, and 1 compound was involved in organic systems pathway (Figure 2B).

The LIPID MAPS annotation results showed that 34 compounds belonged to fatty acyls (FA), 1 compound belonged to glycerophospholipids (GP), 112 compounds belonged to polyketides (PK), 29 compounds belonged to prenol lipids (PR), and 13 compounds belonged to sterols (ST) (Figure 2C).

In general, this study not only identified the common natural products in licorice, but also found a lot of novel compounds produced by fermentation, which laid the foundation for the discovery of new active ingredients.

And more importantly, further sorting and classifying the compounds, we identified a total of 424 natural medicinal products with potentially important bioactivities, including 11 anthocyanins, 10 chalcones and dihydrochalcones, 25 flavanones, 45 flavones and flavonols, 117 flavonoids, 34 isoflavonoids, 21 phenols and its derivatives, 20 phenylpropanoids and polyketides, 96 terpenoids and 25 coumarins and derivatives (Figure 2D). These results demonstrated that the quasi-targeted metabolomics developed in this research was very suitable for the analysis of natural medicinal products, which could provide important support for the research on the new efficacy of fermented licorice and the development of new products.

3.3. Effect of fermentation on licorice chemical constituents

In order to further analyze the effect of fermentation on the chemical constituents of licorice, we conducted a differential analysis of the chemical constituents before and after fermentation, and the results showed that 151 compounds were significantly increased (Figure 3A; Supplementary Dataset S2), including probiotic metabolites that are potentially beneficial to the body, involving 9 kinds of carbohydrates and its derivatives, 8 organic acid and its derivatives, including important natural medicinal products, involving 1 anthocyanins, 9 flavanones, 13 flavones and flavonols, 16 flavonoids,

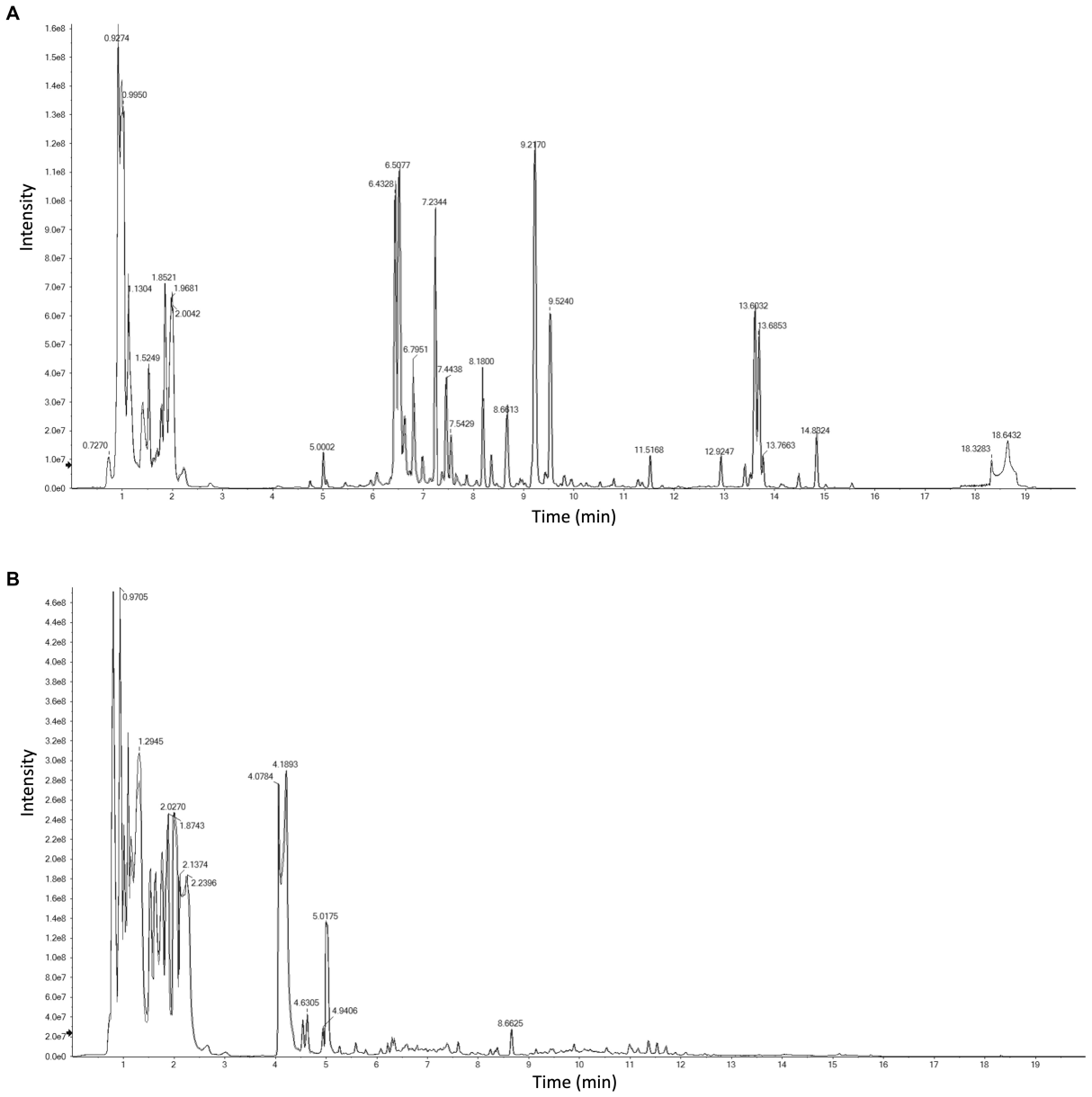

FIGURE 1
Total ion chromatorgraphy of mixed quality control sample of fermented licorice in positive **(A)** and negative **(B)** polarity mode.

12 isoflavonoids, 4 phenols and its derivatives, 3 phenylpropanoids (Figure 3B). The results suggested that fermented licorice might enhance some medicinal effects of licorice.

3.4. In-depth prediction of potential efficacy of fermented licorice via bioinformatics

In order to further predict the potential efficacy of fermented licorice, we used bioinformatics to predict the potential targets of fermented licorice chemical constituents and potential therapeutic diseases. KEGG enrichment analysis showed that the targets of these chemical constituents mainly involved pathways of amino acid metabolism, metabolism of other amino acids, arginine and proline metabolism, carbon metabolism, metabolism of cofactors and vitamins, biosynthesis of amino acids, valine, leucine and isoleucine degradation, calcium signaling and glutathione metabolism (Figure 3C; Supplementary Dataset S3). GO enrichment analysis showed that the targets of these chemical constituents mainly involved small molecule metabolic process, cellular amino acid metabolic process, cell–cell signaling, transmembrane transport, transport, transmembrane transporter activity, cytoplasm, lipid metabolic process and homeostatic process (Figure 3D; Supplementary Dataset S4).

Interestingly, we found that these targets were also related to neuroactive ligand-receptor interaction, nervous system, oxidoreductase activity, neurological system process and response to stress (Figures 3C–E).

Therefore, we further performed disease enrichment analysis on these targets, and the results showed that these targets were indeed

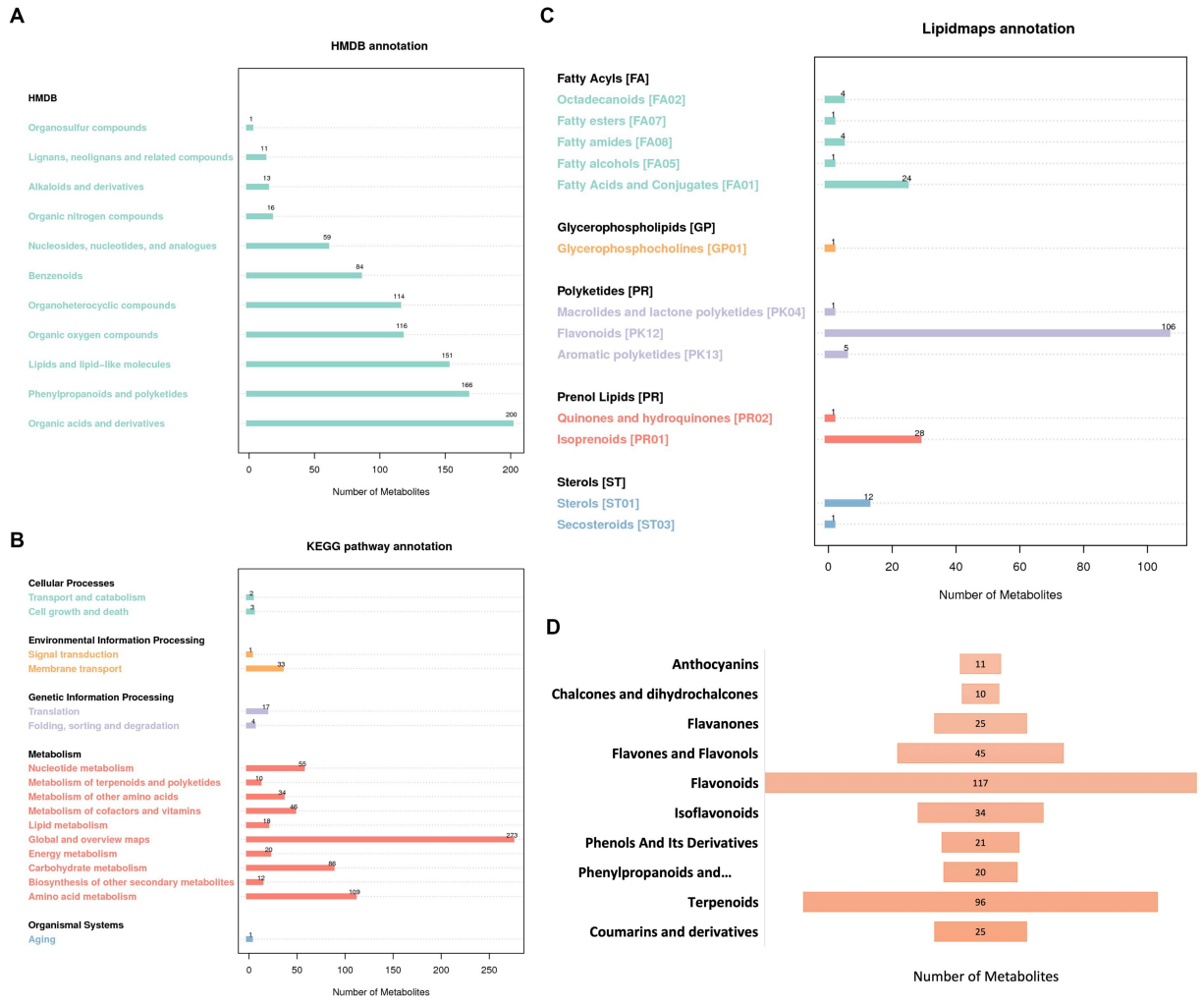

FIGURE 2
Annotation of 1,435 identified chemicals. **(A)** HMDB annotation. **(B)** KEGG pathway annotation. **(C)** Lipidmaps annotation. **(D)** Classification of 424 natural medicinal products.

related to neurodegenerative diseases, including Alzheimer's disease, Parkinson's disease, Multiple Sclerosis and Amyotrophic Lateral Sclerosis (Figure 4A; Supplementary Dataset S5).

Biological process analysis showed that they mainly involved synaptic signaling, anterograde trans-synaptic signaling, chemical synaptic transmission, trans-synaptic signaling and behavior (Figure 4B; Supplementary Dataset S6). Cellular component analysis showed that they mainly involve neuron projection, somatodendritic compartment, synapse, integral component of plasma membrane and intrinsic component of plasma membrane (Figure 4C; Supplementary Dataset S6). Molecular function analysis showed that they mainly involved neurotransmitter receptor activity, postsynaptic neurotransmitter receptor activity, gated channel activity, ion channel activity and transmembrane signaling receptor activity (Figure 4D; Supplementary Dataset S6).

3.5. Verification of potential efficacy of fermented licorice via *in vitro* and *in vivo* experiments

Bioinformatic prediction showed that the targets of fermented licorice chemical constituents involved oxidoreductase activity. To verify this predicted result, we further performed *in vitro* experiment, by using vitamin C as a positive control. The DPPH clearance test showed that fermented licorice had a DPPH clearance ability comparable to that of vitamin C (Figure 5A). The reducing ability test showed that the total antioxidant capacity and ROS clearance rate of fermented licorice could reach 50% of Vitamin C (Figures 5B,C). These results proved that fermented licorice had excellent DPPH scavenging ability and antioxidative ability. Moreover, toxicity testing showed that cell viability could be improved at low concentrations, while at high concentrations there was damage to the cells, which indicated that fermented licorice had excellent safety performance at low concentrations (Figure 5D).

Bioinformatic prediction also showed that the targets of fermented licorice chemical constituents involved neurological system process, response to stress and neurodegenerative diseases. In order to verify the predicted results, we further used the inducible neurodegenerative *C. elegans* model to study the effect of fermented licorice on neurodegenerative diseases. The results showed that fermented licorice at both medium and low concentrations could rescue neurodegenerative-related movement disorders (Figures 5E,F), and could also significantly improve the ability of heat stress

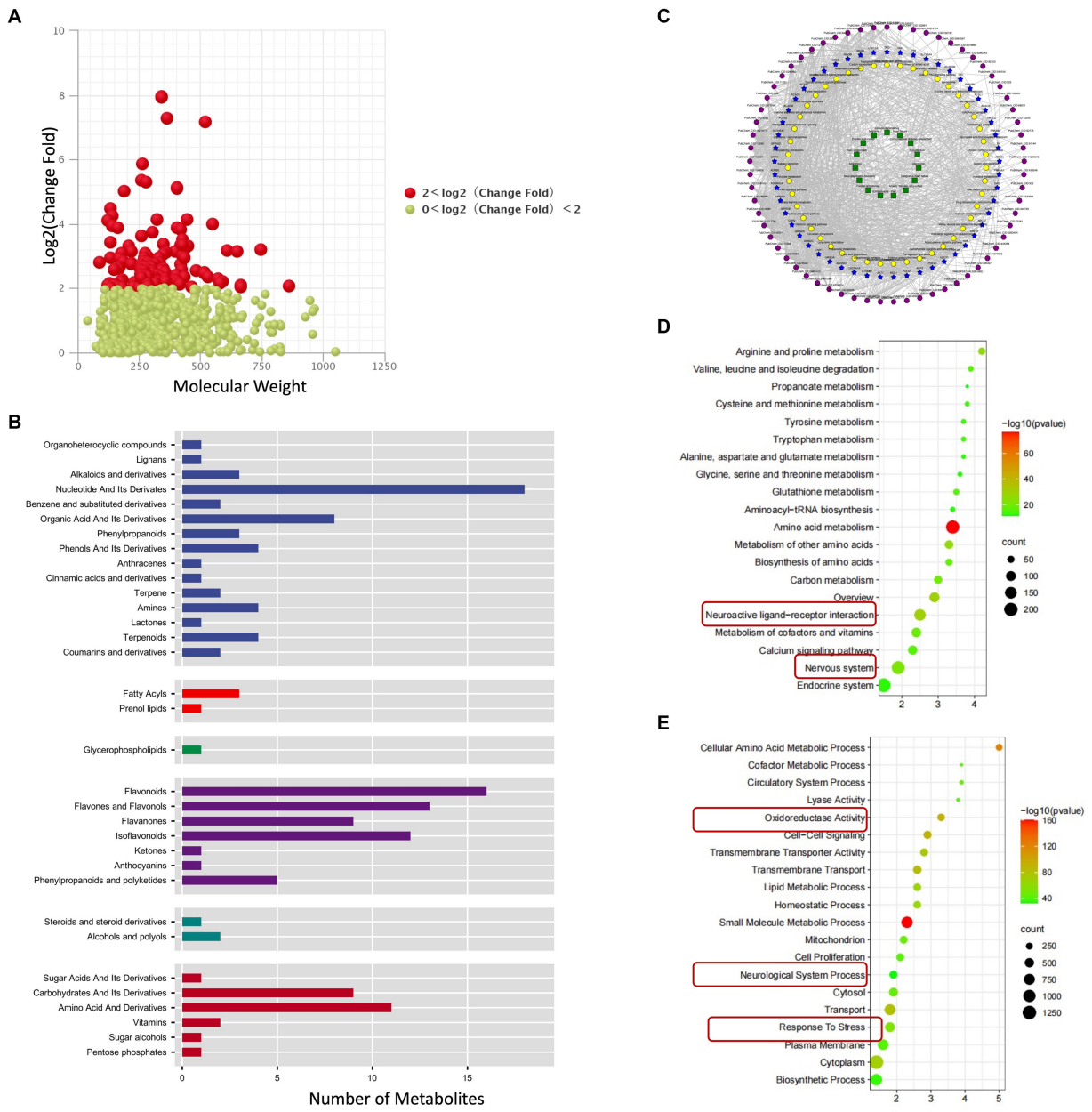

FIGURE 3
Effect of fermentation on licorice chemical constituents. **(A)** Significantly increased chemicals in the process of fermentation. **(B)** Classification of increased chemicals. **(C)** Bioinformatic prediction of increased chemicals. **(D)** KEGG Enrichment analysis of target genes of highly increased chemicals. **(E)** GO Enrichment analysis of target genes of highly increased chemicals.

(Figure 5G). The results proved that fermented licorice could effectively improve neurodegenerative related movement ability and anti-stress ability.

No studies were focused on the efficacy of probiotic fermented licorice to date. This study firstly discovered and verified that probiotic fermented licorice had excellent DPPH scavenging ability and anti-oxidation ability comparable to that of vitamin C, and had excellent anti-neurodegeneration and anti-stress ability. This discovery would help the development of licorice-related products and promote the development of licorice industry.

Data availability statement

The datasets presented in this study can be found in online repositories. The names of the repository/repositories and accession number(s) can be found in the article/Supplementary material.

Author contributions

GX conceived the study. YL participated in design. XW conducted most of the experiments. NK conducted a part of the

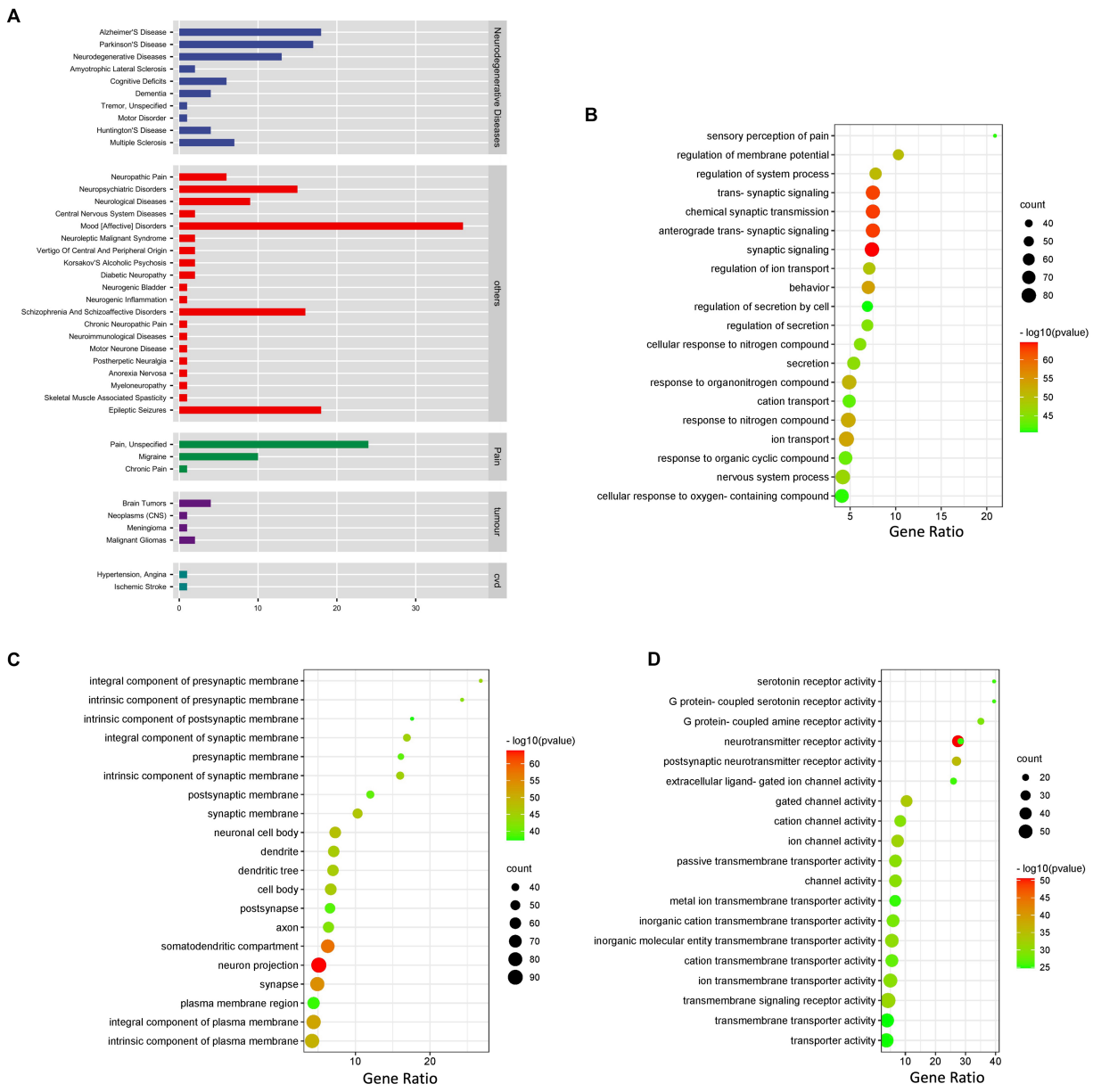

FIGURE 4
In-depth prediction of potential efficacy of fermented licorice. **(A)** Disease enrichment analysis of target genes. **(B)** Biological process enrichment analysis of target genes associated with neurological diseases. **(C)** Cellular component enrichment analysis of target genes associated with neurological diseases. **(D)** Molecular function enrichment analysis of target genes associated with neurological diseases.

experiments. GX and YL wrote and revised the manuscript. All authors contributed to the article and approved the submittedversion.

Funding

This study was supported by National Natural Science Foundation of China (no. 81903738) and the Fundamental Research Funds for the Central Universities (no. 2022-JYB-XJSJJ-031).

Conflict of interest

The authors declare that the research was conducted in the absence of any commercial or financial relationships that could be construed as a potential conflict of interest.

Publisher's note

Supplementary material

The Supplementary material for this article can be found online at: https://www.frontiersin.org/articles/10.3389/fnins.2023.1156037/full#supplementary-material

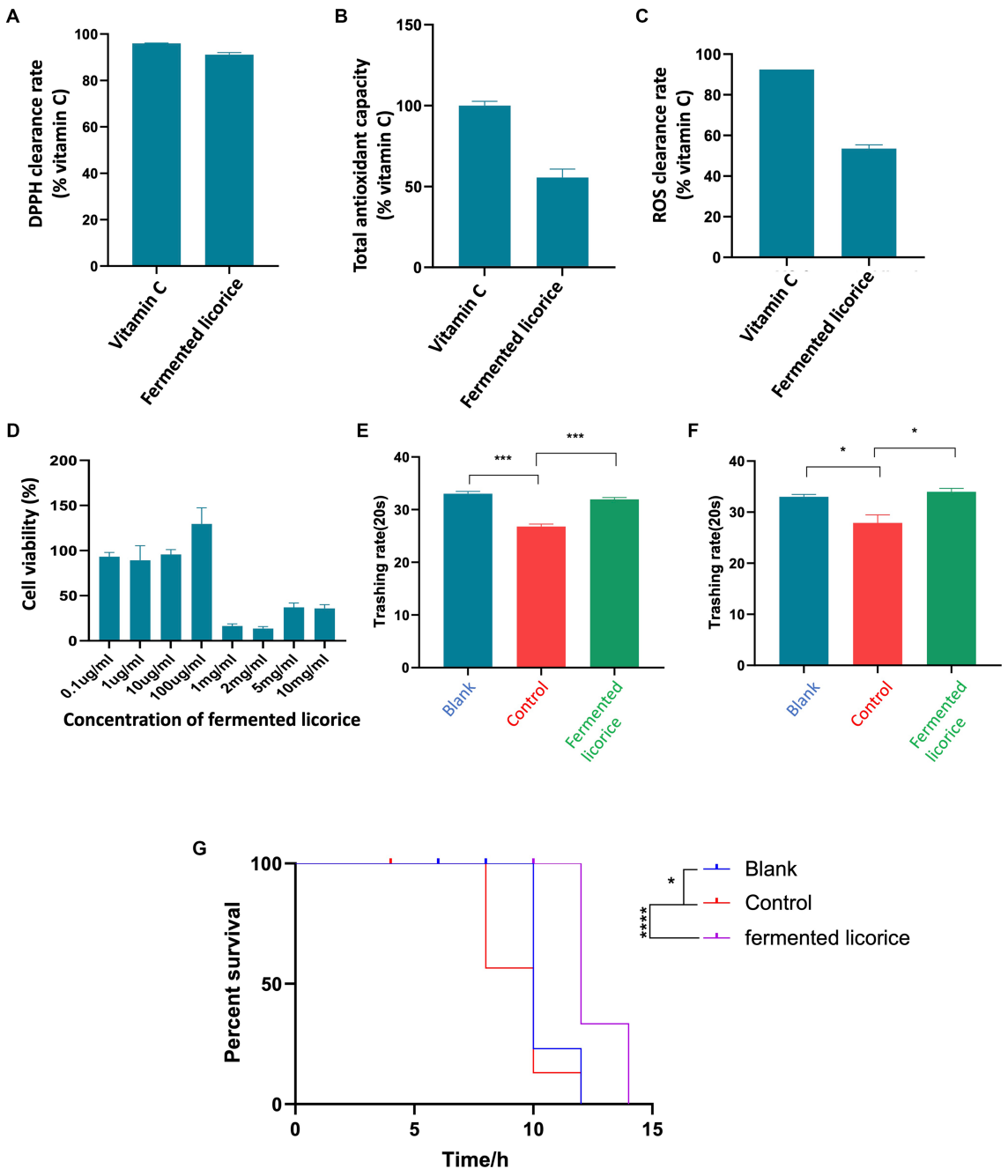

FIGURE 5
In vitro and *in vivo* test of fermented licorice. **(A)** Test of DPPH clearance rate of fermented licorice. **(B)** Test of total antioxidant capacity of fermented licorice. **(C)** Test of ROS clearance rate of fermented licorice. **(D)** SH-SY5Y cell viability under treatment of different concentration of fermented licorice. **(E)** Beneficial effect of fermented licorice on neurodegenerative model of *Caenorhabditis elegans*. **(F)** Beneficial effect of fermented licorice on Alzheimer's model of *C. elegans*. **(G)** The percent survival of *C. elegans* under heat-stress.

References

Abraham, J., and Florentine, S. (2021). Licorice (*Glycyrrhiza glabra*) extracts-suitable pharmacological interventions for COVID-19? A review. *Plants (Basel)* 10:2600. doi: 10.3390/plants10122600

Asl, M. N., and Hosseinzadeh, H. (2008). Review of pharmacological effects of Glycyrrhiza sp. and its bioactive compounds. *Phytother. Res.* 22, 709–724. doi: 10.1002/ptr.2362

Barri, T., and Dragsted, L. O. (2013). UPLC-ESI-QTOF/MS and multivariate data analysis for blood plasma and serum metabolomics: effect of experimental artefacts and anticoagulant. *Anal. Chim. Acta* 768, 118–128. doi: 10.1016/j.aca.2013.01.015

Boozari, M., and Hosseinzadeh, H. (2021). Natural products for COVID-19 prevention and treatment regarding to previous coronavirus infections and novel studies. *Phytother. Res.* 35, 864–876. doi: 10.1002/ptr.6873

Brendler, T., Al-Harrasi, A., Bauer, R., Gafner, S., Hardy, M. L., Heinrich, M., et al. (2021). Botanical drugs and supplements affecting the immune response in the time of COVID-19: implications for research and clinical practice. *Phytother. Res.* 35, 3013–3031. doi: 10.1002/ptr.7008

Caldwell, K. A., Willicott, C. W., and Caldwell, G. A. (2020). Modeling neurodegeneration in *Caenorhabditis elegans*. *Dis. Model. Mech.* 13:dmm046110. doi: 10.1242/dmm.046110

Cao, Y., Li, W., Gong, X., Niu, X., Zheng, J., Yu, J., et al. (2022). Widely quasi-quantitative analysis enables temporal bile acids-targeted metabolomics in rat after oral administration of ursodeoxycholic acid. *Anal. Chim. Acta* 1212:339885. doi: 10.1016/j.aca.2022.339885

Chen, J., Aronow, B. J., and Jegga, A. G. (2009a). Disease candidate gene identification and prioritization using protein interaction networks. *BMC Bioinformatics* 10:73. doi: 10.1186/1471-2105-10-73

Chen, J., Bardes, E. E., Aronow, B. J., and Jegga, A. G. (2009b). ToppGene suite for gene list enrichment analysis and candidate gene prioritization. *Nucleic Acids Res.* 37, W305–W311. doi: 10.1093/nar/gkp427

Chen, J., Xu, H., Aronow, B. J., and Jegga, A. G. (2007). Improved human disease candidate gene prioritization using mouse phenotype. *BMC Bioinformatics* 8:392. doi: 10.1186/1471-2105-8-392

Cheng, M., Zhang, J., Yang, L., Shen, S., Li, P., Yao, S., et al. (2021). Recent advances in chemical analysis of licorice (Gan-Cao). *Fitoterapia* 149:104803. doi: 10.1016/j.fitote.2020.104803

Cui, X., Zuo, P., Zhang, Q., Li, X., Hu, Y., Long, J., et al. (2006). Chronic systemic D-galactose exposure induces memory loss, neurodegeneration, and oxidative damage in mice: protective effects of R-alpha-lipoic acid. *J. Neurosci. Res.* 83, 1584–1590. doi: 10.1002/jnr.20845

Dunn, W. B., Broadhurst, D., Begley, P., Zelena, E., Francis-McIntyre, S., Anderson, N., et al. (2011). Procedures for large-scale metabolic profiling of serum and plasma using gas chromatography and liquid chromatography coupled to mass spectrometry. *Nat. Protoc.* 6, 1060–1083. doi: 10.1038/nprot.2011.335

Fiore, C., Eisenhut, M., Krausse, R., Ragazzi, E., Pellati, D., Armanini, D., et al. (2008). Antiviral effects of *Glycyrrhiza* species. *Phytother. Res.* 22, 141–148. doi: 10.1002/ptr.2295

Han, M. J., and Kim, D. H. (2020). Effects of red and fermented ginseng and Ginsenosides on allergic disorders. *Biomol. Ther.* 10:634. doi: 10.3390/biom10040634

Heidari, S., Mehri, S., and Hosseinzadeh, H. (2021). The genus Glycyrrhiza (Fabaceae family) and its active constituents as protective agents against natural or chemical toxicities. *Phytother. Res.* 35, 6552–6571. doi: 10.1002/ptr.7238

Hosseinzadeh, H., and Nassiri-Asl, M. (2015). Pharmacological effects ofGlycyrrhizaspp. And its bioactive constituents: update and review. *Phytother. Res.* 29, 1868–1886. doi: 10.1002/ptr.5487

Jalali, A., Dabaghian, F., Akbrialiabad, H., Foroughinia, F., and Zarshenas, M. M. (2021). A pharmacology-based comprehensive review on medicinal plants and phytoactive constituents possibly effective in the management of COVID-19. *Phytother. Res.* 35, 1925–1938. doi: 10.1002/ptr.6936

Liana, D., and Phanumartwiwath, A. (2022). Leveraging knowledge of Asian herbal medicine and its active compounds as COVID-19 treatment and prevention. *J. Nat. Med.* 76, 20–37. doi: 10.1007/s11418-021-01575-1

Liu, Z., Guo, F., Wang, Y., Li, C., Zhang, X., Li, H., et al. (2016). BATMAN-TCM: a bioinformatics analysis tool for molecular mechANism of traditional Chinese medicine. *Sci. Rep.* 6:21146. doi: 10.1038/srep21146

Luo, P., Dai, W., Yin, P., Zeng, Z., Kong, H., Zhou, L., et al. (2015). Multiple reaction monitoring-ion pair finder: a systematic approach to transform nontargeted mode to pseudotargeted mode for metabolomics study based on liquid chromatography-mass spectrometry. *Anal. Chem.* 87, 5050–5055. doi: 10.1021/acs.analchem.5b00615

Montoro, P., Maldini, M., Russo, M., Postorino, S., Piacente, S., and Pizza, C. (2011). Metabolic profiling of roots of liquorice (*Glycyrrhiza glabra*) from different geographical areas by ESI/MS/MS and determination of major metabolites by LC-ESI/MS and LC-ESI/MS/MS. *J. Pharm. Biomed. Anal.* 54, 535–544. doi: 10.1016/j.jpba.2010.10.004

Pastorino, G., Cornara, L., Soares, S., Rodrigues, F., and Oliveira, M. (2018). Liquorice (*Glycyrrhiza glabra*): a phytochemical and pharmacological review. *Phytother. Res.* 32, 2323–2339. doi: 10.1002/ptr.6178

Sarao, L. K., and Arora, M. (2017). Probiotics, prebiotics, and microencapsulation: a review. *Crit. Rev. Food Sci. Nutr.* 57, 344–371. doi: 10.1080/10408398.2014.887055

Shang, Z., Liu, C., Qiao, X., and Ye, M. (2022a). Chemical analysis of the Chinese herbal medicine licorice (Gan-Cao): an update review. *J. Ethnopharmacol.* 299:115686. doi: 10.1016/j.jep.2022.115686

Shang, Z., Tian, Y., Yi, Y., Li, K., Qiao, X., and Ye, M. (2022b). Comparative bioactivity evaluation and chemical profiling of different parts of the medicinal plant *Glycyrrhiza uralensis*. *J. Pharm. Biomed. Anal.* 215:114793. doi: 10.1016/j.jpba.2022.114793

Sharifi-Rad, J., Quispe, C., Herrera-Bravo, J., Belén, L. H., Kaur, R., Kregiel, D., et al. (2021). *Glycyrrhiza* genus: enlightening phytochemical components for pharmacological and health-promoting abilities. *Oxidative Med. Cell. Longev.* 2021:7571132. doi: 10.1155/2021/7571132

Shibata, S. (2000). A drug over the millennia: pharmacognosy, chemistry, and pharmacology of licorice. *Yakugaku Zasshi* 120, 849–862. doi: 10.1248/yakushi1947.120.10_849

Suez, J., Zmora, N., Segal, E., and Elinav, E. (2019). The pros, cons, and many unknowns of probiotics. *Nat. Med.* 25, 716–729. doi: 10.1038/s41591-019-0439-x

Wahab, S., Annadurai, S., Abullais, S. S., Das, G., Ahmad, W., Ahmad, M. F., et al. (2021). *Glycyrrhiza glabra* (licorice): a comprehensive review on its Phytochemistry, biological activities, clinical evidence and toxicology. *Plants (Basel)* 10:2751. doi: 10.3390/plants10122751

Wang, C., Qiu, J., Li, G., Wang, J., Liu, D., Chen, L., et al. (2022). Application and prospect of quasi-targeted metabolomics in age-related hearing loss. *Hear. Res.* 424:108604. doi: 10.1016/j.heares.2022.108604

Want, E. J., O'Maille, G., Smith, C. A., Brandon, T. R., Uritboonthai, W., Qin, C., et al. (2006). Solvent-dependent metabolite distribution, clustering, and protein extraction for serum profiling with mass spectrometry. *Anal. Chem.* 78, 743–752. doi: 10.1021/ac051312t

Want, E. J., Wilson, I. D., Gika, H., Theodoridis, G., Plumb, R. S., Shockcor, J., et al. (2010). Global metabolic profiling procedures for urine using UPLC-MS. *Nat. Protoc.* 5, 1005–1018. doi: 10.1038/nprot.2010.50

Wen, B., Mei, Z., Zeng, C., and Liu, S. (2017). metaX: a flexible and comprehensive software for processing metabolomics data. *BMC Bioinformatics* 18:183. doi: 10.1186/s12859-017-1579-y

Wieërs, G., Belkhir, L., Enaud, R., Leclercq, S., Philippart de Foy, J. M., Dequenne, I., et al. (2019). How probiotics affect the microbiota. *Front. Cell. Infect. Microbiol.* 9:454. doi: 10.3389/fcimb.2019.00454

Xiao, D., Xiu, Y., Yue, H., Sun, X., Zhao, H., and Liu, S. (2017). A comparative study on chemical composition of total saponins extracted from fermented and white ginseng under the effect of macrophage phagocytotic function. *J. Ginseng Res.* 41, 379–385. doi: 10.1016/j.jgr.2017.03.009

Xu, T., Yang, M., Li, Y., Chen, X., Wang, Q., Deng, W., et al. (2013). An integrated exact mass spectrometric strategy for comprehensive and rapid characterization of phenolic compounds in licorice. *Rapid Commun. Mass Spectrom.* 27, 2297–2309. doi: 10.1002/rcm.6696

Yu, Y., Dunaway, S., Champer, J., Kim, J., and Alikhan, A. (2020). Changing our microbiome: probiotics in dermatology. *Br. J. Dermatol.* 182, 39–46. doi: 10.1111/bjd.18088

Żółkiewicz, J., Marzec, A., Ruszczyński, M., and Feleszko, W. (2020). Postbiotics-a step beyond pre- and probiotics. *Nutrients* 12:2189. doi: 10.3390/nu12082189

Frontiers in Neuroscience

Provides a holistic understanding of brain function from genes to behavior

Part of the most cited neuroscience journal series which explores the brain - from the new eras of causation and anatomical neurosciences to neuroeconomics and neuroenergetics.

Discover the latest Research Topics

See more →

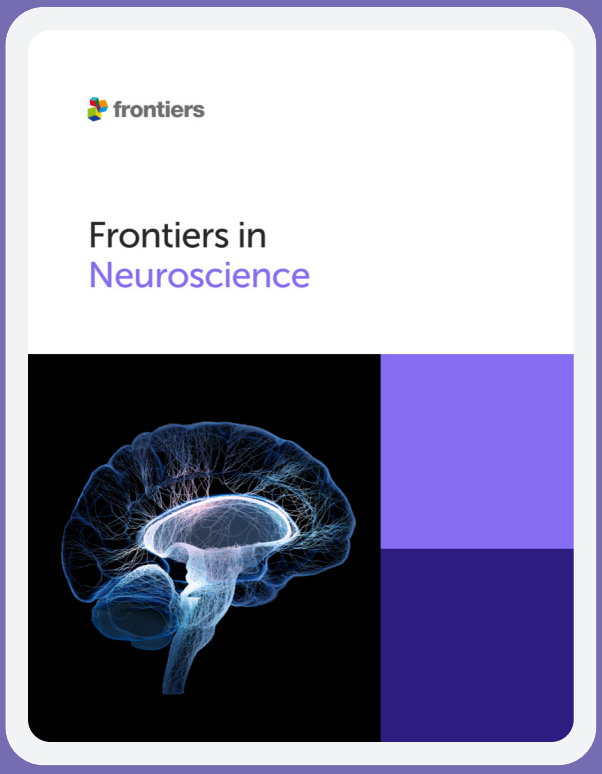

Frontiers

Avenue du Tribunal-Fédéral 34
1005 Lausanne, Switzerland
frontiersin.org

Contact us

+41 (0)21 510 17 00
frontiersin.org/about/contact